

In this Issue

Highlights from this issue of *A&R* | By Lara C. Pullen, PhD

Association Between Rheumatoid Arthritis Morning Stiffness, Synovial Fibrin, and Neutrophils

While rheumatologists know that patients with rheumatoid arthritis (RA) experience morning stiffness, the etiology of this stiffness is poorly understood. In this issue, Orange et al (p. 557) report the results of their study designed to determine whether histologic features of the synovium are associated with morning stiffness. They found that, for patients with RA, morning stiffness may be related to impaired fibrinolysis of neutrophil-enmeshed fibrin deposits along the synovial membrane.

The investigators began by documenting the significant association of both stiffness severity and morning stiffness duration with Disease Activity Score in 28 joints (DAS28). While no synovial feature was associated with stiffness severity, synovial neutrophils and fibrin were associated with patient report of >1 hour of morning stiffness. Moreover, 73% of patients with both synovial fibrin and neutrophils reported morning stiffness of ≥ 1 hour.

Fibrin is the final product of the clotting cascade, and rheumatologists have previously observed it along the surface

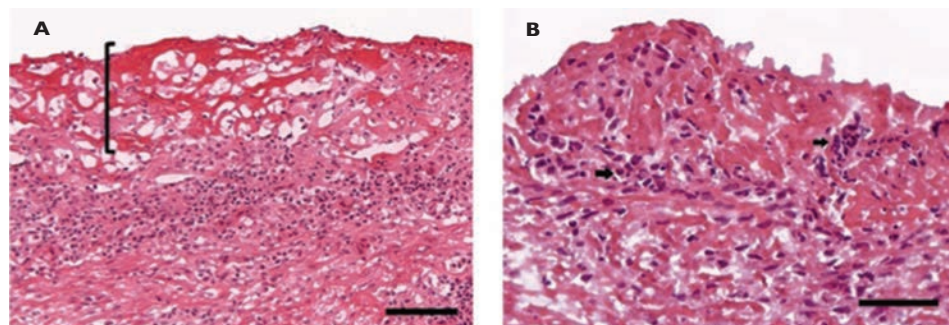


Figure 1. Neutrophils colocalize with fibrin deposit along the synovial lining. Representative images of rheumatoid arthritis synovial tissue. In **A**, bracket highlights eosinophilic synovial fibrin deposition along the synovial membrane. Bar = 100 μm . In **B**, arrows highlight neutrophils intermixed within fibrin, which appears as pink fibrillary material along the synovial lining. Bar = 50 μm .

of inflamed synovium in patients with RA. The current study revealed that these fibrin deposits colocalize with neutrophils. When the researchers performed *in vitro* analyses, they found that fibrin clots seeded with necrotic neutrophils were more resistant to fibrinolysis than those seeded with living neutrophils or no cells. Moreover, DNase I treatment of necrotic neutrophils was able to abrogate the delay in fibrinolysis. The

authors point out that while neutrophils are not unexpected in synovial tissue, their finding suggests that neutrophil DNA confers increased stability and rigidity to fibrin deposits along the synovial surface, thereby contributing to the perception of stiffness. An additional implication of these findings is that implication of these findings is that morning stiffness severity and duration may reflect distinct pathophysiologic phenomena.

Use of the Systemic Lupus International Collaborating Clinics Frailty Index to Predict Damage Accrual

Previous studies have demonstrated an association between the Systemic Lupus International Collaborating Clinics (SLICC) Frailty Index (FI) and mortality in systemic lupus erythematosus (SLE). Its association with other important outcomes, however, has been unknown until now. In this issue, Legge et al (p. 658) report that the SLICC FI predicts damage accrual in incident SLE, extending support for the SLICC FI as a valid health measure for individuals with SLE.

The investigators performed their study in a well-characterized, international cohort of recently diagnosed SLE patients. The 1,549 SLE patients (88.7% female) who were eligible for the analysis had a mean age of 35.7 years, a median disease duration of 1.2 years

at baseline, and a mean baseline SLICC FI of 0.17. The researchers followed the cohort for a mean of 7.2 years. During that time, 653 patients had an increase in SLICC/American College of Rheumatology Damage Index (SDI). Higher baseline SLICC FI values were associated with higher rates of increase in the SDI during follow-up, and this association held true after the investigators adjusted for age, sex, ethnicity/region, education, baseline SLE Disease Activity Index 2000, baseline SDI, and baseline use of glucocorticoids, anti-malarials, and immunosuppressive agents. The authors emphasize in their discussion that, following external validation, the SLICC FI may be a useful prognostic tool for identifying SLE patients at increased risk for future morbidity and mortality.

Autoantibody Diversity Associated With Disease Severity in IgG4-Related Disease

Although rheumatologists have learned a great deal about the immunologic mechanisms of IgG4-related disease (IgG4-RD), there have been few systemic efforts to identify the antigens driving the immune response. Moreover, several autoantigens that have recently been identified have not yet been subjected to external validation, leaving open the possibility that some individuals break tolerance to >1 autoantigen. In this issue, Liu et al (p. 687) report on their efforts to evaluate the relative frequencies of antibody responses against these autoantigens and explore the role of the adaptive immune response in IgG4-RD.

The investigators found antibodies against prohibitin, annexin A11, and laminin 511-E8 in only a small portion of patients with IgG4-RD. Moreover, they found similar levels of these autoantibodies in controls. The authors conclude that none of these autoantigens constitutes a dominant antigen in the context of IgG4-RD.

The researchers had previously analyzed a portion of the cohort (n = 86) for anti-galectin-3 antibody responses and

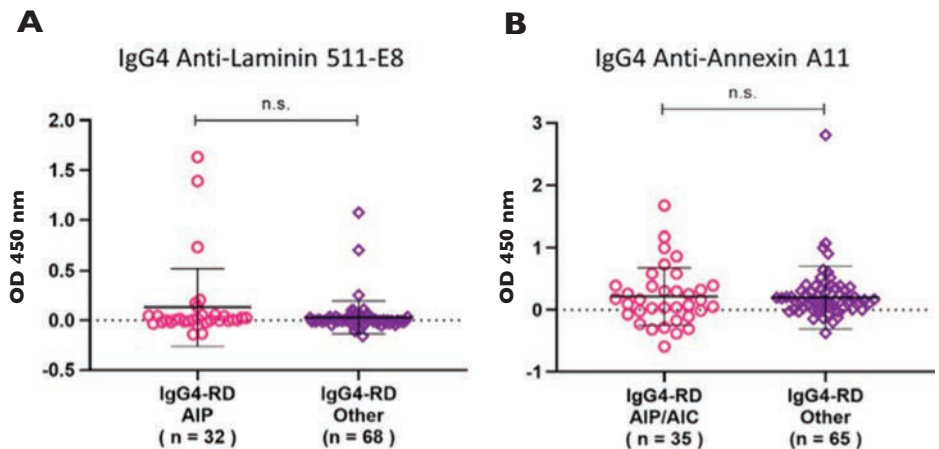


Figure 1. Responses to annexin A11 and laminin 511-E8 autoantibodies according to pancreatobiliary involvement (autoimmune pancreatitis [AIP] or autoimmune cholangitis [AIC]). IgG4 anti-laminin 511-E8 (A) and IgG4 anti-annexin A11 (B) antibody responses between IgG4-related disease (IgG4-RD) patients with pancreatic or biliary involvement and those without such involvement are shown. Symbols represent individual subjects; bars show the mean \pm SD. NS = not significant.

found that 29% had IgG4 anti-galectin-3 antibodies. Of these 86 patients, 37% had IgG4 antibodies to ≥ 1 of the 4 autoantigens (prohibitin, annexin A11, laminin 511-E8, and galectin-3) and 14% showed reactivity with ≥ 2 of the tested antigens. The subset of IgG4-RD patients that had

IgG4 antibodies against ≥ 2 autoantigens presented with robust IgG subclass elevations, complement consumption, and visceral organ involvement. This led the authors to conclude that this broader break in immunologic tolerance was associated with more severe disease.

Biologic Therapies Alter Microbiome of Patients with SpA

In this issue, Manasson et al (p. 645) report the results of their study designed to characterize the ecological effects of biologic therapies on the gut bacterial and fungal microbiome in psoriatic arthritis (PsA)/spondyloarthritis (SpA) patients. They found that, in a subgroup of SpA patients, the initiation of interleukin-17A (IL-17A) blockade correlated with features of subclinical gut inflammation as well as intestinal dysbiosis of certain bacterial and fungal taxa. The most notable microbial shift occurred as a result of a robust expansion of Clostridiales and *Candida albicans*. Nevertheless, the researchers found that a few patients demonstrated a reduction of these microbes in response to IL-17A blockade.

For their study, the investigators analyzed pre- and posttreatment fecal samples from 15 patients treated with tumor necrosis factor inhibitors (TNFi) and 14 treated with IL-17i. They sequenced the fecal microbiome and performed computational microbiome analysis. The researchers then analyzed fecal levels of fatty acid metabolites and

cytokines/proteins implicated in PsA/SpA pathogenesis or intestinal inflammation and correlated these findings with the sequence data. Lastly, they obtained ileal biopsy samples from SpA patients who developed clinically overt Crohn's disease (CD) after treatment with IL-17i and analyzed the samples for expression of IL-23/Th17-related cytokines, IL-25/IL-17E-producing cells, and type 2 innate lymphoid cells (ILC2s).

The researchers found that IL-17i-related CD was associated with overexpression of IL-25/IL-17E-producing tuft cells and ILC2s, compared to pre-IL-17i treatment levels. This is the first study to describe the effects of 2 biologic therapies (TNFi and IL-17i) on the intestinal microbiome of PsA and SpA patients. It revealed that subclinical alterations correlated with changes in bacterial community co-occurrence, metabolic pathways, IL-23/Th17-related cytokines, and various fatty acids. Taken together, the results may explain the potential link between inhibition of a specific IL-17 pathway and the (sub)clinical gut inflammation observed in SpA.

Clinical Connections

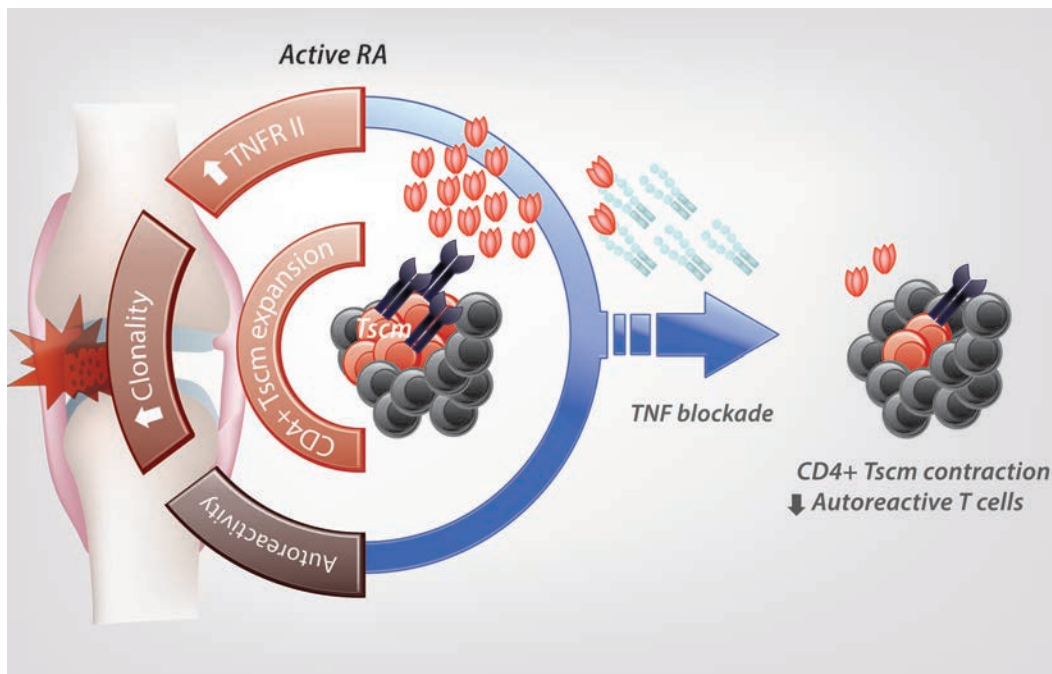
CD4+ Memory Stem T Cells Recognizing Citrullinated Epitopes Are Expanded in Patients With Rheumatoid Arthritis and Sensitive to Tumor Necrosis Factor Blockade

Cianciotti et al, *Arthritis Rheumatol* 2020;75:565–575

CORRESPONDENCE

Nicoletta Cieri, MD, PhD: nicoletta_cieri@dfci.harvard.edu

Chiara Bonini, MD: bonini.chiara@hsr.it



KEY POINTS

- Long-lived self-renewing CD4+ Tscm cells are expanded in patients with active RA.
- Expanded CD4+ Tscm cells are enriched in putative autoreactive clones, express the costimulatory TNFR II, and display an oligoclonal TCR repertoire.
- Effective TNF blockade reduces CD4+ Tscm cell numbers in RA patients.

SUMMARY

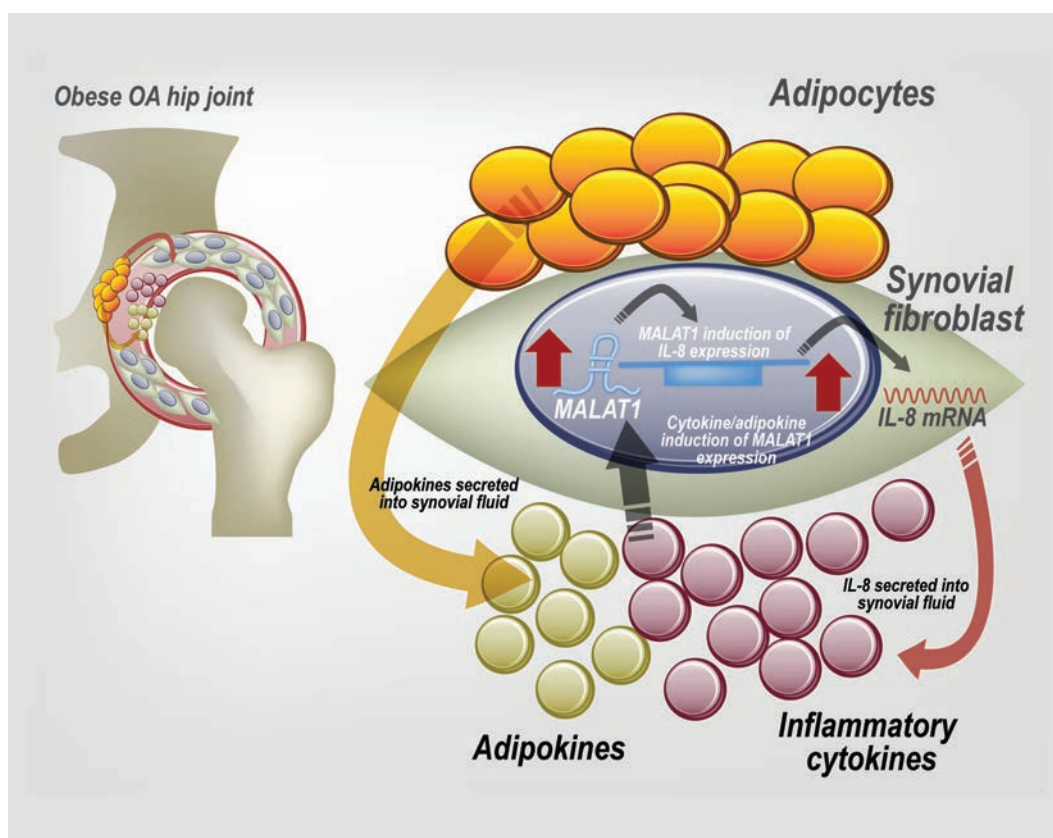
Memory stem T (TSCM) cells are antigen-experienced, self-renewing T cells. While their role in the generation of a long-lasting protective immunity is highly desirable in cancer and infections, Tscm cells might represent a reservoir of long-lived lymphocytes with detrimental antigen specificities responsible for the perpetuation of autoimmunity. Cianciotti et al investigated the role of Tscm cells in rheumatoid arthritis (RA). The authors analyzed the dynamics of Tscm cells in 27 patients with active RA, 16 of whom were also studied during treatment with an anti-tumor necrosis factor (anti-TNF) biologic agent. CD4+ Tscm cells are numerically expanded in RA patients with active disease and display a preferential inflammatory Th17 polarization. Expanded CD4+ Tscm cells express higher levels of the costimulatory TNF receptor II (TNFR II) compared to other memory cells and include autoreactive clones specific for an arthritogenic peptide derived from citrullinated vimentin. T cell receptor (TCR) sequencing of sorted CD4+ memory subsets revealed that Tscm cells are selectively biased toward an oligoclonal TCR repertoire. The autoreactive and oligoclonal CD4+ Tscm cell subpopulation contracts after anti-TNF treatment, supporting the importance of this memory subset in disease maintenance.

Regulation of the Inflammatory Synovial Fibroblast Phenotype by Metastasis-Associated Lung Adenocarcinoma Transcript 1 Long Noncoding RNA in Obese Patients With Osteoarthritis

Nanus et al, *Arthritis Rheumatol* 2020;75:609–619

CORRESPONDENCE

Simon W. Jones, PhD: s.w.jones@bham.ac.uk



KEY POINTS

- Synovial fibroblasts from obese OA patients have an inflammatory phenotype.
- The inflammation-associated MALAT1 lncRNA is highly abundant in obese OA synovial fibroblasts and is produced in response to inflammatory cytokine stimulation.
- Inhibition of MALAT1 reduces the synovial fibroblast inflammatory phenotype by inhibiting cytokine production.
- Targeted inhibition of MALAT1 could be a therapeutic approach to reducing synovitis in obese OA patients.

SUMMARY

Inflammation and enlargement of the synovium (synovitis) is a frequent pathologic feature of osteoarthritis (OA). Nanus et al found synovitis to be greater in hip OA patients who are obese, where the synovial fibroblasts exhibit an inflammatory phenotype with increased production of inflammatory cytokines such as interleukin-6 and CXCL8, compared to either normal-weight OA patients or normal-weight controls.

The inflammatory synovial fibroblast phenotype is associated with the expression of specific long noncoding RNAs (lncRNAs), a new class of gene regulators. The lncRNA for metastasis-associated lung adenocarcinoma transcript 1 (MALAT1) is rapidly produced in OA synovial fibroblasts in response to inflammatory stimulation with inflammatory cytokines. Inhibition of MALAT1 reduces the rate of synovial fibroblast growth and decreases the production and release of inflammatory proteins. These findings demonstrate that obese hip OA patients have an inflammatory synovial fibroblast phenotype and that MALAT1 lncRNA is a central regulator in mediating synovitis in OA patients who are obese.

Arthritis & Rheumatology

An Official Journal of the American College of Rheumatology
www.arthritisrheum.org and wileyonlinelibrary.com

Editor

Richard J. Bucala, MD, PhD
Yale University School of Medicine, New Haven

Deputy Editor

Daniel H. Solomon, MD, MPH, *Boston*

Co-Editors

Joseph E. Craft, MD, *New Haven*
David T. Felson, MD, MPH, *Boston*
Richard F. Loeser Jr., MD, *Chapel Hill*
Peter A. Nigrovic, MD, *Boston*
Janet E. Pope, MD, MPH, FRCPC, *London, Ontario*
Christopher T. Ritchlin, MD, MPH, *Rochester*
Betty P. Tsao, PhD, *Charleston*
John Varga, MD, *Chicago*

Co-Editor and Review Article Editor

Robert Terkeltaub, MD, *San Diego*

Clinical Trials Advisor

Michael E. Weinblatt, MD, *Boston*

Social Media Editor

Paul H. Sufka, MD, *St. Paul*

Journal Publications Committee

Shervin Assassi, MD, MS, *Chair, Houston*
Vivian Bykerk, MD, FRCPC, *New York*
Kristin D'Silva, MD, *Boston*
Deborah Feldman, PhD, *Montreal*
Meenakshi Jolly, MD, MS, *Chicago*
Linda C. Li, PT, MSc, PhD, *Vancouver*
Uyen-Sa Nguyen, MPH, DSc, *Fort Worth*
R. Hal Scofield, MD, *Oklahoma City*

Editorial Staff

Jane S. Diamond, MPH, *Managing Editor, Atlanta*
Ilani S. Lorber, MA, *Assistant Managing Editor, Atlanta*
Lesley W. Allen, *Senior Manuscript Editor, Atlanta*
Kelly Barraza, *Manuscript Editor, Atlanta*
Jessica Hamilton, *Manuscript Editor, Atlanta*
Sara Omer, *Manuscript Editor, Atlanta*
Emily W. Wehby, MA, *Manuscript Editor, Atlanta*
Stefanie L. McKain, *Editorial Coordinator, Atlanta*
Brittany Swett, *Assistant Editor, New Haven*
Will Galanis, *Production Editor, Boston*

Associate Editors

Daniel Aletaha, MD, MS, *Vienna*
Heather G. Allore, PhD, *New Haven*
Daniel J. Clauw, MD, *Ann Arbor*
Robert A. Colbert, MD, PhD, *Bethesda*
Karen H. Costenbader, MD, MPH, *Boston*
Nicola Dalbeth, MD, FRACP, *Auckland*
Kevin D. Deane, MD, *Denver*
Mark C. Genovese, MD, *Palo Alto*
Insoo Kang, MD, *New Haven*
Wan-Uk Kim, MD, PhD, *Seoul*
Carol Langford, MD, MHS, *Cleveland*
Katherine Liao, MD, MPH, *Boston*
S. Sam Lim, MD, MPH, *Atlanta*
Anne-Marie Malfait, MD, PhD, *Chicago*
Paul A. Monach, MD, PhD, *Boston*
Chester V. Oddis, MD, *Pittsburgh*
Andras Perl, MD, PhD, *Syracuse*
Jack Porrino, MD, *New Haven*
Timothy R. D. J. Radstake, MD, PhD, *Utrecht*
William Robinson, MD, PhD, *Palo Alto*
Georg Schett, MD, *Erlangen*
Nan Shen, MD, *Shanghai*
Ronald van Vollenhoven, MD, PhD, *Amsterdam*
Fredrick M. Wigley, MD, *Baltimore*

Advisory Editors

Abhishek Abhishek, MD, PhD, *Nottingham*
Tom Appleton, MD, PhD, *London, Ontario*
Bonnie Bermas, MD, *Dallas*
Liana Fraenkel, MD, MPH, *New Haven*
Monica Guma, MD, PhD, *La Jolla*
Nigil Haroon, MD, PhD, *Toronto*
Erica Herzog, MD, PhD, *New Haven*
Hui-Chen Hsu, PhD, *Birmingham*
J. Michelle Kahlenberg, MD, PhD, *Ann Arbor*
Mariana J. Kaplan, MD, *Bethesda*
Jonathan Kay, MD, *Worcester*
Francis Lee, MD, PhD, *New Haven*
Sang-Il Lee, MD, PhD, *Jinju*
Rik Lories, MD, PhD, *Leuven*
Bing Lu, PhD, *Boston*
Suresh Mahalingam, PhD, *Southport, Queensland*
Aridaman Pandit, PhD, *Utrecht*
Kevin Winthrop, MD, MPH, *Portland*
Kazuki Yoshida, MD, MPH, MS, *Boston*

AMERICAN COLLEGE OF RHEUMATOLOGY

Ellen M. Gravallese, MD, *Boston*, **President**
David R. Karp, MD, PhD, *Dallas*, **President-Elect**
Douglas White, MD, PhD, *La Crosse*, **Treasurer**

Kenneth G. Saag, MD, MSc, *Birmingham*, **Secretary**
Steven Echard, IOM, CAE, *Atlanta*, **Executive Vice-President**

© 2020 American College of Rheumatology. All rights reserved. No part of this publication may be reproduced, stored or transmitted in any form or by any means without the prior permission in writing from the copyright holder. Authorization to copy items for internal and personal use is granted by the copyright holder for libraries and other users registered with their local Reproduction Rights Organization (RRO), e.g. Copyright Clearance Center (CCC), 222 Rosewood Drive, Danvers, MA 01923, USA (www.copyright.com), provided the appropriate fee is paid directly to the RRO. This consent does not extend to other kinds of copying such as copying for general distribution, for advertising or promotional purposes, for creating new collective works or for resale. Special requests should be addressed to: permissions@wiley.com

Access Policy: Subject to restrictions on certain backfiles, access to the online version of this issue is available to all registered Wiley Online Library users 12 months after publication. Subscribers and eligible users at subscribing institutions have immediate access in accordance with the relevant subscription type. Please go to onlinelibrary.wiley.com for details.

The views and recommendations expressed in articles, letters, and other communications published in *Arthritis & Rheumatology* are those of the authors and do not necessarily reflect the opinions of the editors, publisher, or American College of Rheumatology. The publisher and the American College of Rheumatology do not investigate the information contained in the classified advertisements in this journal and assume no responsibility concerning them. Further, the publisher and the American College of Rheumatology do not guarantee, warrant, or endorse any product or service advertised in this journal.

Cover design: Todd Machen

©This journal is printed on acid-free paper.

Arthritis & Rheumatology

An Official Journal of the American College of Rheumatology
www.arthritisrheum.org and wileyonlinelibrary.com

VOLUME 72 • April 2020 • NO. 4

In This Issue	A13
Clinical Connections	A15
Special Articles	
Editorial: Less Pain, More Gain: Should Placebo Be a Clinical Therapeutic? <i>Stacy N. Uchendu and Andrew Wang</i>	511
Editorial: Bugs, Drugs, and Shrugs <i>James T. Rosenbaum and Lisa Karstens</i>	515
New Perspectives In Rheumatology: Nonsteroidal Antiinflammatory Drugs as Potential Disease-Modifying Medications in Axial Spondyloarthritis <i>Runsheng Wang, Joan M. Bathon, and Michael M. Ward</i>	518
2020 American College of Rheumatology Guideline for the Management of Reproductive Health in Rheumatic and Musculoskeletal Diseases <i>Lisa R. Sammaritano, Bonnie L. Bermas, Eliza E. Chakravarty, Christina Chambers, Megan E. B. Clowse, Michael D. Lockshin, Wendy Marder, Gordon Guyatt, D. Ware Branch, Jill Buyon, Lisa Christopher-Stine, Rachelle Crow-Hercher, John Cush, Maurice Druzin, Arthur Kavanaugh, Carl A. Laskin, Lauren Plante, Jane Salmon, Julia Simard, Emily C. Somers, Virginia Steen, Sara K. Tedeschi, Evelynne Vinet, C. Whitney White, Jinoos Yazdany, Medha Barbhuiya, Brittany Bettendorf, Amanda Eudy, Arundathi Jayatilleke, Amit Aakash Shah, Nancy Sullivan, Laura L. Tarter, Mehret Birru Talabi, Marat Turgunbaev, Amy Turner, and Kristen E. D'Anci</i>	529
Rheumatoid Arthritis	
Rheumatoid Arthritis Morning Stiffness Is Associated With Synovial Fibrin and Neutrophils <i>Dana E. Orange, Nathalie E. Blachere, Edward F. DiCarlo, Serene Mirza, Tania Pannellini, Caroline S. Jiang, Mayu O. Frank, Salina Parveen, Mark P. Figgie, Ellen M. Gravallese, Vivian P. Bykerk, Ana-Maria Orbai, Sarah L. Mackie, and Susan M. Goodman</i>	557
CD4+ Memory Stem T Cells Recognizing Citrullinated Epitopes Are Expanded in Patients With Rheumatoid Arthritis and Sensitive to Tumor Necrosis Factor Blockade <i>Beatrice C. Cianciotti, Eliana Ruggiero, Corrado Campochiaro, Giacomo Oliveira, Zulma I. Magnani, Mattia Baldini, Matteo Doglio, Michela Tassara, Angelo A. Manfredi, Elena Baldissera, Fabio Ciceri, Nicoletta Cieri, and Chiara Bonini</i>	565
Involvement of Tumor Necrosis Factor Receptor Type II in FoxP3 Stability and as a Marker of Treg Cells Specifically Expanded by Anti-Tumor Necrosis Factor Treatments in Rheumatoid Arthritis <i>François Santinon, Maxime Batignes, Majda Lyna Mebrek, Jérôme Biton, Gaëlle Clavel, Roxane Hervé, Delphine Lemeiter, Magali Breckler, Florence Busato, Jorg Tost, Marianne Zioli, Marie-Christophe Boissier, Patrice Decker, Luca Semerano, and Natacha Bessis</i>	576
Learned Immunosuppressive Placebo Response Attenuates Disease Progression in a Rodent Model of Rheumatoid Arthritis <i>Laura Lückemann, Hubert Stangl, Rainer H. Straub, Manfred Schedlowski, and Martin Hadamitzky</i>	588
Errata	
Errors in Two Sentences in the Patients and Methods Section of the Article by Duarte-García et al (Arthritis Rheumatol, September 2019)	597
Omitted Acknowledgment in the Article by Mecoli et al (Arthritis Rheumatol, January 2020).....	597
Omission of Fifth Author in the Reply Letter by Mathian et al (Arthritis Rheumatol, January 2020).....	597
Incorrect Spelling of Author's First Name in the Article by Kass et al (Arthritis Rheumatol, March 2020)	597
Osteoarthritis	
Multiparameter Analysis Identifies Heterogeneity in Knee Osteoarthritis Synovial Responses <i>Hannah Labinsky, Paul M. Panipinto, Kaytlyn A. Ly, Deric K. Khuat, Bhanupriya Madarampalli, Vineet Mahajan, Jonathan Clabeaux, Kevin MacDonald, Peter J. Verdin, Jane H. Buckner, and Erika H. Noss</i>	598
Regulation of the Inflammatory Synovial Fibroblast Phenotype by Metastasis-Associated Lung Adenocarcinoma Transcript 1 Long Noncoding RNA in Obese Patients With Osteoarthritis <i>Dominika E. Nanus, Susanne N. Wijesinghe, Mark J. Pearson, Marina R. Hadjicharalambous, Alex Rosser, Edward T. Davis, Mark A. Lindsay, and Simon W. Jones</i>	609
GRK5 Inhibition Attenuates Cartilage Degradation via Decreased NF-κB Signaling <i>Takuya Sueishi, Yukio Akasaki, Norio Goto, Ichiro Kurakazu, Masakazu Toya, Masanari Kuwahara, Taisuke Uchida, Mitsumasa Hayashida, Hidetoshi Tsushima, Hirofumi Bekki, Martin K. Lotz, and Yasuharu Nakashima</i>	620
Intergenerational Transmission of Diet-Induced Obesity, Metabolic Imbalance, and Osteoarthritis in Mice <i>Natalia S. Harasymowicz, Yun-Rak Choi, Chia-Lung Wu, Leanne Iannucci, Ruhang Tang, and Farshid Guilak</i>	632

Psoriatic Arthritis

Interleukin-17 Inhibition in Spondyloarthritis Is Associated With Subclinical Gut Microbiome Perturbations and a Distinctive Interleukin-25–Driven Intestinal Inflammation

Julia Manasson, David S. Wallach, Giuliana Guggino, Matthew Stapylton, Michelle H. Badri, Gary Solomon, Soumya M. Reddy, Roxana Coras, Alexander A. Aksenov, Drew R. Jones, Parvathy V. Girija, Andrea L. Neimann, Adriana Heguy, Leopoldo N. Segal, Pieter C. Dorrestein, Richard Bonneau, Monica Guma, Francesco Ciccia, Carles Ubeda, Jose C. Clemente, and Jose U. Scher..... 645

Systemic Lupus Erythematosus

Prediction of Damage Accrual in Systemic Lupus Erythematosus Using the Systemic Lupus International Collaborating Clinics Frailty Index

Alexandra Legge, Susan Kirkland, Kenneth Rockwood, Pantelis Andreou, Sang-Cheol Bae, Caroline Gordon, Juanita Romero-Diaz, Jorge Sanchez-Guerrero, Daniel J. Wallace, Sasha Bernatsky, Ann E. Clarke, Joan T. Merrill, Ellen M. Ginzler, Paul R. Fortin, Dafna D. Gladman, Murray B. Urowitz, Ian N. Bruce, David A. Isenberg, Anisur Rahman, Graciela S. Alarcón, Michelle Petri, Munther A. Khamashta, M. A. Dooley, Rosalind Ramsey-Goldman, Susan Manzi, Asad A. Zoma, Cynthia Aranow, Meggan Mackay, Guillermo Ruiz-Irastorza, S. Sam Lim, Murat Inanc, Ronald F. van Vollenhoven, Andreas Jonsen, Ola Nived, Manuel Ramos-Casals, Diane L. Kamen, Kenneth C. Kalunian, Soren Jacobsen, Christine A. Peschken, Anca Askanase, and John G. Hanly..... 658

Clinical Images

Jaccoud's Arthropathy

Wen Shi and Yang Jiao..... 666

Vasculitis

Diagnostic Assessment Strategies and Disease Subsets in Giant Cell Arteritis: Data From an International Observational Cohort

K. Bates Gribbons, Cristina Ponte, Anthea Craven, Joanna C. Robson, Ravi Suppiah, Raashid Luqmani, Richard Watts, Peter A. Merkel, and Peter C. Grayson..... 667

Pediatric Rheumatology

Increased T Cell Plasticity With Dysregulation of Follicular Helper T, Peripheral Helper T, and Treg Cell Responses in Children With Juvenile Idiopathic Arthritis and Down Syndrome–Associated Arthritis

C. Foley, A. Floudas, M. Canavan, M. Biniiecka, E. J. MacDermott, D. J. Veale, R. H. Mullan, O. G. Killeen, and U. Fearon..... 677

IgG4-Related Disease

Disease Severity Linked to Increase in Autoantibody Diversity in IgG4-Related Disease

Hang Liu, Cory A. Perugino, Musie Ghebremichael, Zachary S. Wallace, Sydney B. Montesi, John H. Stone, and Shiv Pillai..... 687

Letters

Additional Analyses to Confirm Relationship of Hydroxychloroquine Blood Levels to Retinopathy: Comment on the Article by Petri et al

Wen-hui Xie and Zhuo-li Zhang..... 694

Reply

Michelle Petri, Jessica Li, Laurence S. Magder, and Daniel W. Goldman..... 694

Does Leukopenia Influence Performance of the New European League Against Rheumatism/American College of Rheumatology Classification Criteria in an African-Descendent Population With Childhood-Onset Systemic Lupus Erythematosus? Comment on the Article by Aringer et al

Adriana R. Fonseca, Marta C. F. Rodrigues, Flavio Sztajn bok, Marcelo G. P. Land, and Sheila K. F. de Oliveira..... 694

Reply

Martin Aringer, Karen H. Costenbader, Thomas Dörner, and Sindhu R. Johnson..... 695

CD4+ T Cells as Key Players in the Immunopathology of Takayasu Arteritis: Comment on the Article by Zhang et al

Ryu Watanabe..... 696

Reply

Xiyu Liu, Wanwan Jiang, Ying Wang, Mengyao Sun, Zhibo Li, and Zhenke Wen..... 697

ACR Announcements A18

Cover image: The figure on the cover is the painting *Mother and Child (Baby in Dark Blue Suit, Looking Over His Mother's Shoulder)* (c. 1889) by Mary Cassatt (1844–1926), an American painter and printmaker who lived much of her adult life in France. This issue of *Arthritis & Rheumatology* features the 2020 American College of Rheumatology Guideline for the Management of Reproductive Health in Rheumatic and Musculoskeletal Diseases (Sammaritano et al, pages 529–556).

EDITORIAL

Less Pain, More Gain: Should Placebo Be a Clinical Therapeutic?

Stacy N. Uchendu  and Andrew Wang 

Placebo and nocebo effects are potent, prevalent, and poorly understood. Respectively defined as the therapeutic and harmful effects of being given a physiologically inert treatment, placebo and nocebo effects can result from any type of medical intervention. They are thought to be caused by the context surrounding medical interventions on disease trajectories, as opposed to properties inherent to the medical intervention themselves. The placebo effect has been recognized since antiquity—the Greek physician and medical researcher, Galen of Pergamon, famously wrote that “the patient’s trust in the doctor and in the medicine employed was more important than the treatment method itself” (1). Throughout the history of medicine, physicians were aware of the placebo effect, and some have used it intentionally, although the practice was ethically controversial due to the questionable morality of deceiving patients (2).

Advances in chemistry, physiology, and biology in the early 20th century have made it possible to rigorously test the therapeutic efficacy intrinsic to pharmaceutically active interventions. The first placebo-controlled trial was completed in 1931 and investigated the anti-tuberculosis effects of the drug sanocrysin (3). Since then, placebo-controlled trials have become a gold standard to evaluate the efficacy of medical interventions. Placebo response has been documented across a vast number of disease states, such as in inflammatory diseases (4–6), chronic pain syndromes (7,8), and Parkinson’s disease (7,9), with varying degrees of placebo efficacy between these conditions. In these trials, placebo responses can occur in ~30–70% of subjects, with an effect size ranging from ~50% to 100% of that observed with the pharmaceutical treatment in conditions such as osteoarthritis (10) and chronic pain (11), while in other diseases, placebo responses are not observed (12). Moreover, the same disease studied at different geographic locations produces significantly different placebo responses, and it remains unclear if this is a function of the context of medical intervention or of the patient populations themselves (13). Importantly, placebo response can lead not only to

improvements in “subjective” symptoms, but also in measurable indices of disease activity that reflect underlying disease pathogenesis (such as reductions of proinflammatory cytokine levels in inflammatory diseases [14]), suggesting that neuronal inputs lead to quantitative changes in physiology.

Despite this wealth of observations spanning over 2,000 years, surprisingly little is known about the mechanisms of placebo biology. Much of the research on placebo biology has been motivated by the desire to eliminate the large confounding effect that placebo responders cause in clinical trials for pharmaceutical drugs (15,16). However, alongside this research exists a growing body of work that aims to understand the mechanism of placebo biology in order to harness it for therapeutic use. With the recent advent of sophisticated tools that allow for detailed molecular probing of neurobiologic and physiologic processes, we are now poised to embark upon understanding the molecular mechanisms of placebo and nocebo biology.

In the last few decades, much of the placebo research has been directed toward mapping the neurofunctional networks associated with placebo response through imaging studies in humans and animal models (11,17). It is generally agreed upon that there is involvement of the prefrontal cortex, the orbitofrontal cortex, the dopaminergic reward pathway, and the anterior cingulate cortex (ACC), which has connections to emotional processing, memory, autonomic functions, and reward processing (18,19). Although this network provides a basic skeleton for understanding the neurobiology of placebo response, the brain structures involved vary between different diseases and conditions. For example, placebo analgesia is mostly associated with the dorsal and ventral lateral prefrontal cortex, rostral ACC, and the periaqueductal gray matter in humans, whereas placebo effects on immunosuppression in a rodent model appear to involve the insular cortex, the amygdala, and the ventromedial nucleus of the hypothalamus (17). It is becoming increasingly clear that placebo effects are not the same across various diseases, and that they likely utilize similar

Supported by the NIH (National Institute of Arthritis and Musculoskeletal and Skin Diseases grant K08-AI-128745).

Stacy N. Uchendu, BA, Andrew Wang, MD, PhD: Department of Internal Medicine (Rheumatology, Allergy, & Immunology) and Department of Immunobiology, Yale University, New Haven, Connecticut.

No potential conflicts of interest relevant to this article were reported.
Address correspondence to Andrew Wang, MD, PhD, 330 Cedar Street, PO Box 208056, New Haven, CT 06510. E-mail: andrew.wang@yale.edu.
Submitted for publication November 4, 2019; accepted in revised form November 7, 2019.

but distinct mechanisms to manifest the placebo response as a function of the biologic variable that is improved (perceived pain, magnitude of inflammation, etc.) (Figure 1).

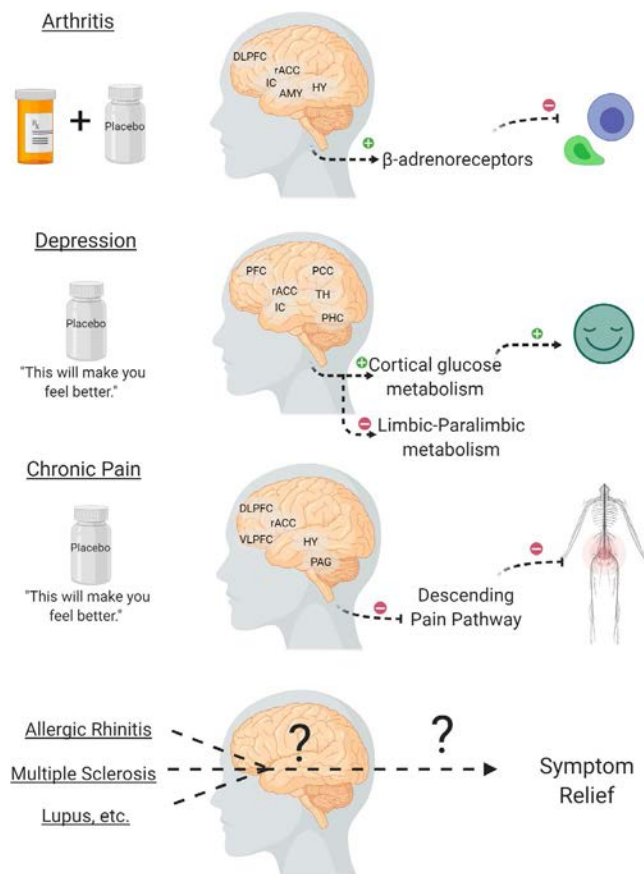


Figure 1. Through various imaging methods such as functional magnetic resonance imaging (fMRI) and positron emission tomography (PET), brain regions associated with placebo response in different conditions have been described. In a rodent model of classically conditioned immunosuppression in which active pharmaceutical agents are paired with placebo, the insular cortex (IC) is shown to be necessary for both acquisition and evocation of conditioned immunosuppression, while the amygdala (AMY) and hypothalamus (HY) are implicated in affective and effective processes, respectively, during conditioning (17). With a placebo antidepressant, the placebo effect can be elicited with positive expectation alone. PET studies show that glucose metabolism increases in cortical structures (such as the prefrontal cortex [PFC] and posterior cingulate cortex [PCC]) and decreases in subcortical and limbic structures (such as the thalamus [TH] and parahippocampal cortex [PHC]) are associated with both placebo and active antidepressant response (37). Similar to depression symptom relief, placebo analgesia can be elicited with positive expectation. Studies with fMRI show that the endogenous opioid system inhibits the descending pain pathway via periaqueductal gray (PAG) matter and is combined with higher-order frontal structures, such as the dorsolateral PFC (DLPPFC), as well as subcortical structures involved in the reward prediction network (11,19). Other conditions associated with placebo response, such as allergic rhinitis and multiple sclerosis, have yet to be neurobiologically characterized. rACC = rostral anterior cingulate cortex; VLPFC = ventrolateral PFC.

There has been continued debate about whether placebo effects work through expectancy or classic conditioning. This distinction is important because it dictates the modality by which placebo is given to a patient in clinic. The answer to this question is likely that they both are important, but to different degrees depending on the disease. For example, conditions that are mostly centrally processed, such as pain or depression, might require that placebo be given in a way that elicits positive expectation (20). For diseases that largely effect peripheral systems such as rheumatoid arthritis, placebo might be best given in conjunction with a pharmaceutically active drug in a classic conditioning modality (14). For example, results of a study performed by Benedetti and colleagues suggest that in Parkinson's disease, neurons can be taught to respond to placebo such that increased exposure to an active drug (apomorphine) prior to placebo exposure causes a more robust and sustained placebo response (21). This suggests that a model in which a patient intermittently receives placebo between periods of active drug treatment may be useful in cases where long-term use of a drug presents issues with toxicity or drug tolerance (14).

In this issue of *Arthritis & Rheumatology*, Lückemann et al report that rats with collagen-induced arthritis can be behaviorally conditioned to respond to placebo when the immunosuppressant cyclosporin A (CSA) is paired with saccharin solution (22). Clinical symptoms of arthritis, such as diminished grip strength, as well as objective measures of inflammation, such as interferon- γ activation and histologic changes, were significantly improved in the conditioned group, achieving 75–100% of the therapeutic effect of high-dose CSA treatment (unconditioned stimulus). This conditioned response was extended by giving the rats subtherapeutic doses of CSA paired with the saccharin solution, thus avoiding extinction. Furthermore, learned immunosuppression was reversed with nadolol, a β -adrenoreceptor (β -AR) antagonist, suggesting that conditioned immunosuppression is mediated by adrenergic signaling, presumably from the central nervous system.

Lückemann and colleagues' work elegantly demonstrates a clear therapeutic use for leveraging placebo biology in minimizing drug toxicity in patients with chronic inflammatory diseases. The finding that central processes could be distilled to β -adrenergic signaling is quite interesting. Traditionally, β -adrenergic engagement on immune cells leads to immunosuppression (23–25). Adrenergic signaling, and in particular, β_2 -AR signaling on macrophages and T cells (cell types implicated in the pathogenesis of inflammatory arthritis), suppresses activation of these cells. Lückemann and colleagues' observation that the conditioned immunosuppression is ablated with β_2 -adrenergic antagonism is consistent with previous findings. Additionally, previous studies have shown that learning is impaired in the presence of β -blockade (26–28). Thus, in addition to intriguing mechanistic possibilities for how central processing may be "translated" into physiologic responses in rheumatoid arthritis particularly, this is

evidence of the possible necessity of sympathetic involvement for certain placebo responses in general. Although placebo biology is becoming increasingly characterized, and evidence for the clinical utility of placebo is mounting, there still remains uncertainty regarding the ideal candidate and disease for placebo.

With such varied placebo efficacy between and within different diseases, a predictive model should be created to assess who might benefit most from placebo and who might be best suited for traditional pharmaceutical therapy. Tétrault et al have attempted this by using whole-brain connectivity to determine brain regions that predict placebo response and magnitude a priori in chronic pain patients (29). Furthermore, when machine learning was applied to psychologic and neurofunctional connectivity profiles of placebo responders and nonresponders, the magnitude of placebo response could be predicted (11). Another method of predicting placebo response is combining genotyping with positron emission tomography imaging. In a study of placebo in anxiety disorders, placebo response was associated with decreased regional blood flow to the left amygdala during a stressful task, in comparison to nonresponders. These responders were exclusively homozygous for the I allele of the serotonin transporter polymorphic gene (5HTTLPR I/I) and the G allele for the tryptophan hydroxylase 2 polymorphic gene (TPH2 G/G)—2 important proteins that regulate the serotonin network (30). This finding implies that genetic control of the neural networks specific to a disease or condition may have an important role in determining who would be an ideal candidate for placebo.

While there is promise in harnessing the clinical potential of placebo response, there are valid concerns about the uncertainty of the biologic mechanism of placebo, the lack of clarity on who are potential placebo responders versus who are likely to be nonresponders, and the questionable ethics of deceiving patients about the treatments they are given. Even with the remaining uncertainties regarding placebo biology, lack of clarity on the mechanisms of action would not be a clear moral deterrent to its clinical use. Take the case of acetaminophen's widespread use as an example. As one of the most commonly ingested drugs, there remains a surprising amount of ambiguity around the mechanism of action. With only a general consensus that it inhibits the synthesis of prostaglandins, acetaminophen is taken with relatively lax precaution. Placebo exists in the same arena as drugs such as acetaminophen—although the exact mechanism is unclear, there is an apparent beneficial effect in a significant population, and there are typically no major side effects when used properly in the right person.

Although the mechanism of placebo is being increasingly defined, with ongoing development of methods to predict possible placebo responders, the question still remains: should we be using placebo? There are ethical concerns that may hinder the widespread adoption of placebo's clinical use, particularly regarding physicians deceiving patients when giving a placebo.

However, it has been shown that placebo response still occurs when patients fully know that they are getting a placebo, known as an "open-label placebo" (31,32). In fact, the psychosocial element of the physician suggesting that placebo ingestion will make the patient feel better increases the positive expectation, which is a large element of the placebo effect. This might eliminate the questionable ethics of giving a placebo to patients, as an open-label placebo only carries the risk of not causing a response in the patient, which is less than the wide range of serious side effects of many active pharmaceutical agents.

However, prominent placebo researcher Benedetti has warned that if positive expectancy is all that is needed to cause placebo response, the door would be open to anything serving as a placebo, like snake oils or talismans (33). Are we embarking on a slippery slope that will return medicine to the late 19th and early 20th centuries when quack doctors and con artists prevailed? In diseases like Parkinson's or arthritis, in which placebo is best paired intermittently with active drugs, a clinician would be working closely with a patient to manage the schedule and prescription, thus leaving less room for deceptive placebo practices. However, in conditions like chronic pain that mainly involve centrally based perception and do not have negative consequences in the peripheral systems, does it truly matter in what form the placebo is? A caregiver's kiss on a toddler's scraped knee could be just as effective in analgesia as a sugar pill prescribed by a doctor. It is of paramount importance that clinicians and scientists clearly communicate the science of placebo to the general public, particularly to avoid the rise of potentially harmful products marketed as placebos.

Beyond the potential for clinical use, understanding placebo biology can lay the foundation for exploring the interface of psychosocial context with physiology, such as understanding the relationship between psychological stressors and autoimmune flares (34–36). Placebo offers clinicians and researchers alike the opportunity to collapse the false dichotomy of the mind and body and take up an integrated understanding of human health and disease.

AUTHOR CONTRIBUTIONS

Ms Uchendu and Dr. Wang drafted the article, revised it critically for important intellectual content, and approved the final version to be published.

REFERENCES

1. Nutton V. The fatal embrace: Galen and the history of ancient medicine. *Sci Context* 2005;18:111–21.
2. Macedo A, Farré M, Baños JE. Placebo effect and placebos: what are we talking about? Some conceptual and historical considerations. *Eur J Clin Pharmacol* 2003;59:337–42.
3. Amberson JB Jr, McMahon BT, Pinner M. A clinical trial of sanocrysin in pulmonary tuberculosis. *Am Rev Tuberc* 1931;24:401–35.
4. Lee EB, Fleischmann R, Hall S, Wilkinson B, Bradley JD, Gruben D, et al. Tofacitinib versus methotrexate in rheumatoid arthritis. *N Engl J Med* 2014;370:2377–86.

5. Ader R, Cohen N. Behaviorally conditioned immunosuppression. *Psychosom Med* 1975;37:333–40.
6. Furie R, Petri M, Zamani O, Cervera R, Wallace DJ, Tegzová D, et al. A phase III, randomized, placebo-controlled study of belimumab, a monoclonal antibody that inhibits B lymphocyte stimulator, in patients with systemic lupus erythematosus. *Arthritis Rheum* 2011;63:3918–30.
7. Holmes RD, Tiwari AK, Kennedy JL. Mechanisms of the placebo effect in pain and psychiatric disorders. *Pharmacogenomics J* 2016;16:491–500.
8. Benedetti F, Amanzio M. The neurobiology of placebo analgesia: from endogenous opioids to cholecystokinin. *Prog Neurobiol* 1997;52:109–25.
9. De la Fuente-Fernández R, Ruth TJ, Sossi V, Schulzer M, Calne DB, Stoessl AJ. Expectation and dopamine release: mechanism of the placebo effect in Parkinson's disease. *Science* 2001;293:1164–6.
10. Zhang W, Robertson J, Jones AC, Dieppe PA, Doherty M. The placebo effect and its determinants in osteoarthritis: meta-analysis of randomised controlled trials. *Ann Rheum Dis* 2008;67:1716–23.
11. Vachon-Preseau E, Berger SE, Abdullah TB, Huang L, Cecchi GA, Griffith JW, et al. Brain and psychological determinants of placebo pill response in chronic pain patients. *Nat Commun* 2018;9:3397.
12. Hróbjartsson A, Gøtzsche PC. Placebo interventions for all clinical conditions. *Cochrane Database Syst Rev* 2010;CD003974.
13. Han MA, Altayar O, Hamdeh S, Takyar V, Rotman Y, Etzion O, et al. Rates of and factors associated with placebo response in trials of pharmacotherapies for nonalcoholic steatohepatitis: systematic review and meta-analysis. *Clin Gastroenterol Hepatol* 2019;17:616–29.
14. Albring A, Wendt L, Benson S, Nissen S, Yavuz Z, Engler H, et al. Preserving learned immunosuppressive placebo response: perspectives for clinical application. *Clin Pharmacol Ther* 2014;96:247–55.
15. Rutherford BR, Roose SP. A model of placebo response in antidepressant clinical trials. *Am J Psychiatry* 2013;170:723–33.
16. Carlino E, Vase L. Can knowledge of placebo and nocebo mechanisms help improve randomized clinical trials? *Int Rev Neurobiol* 2018;138:329–57.
17. Pacheco-López G, Niemi MB, Kou W, Härting M, Fandrey J, Schedlowski M. Neural substrates for behaviorally conditioned immunosuppression in the rat. *J Neurosci* 2005;25:2330–7.
18. Stevens FL, Hurley RA, Taber KH. Anterior cingulate cortex: unique role in cognition and emotion. *J Neuropsychiatry Clin Neurosci* 2011;23:121–5.
19. Wager TD, Atlas LY. The neuroscience of placebo effects: connecting context, learning and health. *Nat Rev Neurosci* 2015;16:403–18.
20. Benedetti F, Arduino C, Costa S, Vighetti S, Tarenzi L, Rainero I, et al. Loss of expectation-related mechanisms in Alzheimer's disease makes analgesic therapies less effective. *Pain* 2006;121:133–44.
21. Benedetti F, Frisaldi E, Carlino E, Giudetti L, Pampallona A, Zibetti M, et al. Teaching neurons to respond to placebos. *J Physiol* 2016;594:5647–60.
22. Lückemann L, Stangl H, Straub RH, Schedlowski M, Hadamitzky M. Learned immunosuppressive placebo response attenuates disease progression in a rodent model of rheumatoid arthritis. *Arthritis Rheumatol* 2020;72:588–97.
23. Ağaç D, Estrada LD, Maples R, Hooper LV, Farrar JD. The β 2-adrenergic receptor controls inflammation by driving rapid IL-10 secretion. *Brain Behav Immun* 2018;74:176–85.
24. Estrada LD, Ağaç D, Farrar JD. Sympathetic neural signaling via the β 2-adrenergic receptor suppresses T-cell receptor-mediated human and mouse CD8⁺ T-cell effector function. *Eur J Immunol* 2016;46:1948–58.
25. Araujo LP, Maricato JT, Guerreschi MG, Takenaka MC, Nascimento VM, de Melo FM, et al. The sympathetic nervous system mitigates CNS autoimmunity via β 2-adrenergic receptor signaling in immune cells. *Cell Rep* 2019;28:3120–30.
26. Villain H, Benkahoul A, Drougard A, Lafragette M, Muzotte E, Pech S, et al. Effects of propranolol, a β -noradrenergic antagonist, on memory consolidation and reconsolidation in mice. *Front Behav Neurosci* 2016;10:49.
27. Kroes MC, Tona KD, den Ouden HE, Vogel S, van Wingen GA, Fernández G. How administration of the β -blocker propranolol before extinction can prevent the return of fear. *Neuropsychopharmacology* 2016;41:1569–78.
28. Lonergan MH, Olivera-Figueroa LA, Pitman RK, Brunet A. Propranolol's effects on the consolidation and reconsolidation of long-term emotional memory in healthy participants: a meta-analysis. *J Psychiatry Neurosci* 2013;38:222–31.
29. Tétéreault P, Mansour A, Vachon-Preseau E, Schnitzer TJ, Apkarian AV, Baliki MN. Brain connectivity predicts placebo response across chronic pain clinical trials. *PLoS Biol* 2016;14:e1002570.
30. Furmark T, Appel L, Henningsson S, Ahs F, Faria V, Linnman C, et al. A link between serotonin-related gene polymorphisms, amygdala activity, and placebo-induced relief from social anxiety. *J Neurosci* 2008;28:13066–74.
31. Meeuwis SH, van Middendorp H, van Laarhoven AI, Veldhuijzen DS, Lavrijsen AP, Evers AW. Effects of open- and closed-label nocebo and placebo suggestions on itch and itch expectations. *Front Psychiatry* 2019;10:436.
32. Carvalho C, Caetano JM, Cunha L, Rebouta P, Kaptchuk TJ, Kirsch I. Open-label placebo treatment in chronic low back pain: a randomized controlled trial. *Pain* 2016;157:2766–72.
33. Benedetti F. The placebo response: science versus ethics and the vulnerability of the patient. *World Psychiatry* 2012;11:70–2.
34. Stojanovich L, Marisavljevic D. Stress as a trigger of autoimmune disease. *Autoimmun Rev* 2008;7:209–13.
35. Bou Khalil R, Khoury E, Richa S. Do fibromyalgia flares have a neurobiological substrate? *Pain Med* 2016;17:469–75.
36. Wang Z, Young MR. PTSD, a disorder with an immunological component. *Front Immunol* 2016;7:219.
37. Mayberg HS, Silva JA, Brannan SK, Tekell JL, Mahurin RK, McGinnis S, et al. The functional neuroanatomy of the placebo effect. *Am J Psychiatry* 2002;159:728–37.

EDITORIAL

Bugs, Drugs, and Shrugs

James T. Rosenbaum¹  and Lisa Karstens² 

“For every action, there is an equal and opposite reaction” is Newton’s third law of thermodynamics. Do the laws of physics have an extrapolation to human biology?

Experimental evidence indicates that interleukin-17 (IL-17) plays a critical role in the pathogenesis of inflammatory bowel disease, but blocking IL-17 makes Crohn’s disease (CD) worse (1,2). Only a subset of patients with melanoma benefit from checkpoint inhibitors (3), and only a subset of patients with any type of rheumatic disease benefit from a specific therapy. A scientist at the NIH using a rodent model couldn’t replicate the experimental results of a scientist at Harvard. The intestinal microbiome might provide the explanation for each of these seemingly disparate conundrums.

These enigmas are not each directly addressed by Manasson and a large talented group of international colleagues in their study on the effect of biologics, specifically tumor necrosis inhibitors (TNFi) or anti-IL-17, on the gut microbiome, in this issue of *Arthritis & Rheumatology* (4). Nonetheless, their findings support the hypothesis that unintentional effects on the microbiome could be the solution to many puzzling therapeutic observations. The “shrug” in our title reflects being flummoxed, i.e., how many of us respond to experimental or clinical data that seem to defy our theoretical predictions.

As discussed in their report (4), Manasson and colleagues are not the first to examine how biologic therapies influence the microbiome (5,6). A dysbiosis or alteration in the gut microbiome is characteristic of the majority of immune-mediated diseases (7). Moreover, in many cases, successful biologic therapy has been associated with a “normalization” of the gut microbiome (5). To appreciate the implications of the Manasson study, we first provide some background about the microbiome and its relevance to rheumatic diseases.

We each possess 2 genomes that influence our health. The most obvious genome is the one we inherit from our parents. The technology to alter this genome is just now emerging. The sec-

ond genome is acquired. It is defined by the microbial world that cohabits our bodies. If the importance of a genome could be determined by the number of unique RNA transcripts it produces, the second genome would be around 150 times more important than the first (8). The second genome also is not easy to alter, although it is certainly easier to manipulate (e.g., by diet) than our mammalian genome. The concept of a second genome has led to the recognition that we are holobionts, a product affected by both genome 1 and genome 2. To understand the efficacy of a pharmaceutical, we need to know not only how the medication affects genome 1 but also how it affects genome 2. Furthermore, we need to recognize the reciprocal, or how genome 2 affects the medication (Figure 1).

Acetaminophen (9) and methotrexate (10) are 2 widely used medications that are both metabolized by the microbiome. Even if a medication is not taken orally, the microbiome can still impact its efficacy. For example, the gut microbiome has a marked effect on the success of monoclonal antibodies in the form of checkpoint inhibitors in animal models of cancer (11,12), as discussed below.

The limited reproducibility of basic research has been widely hailed as a failing of modern science (13). But what if the bacteria that dwell inside a mouse housed in St. Louis are vastly different from the bacteria living in a mouse from New Haven? Unlikely, you scoff. But it turns out that segmented filamentous bacteria (SFB) that live in the mouse gut have a profound effect on the immune system (14). Moreover, if you purchase C57BL/6 mice from Taconic Farms, they are unlikely to harbor SFB, but the opposite is true if the mice are purchased from another major research animal vendor, The Jackson Laboratory (15). Differences in the microbiome that result from vendor, climate, diet, bacteria from the skin of a caretaker in a vivarium, or any one of limitless variables could potentially explain many examples of rodent research that suffer from poor reproducibility.

Perhaps the most direct extrapolation from the study by Manasson et al relates to the explanation about why blocking

Supported by the NIH (grant R01-EY-029266 from the National Eye Institute and grant DK-116706 from the National Institute of Diabetes and Digestive and Kidney Diseases), the Spondylitis Association of America, the Rheumatology Research Foundation, the Grandmaison Fund for Autoimmunity Research, the William and Mary Bauman Foundation, and the Stan and Madelle Rosenfeld Family Trust.

¹James T. Rosenbaum, MD: Oregon Health & Science University and Legacy Devers Eye Institute, Portland; ²Lisa Karstens, PhD: Oregon Health & Science University, Portland.

Dr. Rosenbaum is an unpaid collaborator with Viome. No other potential conflicts of interest relevant to this article were reported.

Address correspondence to James T. Rosenbaum, MD, Oregon Health & Science University, 3181 SW Sam Jackson Park Road, Portland, OR 97239. E-mail: rosenbaj@ohsu.edu.

Submitted for publication November 2, 2019; accepted November 7, 2019.

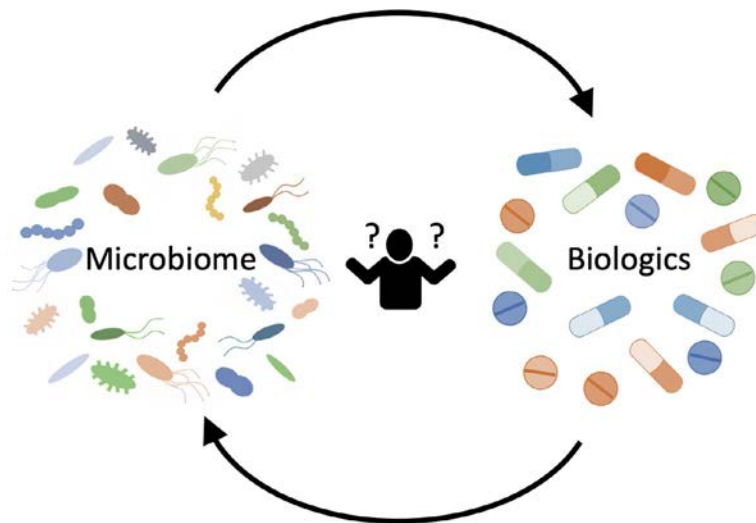


Figure 1. Positive feedback loop. The microbiome alters the effects of biologics, while biologics alter the effects of the microbiome. The confused figure in the center is puzzling to understand the implications of these interactions and wondering if many seemingly disparate observations could each be explained by changes in the microbiome.

IL-17 does not ameliorate CD. Data from animal models show a prominent role for IL-17 in several mouse studies of bowel inflammation (16). The genetics of CD implicates the IL-23 receptor (16), and IL-23 is a major driver for IL-17 synthesis (17). Immunohistology from human tissue supports the importance of IL-17 in the pathogenesis of CD (16). Considering this compelling rationale, many were shocked when inhibiting either IL-17A (1) or the receptor for IL-17 (2) actually exacerbated CD. Recent data point to a role for yeast or fungi, especially *Malassezia*, in the pathogenesis of CD (18). IL-17 plays a major role in the control of fungal infections (19). The data provided by the study in this issue indicate that blocking IL-17 increases the growth of *Candida* in the bowel, and thus could explain why CD is exacerbated by inhibition of IL-17 (20).

While it is not difficult to understand how bacteria could metabolize a medication taken orally, it is a greater challenge to theorize how the intestinal microbiome could alter the efficacy of a monoclonal antibody. However, bacteria in the gut seem to have a dramatic effect on the benefit of checkpoint inhibitors which are being used to bolster the immune response as a treatment for a variety of cancers (21). The evidence for this effect is strong enough to support the rationale to study fecal microbiota transplants as a means to enhance the success of checkpoint inhibitor therapy (22).

As such, the study by Manasson and colleagues is a welcome addition to our understanding of the actions of 2 classes of biologics, those that inhibit TNF and those that neutralize IL-17A. Because both TNF and IL-17A are vital components of our immune system, neutralizing either would be expected to impact the microbiome. It behooves the rheumatology community to define the impact on the microbiome from all medications including biologics. Is it all an epiphenomenon that we can largely ignore? Or is the alteration of the microbiome influential in

determining who benefits from a medication and who does not? Who requires or tolerates an increased dosage? Who is likely to suffer an adverse effect?

Undoubtedly the greatest reward from biologics has derived from their impact on disease. But an unanticipated benefit has come from the lessons that have resulted from the adverse effects of this class of medications. For example, the association between TNFi and demyelinating disease has forced biomedical scientists to gain a better understanding of the role of TNF in the nervous system (23).

Isaac Newton's laws have been applied to physics, but they also relate to biology. We are grateful to Manasson and colleagues for helping us better understand the multitude of unanticipated effects from biologic therapies.

AUTHOR CONTRIBUTIONS

Drs. Rosenbaum and Karstens drafted the article, revised it critically for important intellectual content, and approved the final version to be published.

REFERENCES

1. Hueber W, Sands BE, Lewitzky S, Vandemeulebroecke M, Reinisch W, Higgins PD, et al. Secukinumab, a human anti-IL-17A monoclonal antibody, for moderate to severe Crohn's disease: unexpected results of a randomised, double-blind placebo-controlled trial. *Gut* 2012;61:1693–700.
2. Targan SR, Feagan BG, Vermeire S, Panaccione R, Melmed GY, Blosch C, et al. A randomized, double-blind, placebo-controlled study to evaluate the safety, tolerability, and efficacy of AMG 827 in subjects with moderate to severe Crohn's disease [abstract]. *Gastroenterology* 2012;143:E26.
3. Gopalakrishnan V, Spencer CN, Nezi L, Reuben A, Andrews MC, Karpinets TV, et al. Gut microbiome modulates response to anti-PD-1 immunotherapy in melanoma patients. *Science* 2018;359:97–103.

4. Manasson J, Wallach DS, Guggino G, Stapylton M, Badri MH, Solomon G, et al. Interleukin-17 inhibition in spondyloarthritis associated with subclinical gut microbiome perturbations and a distinctive interleukin-25-driven intestinal inflammation. *Arthritis Rheumatol* 2020;72:645–57.
5. Zhang X, Zhang D, Jia H, Feng Q, Wang D, Liang D, et al. The oral and gut microbiomes are perturbed in rheumatoid arthritis and partly normalized after treatment. *Nat Med* 2015;21:895–905.
6. Busquets D, Mas-de-Xaxars T, López-Siles M, Martínez-Medina M, Bahí A, Sàbat M, et al. Anti-tumour necrosis factor treatment with adalimumab induces changes in the microbiota of Crohn's disease. *J Crohns Colitis* 2015;9:899–906.
7. Rosenbaum JT, Asquith MJ. The microbiome: a revolution in treatment for rheumatic diseases? *Curr Rheumatol Rep* 2016;18:62.
8. Gill SR, Pop M, Deboy RT, Eckburg PB, Turnbaugh PJ, Samuel BS, et al. Metagenomic analysis of the human distal gut microbiome. *Science* 2006;312:1355–9.
9. Clayton TA, Baker D, Lindon JC, Everett JR, Nicholson JK. Pharmacometabonomic identification of a significant host-microbiome metabolic interaction affecting human drug metabolism. *Proc Natl Acad Sci U S A* 2009;106:14728–33.
10. Alexander JL, Wilson ID, Teare J, Marchesi JR, Nicholson JK, Kinross JM. Gut microbiota modulation of chemotherapy efficacy and toxicity [review]. *Nat Rev Gastroenterol Hepatol* 2017;14:356–65.
11. Routy B, Le Chatelier E, Derosa L, Duong CP, Alou MT, Daillère R, et al. Gut microbiome influences efficacy of PD-1-based immunotherapy against epithelial tumors. *Science* 2018;359:91–7.
12. Tanoue T, Morita S, Plichta DR, Skelly AN, Suda W, Sugiura Y, et al. A defined commensal consortium elicits CD8 T cells and anti-cancer immunity. *Nature* 2019;565:600–5.
13. McNutt M. Reproducibility [editorial]. *Science* 2014;343:229.
14. Wu HJ, Ivanov II, Darce J, Hattori K, Shima T, Umesaki Y, et al. Gut-residing segmented filamentous bacteria drive autoimmune arthritis via T helper 17 cells. *Immunity* 2010;32:815–27.
15. Ivanov II, de Llanos Frutos R, Manel N, Yoshinaga K, Rifkin DB, Sartor RB, et al. Specific microbiota direct the differentiation of IL-17-producing T-helper cells in the mucosa of the small intestine. *Cell Host Microbe* 2008;4:337–49.
16. Moschen AR, Tilg H, Raine T. IL-12, IL-23 and IL-17 in IBD: immunobiology and therapeutic targeting. *Nat Rev Gastroenterol Hepatol* 2019;16:185–96.
17. Zhou L, Ivanov II, Spolski R, Min R, Shenderov K, Egawa T, et al. IL-6 programs T_H-17 cell differentiation by promoting sequential engagement of the IL-21 and IL-23 pathways. *Nat Immunol* 2007;8:967–74.
18. Limon JJ, Tang J, Li D, Wolf AJ, Michelsen KS, Funari V, et al. Malassezia is associated with Crohn's disease and exacerbates colitis in mouse models. *Cell Host Microbe* 2019;25:377–88.
19. Conti HR, Gaffen SL. IL-17-mediated immunity to the opportunistic fungal pathogen *Candida albicans*. *J Immunol* 2015;195:780–8.
20. Colombel JF, Sendid B, Jouault T, Poulain D. Secukinumab failure in Crohn's disease: the yeast connection? [letter]. *Gut* 2013;62:800–1.
21. Gravbrot N, Gilbert-Gard K, Mehta P, Ghotmi Y, Banerjee M, Mazis C, et al. Therapeutic monoclonal antibodies targeting immune checkpoints for the treatment of solid tumors [review]. *Antibodies (Basel)* 2019;8:51.
22. Gori S, Inno A, Belluomini L, Bocus P, Bisoffi Z, Russo A, et al. Gut microbiota and cancer: how gut microbiota modulates activity, efficacy and toxicity of antitumoral therapy. *Crit Rev Oncol Hematol* 2019;143:139–47.
23. Valentin-Torres A, Savarin C, Barnett J, Bergmann CC. Blockade of sustained tumor necrosis factor in a transgenic model of progressive autoimmune encephalomyelitis limits oligodendrocyte apoptosis and promotes oligodendrocyte maturation. *J Neuroinflammation* 2018;15:121.

NEW PERSPECTIVES IN RHEUMATOLOGY

Nonsteroidal Antiinflammatory Drugs as Potential Disease-Modifying Medications in Axial Spondyloarthritis

Runsheng Wang,¹  Joan M. Bathon,¹ and Michael M. Ward² 

Nonsteroidal antiinflammatory drugs (NSAIDs) are the first-line pharmacotherapy for patients with axial spondyloarthritis (SpA). In recent years, treatment options have expanded with the availability of biologic agents, including tumor necrosis factor inhibitors and interleukin-17 inhibitors. However, a treatment strategy that clearly prevents syndesmophyte formation has not been established. Observational studies of patients with ankylosing spondylitis indicated potential disease-modifying effects of NSAIDs, but two randomized trials came to different conclusions. More broadly, whether any of the currently available medications for axial SpA have an effect on spine radiographic progression, beyond symptom control, remains inconclusive. In this article, we will review clinical studies of the disease modification effects of NSAIDs and biologics in axial SpA; examine genetic, animal, and clinical evidence of the effects of NSAIDs on bone formation; and discuss how future studies may investigate the question of disease modification in axial SpA.

Introduction

Axial spondyloarthritis (SpA) is a chronic inflammatory spine condition with a prevalence of 0.9–1.4% in the adult population (1). Patients with ankylosing spondylitis (AS), also called radiographic axial SpA, the prototypical form of axial SpA, may develop features of new bone formation, such as ankylosis of the sacroiliac joints, syndesmophytes, and even fusion of the spine (2,3). Pharmacotherapy for axial SpA has significantly broadened beyond nonsteroidal antiinflammatory drugs (NSAIDs) in the past two decades with the availability of biologic agents, including tumor necrosis factor inhibitors (TNFi) and interleukin-17 (IL-17) inhibitors, and more recently, JAK inhibitors (4).

Despite these new treatments, NSAIDs remain the first-line treatment and cornerstone for the management of axial SpA, including early disease and well-established AS. In observational cohorts of patients with early axial SpA, 73.0–92.8% of patients took NSAIDs (5,6). Similarly, in a prospective cohort of patients with established AS, 70.3% of the patients were taking NSAIDs (7). These frequencies are not surprising given the efficacy of NSAIDs, as shown in many clinical trials. In a recent trial of full-dose naproxen

in patients with early axial SpA with active inflammation of the sacroiliac joints, a moderate response was achieved in 56.9% of the patients, as measured by the Assessment of SpondyloArthritis international Society criteria for 40% improvement (ASAS40) (8) (Table 1), and 35.3% of the patients were in ASAS partial remission (Table 1), after 28 weeks of treatment (9). In an open-label study of NSAIDs in patients with axial SpA (including both radiographic and nonradiographic axial SpA), an ASAS40 response was achieved in 35% of the participants after 4 weeks of NSAID treatment (10). In comparison, in the major phase III clinical trials of biologics (TNFi and IL-17 inhibitors) in AS or radiographic axial SpA, ASAS40 was achieved in 39.4–58.1% of the participants at 12 weeks to 24 weeks (11,12), indicating that the rest of the participants, at least 40–60%, needed to optimize their NSAID use in addition to the study drugs or try a different biologic. Although these results were extracted from different studies and cannot be compared directly, they support the notion that, for short-term symptom relief, NSAIDs are not only effective as a first-line treatment but are also important as combination therapy with biologics.

It is less clear, however, whether NSAIDs slow disease progression in patients with axial SpA. In an early retrospective

Dr. Wang's work was supported by a Rheumatology Research Foundation Scientist Development Award. Dr. Ward's work was supported by the Intramural Research Program of the National Institute of Arthritis and Musculoskeletal and Skin Diseases, NIH.

¹Runsheng Wang, MD, MHS, Joan M. Bathon, MD: Columbia University College of Physicians and Surgeons, New York, New York; ²Michael M. Ward, MD, MPH: National Institute of Arthritis and Musculoskeletal and Skin Diseases, NIH, Bethesda, Maryland.

Dr. Wang has received consulting fees from Novartis and Eli Lilly (less than \$10,000 each). No other disclosures relevant to this article were reported.

Address correspondence to Runsheng Wang, MD, MHS, Columbia University College of Physicians and Surgeons, P & S Building, Suite 3450, 630 West 168th Street, New York, NY 10032. E-mail: rw2646@cumc.columbia.edu.

Submitted for publication May 29, 2019; accepted in revised form November 7, 2019.

Table 1. Major outcome measures in clinical research on ankylosing spondylitis or radiographic axial spondyloarthritis*

Outcome measure (ref.)	Description
ASDAS (29)	A composite score, including assessment of total back pain, patient global assessment of disease activity, peripheral pain and swelling, duration of morning stiffness, and C-reactive protein or erythrocyte sedimentation rate
BASDAI (37)	A 6-question, self-administered questionnaire, assessing fatigue, spinal pain, peripheral arthritis, enthesitis, and intensity and duration of morning stiffness
ASAS40 response criteria (8)	On a scale of 10, improvement of $\geq 40\%$ and ≥ 2 units in at least 3 of the 4 domains (patient global assessment, pain, function, and inflammation†), and no worsening in any scores
ASAS partial remission (8)	On a scale of 10, a score in each domain (patient global assessment, pain, function, and inflammation†) of ≤ 2 units

* ASDAS = Ankylosing Spondylitis Disease Activity Score; ASAS40 = Assessment of SpondyloArthritis international Society criteria for 40% improvement.

† Average score of severity and duration of morning stiffness in the Bath Ankylosing Spondylitis Disease Activity Index (BASDAI).

cohort of 40 patients with AS, continuous use of phenylbutazone delayed or arrested radiographic progression compared to no or only intermittent use of phenylbutazone (13). Two randomized trials examined the effects of continuous use versus on-demand use of NSAIDs on disease progression in AS, and came to opposite conclusions (14,15). This uncertainty prompted us to examine the clinical studies of disease modification in AS and the state of knowledge about the effects of NSAIDs on bone growth in general, and in axial SpA in particular. We review the clinical evidence of the effects of NSAIDs and biologic agents on radiographic progression in patients with AS, examine in vitro and in vivo evidence of the effects of NSAIDs on bone formation, and discuss how future studies may evaluate disease modification in axial SpA. Biomarkers for radiographic progression in axial SpA theoretically may be used as surrogate end points for disease modification in clinical studies; however, it is a broad topic in itself, and will not be discussed in this review.

Background

Measurement of disease progression in AS. Syndesmophyte formation and ankylosis of the spine are the key features of AS, and are associated with long-term functional impairment; thus, disease modification to slow or stop syndesmophyte growth is an important goal. The modified Stoke AS Spine Score (mSASSS) (16) has been widely used to evaluate syndesmophyte growth and radiographic progression. The mSASSS is a semiquantitative scoring system based on features of the anterior vertebral corners on lateral projections of cervical and lumbar spine radiographs. Each of the 24 corners (12 in the cervical spine and 12 in the lumbar spine) is graded on a scale of 0–3, where 0 = normal; 1 = erosion, sclerosis, or squaring; 2 = syndesmophyte; and 3 = bony bridging between adjacent vertebrae, for a total score of 0–72 (16). Radiographic progression is usually defined as an increase of ≥ 2 units in the mSASSS; alternatively, the absolute change from baseline in the mSASSS has commonly been used as a radiographic end point (16). When assessed longitudinally, in 2 years, 30–40% of patients demonstrate an increase of any amount in the mSASSS, and ~20% of patients have an increase of ≥ 2 in the mSASSS (16–19). The

rate of change in mSASSS ranges from ~ 1.0 unit in 2 years to 0.98 units/year (17,18,20). The spine has been used as the preferred site to assess radiographic progression, rather than the sacroiliac joints, because it provides a greater range and most patients are eligible to demonstrate change, while changes in joint space or fusion of the sacroiliac joints are difficult to detect.

Although the mSASSS has been shown to have face and construct validity, its reliability and sensitivity to change have been challenged. When assessing progression over 2 years, 2 readers were in agreement in only 54% of the cases (18). Interreader reliability of mSASSS change over 2 years was poor to moderate, with kappa values ranging from 0.17 to 0.67 (19,21–23). Assessing the radiographs in chronological sequence also affects the reading and results in higher apparent progression (17). In addition, it was estimated that in a 2-year randomized controlled trial, a sample size of 100 in each group would be needed to detect a difference between the groups (24), reflecting the slow progression of the disease and relative insensitivity to change of the method.

Risk factors for disease progression in AS. Using the mSASSS as the measure of disease progression, several risk factors have been associated with AS disease progression in longitudinal studies, including the presence of syndesmophytes at baseline (25–28), elevated levels of markers of inflammation (25,27), smoking (25–27), low bone mineral density (26), and high disease activity as measured by the AS Disease Activity Score (29,30) (Table 1). In addition, mechanical stress has been associated with worse radiographic outcomes, both in AS cohorts and animal studies (31–33). Certain occupational and physical activities, such as bending, twisting, and stretching, as well as exposure to whole body vibration, were associated with worse radiographic outcomes, and physically demanding jobs seem to amplify radiographic progression (31).

Heterogeneity in syndesmophyte growth. Increasing evidence suggests that radiographic progression and syndesmophyte growth in AS is a highly heterogeneous process, both temporally and spatially. In a study that evaluated 12-year radiographic progression in patients with AS, new syndesmophytes,

detected based on mSASSS change, were observed in ~60% of patients and 40% of time intervals. At the same time, in ~24% of patients and 40% of time intervals, no radiographic progression was observed, indicating high variability in individual patients and at different time intervals (21). Within the same intervertebral disc spaces, some syndesmophytes were seen to grow substantially while others did not grow, suggesting that local factors, possibly including mechanical forces and local pro-proliferation and anti-proliferation factors, influence syndesmophyte growth (34). This heterogeneity adds further challenges to studying radiographic progression in AS.

Long-term effect of NSAIDs and biologic agents on AS disease modification

Observational studies and clinical trials investigating a disease modification effect of NSAIDs. Since there are more than 20 different NSAIDs used in various dosages, an NSAID intake index has been developed to quantify the dosage in equivalency and duration of NSAID use, with a range of 0–100 (35). For example, daily NSAID use equivalent to 150 mg diclofenac over the whole study period is scored as 100. Using this index, in the German Spondyloarthritis Inception Cohort, the odds of an increase in the mSASSS over 2 years were much lower in patients with high NSAID intake (index ≥ 50) compared to those with low NSAID intake (index < 50) (odds ratio [OR] 0.15 [95% confidence interval (95% CI) 0.02, 0.96]) (total $n = 88$) (36). The results support the hypothesis that NSAIDs have a protective effect on spine radiographic progression in patients with AS. In that study, a similar protective effect was not observed between patients with high AS activity versus those with low AS activity, as measured by the Bath AS Disease Activity Index (36,37) (Table 1), suggesting that subjective symptoms may not be directly associated with radiographic progression, or that the mechanisms by which NSAIDs may act on progression are other than symptom control.

Two separate randomized trials, one with the cyclooxygenase 2 (COX-2) selective NSAID celecoxib (14), and the other with the nonselective NSAID diclofenac (15), examined the efficacy of NSAIDs on radiographic progression (Table 2). In the celecoxib trial, TNFi-naive patients with AS were randomized to receive continuous versus on-demand celecoxib 100 mg twice daily or higher. After 2 years, patients in the continuous use group had less radiographic progression than those in the on-demand group ($P = 0.002$) (14). Post hoc analysis of that trial showed that slowing of progression with continuous treatment was greater in patients with elevated levels of markers of inflammation (erythrocyte sedimentation rate or C-reactive protein [CRP]) (38). The diclofenac trial (Effects of NSAIDs on Radiographic Damage in AS [ENRADAS]) (15) used a similar design, in that TNFi-naive patients with AS were randomized to receive continuous versus on-demand diclofenac 150 mg daily for 2 years. However, in contrast to the findings of the celecoxib study, the group that received continuous diclofenac

treatment had more progression numerically over 2 years ($P = 0.39$). Findings were similar in subgroups of patients with or without syndesmophytes at baseline and in those with or without elevated CRP levels (15). The authors stated that since “not even a trend for less radiographic progression was seen for the continuous group in our study, it is rather unlikely that inclusion of more patients would have changed the result” (15).

The results from both studies might suggest that only COX-2 selective NSAIDs have a disease modification effect, but several caveats should be considered. First, the absence of a dose effect makes the trial results difficult to interpret. When using change in the mSASSS as the study outcome, at least 2 years are proposed to detect a significant change with a sample size of 100 patients in each treatment group. Because it would be unethical to conduct placebo-controlled trials lasting 2 years, both NSAID trials compared continuous use versus on-demand use, to approximate the ideal placebo-controlled study, with the intention to see whether the difference in NSAID intake between the 2 groups was correlated with the difference in mSASSS increase. The result from the celecoxib trial did show a lower rate of mSASSS increase with continuous use; however, a dose effect of NSAIDs was not demonstrated. The average dose in the continuous group (243 mg) was only modestly higher than that in the on-demand group (201 mg), despite the significant difference in the outcome (mean mSASSS change +0.4 in the continuous group versus +1.5 in the on-demand group). The diclofenac trial groups had a difference in NSAID dose, with an NSAID index of 77 in the continuous group versus 44 in the on-demand group, but did not show a corresponding decrease in radiographic progression (mean mSASSS change +1.3 in the continuous group versus +0.8 in the on-demand group).

Further, in the event of imbalance in randomization, risk factors that are associated with spine radiographic progression could lead to bias when assessing treatment effects. For example, in the diclofenac study, the continuous use group had a significantly higher proportion of current smokers at baseline, compared to the on-demand group. Whether the difference in smoking between the groups was enough to overwhelm a potential inhibitory effect of continuous diclofenac use is unclear (15).

A third clinical trial, the Comparison of the Effect of Treatment with Nonsteroidal Antiinflammatory Drugs Added to Anti-Tumor Necrosis Factor α Therapy Alone on Progression of Structural Damage in the Spine Over Two Years in Patients with Ankylosing Spondylitis (CONSUL trial; ClinicalTrials.gov identifier: NCT02758782), evaluating the effect of celecoxib with golimumab compared to golimumab alone on radiographic progression in patients with AS, is ongoing.

Disease modification effects of biologics. With regard to biologics, 2 strategies have been used to retrospectively analyze radiographic data from long-term extensions of clinical trials. The first strategy was to compare radiographic progression among participants in trials of biologics to that in biologic-naive,

Table 2. Comparison of studies of radiographic progression in patients with ankylosing spondylitis*

Author, year (ref.) and study group	No. of participants	Study length	Baseline mSASSS, mean \pm SD	Ever smoker, %	Male, %	HLA-B27 positive, %	mSASSS change, mean \pm SD
NSAIDs (randomized controlled trials)							
Wanders et al, 2005 (14)							
Continuous celecoxib	76	2 years	7.9 \pm 14.7	NR	66	88	0.4 \pm 1.7
On-demand celecoxib	74	2 years	9.3 \pm 15.2	NR	70	88	1.5 \pm 2.5
Sieper et al, 2016 (15)							
Continuous diclofenac	62	2 years	10.9 \pm 15.5	59	71.0	88.7	1.3 (0.7–1.9)†
On-demand diclofenac	60	2 years	16.4 \pm 18.2	33	66.7	91.7	0.8 (0.2–1.4)†
TNFi (retrospective analyses of clinical trials/long-term extension of clinical trial data)							
Baraliakos et al, 2005 (39)							
Infliximab	41	2 years	12.1‡	NR	63	90	0.4 \pm 2.7
GESPIC cohort	41	2 years	5.9‡	NR	71	85	0.7 \pm 2.8
Van der Heijde et al, 2008 (19)							
Infliximab	201	2 years	17.7 \pm 17.9	NR	78.1	86.5	0.9 \pm 2.6
OASIS cohort	192	2 years	15.8 \pm 18.1	NR	67.7	84.4	1.0 \pm 3.2
Van der Heijde et al, 2008 (40)							
Etanercept	257	2 years	16 \pm 18.3	NR	75.5	78.2	0.91 \pm 2.45
OASIS cohort	175	2 years	14 \pm 17.6	NR	69.1	71.1	0.95 \pm 3.18
Van der Heijde et al, 2009 (21)							
Adalimumab	307	2 years	19.8 \pm 19.3	NR	76.5	NR	0.8 \pm 2.6
OASIS cohort	169	2 years	15.8 \pm 17.6	NR	69.2	NR	0.9 \pm 3.3
Braun et al, 2014 (41)							
Placebo \rightarrow golimumab 50 mg	66	208 weeks	16.1 \pm 18.7	NR	NR	NR	2.1 \pm 5.2
Golimumab 50 mg	111	208 weeks	11.7 \pm 16.4	NR	NR	NR	1.3 \pm 4.1
Golimumab 100 mg	112	208 weeks	13.5 \pm 18.9	NR	NR	NR	2.0 \pm 5.6
IL-17A inhibitor (retrospective analyses of clinical trials/long-term extension of clinical trial data)							
Braun et al, 2019 (42)							
Secukinumab 75 mg	61	208 weeks	10.7 \pm 17.82	39.3	87.0	NR	1.6 \pm 5.67
Secukinumab 75 mg \rightarrow 150 mg	23	208 weeks	10.7 \pm 17.82	34.8	70.5	NR	1.8 \pm 4.32
Secukinumab 150 mg	71	208 weeks	8.6 \pm 16.23	29.6	63.4	NR	1.2 \pm 3.91
Braun et al, 2019 (23)							
Secukinumab	168	2 years	NR	25	73.2	82.9	60.7§
ENRADAS cohort	69	2 years	NR	44.9	66.7	88.4	52.2§¶

* NSAIDs = nonsteroidal antiinflammatory drugs; NR = not reported; TNFi = tumor necrosis factor inhibitor; GESPIC = German Spondyloarthritis Inception Cohort; OASIS = Outcomes in Ankylosing Spondylitis International Study; IL-17A = interleukin-17A; ENRADAS = Effects of NSAIDs on Radiographic Damage in Ankylosing Spondylitis.

† Values are the mean (95% confidence interval).

‡ Values are the mean.

§ Proportion of patients with no radiographic progression (least squares mean change in modified Stoke Ankylosing Spondylitis Spine Score [mSASSS] \leq 0).

¶ $P = 0.2430$ versus patients receiving secukinumab.

historical cohorts (19,20,23,39,40) (Table 2). Most of those studies used the change in the mSASSS over 2 years as the primary radiographic end point and did not find any significant difference in radiographic progression between groups. One of the studies, of patients treated with secukinumab versus the ENRADAS cohort, used the proportion of patients with no radiographic progression (defined as least squares mean change in mSASSS \leq 0) as the end point, and indicated that there were more nonprogressors in the secukinumab group (60.7% versus 52.2%; $P = 0.2430$). Notably, the interreader agreement

for change in the mSASSS in that study was poor ($\kappa = 0.17$), and the ENRADAS cohort had a much higher percentage of smokers (23).

The second strategy, similar to that used in the NSAIDs trials, was to compare different dosing regimens with the question of whether there was a dose effect (41,42) (Table 2). However, this approach has not shown associations between the dose of biologics and progression. In a 4-year secukinumab study (42), although the 150 mg group had marginally less radiographic progression than the 75 mg groups as measured by mSASSS, the

75 mg groups had higher mSASSS at baseline, which is a risk factor for radiographic progression. In addition, similar proportions of patients in each dosing group (78.9% versus 78.6%) had no radiographic progression (mSASSS change ≤ 2). In an open-label extension of a study of certolizumab, 80.6% of the patients had no radiographic progression at 4 years, although there was no comparison group (43).

Two observational studies examined the effect of TNFi on spine radiographic progression, with somewhat conflicting results. In a prospective cohort of 334 patients with AS in North America, after adjustment for baseline mSASSS and propensity to receive TNFi, patients who were taking a TNFi had a 50% lower odds of progression compared to those who never received a TNFi. Also, patients who received TNFi for a larger proportion of their disease course had less mSASSS progression (44). In contrast, in a recent observational study of 432 patients with AS from the Swiss Clinical Quality Management Cohort, no contemporaneous association between TNFi use and radiographic progression was found (45). Instead, treatment with TNFi prior to the radiographic interval was protective, as was longer duration of prior use of TNFi. The data did not detect an association with TNFi during the radiographic interval, perhaps indicating that prolonged treatment is needed to see an effect (45).

In summary, current evidence for a disease-modifying effect of biologics, including TNFi and IL-17 inhibitors, is lacking, and the effect of the different classes of biologics on radiographic progression has not been compared directly. A direct comparison of the effects of secukinumab to the effects of an adalimumab biosimilar on radiographic progression is ongoing (ClinicalTrials.gov identifier: NCT03259074).

NSAIDs and bone formation

The inconclusive results of clinical studies of the effect of NSAIDs on radiographic disease progression in AS prompts a review of preclinical, biologic evidence that would support the notion of an inhibitory effect of NSAIDs on syndesmophyte formation in AS. At the genetic level, in an experiment-wide genetic association study that examined genes related to radiographic severity in AS, a single-nucleotide polymorphism (SNP) rs1236913 was found to have a protective association with the degree of radiographic damage (46). This SNP lies in the *PTGS1* gene, encoding prostaglandin-endoperoxide synthase 1, also known as COX-1. Although extensive functional studies are not available, the association at least suggests that COX-1 might be involved in radiographic progression in AS.

NSAIDs are COX inhibitors, blocking the synthesis of prostaglandin G_2/H_2 (PGG_2/H_2) from arachidonic acid, the main precursor of prostanoids. Arachidonic acid is first hydrolyzed by secretory or cytoplasmic phospholipase A_2 , then oxygenated to PGG_2/H_2 by COX, which is then further converted to PGD_2 , PGE_2 , PGF_2 , PGL_2 or thromboxane A_2 by different synthases (47). Among them, PGE_2

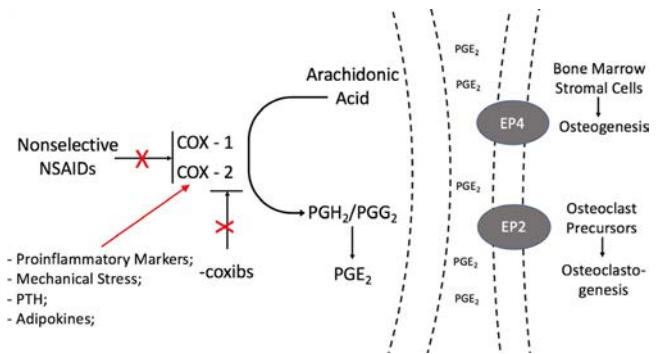


Figure 1. Prostaglandin (PG) pathway and bone metabolism. NSAIDs = nonsteroidal antiinflammatory drugs; COX-1 = cyclooxygenase 1; PTH = parathyroid hormone; PGH_2 = prostaglandin H_2 ; EP_4 = prostaglandin E receptor 4.

is the most studied prostanoid involved in inflammation and bone formation. Local administration of PGE_2 into long bones in rats stimulates bone formation by increasing osteoblast number and activity, and systemic administration of PGE_2 has been shown to increase the osteogenic capacity of bone marrow in ex vivo culture systems (48,49). However, in some experimental systems, PGE_2 is also a potent stimulator of bone resorption, by inducing RANKL expression in primary osteoblastic cell cultures via prostaglandin E receptor 2 (EP_2)/ EP_4 (50,51). Figure 1 illustrates the prostaglandin pathway and effects on bone metabolism.

In vitro evidence of involvement of the prostaglandin pathway and bone metabolism.

Two isoenzymes, COX-1 and COX-2, are traditionally considered the main rate-limiting enzymes in the generation of PGE_2 . COX-1 is constitutively expressed, while COX-2 expression is induced under certain conditions. Proinflammatory cytokines, including IL-1, TNF, and IL-17, have been shown to induce COX-2 expression and PGE_2 production in bone marrow cultures and osteoclast precursors, osteoblastic cells, and synoviocytes (52–54). In addition, mechanical loading of human osteoblastic cell line and primary bone cell cultures derived from the iliac crest triggered the expression of COX-2 and prostaglandin synthesis, and induced bone nodule formation (55,56). In human periodontal ligament cells, cyclic tension force increased PGE_2 expression as well as RANKL messenger RNA expression, but not osteoprotegerin expression, in a COX-2–dependent manner, suggesting a potential for increased osteoclastogenesis (57,58). However, as the skeletal system constantly undergoes remodeling, and COX-2, triggered by proinflammatory cytokines and mechanical force, regulates PGE_2 expression in osteoblasts as well as osteoclasts, these in vitro experiments did not address the net effect of these factors on osteogenesis and osteoclastogenesis.

In vivo evidence of COX inhibition and bone formation.

COX-1^{-/-} and COX-2^{-/-} mice are useful tools to study the net effect of inhibition of COX on bone formation. Using fracture healing models in these mice, COX-2 was shown to be critical for

Table 3. Meta-analyses of the effect of NSAIDs on fracture healing and heterotopic ossification*

Author, year (ref.)	Condition	Study type	Length of follow-up	Type of NSAIDs	No. of studies/no. of participants	Result
Dodwell et al, 2010 (69)	Fracture healing	Mostly retrospective cohort; 1 prospective cohort study	5 months to 3.8 years	Diclofenac, indomethacin, ibuprofen, ketorolac, and not defined	11/2,067 patients exposed to NSAIDs	Increased risk of nonunion (OR 3.0 [95% CI 1.6, 5.6]); in 7 high-quality studies, no significant risk (OR 2.2 [95% CI 0.8, 6.3])
Wheatley et al, 2019 (70)	Fracture healing	RCTs, cohort studies, and case-control studies	>6 months	All types	16 studies/3,283 bones exposed to NSAIDs	Increased risk of delayed union or nonunion (OR 2.07 [95% CI 1.19, 3.61]). No risk for low-dose NSAIDs (<125 mg/day diclofenac, <150 mg/day indomethacin, or <120 mg/day ketorolac) or shorter duration (<1 week) (OR 1.68 [95% CI 0.63, 4.46])
Ma et al, 2018 (71)	Heterotopic ossification	RCTs	1.5–12 months	Naproxen vs. placebo	4/269	Decreased risk of heterotopic ossification at 12 months (RR 0.21 [95% CI 0.12, 0.35])
Joice et al, 2018 (72)	Heterotopic ossification	RCTs	3–24 months	Nonselective NSAIDs vs. placebo	17/4,979	Decreased risk of heterotopic ossification (log OR -1.35 [95% CI -1.83, -0.86])
Joice et al, 2018 (72)	Heterotopic ossification	RCTs	3–24 months	Selective NSAIDs vs. placebo	5/628	Decreased risk of heterotopic ossification (log OR -1.58 [95% CI -2.41, -0.75])
Joice et al, 2018 (72)	Heterotopic ossification	RCTs	3–24 months	Nonselective vs. selective NSAIDs	7/1,096	No difference in risk of heterotopic ossification (log OR 0.22 [95% CI -0.36, 0.79])

* NSAIDs = nonsteroidal antiinflammatory drugs; OR = odds ratio; 95% CI = 95% confidence interval; RCTs = randomized controlled trials; RR = relative risk.

fracture healing, but COX-1 was not (59,60). Consistent with these findings, both nonselective COX inhibitors (e.g., diclofenac, indomethacin, and ketorolac) and COX-2 selective inhibitors (e.g., celecoxib, rofecoxib, and valdecoxib) exerted a delayed or inhibitory effect on fracture healing in rat or rabbit models when given over 4–10 weeks (60–65). Interestingly, when patients were treated with COX selective NSAIDs (rofecoxib or valdecoxib) for 1–2 weeks, or with diclofenac for 1 week, the inhibitory effect of NSAIDs on bone growth was either reversible or less profound (66–68), suggesting a temporal effect of NSAIDs on bone formation.

The effect of NSAIDs on fracture healing in humans has been assessed in randomized controlled trials (RCTs), case-control studies, and cohort studies, with somewhat different results (Table 3). Dodwell et al reported an increased risk of nonunion among NSAID-treated patients in the pooled effect of 11 studies (OR 3.0 [95% CI 1.6, 5.6]), but no effect was observed when only 7 high-quality studies were included (69). Another meta-analysis by Wheatley et al also showed that NSAID use was associated with an increased risk of nonunion or delayed union (OR 2.07 [95% CI 1.19, 3.61]), but similar to the temporal effect observed in the animal studies, no association was found in studies with a short duration of NSAID treatment (70). In addition, no association was observed in studies with low-dose NSAIDs or in pediatric groups (70). Neither of these two meta-analyses examined the difference between the effects of COX-2 selective NSAIDs and nonselective NSAIDs.

The effects of NSAIDs on bone formation have also been examined in the prevention of heterotopic ossification, an abnormal localized growth of bone in muscles and tendons. Systematic reviews and meta-analysis of RCTs (Table 3) have shown that postoperative use of NSAIDs, including indomethacin and naproxen, as well as COX-2 selective NSAIDs, was effective in preventing severe heterotopic ossification after total hip arthroplasty (71,72). In the most recent meta-analysis of the effects of NSAIDs on the

prevention of heterotopic ossification, the effects of nonselective NSAIDs and COX-2 selective NSAIDs were directly compared, based on 7 RCTs and 1,096 participants, and no difference was found between these classes in preventing postoperative heterotopic ossification (72).

Animal studies and clinical evidence from studies of fracture healing and heterotopic ossification formation support the notion that NSAIDs have an inhibitory effect on new bone formation, with no difference between selective and nonselective NSAIDs, at least as clinically evident in humans. A temporal effect of NSAIDs on bone formation has been suggested in studies of fracture healing in animals and humans, i.e., that short duration of NSAID use had a less profound or reversible effect on bone growth, but definitive proof is needed.

Future studies on disease modification in patients with axial SpA

Whether NSAIDs or biologics have a disease modification effect, or more fundamentally, whether suppressing inflammation is sufficient to prevent bone formation in AS, remains unclear. Further studies on disease modification are needed to identify treatment strategies that effectively prevent radiographic progression with the least side effects. How can we improve future studies?

New imaging modalities for evaluating radiographic outcome measures. In recent years, 3-dimensional imaging modalities, including full-dose computed tomography (CT) and low-dose CT of the spine, have been evaluated to improve the measurement of radiographic progression of AS (73,74) (Table 4). The thoracic spine has been omitted from radiographic studies because of the difficulty in seeing vertebral changes on conventional radiographs. In contrast, CT scan methods provide a 360-degree

Table 4. Comparison of radiographic measures for new bone formation in ankylosing spondylitis or radiographic axial spondyloarthritis*

	mSASSS	CTSS	Quantitative syndesmophyte height volume
Imaging modality	Spine radiograph	Low-dose CT	Full-dose CT
Spine segments	Cervical and lumbar spine	Cervical, thoracic, and lumbar spine	Thoracic and lumbar spine
Number of scored IVD spaces (IVD spaces)	12 (C2/3 to C7/T1, T12/L1 to L5/S1)	23 (C2/3 to L5/S1)	13 (T3/4 to L3/4)
Number of scoring sites per IVD space	2	8	Circumferential
Total score (range)	0–72	0–552	NA
Training human readers	Needed	Needed	Not needed
Sensitivity to change (in 2 years)	Increase in 30–40% of patients	Any net change in 61–76% of patients; SDC in 37–43% of patients	Volume increase in >70% of patients
Interreader ICC for change scores	0.17–0.67	0.77 (whole spine) 0.32–0.75 (spine segments)	NA†
Radiation, mSV	1.5‡	4	8

* Magnetic resonance imaging is not included because it does not measure new bone formation. mSASSS = modified Stoke Ankylosing Spondylitis Spine Score; CTSS = computed tomography syndesmophyte score; IVD = intervertebral disc; NA = not applicable; SDC = smallest detectable change; ICC = intraclass correlation coefficient.

† Measured by computer algorithm; no human readers were involved.

‡ For 2 views.

evaluation of the entire vertebral body, and a better visualization of thoracic spine. Using CT scanning, it has been shown that syndesmophytes develop more commonly at the thoracolumbar junction and thoracic spine, rather than the lumbar spine, offering the potential to detect more patients with abnormalities (75,76). In the full-dose CT scan method, syndesmophyte volume was directly quantified and compared over time using a computer algorithm (77). In the low-dose CT method, a CT syndesmophyte score has been developed to measure the radiographic damage in the entire spine by human readers, with moderate interreader intraclass correlation coefficient for change score (76). Both CT methods have been shown to be more sensitive to change than the mSASSS (76,77), which makes it possible to detect a treatment effect in a clinical trial with fewer participants and/or a shorter study length. Notably, the full-dose CT scan method has a radiation exposure of 8 mSv per scan, which is comparable to 3 years of natural background radiation, and about one-third of a positron emission tomography/CT scan, while the low-dose CT has a radiation exposure of 4 mSv per scan. To date, no RCT data have been reported using these new measurements for disease modification effects.

Magnetic resonance imaging (MRI) is a useful imaging tool to detect bone marrow edema in the spine and pelvis. However, it is less sensitive to signals from calcification, so is not as useful to measure new bone formation. A sequential process in which bone marrow edema proceeds the development of fat metaplasia and new bone formation has been proposed, but with mixed evidence (78,79). It is unclear whether the presence of bone marrow edema or its resolution closely correlates with the future development of syndesmophytes.

Identifying subsets of disease. Studies have consistently shown that 30–40% of patients have an increase in mSASSS in a 2-year period. A handful of risk factors for radiographic progression have been identified from previous longitudinal studies, including male sex, HLA-B27 positivity, smoking, elevated CRP, and presence of syndesmophytes at baseline. These risk factors can be used to identify the subset of potential candidates who are more likely to have disease progression, and hence, a higher chance of detecting a difference in radiographic progression in a given time frame. The trial design most likely to detect an NSAID effect would be a study of patients with high risk for progression treated with either minimal-dose or full-dose NSAIDs and assessed with spinal CT.

Identifying novel risk factors and potential interactions. Another methodologic aspect is to identify potential risk factors and their interactions, and include them as covariates in future observational studies. Recent cross-sectional studies have shed light on several new possible risk factors for disease progression, such as crystals, parathyroid hormone (PTH) and vitamin D, and adipokines, but these have not been examined in longitudinal studies. Monosodium urate microcrystals have been shown to

induce COX-2 expression in human monocytes and osteoblast-like cells, and have a synergistic effect with IL-1 on osteoblasts to overexpress COX-2 (80,81). In patients with AS but not a clinical diagnosis of gout, urate crystal deposition at the sacroiliac joint was associated with the progression of sacroiliac joint fusion (82). Both PTH and vitamin D have direct and indirect effects on COX expression, and hence PGE₂ level. A systematic review of cross-sectional studies showed that patients with AS commonly have low vitamin D levels (83). In a cross-sectional study, serum PTH levels were found to be significantly higher in patients with AS than in healthy controls (84). Consistent with this finding, PTH was reported to modulate the response to mechanical stress in osteoblast-like cells (85). Syndesmophyte formation and its association with serum adipokine levels have been investigated in several studies, but the results were inconsistent (86,87).

Conclusions

Despite new therapies that are effective in relieving symptoms in patients with axial SpA, treatments to prevent radiographic progression remain elusive. Observational studies have suggested that NSAIDs might slow syndesmophyte formation in patients with AS; however, two clinical trials had inconsistent results. Genetic and animal studies suggested potential effects of NSAIDs on bone formation, and clinical studies have indicated that NSAIDs may potentially modify disease progression, particularly in patients at higher risk of syndesmophyte growth. Better quantification of syndesmophyte growth, disease subsets with higher risk for radiographic progression, and potential risk factors and their interactions should be considered when designing future studies of disease progression in patients with axial SpA.

AUTHOR CONTRIBUTIONS

All authors were involved in drafting the article or revising it critically for important intellectual content, and all authors approved the final version to be published.

REFERENCES

1. Reveille JD, Witter JP, Weisman MH. Prevalence of axial spondylarthritis in the United States: estimates from a cross-sectional survey. *Arthritis Care Res (Hoboken)* 2012;64:905–10.
2. Taurog JD, Chhabra A, Colbert RA. Ankylosing spondylitis and axial spondyloarthritis. *N Engl J Med* 2016;374:2563–74.
3. Boel A, Molto A, van der Heijde D, Ciurea A, Dougados M, Gensler LS, et al. Do patients with axial spondyloarthritis with radiographic sacroiliitis fulfill both the modified New York criteria and the ASAS axial spondyloarthritis criteria? Results from eight cohorts. *Ann Rheum Dis* 2019;78:1545–9.
4. Ward MM, Deodhar A, Gensler LS, Dubreuil M, Yu D, Khan MA, et al. 2019 update of the American College of Rheumatology/Spondylitis Association of America/Spondyloarthritis research and treatment network recommendations for the treatment of ankylosing spondylitis and nonradiographic axial spondyloarthritis. *Arthritis Rheumatol* 2019;71:1599–613.

5. Moltó A, Paternotte S, van der Heijde D, Claudepierre P, Rudwaleit M, Dougados M. Evaluation of the validity of the different arms of the ASAS set of criteria for axial spondyloarthritis and description of the different imaging abnormalities suggestive of spondyloarthritis: data from the DESIR cohort. *Ann Rheum Dis* 2015;74:746–51.
6. Fongen C, Dagfinrud H, Berg IJ, Ramiro S, van Gaalen F, Landewé R, et al. Frequency of impaired spinal mobility in patients with chronic back pain compared to patients with early axial spondyloarthritis. *J Rheumatol* 2018;45:1643–50.
7. Dau JD, Lee M, Ward MM, Gensler LS, Brown MA, Learch TJ, et al. Opioid analgesic use in patients with ankylosing spondylitis: an analysis of the prospective study of outcomes in an ankylosing spondylitis cohort. *J Rheumatol* 2018;45:188–94.
8. Sieper J, Rudwaleit M, Baraliakos X, Brandt J, Braun J, Burgos-Vargas R, et al. The Assessment of SpondyloArthritis international Society (ASAS) handbook: a guide to assess spondyloarthritis. *Ann Rheum Dis* 2009;68 Suppl 2:ii1–44.
9. Sieper J, Lenaerts J, Wollenhaupt J, Rudwaleit M, Mazurov VI, Myasoutova L, et al. Efficacy and safety of infliximab plus naproxen versus naproxen alone in patients with early, active axial spondyloarthritis: results from the double-blind, placebo-controlled INFAST study—part 1. *Ann Rheum Dis* 2014;73:101–7.
10. Baraliakos X, Kiltz U, Peters S, Appel H, Dybowski F, Igelmann M, et al. Efficiency of treatment with non-steroidal anti-inflammatory drugs according to current recommendations in patients with radiographic and non-radiographic axial spondyloarthritis. *Rheumatology (Oxford)* 2017;56:95–102.
11. Van der Heijde D, Kivitz A, Schiff MH, Sieper J, Dijkmans BA, Braun J, et al, for the ATLAS Study Group. Efficacy and safety of adalimumab in patients with ankylosing spondylitis: results of a multicenter, randomized, double-blind, placebo-controlled trial. *Arthritis Rheum* 2006;54:2136–46.
12. Van der Heijde D, Da Silva JC, Dougados M, Geher P, van der Horst-Bruinsma I, Juanola X, et al. Etanercept 50 mg once weekly is as effective as 25 mg twice weekly in patients with ankylosing spondylitis. *Ann Rheum Dis* 2006;65:1572–7.
13. Boersma JW. Retardation of ossification of the lumbar vertebral column in ankylosing spondylitis by means of phenylbutazone. *Scand J Rheumatol* 1976;5:60–4.
14. Wanders A, van der Heijde D, Landewé R, Béhier JM, Calin A, Olivieri I, et al. Nonsteroidal antiinflammatory drugs reduce radiographic progression in patients with ankylosing spondylitis: a randomized clinical trial. *Arthritis Rheum* 2005;52:1756–65.
15. Sieper J, Listing J, Poddubny D, Song IH, Hermann KG, Callhoff J, et al. Effect of continuous versus on-demand treatment of ankylosing spondylitis with diclofenac over 2 years on radiographic progression of the spine: results from a randomised multicentre trial (ENRADAS). *Ann Rheum Dis* 2016;75:1438–43.
16. Creemers MC, Franssen MJ, van 't Hof MA, Gribnau FW, van de Putte LB, van Riel PL. Assessment of outcome in ankylosing spondylitis: an extended radiographic scoring system. *Ann Rheum Dis* 2005;64:127–9.
17. Wanders A, Landewé R, Spoorenberg A, de Vlam K, Mielants H, Dougados M, et al. Scoring of radiographic progression in randomised clinical trials in ankylosing spondylitis: a preference for paired reading order. *Ann Rheum Dis* 2004;63:1601–4.
18. Baraliakos X, Listing J, Rudwaleit M, Haibel H, Brandt J, Sieper J, et al. Progression of radiographic damage in patients with ankylosing spondylitis: defining the central role of syndesmophytes. *Ann Rheum Dis* 2007;66:910–5.
19. Van der Heijde D, Landewé R, Baraliakos X, Houben H, van Tubergen A, Williamson P, et al. Radiographic findings following two years of infliximab therapy in patients with ankylosing spondylitis. *Arthritis Rheum* 2008;58:3063–70.
20. Ramiro S, Stolwijk C, van Tubergen A, van der Heijde D, Dougados M, van den Bosch F, et al. Evolution of radiographic damage in ankylosing spondylitis: a 12 year prospective follow-up of the OASIS study. *Ann Rheum Dis* 2015;74:52–9.
21. Van der Heijde D, Salonen D, Weissman BN, Landewé R, Maksymowych WP, Kupper H, et al. Assessment of radiographic progression in the spines of patients with ankylosing spondylitis treated with adalimumab for up to 2 years. *Arthritis Res Ther* 2009;11:R127.
22. Braun J, Baraliakos X, Deodhar A, Baeten D, Sieper J, Emery P, et al. Effect of secukinumab on clinical and radiographic outcomes in ankylosing spondylitis: 2-year results from the randomised phase III MEASURE 1 study. *Ann Rheum Dis* 2017;76:1070–7.
23. Braun J, Haibel H, de Hooge M, Landewé R, Rudwaleit M, Fox T, et al. Spinal radiographic progression over 2 years in ankylosing spondylitis patients treated with secukinumab: a historical cohort comparison. *Arthritis Res Ther* 2019;21:142.
24. Wanders AJ, Landewé RB, Spoorenberg A, Dougados M, van der Linden S, Mielants H, et al. What is the most appropriate radiologic scoring method for ankylosing spondylitis? A comparison of the available methods based on the Outcome Measures in Rheumatology Clinical Trials filter. *Arthritis Rheum* 2004;50:2622–32.
25. Poddubny D, Haibel H, Listing J, Märker-Hermann E, Zeidler H, Braun J, et al. Baseline radiographic damage, elevated acute-phase reactant levels, and cigarette smoking status predict spinal radiographic progression in early axial spondylarthritis. *Arthritis Rheum* 2012;64:1388–98.
26. Kim HR, Hong YS, Park SH, Ju JH, Kang KY. Low bone mineral density predicts the formation of new syndesmophytes in patients with axial spondyloarthritis. *Arthritis Res Ther* 2018;20:231.
27. Deminger A, Klingberg E, Geijer M, Göthlin J, Hedberg M, Rehnberg E, et al. A five-year prospective study of spinal radiographic progression and its predictors in men and women with ankylosing spondylitis. *Arthritis Res Ther* 2018;20:162.
28. Van Tubergen A, Ramiro S, van der Heijde D, Dougados M, Mielants H, Landewé R. Development of new syndesmophytes and bridges in ankylosing spondylitis and their predictors: a longitudinal study. *Ann Rheum Dis* 2012;71:518–23.
29. Lukas C, Landewé R, Sieper J, Dougados M, Davis J, Braun J, et al, for the Assessment of SpondyloArthritis international Society. Development of an ASAS-endorsed disease activity score (ASDAS) in patients with ankylosing spondylitis. *Ann Rheum Dis* 2009;68:18–24.
30. Ramiro S, van der Heijde D, van Tubergen A, Stolwijk C, Dougados M, van den Bosch F, et al. Higher disease activity leads to more structural damage in the spine in ankylosing spondylitis: 12-year longitudinal data from the OASIS cohort. *Ann Rheum Dis* 2014;73:1455–61.
31. Ward MM, Reveille JD, Learch TJ, Davis JC Jr, Weisman MH. Occupational physical activities and long-term functional and radiographic outcomes in patients with ankylosing spondylitis. *Arthritis Rheum* 2008;59:822–32.
32. Ramiro S, Landewé R, van Tubergen A, Boonen A, Stolwijk C, Dougados M, et al. Lifestyle factors may modify the effect of disease activity on radiographic progression in patients with ankylosing spondylitis: a longitudinal analysis. *RMD Open* 2015;1:e000153.
33. Jacques P, Lambrecht S, Verheugen E, Pauwels E, Kollias G, Armaka M, et al. Proof of concept: enthesitis and new bone formation in spondyloarthritis are driven by mechanical strain and stromal cells. *Ann Rheum Dis* 2014;73:437–45.
34. Tan S, Yao J, Flynn JA, Yao L, Ward MM. Dynamics of syndesmophyte growth in AS measured by quantitative CT: heterogeneity within and among vertebral disc spaces. *Rheumatology (Oxford)* 2015;54:972–80.
35. Dougados M, Simon P, Braun J, Burgos-Vargas R, Maksymowych WP, Sieper J, et al. ASAS recommendations for collecting, analysing and

- reporting NSAID intake in clinical trials/epidemiological studies in axial spondyloarthritis. *Ann Rheum Dis* 2011;70:249–51.
36. Poddubnyy D, Rudwaleit M, Haibel H, Listing J, Märker-Hermann E, Zeidler H, et al. Effect of non-steroidal anti-inflammatory drugs on radiographic spinal progression in patients with axial spondyloarthritis: results from the German Spondyloarthritis Inception Cohort. *Ann Rheum Dis* 2012;71:1616–22.
 37. Garrett S, Jenkinson T, Kennedy LG, Whitelock H, Gaisford P, Calin A. A new approach to defining disease status in ankylosing spondylitis: the Bath Ankylosing Spondylitis Disease Activity Index. *J Rheumatol* 1994;21:2286–91.
 38. Kroon F, Landewé R, Dougados M, van der Heijde D. Continuous NSAID use reverts the effects of inflammation on radiographic progression in patients with ankylosing spondylitis. *Ann Rheum Dis* 2012;71:1623–9.
 39. Baraliakos X, Listing J, Rudwaleit M, Brandt J, Sieper J, Braun J. Radiographic progression in patients with ankylosing spondylitis after 2 years of treatment with the tumour necrosis factor α antibody infliximab. *Ann Rheum Dis* 2005;64:1462–6.
 40. Van der Heijde D, Landewé R, Einstein S, Ory P, Vosse D, Ni L, et al. Radiographic progression of ankylosing spondylitis after up to two years of treatment with etanercept. *Arthritis Rheum* 2008;58:1324–31.
 41. Braun J, Baraliakos X, Hermann KG, Deodhar A, van der Heijde D, Inman R, et al. The effect of two golimumab doses on radiographic progression in ankylosing spondylitis: results through 4 years of the GO-RAISE trial. *Ann Rheum Dis* 2014;73:1107–13.
 42. Braun J, Baraliakos X, Deodhar A, Poddubnyy D, Emery P, Delicha EM, et al. Secukinumab shows sustained efficacy and low structural progression in ankylosing spondylitis: 4-year results from the MEASURE 1 study. *Rheumatology (Oxford)* 2019;58:859–68.
 43. Van der Heijde D, Baraliakos X, Hermann KA, Landewé RB, Machado PM, Maksymowych WP, et al. Limited radiographic progression and sustained reductions in MRI inflammation in patients with axial spondyloarthritis: 4-year imaging outcomes from the RAPID-axSpA phase III randomised trial. *Ann Rheum Dis* 2018;77:699–705.
 44. Haroon N, Inman RD, Learch TJ, Weisman MH, Lee M, Rahbar MH, et al. The impact of tumor necrosis factor α inhibitors on radiographic progression in ankylosing spondylitis. *Arthritis Rheum* 2013;65:2645–54.
 45. Molnar C, Scherer A, Baraliakos X, de Hooge M, Micheroli R, Exer P, et al. TNF blockers inhibit spinal radiographic progression in ankylosing spondylitis by reducing disease activity: results from the Swiss Clinical Quality Management cohort. *Ann Rheum Dis* 2018;77:63–9.
 46. Cortes A, Maksymowych WP, Wordsworth BP, Inman RD, Danoy P, Rahman P, et al. Association study of genes related to bone formation and resorption and the extent of radiographic change in ankylosing spondylitis. *Ann Rheum Dis* 2015;74:1387–93.
 47. Smith WL, DeWitt DL, Garavito RM. Cyclooxygenases: structural, cellular, and molecular biology. *Annu Rev Biochem* 2000;69:145–82.
 48. Weinreb M, Saponitzky I, Keila S. Systemic administration of an anabolic dose of PGE2 in young rats increases the osteogenic capacity of bone marrow. *Bone* 1997;20:521–6.
 49. Saponitzky I, Weinreb M. Differential effects of systemic prostaglandin E2 on bone mass in rat long bones and calvariae. *J Endocrinol* 1998;156:51–7.
 50. Li X, Pilbeam CC, Pan L, Breyer RM, Raisz LG. Effects of prostaglandin E2 on gene expression in primary osteoblastic cells from prostaglandin receptor knockout mice. *Bone* 2002;30:567–73.
 51. Miyaoura C, Inada M, Suzawa T, Sugimoto Y, Ushikubi F, Ichikawa A, et al. Impaired bone resorption to prostaglandin E2 in prostaglandin E receptor EP4-knockout mice. *J Biol Chem* 2000;275:19819–23.
 52. Min YK, Rao Y, Okada Y, Raisz LG, Pilbeam CC. Regulation of prostaglandin G/H synthase-2 expression by interleukin-1 in human osteoblast-like cells. *J Bone Miner Res* 1998;13:1066–75.
 53. Kotake S, Udagawa N, Takahashi N, Matsuzaki K, Itoh K, Ishiyama S, et al. IL-17 in synovial fluids from patients with rheumatoid arthritis is a potent stimulator of osteoclastogenesis. *J Clin Invest* 1999;103:1345–52.
 54. LeGrand A, Fermor B, Fink C, Pisetsky DS, Weinberg JB, Vail TP, et al. Interleukin-1, tumor necrosis factor α , and interleukin-17 synergistically up-regulate nitric oxide and prostaglandin E2 production in explants of human osteoarthritic knee menisci. *Arthritis Rheum* 2001;44:2078–83.
 55. Joldersma M, Burger EH, Semeins CM, Klein-Nulend J. Mechanical stress induces COX-2 mRNA expression in bone cells from elderly women. *J Biomech* 2000;33:53–61.
 56. Siddhivarn C, Banas A, Champagne C, Riché EL, Weerapradist W, Offenbacher S. Prostaglandin D2 pathway and peroxisome proliferator-activated receptor γ -1 expression are induced by mechanical loading in an osteoblastic cell line. *J Periodontol Res* 2006;41:92–100.
 57. Shimizu N, Ozawa Y, Yamaguchi M, Goseki T, Ohzeki K, Abiko Y. Induction of COX-2 expression by mechanical tension force in human periodontal ligament cells. *J Periodontol* 1998;69:670–7.
 58. Kanzaki H, Chiba M, Shimizu Y, Mitani H. Periodontal ligament cells under mechanical stress induce osteoclastogenesis by receptor activator of nuclear factor κ B ligand up-regulation via prostaglandin E2 synthesis. *J Bone Miner Res* 2002;17:210–20.
 59. Zhang X, Schwarz EM, Young DA, Puzas JE, Rosier RN, O’Keefe RJ. Cyclooxygenase-2 regulates mesenchymal cell differentiation into the osteoblast lineage and is critically involved in bone repair. *J Clin Invest* 2002;109:1405–15.
 60. Simon AM, Manigrasso MB, O’Connor JP. Cyclo-oxygenase 2 function is essential for bone fracture healing. *J Bone Miner Res* 2002;17:963–76.
 61. Goodman S, Ma T, Trindade M, Ikenoue T, Matsuura I, Wong N, et al. COX-2 selective NSAID decreases bone ingrowth in vivo. *J Orthop Res* 2002;20:1164–1169.
 62. Altman RD, Latta LL, Keer R, Renfree K, Hornicek FJ, Banovac K. Effect of nonsteroidal antiinflammatory drugs on fracture healing: a laboratory study in rats. *J Orthop Trauma* 1995;9:392–400.
 63. Gerstenfeld LC, Thiede M, Seibert K, Mielke C, Phippard D, Svagr B, et al. Differential inhibition of fracture healing by non-selective and cyclooxygenase-2 selective non-steroidal anti-inflammatory drugs. *J Orthop Res* 2003;21:670–5.
 64. Beck A, Krischak G, Sorg T, Augat P, Farker K, Merkel U, et al. Influence of diclofenac (group of nonsteroidal anti-inflammatory drugs) on fracture healing. *Arch Orthop Trauma Surg* 2003;123:327–32.
 65. Bergenstock M, Min W, Simon AM, Sabatino C, O’Connor JP. A comparison between the effects of acetaminophen and celecoxib on bone fracture healing in rats. *J Orthop Trauma* 2005;19:717–23.
 66. Gerstenfeld LC, Al-Ghawas M, Alkhiary YM, Cullinane DM, Krall EA, Fitch JL, et al. Selective and nonselective cyclooxygenase-2 inhibitors and experimental fracture-healing: reversibility of effects after short-term treatment. *J Bone Joint Surg Am* 2007;89:114–25.
 67. Goodman SB, Ma T, Mitsunaga L, Miyaniishi K, Genovese MC, Smith RL. Temporal effects of a COX-2-selective NSAID on bone ingrowth. *J Biomed Mater Res A* 2005;72:279–87.
 68. Krischak GD, Augat P, Sorg T, Blakytyn R, Kinzl L, Claes L, et al. Effects of diclofenac on periosteal callus maturation in osteotomy healing in an animal model. *Arch Orthop Trauma Surg* 2007;127:3–9.
 69. Dodwell ER, Latorre JG, Parisini E, Zwettler E, Chandra D, Mulpuri K, et al. NSAID exposure and risk of nonunion: a meta-analysis of case-control and cohort studies. *Calcif Tissue Int* 2010;87:193–202.

70. Wheatley BM, Nappo KE, Christensen DL, Holman AM, Brooks DI, Potter BK. Effect of NSAIDs on bone healing rates: a meta-analysis. *J Am Acad Orthop Surg* 2019;27:e330–6.
71. Ma R, Chen GH, Zhao LJ, Zhai XC. Efficacy of naproxen prophylaxis for the prevention of heterotopic ossification after hip surgery: a meta-analysis. *J Orthop Surg Res* 2018;13:48.
72. Joice M, Vasileiadis GI, Amanatullah DF. Non-steroidal anti-inflammatory drugs for heterotopic ossification prophylaxis after total hip arthroplasty: a systematic review and meta-analysis. *Bone Joint J* 2018;100-B:915–22.
73. Tan S, Yao J, Flynn JA, Yao L, Ward MM. Quantitative measurement of syndesmophyte volume and height in ankylosing spondylitis using CT. *Ann Rheum Dis* 2014;73:544–50.
74. De Bruin F, de Koning A, van den Berg R, Baraliakos X, Braun J, Ramiro S, et al. Development of the CT Syndesmophyte Score (CTSS) in patients with ankylosing spondylitis: data from the SIAS cohort. *Ann Rheum Dis* 2018;77:371–7.
75. Tan S, Yao J, Flynn JA, Yao L, Ward MM. Zygapophyseal joint fusion in ankylosing spondylitis assessed by computed tomography: associations with syndesmophytes and spinal motion. *J Rheumatol* 2017;44:1004–10.
76. De Koning A, de Bruin F, van den Berg R, Ramiro S, Baraliakos X, Braun J, et al. Low-dose CT detects more progression of bone formation in comparison to conventional radiography in patients with ankylosing spondylitis: results from the SIAS cohort. *Ann Rheum Dis* 2018;77:293–9.
77. Tan S, Yao J, Flynn JA, Yao L, Ward MM. Quantitative syndesmophyte measurement in ankylosing spondylitis using CT: longitudinal validity and sensitivity to change over 2 years. *Ann Rheum Dis* 2015;74:437–43.
78. Baraliakos X, Heldmann F, Callhoff J, Listing J, Appelboom T, Brandt J, et al. Which spinal lesions are associated with new bone formation in patients with ankylosing spondylitis treated with anti-TNF agents? A long-term observational study using MRI and conventional radiography. *Ann Rheum Dis* 2014;73:1819–25.
79. Maksymowych WP, Chiowchanwisawakit P, Clare T, Pedersen SJ, Østergaard M, Lambert RG. Inflammatory lesions of the spine on magnetic resonance imaging predict the development of new syndesmophytes in ankylosing spondylitis: evidence of a relationship between inflammation and new bone formation. *Arthritis Rheum* 2009;60:93–102.
80. Bouchard L, de Médicis R, Lussier A, Naccache PH, Poubelle PE. Inflammatory microcrystals alter the functional phenotype of human osteoblast-like cells in vitro: synergism with IL-1 to overexpress cyclooxygenase-2. *J Immunol* 2002;168:5310–7.
81. Pouliot M, James MJ, McColl SR, Naccache PH, Cleland LG. Monosodium urate microcrystals induce cyclooxygenase-2 in human monocytes. *Blood* 1998;91:1769–76.
82. Zhu J, Li A, Jia E, Zhou Y, Xu J, Chen S, et al. Monosodium urate crystal deposition associated with the progress of radiographic grade at the sacroiliac joint in axial SpA: a dual-energy CT study. *Arthritis Res Ther* 2017;19:83.
83. Zhao S, Duffield SJ, Moots RJ, Goodson NJ. Systematic review of association between vitamin D levels and susceptibility and disease activity of ankylosing spondylitis. *Rheumatology (Oxford)* 2014;53:1595–603.
84. Orsolini G, Adami G, Rossini M, Ghellere F, Caimmi C, Fassio A, et al. Parathyroid hormone is a determinant of serum Dickkopf-1 levels in ankylosing spondylitis. *Clin Rheumatol* 2018;37:3093–8.
85. Ryder KD, Duncan RL. Parathyroid hormone modulates the response of osteoblast-like cells to mechanical stimulation. *Calcif Tissue Int* 2000;67:241–6.
86. Hartl A, Sieper J, Syrbe U, Listing J, Hermann KG, Rudwaleit M, et al. Serum levels of leptin and high molecular weight adiponectin are inversely associated with radiographic spinal progression in patients with ankylosing spondylitis: results from the ENRADAS trial. *Arthritis Res Ther* 2017;19:140.
87. Park JH, Lee SG, Jeon YK, Park EK, Suh YS, Kim HO. Relationship between serum adipokine levels and radiographic progression in patients with ankylosing spondylitis. *Medicine (Baltimore)* 2017;96:e7854.

2020 American College of Rheumatology Guideline for the Management of Reproductive Health in Rheumatic and Musculoskeletal Diseases

Lisa R. Sammaritano,¹ Bonnie L. Bermas,² Eliza E. Chakravarty,³ Christina Chambers,⁴ Megan E. B. Clowse,⁵ Michael D. Lockshin,¹ Wendy Marder,⁶ Gordon Guyatt,⁷ D. Ware Branch,⁸ Jill Buyon,⁹ Lisa Christopher-Stine,¹⁰ Rachele Crow-Hercher,¹¹ John Cush,¹² Maurice Druzin,¹³ Arthur Kavanaugh,⁴ Carl A. Laskin,¹⁴ Lauren Plante,¹⁵ Jane Salmon,¹ Julia Simard,¹³ Emily C. Somers,⁶ Virginia Steen,¹⁶ Sara K. Tedeschi,¹⁷ Evelyne Vinet,¹⁸ C. Whitney White,¹⁹ Jinoos Yazdany,²⁰ Medha Barbhuiya,¹ Brittany Bettendorf,²¹ Amanda Eudy,⁵ Arundathi Jayatilleke,¹⁵ Amit Aakash Shah,²² Nancy Sullivan,²³ Laura L. Tarter,¹⁷ Mehret Birru Talabi,²⁴ Marat Turgunbaev,²² Amy Turner,²² and Kristen E. D'Anci²³

Guidelines and recommendations developed and/or endorsed by the American College of Rheumatology (ACR) are intended to provide guidance for patterns of practice and not to dictate the care of a particular patient. The ACR considers adherence to the recommendations within this guideline to be voluntary, with the ultimate determination regarding their application to be made by the clinician in light of each patient's individual circumstances. Guidelines and recommendations are intended to promote beneficial or desirable outcomes, but cannot guarantee any specific outcome. Guidelines and recommendations developed and endorsed by the ACR are subject to periodic revision, as warranted by the evolution of medical knowledge, technology, and practice. ACR recommendations are not intended to dictate payment or insurance decisions. These recommendations cannot adequately convey all uncertainties and nuances of patient care.

The American College of Rheumatology is an independent, professional, medical and scientific society that does not guarantee, warrant, or endorse any commercial product or service.

Objective. To develop an evidence-based guideline on contraception, assisted reproductive technologies (ART), fertility preservation with gonadotoxic therapy, use of menopausal hormone replacement therapy (HRT), pregnancy assessment and management, and medication use in patients with rheumatic and musculoskeletal disease (RMD).

Methods. We conducted a systematic review of evidence relating to contraception, ART, fertility preservation, HRT, pregnancy and lactation, and medication use in RMD populations, using Grading of Recommendations Assessment, Development and Evaluation methodology to rate the quality of evidence and a group consensus process to determine final recommendations and grade their strength (conditional or strong). Good practice statements were agreed upon when indirect evidence was sufficiently compelling that a formal vote was unnecessary.

Results. This American College of Rheumatology guideline provides 12 ungraded good practice statements and 131 graded recommendations for reproductive health care in RMD patients. These recommendations are intended to guide care for all patients with RMD, except where indicated as being specific for patients with systemic lupus erythematosus, those positive for antiphospholipid antibody, and/or those positive for anti-Ro/SSA and/or anti-La/SSB antibodies. Recommendations and good practice statements support several guiding principles: use of safe and effective contraception to prevent unplanned pregnancy, pre-pregnancy counseling to encourage conception during periods of disease quiescence and while receiving pregnancy-compatible medications, and ongoing physician-patient discussion with obstetrics/gynecology collaboration for all reproductive health issues, given the overall low level of available evidence that relates specifically to RMD.

Conclusion. This guideline provides evidence-based recommendations developed and reviewed by panels of experts and RMD patients. Many recommendations are conditional, reflecting a lack of data or low-level data. We intend that this guideline be used to inform a shared decision-making process between patients and their physicians on issues related to reproductive health that incorporates patients' values, preferences, and comorbidities.

INTRODUCTION

The management of reproductive health issues in patients with rheumatic and musculoskeletal diseases (RMD) differs from that in healthy persons. As a result, rheumatologists and other clinicians caring for these patients must often discuss with and counsel their patients about contraception, pregnancy and lactation (including medications), assisted reproductive technology (ART), fertility preservation, and hormone replacement therapy (HRT), and they must collaborate with specialists in the fields of obstetrics-gynecology, maternal-fetal medicine, and reproductive endocrinology and infertility.

Pregnancy in women with RMD may lead to serious maternal or fetal adverse outcomes; accordingly, contraception, tailored to the individual patient with emphasis on safety and efficacy, should be discussed and encouraged. Because risk for pregnancy complications depends on diagnosis, disease activity and damage, medications, and the presence of anti-Ro/SSA, anti-La/SSB, and antiphospholipid (aPL) antibodies, pre-pregnancy assessment is critical to informing pregnancy management, therapy, and outcomes. The ability to become pregnant may itself be an independent concern for some patients, so minimizing risk of gonadal insufficiency is important. RMD patients with subfertility value

advice from their rheumatologists about oocyte preservation and in vitro fertilization (IVF).

It is difficult to avoid use of medication during pregnancy in patients with RMD. Not all medications are safe for pre-conception use by men and women or during pregnancy and lactation, but uncontrolled systemic inflammatory disease is itself associated with poor pregnancy outcomes (1–6). In addition, patients are vulnerable to disease flare postpartum (7,8), but the American Academy of Pediatrics recommends that infants be exclusively breastfed for 6 months (9). In many cases medication safety is uncertain because most data are derived from case reports, small series, and observational studies; direct data from randomized controlled trials are scarce. As a result, identifying the appropriate screening and management (including medication use) for RMD patients is challenging for clinicians.

Given the primary goal of providing recommendations for care of all adult RMD patients throughout the reproductive lifespan, the scope of this guideline is broad. There has been little attention to aspects of reproductive health care other than pregnancy in patients with RMD, and the American College of Rheumatology (ACR) recognizes the imperative for guidance in reproductive health issues for these patients.

This article is published simultaneously in *Arthritis Care & Research*.

Supported by the American College of Rheumatology.

¹Lisa R. Sammaritano, MD, Michael D. Lockshin, MD, Jane Salmon, MD, Medha Barbhuiya MD, MPH: Weill Cornell Medicine, Hospital for Special Surgery, New York, New York; ²Bonnie L. Bermas, MD: University of Texas Southwestern Medical Center, Dallas; ³Eliza E. Chakravarty, MD, MS: Oklahoma Medical Research Foundation, Oklahoma City; ⁴Christina Chambers, PhD, MPH, Arthur Kavanaugh, MD: University of California, San Diego; ⁵Megan E. B. Clowse, MD, MPH, Amanda Eudy, PhD: Duke University Medical Center, Durham, North Carolina; ⁶Wendy Marder, MD, MS, Emily C. Somers, PhD, ScM: University of Michigan School of Medicine, Ann Arbor; ⁷Gordon Guyatt, MD, MSc: McMaster University, Hamilton, Ontario, Canada; ⁸D. Ware Branch, MD: University of Utah, Salt Lake City; ⁹Jill Buyon, MD: New York University School of Medicine, New York, New York; ¹⁰Lisa Christopher-Stine, MD, MPH: John Hopkins Medicine, Baltimore, Maryland; ¹¹Rachelle Crow-Hercher, MEd: Shelby Township, Michigan; ¹²John Cush, MD: Baylor Research Institute, Dallas, Texas; ¹³Maurice Druzin, MD, Julia Simard, ScD: Stanford Medicine, Stanford, California; ¹⁴Carl A. Laskin, MD: University of Toronto, Toronto, Ontario, Canada; ¹⁵Lauren Plante, MD, MPH, Arundathi Jayatilke, MD, MS: Drexel University College of Medicine, Philadelphia, Pennsylvania; ¹⁶Virginia Steen, MD: Georgetown University Medical Center, Washington, DC; ¹⁷Sara K. Tedeschi, MD, MPH, Laura L. Tarter, MD: Brigham and Women's Hospital, Boston, Massachusetts; ¹⁸Evelyn Vinet, MD, PhD: McGill University Health Center, Montreal, Quebec, Canada; ¹⁹C. Whitney White, PharmD: University of Mississippi, Jackson; ²⁰Jinoos Yazdany, MD, MPH: University of California San Francisco; ²¹Brittany Bettendorf, MD: University of Iowa, Iowa City; ²²Amit Aakash Shah, MD, MPH, Marat Turgunbaev, MD, MPH, Amy Turner: American College of Rheumatology, Atlanta, Georgia; ²³Nancy Sullivan, BA, Kristen E. D'Anci, PhD: ECRl Institute, Plymouth Meeting, Pennsylvania; ²⁴Mehret Birru Talabi, MD, PhD: University of Pittsburgh, Pittsburgh, Pennsylvania.

Dr. Bermas has received consulting fees, speaking fees, and/or honoraria from UCB (less than \$10,000). Dr. Chakravarty has received

consulting fees, speaking fees, and/or honoraria from UCB (less than \$10,000). Dr. Chambers has received research support from Amgen, AstraZeneca, Bristol-Myers Squibb, Celgene, GlaxoSmithKline, Janssen, Pfizer, Regeneron, Hoffmann La-Roche-Genentech, Genzyme-Sanofi-Aventis, Seqirus, Takeda Pharmaceuticals, UCB, Sun Pharma Global FZE, and the Gerber Foundation. Dr. Clowse has received consulting fees, speaking fees, and/or honoraria from AstraZeneca and MotherToBaby (less than \$10,000 each) and from UCB (more than \$10,000) and research support from GlaxoSmithKline (paid to Duke University). Dr. Lockshin has received consulting fees, speaking fees, and/or honoraria from Advance Medical, groupH, Biologische Heilmittel Heel, and Defined Health and has served as an expert witness concerning adverse pregnancy outcome with question of antiphospholipid syndrome. Dr. Branch has received research support from UCB. Dr. Laskin has received consulting fees, speaking fees, and/or honoraria from AbbVie (less than \$10,000) and research support from Ferring Pharmaceuticals. Dr. Salmon has received consulting fees, speaking fees, and/or honoraria from UCB and Bristol-Myers Squibb (less than \$10,000 each) and owns stock or stock options in Bristol-Myers Squibb, Abbott, Pfizer, Eli Lilly, Biogen Idec, and Regeneron. Dr. White has received consulting fees, speaking fees, and/or honoraria from AbbVie (less than \$10,000). Dr. Yazdany has received consulting fees, speaking fees, and/or honoraria from Pfizer, AstraZeneca, and Eli Lilly (less than \$10,000 each). Dr. Eudy has received consulting fees, speaking fees, and/or honoraria from GlaxoSmithKline (more than \$10,000) and research support from GlaxoSmithKline. Dr. Jayatilke has received consulting fees and/or honoraria from GlaxoSmithKline (less than \$10,000). No other disclosures relevant to this article were reported.

Address correspondence to Lisa R. Sammaritano, MD, Hospital for Special Surgery, 535 East 70th Street, New York, NY 10021. E-mail: SammaritanoL@hss.edu.

Submitted for publication July 3, 2019; accepted in revised form December 10, 2019.

METHODS

These recommendations follow the ACR guideline development process, using a systematic literature review and Grading of Recommendations Assessment, Development and Evaluation methodology (for details, see Supplementary Appendices 1, 2, and 3, available on the *Arthritis & Rheumatology* web site at <http://onlinelibrary.wiley.com/doi/10.1002/art.41191/abstract>). When no direct data on RMD patients were available from the systematic literature review, discussion and voting were supplemented with indirect data collected in additional, less formal literature reviews (Supplementary Appendix 4, <http://onlinelibrary.wiley.com/doi/10.1002/art.41191/abstract>) performed by Core Team members (Supplementary Appendix 5, <http://onlinelibrary.wiley.com/doi/10.1002/art.41191/abstract>); these data were not part of the systematic literature review and are listed as “not graded” in evidence tables. Results of the systematic literature review were compiled in an Evidence Report (Supplementary Appendix 6, <http://onlinelibrary.wiley.com/doi/10.1002/art.41191/abstract>).

A *strong recommendation* suggests that most informed patients would choose the recommended management. While usually reflecting a higher level of evidence, it may also reflect the

severity of a potential negative outcome. A *conditional recommendation* suggests that choice will vary with individual values and preferences. Conditional recommendations generally reflect a lack of data, limited data, or conflicting data that lead to uncertainty. Finally, *good practice statements* are those for which indirect evidence is sufficiently compelling that a formal vote is unnecessary. They are presented as “suggestions” rather than formal recommendations. Recommendation numbers are denoted in Supplementary Appendix 7 (<http://onlinelibrary.wiley.com/doi/10.1002/art.41191/abstract>) as numbers in parentheses, allowing for cross-referencing of recommendations with tables/appendices, and referencing the order in the original list (i.e., may not be consecutive in the supplementary appendix.)

RESULTS/RECOMMENDATIONS

The detailed tables of recommendations appear in Supplementary Appendix 7 (available on the *Arthritis & Rheumatology* web site at <http://onlinelibrary.wiley.com/doi/10.1002/art.41191/abstract>). Concise recommendations within this appendix and throughout the article are grouped into categories of contraception,

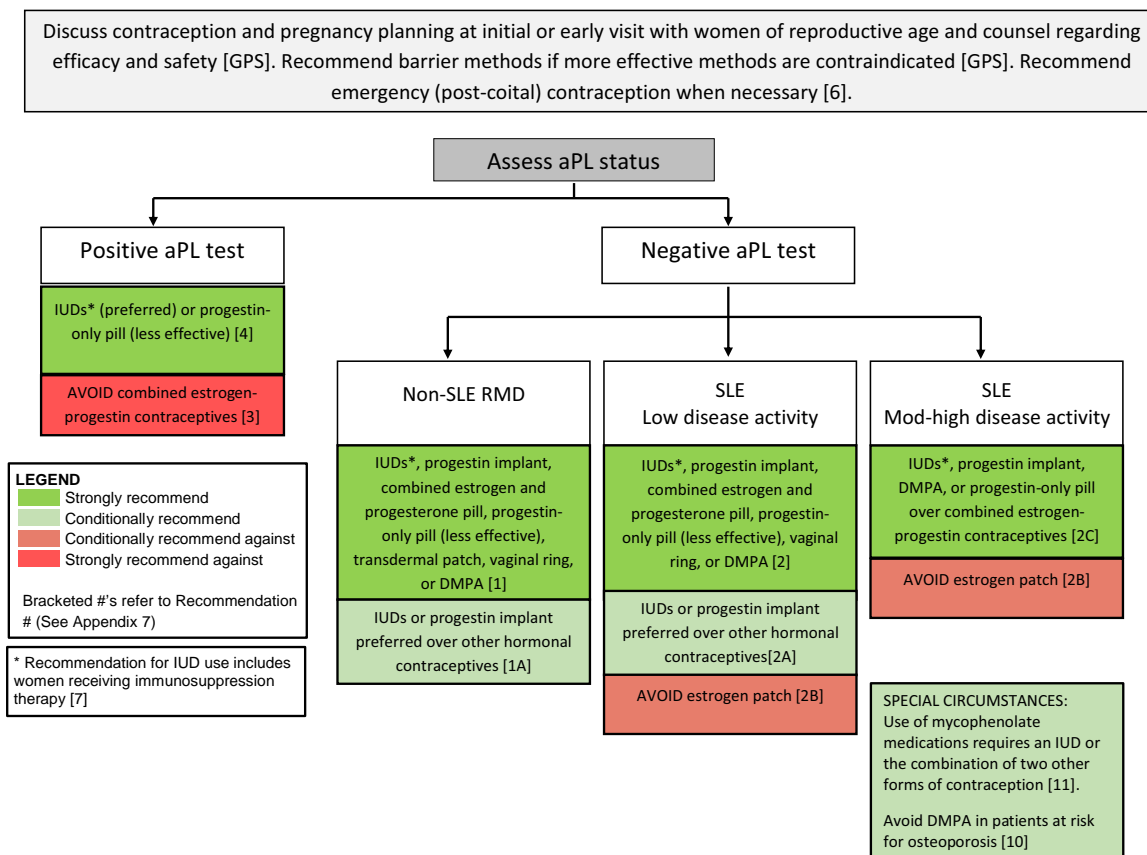


Figure 1. Recommendations and good practice statements (GPS) for use of contraception in women with rheumatic and musculoskeletal disease (RMD). aPL = antiphospholipid antibody (persistent moderate [Mod]–to–high–titer anticardiolipin or anti-β₂-glycoprotein I antibody or persistent positive lupus anticoagulant); IUDs = intrauterine devices (copper or progestin); SLE = systemic lupus erythematosus; DMPA = depot medroxyprogesterone acetate.

ART, fertility preservation with gonadotoxic therapy, use of menopausal HRT, pregnancy assessment and management, and medication use (compatibilities for paternal, maternal, and breastfeeding use are reported).

Most recommendations are general; when relevant, RMDs are specifically identified, most often for systemic lupus erythematosus (SLE) or according to presence of specific autoantibodies (aPL and anti-Ro/SSA and anti-La/SSB antibodies). In general, testing for aPL should be performed in patients with SLE or SLE-like disease and in patients with suggestive histories or physical findings; whether to check these antibodies in other RMD patients with a lower likelihood of positive results should be decided by physician-patient discussion. The presence of aPL modifies the recommendations in many circumstances, and therefore is considered separately. "Positive aPL" throughout this guideline refers to laboratory criteria only (10): persistent (2 positive test results at least 12 weeks apart) moderate-high-titer anticardiolipin antibody (aCL) (≥ 40 units or ≥ 99 th percentile), moderate-high-titer anti- β_2 -glycoprotein I (anti- β_2 GPI) (≥ 40 units or ≥ 99 th percentile), or positive lupus anticoagulant (LAC).

Detailed definitions of aPL and antiphospholipid syndrome (APS) are presented in Supplementary Appendix 8 (available on the *Arthritis & Rheumatology* web site at <http://onlinelibrary.wiley.com/doi/10.1002/art.41191/abstract>). Briefly, included within the positive aPL group are patients with asymptomatic aPL who have no history of thrombosis or pregnancy morbidity (i.e., meet laboratory but not clinical APS criteria), patients with obstetric APS (OB APS), and patients with thrombotic APS. OB APS refers to patients

who meet laboratory criteria for APS and have experienced prior pregnancy complications consistent with APS (with other causes ruled out). These include 3 consecutive losses prior to 10 weeks' gestation, a fetal loss at or after 10 weeks' gestation, or delivery at < 34 weeks due to preeclampsia, intrauterine growth restriction, or fetal distress. Thrombotic APS refers to patients who meet laboratory criteria for APS and have experienced a prior thrombotic event (arterial or venous), regardless of whether they have had obstetric complications. The aPL definitions in the guideline include both patients with and patients without other underlying autoimmune disease, unless specifically stated.

Patients with lower-titer aCL and/or anti- β_2 GPI (or non-criteria aPL) who do not meet laboratory classification criteria may still have some degree of risk that is difficult to quantify. Recommendations for these patients are not offered in this guideline; decisions regarding therapy rest on discussion between the patient and the physician, taking into account additional relevant risk factors.

Contraception

Supplementary Appendix 7, Table A (on the *Arthritis & Rheumatology* web site at <http://onlinelibrary.wiley.com/doi/10.1002/art.41191/abstract>) presents formal recommendations regarding contraception; strength of evidence and justifications for strong and conditional recommendations are shown in Supplementary Appendix 9 (<http://onlinelibrary.wiley.com/doi/10.1002/art.41191/abstract>). Figure 1 details the contraception decision-making

Table 1. Safety and efficacy of various contraceptive methods in women with RMD*

Method	Safety in women with RMD	1-year failure rate, %†
Highly effective (LARC)		
Copper IUD	Safe in all women with RMD; may increase menstrual bleeding	<1
Progestin IUD	Safe in all women with RMD; may decrease menstrual bleeding	<1
Progestin implant	Limited data, but likely safe in all women with RMD	<1
Effective		
Progestin-only pill (daily)	Safe in all women with RMD; higher rate of breakthrough bleeding than with combined contraceptives; must take same time every day for efficacy	5–8
DMPA (IM injection every 12 weeks)	Safe in most women with RMD; <u>exceptions</u> : positive aPL, at high risk for OP	3
Combined estrogen and progesterone pill (daily)	Safe in most women with RMD; <u>exceptions</u> : positive aPL, very active SLE	5–8
Transdermal patch (weekly)	Safe in most women with RMD; <u>exceptions</u> : positive aPL, SLE; serum estrogen levels higher than with pill or vaginal ring	5–8
Vaginal ring (monthly)	Safe in most women with RMD; <u>exceptions</u> : positive aPL, very active SLE	5–8
Less effective		
Diaphragm	Safe in all women with RMD	12
Condom	Safe in all women with RMD; only form to prevent STD	18
Fertility awareness-based methods‡	Safe in all women with RMD; limited efficacy, especially if menses are irregular	24
Spermicide	Safe in all women with RMD; use with condoms or diaphragm to improve efficacy	28

* RMD = rheumatic and musculoskeletal disease; LARC = long-acting reversible contraception; IUD = intrauterine device; DMPA = depot medroxyprogesterone acetate; IM = intramuscular; aPL = antiphospholipid antibody; OP = osteoporosis; SLE = systemic lupus erythematosus; STD = sexually transmitted disease.

† Percent of women who will become pregnant within the first year of typical use.

‡ Methods based on the timing of the menstrual cycle.

process, and Table 1 provides efficacy data and comments on available contraceptives.

RMD patients typically underutilize effective contraception (11–13). The most important reason for effective contraception in women with RMD is to avoid risks of unplanned pregnancy, which include worsening disease activity that may threaten maternal organ function or life, adverse pregnancy outcomes (pregnancy loss, severe prematurity, and growth restriction), and teratogenesis. Members of a 1-day patient focus group, convened as part of the guideline process, emphasized their desire that clinicians caring for patients with RMD routinely discuss family planning, as they view their rheumatologists as “the doctors who know them and their medications best.” We suggest that rheumatologists treating reproductive-age women with RMD discuss contraception and pregnancy plans at an initial or early visit and periodically thereafter, and always when initiating treatment with potentially teratogenic medications. One Key Question (www.powertodecide.org) has been suggested in the literature as a simple way of addressing the issue of family planning with patients: “Would you like to become pregnant in the next year?” (14). In whatever way one chooses to discuss this topic, counseling regarding contraception should include issues of efficacy and safety, with consideration of individual values and preferences.

Effectiveness of reversible forms of contraception varies. For long-acting reversible contraceptives (copper or progestin intrauterine devices [IUDs] and subdermal progestin implants), ideal use and “real-world” use effectiveness are similar, with pregnancy rates of <1% per year (“highly effective”). Combined estrogen-progestin methods, depot medroxyprogesterone acetate (DMPA) injections, and progestin-only pills yield pregnancy rates of 3–8% per year (“effective”) (15,16). Condoms, fertility-based methods (e.g., “rhythm”), and spermicide are less effective and yield pregnancy rates of 18–28% per year (17). Barrier methods confer some protection against sexually transmitted diseases.

While long-acting reversible contraceptives are encouraged as first-line contraceptives for all appropriate candidates, including nulliparous women and adolescents (17), lack of data specific to RMD and variability in clinical situations, values, and preferences may affect a patient’s choice. Clinical factors that affect appropriateness of various contraceptive methods include diagnosis and activity of SLE, presence of aPL, osteoporosis, and some potentially interacting medications (see Special RMD Situations below and Supplementary Appendix 10, on the *Arthritis & Rheumatology* web site at <http://onlinelibrary.wiley.com/doi/10.1002/art.41191/abstract>). “Hormonal contraceptives” refers to any contraception containing a hormone, including estrogen-progestin contraceptives and progestin-only contraceptives. The term “fertile women” refers to women of reproductive age who do not have documented menopause,

hysterectomy, or permanent sterilization (i.e., women who may become pregnant).

In fertile women with RMD who have neither SLE nor positive aPL, we strongly recommend use of effective contraceptives (i.e., hormonal contraceptives or IUDs) over less effective options or no contraception; among effective methods, we conditionally recommend the highly effective IUDs or subdermal progestin implant (long-acting reversible contraceptives) because they have the lowest failure rates.

We strongly recommend discussing use of emergency contraception with all patients, including those with SLE or positive aPL, because risks of emergency contraception are low compared to those of unplanned pregnancy.

Levonorgestrel, the over-the-counter option, is widely available and has no medical contraindications to use, including thrombophilia (18).

SLE patients. Controlled studies of estrogen-progestin contraceptives in SLE have enrolled only women with stable, low disease activity; they specifically excluded those with high disease activity and history of thrombosis (19,20). Prospective studies (evidence level moderate) in patients with stable SLE showed no increased risk of flare related to estrogen-progestin pills (19,20), and there are no data suggesting increased SLE flare risk with progestin-only pills or copper IUDs (20,21).

In SLE patients with stable or low disease activity who are not positive for aPL, we strongly recommend use of effective contraceptives (i.e., hormonal contraceptives or IUDs) over less effective options or no contraception, and we conditionally recommend the highly effective IUDs or subdermal progestin implant because they have the lowest failure rates.

We conditionally recommend against use of the transdermal estrogen-progestin patch in patients with SLE.

Although not directly studied in SLE patients, the transdermal estrogen-progestin patch results in greater estrogen exposure than do oral or transvaginal methods (22,23), raising concern regarding potential increased risk of flare or thrombosis.

We strongly recommend progestin-only or IUD contraceptives over combined estrogen-progestin contraception in SLE patients with moderate or severe disease activity, including nephritis, because estrogen-containing contraceptives have not been studied in SLE patients with moderate or severe disease activity.

Antiphospholipid antibody-positive patients. Presence of aPL, with or without history of clinical complications, is a contraindication to use of estrogen-containing contraceptives due to the potential further increase in thrombosis risk.

We strongly recommend *against* combined estrogen-progestin contraceptives in women with positive aPL because estrogen increases risk of thromboembolism.

We strongly recommend IUDs (levonorgestrel or copper) or the progestin-only pill in women with positive aPL.

In aPL-positive patients, we do not recommend DMPA due to concern regarding thrombogenicity. We do not comment on the relatively new progestin implant due to lack of data.

The risk of venous thromboembolism (VTE) in healthy women taking combined estrogen-progestin contraceptives is 36 times higher than the baseline annual risk of 1/10,000 women (24). Although whether there is any increase in thrombosis risk with progestin-only contraception is debated, progestin-only methods are widely accepted as a lower-risk option in patients for whom estrogens are contraindicated but who still need effective contraception (18,25,26). The specific progestin and its serum level affect thrombosis risk: in healthy women taking estrogen-progestin contraceptive pills that vary progestin type but not estrogen, VTE risk odds ratios range from 2.2 to 6.6 (24). However, VTE risk in healthy women using either the progestin-only pill or the progestin IUD is not increased, with relative risks (RRs) of 0.90 (95% confidence interval [95% CI] 0.57–1.45) and 0.61 (95% CI 0.24–1.53), respectively (27). Furthermore, thrombosis frequency does not increase when progestin (levonorgestrel) IUDs are used in non-RMD patients with increased (non-aPL-associated) thrombosis risk (27–29). VTE data on the newer progestin (etonogestrel) subdermal implant are inadequate to permit recommendations (the prior progestin implant containing levonorgestrel is no longer available in the US). Very limited data on non-RMD patients suggest that injectable DMPA imparts a higher VTE risk than do other progestin-only contraceptives (RR 2.67 [95% CI 1.29–5.53]), similar to that with oral estrogen-progestin contraceptives (27). For this reason, we do not include DMPA among the progestin contraceptives recommended for use in patients with positive aPL.

The copper IUD is a highly effective alternative that does not increase risk of VTE, but it may increase menstrual bleeding and cramping for several months after insertion. Progestin IUDs may decrease these symptoms (30), a potential benefit for patients receiving anticoagulation therapy.

We suggest the progestin-only pill (which is an effective, but not highly effective, contraceptive) as a low-risk alternative for patients who are unable or unwilling to use an IUD. The lack of data specific to aPL-positive patients using the progestin-only pill or IUD must be weighed against the risk of

pregnancy-related VTE in the general population, which is >10 times that seen with estrogen-progestin contraceptive use. Pregnancy-related thrombosis risk in aPL-positive patients is not well quantified, but VTE risk is 197/10,000 women-years for pregnant patients with a single prothrombotic mutation and 776/10,000 women-years (31) if there are multiple prothrombotic mutations.

Other special RMD situations. Factors other than diagnosis of SLE or presence of aPL may influence the choice of contraception in women with RMD. These include use of medications and presence or risk of osteoporosis. Immunosuppressive therapy does not preclude use of any contraceptive method, but there is concern that mycophenolate-containing medications may interfere with hormonal contraceptive efficacy.

Since IUDs are the most effective contraceptive options, we strongly recommend the IUD (copper or progestin) for women with RMD who are receiving immunosuppressive therapy, despite hypothetical infection risk.

IUD-associated infection risk in RMD patients receiving immunosuppressive therapy has not been specifically studied, but studies in women with HIV show no increase (32), and IUDs are recommended for all solid organ transplant patients, including adolescents (33,34). In one arm of an SLE contraceptive trial a copper IUD was used; although the number of patients receiving immunosuppressive agents was not reported, there were no cases of pelvic inflammatory disease (20).

In women with RMD who are at increased risk for osteoporosis from glucocorticoid use or underlying disease, we conditionally recommend against using DMPA as a long-term contraceptive because data suggest that bone mineral density declines by up to 7.5% over 2 years of use in a healthy population (35).

Although there are no published data suggesting increased fracture risk, the American College of Obstetricians and Gynecologists recommends caution regarding DMPA use in women with or at increased risk for osteoporosis (17).

We conditionally recommend that women with RMD taking mycophenolate mofetil/mycophenolic acid (MMF) use an IUD alone or 2 other methods of contraception together, because MMF may reduce serum estrogen and progesterone levels (in turn reducing the efficacy of oral contraceptives).

The Mycophenolate Risk Evaluation and Mitigation Strategy program suggests use of an IUD alone (copper or progestin is not specified), or an estrogen-progestin contraceptive or the progestin implant together with a barrier contraceptive (36). It is not known whether these medications reduce efficacy of progestin IUDs, which contain varying amounts of hormone and have a largely

intrauterine effect. Other recommendations vary: while the package insert states that MMF may reduce effectiveness of oral contraceptives and use of additional barrier contraceptive methods is recommended (37), the European Medicine Agency recently updated recommendations regarding use of contraception for women taking MMF to state that “two forms of contraception are preferred but no longer mandatory”(38). Voting Panel members disagreed on the need to use additional contraceptive measures. As befits a conditional recommendation, clinicians should be aware of and discuss this hypothetical risk with their patients.

Assisted reproductive technology

Supplementary Appendix 7, Table B (<http://onlinelibrary.wiley.com/doi/10.1002/art.41191/abstract>) presents the ART recommendations with strength of supporting evidence; detailed justifications for strong and conditional recommendations are shown in Supplementary Appendix 9 (<http://onlinelibrary.wiley.com/doi/10.1002/art.41191/abstract>). Figure 2 details the ART decision-making process.

While fertility is typically normal in women with RMD (who have not been treated with cyclophosphamide [CYC]), it decreases with age, and ART may be needed by some RMD

patients. ART techniques include ovarian stimulation, which elevates estrogen levels, IVF, and embryo transfer. Ovarian stimulation cycles for IVF generally require more aggressive stimulation than do those for intrauterine insemination; they involve surgical extraction of oocytes and IVF, followed by embryo transfer. Frozen embryo transfer does not usually require ovarian stimulation.

As is the case with any underlying significant medical disease, women undertaking ovarian stimulation must be cleared medically by the appropriate specialist. Similarly, women with APS, thrombotic or otherwise, should be cleared medically by their rheumatologist. The rheumatologist should consult with the reproductive endocrinology and infertility specialist regarding adjustments to the ovarian stimulation protocol in order to minimize the risk to the patient. Women with these underlying conditions who undergo fertility therapy should do so only in centers where the appropriate expertise is readily available.

We strongly recommend proceeding with ART if needed in women with uncomplicated RMD who are receiving pregnancy-compatible medications, whose disease is stable/quiescent, and who are negative for aPL.

Compared to the benefit of a successful pregnancy, the risk of ART for subfertile patients with RMD is low; nonetheless,

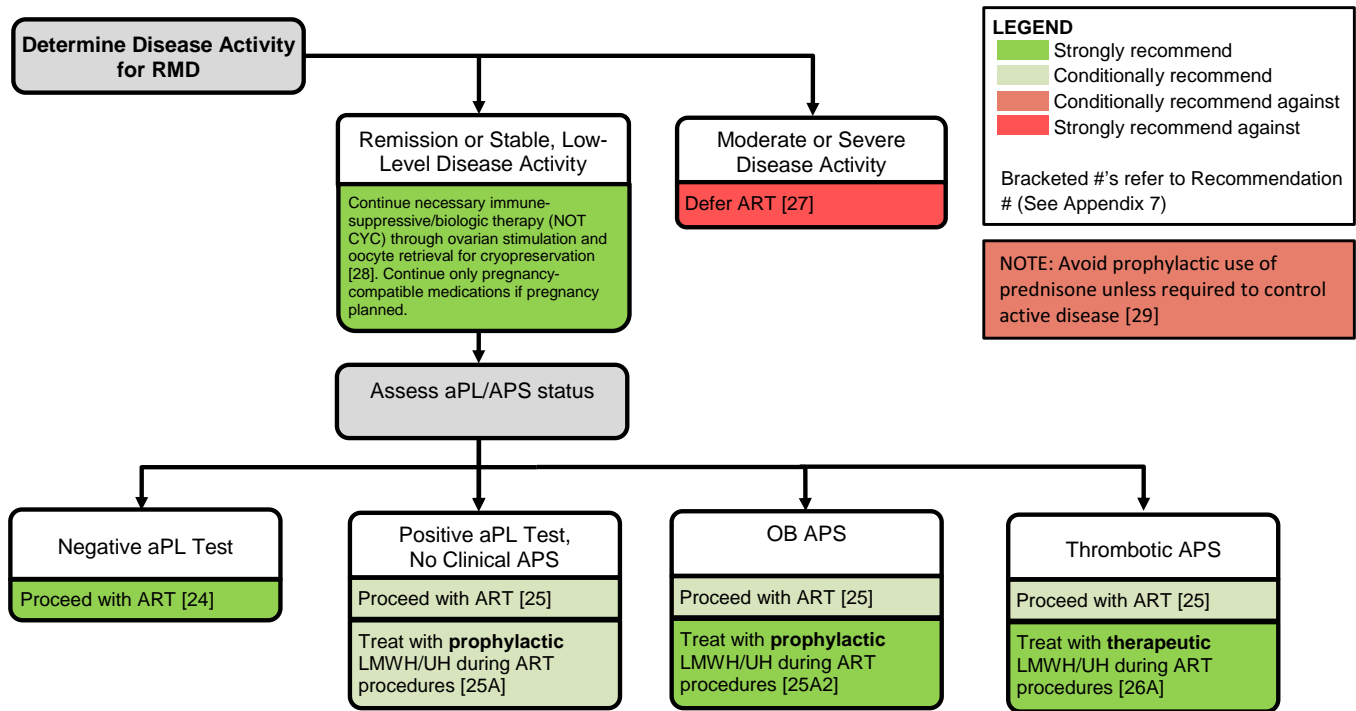


Figure 2. Recommendations for use of assisted reproductive technology (ART) in women with rheumatic and musculoskeletal disease (RMD). CYC = cyclophosphamide; aPL = antiphospholipid antibody (persistent moderate-to-high-titer anticardiolipin or anti-β₂-glycoprotein I antibody or persistent positive lupus anticoagulant); APS = antiphospholipid syndrome (obstetric and/or thrombotic); obstetric APS (OB APS) = patients meeting laboratory criteria for APS and having prior consistent pregnancy complications (≥3 consecutive losses prior to 10 weeks’ gestation, fetal loss at or after 10 weeks’ gestation, or delivery at <34 weeks due to preeclampsia, intrauterine growth restriction, or fetal distress) and with no history of thrombosis; thrombotic APS = patients meeting laboratory criteria for APS and having a prior thrombotic event (arterial or venous), regardless of whether they have had obstetric complications; LMWH = low molecular weight heparin; UH = unfractionated heparin.

risks associated with ART, especially thrombosis and lupus flare (39,40), should be discussed with patients. The level of evidence specific to RMD patients is very low (41,42), but evidence supports the safety of ART in a general population (43,44).

SLE patients. Data on IVF cycles in RMD patients are limited; however, the intended outcome of IVF, pregnancy, may be adversely affected by the presence of active RMD. In addition, there is concern that flare in SLE patients might be worsened in the setting of elevated estrogen levels.

We strongly recommend deferring ART procedures in patients with any RMD while disease is moderately or severely active; this recommendation is based on extrapolated evidence that RMD disease activity increases pregnancy risks.

For pregnancy planning, 6 months of stable inactive or low-level disease is most often suggested, but individual clinical factors may influence this decision. In patients with SLE, there is theoretical concern that ovarian stimulation with elevated estrogen levels may worsen active disease.

We conditionally recommend *against* an empiric dosage increase of prednisone during ART procedures in patients with SLE; instead, we suggest monitoring the patient carefully and treating for flare if it occurs.

No studies have evaluated prescription of prophylactic prednisone to prevent SLE flare during ART.

Antiphospholipid antibody-positive patients. Patients who are positive for aPL are at increased risk for thrombosis. Most reports of aPL-positive patients undergoing IVF describe the use of empiric prophylactic anticoagulation due to concern regarding further increased risk of potentially life-threatening thrombosis from elevated estrogen levels during ovarian stimulation.

In subfertile patients with RMD who desire pregnancy, have stable/quiescent disease, and have asymptomatic positive aPL, OB APS, or treated thrombotic APS, we conditionally recommend ART with anticoagulation, as described below.

We conditionally recommend prophylactic anticoagulation therapy with heparin or low molecular weight heparin in asymptomatic aPL-positive patients during ART procedures (41,42).

The increased risk of organ- or life-threatening thrombosis due to high estrogen levels greatly outweighs the low risk of bleeding or other complications of unfractionated heparin or low molecular weight heparin (LMWH).

We strongly recommend prophylactic anticoagulation with heparin or LMWH in women with OB APS, and we strongly recommend therapeutic anticoagulation in women with thrombotic APS, during ART procedures.

The strength of these recommendations rests on the severity of the risk of organ- or life-threatening thrombosis during ovarian stimulation. An added risk for thrombosis is ovarian hyperstimulation syndrome, an important, uncommon complication consisting of capillary leak syndrome (with pleural effusion and ascites) and, in severe cases, arterial and venous thrombosis and renal failure (43). Underlying thrombophilia increases the risk of severe ovarian hyperstimulation syndrome (44). While there are few data to guide prophylactic anticoagulation in aPL-positive patients, thromboprophylaxis is recommended to prevent thrombotic complications of moderate-to-severe ovarian hyperstimulation syndrome, as it is for patients with known inherited or acquired thrombophilia (45,46). Reports of thrombosis in aPL-positive patients undergoing IVF are uncommon, but most reported patients received empiric anticoagulation (41,42). In a recent series, 2 of 4 reported thromboses occurred in women who, on their own decision, discontinued LMWH after oocyte retrieval (41).

LMWH is used most commonly. Prophylactic dosing of enoxaparin is usually 40 mg daily, started at the beginning of ovarian stimulation, withheld 24–36 hours prior to oocyte retrieval, and resumed following retrieval. Optimal duration of prophylactic LMWH for asymptomatic aPL-positive patients undergoing ovarian stimulation has not been studied; this is a decision best made in consultation with the reproductive endocrinology and infertility specialist. The treatment is often continued until estrogen levels return to near-physiologic levels if no pregnancy occurs. Patients with OB APS will continue therapy throughout pregnancy. Aspirin is not commonly used prior to oocyte retrieval (it will be started after retrieval if indicated) given concern that its prolonged action may increase bleeding risk at the time of the retrieval. Patients receiving regular anticoagulation therapy with vitamin K antagonists for thrombotic APS should transition to therapeutic-dose LMWH for ART (usually enoxaparin 1 mg/kg subcutaneously every 12 hours), with this treatment withheld for retrieval and resumed subsequently, to continue throughout pregnancy. Since ovarian stimulation protocols vary, discussion with the reproductive endocrinology and infertility specialist is appropriate. In addition to anticoagulation, patients at risk for thrombosis or ovarian hyperstimulation syndrome may benefit from ovarian stimulation protocols that yield lower peak serum estrogen levels, such as those incorporating aromatase inhibitors (47).

Embryo and oocyte cryopreservation. Embryo and oocyte cryopreservation are good options to preserve fertility in patients whose condition is stable enough for them to undergo ovarian stimulation but who are either not able or not ready to pursue pregnancy at the time of stimulation. A carefully monitored ovarian

stimulation/IVF cycle followed by embryo transfer to a surrogate is an option, if available, for patients with severe disease-related damage who desire a biologic child and are able to undergo ovarian stimulation and oocyte retrieval, but cannot safely undergo pregnancy.

We strongly recommend continuation of necessary immunosuppressive and/or biologic therapies (except CYC, which directly impacts maturing follicles) in treated patients whose condition is stable, when the purpose of ovarian stimulation is oocyte retrieval for oocyte or embryo cryopreservation.

This includes continuation of mycophenolate or methotrexate (MTX). There is an anticipated risk of uncontrolled disease from withdrawal of effective medication. However, there are no published data that directly address oocyte retrieval during treatment with most immunosuppressive or biologic therapies other than CYC.

Fertility preservation with cyclophosphamide

Supplementary Appendix 7, Table C (on the *Arthritis & Rheumatology* web site at <http://onlinelibrary.wiley.com/doi/10.1002/art.41191/abstract>) presents the formal recommendations regarding fertility preservation with CYC treatment and strength of supporting evidence. Detailed justifications for strong and conditional recommendations are shown in Supplementary Appendix 9 (<http://onlinelibrary.wiley.com/doi/10.1002/art.41191/abstract>).

Fertility preservation in women with RMD treated with CYC. Although CYC is used less frequently than in the past due to availability of alternative treatments, it remains a mainstay of therapy for severe or life-threatening RMD. Ovarian insufficiency is a potential long-term complication of monthly intravenous CYC therapy. Hormonal co-therapy during the course of CYC is suggested to reduce risk of ovarian insufficiency.

To prevent inducing primary ovarian insufficiency in premenopausal women with RMD receiving monthly intravenous CYC, we conditionally recommend monthly gonadotropin-releasing hormone agonist co-therapy.

Ovarian insufficiency risk with CYC treatment depends on patient age and cumulative monthly CYC dose (48); measures of ovarian function remained stable during treatment according to the Euro-Lupus protocol (49). The recommendation of gonadotropin-releasing hormone agonist therapy for ovarian protection during monthly CYC therapy is based on evidence supporting benefit in early breast cancer (50,51); evidence more specific to RMD patients is less robust but positive, with limited clinical trials of gonadotropin-releasing hormone agonist (usually leuprolide acetate) that included patients with SLE and other RMD populations and used a number of different outcome measures (52–56).

Thus far, studies have addressed gonadotropin-releasing hormone agonist co-therapy only in CYC-treated RMD patients who receive CYC monthly by intravenous administration. Acknowledging this lack of data on oral CYC-treated patients, it is reasonable to consider gonadotropin-releasing hormone agonist use for these patients. Theoretically, gonadotropin-releasing hormone agonist co-therapy may not be necessary for patients receiving the lower cumulative CYC dose in the Euro-Lupus regimen (49). Expense including insurance coverage issues and difficulty coordinating administration (preferred timing is 10–14 days prior to CYC administration) may impact the ability to administer gonadotropin-releasing hormone agonist for the first CYC infusion, especially in the setting of urgent need for therapy.

Fertility preservation in men with RMD treated with CYC. CYC may cause infertility and long-term gonadal damage in treated men. Options for fertility preservation should be presented to male patients in whom CYC therapy is required.

We conditionally recommend against testosterone co-therapy in men with RMD receiving CYC, as it does not preserve fertility in men undergoing chemotherapy for malignancy (57).

Because sperm cryopreservation prior to treatment preserves a man's ability to conceive a healthy child, we strongly suggest sperm cryopreservation as good practice for CYC-treated men who desire it.

We acknowledge the difficulty of coordinating sperm banking when CYC therapy is urgently indicated. Because CYC causes the most damage to the postmeiosis spermatids and sperm developing during therapy have the highest degree of genetic damage (58), sperm should be collected prior to CYC treatment. If sperm is collected after CYC treatment, urologists recommend waiting a minimum of 3 months after completion of therapy (59).

Menopause and hormone replacement therapy

Supplementary Appendix 7, Table D (<http://onlinelibrary.wiley.com/doi/10.1002/art.41191/abstract>) presents formal recommendations regarding menopause and HRT with strength of supporting evidence. Detailed justifications for strong and conditional recommendations are shown in Supplementary Appendix 9 (<http://onlinelibrary.wiley.com/doi/10.1002/art.41191/abstract>). Figure 3 details the HRT decision-making process. In this guideline, postmenopausal women include women with surgically induced menopause.

Current population recommendations (60–62) suggest limiting HRT use in healthy postmenopausal women and using the lowest dose that alleviates symptoms for the minimum time necessary. Studies of long-term HRT show that risks, including stroke and breast cancer, outweigh benefits (63). Risks of HRT

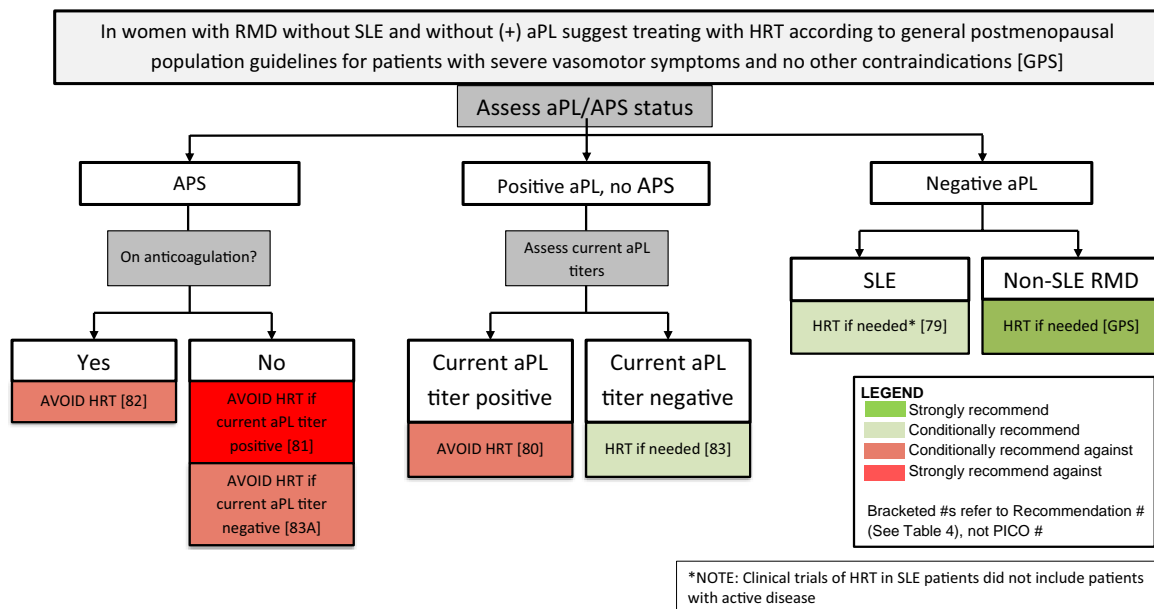


Figure 3. Recommendations and good practice statements (GPS) for hormone replacement therapy (HRT) use in postmenopausal women with rheumatic and musculoskeletal disease (RMD). SLE = systemic lupus erythematosus; aPL = antiphospholipid antibody (persistent moderate-to-high-titer anticardiolipin or anti- β_2 -glycoprotein I antibody or persistent positive lupus anticoagulant); APS = antiphospholipid syndrome (obstetric and/or thrombotic); PICO = population, intervention, comparator, outcomes.

depend on the type, dose, route of administration, duration of use, and timing of initiation. Benefit-risk balance is most favorable for severe vasomotor symptoms in women ≤ 60 years old or within 10 years of menopause onset (61).

Vasomotor symptoms, as defined by the North American Menopause Society, include hot flashes and night sweats. Hot flashes are recurrent, transient episodes of flushing, perspiration, and a sensation ranging from warmth to intense heat on the upper body and face, sometimes followed by chills. Night sweats are hot flashes that occur with perspiration during sleep (64). General contraindications to use of HRT include history of breast cancer, coronary heart disease, previous venous thromboembolic event or stroke, or active liver disease.

We strongly suggest as good practice the use of HRT in postmenopausal women with RMD without SLE or positive aPL who have severe vasomotor symptoms, have no contraindications, and desire treatment with HRT.

SLE patients. Use of HRT in symptomatic postmenopausal SLE patients may raise concerns regarding increased risk of flare and/or thrombosis; however, HRT use in aPL-negative women with quiescent SLE may be considered.

In SLE patients without positive aPL who desire HRT due to severe vasomotor symptoms and have no contraindications, we conditionally recommend HRT treatment.

Moderate-quality direct evidence supports use of oral HRT in aPL-negative women with SLE who have stable low-level disease

activity and no contraindication to use (65–68), although no studies have directly addressed use of HRT in patients with moderate-to-high disease activity. The recommendation is conditional because there was a small increase in risk of mild-to-moderate (but not severe) lupus flares with use of oral HRT in the Safety of Estrogens in Lupus Erythematosus National Assessment study (65), and because the studies did not include women with active disease.

aPL-positive patients. Estrogen use in aPL-positive patients should be avoided due to the potential increased risk of thrombosis. Data are limited, however, for many clinical situations, and specific recommendations vary in strength for this reason.

In women with asymptomatic aPL, we conditionally recommend *against* treating with HRT.

We strongly recommend *against* use of HRT in women with obstetric and/or thrombotic APS.

We conditionally recommend *against* HRT use in patients with APS who are receiving anticoagulation treatment and in patients with APS who are currently negative for aPL.

We conditionally recommend consideration of HRT, if desired, in women who have a history of positive aPL but are currently testing negative for aPL and have no history of clinical APS.

Risk of VTE may be increased with HRT use in the general population (69,70). Types of estrogen and progestin and route of administration (71–74) affect risk. In the Women's Health Initiative study, VTE risk with oral estrogen-progestin increased 2-fold over placebo (70), and oral HRT in patients with factor V Leiden or prothrombin G20210A mutations increases VTE risk 25-fold compared to mutation-free women not receiving HRT (75,76). In contrast, recent studies show that transdermal estrogen does not increase VTE risk in healthy women (71,74), even those with prothrombotic mutations or high body mass index (75,77). No studies, however, have specifically assessed thrombosis risk with oral or transdermal HRT in women with aPL.

Direct evidence regarding thrombosis risk with HRT in SLE patients with or without aPL is low, as studies have addressed risk of flare in SLE but not thrombosis, and some studies excluded patients with prior thrombosis (65,67). In one study 106 SLE patients, regardless of aPL status but excluding those with recent thrombosis, were randomized to receive oral estrogen-progestin HRT or placebo. Approximately one-third of the patients in each group had some degree of positivity for aPL (level unreported) (78). During 24 months of follow-up 3 thrombotic events occurred in the HRT group and 1 in the placebo group, a nonsignificant difference.

Available evidence supports the use, when indicated and desired, of HRT in RMD patients without aPL, including those with SLE (65). Given the demonstrated lower VTE risk with transdermal administration as opposed to oral estrogen-progestin preparations even in women at increased prothrombotic risk (77), it may be reasonable to consider transdermal estrogen as initial therapy.

Pregnancy: general assessment, counseling, and management

Obstetrics-gynecology or maternal-fetal medicine specialists necessarily assume primary medical management of pregnancy in a woman with RMD. An understanding of basic pregnancy physiology is helpful for rheumatologists to identify and treat active disease during pregnancy and coordinate care with obstetric providers.

Pregnancy changes may impact manifestations of RMD. Pregnancy-related increased intravascular volume may worsen already abnormal cardiac or renal function. The expected 50% increase in glomerular filtration rate during pregnancy may worsen preexisting stable proteinuria. Pregnancy-induced hypercoagulability increases RMD-associated thrombosis risk. The calcium demand of fetal bone development and breastfeeding may worsen maternal osteoporosis. In addition, normal pregnancy symptoms such as malar erythema, chloasma gravidarum, anemia, elevated erythrocyte sedimentation, and diffuse arthralgias may falsely mimic symptoms of active RMD. Pregnancy-induced hypertension syndromes (preeclampsia) may be confused with

lupus nephritis, scleroderma renal crisis, or vasculitis flare. HELLP syndrome (hemolysis, elevated liver enzymes, and low platelets) or eclampsia may resemble severe disease flare. Distinguishing among these syndromes requires the expertise of rheumatologists and obstetrics-gynecology or maternal-fetal medicine physicians working together.

Most information regarding pregnancy management in RMD comes from observational studies, primarily in patients with SLE and APS. There have been very few controlled trials. Data about pregnancies in rare rheumatic diseases usually derive from small case series. For these reasons, many recommendations are conditional, supported by collective experience of the Voting Panel members and patient input. Supplementary Appendix 7, Table E (<http://onlinelibrary.wiley.com/doi/10.1002/art.41191/abstract>) presents formal recommendations regarding pregnancy in patients with RMD with strength of supporting evidence. Detailed justifications for strong and conditional recommendations are shown in Supplementary Appendix 11 (<http://onlinelibrary.wiley.com/doi/10.1002/art.41191/abstract>). Figure 4 details the pregnancy management process in patients with RMD. Supplementary Appendix 10 (<http://onlinelibrary.wiley.com/doi/10.1002/art.41191/abstract>) provides assessment and management suggestions for specific RMDs.

As standard good practice, we strongly suggest counseling women with RMD who are considering pregnancy regarding the improved maternal and fetal outcomes (based on many studies) associated with entering pregnancy with quiescent/low activity disease (75,77,79–98). As additional good practice, we suggest maintaining concurrent care with specialists in obstetrics-gynecology, maternal-fetal medicine, neonatology, and other specialists as appropriate.

Patient participants expressed a strong desire that their physicians discuss family planning “early and often,” including before planning of pregnancy. Discussion with patients should include information on medications and impact of disease activity, autoantibodies, and organ system abnormalities on maternal and fetal health. In rare situations with significant disease-related damage, such as pulmonary arterial hypertension, renal dysfunction, heart failure, or other severe organ damage, pregnancy may be contraindicated due to high risk of maternal morbidity and mortality.

In women with RMD planning pregnancy who are receiving medication that is incompatible with pregnancy, we strongly recommend switching to a pregnancy-compatible medication and observing for sufficient time to assess efficacy and tolerability of the new medication.

There are no data to support a specific period of time for observation with pregnancy-compatible medications. Timing will vary depending on individual clinical factors; in clinical practice this is usually a minimum of several months.

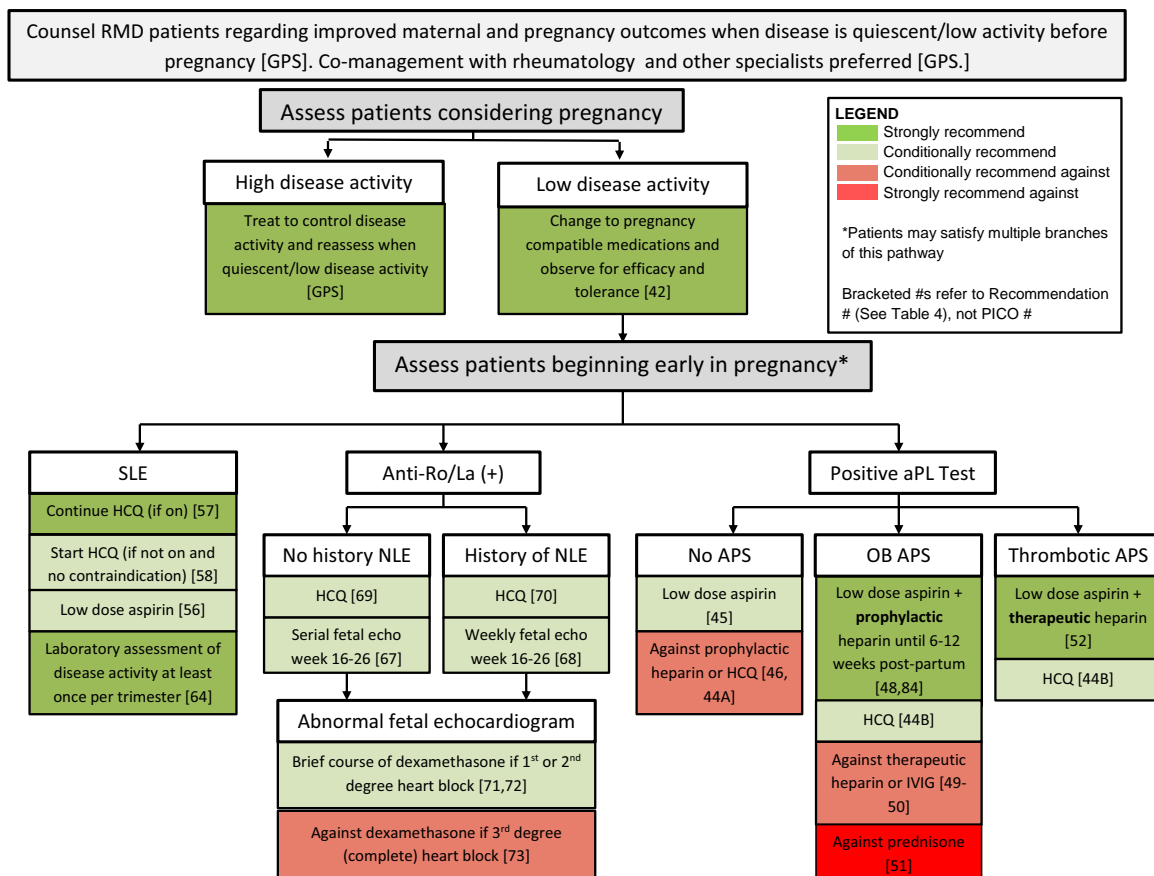


Figure 4. Recommendations and good practice statements (GPS) for pregnancy counseling, assessment, and management in women with rheumatic and musculoskeletal disease (RMD). SLE = systemic lupus erythematosus; HCQ = hydroxychloroquine; NLE = neonatal lupus erythematosus; aPL = antiphospholipid antibody (persistent moderate-to-high-titer anticardiolipin or anti- β_2 -glycoprotein I antibody or persistent positive lupus anticoagulant); APS = antiphospholipid syndrome (obstetric and/or thrombotic); obstetric APS (OB APS) = patients meeting laboratory criteria for APS and having prior consistent pregnancy complications (≥ 3 consecutive losses prior to 10 weeks' gestation, fetal loss at or after 10 weeks' gestation, or delivery at <34 weeks due to preeclampsia, intrauterine growth restriction, or fetal distress) and with no history of thrombosis; thrombotic APS = patients meeting laboratory criteria for APS and having a prior thrombotic event (arterial or venous), regardless of whether they have had obstetric complications; IVIG = intravenous immunoglobulin; PICO = population, intervention, comparator, outcomes.

In women with RMD who are currently pregnant and have active disease that requires medical therapy, we strongly recommend initiating or continuing a pregnancy-compatible steroid-sparing medication, as both active RMD and continuous high-dose glucocorticoid treatment have potential for maternal and fetal harm (99).

Pre-pregnancy or early pregnancy laboratory testing for relevant autoantibodies is recommended. Ascertaining anti-Ro/SSA, anti-La/SSB, and aPL status improves counseling regarding pregnancy and fetal risk.

We strongly recommend testing for anti-Ro/SSA and anti-La/SSB once before or early in pregnancy in women with SLE or SLE-like disorders, Sjögren's syndrome, systemic sclerosis, and rheumatoid arthritis. Given the relative persistence and unchanged titers of these antibodies, we strongly recommend *against* repeating the test during pregnancy.

Patients with scleroderma renal crisis. Most disease-specific recommendations for RMD pregnancy management focus on presence of underlying SLE or positive aPL. One aspect of disease in systemic sclerosis, however, is of particular importance during pregnancy: the development of scleroderma renal crisis. While effective medications are usually contraindicated during pregnancy due to risk of adverse fetal effects, they should be considered in this unusual and life-threatening circumstance.

We strongly recommend use of angiotensin-converting enzyme inhibitor or angiotensin receptor blockade therapy to treat active scleroderma renal crisis in pregnancy, because the risk of maternal or fetal death with untreated disease is higher than the risk associated with use of these medications during pregnancy.

While scleroderma renal crisis is rare in pregnancy (an estimated 2% of scleroderma pregnancies), it can easily be confused

with preeclampsia. Angiotensin-converting enzyme inhibitors can be renal-protective and life saving (100); however, they are contraindicated in the second and third trimesters of pregnancy because of potential oligohydramnios or permanent fetal renal damage (101), and should be considered only for active scleroderma renal crisis.

SLE patients. Supplementary Appendix 7, Table E (<http://onlinelibrary.wiley.com/doi/10.1002/art.41191/abstract>) presents formal recommendations for SLE pregnancy management, with strength of supporting evidence. Detailed justifications for strong and conditional recommendations are shown in Supplementary Appendix 11 (<http://onlinelibrary.wiley.com/doi/10.1002/art.41191/abstract>).

In women with SLE who are considering pregnancy or are pregnant, we strongly recommend testing for LAC, aCL, and anti- β_2 GPI antibodies once before or early in pregnancy, and *against* repeating these tests during pregnancy.

We recommend that all women with SLE take hydroxychloroquine (HCQ) during pregnancy if possible. If a patient is already taking HCQ, we strongly recommend continuing it during pregnancy; if she is not taking HCQ, we conditionally recommend starting it if there is no contraindication.

Many studies support maternal and pregnancy benefit of HCQ and low risk for mother and fetus (84,102–111). Potential contraindications include allergy, adverse side effects, or intolerance.

We conditionally recommend treating SLE patients with low-dose aspirin (81 or 100 mg daily), beginning in the first trimester.

The American College of Obstetricians and Gynecologists and US Protective Health Task Force recommend aspirin 81 mg daily as prophylaxis in all patients at high risk for preeclampsia (97,112–117). Treatment with low-dose aspirin during pregnancy to prevent or delay the onset of gestational hypertensive disease is recommended for those with SLE or APS because of their increased risk and may be considered for women with other RMD diagnoses depending on individual clinical risk factors. Some investigators have used doses of aspirin up to 150 mg daily, but both the American College of Obstetricians and Gynecologists and the U.S. Preventive Services Task Force note that there is a lack of appropriate comparative studies to show the superiority of doses >100 mg per day. Low-dose aspirin is not thought to complicate anesthesia or delivery (112); however, a decision regarding discontinuation prior to delivery should be made by the obstetrician-gynecologist and anesthesiologist according to the patient's specific clinical situation.

Because active disease affects maternal and pregnancy outcome, we strongly suggest, as good practice,

monitoring SLE disease activity with clinical history, examination, and laboratory tests at least once per trimester.

Abnormalities in the complete blood cell count, differential cell count, urinalysis results and urinary protein:creatinine ratio, or anti-DNA, C3, or C4 levels may indicate possible SLE flare and/or preeclampsia despite absence of clinical symptoms. Frequency of laboratory monitoring and rheumatology follow-up may vary with an individual patient's clinical status and medications.

Antiphospholipid antibody-positive patients. Pregnancies in patients with positive aPL or APS present specific challenges and may require additional monitoring and therapy. Supplementary Appendix 7, Table F (<http://onlinelibrary.wiley.com/doi/10.1002/art.41191/abstract>) presents formal recommendations, with strength of supporting evidence. Detailed justifications for strong and conditional recommendations are shown in Supplementary Appendix 11 (<http://onlinelibrary.wiley.com/doi/10.1002/art.41191/abstract>).

Antiphospholipid antibody is a major risk factor for pregnancy loss and other adverse pregnancy outcomes, especially in SLE patients (118). Anti- β_2 GPI, aCL, and LAC should all be tested. Among aPLs, LAC conveys the greatest risk for adverse pregnancy outcome in women with or without SLE: the RR for adverse pregnancy outcome with LAC was 12.15 (95% CI 2.92–50.54, $P = 0.0006$) in the PROMISSE (Predictors of Pregnancy Outcome: Biomarkers in APL syndrome and SLE) study (118). Other independent risk factors in aPL-positive women were younger age, history of thrombosis, and SLE.

Antiphospholipid antibody-positive patients without thrombosis or obstetric complications. Asymptomatic aPL-positive patients (those without pregnancy complications or history of thrombosis) are not generally treated with prophylactic therapy to prevent pregnancy loss. However, presence of aPL regardless of clinical history is considered a risk factor for development of preeclampsia.

In pregnant women with positive aPL who do not meet criteria for obstetric or thrombotic APS, we conditionally recommend treating with prophylactic aspirin, 81 or 100 mg daily, during pregnancy as preeclampsia prophylaxis.

Treatment should begin early in pregnancy (before 16 weeks) and continue through delivery.

Patients with obstetric and thrombotic APS. Pregnancy increases the risk of thrombosis due to both hemostatic and anatomic factors. Patients who meet criteria for APS—whether obstetric or thrombotic—should receive therapy with heparin (usually LMWH) to improve pregnancy outcome and/or reduce risk of thrombosis.

We strongly recommend combined low-dose aspirin and prophylactic-dose heparin (usually LMWH) for patients meeting criteria for OB APS (119–126).

This is based on evidence of moderate strength.

In women with OB APS, we further strongly recommend treating with prophylactic-dose anticoagulation for 6–12 weeks post partum (127).

In pregnant women with thrombotic APS, we strongly recommend treating with low-dose aspirin and therapeutic-dose heparin (usually LMWH) throughout pregnancy and post partum.

We conditionally recommend *against* using the combination of prophylactic-dose heparin and low-dose aspirin therapy for patients with positive aPL who do not meet criteria for OB APS.

We appreciate and stress, however, that benefit in individual high-risk circumstances, such as triple-positive aPL or strongly positive LAC results, advanced maternal age, or IVF pregnancy, may outweigh risks of this therapy, and decisions should be made with discussion between physician and patient, weighing potential risks and benefits.

Other therapies for refractory OB APS. Despite improved outcomes with standard therapy with low-dose aspirin and prophylactic heparin/LMWH, additional treatments are needed for patients who do not respond to standard therapy. Intravenous immunoglobulin, low-dose prednisone, increased dose of heparin/LMWH, and HCQ have all been suggested as additional or alternative treatments.

We conditionally recommend *against* treatment with intravenous immunoglobulin or an increased LMWH dose, as these have not been demonstrably helpful in cases of pregnancy loss despite standard therapy with low-dose aspirin and prophylactic heparin or LMWH.

Prophylactic-dose heparin and aspirin therapy for OB APS improves likelihood of live birth, but not necessarily full-term birth. Pregnancy loss occurs, despite treatment, in 25% of OB APS pregnancies. There are no data demonstrating improved outcomes with a higher dose of heparin, and only anecdotal data support the use of intravenous immunoglobulin.

We strongly recommend *against* adding prednisone to prophylactic-dose heparin or LMWH and low-dose aspirin in patients in whom standard therapy has been unsuccessful, since there are no controlled studies demonstrating a benefit.

We acknowledge, however, that this recommendation is based on a lack of compelling data rather than data showing no clear benefit, and also that potential risk with this therapy is likely

to be strongly affected by daily dosage, with higher doses imparting greater risk of side effects.

We conditionally recommend the addition of HCQ to prophylactic-dose heparin or LMWH and low-dose aspirin therapy for patients with primary APS.

Recent small studies of APS pregnancies suggest that HCQ may decrease complications (111).

In pregnant women with positive aPL who do not meet criteria for APS and do not have another indication for the drug (such as SLE), we conditionally recommend *against* treating with prophylactic HCQ.

As with any unproven treatment, this therapy may be considered in specific circumstances, depending on a patient's values and preferences and after a discussion about risks and benefits.

Anti-Ro/SSA and/or anti-La/SSB antibodies in pregnancy. Neonatal lupus erythematosus (NLE) describes several fetal and infant manifestations caused by or associated with maternal anti-Ro/SSA (commonly) and anti-La/SSB auto-antibodies. While isolated anti-La/SSB rarely imposes risk, when combined with anti-Ro/SSA, La/SSB antibodies may increase fetal risk (128). Prospective studies of infants born to women with anti-Ro/SSA and/or anti-La/SSB antibodies show that ~10% develop an NLE rash, 20% transient cytopenias, and 30% mild transient transaminitis (estimates vary widely between reports). These complications are short-lived and spontaneously resolve as the child's maternal antibodies disappear (129).

Complete (third-degree) heart block (CHB) occurs in ~2% of pregnancies of women with anti-Ro/SSA and/or anti-La/SSB antibodies who have not had a prior infant with NLE, and in 13–18% of pregnancies of women with a prior infant who had either cutaneous or cardiac NLE (130). Low-titer antibodies are probably not associated with the same risk of CHB as higher titers (131). CHB rarely occurs after week 26. It is irreversible, and management transfers to pediatric cardiologists. Approximately 20% of children with CHB die in utero or in the first year of life; more than half will need a pacemaker (128).

Supplementary Appendix 7, Table G (<http://onlinelibrary.wiley.com/doi/10.1002/art.41191/abstract>) presents formal recommendations regarding pregnancy in women with anti-Ro/SSA and/or anti-La/SSB antibodies, with strength of supporting evidence. Detailed justifications for strong and conditional recommendations are shown in Supplementary Appendix 11 (<http://onlinelibrary.wiley.com/doi/10.1002/art.41191/abstract>).

In pregnant women with anti-Ro/SSA and/or anti-La/SSB antibodies but no history of an infant with CHB or NLE, we conditionally recommend serial fetal echocardiography (less frequent than weekly; interval not determined) starting between 16 and 18 weeks and continuing

through week 26. For women with a prior infant with CHB or other NLE we conditionally recommend fetal echocardiography weekly, starting at week 16–18 and continuing through week 26.

Recommendations regarding monitoring for and treatment of CHB in women with anti-Ro/SSA and/or anti-La/SSB are all conditional. Given the rarity of CHB, large case series are not available; most studies are retrospective and not randomized. An argument against screening includes the risk of identification and treatment of artifacts that do not impact offspring health, thus exposing both fetus and mother to long-term side effects of dexamethasone; this risk must be balanced against the potentially devastating impact of CHB. All discussions should acknowledge the limited data and consider the patient's values and preferences.

We conditionally recommend treating all women who are positive for anti-Ro/SSA and/or anti-La/SSB antibodies with HCQ during pregnancy.

This is based on early and limited data and the low risk profile of HCQ. Retrospective studies demonstrate that in pregnant women with a prior child with cardiac NLE who take HCQ, there is a lower risk of the current fetus developing CHB (132).

For pregnant women with anti-Ro/SSA and/or anti-La/SSB antibodies and fetal first- or second-degree heart block shown on echocardiography, we conditionally recommend treatment with oral dexamethasone 4 mg daily. If CHB (without other cardiac inflammation) is present, we conditionally recommend *against* treating with dexamethasone.

Fluorinated glucocorticoids, such as dexamethasone and betamethasone, cross the placenta; low-to-moderate-dose

nonfluorinated glucocorticoids, such as prednisone and prednisolone, are largely metabolized before they reach the fetus. Whether dexamethasone given for fetal first- or second-degree heart block changes outcome is a matter of controversy. Treatment should be limited to several weeks, depending on response, because of the risk of irreversible fetal and maternal toxicity. Whether dexamethasone improves long-term survival for a fetus with CHB is controversial (133,134), but recent analyses do not support its use (135).

Medication use

Paternal medication use. Supplementary Appendix 7, Table H (<http://onlinelibrary.wiley.com/doi/10.1002/art.41191/abstract>) presents best practice statements and recommendations regarding paternal medication use in men with RMD, with strength of supporting evidence. Detailed justifications for strong and conditional recommendations are shown in Supplementary Appendix 12 (<http://onlinelibrary.wiley.com/doi/10.1002/art.41191/abstract>). Table 2 summarizes recommendations for paternal medication use.

Medication issues differ between men with RMD who are planning to father a pregnancy and those whose sexual partner is pregnant. Pre-conception, the concerns are potential effects on male fertility and medication-associated teratogenicity. There are few published data addressing these potential effects of medications for RMD. A decision to stop a medication must be weighed against the impact it may have on paternal disease activity.

When the man's partner is pregnant, the concern is whether his medication is present in seminal fluid and can transfer through vaginal mucosa, cross the placenta, and be teratogenic. In fact, post-conception exposure of the embryo or fetus is likely minimal,

Table 2. Recommendations regarding medication use for men with rheumatic and musculoskeletal disease who are planning to father a child

Strongly recommend continuing	Conditionally recommend continuing	Strongly recommend discontinuing	Conditionally recommend discontinuing	Unable to make a recommendation due to limited data
Azathioprine/ 6-mercaptopurine Colchicine Hydroxychloroquine Tumor necrosis factor inhibitors (all)	Anakinra Cyclooxygenase 2 inhibitors Cyclosporine Leflunomide Methotrexate Mycophenolate mofetil Mycophenolic acid Nonsteroidal anti-inflammatory drugs Rituximab Sulfasalazine (semen analysis if delayed conception) Tacrolimus	Cyclophosphamide (discontinue 12 weeks prior to attempted conception)	Thalidomide (discontinue 4 weeks prior to attempted conception)	Abatacept Apremilast Baricitinib Belimumab Secukinumab Tocilizumab Tofacitinib Ustekinumab

Table 3. Maternal medication use: overview of medication use before and during pregnancy, and during breastfeeding

Medication	Pre-conception	During pregnancy	Breastfeeding
Conventional medications			
Hydroxychloroquine	++	++	++
Sulfasalazine	++	++	++
Colchicine	++	++	++
Azathioprine, 6-mercaptopurine	++	++	+ Low transfer
Prednisone	+ Taper to <20 mg/day by adding pregnancy-compatible immunosuppressants	+ Taper to <20 mg/day by adding pregnancy-compatible immunosuppressants	+ After a dose of >20 mg, delay breastfeeding for 4 hours
Cyclosporine, tacrolimus	+ Monitor blood pressure	+ Monitor blood pressure	+ Low transfer
Nonsteroidal antiinflammatory drugs (cyclooxygenase 2 inhibitors not preferred)	+ Discontinue if the woman is having difficulty conceiving	+ Continue in first and second trimesters; discontinue in third trimester	+ Ibuprofen preferred
Tumor necrosis factor inhibitors (tumor necrosis factor inhibitors are considered compatible with pregnancy)			
Certolizumab	++	++	++
Infliximab, etanercept, adalimumab, golimumab	+ Continue through conception	+ Continue in first and second trimesters; discontinue in third trimester several half-lives prior to delivery	++
Rituximab	+ Discontinue at conception	+ Life-/organ-threatening disease	++
Other biologics (limited safety data; limited transfer in early pregnancy but high transfer in second half of pregnancy)			
Anakinra, belimumab, abatacept, tocilizumab, secukinumab, ustekinumab	+ Discontinue at conception	X Discontinue during pregnancy	+ Expect minimal transfer due to large molecular size, but no available data
Not compatible with pregnancy			
Methotrexate	XX Stop 1–3 months prior to conception	XX Stop and give folic acid 5 mg/day	X Limited data suggest low transfer
Leflunomide	XX Cholestyramine washout if detectable levels	XX Stop and give cholestyramine washout	XX
Mycophenolate mofetil and mycophenolic acid	XX Stop >6 weeks prior to conception to assess disease stability	XX	XX
Cyclophosphamide	XX Stop 3 months prior to conception	+ Life-/organ-threatening disease in second and third trimesters	XX
Thalidomide	XX Stop 1–3 months prior to conception	XX	XX
Tofacitinib, apremilast, baricitinib	Unable to determine due to lack of data; small molecular size suggests transfer across the placenta and into breast milk		

	++ Strongly recommend
	+ Conditionally recommend
	X Conditionally recommend against
	XX Strongly recommend against

as seminal concentrations of medications and volumes transferred are small (136). There are no reports of post-conception teratogenesis attributable to medications taken by a man with RMD. When a man's sexual partner is pregnant, reassurance regarding low risk associated with his RMD treatment is generally warranted.

In the absence of adequate data regarding paternal exposure for most medications used for RMD, we developed recommendation statements when 1) at least some data on paternal exposure were available, 2) accumulated clinical experience of paternal exposure could guide the recommendation, or 3) there were no data on paternal exposure, but maternal exposure demonstrates teratogenicity. We do not present recommendations for new medications with no available class-level or drug-specific data.

We strongly recommend against use of CYC and thalidomide in men prior to attempting conception.

Paternal use of CYC may impair spermatogenesis or be mutagenic for DNA (137) and should be discontinued 3 months prior to attempting conception. Thalidomide is detectable in seminal fluid and is strongly teratogenic when given to pregnant women (138,139), and should be discontinued at least 1 month prior to attempting conception. The remaining medications are recommended either strongly or conditionally for continuation during peri- and post-conception periods.

In men with RMD who are planning to father a pregnancy, we strongly recommend continuation of HCQ, azathioprine, 6-mercaptopurine, colchicine, and tumor necrosis factor inhibitors (140–142).

In men with RMD who are planning to father a pregnancy, we conditionally recommend, based on a smaller body of evidence, continuing treatment with MTX, MMF, leflunomide, sulfasalazine, calcineurin inhibitors, and non-steroidal antiinflammatory drugs (NSAIDs) (142–149).

Although the drug label suggests discontinuation of MTX before attempting pregnancy, data show no evidence for mutagenesis or teratogenicity (143–145).

Although sulfasalazine may affect sperm count and quality, there are no data suggesting teratogenicity (146,150), and we conditionally recommend its continuation. If conception does not occur, semen analysis should be considered.

We conditionally recommend continuation of anakinra and rituximab based on limited data (151,152).

Maternal medication use. Supplementary Appendix 7, Tables I (conventional rheumatology medications), J (biologic rheumatology medications), and K (glucocorticoids) (<http://onlinelibrary.wiley.com/doi/10.1002/art.41191/abstract>) present formal best practice statements and recommendations regarding maternal medication use in patients with RMD, with strength of sup-

porting evidence. Detailed justifications for strong and conditional recommendations are shown in Supplementary Appendix 12 (<http://onlinelibrary.wiley.com/doi/10.1002/art.41191/abstract>). Table 3 summarizes recommendations for maternal medication use.

As standard good practice, we suggest discussing medications well before the patient attempts to conceive; we also suggest discussing pregnancy plans prior to initiating treatment with medications that may affect gonadal function, such as CYC.

There are no published data regarding specific timing for medication discussion, which will vary according to the individual clinical situation, but in general we suggest adequate time to allow for appropriate medication changes and demonstration of tolerability and disease stability, usually a minimum of several months.

MTX, MMF, CYC, and thalidomide are known teratogens. We strongly recommend discontinuation of these within 3 months prior to conception (153–156).

Data regarding timing of discontinuation are conflicting and do not permit more specific recommendations. However, discontinuation within 1 menstrual cycle would represent the minimum, and 3 months the most common, period for discontinuation. In addition to concerns about teratogenicity, it is optimal to allow adequate time for observation of disease stability without medication.

For women treated with leflunomide, we strongly recommend cholestyramine washout if there are detectable serum levels of metabolite prior to or as soon as pregnancy is confirmed. Once metabolite is not detectable in the serum, the risks of pregnancy loss and birth defects are not elevated (157,158).

We conditionally recommend treatment with CYC for life-threatening conditions in the second or third trimester (86).

When potentially teratogenic medications are discontinued prior to pregnancy, we strongly recommend a period of observation without medication or transition to pregnancy-compatible medications to ensure disease stability (as discussed above). In women with inadvertent exposure to teratogenic medications we strongly suggest immediate referral to a maternal-fetal medicine specialist, pregnancy medication specialist, or genetics counselor as standard good practice.

We strongly recommend HCQ, azathioprine/6-mercaptopurine, colchicine, and sulfasalazine, medications commonly used for RMD, as compatible for use throughout pregnancy (104,106,159–161).

We conditionally recommend calcineurin inhibitors (tacrolimus and cyclosporine) and NSAIDs as compatible for use during pregnancy (154).

We conditionally recommend discontinuation of NSAIDs pre-conception if the patient is having difficulty conceiving (and if disease control would not be compromised), due to the possibility of NSAID-induced unruptured follicle syndrome, a cause of subfertility (162).

We strongly recommend *against* use of NSAIDs in the third trimester because of the risk of premature closure of the ductus arteriosus (163).

We conditionally recommend nonselective NSAIDs over cyclooxygenase 2-specific inhibitors in the first 2 trimesters, due to lack of data on cyclooxygenase 2-specific inhibitors.

Nonfluorinated glucocorticoids should be used when needed, but substitution of steroid-sparing pregnancy-compatible immunosuppressive therapy is desirable when high-dose or prolonged use is required.

We conditionally recommend continuing low-dose glucocorticoid treatment (≤ 10 mg daily of prednisone or nonfluorinated equivalent) during pregnancy if clinically indicated. We strongly recommend tapering higher doses of nonfluorinated glucocorticoids to < 20 mg daily of prednisone, adding a pregnancy-compatible glucocorticoid-sparing agent if necessary. Although there are only minimal data regarding prolonged treatment with low-dose glucocorticoids during pregnancy, we conditionally recommend *against* routine administration of stress-dose glucocorticoids at the time of vaginal delivery, but conditionally do recommend such treatment for surgical (cesarean) delivery.

We conditionally recommend continuing tumor necrosis factor inhibitor therapy with infliximab, etanercept, adalimumab, or golimumab prior to and during pregnancy (164,165). The tumor necrosis factor inhibitor certolizumab does not contain an Fc chain and thus has minimal placental transfer (166). We strongly recommend continuation of certolizumab therapy prior to and during pregnancy.

Placental transfer and fetal exposure for most biologic therapies vary with gestational stage. The majority of RMD biologic therapies contain an Fc IgG1 construct that does not cross into the fetal circulation in significant concentrations until the second trimester (167). Use of the tumor necrosis factor (TNF) inhibitors that include an IgG1 Fc construct during the third trimester (infliximab, etanercept, adalimumab, and golimumab) results in high levels of placental transfer and significant drug levels in

the neonate. A modest amount of evidence suggests that these TNF inhibitors cause no adverse effects, especially in the first trimester. There was extensive Voting Panel discussion regarding if, and when, these medications should be discontinued prior to delivery. The Voting Panel agreed that if the patient's disease is under good control, these medications may be discontinued in the third trimester. While there is a paucity of safety data, continuing TNF inhibitors through delivery if the patient's disease is active can be considered, with the understanding that the neonate will have significant serum levels of drug for a period of time.

There are limited data on the compatibility of other biologics with pregnancy. Given that these agents likely do not cross the placenta until the second trimester, the panel conditionally recommends that non-TNF inhibitor IgG-based molecules are compatible in the periconception period but should be discontinued during pregnancy (i.e. at the time of the first positive pregnancy test result).

We conditionally recommend continuing treatment with anakinra, belimumab, abatacept, tocilizumab, secukinumab, and ustekinumab while a woman is trying to conceive, but discontinuing once she is found to be pregnant.

If disease cannot be controlled with medications considered compatible with pregnancy, the physician and patient should discuss and weigh the possible risks from these medications versus the risks of uncontrolled disease during pregnancy.

We conditionally recommend continuing treatment with rituximab while a woman is trying to conceive, and we conditionally recommend continuing rituximab during pregnancy if severe life- or organ-threatening maternal disease so warrants.

Dosing in the second half of pregnancy puts the fetus at high risk of having minimal B cells at delivery (168).

There is no available evidence regarding use or safety of the new small-molecule agents, tofacitinib, baricitinib, and apremilast, during pregnancy. The Voting Panel elected not to offer recommendations regarding these drugs. It should be noted, however, that small molecules are likely to pass through the placenta.

Medication use during breastfeeding. The benefits of breastfeeding are numerous (169–175); the American Academy of Pediatrics recommends exclusive breastfeeding for the first 6 months and continued breastfeeding until 1 year (9). Because women with RMD may experience disease flare post partum and require treatment, it is important to balance benefits of disease control with risk of infant exposure through breast milk.

Infant serum levels of drugs ingested by the mother depend on multiple variables and are a function of drug concentration in breast milk, quantity of breast milk ingested, and drug absorption through the infant's gastrointestinal tract. Premature infants

Table 4. Reproductive health care in patients with RMD: concise recommendation summary*

Topic	Recommendation	Strength	
Contraception All RMD	Contraception/pregnancy discussion early and regularly; choose contraception based on safety, efficacy, and patient preference	GPS	
	Use barrier methods if unable to use other methods	GPS	
	Use emergency contraception if necessary [6]	Strong	
	Women receiving immunosuppressive medications: Use IUD if desired [7]	Strong	
	Women at risk for osteoporosis: <i>Avoid</i> DMPA [10]	Conditional	
	Women receiving MMF: Use IUD or 2 other methods together [11]	Conditional	
	RMD without SLE or aPL: Use highly effective or effective methods† [1]	Strong	
	Highly effective methods preferred to effective methods [1A]	Conditional	
SLE	SLE with negative aPL and low/stable disease activity: Use highly effective or effective methods† [2]	Strong	
	Highly effective methods preferred to effective methods [2A]	Conditional	
	<i>Avoid</i> transdermal estrogen-progestin patch [2B]	Conditional	
	SLE with negative aPL and moderate-to-high disease activity: Use progestin-only contraceptives or IUD [2C]	Strong	
Positive aPL	Do <i>not</i> use combined estrogen-progestin contraceptives [3]; use IUD or progestin-only pill [4]	Strong	
Assisted reproductive technology All RMD	Stable disease and negative aPL: Proceed with assisted reproductive technology: IVF if pregnancy-compatible medications [24]	Strong	
	Oocyte cryopreservation: Continue medications except CYC [28]	Strong	
	Active disease: Defer assisted reproductive technology until disease is stable/quiescent [27]	Strong	
	SLE	Active SLE: Defer assisted reproductive technology until disease is stable/quiescent [27]	Strong
		Do <i>not</i> treat with prophylactic prednisone [29]	Conditional
	Positive aPL	No prior thromboses or OB APS: Prophylactic heparin or LMWH [25A]	Conditional
No prior thromboses but history of OB APS: Prophylactic heparin or LMWH [25A2]		Strong	
Prior thromboses: Therapeutic heparin or LMWH [26A]		Strong	
Fertility preservation	Women: Use gonadotropin-releasing hormone agonist therapy during IV CYC treatment [31]	Conditional	
	Men: Sperm cryopreservation pre-CYC treatment	GPS	
	Do <i>not</i> use gonadotropin-releasing hormone agonist therapy [35]	Conditional	
Menopause/hormone replacement therapy All RMD	RMD without SLE or aPL: Treat with hormone replacement therapy if indicated‡	GPS	
	SLE	SLE and negative aPL: Treat with hormone replacement therapy if indicated‡ [79]	Conditional
	Positive aPL	If no prior thrombosis or OB APS: Do <i>not</i> treat with hormone replacement therapy [80]	Conditional
		If current titers negative, treat with hormone replacement therapy if indicated‡ [83]	Conditional
If prior thrombosis or OB APS and not receiving anticoagulation treatment: Do <i>not</i> treat with hormone replacement therapy [81]		Strong	
	If current titers negative, do <i>not</i> treat with hormone replacement therapy [83A]	Conditional	
	If prior thrombosis or OB APS and receiving anticoagulation treatment: Do <i>not</i> treat with hormone replacement therapy [82]	Conditional	
Pregnancy All RMD	Counseling: Outcomes improved with pregnancy planning, stable disease, compatible medications, and co-management by rheumatology and obstetrics-gynecology/maternal-fetal medicine	GPS	
	Pre-pregnancy: Change to pregnancy-compatible medication and observe for stability [42]	Strong	
	If active disease during pregnancy: Initiate pregnancy-compatible medication [54]	Strong	
	If SLE or SLE-like disease, SS, SSc, or RA: Test once (early) for anti-Ro/SSA and anti-La/SSB [60, 62]	Strong	
	If SSc and renal crisis during pregnancy: Treat with ACE inhibitor or ARB for life-threatening disease [55]	Strong	

(Continued)

Table 4. (Cont'd)

Topic	Recommendation	Strength
SLE	SLE or SLE-like disease: Test once (early) for aPL (aCL, anti- β_2 GPI, LAC) [59, 61]	Strong
	Continue HCQ during pregnancy [57]	Strong
	If not taking HCQ, start HCQ during pregnancy if no contraindications [58]	Conditional
	Monitor laboratory values at least once per trimester	GPS
	Treat with low-dose aspirin starting in first trimester [56]	Conditional
Positive aPL	Positive aPL only: If no prior thrombosis or OB APS, treat with low-dose aspirin starting in first trimester [45]	Conditional
	Do <i>not</i> treat with combination prophylactic heparin or LMWH/low-dose aspirin [46]	Conditional
	Do <i>not</i> treat with HCQ [44A]	Conditional
	OB APS: If no thrombosis but meet OB APS criteria, treat with combination prophylactic heparin or LMWH/low-dose aspirin [48]	Strong
	Do <i>not</i> treat with combination therapeutic heparin or LMWH/low-dose aspirin [49]	Conditional
	Do <i>not</i> treat with addition of IVIG [50]	Conditional
	Do <i>not</i> treat with addition of prednisone [51]	Strong
	Treat with addition of HCQ for combination heparin/low-dose aspirin failure [44B]	Conditional
	Treat with prophylactic anticoagulation during post partum period [84]	Strong
	Thrombotic APS: If prior thrombosis (meeting or not meeting OB APS criteria), treat with therapeutic heparin or LMWH/low-dose aspirin [52]	Strong
	Treat with addition of HCQ for therapeutic heparin or LMWH/low-dose aspirin therapy failure [44B]	Conditional
Positive anti-Ro/SSA with or without anti-La/SSB	Treat with HCQ during pregnancy [69, 70]	Conditional
	If no prior history of neonatal lupus: Serial (interval uncertain) fetal echocardiography in weeks 16–26 [67]	Conditional
	If prior history of neonatal lupus: Weekly fetal echocardiography in weeks 16–26 [68]	Conditional
	Abnormal fetal echocardiography: If first- or second-degree heart block, treat with dexamethasone 4 mg daily [71, 72]	Conditional
	If isolated third-degree heart block (and no other cardiac inflammation), do <i>not</i> treat with dexamethasone [73]	Conditional
Medication		
Paternal medication	If planning to father a child: Discuss medication use including CYC	GPS
	Discontinue CYC and thalidomide [133, 139]	Strong/conditional
	Continue HCQ, AZA, infliximab, etanercept, adalimumab, golimumab, certolizumab, colchicine [90, 115, 143, 146, 149, 152, 155, 97]	Strong
	Continue leflunomide, MMF, NSAIDs, sulfasalazine, cyclosporine, tacrolimus, anakinra, rituximab [108, 119, 85, 94, 126, 130, 159, 163]	Conditional
Maternal medication	If planning pregnancy: Discuss medication use including CYC	GPS
	If pregnant and exposed to teratogenic medications: Discontinue immediately, pursue counseling	GPS
	Discontinue NSAIDs if difficulty conceiving [86]	Conditional
	Avoid NSAIDs in third trimester [87]	Strong
	Use nonselective rather than COX-2-specific NSAIDs [88]	Conditional
	Discontinue MTX, MMF, thalidomide, CYC prior to conception [102, 120, 140, 134]	Strong
	Use CYC for life-threatening disease only in second and third trimester [136]	Conditional
	Discontinue leflunomide 24 months prior to conception or check serum metabolite levels and treat with cholestyramine washout [109, 110]	Strong
	Continue HCQ, sulfasalazine, AZA, colchicine [91, 95, 116, 98]	Strong
	Continue cyclosporine and tacrolimus [127, 131]	Conditional
	Continue certolizumab [156]	Strong
	Continue infliximab, etanercept, adalimumab, golimumab [144, 147, 150, 153]	Conditional
	Stop when pregnancy confirmed: rituximab, belimumab, anakinra, abatacept, tocilizumab, secukinumab, ustekinumab [164, 169, 160, 173, 177, 181, 185]	Conditional
Use rituximab for organ- or life-threatening disease during pregnancy [165]	Conditional	
No recommendations for tofacitinib, baricitinib, apremilast due to lack of data [189, 193, 197]		
Continue regular low-dose prednisone [201]	Conditional	

(Continued)

Table 4. (Cont'd)

Topic	Recommendation	Strength
Breastfeeding	Taper high-dose prednisone with addition of pregnancy-compatible drug if needed [202]	Strong
	Stress-dose steroid at delivery: do <i>not</i> treat for vaginal delivery, do treat for cesarean delivery [206, 207]	Conditional
	Encourage breastfeeding and maintain disease control with compatible medications if possible	GPS
	Compatible medications: HCQ, infliximab, etanercept, adalimumab, golimumab, certolizumab, rituximab [92, 143, 146, 149, 152, 155]	Strong
	NSAIDs, sulfasalazine, colchicine, AZA, cyclosporine, tacrolimus, anakinra, belimumab, abatacept, tocilizumab, secukinumab, ustekinumab [89, 96, 99, 117, 128, 132, 161, 170, 174, 178, 182, 186]	Conditional
	Prednisone or nonfluorinated steroid equivalent <20 mg daily [204]	Strong
	For prednisone ≥20 mg daily, discard breast milk obtained within 4 hours following medication [205]	Strong
	Do <i>not</i> treat with leflunomide, MMF, CYC, thalidomide [113, 124, 137, 142] Do <i>not</i> treat with MTX [106]	Strong Conditional

* Recommendation numbers, shown in brackets, allow for cross-referencing with supplementary appendices. For more detailed/complete recommendations, see text or Supplementary Appendix 7 (on the *Arthritis & Rheumatology* web site at <http://onlinelibrary.wiley.com/doi/10.1002/art.41191/abstract>). RMD = rheumatic and musculoskeletal disease; GPS = good practice statement; MMF = mycophenolate mofetil (and mycophenolic acid); SLE = systemic lupus erythematosus; aPL = antiphospholipid antibody, meeting laboratory criteria for antiphospholipid syndrome (APS) (Supplementary Appendix 8, <http://onlinelibrary.wiley.com/doi/10.1002/art.41191/abstract>); IVF = in vitro fertilization; CYC = cyclophosphamide; OB APS = APS meeting laboratory criteria and clinical obstetric criteria (Supplementary Appendix 8); LMWH = low molecular weight heparin; IV = intravenous; SS = Sjögren's syndrome; SSc = systemic sclerosis; RA = rheumatoid arthritis; ACE inhibitor = angiotensin-converting enzyme inhibitor; ARB = angiotensin receptor blocker; aCL = anticardiolipin antibody; anti-β₂GPI = anti-β₂-glycoprotein I; LAC = lupus anticoagulant; HCQ = hydroxychloroquine; IVIG = IV immunoglobulin; AZA = azathioprine (and 5-fluorouracil); NSAIDs = nonsteroidal antiinflammatory drugs; COX-2 = cyclooxygenase 2; MTX = methotrexate.

† Highly effective contraceptives are long-acting reversible contraceptives including progestin or copper intrauterine device (IUD) and progestin implant. Effective contraceptives are estrogen-progestin contraceptives (oral, patch, or vaginal ring) and progestin-only (oral, depot medroxyprogesterone acetate [DMPA]).

‡ General indication for hormone replacement therapy: Current recommendations suggest limiting hormone replacement therapy use in healthy postmenopausal women and using the lowest dose that alleviates symptoms for the minimum time necessary. Benefit-risk balance is most favorable for severe vasomotor symptoms in women ≤60 years old or within 10 years of menopause onset (ref. 61).

or those with gastrointestinal disorders may absorb medication differently. Rheumatologists should collaborate with pediatricians when making recommendations (176). Levels of drug in breast milk are routinely expressed as the relative infant dose (infant dose mg/kg/day divided by maternal dose mg/kg/day) and are available in reference publications; a value of <10% is considered safe.

Supplementary Appendix 7, Table L (<http://onlinelibrary.wiley.com/doi/10.1002/art.41191/abstract>) presents formal best practice statements and recommendations for use of medications during breastfeeding, with strength of supporting evidence. Detailed justifications for strong and conditional recommendations are shown in Supplementary Appendix 12 (<http://onlinelibrary.wiley.com/doi/10.1002/art.41191/abstract>).

We suggest as standard good practice that women with RMD be encouraged to breastfeed if they so desire and are able to do so. In addition, we suggest that disease control be maintained with lactation-compatible medications and that individualized risks and benefits be reviewed with each patient.

Fortunately, many RMD medications may be initiated or continued during lactation.

We strongly recommend treatment with HCQ, colchicine, sulfasalazine, rituximab, and all TNF inhibitors as compatible with breastfeeding (177–181).

We also recommend prednisone <20 mg daily (or equivalent nonfluorinated glucocorticoid) as compatible with breastfeeding, but strongly recommend that with doses of prednisone ≥20 mg a day (or equivalent), women delay breastfeeding or discard breast milk accumulated in the 4 hours following glucocorticoid administration.

We conditionally recommend treatment with azathioprine/6-mercaptopurine, calcineurin inhibitors, NSAIDs and the non-TNF inhibitor biologic agents (anakinra, rituximab, belimumab, abatacept, tocilizumab, secukinumab, and ustekinumab) as compatible with breastfeeding (182–184).

We strongly recommend *against* use of CYC, leflunomide, MMF, and thalidomide while breastfeeding. We conditionally recommend *against* use of MTX while breastfeeding.

Despite minimal passage of MTX into breast milk, especially with once-weekly dosing, this medication may accumulate in neonatal tissues (185,186).

The Voting Panel declined to vote on the compatibility of new small-molecule agents regarding use during breastfeeding due to absence of data. In theory, however, these medications may transfer into breast milk because of their low molecular weights.

DISCUSSION

Patients' reproductive health concerns are relevant for all practicing rheumatologists. Issues regarding contraception, fertility, pregnancy, lactation, and the offspring's health affect almost every patient across all RMD diagnoses. The importance of this area is highlighted by recent publications that have addressed key elements of reproductive health for some or all RMD patients. The European League Against Rheumatism (EULAR) published recommendations regarding women's health issues in patients with SLE and APS (187), and both EULAR (with points to consider) and the British Society for Rheumatology/British Health Professionals in Rheumatology (with guideline recommendations) addressed use of medications before, during, and after RMD pregnancy (188–190). Here, we address broad reproductive health concerns as well as medication use surrounding pregnancy for all RMD patients, with special attention, when indicated, for patients with specific disorders such as SLE or APS.

Even with the wide spectrum of reproductive issues addressed here (Table 4), this project has important limitations. This guideline was developed, and the literature review conducted, in the adult population. An important future step will be to consider these issues among adolescents, as counseling and care for these patients may differ.

Another important limitation is the inability to include recommendations for uncommon but important clinical situations. Although our mandate was broad, our task was to derive and support our recommendations with available evidence, but many uncommon clinical scenarios have little published data. One such situation that reflects an ongoing research need is the challenge of reproductive health issues specific to transgender individuals, especially regarding hormonal therapies.

A relatively rare but important scenario is the therapeutic termination of pregnancy in patients with life-threatening disease damage or flare. Pregnancy in patients with preexisting severe organ damage carries profound maternal risk. Pulmonary arterial hypertension is associated with a particularly high risk of maternal mortality, estimated at up to 20% even with aggressive therapy (191). Other high-risk scenarios include severe renal insufficiency, cardiomyopathy, or valvular dysfunction. Severe autoimmune disease flare occurring during pregnancy—including diffuse alveolar hemorrhage, active nephritis or vasculitis, or central nervous system inflammation—also carries high risk for maternal morbidity and mortality (55,192–194). In these and other high-risk situations, the option of therapeutic termination of pregnancy may be lifesaving and should be discussed with the patient (195). Decisions regarding pregnancy termination in the setting of teratogenic

medication exposure will depend on the specific medication, timing of exposure, and the patient's assessment of the available data; counseling by expert professionals such as maternal-fetal medicine or genetics specialists regarding degree of risk based on specific circumstances is suggested in these cases.

We provide data-derived recommendations for common clinical reproductive health decisions including recent advances in this area and emphasize the need for early involvement of the rheumatologist in reproductive health discussions involving patients with RMD, for instance, the importance of effective contraception. Almost half of pregnancies in the US are unplanned (196). In RMD patients unplanned pregnancies carry greater risk than do planned pregnancies in periods of low disease activity treated with compatible medications. Whether considering pregnancy or not, patients should know maternal and fetal risks, including fetal exposure to teratogenic medications and their safest and most effective contraception options.

Asking a patient about desire for pregnancy early and periodically (not only during perceived periods of change) and acknowledging her personal risk factors will ensure open dialog. New information supports a shift from the paradigm of discontinuing all RMD medications except prednisone, since pregnancy-compatible steroid-sparing disease-modifying antirheumatic drugs and biologic agents pose fewer short- and long-term risks to mother and infant. With adequate planning, treatment, and monitoring, most women with RMD can have successful pregnancies. Recent data indicate compatibility of many rheumatology medications both with lactation and with paternal use. The rheumatologist's familiarity with drug safety during these periods is important to maintain disease control and minimize mother and infant risk.

Fertility and postmenopausal issues are not uncommon in RMD patients. Recommendations regarding ART reflect a growing demand among patients with RMD for fertility therapies. Oocyte freezing is now widely available (197). Attention to disease activity and aPL status and discussion with reproductive endocrinology and infertility specialists will optimize safety. For patients undergoing CYC therapy, the greatest challenge is to consider preservation of gonadal function and to initiate protective treatment protocols. HRT is another issue of importance for postmenopausal RMD patients. Severe vasomotor symptoms may be debilitating and if affected patients do not have aPL, HRT may improve quality of life.

The strength of evidence on reproductive health topics in RMD patients is moderate at best, and usually low, very low, or nonexistent for many topics of interest. Identification of areas with weak evidence highlights research priorities. One need is to establish the long-term safety profile of highly effective contraceptives in RMD patients with and without aPL. Although low-dose aspirin for preeclampsia prophylaxis in SLE and aPL patients is a low-risk intervention, its effectiveness is not known. Management of OB APS is one area with moderately strong evidence, but treatment for women with recurring adverse

outcomes despite standard therapy is needed. Much in the field of prevention, screening, and management of NLE requires further study. There are very limited data on RMD medication effects on fertility and teratogenicity in men with RMD. Because women with RMD who plan to conceive, are pregnant, or are lactating are usually excluded from clinical trials, large-scale data about medication use in these populations are also lacking. Pregnancy registries collect these data but suffer reporting bias and may not reflect the racial and ethnic make-up of the patient population. Given the difficulties of collecting clinical data, research that focuses on better understanding of placental and breast physiology, as well as drug and antibody transport, may help inform decision-making.

With the development of this guideline, the ACR recognizes the key role of clinical rheumatologists not only in managing disease activity but also in understanding the interactions of RMDs and their therapies in the context of reproductive health. The most important goal of this guideline is to provide substance and direction for discussion between clinicians and patients. A second goal is to encourage development of close working relationships among rheumatologists, specialists in obstetrics-gynecology, maternal-fetal medicine, and reproductive endocrinology and infertility, and other involved clinicians. We present this guideline as a resource to share, discuss, and disseminate across specialties and patient groups.

ACKNOWLEDGMENTS

We thank Adegbeniga Bankole, MD, Karen Costenbader, MD, MPH, and Michael Weisman, MD for serving on the Expert Panel. We thank Roger Levy, MD, PhD for participating in the initial guideline scoping meeting. We thank Liana Frankel, MD for leading the Patient Panel meeting, as well the patients who (along with authors Rachelle Crow-Hercher and C. Whitney White) participated in this meeting: Jenee Johnson, Kamanta Kettle, Nicole Lumpkin, Teona Osborne, Melissa Perry-Bell, Mera Ramkissoon, Zenethia Roberts, Kaci Jackson Sanderson, Paula Sosin, and Bene Williams. We thank the ACR staff, including Regina Parker for assistance in organizing the face-to-face Patient Panel and Voting Panel meetings and coordinating the administrative aspects of the project and Robin Lane for assistance in manuscript preparation. We thank Janet Waters for help in developing the literature search strategy and performing the literature search and updates, and Janet Joyce for peer-reviewing the literature search strategy.

AUTHOR CONTRIBUTIONS

All authors were involved in drafting the article or revising it critically for important intellectual content, and all authors approved the final version to be published. Dr. Sammaritano had full access to all of the data in the study and takes responsibility for the integrity of the data and the accuracy of the data analysis.

Study conception and design. Sammaritano, Bermas, Chakravarty, Chambers, Clowse, Lockshin, Marder, Kavanaugh, Simard, Somers, Steen, Yazdany, Turner, D'Anci.

Acquisition of data. Sammaritano, Bermas, Chakravarty, Chambers, Clowse, Lockshin, Marder, Laskin, Tedeschi, Barbhैया, Bettendorf, Eudy, Jayatileke, Shah, Sullivan, Tarter, Turgunbaev, D'Anci.

Analysis and interpretation of data. Sammaritano, Bermas, Chakravarty, Chambers, Clowse, Lockshin, Marder, Guyatt, Branch, Buyon, Christopher-Stine, Crow-Hercher, Cush, Druzin, Kavanaugh, Laskin, Plante, Salmon, Simard, Somers, Steen, Tedeschi, Vinet, White, Barbhैया, Bettendorf, Eudy, Jayatileke, Shah, Sullivan, Tarter, Birru Talabi, Turgunbaev, D'Anci.

REFERENCES

- Smyth A, Oliveira GH, Lahr BD, Bailey KR, Norby SM, Garovic VD. A systematic review and meta-analysis of pregnancy outcomes in patients with systemic lupus erythematosus and lupus nephritis. *Clin J Am Soc Nephrol* 2010;5:2060–8.
- Smith CJ, Förger F, Bandoli G, Chambers CD. Factors associated with preterm delivery among women with rheumatoid arthritis and women with juvenile idiopathic arthritis. *Arthritis Care Res (Hoboken)* 2019;71:1019–27.
- Langen ES, Chakravarty EF, Liaquat M, El-Sayed YY, Druzin ML. High rate of preterm birth in pregnancies complicated by rheumatoid arthritis. *Am J Perinatol* 2014;31:9–13.
- Chakravarty EF, Nelson L, Krishnan E. Obstetric hospitalizations in the United States for women with systemic lupus erythematosus and rheumatoid arthritis. *Arthritis Rheum* 2006;54:899–907.
- Bharti B, Lee SJ, Lindsay SP, Wingard DL, Jones KL, Lemus H, et al. Disease severity and pregnancy outcomes in women with rheumatoid arthritis: results from the Organization of Teratology Information Specialists Autoimmune Diseases in Pregnancy Project. *J Rheumatol* 2015;42:1376–82.
- Borella E, Lojaco A, Gatto M, Andreoli L, Taglietti M, Iaccarino L, et al. Predictors of maternal and fetal complications in SLE patients: a prospective study. *Immunol Res* 2014;60:170–6.
- Ruiz-Irastorza G, Lima F, Alves J, Khamashta MA, Simpson J, Hughes GR, et al. Increased rate of lupus flare during pregnancy and the puerperium: a prospective study of 78 pregnancies. *Br J Rheumatol* 1996;35:133–8.
- Barrett JH, Brennan P, Fiddler M, Silman AJ. Does rheumatoid arthritis remit during pregnancy and relapse postpartum? Results from a nationwide study in the United Kingdom performed prospectively from late pregnancy. *Arthritis Rheum* 1999;42:1219–27.
- Section on Breastfeeding. Breastfeeding and the use of human milk. *Pediatrics* 2012;129:e827–41.
- Miyakis S, Lockshin MD, Atsumi T, Branch DW, Brey RL, Cervera R, et al. International consensus statement on an update of the classification criteria for definite antiphospholipid syndrome (APS). *J Thromb Haemost* 2006;4:295–306.
- Schwarz EB, Manzi S. Risk of unintended pregnancy among women with systemic lupus erythematosus. *Arthritis Rheum* 2008;59:863–6.
- Yazdany J, Trupin L, Kaiser R, Schmajuk G, Gillis JZ, Chakravarty E, et al. Contraceptive counseling and use among women with systemic lupus erythematosus: a gap in health care quality? *Arthritis Care Res (Hoboken)* 2011;63:358–65.
- Østensen M, von Esbeck M, Villiger PM. Therapy with immunosuppressive drugs and biological agents and use of contraception in patients with rheumatic disease. *J Rheumatol* 2007;34:1266–9.
- Allen D, Hunter MS, Wood S, Beeson T. One Key Question[®]: first things first in reproductive health. *Matern Child Health J* 2017;21:387–92.

15. Amy JJ, Tripathi V. Contraception for women: an evidence based overview. *BMJ* 2009;339:b2895.
16. Winner B, Peipert JF, Zhao Q, Buckel C, Madden T, Allsworth JE, et al. Effectiveness of long-acting reversible contraception. *N Engl J Med* 2012;366:1998–2007.
17. Committee on Gynecologic Practice Long-Acting Reversible Contraception Working Group. Committee opinion no. 642: increasing access to contraceptive implants and intrauterine devices to reduce unintended pregnancy. *Obstet Gynecol* 2015;126:e44–8.
18. Curtis KM, Tepper NK, Jatlaoui TC, Berry-Bibee E, Horton LG, Zapata LB, et al. U.S. medical eligibility criteria for contraceptive use, 2016. *MMWR Recomm Rep* 2016;65:1–103.
19. Petri M, Kim MY, Kalunian KC, Grossman J, Hahn BH, Sammaritano LR, et al. Combined oral contraceptives in women with systemic lupus erythematosus. *N Engl J Med* 2005;353:2550–8.
20. Sánchez-Guerrero J, Uribe AG, Jiménez-Santana L, Mestanza-Peralta M, Lara-Reyes P, Seuc AH, et al. A trial of contraceptive methods in women with systemic lupus erythematosus. *N Engl J Med* 2005;353:2539–49.
21. Julkunen HA, Kaaja R, Friman C. Contraceptive practice in women with systemic lupus erythematosus. *Br J Rheumatol* 1993;32:227–30.
22. Galzote RM, Rafie S, Teal R, Mody SK. Transdermal delivery of combined hormonal contraception: a review of the current literature. *Int J Womens Health* 2017;9:315–21.
23. Van den Heuvel MW, van Bragt AJ, Alnabawy AK, Kaptein MC. Comparison of ethinylestradiol pharmacokinetics in three hormonal contraceptive formulations: the vaginal ring, the transdermal patch and an oral contraceptive. *Contraception* 2005;72:168–74.
24. Stam-Slob MC, Lambalk CB, van de Ree MA. Contraceptive and hormonal treatment options for women with history of venous thromboembolism. *BMJ* 2015;351:h4847.
25. ACOG Committee on Practice Bulletins-Gynecology. ACOG practice bulletin no. 73: use of hormonal contraception in women with coexisting medical conditions. *Obstet Gynecol* 2006;107:1453–72.
26. World Health Organization Department of Reproductive Health. Medical eligibility criteria for contraceptive use. 5th ed. 2015.
27. Mantha S, Karp R, Raghavan V, Terrin N, Bauer KA, Zwicker JI. Assessing the risk of venous thromboembolic events in women taking progestin-only contraception: a meta-analysis. *BMJ* 2012;345:e4944.
28. Conard J, Plu-Bureau G, Bahi N, Horellou MH, Pellissier C, Thalabard JC. Progestogen-only contraception in women at high risk of venous thromboembolism. *Contraception* 2004;70:437–41.
29. Le Moigne E, Tromeur C, Delluc A, Gouillou M, Alavi Z, Lacut K, et al. Risk of recurrent venous thromboembolism on progestin-only contraception: a cohort study. *Haematologica* 2016;101:e12–4.
30. Pisoni CN, Cuadrado MJ, Khamashta MA, Hunt BJ. Treatment of menorrhagia associated with oral anticoagulation: efficacy and safety of the levonorgestrel releasing intrauterine device (Mirena coil). *Lupus* 2006;15:877–80.
31. Van Vlijmen EF, Veeger NJ, Middeldorp S, Hamulyák K, Prins MH, Büller HR, et al. Thrombotic risk during oral contraceptive use and pregnancy in women with factor V Leiden or prothrombin mutation: a rational approach to contraception. *Blood* 2011;118:2055–61.
32. Stringer EM, Kaseba C, Levy J, Sinkala M, Goldenberg RL, Chi BH, et al. A randomized trial of the intrauterine contraceptive device vs hormonal contraception in women who are infected with the human immunodeficiency virus. *Am J Obstet Gynecol* 2007;197:144.e1–8.
33. Krajewski CM, Geetha D, Gomez-Lobo V. Contraceptive options for women with a history of solid-organ transplantation. *Transplantation* 2013;95:1183–6.
34. Huguélet PS, Sheehan C, Spitzer RF, Scott S. Use of the levonorgestrel 52-mg intrauterine system in adolescent and young adult solid organ transplant recipients: a case series. *Contraception* 2017;95:378–81.
35. Clark M, Sowers M, Levy B, Nichols S. Bone mineral density loss and recovery during 48 months in first-time users of depot medroxyprogesterone acetate. *Fertil Steril* 2006;86:1466–74.
36. Welcome to the mycophenolate REMS (Risk Evaluation and Mitigation Strategy). URL: <https://www.mycophenolaterems.com/>.
37. Cellcept (mycophenolate mofetil) prescribing information. San Francisco (CA): 2019. Genentech; 2019. URL: gene.com/download/pdf/cellcept_prescribing.pdf.
38. Mycophenolate: updated recommendations for contraception for men and women. December 2017. URL: <https://www.ema.europa.eu/en/news/mycophenolate-updated-recommendations-contraception-men-women>.
39. Bellver J, Pellicer A. Ovarian stimulation for ovulation induction and in vitro fertilization in patients with systemic lupus erythematosus and antiphospholipid syndrome. *Fertil Steril* 2009;92:1803–10.
40. Huong DL, Wechsler B, Vauthier-Brouzes D, Duhaut P, Costedoat N, Lefebvre G, et al. Importance of planning ovulation induction therapy in systemic lupus erythematosus and antiphospholipid syndrome: a single center retrospective study of 21 cases and 114 cycles. *Semin Arthritis Rheum* 2002;32:174–88.
41. Orquevaux P, Masseau A, Le Guern V, Gayet V, Vauthier D, Guettrot-Imbert G, et al. In vitro fertilization in 37 women with systemic lupus erythematosus or antiphospholipid syndrome: a series of 97 procedures. *J Rheumatol* 2017;44:613–8.
42. Guballa N, Sammaritano L, Schwartzman S, Buyon J, Lockshin MD. Ovulation induction and in vitro fertilization in systemic lupus erythematosus and antiphospholipid syndrome. *Arthritis Rheum* 2000;43:550–6.
43. Chan WS, Dixon ME. The “ART” of thromboembolism: a review of assisted reproductive technology and thromboembolic complications. *Thromb Res* 2008;121:713–26.
44. Nelson SM, Greer IA. Artificial reproductive technology and the risk of venous thromboembolic disease. *J Thromb Haemost* 2006;4:1661–3.
45. Chan WS. The ‘ART’ of thrombosis: a review of arterial and venous thrombosis in assisted reproductive technology. *Curr Opin Obstet Gynecol* 2009;21:207–18.
46. Yinon Y, Pauzner R, Dulitzky M, Elizur SE, Dor J, Shulman A. Safety of IVF under anticoagulant therapy in patients at risk for thrombo-embolic events. *Reprod Biomed Online* 2006;12:354–8.
47. Nelson SM. Venous thrombosis during assisted reproduction: novel risk reduction strategies. *Thromb Res* 2013;131 Suppl 1:S1–3.
48. Mok CC, Lau CS, Wong RW. Risk factors for ovarian failure in patients with systemic lupus erythematosus receiving cyclophosphamide therapy. *Arthritis Rheum* 1998;41:831–7.
49. Tamirou F, Husson SN, Gruson D, Debiève F, Lauwerys BR, Houssiau FA. The Euro-Lupus low-dose intravenous cyclophosphamide regimen does not impact the ovarian reserve, as measured by serum levels of anti-Müllerian hormone. *Arthritis Rheumatol* 2017;69:1267–71.
50. Oktay K, Harvey BE, Partridge AH, Quinn GP, Reinecke J, Taylor HS, et al. Fertility preservation in patients with cancer: ASCO clinical practice guideline update. *J Clin Oncol* 2018;36:1994–2001.
51. Moore HC, Unger JM, Phillips KA, Boyle F, Hitre E, Porter D, et al. Goserelin for ovarian protection during breast-cancer adjuvant chemotherapy. *N Engl J Med* 2015;372:923–32.
52. Blumenfeld Z, Mischari O, Schultz N, Boulman N, Balbir-Gurman A. Gonadotropin releasing hormone agonists may minimize cyclophosphamide associated gonadotoxicity in SLE and autoimmune diseases. *Semin Arthritis Rheum* 2011;41:346–52.




53. Brunner HI, Silva CA, Reiff A, Higgins GC, Imundo L, Williams CB, et al. Randomized, double-blind, dose-escalation trial of triptorelin for ovary protection in childhood-onset systemic lupus erythematosus. *Arthritis Rheumatol* 2015;67:1377–85.
54. Koga T, Umeda M, Endo Y, Ishida M, Fujita Y, Tsuji S, et al. Effect of a gonadotropin-releasing hormone analog for ovarian function preservation after intravenous cyclophosphamide therapy in systemic lupus erythematosus patients: a retrospective inception cohort study. *Int J Rheum Dis* 2018;21:1287–92.
55. Pagnoux C, Le Guern V, Goffinet F, Diot E, Limal N, Pannier E, et al. Pregnancies in systemic necrotizing vasculitides: report on 12 women and their 20 pregnancies. *Rheumatology (Oxford)* 2011;50:953–61.
56. Somers EC, Marder W, Christman GM, Ognenovski V, McCune WJ. Use of a gonadotropin-releasing hormone analog for protection against premature ovarian failure during cyclophosphamide therapy in women with severe lupus. *Arthritis Rheum* 2005;52:2761–7.
57. Soares PM, Borba EF, Bonfa E, Hallak J, Corrêa AL, Silva CA. Gonad evaluation in male systemic lupus erythematosus. *Arthritis Rheum* 2007;56:2352–61.
58. Wyrobek AJ, Schmid TE, Marchetti F. Relative susceptibilities of male germ cells to genetic defects induced by cancer chemotherapies. *J Natl Cancer Inst Monogr* 2005;2005:31–5.
59. Stahl PJ, Stember DS, Hsiao W, Schlegel PN. Indications and strategies for fertility preservation in men. *Clin Obstet Gynecol* 2010;53:815–27.
60. ACOG Practice Bulletin no. 141: management of menopausal symptoms. *Obstet Gynecol* 2014;123:202–16.
61. The NAMS 2017 Hormone Therapy Position Statement Advisory Panel. The 2017 hormone therapy position statement of the North American Menopause Society. *Menopause* 2017;24:728–53.
62. U.S. Preventive Services Task Force. Hormone therapy for the prevention of chronic conditions in postmenopausal women: recommendations from the U.S. Preventive Services Task Force. *Ann Intern Med* 2005;142:855–60.
63. Beral V, Million Women Study Collaborators. Breast cancer and hormone-replacement therapy in the Million Women Study. *Lancet* 2003;362:419–27.
64. North American Menopause Society. The 2012 hormone therapy position statement of the North American Menopause Society. *Menopause* 2012;19:257–71.
65. Buyon JP, Petri MA, Kim MY, Kalunian KC, Grossman J, Hahn BH, et al. The effect of combined estrogen and progesterone hormone replacement therapy on disease activity in systemic lupus erythematosus: a randomized trial. *Ann Intern Med* 2005;142:953–62.
66. Mok CC, Lau CS, Ho CT, Lee KW, Mok MY, Wong RW. Safety of hormonal replacement therapy in postmenopausal patients with systemic lupus erythematosus. *Scand J Rheumatol* 1998;27:342–6.
67. Sánchez-Guerrero J, González-Pérez M, Durand-Carbajal M, Lara-Reyes P, Jiménez-Santana L, Romero-Díaz J, et al. Menopause hormonal therapy in women with systemic lupus erythematosus. *Arthritis Rheum* 2007;56:3070–9.
68. Kreidstein S, Urowitz MB, Gladman DD, Gough J. Hormone replacement therapy in systemic lupus erythematosus. *J Rheumatol* 1997;24:2149–52.
69. Marjoribanks J, Farquhar C, Roberts H, Lethaby A, Lee J. Long-term hormone therapy for perimenopausal and postmenopausal women. *Cochrane Database Syst Rev* 2017;1:CD004143.
70. Cushman M, Kuller LH, Prentice R, Rodabough RJ, Psaty BM, Stafford RS, et al. Estrogen plus progestin and risk of venous thrombosis. *JAMA* 2004;292:1573–80.
71. Canonico M, Oger E, Plu-Bureau G, Conard J, Meyer G, Lévesque H, et al, for the Estrogen and Thromboembolism Risk (ESTHER) Study Group. Hormone therapy and venous thromboembolism among postmenopausal women—impact of the route of estrogen administration and progestogens: the ESTHER study. *Circulation* 2007;20;115:840–5.
72. Sweetland S, Beral V, Balkwill A, Liu B, Benson VS, Canonico M, et al. Venous thromboembolism risk in relation to use of different types of postmenopausal hormone therapy in a large prospective study. *J Thromb Haemost* 2012;10:2277–86.
73. Smith NL, Heckbert SR, Lemaitre RN, Reiner AP, Lumley T, Weiss NS, et al. Esterified estrogens and conjugated equine estrogens and the risk of venous thrombosis. *JAMA* 2004;292:1581–7.
74. Rovinski D, Ramos RB, Figuera TM, Casanova GK, Spritzer PM. Risk of venous thromboembolism events in postmenopausal women using oral versus non-oral hormone therapy: a systematic review and meta-analysis. *Thromb Res* 2018;168:83–95.
75. Straczek C, Oger E, Yon de Jonage-Canonico MB, Plu-Bureau G, Conard J, Meyer G, et al, for the Estrogen and Thromboembolism Risk (ESTHER) Study Group. Prothrombotic mutations, hormone therapy, and venous thromboembolism among postmenopausal women: impact of the route of estrogen administration. *Circulation* 2005;112:3495–500.
76. Rosendaal FR, Vessey M, Rumley A, Daly E, Woodward M, Helmerhorst FM, et al. Hormonal replacement therapy, prothrombotic mutations and the risk of venous thrombosis. *Br J Haematol* 2002;116:851–4.
77. Canonico M, Plu-Bureau G, Lowe GD, Scarabin PY. Hormone replacement therapy and risk of venous thromboembolism in postmenopausal women: systematic review and meta-analysis. *BMJ* 2008;336:1227–31.
78. Cravioto MD, Durand-Carbajal M, Jiménez-Santana L, Lara-Reyes P, Seuc AH, Sánchez-Guerrero J. Efficacy of estrogen plus progestin on menopausal symptoms in women with systemic lupus erythematosus: a randomized, double-blind, controlled trial. *Arthritis Care Res (Hoboken)* 2011;63:1654–63.
79. Gupta R, Deepanjali S, Kumar A, Dadhwal V, Agarwal SK, Pandey RM, et al. A comparative study of pregnancy outcomes and menstrual irregularities in northern Indian patients with systemic lupus erythematosus and rheumatoid arthritis. *Rheumatol Int* 2010;30:1581–5.
80. Lockshin MD. Pregnancy does not cause systemic lupus erythematosus to worsen. *Arthritis Rheum* 1989;32:665–70.
81. Le Thi Huong D, Wechsler B, Piette JC, Bletry O, Godeau P. Pregnancy and its outcome in systemic lupus erythematosus. *QJM* 1994;87:721–9.
82. Hussein Aly EA, Mohamed Riyad R, Nabil Mokbel A. Pregnancy outcome in patients with systemic lupus erythematosus: a single center study in the High Risk Pregnancy unit. *Middle East Fertil Soc J* 2016;21:168–74.
83. Mintz G, Niz J, Gutierrez G, Garcia-Alonso A, Karchmer S. Prospective study of pregnancy in systemic lupus erythematosus: results of a multidisciplinary approach. *J Rheumatol* 1986;13:732–9.
84. Mokbel A, Geilan AM, AboElgeith S. Could women with systemic lupus erythematosus (SLE) have successful pregnancy outcomes? Prospective observational study. *Egypt Rheumatologist* 2013;35:133–9.
85. Mankee A, Petri M, Magder LS. Lupus anticoagulant, disease activity and low complement in the first trimester are predictive of pregnancy loss. *Lupus Sci Med* 2015;2:e000095.
86. Tuin J, Sanders JS, de Joode AA, Stegeman CA. Pregnancy in women diagnosed with antineutrophil cytoplasmic antibody-associated vasculitis: outcome for the mother and the child. *Arthritis Care Res (Hoboken)* 2012;64:539–45.

87. Whitelaw DA, Hall D, Kotze T. Pregnancy in systemic lupus erythematosus: a retrospective study from a developing community. *Clin Rheumatol* 2008;27:577–80.
88. Croft AP, Smith SW, Carr S, Youssouf S, Salama AD, Burns A, et al. Successful outcome of pregnancy in patients with anti-neutrophil cytoplasm antibody-associated small vessel vasculitis. *Kidney Int* 2015;87:807–11.
89. Tozman EC, Urowitz MB, Gladman DD. Systemic lupus erythematosus and pregnancy. *J Rheumatol* 1980;7:624–32.
90. Ku M, Guo S, Shang W, Li Q, Zeng R, Han M, et al. Pregnancy outcomes in Chinese patients with systemic lupus erythematosus (SLE): a retrospective study of 109 pregnancies. *PLoS One* 2016;11:e0159364.
91. Kothari R, Digole A, Kamat S, Nandanwar YS, Gokhale Y. Reproductive health in systemic lupus erythematosus, an experience from government hospital in western India. *J Assoc Physicians India* 2016;64:16–20.
92. Skorpen CG, Lydersen S, Gilboe IM, Skomsvoll JF, Salvesen KÅ, Palm Ø, et al. Influence of disease activity and medications on offspring birth weight, pre-eclampsia and preterm birth in systemic lupus erythematosus: a population-based study. *Ann Rheum Dis* 2018;77:264–9.
93. Phansenee S, Sekararithi R, Jatavan P, Tongsong T. Pregnancy outcomes among women with systemic lupus erythematosus: a retrospective cohort study from Thailand. *Lupus* 2018;27:158–64.
94. Rahman FZ, Rahman J, Al-Suleiman SA, Rahman MS. Pregnancy outcome in lupus nephropathy. *Arch Gynecol Obstet* 2005;271:222–6.
95. Bobrie G, Liote F, Houillier P, Grünfeld JP, Jungers P. Pregnancy in lupus nephritis and related disorders. *Am J Kidney Dis* 1987;9:339–43.
96. Jungers P, Dougados M, Pélissier C, Kuttenn F, Tron F, Lesavre P, et al. Lupus nephropathy and pregnancy: report of 104 cases in 36 patients. *Arch Intern Med* 1982;142:771–6.
97. Gaballa HA, El-Shahawy EE, Atta DS, Gerbash EF. Clinical and serological risk factors of systemic lupus erythematosus outcomes during pregnancy. *Egypt Rheumatologist* 2012;34:159–65.
98. Tedeschi SK, Massarotti E, Guan H, Fine A, Bermas BL, Costenbader KH. Specific systemic lupus erythematosus disease manifestations in the six months prior to conception are associated with similar disease manifestations during pregnancy. *Lupus* 2015;24:1283–92.
99. Palmsten K, Rolland M, Hebert MF, Clowse ME, Schatz M, Xu R, et al. Patterns of prednisone use during pregnancy in women with rheumatoid arthritis: daily and cumulative dose. *Pharmacoepidemiol Drug Saf* 2018;27:430–8.
100. Zanatta E, Polito P, Favaro M, Larosa M, Marson P, Cozzi F, et al. Therapy of scleroderma renal crisis: state of the art. *Autoimmun Rev* 2018;17:882–9.
101. Bullo M, Tschumi S, Bucher BS, Bianchetti MG, Simonetti GD. Pregnancy outcome following exposure to angiotensin-converting enzyme inhibitors or angiotensin receptor antagonists: a systematic review. *Hypertension* 2012;60:444–50.
102. Liu EL, Liu Z, Zhou YX. Feasibility of hydroxychloroquine adjuvant therapy in pregnant women with systemic lupus erythematosus. *Biomed Res* 2018;29:980–3.
103. Leroux M, Desveaux C, Parcevaux M, Julliac B, Gouyon JB, Dalley D, et al. Impact of hydroxychloroquine on preterm delivery and intrauterine growth restriction in pregnant women with systemic lupus erythematosus: a descriptive cohort study. *Lupus* 2015;24:1384–91.
104. Eudy AM, Siega-Riz AM, Engel SM, Franceschini N, Howard AG, Clowse ME, et al. Effect of pregnancy on disease flares in patients with systemic lupus erythematosus. *Ann Rheum Dis* 2018;77:855–60.
105. Clowse ME, Magder L, Witter F, Petri M. Hydroxychloroquine in lupus pregnancy. *Arthritis Rheum* 2006;54:3640–7.
106. Diav-Citrin O, Blyakhman S, Shechtman S, Ornoy A. Pregnancy outcome following in utero exposure to hydroxychloroquine: a prospective comparative observational study. *Reprod Toxicol* 2013;39:58–62.
107. Hwang JK, Park HK, Sung YK, Hoh JK, Lee HJ. Maternal outcomes and follow-up of preterm and term neonates born to mothers with systemic lupus erythematosus. *J Matern Fetal Neonatal Med* 2018;31:7–13.
108. Kroese SJ, de Hair MJ, Limper M, Lely AT, van Laar JM, Derksen RH, et al. Hydroxychloroquine use in lupus patients during pregnancy is associated with longer pregnancy duration in preterm births. *J Immunol Res* 2017;2017:2810202.
109. Georgiou PE, Politi EN, Katsimbri P, Sakka V, Drosos AA. Outcome of lupus pregnancy: a controlled study. *Rheumatology (Oxford)* 2000;39:1014–9.
110. Teh CL, Wong JS, Ngeh NK, Loh WL. Systemic lupus erythematosus pregnancies: a case series from a tertiary, East Malaysian hospital. *Lupus* 2009;18:278–82.
111. Ruffatti A, Tonello M, Hoxha A, Sciascia S, Cuadrado M, Latino JO, et al. Effect of additional treatments combined with conventional therapies in pregnant patients with high-risk antiphospholipid syndrome: a multicentre study. *Thromb Haemost* 2018;118:639–46.
112. ACOG committee opinion no. 743: low-dose aspirin use during pregnancy. *Obstet Gynecol* 2018;132:e44–52.
113. LeFevre ML, US Preventive Services Task Force. Low-dose aspirin use for the prevention of morbidity and mortality from preeclampsia: U.S. Preventive Services Task Force recommendation statement. *Ann Intern Med* 2014;161:819–26.
114. Buyon JP, Kim MY, Guerra MM, Laskin CA, Petri M, Lockshin MD, et al. Predictors of pregnancy outcomes in patients with lupus: a cohort study. *Ann Intern Med* 2015;163:153–63.
115. Abheiden CN, Blomjous BS, Kroese SJ, Bultink IE, Fritsch-Stork RD, Lely AT, et al. Low-molecular-weight heparin and aspirin use in relation to pregnancy outcome in women with systemic lupus erythematosus and antiphospholipid syndrome: a cohort study. *Hypertens Pregnancy* 2017;36:8–15.
116. Moroni G, Doria A, Giglio E, Imbasciati E, Tani C, Zen M, et al. Maternal outcome in pregnant women with lupus nephritis: a prospective multicenter study. *J Autoimmun* 2016;74:194–200.
117. Imbasciati E, Tincani A, Gregorini G, Doria A, Moroni G, Cabiddu G, et al. Pregnancy in women with pre-existing lupus nephritis: predictors of fetal and maternal outcome. *Nephrol Dial Transplant* 2009;24:519–25.
118. Lockshin MD, Kim M, Laskin CA, Guerra M, Branch DW, Merrill J, et al. Prediction of adverse pregnancy outcome by the presence of lupus anticoagulant, but not anticardiolipin antibody, in patients with antiphospholipid antibodies. *Arthritis Rheum* 2012;64: 2311–8.
119. Bao SH, Sheng SL, Liao H, Zhou Q, Frempong ST, Tu WY. Use of D-dimer measurement to guide anticoagulant treatment in recurrent pregnancy loss associated with antiphospholipid syndrome. *Am J Reprod Immunol* 2017;78:e12770.
120. Farquharson RG, Quenby S, Greaves M. Antiphospholipid syndrome in pregnancy: a randomized, controlled trial of treatment. *Obstet Gynecol* 2002;100:408–13.
121. Van Hoorn ME, Hague WM, van Pampus MG, Bezemer D, de Vries JI, for the FRUIT investigators. Low-molecular-weight heparin and aspirin in the prevention of recurrent early-onset pre-eclampsia in women with antiphospholipid antibodies: the FRUIT-RCT. *Eur J Obstet Gynecol Reprod Biol* 2016;197:168–73.
122. Naru T, Khan RS, Ali R. Pregnancy outcome in women with antiphospholipid syndrome on low-dose aspirin and heparin: a retrospective study. *East Mediterr Health J* 2010;16:308–12.

123. Goel N, Tuli A, Choudhry R. The role of aspirin versus aspirin and heparin in cases of recurrent abortions with raised anticardiolipin antibodies. *Med Sci Monit* 2006;12:CR132–6.
124. Brewster JA, Shaw NJ, Farquharson RG. Neonatal and pediatric outcome of infants born to mothers with antiphospholipid syndrome. *J Perinat Med* 1999;27:183–7.
125. Cohn DM, Goddijn M, Middeldorp S, Korevaar JC, Dawood F, Farquharson RG. Recurrent miscarriage and antiphospholipid antibodies: prognosis of subsequent pregnancy. *J Thromb Haemost* 2010;8:2208–13.
126. Clark CA, Spitzer KA, Crowther MA, Nadler JN, Laskin MD, Waks JA, et al. Incidence of postpartum thrombosis and preterm delivery in women with antiphospholipid antibodies and recurrent pregnancy loss. *J Rheumatol* 2007;34:992–6.
127. ACOG practice bulletin no. 196: thromboembolism in pregnancy. *Obstet Gynecol* 2018;132:e1–17.
128. Brito-Zerón P, Izmirly PM, Ramos-Casals M, Buyon JP, Khamashta MA. The clinical spectrum of autoimmune congenital heart block. *Nat Rev Rheumatol* 2015;11:301–12.
129. Wahren-Herlenius M, Sonesson SE, Clowse ME. Neonatal lupus erythematosus. In: Wallace D, Hahn B, editors. *Dubois' lupus erythematosus and related syndromes*. 8th ed. Philadelphia: Saunders; 2012. p. 464–72.
130. Izmirly PM, Rivera TL, Buyon JP. Neonatal lupus syndromes. *Rheum Dis Clin North Am* 2007;33:267–85.
131. Kan N, Silverman ED, Kingdom J, Dutil N, Laskin C, Jaeggi E. Serial echocardiography for immune-mediated heart disease in the fetus: results of a risk-based prospective surveillance strategy. *Prenat Diagn* 2017;37:375–82.
132. Izmirly PM, Costedoat-Chalumeau N, Pisoni CN, Khamashta MA, Kim MY, Saxena A, et al. Maternal use of hydroxychloroquine is associated with a reduced risk of recurrent anti-SSA/Ro-antibody-associated cardiac manifestations of neonatal lupus. *Circulation* 2012;126:76–82.
133. Cuneo BF, Lee M, Roberson D, Niksch A, Ovidia M, Parilla BV, et al. A management strategy for fetal immune-mediated atrioventricular block. *J Matern Fetal Neonatal Med* 2010;23:1400–5.
134. Friedman DM, Kim MY, Copel JA, Llanos C, Davis C, Buyon JP. Prospective evaluation of fetuses with autoimmune-associated congenital heart block followed in the PR Interval and Dexamethasone Evaluation (PRIDE) study. *Am J Cardiol* 2009;103:1102–6.
135. Izmirly PM, Saxena A, Sahl SK, Shah U, Friedman DM, Kim MY, et al. Assessment of fluorinated steroids to avert progression and mortality in anti-SSA/Ro-associated cardiac injury limited to the fetal conduction system. *Ann Rheum Dis* 2016;75:1161–5.
136. Colie CF. Male mediated teratogenesis. *Reprod Toxicol* 1993;7:3–9.
137. Anderson D, Bishop JB, Garner RC, Ostrosky-Wegman P, Selby PB. Cyclophosphamide: review of its mutagenicity for an assessment of potential germ cell risks. *Mutat Res* 1995;330:115–81.
138. Brandenburg NA, Bwire R, Freeman J, Houn F, Sheehan P, Zeldis JB. Effectiveness of risk evaluation and mitigation strategies (REMS) for lenalidomide and thalidomide: patient comprehension and knowledge retention. *Drug Saf* 2017;40:333–41.
139. Teo SK, Harden JL, Burke AB, Noormohamed FH, Youle M, Johnson MA, et al. Thalidomide is distributed into human semen after oral dosing. *Drug Metab Dispos* 2001;29:1355–7.
140. Larsen MD, Friedman S, Magnussen B, Nørgård BM. Birth outcomes in children fathered by men treated with anti-TNF- α agents before conception. *Am J Gastroenterol* 2016;111:1608–13.
141. Nørgård BM, Magnussen B, Larsen MD, Friedman S. Reassuring results on birth outcomes in children fathered by men treated with azathioprine/6-mercaptopurine within 3 months before conception: a nationwide cohort study. *Gut* 2017;66:1761–6.
142. Ben-Chetrit E, Berkun Y, Ben-Chetrit E, Ben-Chetrit A. The outcome of pregnancy in the wives of men with familial Mediterranean fever treated with colchicine. *Semin Arthritis Rheum* 2004;34:549–52.
143. Weber-Schoendorfer C, Hoeltzenbein M, Wacker E, Meister R, Schaefer C. No evidence for an increased risk of adverse pregnancy outcome after paternal low-dose methotrexate: an observational cohort study. *Rheumatology (Oxford)* 2014;53:757–63.
144. Eck LK, Jensen TB, Mastrogiannis D, Torp-Pedersen A, Askaa B, Nielsen TK, et al. Risk of adverse pregnancy outcome after paternal exposure to methotrexate within 90 days before pregnancy. *Obstet Gynecol* 2017;129:707–14.
145. Winter RW, Larsen MD, Magnussen B, Friedman S, Kammerlander H, Nørgård BM. Birth outcomes after preconception paternal exposure to methotrexate: a nationwide cohort study. *Reprod Toxicol* 2017;74:219–23.
146. Wallenius M, Lie E, Daltveit AK, Salvesen KÅ, Skomsvoll JF, Kalstad S, et al. No excess risks in offspring with paternal preconception exposure to disease-modifying antirheumatic drugs. *Arthritis Rheumatol* 2015;67:296–301.
147. Kieseier BC, Benamor M. Pregnancy outcomes following maternal and paternal exposure to teriflunomide during treatment for relapsing-remitting multiple sclerosis. *Neurol Ther* 2014;3:133–8.
148. Midtvedt K, Bergan S, Reisaeter AV, Vikse BE, Åsberg A. Exposure to mycophenolate and fatherhood. *Transplantation* 2017;101:e214–7.
149. Jones A, Clary MJ, McDermott E, Coscia LA, Constantinescu S, Moritz MJ, et al. Outcomes of pregnancies fathered by solid-organ transplant recipients exposed to mycophenolic acid products. *Prog Transplant* 2013;23:153–7.
150. Sands K, Jansen R, Zaslau S, Greenwald D. The safety of therapeutic drugs in male inflammatory bowel disease patients wishing to conceive [review]. *Aliment Pharmacol Ther* 2015;41:821–34.
151. Youngstein T, Hoffmann P, Gül A, Lane T, Williams R, Rowczenio DM, et al. International multi-centre study of pregnancy outcomes with interleukin-1 inhibitors. *Rheumatology (Oxford)* 2017;56:2102–8.
152. Ciron J, Audoin B, Bourre B, Brassat D, Durand-Dubief F, Laplaud D, et al. Recommendations for the use of rituximab in neuromyelitis optica spectrum disorders. *Rev Neurol (Paris)* 2018;174:255–64.
153. Feldkamp M, Carey JC. Clinical teratology counseling and consultation case report: low dose methotrexate exposure in the early weeks of pregnancy. *Teratology* 1993;47:533–9.
154. Kainz A, Harabacz I, Cowlick IS, Gadgil SD, Hagiwara D. Review of the course and outcome of 100 pregnancies in 84 women treated with tacrolimus. *Transplantation* 2000;70:1718–21.
155. Sifontis NM, Coscia LA, Constantinescu S, Lavelanet AF, Moritz MJ, Armenti VT. Pregnancy outcomes in solid organ transplant recipients with exposure to mycophenolate mofetil or sirolimus. *Transplantation* 2006;82:1698–702.
156. Vargesson N. Thalidomide-induced teratogenesis: history and mechanisms. *Birth Defects Res C Embryo Today* 2015;105:140–56.
157. Bérard A, Zhao JP, Shui I, Colilla S. Leflunomide use during pregnancy and the risk of adverse pregnancy outcomes. *Ann Rheum Dis* 2018;77:500–9.
158. Weber-Schoendorfer C, Beck E, Tissen-Diabaté T, Schaefer C. Leflunomide—a human teratogen? A still not answered question: an evaluation of the German Embryotox pharmacovigilance database. *Reprod Toxicol* 2017;71:101–7.
159. Connell W, Miller A. Treating inflammatory bowel disease during pregnancy: risks and safety of drug therapy. *Drug Saf* 1999;21:311–23.
160. Indraratna PL, Virk S, Gurram D, Day RO. Use of colchicine in pregnancy: a systematic review and meta-analysis. *Rheumatology (Oxford)* 2018;57:382–7.

161. Saavedra MÁ, Sánchez A, Morales S, Ángeles U, Jara LJ. Azathioprine during pregnancy in systemic lupus erythematosus patients is not associated with poor fetal outcome. *Clin Rheumatol* 2015;34:1211–6.
162. Brouwer J, Hazes JM, Laven JS, Dolhain RJ. Fertility in women with rheumatoid arthritis: influence of disease activity and medication. *Ann Rheum Dis* 2015;74:1836–41.
163. Koren G, Florescu A, Costei AM, Boskovic R, Moretti ME. Non-steroidal antiinflammatory drugs during third trimester and the risk of premature closure of the ductus arteriosus: a meta-analysis. *Ann Pharmacother* 2006;40:824–9.
164. Bröms G, Granath F, Ekblom A, Hellgren K, Pedersen L, Sørensen HT, et al. Low risk of birth defects for infants whose mothers are treated with anti-tumor necrosis factor agents during pregnancy. *Clin Gastroenterol Hepatol* 2016;14:234–41.
165. Diav-Citrin O, Otcheretianski-Volodarsky A, Shechtman S, Ornoy A. Pregnancy outcome following gestational exposure to TNF- α inhibitors: a prospective, comparative, observational study. *Reprod Toxicol* 2014;43:78–84.
166. Mariette X, Förger F, Abraham B, Flynn AD, Moltó A, Flipo RM, et al. Lack of placental transfer of certolizumab pegol during pregnancy: results from CRIB, a prospective, postmarketing, pharmacokinetic study. *Ann Rheum Dis* 2018;77:228–33.
167. Kane SV, Acquah LA. Placental transport of immunoglobulins: a clinical review for gastroenterologists who prescribe therapeutic monoclonal antibodies to women during conception and pregnancy. *Am J Gastroenterol* 2009;104:228–33.
168. Chakravarty EF, Murray ER, Kelman A, Farmer P. Pregnancy outcomes after maternal exposure to rituximab. *Blood* 2011;117:1499–506.
169. Sheard NF, Walker WA. The role of breast milk in the development of the gastrointestinal tract. *Nutr Rev* 1988;46:1–8.
170. Hanson LA, Ahlstedt S, Andersson B, Carlsson B, Fällström SP, Mellander L, et al. Protective factors in milk and the development of the immune system. *Pediatrics* 1985;75:172–6.
171. Ladomenou F, Moschandreas J, Kafatos A, Tselentis Y, Galanakis E. Protective effect of exclusive breastfeeding against infections during infancy: a prospective study. *Arch Dis Child* 2010;95:1004–8.
172. Armstrong J, Reilly JJ. The prevalence of obesity and undernutrition in Scottish children: growth monitoring within the Child Health Surveillance Programme. *Scott Med J* 2003;48:32–7.
173. Davis MK, Savitz DA, Graubard BI. Infant feeding and childhood cancer. *Lancet* 1988;2:365–8.
174. Horta BL, Loret de Mola C, Victora CG. Long-term consequences of breastfeeding on cholesterol, obesity, systolic blood pressure and type 2 diabetes: a systematic review and meta-analysis [review]. *Acta Paediatr* 2015;104:30–7.
175. Schwarz EB, Ray RM, Stuebe AM, Allison MA, Ness RB, Freiberg MS, et al. Duration of lactation and risk factors for maternal cardiovascular disease. *Obstet Gynecol* 2009;113:974–82.
176. Newton ER, Hale TW. Drugs in breast milk. *Clin Obstet Gynecol* 2015;58:868–84.
177. Motta M, Tincani A, Faden D, Zinzini E, Lojaco A, Marchesi A, et al. Follow-up of infants exposed to hydroxychloroquine given to mothers during pregnancy and lactation. *J Perinatol* 2005;25:86–9.
178. Ben-Chetrit E, Scherrmann JM, Levy M. Colchicine in breast milk of patients with familial Mediterranean fever. *Arthritis Rheum* 1996;39:1213–7.
179. Bragnes Y, Boshuizen R, de Vries A, Lexberg Å, Østensen M. Low level of rituximab in human breast milk in a patient treated during lactation [letter]. *Rheumatology (Oxford)* 2017;56:1047–8.
180. Berlin CM Jr, Yaffe SJ. Disposition of salicylazosulfapyridine (Azulfidine) and metabolites in human breast milk. *Dev Pharmacol Ther* 1980;1:31–9.
181. Fritzsche J, Pilch A, Mury D, Schaefer C, Weber-Schoendorfer C. Infliximab and adalimumab use during breastfeeding [letter]. *J Clin Gastroenterol* 2012;46:718–9.
182. Gardiner SJ, Geary RB, Roberts RL, Zhang M, Barclay ML, Begg EJ. Comment: breast-feeding during maternal use of azathioprine. *Ann Pharmacother* 2007;41:719–20.
183. Bramham K, Chusney G, Lee J, Lightstone L, Nelson-Piercy C. Breastfeeding and tacrolimus: serial monitoring in breast-fed and bottle-fed infants. *Clin J Am Soc Nephrol* 2013;8:563–7.
184. Matro R, Martin CF, Wolf D, Shah SA, Mahadevan U. Exposure concentrations of infants breastfed by women receiving biologic therapies for inflammatory bowel diseases and effects of breastfeeding on infections and development. *Gastroenterology* 2018;155:696–704.
185. American Academy of Pediatrics Committee on Drugs. Transfer of drugs and other chemicals into human milk. *Pediatrics* 2001;108:776–89.
186. Johns DG, Rutherford LD, Leighton PC, Vogel CL. Secretion of methotrexate into human milk. *Am J Obstet Gynecol* 1972;112:978–80.
187. Andreoli L, Bertsias GK, Agmon-Levin N, Brown S, Cervera R, Costedoat-Chalumeau N, et al. EULAR recommendations for women's health and the management of family planning, assisted reproduction, pregnancy and menopause in patients with systemic lupus erythematosus and/or antiphospholipid syndrome. *Ann Rheum Dis* 2017;76:476–85.
188. Flint J, Panchal S, Hurrell A, van de Venne M, Gayed M, Schreiber K, et al. BSR and BHPR guideline on prescribing drugs in pregnancy and breastfeeding—part I: Standard and biologic disease modifying anti-rheumatic drugs and corticosteroids. *Rheumatology (Oxford)* 2016;55:1693–7.
189. Flint J, Panchal S, Hurrell A, van de Venne M, Gayed M, Schreiber K, et al. BSR and BHPR guideline on prescribing drugs in pregnancy and breastfeeding—part II: analgesics and other drugs used in rheumatology practice. *Rheumatology (Oxford)* 2016;55:1698–702.
190. Götestam Skorpen C, Hoeltzenbein M, Tincani A, Fischer-Betz R, Elefant E, Chambers C, et al. The EULAR points to consider for use of antirheumatic drugs before pregnancy, and during pregnancy and lactation. *Ann Rheum Dis* 2016;75:795–810.
191. Meng ML, Landau R, Viktorsdottir O, Banayan J, Grant T, Bateman B, et al. Pulmonary hypertension in pregnancy: a report of 49 cases at four tertiary North American sites. *Obstet Gynecol* 2017;129:511–20.
192. Sangle SR, Vounotrypidis P, Briley A, Nel L, Lutalo PM, Sanchez-Fernandez S, et al. Pregnancy outcome in patients with systemic vasculitis: a single-centre matched case-control study. *Rheumatology (Oxford)* 2015;54:1582–6.
193. Ritchie J, Smyth A, Tower C, Helbert M, Venning M, Garovic V. Maternal deaths in women with lupus nephritis: a review of published evidence. *Lupus* 2012;21:534–41.
194. El-Sayed YY, Lu EJ, Genovese MC, Lambert RE, Chitkara U, Druzin ML. Central nervous system lupus and pregnancy: 11-year experience at a single center. *J Matern Fetal Neonatal Med* 2002;12:99–103.
195. Society for Maternal-Fetal Medicine (SMFM). Executive summary: Reproductive Services for Women at High Risk for Maternal Mortality Workshop, February 11–12, 2019, Las Vegas, Nevada. *Am J Obstet Gynecol* 2019;221:B2–5.
196. Finer LB, Zolna MR. Declines in unintended pregnancy in the United States, 2008–2011. *N Engl J Med* 2016;374:843–52.
197. Practice Committees of American Society for Reproductive Medicine, Society for Assisted Reproductive Technology. Mature oocyte cryopreservation: a guideline. *Fertil Steril* 2013;99:37–43.

Rheumatoid Arthritis Morning Stiffness Is Associated With Synovial Fibrin and Neutrophils

Dana E. Orange,¹  Nathalie E. Blachere,² Edward F. DiCarlo,³ Serene Mirza,³ Tania Pannellini,³ Caroline S. Jiang,⁴ Mayu O. Frank,² Salina Parveen,² Mark P. Figgie,³ Ellen M. Gravallese,⁵ Vivian P. Bykerk,³ Ana-Maria Orbai,⁶  Sarah L. Mackie,⁷ and Susan M. Goodman³ 

Objective. Morning stiffness is a hallmark symptom of rheumatoid arthritis (RA), but its etiology is poorly understood. This study was undertaken to determine whether any histologic features of synovium are associated with this symptom.

Methods. Data on patient-reported morning stiffness duration and severity, and Disease Activity Score in 28 joints (DAS28) were collected from 176 patients with RA undergoing arthroplasty. Synovium was scored for 10 histopathologic features: synovial lining hyperplasia, lymphocytes, plasma cells, Russell bodies, binucleate plasma cells, fibrin, synovial giant cells, detritus, neutrophils, and mucin. Fibrinolysis of clots seeded with various cell types was measured in turbidimetric lysis assays.

Results. Stiffness severity and morning stiffness duration were both significantly associated with DAS28 ($P = 0.0001$ and $P = 0.001$, respectively). None of the synovial features examined were associated with patient-reported stiffness severity. The presence of neutrophils and fibrin in RA synovial tissue were significantly associated ($P < 0.0001$) with patient-reported morning stiffness of ≥ 1 hour, such that 73% of patients with both synovial fibrin and neutrophils reported morning stiffness of ≥ 1 hour. Further, neutrophils and fibrin deposits colocalized along the synovial lining. In *in vitro* analyses, fibrin clots seeded with necrotic neutrophils were more resistant to fibrinolysis than those seeded with living neutrophils or no cells ($P = 0.008$). DNase I treatment of necrotic neutrophils abrogated the delay in fibrinolysis.

Conclusion. In RA, prolonged morning stiffness may be related to impaired fibrinolysis of neutrophil-enmeshed fibrin deposits along the synovial membrane. Our findings also suggest that morning stiffness severity and duration may reflect distinct pathophysiologic phenomena.

INTRODUCTION

Rheumatoid arthritis (RA) is characterized by symptoms of joint swelling, pain, and stiffness in the morning (1), which improves as the day progresses. Morning stiffness interferes with activities

of daily living such as bathing and dressing, making it difficult for RA patients to get to work on time, and is therefore the most commonly cited reason for early retirement (2,3). Morning stiffness lasting more than 1 hour was one of the 1987 American College of Rheumatology classification criteria for RA (4). This symptom

The views expressed are those of the authors and not necessarily those of the NIH or the UK Department of Health and Social Care.

Supported by the NIH (National Center for Advancing Translational Sciences grant UL1-TR-001866, Clinical Translational Science Center Award grant UL1-TR000457-06, National Institute of Arthritis and Musculoskeletal and Skin Diseases grant P30-AR-07054, and Accelerating Medicines Partnership Program grants 1-UH2-AR-06769 and 11652401), and the Block Family Foundation.

¹Dana E. Orange, MD, MS: Hospital for Special Surgery, Howard Hughes Medical Institute, and The Rockefeller University, New York, New York; ²Nathalie E. Blachere, PhD, Mayu O. Frank, NP, PhD, Salina Parveen, MA: Howard Hughes Medical Institute and The Rockefeller University, New York, New York; ³Edward F. DiCarlo, MD, Serene Mirza, BS, Tania Pannellini, MD, PhD, Mark P. Figgie, MD, Vivian P. Bykerk, MD, Susan M. Goodman, MD: Hospital for Special Surgery, New York, New York; ⁴Caroline S. Jiang, MS: Rockefeller University Hospital, New York, New York; ⁵Ellen M. Gravallese, MD: University of Massachusetts Memorial Medical Center, Worcester; ⁶Ana-Maria Orbai, MD, MHS: Johns Hopkins Medicine,

Baltimore, Maryland; ⁷Sarah L. Mackie, BMBCh: University of Leeds, Leeds NIHR Biomedical Research Centre, and Leeds Teaching Hospitals NHS Trust, Leeds, UK.

Dr. DiCarlo has received consulting fees from Wright Medical Technology (less than \$10,000). Dr. Bykerk has received consulting fees from Bristol-Myers Squibb, Gilead Sciences, UCB, and Sanofi (less than \$10,000 each). Dr. Orbai has received consulting fees from AbbVie, Celgene, Horizon Pharma, Janssen, Eli Lilly, Novartis, Pfizer, and UCB (less than \$10,000 each). Dr. Mackie has received consulting fees from Roche (less than \$10,000) and research support from the NIH, Vasculitis UK, and Sanofi. Dr. Goodman has received consulting fees from Novartis, UCB, and Pfizer (less than \$10,000 each), and research support from Novartis. No other disclosures relevant to this article were reported.

Address correspondence to Dana E. Orange, MD, MS, The Rockefeller University, 1230 York Avenue, New York, NY 10065. E-mail: dorange@rockefeller.edu.

Submitted for publication April 1, 2019; accepted in revised form October 11, 2019.

was removed from the classification criteria update in 2010 (1), in part due to reports noting the lack of specificity for RA, as well as conflicting reports of its association with disease activity (5–8). Though morning stiffness is no longer included in the classification criteria, the symptom is important to patients (9) and is still routinely used by clinical rheumatologists to distinguish inflammatory arthritis from degenerative arthritis. If prolonged morning stiffness is a characteristic of inflammatory arthritis, synovial inflammation might be increased in patients who report morning stiffness. However, histologic descriptions of synovial pathology from RA patients with and without morning stiffness are lacking. We hypothesized that inflammatory features of RA synovium may be associated with morning stiffness, and we reasoned that a more granular understanding of which synovial features correlate with this symptom might provide insights into the mechanism underlying this problem.

We recently demonstrated that 10 synovial features, identified by histologic analysis of hematoxylin and eosin (H&E)-stained synovial tissue sections, can be used to predict inflammatory gene expression subtypes (10). These include scores of cellular and other histologic features, such as synovial lining hyperplasia, lymphocytes, plasma cells, Russell bodies, binucleate plasma cells, synovial giant cells, detritus, mucin, fibrin, and neutrophils. Here, we report our analysis of histologic features and patient-reported morning stiffness in a cohort of 176 RA patients undergoing arthroplasty. We discovered that synovial fibrin and neutrophils correlated with duration of morning stiffness. We also found that neutrophils could be detected within fibrin clots along the lining of the synovial membrane and embedded in synovial fluid rice bodies. Based on this observation, we performed *in vitro* coagulation and lysis assays and found that clots containing necrotic neutrophils were resistant to plasmin-mediated fibrinolysis and that this effect could be abrogated by treatment with DNase I. Taken together, our results demonstrate that neutrophil-laden fibrin deposits are present in RA synovium and are associated with prolonged morning stiffness in patients with RA.

PATIENTS AND METHODS

Patient cohort. One hundred seventy-six patients diagnosed as having RA who underwent arthroplasty, as previously described (11), and responded to questions about morning stiffness were included in this analysis. Disease activity in the patients was measured at the presurgical screening visit, typically 2 weeks prior to receiving arthroplasty or on the day of surgery, by the Disease Activity Score in 28 joints using the erythrocyte sedimentation rate (DAS28-ESR). DAS28 scores were categorized as low (<3.2), moderate (<5.1), or high (≥ 5.1). The Rheumatoid Arthritis Disease Activity Index (12), which includes the questions “Were your joints stiff when you woke up today? If yes, how long did the stiffness last?” and the answer options “no stiffness,” “<30 minutes,” “30–60 minutes,” “1–2 hours,” “2–3 hours,” “3–4 hours,”

“>4 hours,” and “all day,” were used to measure stiffness duration. The Outcome Measures in Rheumatology RA Flare Questionnaire (13), which includes the question “How severe was your stiffness over the past week?” with a 10-point numerical rating scale to respond between no stiffness and severe stiffness, was used to measure stiffness severity.

Histologic scoring. Synovial samples were preferentially obtained from grossly inflamed (dull and opaque) synovium. If no inflammation was apparent, samples were obtained from standardized locations: the femoral aspects of the medial and lateral gutters, and the central supratrochlear region in the suprapatellar pouch. Tissue samples were stained with Harris’ modified hematoxylin solution and eosin Y (both from Sigma-Aldrich). Ten features (synovial lining hyperplasia, lymphocytes, plasma cells, Russell bodies, binucleate plasma cells, fibrin, synovial giant cells, detritus, neutrophils, and mucin) were scored as previously described (10) (www.hss.edu/pathology-synovitis.asp).

Clotting assay. Normal donor plasma was collected using EDTA (Becton Dickinson), which anticoagulates blood by chelating calcium. Plasma was filtered using a 0.45 μm syringe filter (Whatman). Plasma (90 μl) was plated in 4–10 technical replicates with either no cells, live neutrophils (polymorphonuclear neutrophils [PMNs]), or necrotic PMNs (necrosis was induced by 5 successive cycles of freezing and thawing of PMN pellets) at 1.5 million cells per milliliter, in 96-well plates. For experiments using DNase I pretreatment, necrotic PMNs were incubated with 5 units of DNase I (Promega) for 30 minutes at 37°C in Hanks’ balanced salt solution with 6 mM CaCl_2 . Clotting was induced with the addition of 6 mM CaCl_2 (Sigma-Aldrich) diluted in phosphate buffered saline (EMD Millipore). Plates were incubated either rotating at 300 revolutions per minute or without movement. Clotting was confirmed by comparing optical density prior to the addition of calcium.

Fibrinolysis assay. Clots were incubated for 30 minutes at 65°C to denature enzyme activity, and then 570 nM human plasmin (Haematologic Technologies) was added to the clots (1:20), plates were incubated on a rotator at 37°C, and optical density was measured serially over time for up to 270 minutes.

Statistical analysis. The Shapiro-Wilk normality test was used to assess the normality of distribution of clinical features. The difference in the presence of stiffness across the DAS28 score ranges (low, moderate, or high) was tested using a chi-square test. Kruskal-Wallis tests were used to assess differences in morning stiffness duration and severity across DAS28 groups. Morning stiffness duration was modeled as a binary outcome classified as <1 hour versus ≥ 1 hour using logistic regression, and severity was modeled as a continuous outcome using linear regression. Simple regression models were applied first to examine the association

between DAS28-ESR and morning stiffness duration, as well as stiffness severity. Multivariable regression models were performed with the main variable of interest (DAS28-ESR) and the following clinical variables: age, sex, body mass index (BMI), duration since RA diagnosis, anti-cyclic citrullinated peptide (anti-CCP) status, and rheumatoid factor (RF) status. Mann-Whitney or Kruskal-Wallis tests were used to compare stiffness severity according to 10 histologic feature scores. The chi-square test or Fisher's exact test was used to assess the association between the 10 histologic features and the binary classification of morning stiffness duration as <1 hour or ≥ 1 hour. Bonferroni-adjusted *P* values are reported to be correct for multiple testing of the histologic features. The Cochran-Armitage trend test was used to assess the significance of fibrin only, neutrophils only, neither fibrin nor neutrophils, or both fibrin in relation to neutrophils and morning stiffness duration. An unpaired *t*-test was used to assess the significance of the differences in results obtained using plasma with and without the addition of calcium. A mixed-effects model for repeated measures with clot condition, time, and clot condition-by-time interaction was used to determine the effect of various cells on fibrinolysis. Analysis of variance with Dunnett's correction for multiple comparisons was used to assess the effect of clot condition at the final time point. Analyses were performed using SAS Studio, version 3.7.

RESULTS

Clinical characteristics. Patient characteristics are presented in Supplementary Table 1, available on the *Arthritis & Rheumatology* web site at <http://onlinelibrary.wiley.com/doi/10.1002/art.41141/abstract>. The majority of patients were female, and 41% and 70% were seropositive for RF and CCP, respectively. Median disease duration was 11 years, the average DAS28 score was 3.7 (moderate), and 52% of patients were treated with a biologic agent (until 1 dose interval prior to surgery).

Association of severity and duration of morning stiffness with disease activity.

Given inconsistencies in previous studies evaluating the association of morning stiffness with RA-related disease activity, we first evaluated whether the stiffness severity or duration of morning stiffness was associated with disease activity in our cohort. The vast majority of patients (83%) responded that they had experienced stiffness that morning, and there was no significant difference in frequency of any morning stiffness between individuals having low, moderate, or high DAS28 scores (Figure 1A). However, the duration of morning stiffness was significantly longer in patients with high DAS28 (Figure 1B). We also evaluated whether morning stiffness duration was associated with disease activity using logistic regression and found that morning

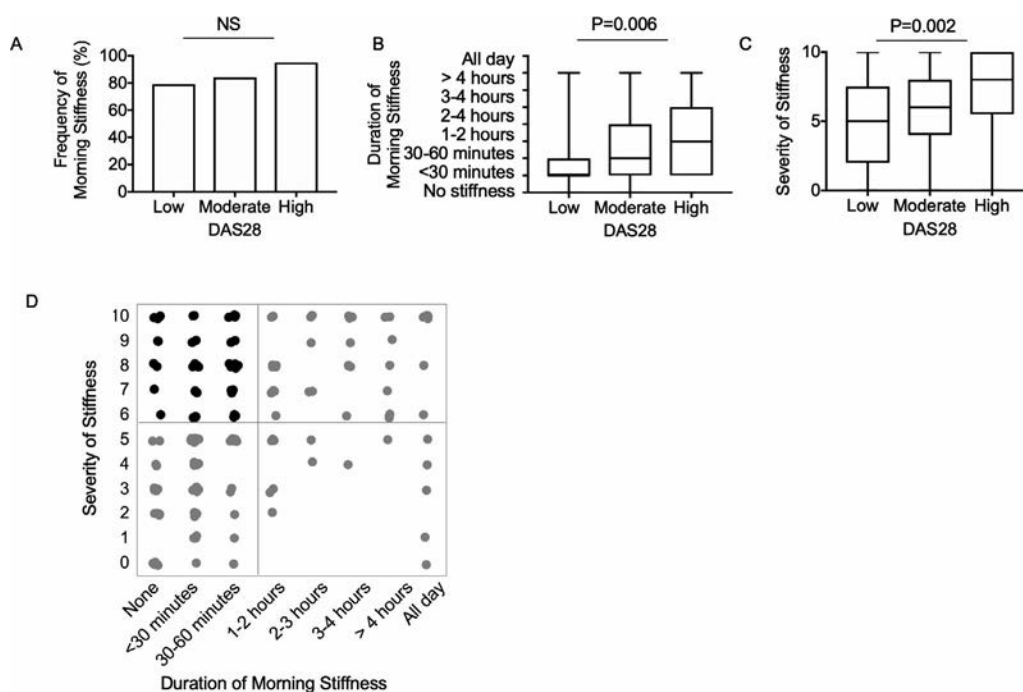


Figure 1. Association of stiffness severity and morning stiffness duration with disease activity. **A**, Frequency of any patient-reported morning stiffness stratified by disease severity according to the Disease Activity Score in 28 joints (DAS28). **B**, Duration of morning stiffness stratified by DAS28. **C**, Severity of stiffness stratified by DAS28. In **B** and **C**, data are shown as box plots. Each box represents the 25th to 75th percentiles. Lines inside the boxes represent the median. Lines outside the boxes represent the 10th and 90th percentiles. **D**, Distribution of responses to questions regarding duration and severity of morning stiffness. Each dot represents 1 patient response. The black dots represent 43% of patients with discordant responses (<1 hour of morning stiffness, but stiffness severity ≥ 6 on a 10-point scale). *P* values were determined by chi-square test (**A**) or Kruskal-Wallis test (**B** and **C**). NS = not significant.

stiffness duration of ≥ 1 hour was significantly associated with DAS28 ($P = 0.001$), and this association remained significant after incorporating covariates including age, sex, BMI, duration of diagnosis, anti-CCP, RF, and smoking status (Table 1). None of these additional covariates were significantly associated with morning stiffness duration.

Stiffness severity also varied significantly across DAS28 groups (Figure 1C). We further evaluated the relationship of stiffness severity with DAS28 using linear regression and found stiffness severity was significantly associated with DAS28 (Table 2) ($P = 0.0001$). This association remained significant after incorporating additional clinical features into the model. Duration of disease was also significantly associated with stiffness severity ($P = 0.003$). Age, BMI, sex, CCP, RF, and smoking status were not significantly associated with stiffness severity.

Though patient-reported stiffness severity tended to increase with duration of morning stiffness, there was notable discordance between reports of severity and duration of stiffness (Figure 1D). Forty-three percent of patients with < 1 hour of morning stiffness considered their stiffness to be severe (≥ 6 on a 10-point scale). The finding that stiffness severity, but not duration of morning stiffness, was associated with disease duration, along with the notable discordance in patient-reported severity and duration, suggest that the 2 questions may capture distinct manifestations of RA.

Association of neutrophils and fibrin with duration of morning stiffness. We next assessed whether there was an association between any of the 10 histologic features, or

Table 1. Logistic regression model of morning stiffness duration (1-hour cutoff) and DAS28-ESR*

Variable	Final model, OR (95% CI)
DAS28-ESR	1.85 (1.29–2.65) [†]
Age, years	1.0 (0.96–1.04)
BMI	0.98 (0.92–1.03)
Duration of diagnosis, years	1.03 (1.0–1.07)
Sex	
Male (referent)	
Female	0.86 (0.27–2.71)
Anti-CCP	
0 (referent)	
1	0.36 (0.12–1.13)
2	1.71 (0.57–5.15)
RF	
0 (referent)	
1	0.76 (0.29–1.98)
Current smoker	
No (referent)	
Yes	0.38 (0.05–2.93)

* The main variable of interest, Disease Activity Score in 28 joints using the erythrocyte sedimentation rate (DAS28-ESR), was examined in an initial model, yielding an odds ratio (OR) of 1.63 (95% confidence interval [95% CI] 1.22–2.19) ($P = 0.001$). Subsequently, the final model (multivariable regression including the DAS28-ESR and other variables as shown) was applied. BMI = body mass index; anti-CCP = anti-cyclic citrullinated peptide; RF = rheumatoid factor.

[†] $P = 0.001$.

Table 2. Linear regression model of stiffness severity and DAS28-ESR*

Variable	Final model, coefficient estimate
Intercept	2.50
DAS28-ESR	0.48 [†]
Age, years	–0.01
BMI	0.03
Duration of diagnosis, years	0.06 [‡]
Sex	
Male (referent)	
Female	0.91
Anti-CCP	
0 (referent)	
1	–0.17
2	–0.33
RF	
0 (referent)	
1	–0.29
Current smoker	
No (referent)	
Yes	1.70
R ²	0.18

* The main variable of interest, Disease Activity Score in 28 joints using the erythrocyte sedimentation rate (DAS28-ESR), was examined in an initial model, yielding a coefficient estimate of 0.66 ($P = 0.0001$) (intercept 3.52 [$P < 0.0001$], R² 0.09). Subsequently, the final model (multivariable regression including the DAS28-ESR and other variables as shown) was applied. BMI = body mass index; anti-CCP = anti-cyclic citrullinated peptide; RF = rheumatoid factor.

[†] $P = 0.008$.

[‡] $P = 0.003$.

a histologic summary score, and reported morning stiffness. Detection of fibrin and detection of neutrophils were significantly associated with ≥ 1 hour of morning stiffness (Figures 2A and B). Fibrin deposition was identified in 41% of cases, while neutrophils were identified in only 15%. We found a significant trend of increasing likelihood of prolonged morning stiffness, comparing synovial samples with neither fibrin nor neutrophils, fibrin only, or neutrophils only to samples with both fibrin and neutrophils (Figure 2C). None of the 10 synovial histologic features assessed (including neutrophils and fibrin, which were associated with stiffness duration), were associated with stiffness severity (Figure 2D).

Colocalization of neutrophils with fibrin deposition along the RA synovial lining.

A shared feature of synovial fibrin deposits and neutrophils is that they are both typically found in RA synovial fluid. Fibrin clots can be found in synovial fluid as “rice bodies,” which appear macroscopically as grains of rice floating in synovial fluid (14), and neutrophils are the most abundant white blood cell type in RA synovial fluid (15) and are comparatively sparse in synovial tissue. Both fibrin and neutrophils (Figures 3A and B) were found along the synovial lining, at the interface with synovial fluid. Further, histologic analysis revealed neutrophils intermixed with synovial lining fibrin deposits (Figure 3B). We also identified neutrophils enmeshed in fibrinous “rice bodies” (Figure 3C).

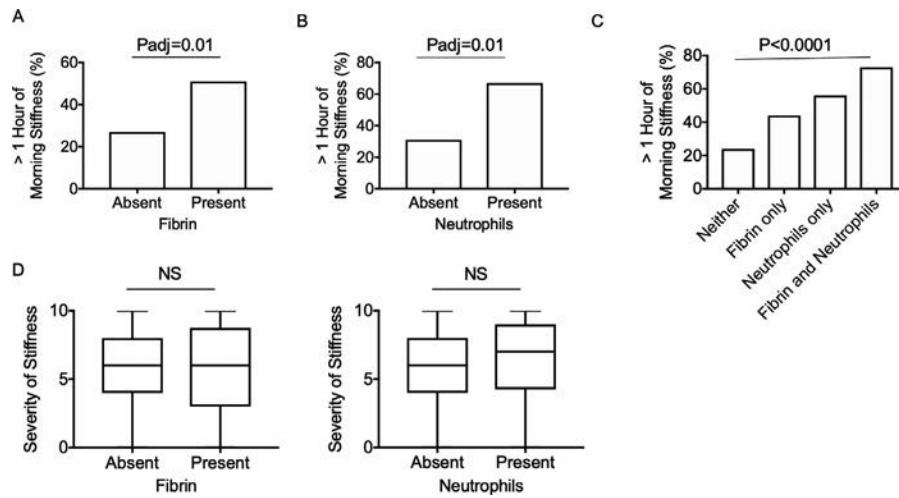


Figure 2. Fibrin and neutrophils are associated with duration of morning stiffness. **A** and **B**, Percentage of patients with ≥ 1 hour of morning stiffness according to the presence of synovial fibrin (**A**) and neutrophils (**B**). **C**, Percentage of patients with ≥ 1 hour of morning stiffness according to the presence of neither fibrin nor neutrophils, fibrin only, neutrophils only, or both fibrin and neutrophils in synovium. **D**, Severity of stiffness according to the presence of fibrin and neutrophils. Data are shown as box plots. Each box represents the 25th to 75th percentiles. Lines inside the boxes represent the median. Lines outside the boxes represent the 10th and 90th percentiles. Adjusted P values (P_{adj}) were determined by Fisher's exact test with Bonferroni correction for multiple comparisons (**A** and **B**); P values were determined by the Cochran-Armitage trend test (**C**) or the Mann-Whitney test (**D**). NS = not significant.

Neutrophil DNA impedes fibrinolysis. We considered the possibility that fibrin could accumulate along the synovial membrane while patients are relatively sedentary overnight, and that this may improve as the day progresses and as fibrin clots are lysed by plasmin. Recalcifying EDTA-anticoagulated plasma in vitro induced clotting in samples that were incubated without shaking but not in those that were shaken (Figure 4A), which is consistent with extensive clinical data noting immobilization as a risk for thrombosis. We further hypothesized that neutrophils might enhance the stability of fibrin deposits, thereby contributing to the sensation of prolonged morning stiffness. To assess whether neutrophils impede plasmin-mediated fibrinolysis, we generated fibrin clots in vitro by recalcifying EDTA-anticoagulated plasma seeded with either no cells, live

PMNs, or necrotic PMNs. After 1 hour, all samples were clotted (Figure 4B); however, the peak optical density was variable across groups. We next added plasmin to the various clots and measured fibrinolysis over 2 hours. We normalized to the peak optical density for any given well to control for the variability of peak optical density (Figure 4B). We observed a significant difference in the various clot conditions over time ($P < 0.0001$, clot condition \times time). Clots seeded with live PMNs were lysed with kinetics that were similar to those observed in clots with no cells, while clots seeded with necrotic PMNs were resistant to fibrinolysis (Figure 4C), and this effect could be abrogated by pretreatment of the necrotic PMN lysate with DNase I (Figure 4D), demonstrating that DNA derived from necrotic PMNs can render fibrin resistant to fibrinolysis.

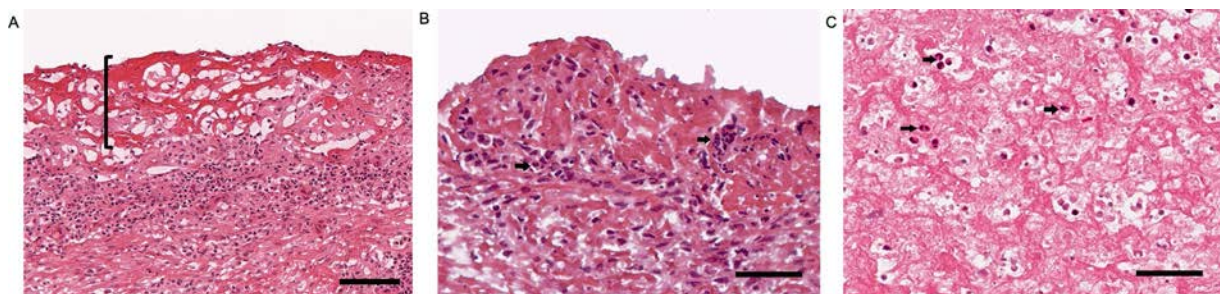


Figure 3. Neutrophils colocalize with fibrin deposits along the synovial lining. **A** and **B**, Representative images of rheumatoid arthritis synovial tissue. In **A**, bracket highlights eosinophilic synovial fibrin deposition along the synovial membrane. Bar = 100 μ m. In **B**, arrows highlight neutrophils intermixed within fibrin, which appear as pink fibrillary material along the synovial lining. Bar = 50 μ m. **C**, Representative image of rice body. Arrows highlight neutrophils intermixed within fibrin. Bar = 50 μ m. Hematoxylin and eosin stained; original magnification $\times 20$ in **A**, $\times 40$ in **B** and **C**.

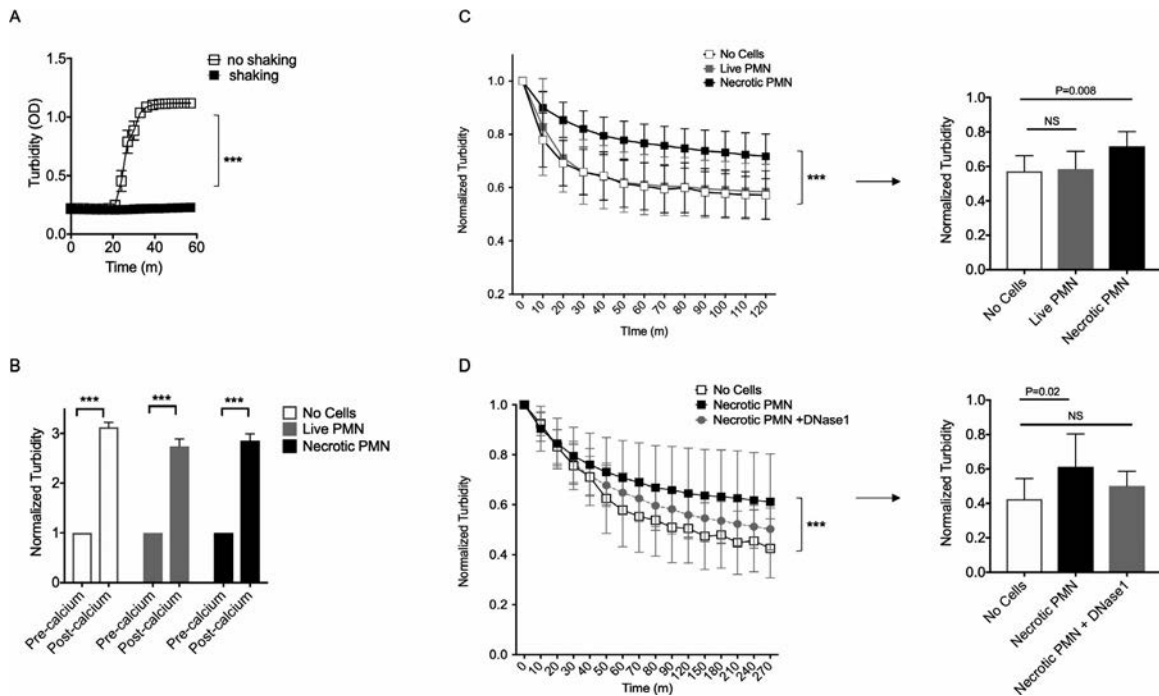


Figure 4. Necrotic neutrophils impede fibrinolysis. **A**, Clotting as measured by turbidity over time of plasma collected using EDTA and incubated with calcium with or without shaking. Values are the mean \pm SD OD (absorbance at 405 nm) and represent 1 of 2 independent experiments. **B**, Clotting as measured by turbidity of plasma alone or seeded with either live polymorphonuclear neutrophils (PMNs) or necrotic PMNs, before and after incubation with calcium for 1 hour. Values are the mean \pm SD OD (absorbance at 405 nm), normalized to the value obtained just prior to addition of calcium. In **A** and **B**, $*** = P < 0.0001$ by unpaired *t*-test. **C**, Left, Fibrinolysis as measured by normalized turbidity of clots alone or seeded with either live PMNs or necrotic PMNs and treated with plasmin. Right, Normalized turbidity of fibrin clots (from left panel) at 120 minutes. Data represent 1 of 6 independent experiments. **D**, Left, Fibrinolysis as measured by normalized turbidity of clots alone or seeded with either necrotic PMNs or necrotic PMNs pretreated with DNase I and then lysed with plasmin. Right, Normalized turbidity of fibrin clots (from left panel) at 270 minutes. Data represent 1 of 3 independent experiments. In **C** and **D**, values are the mean \pm SD OD (absorbance at 405 nm), normalized to the value obtained at time 0, following the addition of plasmin. $*** = P < 0.0001$ in a mixed-effects model for clot conditions by time. *P* values in right panel were determined by analysis of variance with Dunnett's multiple comparisons test, using the no cells group as the reference. NS = not significant.

DISCUSSION

Morning stiffness is a hallmark clinical symptom experienced by RA patients. Here we report that in a cohort of 176 patients with RA undergoing arthroplasty, 83% experienced morning stiffness, and both morning stiffness duration and stiffness severity were significantly associated with disease activity.

We found that synovial neutrophils and fibrin were significantly associated with patient-reported morning stiffness of ≥ 1 hour. Fibrin, the final product of the clotting cascade, is a gel-like substance frequently observed along the surface of inflamed synovium in RA (10). Neutrophils are short-lived cells programmed to die within hours after infiltrating tissue. Therefore, the association of synovial neutrophils with prolonged morning stiffness suggests that acute synovial inflammation or ongoing neutrophil recruitment may play a role in mediating this symptom. Such a possibility is consistent with our finding that patient-reported stiffness was significantly associated with disease activity. Indeed, one of the principal mechanisms of glucocorticoids is to inhibit access of neutrophils to sites of inflammation

(16), and in a clinical trial of delayed-release prednisone, this treatment produced a significant reduction in duration of morning stiffness (17).

We further demonstrated that neutrophils can be found enmeshed in fibrin deposits along the synovial membrane. It is not unexpected that neutrophils can be found in this location, as it is well established from extensive clinical experience that inflamed synovial fluid is laden with neutrophils, and since neutrophils reach the synovial fluid by extravasating through blood vessels in synovium, they must cross the synovial lining to reach the synovial fluid space. We report here that necrotic neutrophil DNA can render fibrin deposits resistant to fibrinolysis. This result is consistent with prior reports demonstrating that clots containing histones and DNA have thicker fibers, increased clot stability, and greater rigidity (18, 19). It is plausible that when neutrophils infiltrate the joint, their DNA confers increased stability and rigidity to fibrin deposits along the synovial surface, contributing to the sensation of stiffness by altering the mechanics of articular movement. Interestingly, no plasma cell features or RA-associated autoantibodies were significantly associated with duration of morning stiffness.

The lack of association of markers typical of an adaptive immune response (plasma cells and autoantibodies), along with the fact that fibrin deposition is a finding common to a spectrum of inflammatory states, raises the possibility that neutrophil-enmeshed fibrin could represent a generic cause of stiffness that may also mediate morning stiffness in other rheumatologic diseases, such as ankylosing spondylitis or psoriatic arthritis.

Another interesting finding of our study was that RA patients who rated their stiffness severity as high did not necessarily experience prolonged duration of morning stiffness. It is possible that the discrepancy between these 2 reported symptoms is because the stiffness severity question was worded to capture stiffness over the past week rather than that particular day, while the stiffness duration question was worded to capture symptoms that day. Alternatively, severity and duration of morning stiffness may reflect distinct pathophysiologic mechanisms of inflammation and damage, and thereby representing different clinical symptom constructs. This hypothesis is supported by our finding that stiffness severity was associated with disease duration but not with any of the synovial histologic features assessed in this study.

An important limitation of our work is that we only assessed a small section of a relatively large synovial membrane in each patient. There could be variability within any given synovium that was not assessed in this study. Further, there are other important structures in joints that might affect the sensation of morning stiffness such as the joint capsule, tendons, ligaments, vasculature, cartilage, and bone, none of which were included in this analysis. Finally, it is important to note that the joints studied in this analysis were limited to large joints (hips and knees) in patients with relatively long disease duration (median 11 years). It is not known whether neutrophils and fibrin are also associated with morning stiffness duration in small joints such as hands and feet, or in patients with early arthritis.

In summary, we investigated the association of morning stiffness with clinical and synovial histologic features of RA in a cohort of patients undergoing arthroplasty. We found that both synovial tissue neutrophils and fibrin are associated with duration of morning stiffness and that neutrophil-derived DNA renders fibrin resistant to fibrinolysis. Our observations identify histologic findings that are significantly associated with patient-reported morning stiffness, and thereby provide insights into potential mechanisms mediating a vexing clinical symptom that is frequently experienced by patients with RA and other types of inflammatory arthritis.

AUTHOR CONTRIBUTIONS

All authors were involved in drafting the article or revising it critically for important intellectual content, and all authors approved the final version to be published. Dr. Orange had full access to all the data in the study and takes responsibility for the integrity of the data and the accuracy of the data analysis.

Study conception and design. Orange, Bykerk, Goodman.

Acquisition of data. Orange, Blachere, DiCarlo, Mirza, Pannellini, Parveen, Figgie, Gravallesse, Goodman.



Analysis and interpretation of data. Orange, Jiang, Frank, Orbai, Mackie, Goodman.

REFERENCES

1. Aletaha D, Neogi T, Silman AJ, Funovits J, Felson DT, Bingham CO III, et al. 2010 rheumatoid arthritis classification criteria: an American College of Rheumatology/European League Against Rheumatism collaborative initiative. *Arthritis Rheum* 2010;62:2569–81.
2. Mattila K, Buttgerit F, Tuominen R. Impact of morning stiffness on working behaviour and performance in people with rheumatoid arthritis. *Rheumatol Int* 2014;34:1751–8.
3. Mattila K, Buttgerit F, Tuominen R. Influence of rheumatoid arthritis-related morning stiffness on productivity at work: results from a survey in 11 European countries. *Rheumatol Int* 2015;35:1791–7.
4. Arnett FC, Edworthy SM, Bloch DA, McShane DJ, Fries JF, Cooper NS, et al. The American Rheumatism Association 1987 revised criteria for the classification of rheumatoid arthritis. *Arthritis Rheum* 1988;31:315–24.
5. Hazes JM, Hayton R, Silman AJ. A reevaluation of the symptom of morning stiffness. *J Rheumatol* 1993;20:1138–42.
6. Boers M, Buttgerit F, Saag K, Alten R, Grahn A, Storey D, et al. What is the relationship between morning symptoms and measures of disease activity in patients with rheumatoid arthritis? *Arthritis Care Res (Hoboken)* 2015;67:1202–9.
7. Khan NA, Yazici Y, Calvo-Alen J, Dadoniene J, Gossec L, Hansen TM, et al. Reevaluation of the role of duration of morning stiffness in the assessment of rheumatoid arthritis activity. *J Rheumatol* 2009;36:2435–42.
8. Yazici Y, Erkan D, Peterson MG, Kagen LJ. Morning stiffness: how common is it and does it correlate with physician and patient global assessment of disease activity? [letter]. *J Rheumatol* 2001;28:1468–9.
9. Orbai AM, Smith KC, Bartlett SJ, De Leon E, Bingham CO III. “Stiffness has different meanings, I think, to everyone”: examining stiffness from the perspective of people living with rheumatoid arthritis. *Arthritis Care Res (Hoboken)* 2014;6:1662–72.
10. Orange DE, Agius P, DiCarlo EF, Robine N, Geiger H, Szymonifka J, et al. Identification of three rheumatoid arthritis disease subtypes by machine learning integration of synovial histologic features and RNA sequencing data. *Arthritis Rheumatol* 2018;70:690–701.
11. Goodman SM, Bykerk VP, DiCarlo E, Cummings RW, Donlin LT, Orange DE, et al. Flares in patients with rheumatoid arthritis after total hip and total knee arthroplasty: rates, characteristics, and risk factors. *J Rheumatol* 2018;45:604–11.
12. Stucki G, Liang MH, Stucki S, Brühlmann P, Michel BA. A self-administered Rheumatoid Arthritis Disease Activity Index (RADAI) for epidemiologic research: psychometric properties and correlation with parameters of disease activity. *Arthritis Rheum* 1995;38:795–8.
13. Bykerk VP, Bingham CO, Choy EH, Lin D, Alten R, Christensen R, et al. Identifying flares in rheumatoid arthritis: reliability and construct validation of the OMERACT RA Flare Core Domain Set. *RMD Open* 2016;2:e000225.
14. Popert AJ, Scott DL, Wainwright AC, Walton KW, Williamson N, Chapman JH. Frequency of occurrence, mode of development, and significance of rice bodies in rheumatoid joints. *Ann Rheum Dis* 1982;41:109–17.
15. Dougados M. Synovial fluid cell analysis. *Baillieres Clin Rheumatol* 1996;10:519–34.
16. Fauci AS, Dale DC, Balow JE. Glucocorticosteroid therapy: mechanisms of action and clinical considerations. *Ann Intern Med* 1976; 84:304–15.

17. Buttgereit F, Doering G, Schaeffler A, Witte S, Sierakowski S, Gromnica-Ihle E, et al. Targeting pathophysiological rhythms: prednisone chronotherapy shows sustained efficacy in rheumatoid arthritis. *Ann Rheum Dis* 2010;69:1275–80.
18. Longstaff C, Varjú I, Sótonyi P, Szabó L, Krumrey M, Hoell A, et al. Mechanical stability and fibrinolytic resistance of clots containing fibrin, DNA, and histones. *J Biol Chem* 2013;288:6946–56.
19. Varjú I, Longstaff C, Szabó L, Farkas ÁZ, Varga-Szabó VJ, Tanka-Salamon A, et al. DNA, histones and neutrophil extracellular traps exert anti-fibrinolytic effects in a plasma environment. *Thromb Haemost* 2015;113:1289–98.

CD4+ Memory Stem T Cells Recognizing Citrullinated Epitopes Are Expanded in Patients With Rheumatoid Arthritis and Sensitive to Tumor Necrosis Factor Blockade

Beatrice C. Cianciotti,¹  Eliana Ruggiero,² Corrado Campochiaro,¹ Giacomo Oliveira,² Zulma I. Magnani,² Mattia Baldini,² Matteo Doglio,² Michela Tassara,² Angelo A. Manfredi,¹ Elena Baldissera,² Fabio Ciceri,¹ Nicoletta Cieri,²  and Chiara Bonini¹ 

Objective. Memory stem T (Tscm) cells are long-lived, self-renewing T cells that play a relevant role in immunologic memory. This study was undertaken to investigate whether Tscm cells accumulate in rheumatoid arthritis (RA).

Methods. The polarization and differentiation profiles of circulating T cells were assessed by flow cytometry. Antigen-specific T cells were characterized by staining with major histocompatibility complex class II tetramers. The T cell receptor (TCR) repertoire was analyzed by high-throughput sequencing using an unbiased RNA-based approach in CD4+ T cell subpopulations sorted by fluorescence-activated cell sorting.

Results. We analyzed the dynamics of circulating Tscm cells (identified as CD45RA+CD62L+CD95+ T cells) by flow cytometry in 27 RA patients, 16 of whom were also studied during treatment with the anti-tumor necrosis factor (anti-TNF) agent etanercept. Age-matched healthy donors were used as controls. CD4+ Tscm cells were selectively and significantly expanded in RA patients in terms of frequency and absolute numbers, and significantly contracted upon anti-TNF treatment. Expanded CD4+ Tscm cells displayed a prevalent Th17 phenotype and a skewed TCR repertoire in RA patients, with the 10 most abundant clones representing up to 53.7% of the detected sequences. CD4+ lymphocytes specific for a citrullinated vimentin (Cit-vimentin) epitope were expanded in RA patients with active disease. Tscm cells accounted for a large fraction of Cit-vimentin-specific CD4+ cells.

Conclusion. Our results indicate that Tscm cells, including expanded clones specific for relevant autoantigens, accumulate in RA patients not exposed to biologic agents, and might be involved in the natural history of the disease. Further analysis of Tscm cell dynamics in autoimmune disorders may have implications for the design and efficacy assessment of innovative therapies.

INTRODUCTION

Memory stem T (Tscm) cells represent a population of antigen-experienced CD45RA+CD62L+CCR7+IL7R α +CD95+ T lymphocytes endowed with exceptional persistence and self-renewing ability (1,2). Indeed, in models of genetic diseases (3), cancer (4–6), and infections (7), Tscm cells proved hierarchically superior to other antigen-experienced T cell subsets and endowed with a long-lasting protective role. Nevertheless, this very same cell population might represent a foe in T cell-mediated pathologies. In the first report on Tscm cells, Zhang and col-

leagues (8) identified this T cell subset as a dominant reservoir of alloreactive lymphocytes in a murine model of graft-versus-host disease, a major T cell-mediated complication of hematopoietic stem cell transplantation (HSCT); subsequently, we observed a selective accumulation of Tscm cells early after HSCT in humans (9). While a number of reports have highlighted the beneficial role of Tscm cells in cancer and infections, very little is known about the dynamics of Tscm cells in the context of chronic inflammatory conditions and autoimmune diseases. A high frequency of CD8+ Tscm cells has been associated with failure of immunosuppressive treatment in patients with aplastic anemia (10)

Presented by Ms Cianciotti in partial fulfillment of the requirements for a PhD degree, Vita-Salute San Raffaele University, Milan.

Supported by the Italian Ministry of Education, University and Research.

¹Beatrice C. Cianciotti, MSc, Corrado Campochiaro, MD, Angelo A. Manfredi, MD, Fabio Ciceri, MD, Chiara Bonini, MD: IRCCS Ospedale San Raffaele and Vita-Salute San Raffaele University, Milan, Italy; ²Eliana Ruggiero, PhD, Giacomo Oliveira, PhD, Zulma I. Magnani, MSc, Mattia Baldini, MD, MRCEM, Matteo Doglio, MD, Michela Tassara, MD, Elena

Baldissera, MD, Nicoletta Cieri, MD, PhD: IRCCS Ospedale San Raffaele, Milan, Italy.

Drs. Cieri and Bonini contributed equally to this work.

No disclosures relevant to this article were reported.

Address correspondence to Nicoletta Cieri, MD, PhD, or Chiara Bonini, MD, Via Olgettina 60, 20132 Milan MI, Italy. E-mail: nicolettacieri@dfci.harvard.edu or chiara.bonini@hsr.it.

Submitted for publication August 24, 2018; accepted in revised form October 31, 2019.

and increased CD8+ Tscm cell numbers have recently been described in patients with type 1 diabetes mellitus (11).

Rheumatoid arthritis (RA) is one of the most common autoimmune diseases, affecting ~1% of the worldwide population. It is characterized by autoantibody production and cartilage and bone destruction, resulting in disability and reduced quality of life and life expectancy (12). The predominant target tissues are the synovial joints, which are massively infiltrated by T cells, representing ~30–50% of cells in the RA synovium, and macrophages. B cells, plasma cells, and dendritic cells are also detected. The recruitment of activated T cells in synovial lesions, the well-established association of RA with HLA class II alleles, and the recent genome-wide scanning studies linking RA susceptibility to polymorphisms in genes related to T cell function point to a critical role of adaptive immunity, and of CD4+ T lymphocytes in particular, in RA pathogenesis (13).

Building on these findings, we hypothesized that T lymphocytes specific for relevant autoantigens and endowed with enhanced self-renewal capacities, such as Tscm cells, may be pathogenic in the context of T cell-mediated autoimmune disorders. We thus investigated the frequencies, dynamics, and repertoire of Tscm cells in patients affected by RA, and their sensitivity to anti-tumor necrosis factor (anti-TNF) agents.

MATERIALS AND METHODS

Patient population. We studied 27 patients with RA who fulfilled both the American College of Rheumatology (ACR) 1987 criteria (14) and the ACR/European League Against Rheumatism 2010 criteria (15). Sixteen patients were analyzed longitudinally before and during anti-TNF administration (etanercept, given at a dose of 50 mg/week subcutaneously). Twenty age-matched healthy donors were studied in parallel as controls. All subjects signed informed consent forms approved by the Ospedale San Raffaele Ethics Committee, in accordance with the Declaration of Helsinki. Disease activity and clinical responses were assessed using the Disease Activity Score in 28 joints (DAS28) (16). Clinical characteristics of the patients included in the study are summarized in Table 1.

T cell isolation and sorting. Peripheral blood mononuclear cells (PBMCs) were isolated by Ficoll-Hypaque separation (Lymphoprep; Fresenius) from peripheral blood samples from healthy donors and RA patients, stained with fluorochrome-conjugated antibodies, and subjected to flow cytometric analysis. For T cell sorting, PBMCs were labeled with anti-CD3, anti-CD4, anti-CD45RA, anti-CD62L, and anti-CD95 antibodies (BioLegend) and sorted on MoFlo-MLS or XDP cell sorters (Dako) with a purity of >95%.

Absolute cell counts. Absolute quantification of PBMCs was determined using Flow-Count technology (Beckman Coulter). Briefly, anti-human fluorescein isothiocyanate-conjugated T cell receptor $\alpha\beta$ (TCR $\alpha\beta$) (BD Biosciences), phycoerythrin (PE)-Texas

Table 1. Clinical characteristics of the patients with rheumatoid arthritis (n = 27)*

No. of patients followed up during ETN treatment (50 mg/week)	16
Age, median (range) years	55 (24–74)
Female, no. (%)	24 (89)
Time from diagnosis to first sample, median (range) years	5 (2–26)
Time from first sample to follow-up sample, median (range) days	99 (46–116)
Time from ETN initiation to follow-up sample, median (range) days	95 (46–116)
Baseline DAS28, median (range)	4.34 (2.28–6.39)
DAS28 during ETN treatment, median (range)	2.86 (1.27–5.4)†
Ever smoked, no. (%)	13 (48)
No. of current smokers	6
No. of ex-smokers	7
RF positive, no. (%)	24 (89)
ACPA positive, no. (%)	20 (74)
Concomitant treatment, no. %	
Methotrexate (10–20 mg/week)	12 (44)
Leflunomide (20 mg/day)	7 (26)
Plaquenil (200 mg/day)	4 (15)
Prednisone equivalent (0.07 mg/kg/day)	12 (44)

* ETN = etanercept; RF = rheumatoid factor; ACPA = anti-citrullinated protein antibody.

† $P < 0.001$ versus baseline Disease Activity Score in 28 joints (DAS28), by Wilcoxon's test.

Red-conjugated CD4 (Invitrogen), PerCP-Cy5.5-conjugated CD8, PE-Cy7-conjugated CD19, allophycocyanin (APC)-conjugated TCR $\gamma\delta$, APC-Cy7-conjugated CD14, A700-conjugated CD15, Pacific Blue-conjugated CD56, and BV510-conjugated CD3 antibodies (all from BioLegend) were added to 50 μ l of EDTA-treated whole blood, previously diluted in a 1:3 ratio with in-house produced Fc-block (2.4G2 hybridoma; ATCC), and incubated for 15 minutes at room temperature. Red blood cells were then lysed with ACK lysing buffer for 10 minutes at room temperature. After centrifugation to remove cell debris, 25 μ l of Flow-Count Fluorospheres (Beckman Coulter) were added. Samples were acquired using a Gallios cytometer and analyzed with Kaluza software (Beckman Coulter).

Multiparameter flow cytometric analysis and intracellular staining. PBMCs were labeled with anti-CD3, anti-CD4, anti-CD8, anti-CD45RA, anti-CD62L, anti-CD95 (all from BioLegend), anti-CD120a (Beckman Coulter and BD Biosciences), and anti-CD120b (BD Biosciences and Miltenyi) antibodies. Viable lymphocytes were identified based on forward scatter and side scatter properties. CD4+ and CD8+ T cells were gated within CD3+ lymphocytes. Expression of CD45RA and CD62L in gated CD4+ and CD8+ T cells was used to identify naive T cells and Tscm (CD45RA+CD62L+) cells, central memory T (Tcm; CD45RA-CD62L+) cells, effector memory T (Tem; CD45RA-CD62L-) cells, and terminal effector T (Temra; CD45RA+CD62L-) cells. CD95 expression on gated total CD4+ and CD8+ cells was used to discriminate between naive (CD95-) and antigen-experienced (CD95+) T cell subpopulations. The use of the same CD95 gate in selected CD45RA+CD62L+ cells allowed reproducible discrimination

between naive T (CD45RA+CD62L+CD95-) cells and Tscm (CD45RA+CD62L+CD95+) cells. CD4+ cells specific for the previously described Epstein-Barr virus (EBV) peptide BHRF1¹²²⁻¹³³ and for the citrullinated vimentin peptide Cit-vimentin⁶⁵⁻⁷⁷ (17,18) were detected using custom APC- or PE-conjugated HLA-DRB1*04:01-restricted tetramers (ProImmune), respectively. CD8+ viral-specific lymphocytes were quantified with HLA-A2*0201-restricted, PE-conjugated dextramers (Immudex) specific for the following viral peptides: NLVPMVATV (CMV-pp65), GILGFVFTL (Flu-MP), and GLCTLVAML (EBV-BMLF1).

To identify the cytokine secretion profile of discrete T cell subsets, 0.4×10^6 PBMCs were preincubated with TNF proteinase inhibitor 2 as previously described (19), then exposed to phorbol myristate acetate/ionomycin for 4 hours at 37°C. Brefeldin A was added for 2 additional hours. Cells were subsequently stained with fluorochrome-conjugated antibodies specific for surface antigens, washed, and then fixed and permeabilized with FoxP3 Fix/Perm Buffer Set (BioLegend). Intracellular staining was then performed and samples were acquired on an LSRFortessa cytometer (BD Biosciences). Each acquisition was calibrated using Rainbow Calibration Particles (Spherotech) to correct for day-to-day variation. Data were analyzed using FlowJo version X.0.7 (TreeStar).

HLA-DRB 04:01 typing. RA patients and healthy donors were screened by flow cytometry for HLA-DRB1*04:01 expression by staining PBMCs with a biotinylated HLA-DRB1*04:01-specific monoclonal antibody (One Lambda) followed by PE-conjugated streptavidin (BioLegend). For positive samples, molecular HLA typing was performed by the HLA typing and chimerism laboratory of San Raffaele Scientific Institute. HLA typing was performed at high resolution (4 digits) with a standard Sequence-Specific Priming (SSP) technique. Briefly, CareDx (Olerup SSP) DRB1*04-specific kits were used for performing the sequence-specific polymerase chain reaction (PCR); the presence or absence of the sequence-specific PCR products was determined by capillary electrophoresis (QIAxcel Advanced System; Qiagen). Results were interpreted using Helmborg Score SSP software.

TCR sequencing. TCR α and β chains were sequenced using a modified rapid amplification of complementary DNA (cDNA) ends PCR protocol, independent of multiplex PCRs (20,21). Total RNA extracted from sorted memory subpopulations was reverse transcribed and amplified using primers specific for α/β -chain constant regions and for the template-switching sequence added during cDNA synthesis. Individual samples were unequivocally tagged using a barcoded fusion primer specific for constant TCR genes in addition to the barcoded template-switching primer. PCR amplicons were purified with AMPure beads (Beckman Coulter) and sequenced on a MiSeq platform (Illumina). Raw reads were sorted according to the individual barcode combination used for each specimen. Data were analyzed using MiXCR software (22).

Statistical analysis. Nonparametric continuous variables were analyzed by Mann-Whitney U test or Wilcoxon's rank sum test for comparing 2 independent groups and Wilcoxon's signed rank test for comparing 2 dependent groups. Data were analyzed using JMP, version 10, and *P* values less than or equal to 0.05 were considered significant. Graphs were created using GraphPad Prism 8 software.

RESULTS

CD4+ Tscm cells are expanded in RA patients and contract upon TNF blockade. We analyzed the T cell subset distribution in 27 patients with RA who had not been previously treated with biologic disease-modifying antirheumatic drugs (DMARDs). The median DAS28 score was 4.34, indicating moderate disease activity. We tracked T cell dynamics in 16 of the 27 patients upon treatment with the anti-TNF agent etanercept. Clinical characteristics of the patients studied are summarized in Table 1. A significant reduction in DAS28 upon etanercept administration (mean DAS28 reduction -1.64 [range $-3.37, 0.65$]) was observed, with 15 of the 16 patients responding to treatment a median of 3 months after initiation.

We first quantitatively evaluated the circulating lymphoid and myeloid cells in RA patients before and during TNF blockade. RA patients' absolute numbers of circulating CD4+, CD8+, $\gamma\delta$ T cells, CD56+ natural killer cells, CD19+ B cells, and CD14+ monocytes were similar to those of age-matched healthy donors, with the only exception being CD15+ granulocytes, which were significantly increased in patients with active disease, possibly due to concomitant steroid therapy in a fraction of patients. No significant differences in circulating leukocyte subsets were observed before or during anti-TNF treatment (Supplementary Figures 1A–C, available on the *Arthritis & Rheumatology* web site at <http://onlinelibrary.wiley.com/doi/10.1002/art.41157/abstract>).

As expected, RA patients showed a significant increase in the CD4:CD8 cell ratio compared to healthy donors, independent of treatment (Supplementary Figure 1D). We analyzed the expression of CD45RA, CD62L, and CD95 in CD4+ and CD8+ lymphocytes by multiparameter flow cytometry (Supplementary Figure 2, available on the *Arthritis & Rheumatology* web site at <http://onlinelibrary.wiley.com/doi/10.1002/art.41157/abstract>). In our patient cohort, the CD4+ Tscm cell subset was the only T cell subset significantly expanded in RA patients compared to controls, both in terms of percentages (Figure 1A) and absolute numbers (Figure 1B). In contrast, the percentages and numbers of naive T cells, Tcm cells, Tem cells, and Temra cells did not differ between patients and controls.

The CD4+ Tscm compartment contracted upon TNF blockade (Figures 1A–C and Supplementary Figure 3, available on the *Arthritis & Rheumatology* web site at <http://onlinelibrary.wiley.com/doi/10.1002/art.41157/abstract>). Consistent with the prevalent role of CD4+ lymphocytes in RA, there was only a slight, nonsignificant increase in

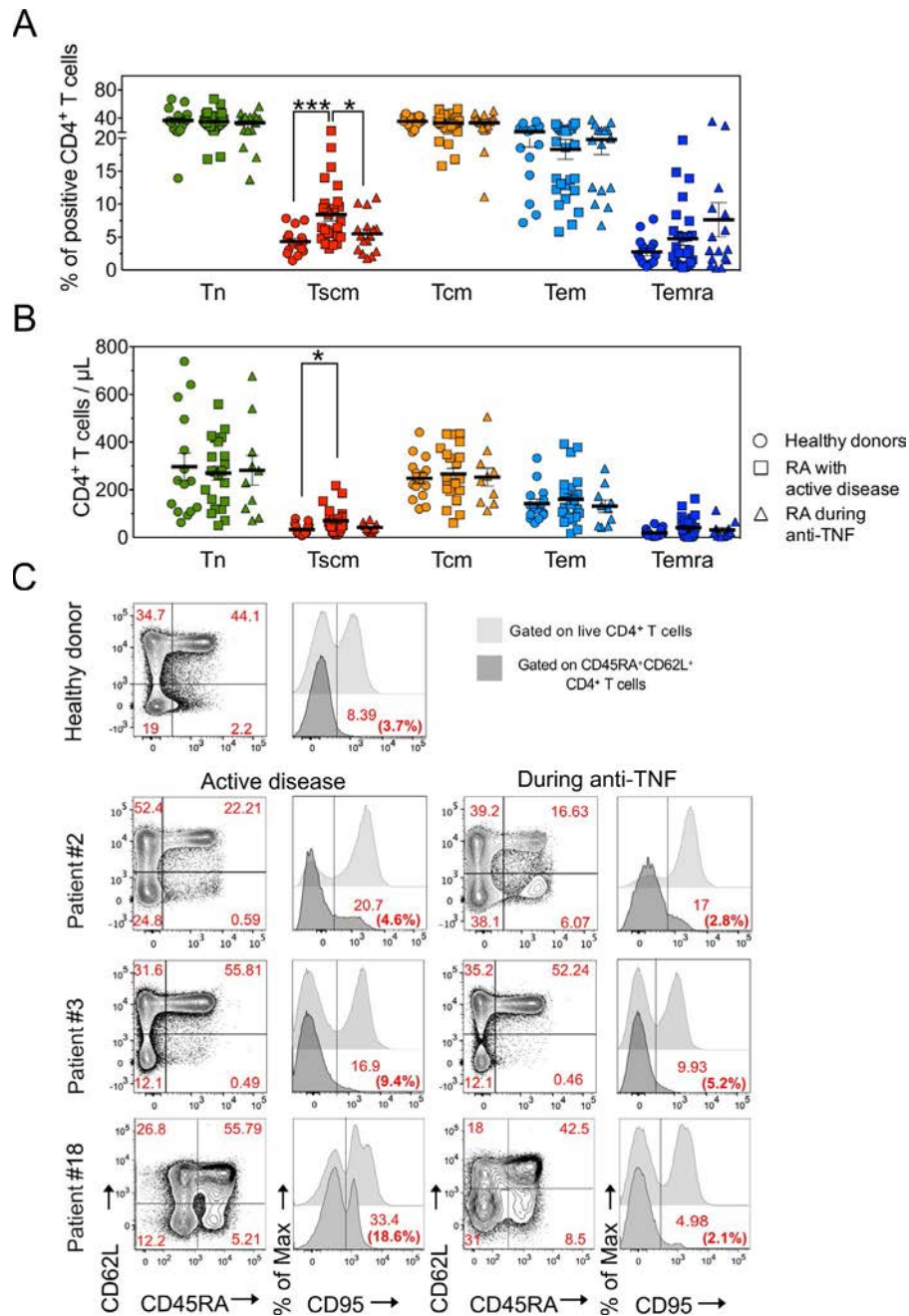


Figure 1. CD4⁺ memory stem T (Tscm) cells in patients with rheumatoid arthritis (RA). The percentages and numbers of CD4⁺ Tscm cells were increased in patients with active RA and significantly decreased during anti-tumor necrosis factor (anti-TNF) treatment. **A** and **B**, Percentage (**A**) and absolute number (**B**) of each T cell subset on total CD4⁺ T cells in patients with active RA (n = 27), patients with RA receiving anti-TNF treatment (n = 16), and age-matched healthy donors (n = 15). The T cell subsets were defined as naive T (Tn; CD45RA⁺CD62L⁺CD95⁻) cells, Tscm (CD45RA⁺CD62L⁺CD95⁺) cells, central memory T (Tcm; CD45RA⁻CD62L⁺) cells, effector memory T (Tem; CD45RA⁻CD62L⁻) cells, and terminal effector T (Temra; CD45RA⁺CD62L⁻) cells. Symbols represent individual subjects; horizontal lines and error bars show the mean \pm SEM. * = $P \leq 0.05$; *** = $P \leq 0.001$. **C**, Representative fluorescence-activated cell sorting results showing the T cell subset composition in a healthy donor and in patients 2, 3, and 18 during active disease and upon TNF blockade. The numbers in parentheses are the frequency of Tscm cells among total CD4⁺ T cells.

CD8⁺ Tscm cells in RA patient samples compared to controls (Supplementary Figure 4, available on the *Arthritis & Rheumatology* web site at <http://onlinelibrary.wiley.com/doi/10.1002/art.41157/abstract>). These observations suggest that CD4⁺ long-lived, self-renewing Tscm cells may be selectively modulated depending on RA activity.

Preferential Th17 polarization of CD4⁺ Tscm cells in RA patients. Since we observed a significant expansion of CD4⁺ Tscm cells in RA, we next sought to determine the cytokine secretion profile of this expanded T cell subset. Consistent with previous observations on bulk CD4⁺ cells (23), we observed a

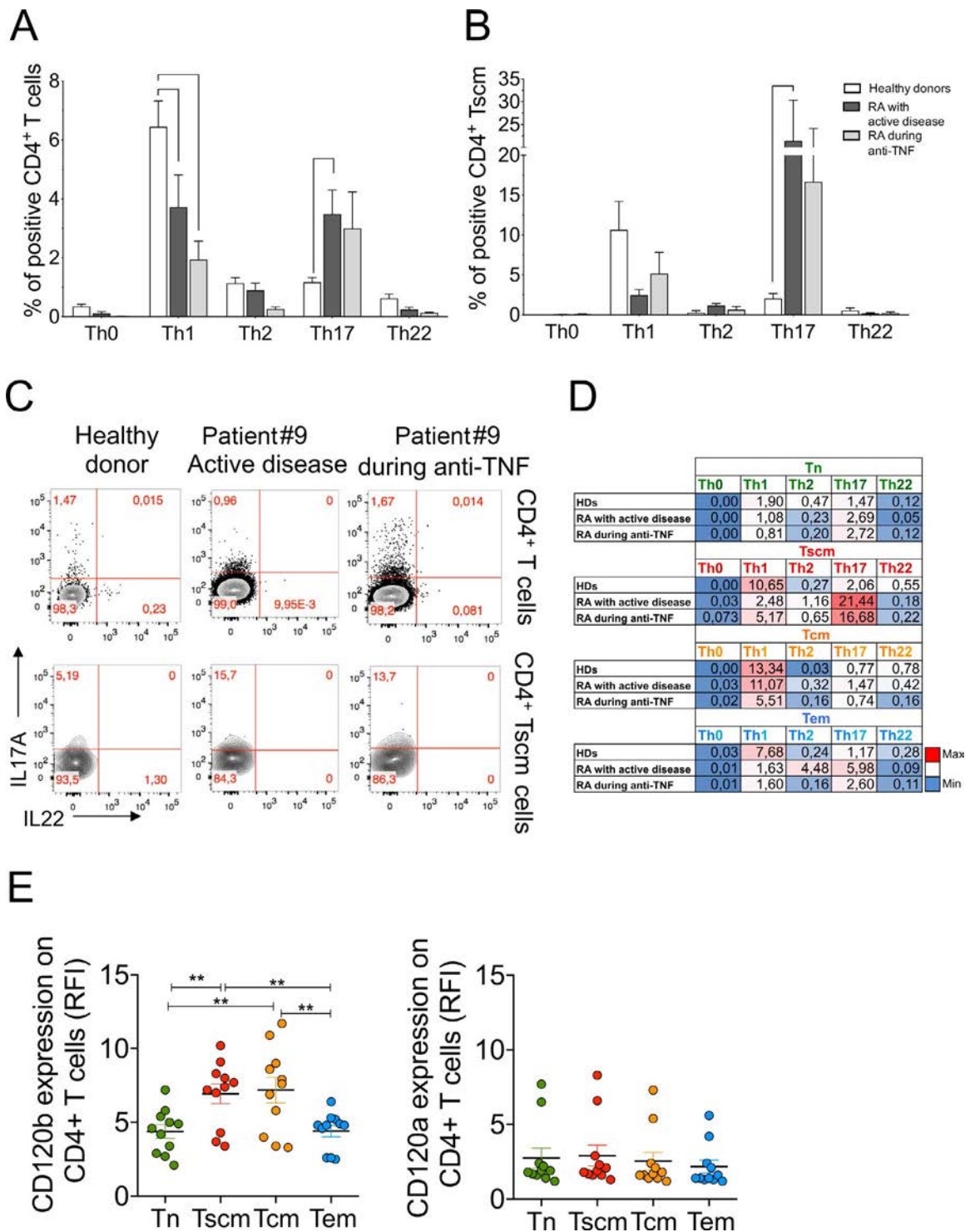


Figure 2. Skewing of CD4+ Tscm cells toward a Th17 phenotype in RA patients. **A** and **B**, Polarization profile of total CD4+ T cells (**A**) and gated CD4+ Tscm cells (**B**) in patients with active RA (n = 9), patients with RA receiving anti-TNF treatment (n = 5), and age-matched healthy donors (HDs; n = 23 in **A** and n = 7 in **B**). T cells were classified as Th0 (IFN γ +IL-4-) cells, Th1 (IFN γ +IL-4-) cells, Th2 (IFN γ -IL-4+) cells, Th17 (IL-17+) cells, or Th22 (IL22+) cells. Bars show the mean \pm SEM. **C**, Representative fluorescence-activated cell sorting plots showing T cell polarity on total CD4+ T cells and on gated CD4+ Tscm cells in a healthy donor, patient 9 during active disease, and patient 9 during anti-TNF treatment. **D**, Percentages of Th0, Th1, Th2, Th17, and Th22 cells quantified on naive T cells, Tscm cells, Tcm cells, and Tem cells in healthy donors, patients with active RA, and patients with RA receiving anti-TNF treatment. The color gradient denotes the relative frequency of each cell population, with blue and red indicating the lowest and the highest percentages, respectively. **E**, CD120b (TNF receptor type II [TNFRII]) and CD120a (TNFR1) expression measured as relative fluorescence intensity (RFI) on naive T, Tscm, Tcm, and Tem cells from patients with active RA. The RFI was defined as mean fluorescence intensity of the stained patient sample/mean fluorescence intensity of a fluorescence minus 1 control sample. Symbols represent individual patients; horizontal lines and error bars show the mean \pm SEM. ** = $P \leq 0.01$; **** = $P \leq 0.0001$. See Figure 1 for other definitions.

significant increase in Th17+ lymphocytes in RA patients compared to healthy donors, accompanied by a concomitant underrepresentation of Th1 cells (Figure 2A). When focusing on CD4+ Tscm cells, we observed a significant skewing toward a Th17 polarization in RA patients compared to healthy donors (Figures 2B and C). As shown in the heatmap in Figure 2D, Th17 polarization preferentially segregated within the CD4+ Tscm cell compartment, thus supporting the notion of elevated Th17 potential of CD4+ Tscm lymphocytes in the inflammatory events associated with active RA. Given the significant reduction in Tscm cells upon anti-TNF administration, we hypothesized that TNF may act as a prosurvival factor for this T cell subpopulation. Consistent with this hypothesis, we observed that the expression of the prosurvival TNF receptor type II (TNFR2) (CD120b) but not that of the proapoptotic TNFR1 (CD120a), was significantly higher in early differentiated Tscm and Tcm cells than in the other T cell subpopulations (Figure 2E).

Enrichment of circulating Cit-vimentin-specific CD4+ T cells in Tscm cells in RA patients. We next investigated whether Tscm cells were enriched in putative autoreactive specificities. To this end we exploited a published synthetic epitope derived from Cit-vimentin restricted to HLA-DRB1*04:01 (18,24). Cit-vimentin-specific CD4+ lymphocytes were detected only in HLA-DRB1*04:01-positive RA patients and not in HLA-DRB1*04:01-negative subjects. Additionally, Cit-vimentin-specific CD4+ cells were not detectable in HLA-DRB1*04:01-positive healthy donors. In contrast, CD4+ EBV^{BHFRF1}-specific, HLA-DRB1*04:01-restricted lymphocytes could be quantified in both RA patients and healthy donors (Figures 3A–C). Notably, in RA patients, we observed a trend toward contraction of Cit-vimentin-specific T cells upon anti-TNF treatment.

Within the Cit-vimentin-specific lymphocyte pool, Tscm cells were a major contributor, representing 31% of total antigen-specific T cells, while only 24% of EBV^{BHFRF1}-specific CD4+ T cells displayed a Tscm phenotype (Figure 3C); although, given the limited number of HLA-DRB1*04:01-positive patients, this difference did not reach significance. Interestingly, Cit-vimentin-specific Tscm cells showed a trend toward contraction upon TNF blockade, while EBV^{BHFRF1}-specific T cells did not fluctuate to the same extent (Figures 3D and E).

To explore the potential antigen-specific T cell response to anti-TNF therapy, we analyzed the expression of CD120b and CD120a on both Cit-vimentin-specific and EBV^{BHFRF1}-specific CD4+ T cells for 2 HLA-DRB1*04:01-positive RA patients with active disease and during anti-TNF treatment. We detected a higher frequency of CD120b in Cit-vimentin-specific than in EBV^{BHFRF1}-specific T cells in RA patients with active disease, though the difference was not significant. In contrast, CD120a appeared to be expressed at lower levels in both Cit-vimentin-specific and EBV^{BHFRF1}-specific CD4+ T cells. Although the limited number of samples available did not allow definite conclusions, these data suggest a potential mechanism for antigen-specific T cell response to TNF (Figure 3F).

We also traced the dynamics of viral-specific (EBV_{BMLF-1}, CMV_{pp65}, Flu) CD8+ T cells in 5 HLA-A2-positive RA patients. Most viral-specific CD8+ T cells displayed a more differentiated Tcm or Tem phenotype, and their frequency did not vary upon anti-TNF blockade. These results further support the notion of a selective response of CD4+ T cells, which include Cit-vimentin-specific T cells, to anti-TNF treatment (Supplementary Figures 5A and B, available on the *Arthritis & Rheumatology* web site at <http://onlinelibrary.wiley.com/doi/10.1002/art.41157/abstract>).

Oligoclonal TCR repertoire of CD4+ Tscm cells in RA patients. We sorted circulating CD4+ naïve T cells, Tscm cells, Tcm cells, and Tem cells from 5 RA patients and performed unbiased high-throughput RNA-based TCR sequencing (21). Analysis of third complementarity-determining region (CDR3) clonotype contribution revealed an oligoclonal α and β TCR repertoire in Tscm cells isolated from RA patients, with the 10 most abundant clonotypes accounting for up to 53.7% of the total retrieved CDR3 sequences. In contrast, healthy donor samples revealed an expected highly polyclonal TCR repertoire (Figure 4A). Accordingly, the Shannon index, which measures TCR repertoire richness (i.e., number of different CDR3 clonotypes), confirmed a significant reduction in TCR diversity in the Tscm compartment and not in the other memory subsets (Figure 4B and Supplementary Table 1, available on the *Arthritis & Rheumatology* web site at <http://onlinelibrary.wiley.com/doi/10.1002/art.41157/abstract>). For 2 additional RA patients, we also analyzed CDR3 clonotype richness on sorted memory T cell subpopulations within the first 100 days after anti-TNF administration. We did not observe a normalization of TCR diversity in Tscm cells, suggesting that, in this short timeframe (3 months), anti-TNF treatment induces a normalization in the frequency of circulating Tscm cells, but not in their clonality (Supplementary Figure 6, available on the *Arthritis & Rheumatology* web site at <http://onlinelibrary.wiley.com/doi/10.1002/art.41157/abstract>).

We next characterized CDR3 sequences shared between Tscm cells and at least one other T cell subset. Despite the fact that shared CDR3 sequences were more frequent in healthy donors than in RA patients (data not shown), their relative sequence counts for α and β chains reached 0.27% and 0.55%, respectively, in Tscm from healthy donors, while they accounted for up to 3.34% and 3.11%, respectively, in Tscm cells from RA patients (Figure 4C). This finding further confirmed that Tscm cells from RA patients harbor a skewed TCR repertoire. Taken together, these data highlight Tscm cells from RA patients as a putative reservoir of autoreactive T cell clones, oligoclonally expanded as a consequence of autoantigen recognition.

DISCUSSION

In this study, we showed that RA patients have high frequencies and numbers of circulating Th17-polarized CD4+ Tscm cells,

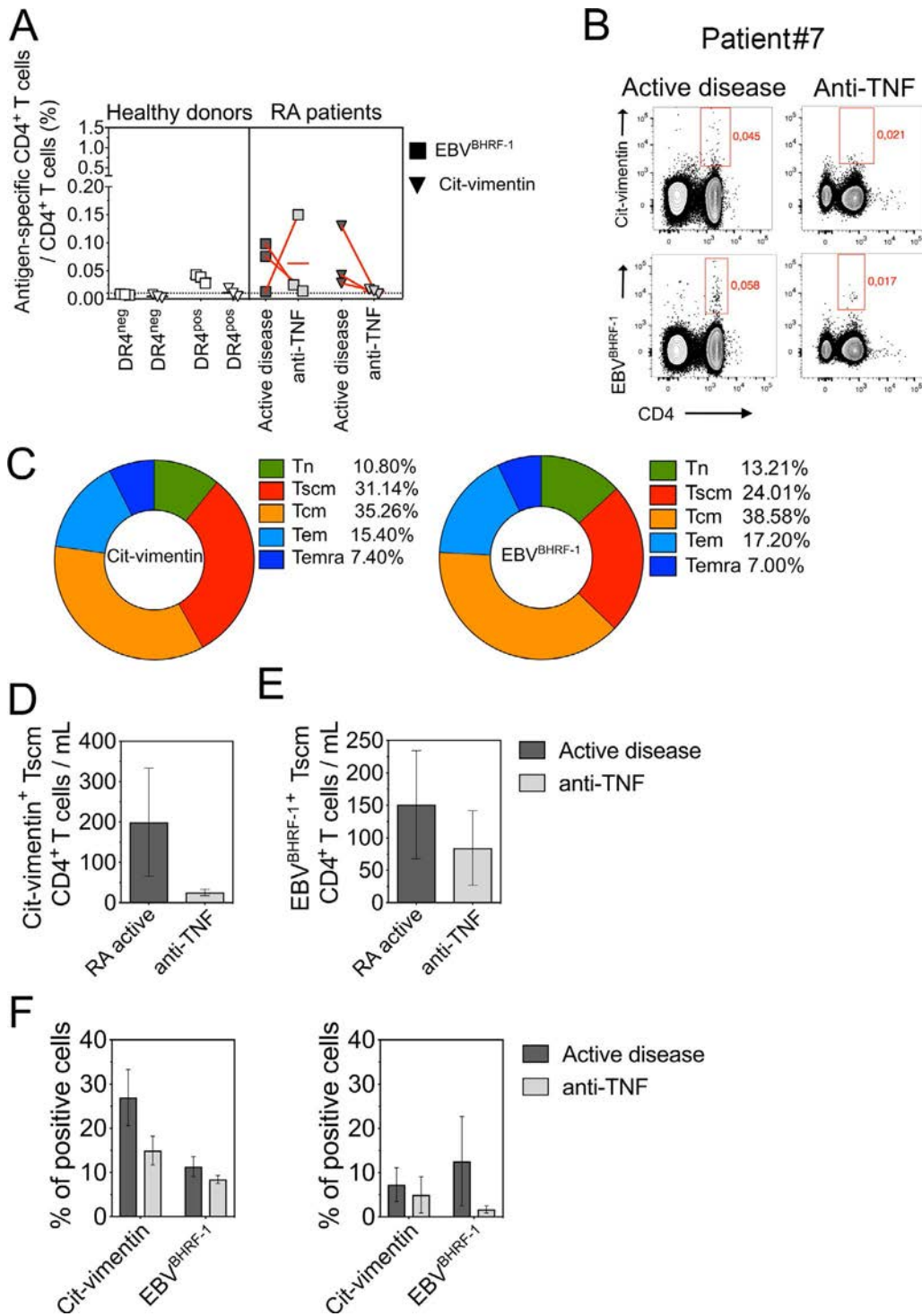


Figure 3. Circulating citrullinated vimentin (Cit-vimentin)-specific CD4⁺ Tscm and Epstein-Barr virus^{BHRF1} (EBV^{BHRF1})-specific CD4⁺ Tscm cells in RA patients. **A**, Frequencies of EBV^{BHRF1}-specific and Cit-vimentin-specific CD4⁺ T cells in HLA-DRB1*04:01-negative (DR4^{neg}) and DRB1*04:01-positive healthy donors and in DRB1*04:01-positive RA patients with active disease and during anti-TNF treatment. **B**, Representative fluorescence-activated cell sorting plots of circulating CD4⁺ antigen-specific T cells from an HLA-DRB1*04:01-positive RA patient with active disease and during anti-TNF treatment. **C**, Distribution of T cell subsets in Cit-vimentin-specific and EBV^{BHRF1}-specific CD4⁺ T cells. **D** and **E**, Absolute numbers of circulating Cit-vimentin-specific (**D**) and EBV^{BHRF1}-specific (**E**) CD4⁺ Tscm cells in RA patients with active disease and during anti-TNF treatment. **F**, Frequencies of Cit-vimentin-specific and EBV^{BHRF1}-specific CD4⁺ T cells expressing CD120b (TNF receptor type II [TNFR2]) or CD120a (TNFR1) in 2 HLA-DRB1*04:01-positive RA patients with active disease and during anti-TNF therapy. In **D-F**, bars show the mean ± SEM. See Figure 1 for other definitions.

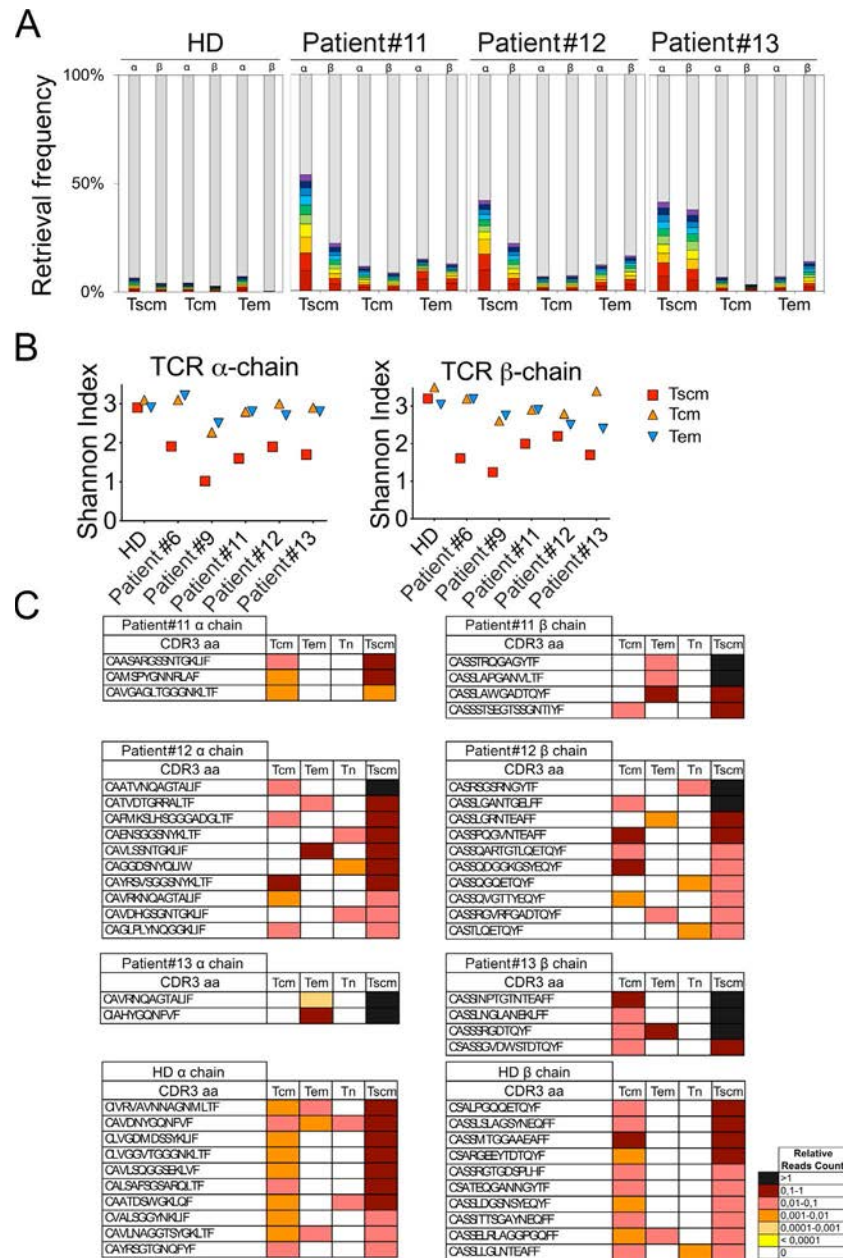


Figure 4. Skewed oligoclonal T cell receptor (TCR) repertoire of CD4⁺ Tscm cells in RA patients. **A**, Composition of the TCR repertoire in 1 healthy donor (HD) and 3 RA patients. Each bar represents an individual third complementarity-determining region (CDR3) amino acid clonotype. Sections shown in color represent the first through tenth most predominant CDR3 sequences, with red indicating the first most predominant and violet indicating the tenth most predominant; gray indicates the remaining sequences identified in the analyzed samples. **B**, Quantification of TCR repertoire richness in the Tscm, Tcm, and Tem cell subsets in a healthy donor and 5 RA patients, calculated using the Shannon Index. **C**, Heatmaps showing CDR3 amino acid (aa) sequences shared between the indicated T cell subpopulations. For patient 12 and the healthy donor, only the 10 shared CDR3 amino acid sequences with the highest relative read counts are shown (the total numbers of shared amino acids were 15 for α -chain and 14 for β -chain for patient 12, and 47 for α -chain and 25 for β -chain for the healthy donor). See Figure 1 for other definitions.

and that Tscm cell accumulation declines early upon TNF blockade. Recently identified, Tscm lymphocytes appear to play important roles across a wide spectrum of clinical conditions, ranging from infectious diseases (25–27), vaccination (7), cancer immunotherapy (1,4), allogeneic HSCT (9,28), and gene therapy (3,5), to adult T cell leukemia (29). While highly desirable in the context of

immunotherapy and infections, it stands to reason that long-lived, self-renewing Tscm cells may be detrimental in T cell-mediated diseases, such as T cell lymphoproliferative dyscrasias or autoimmune diseases, where they may represent a reservoir of long-lived lymphocytes with undesired and detrimental specificities responsible for disease perpetuation. To date, Tscm cells have been reported in

type 1 diabetes mellitus (10,11) and systemic lupus erythematosus (30). The present study is, to our knowledge, the first to demonstrate preferential Tscm cell expansion in patients with RA.

We found that CD4⁺ Tscm lymphocytes were significantly more represented, in terms of both frequencies and absolute numbers, in RA patients than in age-matched healthy controls. However, the extent of Tscm cell expansion did not correlate with disease severity. These results suggest that Tscm cells might contribute to the development and maintenance of RA, while disease activity is reasonably driven by other factors that affect the stimulation or activation status of the overall immune compartment and its interaction with the tissues targeted by the autoimmune attack. Functionally, expanded CD4⁺ Tscm cells displayed a preferential Th17 polarization, which is known to play a pathogenic role in rheumatic synovitis (31,32), thus further corroborating Tscm lymphocytes as potential novel players in RA pathogenesis and maintenance. Notably, we did not find quantitative alterations in the circulating Treg cell pool in our patient cohort, but we cannot exclude functional impairment in the Treg cell compartment as previously described (33).

Interestingly, TNF blockade abated CD4⁺ Tscm cell expansion and restored T cell homeostasis in responder patients at the polyclonal level after a median of 3 months, suggesting that restoration of physiologic circulating Tscm numbers could represent a potential biomarker for response prediction. Unfortunately, we did not have sufficient numbers of nonresponders in our cohort to fully validate Tscm cell decrease upon TNF blockade as a robust biomarker of disease response. Indeed, it would be interesting in future studies to longitudinally track fluctuations in the Tscm cell compartment of responders, inadequate responders, and patients who did not maintain a response not only to anti-TNF agents but also to other biologic therapies, to further define the role of Tscm cells in this context.

In our study, we focused on patients whose disease did not respond to nonbiologic DMARDs and were therefore candidates for TNF blockade, but it would also be relevant to evaluate the influence of first-line nonbiologic DMARDs on the repertoire and frequencies of Tscm cells, to define whether different therapeutic approaches could have a distinct impact on the underlying T cell pathogenic events. We found no significant differences in the expansion or repertoire of Tscm cells between patients who were treated with conventional DMARDs and those who were not, independent of the agent used. However, the apparent lack of effect is difficult to interpret, due to the small size of each group, particularly of the group of untreated patients, and because there were no patients in whom satisfactory clinical control was achieved with conventional DMARDs alone. Further prospective studies that include treatment-naïve patients and longitudinally monitor the possible accumulation and repertoire of Tscm cells will be necessary to address this question.

From a biologic point of view, 2 mechanisms could explain the decrease in Tscm cells upon TNF blockade. First, Tscm lymphocytes might directly benefit from signals emanating from TNF. TNF activates 2 receptors, namely TNFR1 and TNFR2. While TNFR1

preferentially delivers proapoptotic signals by incorporating a death domain in its structure, TNFR2 predominantly acts as a costimulatory molecule on lymphocytes (34). Notably, the expression of the costimulatory TNFR2, but not that of the proapoptotic TNFR1, was significantly higher in early differentiated CD4⁺ Tscm and Tcm cells than in Tem and CD4⁺ naïve T lymphocytes, suggesting that TNF might indeed provide a prosurvival signal to early differentiated Tscm/Tcm cells, possibly including the Cit-vimentin-specific ones, through TNFR2. Alternatively, TNF blockade might exert its beneficial effects by interfering with other cell types supporting Tscm cell expansion, and therefore normalization of Tscm cell frequencies may be only indirectly linked to the normalization of TNF levels. While no experimental data support this latter hypothesis, interesting candidates for intermediate players include activated synovial fibroblasts, which have been shown to produce high levels of interleukin-17 (IL-17), and synovial macrophages, which are responsible for local IL-15 production (35), with both cytokines being instrumental for Tscm generation and maintenance. However, in this hypothesis, it is difficult to reconcile that a local effect of TNF blockade (i.e., at lesion sites) could so dramatically impact the circulating lymphocyte pool, unless the 2 compartments are assumed to be in a state of highly dynamic equilibrium.

Since we hypothesized that Tscm lymphocytes are a reservoir of autoreactive specificities fueling and perpetuating disease, we used HLA class II tetramers to trace and characterize antigen-specific CD4⁺ T cells reactive against a known arthritogenic peptide derived from Cit-vimentin and restricted to the RA-associated HLA class II allele DRB1*0401. In 3 patients carrying the necessary HLA allele, we were able to detect, prior to TNF blockade, Cit-vimentin-specific T cells, which were enriched in Tscm cells compared to the overall CD4⁺ pool. Of note, Cit-vimentin-specific T cells contracted upon TNF blockade in all patients analyzed (albeit the difference did not reach statistical significance). Although these observations need to be confirmed in a larger patient cohort, overall, they suggest that arthritogenic CD4⁺ T cell clones might be susceptible to TNF signaling inhibition. Importantly, preferential curtailment of autoreactive T cells was further corroborated by the absence of fluctuations in the frequencies of viral-specific CD8⁺ T cells.

We next performed TCR sequencing of purified T cell subsets harvested from RA patients with active disease and found that Tscm cells displayed a far more skewed and oligoclonal TCR repertoire than the other memory subsets, further reinforcing the notion that the Tscm cell compartment in RA represents a reservoir of putative autoreactive specificities. These data raise the question of how circulating Tscm cells are linked to the damaged synovial tissue. Early differentiated Tscm cells accumulate selectively in secondary lymphoid organs and appear hierarchically superior to other T cell subsets within a progressive T cell differentiation model (9). In a model of viral infection in nonhuman primates, antigen-specific Tscm cells were found to preferentially localize in lymph nodes, while they were virtually absent in mucosal surfaces (36). Taken together, the results of

the present study and previous studies suggest that Tscm cells identified in the peripheral blood of RA patients might represent the circulating precursors that provide continuous refueling of the more differentiated arthritogenic lymphocytes, such as Tem cells, enriched in the synovia. A longitudinal, as well as cross-sectional, tracking of T cell clonotypes in different anatomic sites might validate this hypothesis. Finally, in future studies, it would be of particular interest to assess whether, in the case of treatment interruption, Tscm cell frequencies would increase again, and whether the reappearing T cell clones within the Tscm cell compartment would be the same prior to treatment.

Overall, our study provides evidence that RA patients harbor an increased circulating CD4+ Tscm cell pool, functionally Th17 polarized, with a skewed TCR repertoire. This CD4+ Tscm cell pool is enriched in arthritogenic clones and declines upon TNF blockade, underscoring the importance of this T cell subset in the pathogenesis and perpetuation of autoimmunity in RA. Additional studies in large patient cohorts are required to validate this finding. Finally, the ongoing revolution in RA therapeutics targeting vulnerable adaptive and downstream cytokine effector pathways will hopefully provide novel avenues for a cure. We envision that Tscm cell clonal composition and dynamics might become useful biomarkers to inform clinicians on the efficacy of and duration of response to novel treatments aimed at the long-sought goal of immunologic homeostasis and drug-free remission in RA.

AUTHOR CONTRIBUTIONS

All authors were involved in drafting the article or revising it critically for important intellectual content, and all authors approved the final version to be published. Dr. Bonini had full access to all of the data in the study and takes responsibility for the integrity of the data and the accuracy of the data analysis.

Study conception and design. Oliveira, Ciceri, Cieri, Bonini.

Acquisition of data. Cianciotti, Ruggiero, Campochiaro, Oliveira, Magnani, Baldini, Tassara, Baldissera, Cieri.



Analysis and interpretation of data. Cianciotti, Ruggiero, Oliveira, Doglio, Manfredi, Ciceri, Cieri, Bonini.

REFERENCES

- Gattinoni L, Lugli E, Ji Y, Pos Z, Paulos CM, Quigley MF, et al. A human memory T cell subset with stem cell-like properties. *Nat Med* 2011;17:1290–7.
- Gattinoni L, Speiser DE, Lichterfeld M, Bonini C. T memory stem cells in health and disease. *Nat Med* 2017;23:18–27.
- Biasco L, Scala S, Basso Ricci L, Dionisio F, Baricordi C, Calabria A, et al. In vivo tracking of T cells in humans unveils decade-long survival and activity of genetically modified T memory stem cells. *Sci Transl Med* 2015;7:273ra13.
- Cieri N, Camisa B, Cocchiarella F, Forcato M, Oliveira G, Provasi E, et al. IL-7 and IL-15 instruct the generation of human memory stem T cells from naive precursors. *Blood* 2013;121:573–84.
- Oliveira G, Ruggiero E, Stanghellini MT, Cieri N, D'Agostino M, Fronza R, et al. Tracking genetically engineered lymphocytes long-term reveals the dynamics of T cell immunological memory. *Sci Transl Med* 2015;7:317ra198.
- Xu Y, Zhang M, Ramos CA, Duret A, Liu E, Dakhova O, et al. Closely related T-memory stem cells correlate with in vivo expansion of CAR-CD19-T cells and are preserved by IL-7 and IL-15. *Blood* 2014;123:3750–9.
- Fuertes-Marraco SA, Soneson C, Cagnon L, Gannon PO, Allard M, Abed Maillard S, et al. Long-lasting stem cell-like memory CD8+ T cells with a naïve-like profile upon yellow fever vaccination. *Sci Transl Med* 2015;7:282ra48.
- Zhang Y, Joe G, Hexner E, Zhu J, Emerson SG. Host-reactive CD8+ memory stem cells in graft-versus-host disease. *Nat Med* 2005;11:1299–305.
- Cieri N, Oliveira G, Greco R, Forcato M, Taccioli C, Cianciotti B, et al. Generation of human memory stem T cells upon haploidentical T-replete hematopoietic stem cell transplantation. *Blood* 2015;125:2865–74.
- Hosokawa K, Muranski P, Feng X, Townsley DM, Liu B, Knickelbein J, et al. Memory stem T cells in autoimmune disease: high frequency of circulating CD8+ memory stem cells in acquired aplastic anemia. *J Immunol* 2016;196:1568–78.
- Vignali D, Cantarelli E, Bordignon C, Canu A, Citro A, Annoni A, et al. Detection and characterization of CD8+ autoreactive memory stem T cells in patients with type 1 diabetes. *Diabetes* 2018;67:936–45.
- McInnes IB, Schett G. Pathogenetic insights from the treatment of rheumatoid arthritis. *Lancet* 2017;389:2328–37.
- Malmström V, Catrina AI, Klareskog L. The immunopathogenesis of seropositive rheumatoid arthritis: from triggering to targeting [review]. *Nat Rev Immunol* 2017;17:60–75.
- Annett FC, Edworthy SM, Bloch DA, McShane DJ, Fries JF, Cooper NS, et al. The American Rheumatism Association 1987 revised criteria for the classification of rheumatoid arthritis. *Arthritis Rheum* 1988;31:315–24.
- Aletaha D, Neogi T, Silman AJ, Funovits J, Felson DT, Bingham CO III, et al. 2010 rheumatoid arthritis classification criteria: an American College of Rheumatology/European League Against Rheumatism collaborative initiative. *Arthritis Rheum* 2010;62:2569–81.
- Prevoe ML, van 't Hof MA, Kuper HH, van Leeuwen MA, van de Putte LB, van Riel PL. Modified disease activity scores that include twenty-eight-joint counts: development and validation in a prospective longitudinal study of patients with rheumatoid arthritis. *Arthritis Rheum* 1995;38:44–8.
- Landais E, Saulquin X, Scotet E, Trautmann L, Peyrat MA, Yates JL, et al. Direct killing of Epstein-Barr virus (EBV)-infected B cells by CD4 T cells directed against the EBV lytic protein BHRF1. *Blood* 2004;103:1408–16.
- Hill JA, Southwood S, Sette A, Jevnikar AM, Bell DA, Cairns E. Cutting edge: the conversion of arginine to citrulline allows for a high-affinity peptide interaction with the rheumatoid arthritis-associated HLA-DRB1*0401 MHC class II molecule. *J Immunol* 2003;171:538–41.
- Jabbari A, Harty JT. Simultaneous assessment of antigen-stimulated cytokine production and memory subset composition of memory CD8 T cells. *J Immunol* 2006;176:161–8.
- Bolotin DA, Mamedov IZ, Britanova OV, Zvyagin IV, Shagin D, Ustyugova SV, et al. Next generation sequencing for TCR repertoire profiling: platform-specific features and correction algorithms. *Eur J Immunol* 2012;42:3073–83.
- Ruggiero E, Nicolay JP, Fronza R, Arens A, Paruzynski A, Nowrouzi A, et al. High-resolution analysis of the human T-cell receptor repertoire. *Nat Commun* 2015;6:8081.
- Bolotin DA, Poslavsky S, Mitrophanov I, Shugay M, Mamedov IZ, Putintseva EV, et al. MiXCR: software for comprehensive adaptive immunity profiling [letter]. *Nat Methods* 2015;12:380–1.
- McInnes IB, Schett G. The pathogenesis of rheumatoid arthritis. *N Engl J Med* 2011;365:2205–19.

24. Snir O, Rieck M, Gebe JA, Yue BB, Rawlings CA, Nepom G, et al. Identification and functional characterization of T cells reactive to citrullinated vimentin in HLA-DRB1*0401-positive humanized mice and rheumatoid arthritis patients. *Arthritis Rheum* 2011;63:2873–83.
25. Buzon MJ, Sun H, Li C, Shaw A, Seiss K, Ouyang Z, et al. HIV-1 persistence in CD4+ T cells with stem cell-like properties. *Nat Med* 2014;20:139–142.
26. Mateus J, Lasso P, Pavia P, Rosas F, Roa N, Valencia-Hernández CA, et al. Low frequency of circulating CD8+ T stem cell memory cells in chronic chagasic patients with severe forms of the disease. *PLoS Negl Trop Dis* 2015;9:e3432.
27. Mpande CA, Dintwe OB, Musvosvi M, Mabwe S, Bilek N, Hatherill M, et al. Functional, antigen-specific stem cell memory (T_{SCM}) CD4+ T cells are induced by human mycobacterium tuberculosis infection. *Front Immunol* 2018;9:324.
28. Roberto A, Castagna L, Zanon V, Bramanti S, Crocchiolo R, McLaren JE, et al. Role of naive-derived T memory stem cells in T-cell reconstitution following allogeneic transplantation. *Blood* 2015;125:2855–64.
29. Nagai Y, Kawahara M, Hishizawa M, Shimazu Y, Sugino N, Fujii S, et al. T memory stem cells are the hierarchical apex of adult T-cell leukemia. *Blood* 2015;125:3527–35.
30. Lee YJ, Park JA, Kwon H, Choi YS, Jung KC, Park SH, et al. Role of stem cell-like memory T cells in systemic lupus erythematosus. *Arthritis Rheumatol* 2018;70:1459–69.
31. Hirota K, Yoshitomi H, Hashimoto M, Maeda S, Teradaira S, Sugimoto N, et al. Preferential recruitment of CCR6-expressing Th17 cells to inflamed joints via CCL20 in rheumatoid arthritis and its animal model. *J Exp Med* 2007;204:2803–12.
32. Van den Berg WB, McInnes IB. Th17 cells and IL-17 A—focus on immunopathogenesis and immunotherapeutics. *Semin Arthritis Rheum* 2013;43:158–70.
33. Nie H, Zheng Y, Li R, Guo TB, He D, Fang L, et al. Phosphorylation of FOXP3 controls regulatory T cell function and is inhibited by TNF- α in rheumatoid arthritis. *Nat Med* 2013;19:322–8.
34. Faustman D, Davis M. TNF receptor 2 pathway: drug target for autoimmune diseases. *Nat Rev Drug Discov* 2010;9:482–93.
35. McInnes IB, Schett G. Cytokines in the pathogenesis of rheumatoid arthritis. *Nat Rev Immunol* 2007;7:429–42.
36. Lugli E, Dominguez MH, Gattinoni L, Chattopadhyay PK, Bolton DL, Song K, et al. Superior T memory stem cell persistence supports long-lived T cell memory. *J Clin Invest* 2013;123:594–99.

Involvement of Tumor Necrosis Factor Receptor Type II in *Foxp3* Stability and as a Marker of Treg Cells Specifically Expanded by Anti-Tumor Necrosis Factor Treatments in Rheumatoid Arthritis

François Santinon,¹ Maxime Batignes,¹ Majda Lyna Mebrek,¹ Jérôme Biton,¹ Gaëlle Clavel,² Roxane Hervé,¹ Delphine Lemeiter,¹ Magali Breckler,¹ Florence Busato,³ Jorg Tost,³  Marianne Zioli,⁴ Marie-Christophe Boissier,⁵ Patrice Decker,¹ Luca Semerano,⁵ and Natacha Bessis¹ 

Objective. To study the involvement of Treg cells expressing tumor necrosis factor receptor type II (TNFR2) in exerting control of inflammation in experimental models and in the response to anti-TNF treatments in patients with rheumatoid arthritis (RA) or spondyloarthritis (SpA).

Methods. The role of TNFR2 in Treg cells was explored using a multilevel translational approach. Treg cell stability was evaluated by analyzing the methylation status of the *Foxp3* locus using bisulfite sequencing. Two models of inflammation (imiquimod-induced skin inflammation and delayed-type hypersensitivity arthritis [DTHA]) were induced in TNFR2^{-/-} mice, with or without transfer of purified CD4+CD25+ cells from wild-type (WT) mice. In patients with RA and those with SpA, the evolution of the TNFR2+ Treg cell population before and after targeted treatment was monitored.

Results. *Foxp3* gene methylation in Treg cells was greater in TNFR2^{-/-} mice than in WT mice (50% versus 36.7%). In cultured Treg cells, TNF enhanced the expression, maintenance, and proliferation of *Foxp3* through TNFR2 signaling. Imiquimod-induced skin inflammation and DTHA were aggravated in TNFR2^{-/-} mice ($P < 0.05$ for mice with skin inflammation and $P < 0.0001$ for mice with ankle swelling during DTHA compared to WT mice). Adoptive transfer of WT mouse Treg cells into TNFR2^{-/-} mice prevented aggravation of arthritis. In patients with RA receiving anti-TNF treatments, but not those receiving tocilizumab, the frequency of TNFR2+ Treg cells was increased at 3 months of treatment compared to baseline (mean \pm SEM 65.2 \pm 3.1% versus 49.1 \pm 5.5%; $P < 0.01$). In contrast, in anti-TNF-treated patients with SpA, the frequency of TNFR2+ Treg cells was not modified.

Conclusion. TNFR2 expression identifies a subset of Treg cells that are characterized by stable expression of *Foxp3* via gene hypomethylation, and adoptive transfer of TNFR2-expressing Treg cells ameliorates inflammation in experimental models. Expansion and activation of TNFR2+ Treg cells may be one of the mechanisms by which anti-TNF agents control inflammation in RA, but not in SpA.

INTRODUCTION

Tumor necrosis factor (TNF) is a potent proinflammatory cytokine involved in the initiation, coordination, and perpetuation of

inflammation and the immune response (1). TNF exerts its effects by binding to 2 cell-membrane TNF receptors (TNFRs), TNFR1 (p55) and TNFR2 (p75) (2). Anti-TNF agents are effective in a broad spectrum of chronic inflammatory diseases such as rheumatoid

Supported by unrestricted research grants from Pfizer (within the Projet Passerelle 2016), Sandoz, the French Society for Rheumatology, and the Institut Fédératif de Recherche Biomédicale of Paris 13 University.

¹François Santinon, PhD, Maxime Batignes, PhD, Majda Lyna Mebrek, MSc, Jérôme Biton, PhD, Roxane Hervé, PhD, Delphine Lemeiter, Magali Breckler, PhD, Patrice Decker, PhD, Natacha Bessis, PhD: INSERM UMR 1125, Université Sorbonne Paris Cité, and Université Paris 13, Bobigny, France; ²Gaëlle Clavel, MD, PhD: INSERM UMR 1125, Université Sorbonne Paris Cité, Université Paris 13, and Fondation Adolphe De Rothschild, Paris, France; ³Florence Busato, MSc, Jorg Tost, PhD: Commissariat à l'énergie atomique et aux énergies alternatives, Evry, France; ⁴Marianne Zioli, MD, PhD: Hôpital Jean-Verdier, AP-HP, Bondy, INSERM UMR 1162, Université Paris Descartes, and Université Paris Diderot, Paris, France; ⁵Marie-Christophe Boissier, MD, PhD, Luca Semerano, MD, PhD: INSERM UMR 1125, Université Sorbonne

Paris Cité, Université Paris 13, Hôpital Avicenne, Hôpital Jean-Verdier, Hôpital René-Muret, and AP-HP, Bobigny, France.

Dr. Batignes and Ms Mebrek contributed equally to this work.

Dr. Boissier has received speaking fees from Novartis, Eli Lilly, and Peptinov (less than \$10,000 each) and research support from Diacurate. Dr. Semerano has received consulting fees, speaking fees, and/or honoraria from Bristol-Myers Squibb, MSD, Pfizer, and Roche-Chugai (less than \$10,000 each) and research support from Pfizer. No other disclosures relevant to this article were reported.

Address correspondence to Natacha Bessis, PhD, Université Paris 13 Université Sorbonne Paris Cité, INSERM UMR 1125, 1 Rue de Chablais, 93000 Bobigny, France. E-mail: natacha.bessis@univ-paris13.fr.

Submitted for publication January 17, 2019; accepted in revised form October 8, 2019.

arthritis (RA), spondyloarthritis (SpA), inflammatory bowel disease, and psoriasis (3–6).

Besides its well-characterized proinflammatory role, TNF also exerts antiinflammatory and immunosuppressive effects (7). Administration of TNF delays the recurrence of diabetes in non-obese diabetic mice (8) and ameliorates lupus in NZB/NZW mice (9), but anti-TNF agents aggravate multiple sclerosis (10).

Most of the proinflammatory effects of TNF are generally considered to be mediated by TNFR1 (11), whereas the immunosuppressive effects of TNF are considered to be mediated by TNFR2 (12). In particular, the antiinflammatory effects of TNF may be dependent on its ability to activate and expand TNFR2-expressing Treg cells (13–15). Treg cells are essential in the control of a variety of immune responses, including allergy, autoimmunity, inflammation, and tumor immunity. Treg cells play a vital role in tolerance to self and are defective in a number of human autoimmune diseases, including RA (16). Moreover, expression of TNFR2 in the joints has been shown to exert a physiologic role in the resolution of inflammation (17). We and others have shown that anti-TNF biologic agents restore the suppressive capacities of Treg cells in a TNF-dependent arthritis model (13) and in RA patients (18). In this context, Nguyen et al recently showed in vitro that adalimumab, an anti-TNF monoclonal antibody, but not the receptor fusion protein etanercept, binds to membrane TNF on RA monocytes and promotes Treg cell expansion via enhanced TNFR2 signaling (19). This result is of paramount interest because it suggests that anti-TNF treatments may block the proinflammatory activity of TNF while, in the meantime, promoting its immunosuppressive properties.

To further characterize TNFR2-positive Treg cells and their involvement in the control of inflammation and response to treatment, we adopted a multilevel translational approach. We first studied the effect of TNFR2 in vitro on Treg cell survival and *Foxp3* methylation, and then explored the effect of TNFR2 deletion in vivo in 2 experimental models of inflammation. Finally, we longitudinally followed up the evolution of TNFR2-positive Treg cell subpopulations during anti-TNF treatments both in patients with RA and in patients with spondyloarthritis (SpA).

MATERIALS AND METHODS

Patients and healthy donors. Individuals meeting the American College of Rheumatology/European League Against Rheumatism (EULAR) revised criteria for RA (20) and qualifying for biologic treatment were selected. Eligible participants were required to have either a Disease Activity Score in 28 joints (DAS28) of ≥ 3.2 (21) or evidence of erosive disease on imaging regardless of the DAS28 score. Seventeen participants starting anti-TNF treatment (8 with etanercept, 5 with infliximab, 2 with golimumab, 1 with adalimumab, and 1 with certolizumab) (mean \pm SD age 56.8 ± 12.4 years [range 29–72 years], mean \pm SD disease duration 15.5 ± 8.3 years [range 2–32 years]; 16 female,

1 male) and 6 participants starting tocilizumab (mean \pm SD age 60.3 ± 13.3 years [range 39–73 years], mean \pm SD disease duration 7 ± 5.2 years [range 2–13 years]; 3 female, 3 male) were recruited. All treatments were administered according to the label dosing recommendation. According to the EULAR response criteria (22), good responders were defined as those who had a decrease in the DAS28 of >1.2 points, moderate responders were those with a decrease in DAS28 of 0.6–1.2 points, and nonresponders were those with a stable increase or decrease in DAS28 of <0.6 points.

We also recruited 20 individuals fulfilling the Assessment of SpondyloArthritis international Society criteria for axial or peripheral SpA (23) who were starting anti-TNF treatment (4 with etanercept, 9 with infliximab, 1 with adalimumab, 2 with certolizumab pegol, and 4 with golimumab) (mean \pm SD age 50 ± 12.6 years [range 36–84 years], mean \pm SD disease duration 13.8 ± 13.3 years [range 12–60 years]; 11 female, 9 male). According to the EULAR recommendations, patients with SpA received anti-TNF treatment if the Bath Ankylosing Spondylitis Disease Activity Index (BASDAI) was >40 (24) or if they needed daily treatment with nonsteroidal antiinflammatory drugs independent of the BASDAI score. Individuals were considered to be responders if they experienced a decrease in the BASDAI score of below 40 (of 100).

All patients underwent 2 blood sample collections: 1 before the first biologic treatment administration, and the second after 3 months of treatment (at the time of first clinical response evaluation). The study was approved by the local ethics committee (CPP Paris Ile de France, approval no. NI-2016-11-01), and informed consent was obtained from all patients before study entry.

In addition, blood samples (stored in EDTA) from random healthy individuals, obtained from a blood bank in Bobigny, France, were used for in vitro culture experiments.

Mice. Homozygous TNFR2^{-/-} mice were generated by crossing wild-type (WT) C57BL/6 mice (Janvier) and TNFR1^{-/-}/TNFR2^{-/-} double-deficient mice (generated and kindly provided by Dr. Muazzam Jacobs) (25). We obtained TNFR1^{+/+}/TNFR2^{-/-} mice and TNFR1^{-/-}/TNFR2^{+/+} mice, but did not obtain any TNFR1^{-/-}/TNFR2^{+/+} mice. The TNFR1^{+/+}/TNFR2^{-/-} mice and the TNFR1^{-/-}/TNFR2^{+/+} mice were simply renamed as TNFR2^{-/-} mice and TNFR1^{-/-} mice, respectively. The genotypes of the different mouse strains were confirmed by polymerase chain reaction (PCR) analysis of tail biopsy specimens (the primer sequences used are available from the corresponding author upon request). TNFR2^{-/-} mice and TNFR1^{-/-} mice were crossed, bred, and housed in our animal facility (agreement no. C93-008-01).

In some experiments, we used 6–12-week-old mice belonging to the C57BL/6 strain (purchased from Janvier). All procedures were approved by the Animal Care and Use Committee of the Paris 13 University and the Charles Darwin National Animal Ethics Committee.

Animal models of inflammation. *Generation of imiquimod-induced psoriasis-like skin inflammation in mice.* Details regarding the induction and evaluation of psoriasis in an animal model of imiquimod-induced psoriasis-like skin inflammation are available from the corresponding author upon request.

Induction and assessment of delayed-type hypersensitivity arthritis (DTHA) in mice. On day -7 , 10-week-old C57BL/6 mice were injected intradermally at the base of the tail with 250 μg methylated bovine serum albumin (mBSA) emulsified in complete Freund's adjuvant (CFA; Difco). Four days later (day -3), the mice received 200 μg anti-mouse type II collagen antibody cocktail (Chondrex), containing the clones A2-10 (IgG2a), F10-21 (IgG2a), D8-6 (IgG2a), D1-2G (IgG2b), and D2-112 (IgG2b), intravenously in 100 μl phosphate buffered saline (PBS) (26). On day 0, mice were challenged with 200 μg mBSA subcutaneously in 20 μl PBS in the left hind foot pad. The right hind foot pad received 20 μl PBS only and was used as a control.

On day 0 just before mBSA challenge, thicknesses of the left paw and left ankle were measured using an electronic caliper (Mitutoyo) (baseline measurement). Subsequently, paw and ankle swelling was measured, with results expressed as the difference in the thickness of the left paw or ankle compared to the baseline measurement.

Histologic changes in the paws were assessed on sections stained with hematoxylin and eosin and Safranin O. The extra-articular infiltration of inflammatory cells and arthritic changes (each scored on a scale of 0–3) were assessed separately. Arthritic changes were assessed on the ankle and tarsal joints, including scores for synovitis, cartilage destruction, and bone erosion. The sum score of histologic features was the mean of the 4 scores (extraarticular infiltration, synovitis, cartilage destruction, and bone erosion).

Cell preparation and flow cytometry. Details on the preparation of cells and tissue samples and the staining of mouse and human cells for flow cytometry, as well as the purification of lymphocytes, are available from the corresponding author upon request.

Adoptive Treg cell transfer experiments and assessment of Treg cell effects. CD4+CD25+ cells in splenocytes obtained from 12 naive mice were purified by magnetic separation. A total of 7×10^5 purified cells (95% purity) was transferred by retro-orbital injection (100 μl) into the left foot pad of 11 TNFR1I $^{-/-}$ mice 2 days before mBSA challenge. Control TNFR1I $^{-/-}$ mice or WT littermate mice (each $n = 12$) received PBS instead. Details on the in vitro culture of cells and measurement of Treg cell proliferation and viability are available from the corresponding author upon request.

CD4+CD25 $-$ effector T (Teff) cells and CD4+CD25+ Treg cells were purified from the spleens of mice with DTHA at the time of euthanasia (details available from the corresponding

author upon request). Teff cells were pre-labeled with 5 mM 5,6-carboxyfluorescein succinimidyl ester (CFSE; Invitrogen) for 10 minutes at 37°C. CFSE-labeled Teff cells (1×10^5) were cocultured in flat-bottomed 96-well plates with Treg cells (1×10^5) (ratio 1:1) in RPMI 1640 with 10% fetal calf serum, 100 units/ml penicillin, 100 mg/ml streptomycin, 50 mM 2-mercaptoethanol, 1M HEPES, and 5 $\mu\text{g}/\text{ml}$ soluble anti-CD3 (clone 2C11; BD Biosciences). Controls were non-CFSE-labeled Teff cells (1×10^5) instead of Treg cells. Antigen-presenting cells (1×10^5 splenocytes from naive C57BL/6 mice) that had been previously treated with mitomycin (50 $\mu\text{g}/\text{ml}$) for 45 minutes at 37°C were added to the culture medium. Cells were then incubated at 37°C in an atmosphere of 5% CO $_2$. After 3 days of culture, the cells were stained with allophycocyanin-labeled anti-CD4 antibody (clone RM4-5; BioLegend) and the proliferation of Teff cells was determined by flow cytometry, to measure CFSE dilution. Data were analyzed using BD FACSDiva software (BD Biosciences).

DNA methylation analysis by pyrosequencing.

Genomic DNA was extracted from purified CD4+CD25+ or CD4+CD25 $-$ cells using an All Prep DNA/RNA mini kit (Qiagen). Quantitative DNA methylation analysis involved pyrosequencing bisulfite-treated DNA (27). DNA (650 ng to 1 μg) was bisulfite-converted using an EpiTect 96 Fast Bisulfite kit (Qiagen) according to the manufacturer's instructions.

The Treg-specific demethylated region (TSDR) of *Foxp3* was amplified using 30 ng bisulfite-treated mouse genomic DNA and 5 pmoles forward and reverse primers, 1 of which was biotinylated (details on the sequences of the oligonucleotides used for PCR amplification and pyrosequencing are available from the corresponding author upon request). Reaction conditions comprised 1 \times HotStarTaq buffer supplemented with 1.6 mM MgCl $_2$, 400 μM dNTPs, and 1.8 units HotStarTaq polymerase (Qiagen) in a 25- μl volume. The PCR program consisted of a denaturing step of 15 minutes at 95°C followed by 50 cycles of 30 seconds at 95°C, 30 seconds at 61°C, and 15 seconds at 72°C, with a final extension of 5 minutes at 72°C. An amount of 10–15 μl PCR product was rendered single-stranded using a previously described method (27), and 4 pmoles of the respective sequencing primer was used for analysis.

Quantitative DNA methylation analysis was carried out on a PyroMark Q24 Advanced system with a PyroMark Q24 Advanced CpG reagent kit (Qiagen). The results were analyzed using PyroMark Q24 Advanced software version 3.0.0.

Statistical analysis. Data distribution was preliminarily checked for normality with the Kolmogorov-Smirnov test. For in vitro and in vivo experiments, according to data distribution and number of groups, a parametric test (analysis of variance [ANOVA], *t*-test) or nonparametric test (Kruskal-Wallis, Mann-Whitney test) was used. For comparison of data in some of the

cell culture experiments, two-way ANOVA was used. For the study of patient-specific parameters (disease activity scores, Treg cell frequency) before and after biologic treatment, a paired *t*-test (Wilcoxon's test) was used. For differences between groups, *P* values less than 0.05 were considered statistically significant. Data are presented as the mean ± SEM. Statistical analyses were performed with GraphPad Prism software version 6.0.

RESULTS

Maintenance of *Foxp3* expression and Treg cell proliferation by TNF in vitro through TNFR11, but not TNFR1, signaling. To assess the effect of TNF on the maintenance of *Foxp3* expression, we evaluated the impact of exogenous TNF on purified Treg cells stimulated with soluble anti-CD3 and anti-CD28 antibodies. Alone, T cell receptor and costimulation signals were not sufficient to maintain *Foxp3* expression after 72 hours

of culture. In contrast, the addition of TNF partly restored the expression of *Foxp3*, exhibiting a dose-response effect, as previously described (15). Moreover, TNF decreased the frequency of CD39+ Treg cells, but not CTLA-4+ Treg cells, with a dose-dependent effect (details available from the corresponding author upon request).

We then investigated whether the effect of TNF on Treg cells was mediated by TNFR11, and not TNFR1, using anti-TNFR1 or anti-TNFR11 neutralizing antibodies. TNF-induced *Foxp3* expression was abolished by anti-TNFR11 antibodies, but not by anti-TNFR1 antibodies (Figures 1A and B).

To determine whether TNF exerts its effect only by preventing the loss of *Foxp3* expression or whether it also can induce Treg cell proliferation, we used a CFSE-labeling assay to assess Treg cells from WT or TNFR11^{-/-} mice. Following stimulation of WT mouse Treg cells with TNF for 96 hours, we observed that TNF induced a stronger proliferation of Treg cells as compared to cells in culture with only anti-CD3 and anti-CD28 monoclonal antibodies

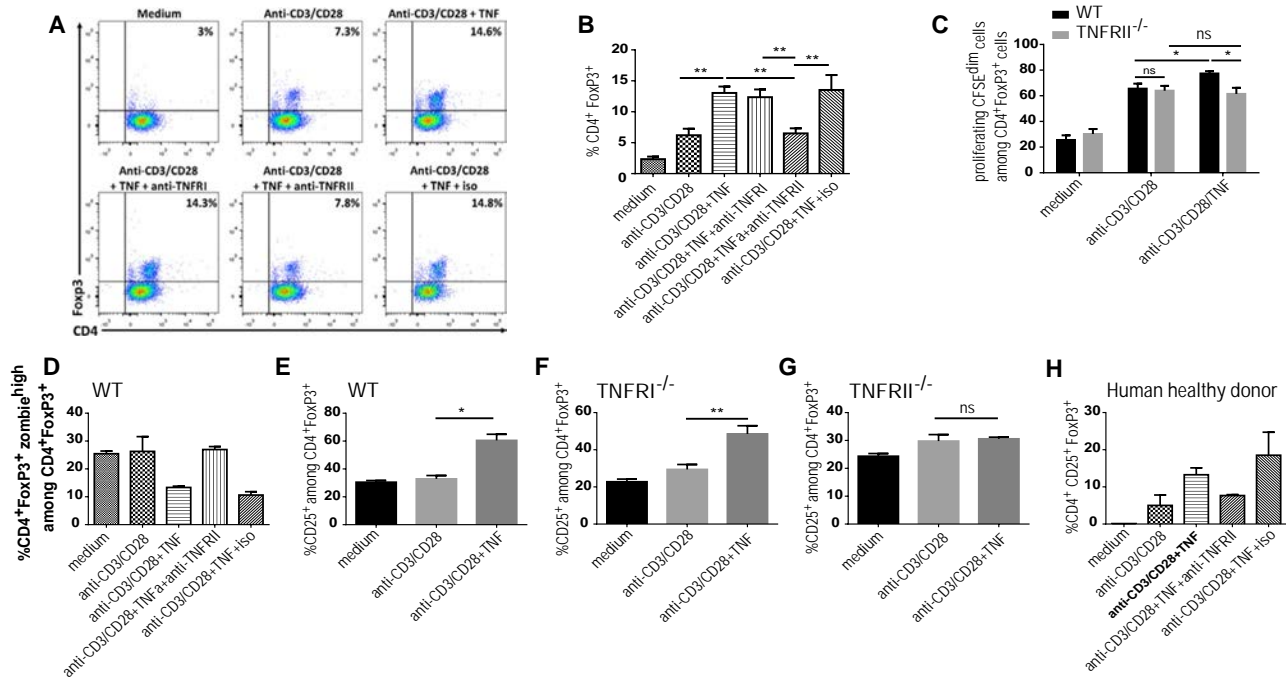


Figure 1. Effect of tumor necrosis factor (TNF) on cultured mouse and human Treg cells. CD4+CD25+ cells were purified from the spleens of wild-type (WT), TNF receptor type I-deficient (TNFR1^{-/-}), and TNFR11^{-/-} mice, and CD4+CD25+CD127⁻ cells were purified from healthy human donor peripheral blood mononuclear cells (PBMCs). In some cases, cells were labeled with 5,6-carboxyfluorescein succinimidyl ester (CFSE). Cells were cultured for 72 hours (A, B, and D–H) or 96 hours (C) with anti-CD3 and anti-CD28 antibodies in the presence of 20 ng/ml recombinant murine TNF (A–G) or with 400 ng/ml recombinant human TNF (H). In some experiments, 10 µg/ml anti-mouse TNFR1 or TNFR11 monoclonal antibodies (A, B, and D) or 40 µg/ml anti-human TNFR11 monoclonal antibodies (H) were added, with isotype (iso) used as a control. A, Representative dot plots of CD4+FoxP3+ cell frequency among total cells. B, CD4+FoxP3+ cell frequency among total cells. Data were pooled from 3 independent experiments. C, Percentage of proliferating CFSE^{dim} cells among CD4+FoxP3+CFSE+ cells. D, Frequency of dead cells (zombie^{high}) among CD4+FoxP3+ cells. E–G, Frequency of CD25+ cells among CD4+FoxP3+ cells in WT (E), TNFR1^{-/-} (F), and TNFR11^{-/-} (G) mice. H, Frequency of CD4+FoxP3+CD25+ cells among total cells in healthy human PBMCs. In D, CD4+CD25+ cells were purified from the spleens pooled from 2 WT mice. Data are representative of 2 independent experiments, each with similar results. In H, Treg cells were purified from PBMCs of 1 healthy donor. Data are representative of 3 individuals, each with similar results. Results in B–H are the mean ± SEM. * = *P* < 0.05; ** = *P* < 0.01, by one-way analysis of variance (ANOVA) with Tukey's post hoc test for multiple comparisons (B and E–G) or two-way ANOVA (C). NS = not significant.

(Figure 1C). Moreover, this TNF-induced Treg cell proliferation was mediated by TNFR11, as indicated by the lack of increase in CFSE^{dim} Treg cell frequency in TNFR11^{-/-} mice (Figure 1C). TNF also protected Treg cells against death, since the frequency of zombie^{high} cells among CD4+Foxp3+ cells was decreased in WT mice (Figure 1D).

In addition, TNF stimulation modified the expression of CD25 by Treg cells, as shown by the induction of an almost doubling of the CD25+ Treg cell proportion by TNF (Figure 1E). Again, this effect was mediated by TNFR11, since it occurred in Treg cells from WT and TNFR11^{-/-} mice only (Figure 1F) but not in Treg cells from TNFR11^{-/-} mice (Figure 1G).

Of note, TNF induced CD25 expression by Treg cells (Figure 1E) and also increased interleukin-2 (IL-2)-induced CD25 and STAT5 phosphorylation in Treg cells (results available from the corresponding author upon request). Subsequently, we confirmed that TNF also sustained the expression of *Foxp3*

in human Treg cells through a TNFR11-dependent pathway (Figure 1H).

Facilitation of TSDR demethylation, a driver of *Foxp3* stability, by TNFR11.

Treg cells with stable suppressive functions are characterized by an unmethylated *Foxp3* TSDR and stable expression of *Foxp3* (28). Because, as discussed above, TNFR11 affected the maintenance of *Foxp3* expression and the proliferative ability of Treg cells, we investigated the effect of deletion of TNFR11 on the methylation of the TSDR site. In isolated CD4+CD25- Teff cells, which served as a control, the proportion of *Foxp3* methylation was 95.4%, as compared to 36.7% in isolated CD4+CD25+ Treg cells (Figure 2A).

We therefore compared the methylation state of the *Foxp3* TSDR of freshly isolated CD4+CD25+ Treg cells from WT and TNFR11^{-/-} mice and in various culture conditions. The

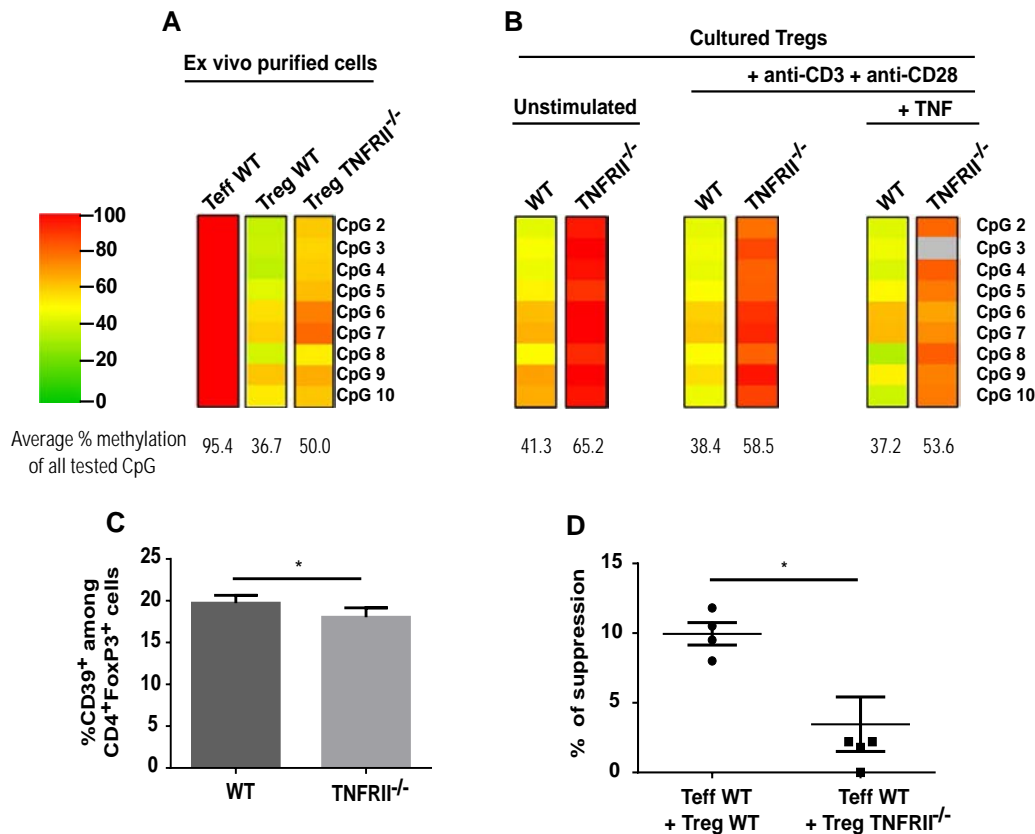


Figure 2. Methylation of the Treg-specific demethylated region and characterization of Treg cells in WT and TNFR11^{-/-} mice. **A** and **B**, Genomic DNA was extracted from CD4+CD25+ cells isolated from WT and TNFR11^{-/-} mouse spleens (**A**) or from Treg cells obtained from WT and TNFR11^{-/-} mice and cultured for 72 hours under the indicated conditions (**B**). In **A**, DNA from CD4+CD25- effector T (Teff) cells isolated from WT mouse spleens served as a control. Amplicons are subdivided by horizontal lines, each representing an individual CpG motif. The methylation status of individual CpG motifs is color coded according to the degree of methylation at that site. The color code ranges from green (0% methylation) to red (100% methylation). Because of sequencing problems, the CpG motif 3 in TNFR11^{-/-} Treg cells cultured with anti-CD3 and anti-CD28 antibodies and stimulated with TNF appears in gray (**B**). Results are representative of 1 of 2 independent experiments. **C**, The frequency of CD39+ cells among CD4+FoxP3+ cells in WT and TNFR11^{-/-} mice was determined by fluorescence-activated cell sorting analysis. Results are the mean \pm SEM of 5 mice per group. **D**, The suppressive effect of CD4+CD25+ Treg cells from WT or TNFR11^{-/-} mice on the proliferation of WT mouse CD4+CD25- Teff cells was determined. Symbols show individual mice ($n = 5$ per group); horizontal lines with bars show the mean \pm SEM. * = $P < 0.05$ by unpaired 2-tailed *t*-test (**C**) or Mann-Whitney test (**D**). See Figure 1 for other definitions. Color figure can be viewed in the online issue, which is available at <http://onlinelibrary.wiley.com/doi/10.1002/art.41134/abstract>.

methylation proportion in the *Foxp3* TSDR was higher in Treg cells ex vivo from TNFR11^{-/-} mice than in those from WT mice (50% versus 36.7%) (Figure 2A). This difference was even more pronounced in cultured cells, especially on unstimulated Treg cells (41.3% in WT mouse Treg cells versus 65.2% in TNFR11^{-/-} mouse Treg cells) (Figure 2B). These data suggest that TNFR11 expression is essential for optimal *Foxp3* TSDR demethylation, and the findings highlight the involvement of TNFR11 in the stabilization of *Foxp3* expression. Of note, greater TSDR methylation in TNFR11^{-/-} mouse Treg cells compared to WT mouse Treg cells was associated with a reduced capacity to inhibit Teff cell proliferation (Figure 2D) and a lower expression of CD39⁺ Treg cells (Figure 2C), whereas the expression of CTLA-4 in Treg cells was similar between the 2 groups (data not shown).

Aggravated skin inflammation in the presence of TNFR11 deficiency in a mouse model of psoriasis. To assess the role of TNFR11 in the development of in vivo inflammation, we first evaluated the effect of TNFR11 deficiency in a short-lasting model of inflammation, namely imiquimod-induced psoriasis. Disease was aggravated in TNFR11^{-/-} mice compared to WT mice (Figures 3A–F). The score of inflammatory cell infiltration was the

most affected factor (Figure 3D), and epidermal thickness, quantified on skin histology slides, was also higher in TNFR11^{-/-} mice compared to WT mice (Figures 3E and F), in accordance with the findings from the clinical analysis.

We then investigated the involvement of Treg cells in the exacerbated skin inflammation observed in TNFR11^{-/-} mice. The frequencies and numbers of Treg cells were decreased in the spleens and lymph nodes (LNs) of TNFR11^{-/-} mice as compared to WT mice (Figures 3G and H), and this was associated with a reduced intensity of *FoxP3* expression (results available from the corresponding author upon request).

With regard to Treg cell activation and/or functionality markers, the proportion of Treg cells expressing CD39 was significantly lower in TNFR11^{-/-} mice than in WT mice, whereas the frequency of CTLA-4⁺ Treg cells was unchanged. Of note, the frequencies and numbers of CD8⁺Foxp3⁺ Treg cells were also lower in TNFR11^{-/-} mice than in WT mice. Moreover, the frequency of CD4⁺IFN γ ⁺ Th1 cells was lower in the spleens of TNFR11^{-/-} mice compared to WT mice. Local skin cell analysis revealed that the frequency of CD45⁺ leukocytes was higher in TNFR11^{-/-} mice than in WT mice, which was related to an increased proportion of F4/80⁺ macrophages, whereas the frequency of CD3⁺ T lymphocytes was comparable between

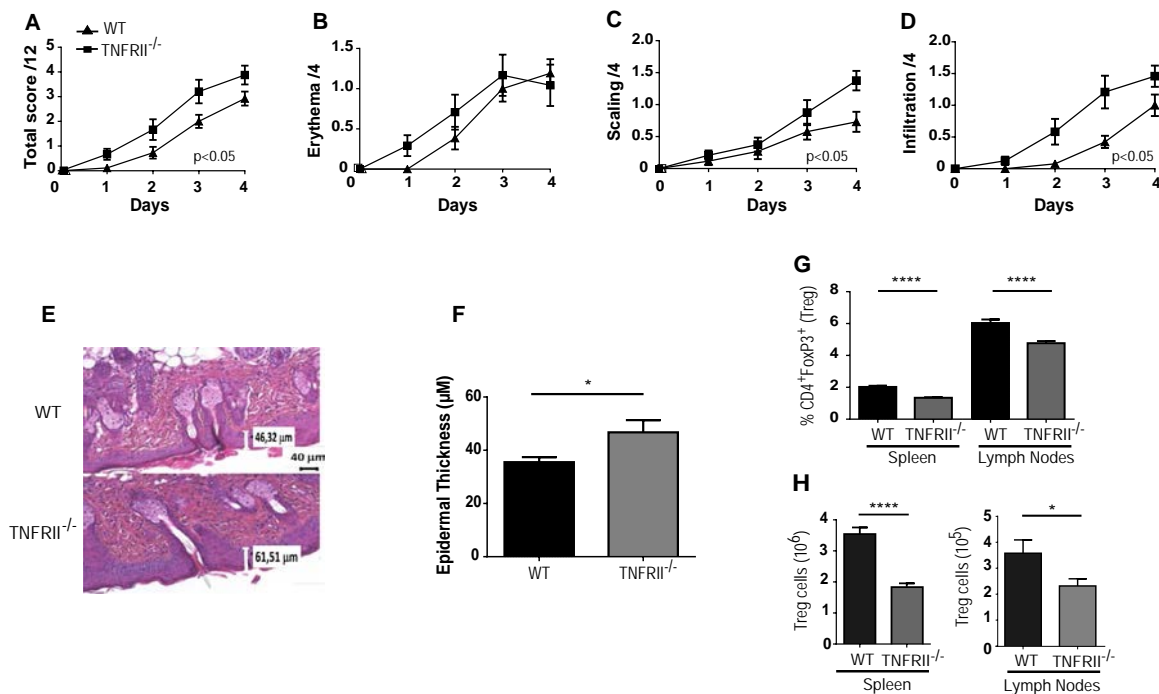


Figure 3. Aggravation of imiquimod-induced skin inflammation in TNFR11^{-/-} mice. Imiquimod cream was applied daily to the skin of TNFR11^{-/-} mice (n = 12) and WT mice (n = 13). **A–D**, The extent of erythema, scales, and infiltration of the back skin was scored daily on a scale of 0–4 (**B–D**), along with calculation of a cumulative score for all 3 features (**A**). **E** and **F**, Epidermal thickness was measured on histology slides of the skin on day 5. In **E**, representative skin samples are shown (original magnification $\times 20$). In **F**, the epidermal thickness was measured in TNFR11^{-/-} and WT mice (n = 8 mice per group). **G** and **H**, Fluorescence-activated cell sorting analysis was used to determine the frequency (**G**) and numbers (**H**) of CD4⁺FoxP3⁺ Treg cells among whole splenocytes and lymph nodes of WT and TNFR11^{-/-} mice on day 5 of skin inflammation. Data are representative of 3 independent experiments. All results are the mean \pm SEM. * = $P < 0.05$; **** = $P < 0.0001$, by Student's *t*-test for area under the curve in each mouse (**A–D**) or by unpaired 2-tailed *t*-test (**F–H**). See Figure 1 for definitions. Color figure can be viewed in the online issue, which is available at <http://onlinelibrary.wiley.com/doi/10.1002/art.41134/abstract>.

the 2 groups (results available from the corresponding author upon request).

Restoration of aggravated experimental arthritis to a normal level in TNFR11^{-/-} mice after adoptive transfer of WT mouse Treg cells. We assessed the effect of TNFR11 deficiency on the development of DTHA in mice. Arthritis developed in all mice of both the WT and TNFR11^{-/-} genotypes as soon as day 1 after administration of mBSA boost in the foot pad, which is usual in the DTHA model (26). Arthritis was aggravated in TNFR11^{-/-} mice, as indicated by a significant increase in both ankle and tarsus swelling compared to that in WT mice (Figures 4A and B). Accordingly, the maximum ankle swelling and maximum tarsus swelling were both higher in TNFR11^{-/-} mice than in WT mice (Figures 4C and D).

Histopathologic analyses were performed to assess the extent of inflammation and cartilage and bone destruction in the mice (26). The sum score of histologic features was higher in TNFR11^{-/-} mice than in WT mice (Figures 4E and F), thus confirming the findings from clinical evaluation.

The frequency of CD4⁺FoxP3⁺ Treg cells was similar in the spleens and LNs of WT and TNFR11^{-/-} mice on day 0. On day 2, the mean Treg cell frequency was lower in TNFR11^{-/-} mice than in WT mice (left LN, mean \pm SEM 1.61 \pm 0.29% versus 2.27 \pm

0.26% [$P < 0.02$]; right LN, 1.75 \pm 0.05% versus 2.05 \pm 0.1% [$P < 0.05$]).

We then evaluated the impact of TNFR11 deficiency on Treg cell suppressive functions. We found that the capacity to inhibit the proliferation of Teff cells was lower for TNFR11^{-/-} mouse Treg cells than for WT mouse Treg cells (Figure 4G).

To assess the role of Treg cell deficiency in the exacerbation of DTHA in TNFR11^{-/-} animals, we evaluated the capacity of WT mouse Treg cells to protect TNFR11^{-/-} mice against arthritis. CD4⁺CD25⁺ cells were purified from the spleens of WT mice and transferred into TNFR11^{-/-} mice at 5 days after immunization with mBSA/CFA. We repeatedly confirmed that more than 90% of the purified CD4⁺CD25⁺ cells expressed *Foxp3*. Thus, CD4⁺CD25⁺ cell transfer can be considered a transfer of Treg cells. As expected, adoptive transfer of WT mouse Treg cells significantly attenuated arthritis as compared to that in TNFR11^{-/-} mice receiving only PBS (Figures 5A–D).

Increased frequency of TNFR11-expressing Treg cells in patients with RA, but not in patients with SpA, during anti-TNF treatment. Some anti-TNF agents have been suggested to promote the immunosuppressive activities of TNF, and therefore we studied the evolution of TNFR11-deficient Treg cells in

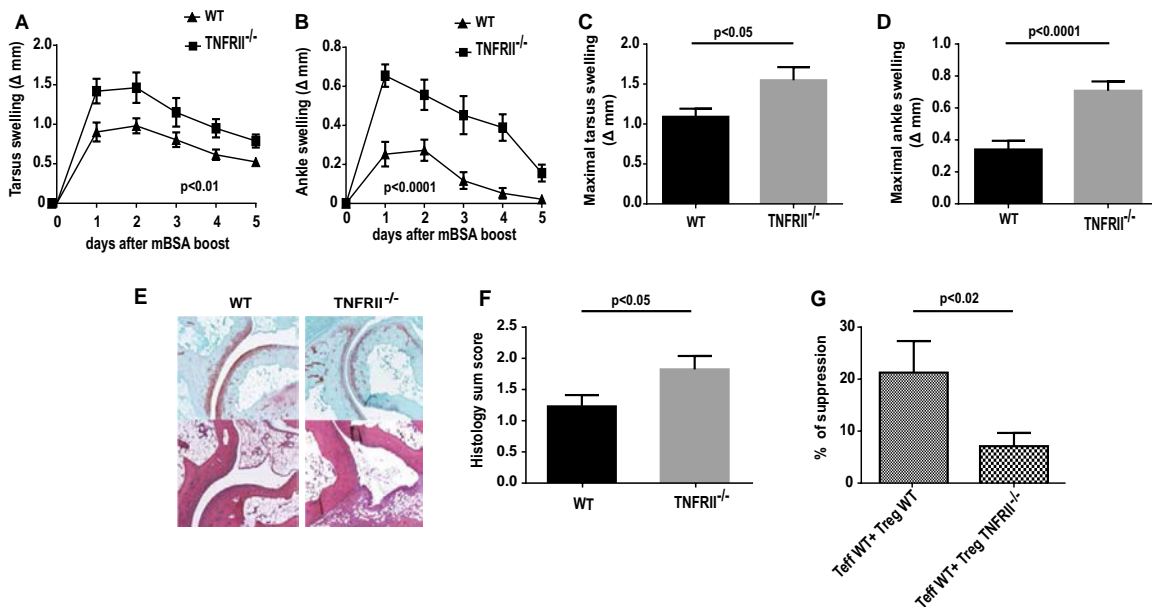


Figure 4. Exacerbation of arthritis in TNFR11^{-/-} mice. Delayed-type hypersensitivity arthritis was induced in WT mice ($n = 15$) and TNFR11^{-/-} mice ($n = 13$). **A–D**, Swelling of the tarsus (**A**) and ankle (**B**) over the duration of the study was examined, and the maximal tarsus (**C**) and ankle (**D**) swelling during the disease course was calculated for each individual mouse. **E**, Ankle and tarsal joints were assessed for histologic changes on day 7 by staining paw sections with Safranin O (upper panels) and hematoxylin and eosin (lower panels). Samples from a representative WT control mouse and TNFR11^{-/-} mouse are shown. **F**, The mean sum score of histologic features was calculated to assess the extent of extraarticular infiltration of inflammatory cells and arthritic changes (synovitis, cartilage destruction, and bone erosion) (score scale 0–3). **G**, The suppressive effect of CD4⁺CD25⁺ cells from WT or TNFR11^{-/-} mice ($n = 8$ randomly chosen mice per group) on the proliferation of WT mouse CD4⁺CD25⁻ effector T (Teff) cells was determined. Results are the mean \pm SEM. In **A–F**, data are representative of 1 of 2 experiments, each yielding similar results. P values were determined by unpaired 2-tailed t -test (**A–D** and **F**) or by Mann-Whitney test (**G**). mBSA = methylated bovine serum albumin (see Figure 1 for other definitions). Color figure can be viewed in the online issue, which is available at <http://onlinelibrary.wiley.com/doi/10.1002/art.41134/abstract>.

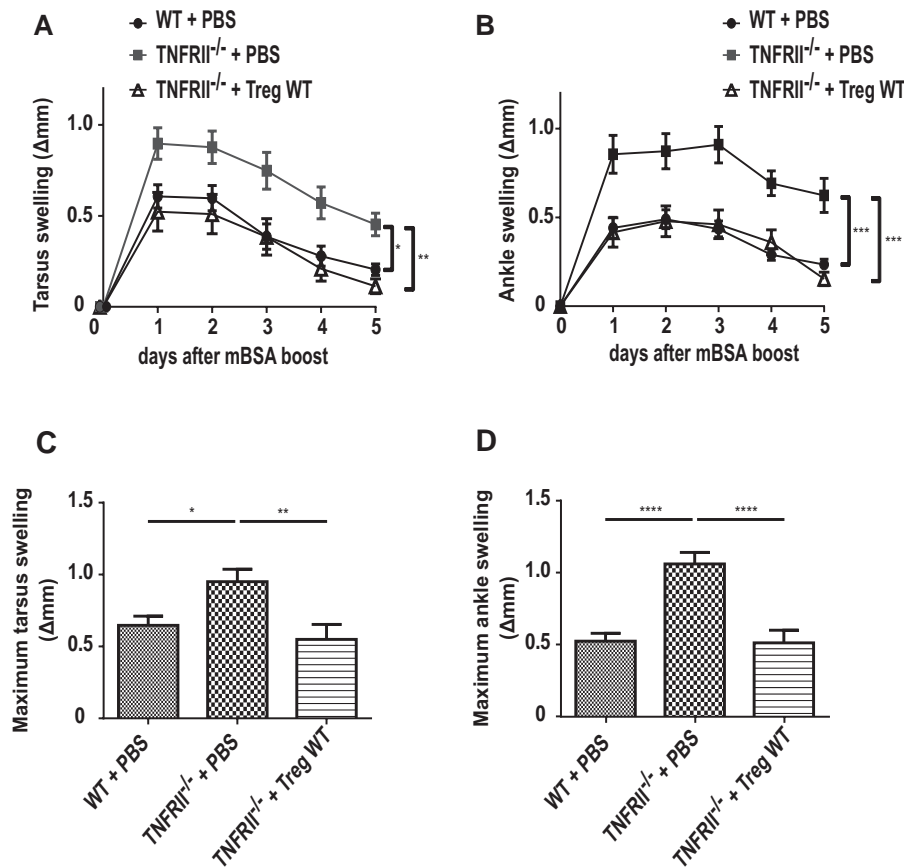


Figure 5. Adoptive transfer of CD4+CD25+ WT mouse Treg cells attenuates arthritis in TNFR11^{-/-} mice. Delayed-type hypersensitivity arthritis (DTHA) was induced in WT mice (n = 12) and TNFR11^{-/-} mice (n = 23). CD4+CD25+ cells (7×10^6) from WT mice without DTHA were intravenously transferred to TNFR11^{-/-} mice (n = 11) at 5 days after subcutaneous immunization with methylated bovine serum albumin (mBSA)/complete Freund's adjuvant; control TNFR11^{-/-} mice with DTHA (n = 12) received only phosphate buffered saline (PBS). Boost mBSA/PBS was administered in the foot pad 2 days later in all mice. Swelling of the tarsus (**A**) and ankle (**B**) was examined over the duration of the study, and maximal tarsus (**C**) and ankle (**D**) swelling during the disease course for each individual mouse was calculated. Results are the mean \pm SEM. * = $P < 0.05$; ** = $P < 0.02$; *** = $P < 0.01$; **** = $P < 0.001$, by one-way analysis of variance (ANOVA) for the area under the curve for each mouse (**A** and **B**) or by one-way ANOVA (**C** and **D**). See Figure 1 for other definitions.

patients with either RA or SpA who had received anti-TNF agents. After 3 months of treatment, anti-TNF-treated patients with RA showed a significantly increased frequency of peripheral blood Treg cells among CD4+ T cells (Figure 6A), more specifically, the TNFR11-positive subpopulation (mean \pm SEM $65.2 \pm 3.1\%$ versus $49.1 \pm 5.5\%$ at baseline; $P < 0.01$) (Figure 6B).

Of the 17 treated patients with RA, 2 were classified as nonresponders, 1 had stable low disease activity, 9 were good responders, and 5 were moderate responders (Figure 6C). We found no clear association between the clinical response and the modified Treg cell frequency or the expression of TNFR11 by Treg cells (data not shown); nevertheless, the number of nonresponders was probably too low to detect a difference. Importantly, the fold increase in TNFR11+ Treg cell frequency did not differ between individuals who received etanercept (n = 8) and those who received anti-TNF monoclonal antibody (n = 9) (mean \pm SEM $1.92 \pm 0.53\%$ versus $1.58 \pm 0.25\%$ from baseline to month 3).

In patients with RA who received tocilizumab, the Treg cell frequency was significantly increased at 3 months of treatment (Figure 6K), with a specific increase in the subpopulation of Treg cells expressing CD39 (Figure 6L), which confirms our previous results (29). Importantly, TNFR11+ Treg cells were not affected by tocilizumab treatment (Figure 6M), which suggests that the increase in this Treg cell subpopulation in patients with RA may be specific to TNF inhibitors.

In patients with SpA, anti-TNF treatment was not associated with a significant modification in either the percentage or frequency of Treg cells expressing TNFR11 (Figures 6F and G). The clinical response in patients with SpA was variable (Figure 6H) and was not associated with Treg cell frequency (data not shown).

DISCUSSION

TNFR11+ Treg cells are a highly suppressive subpopulation of Treg cells that are expanded by anti-TNF monoclonal antibody treatment in RA. Among other findings, our novel data show that

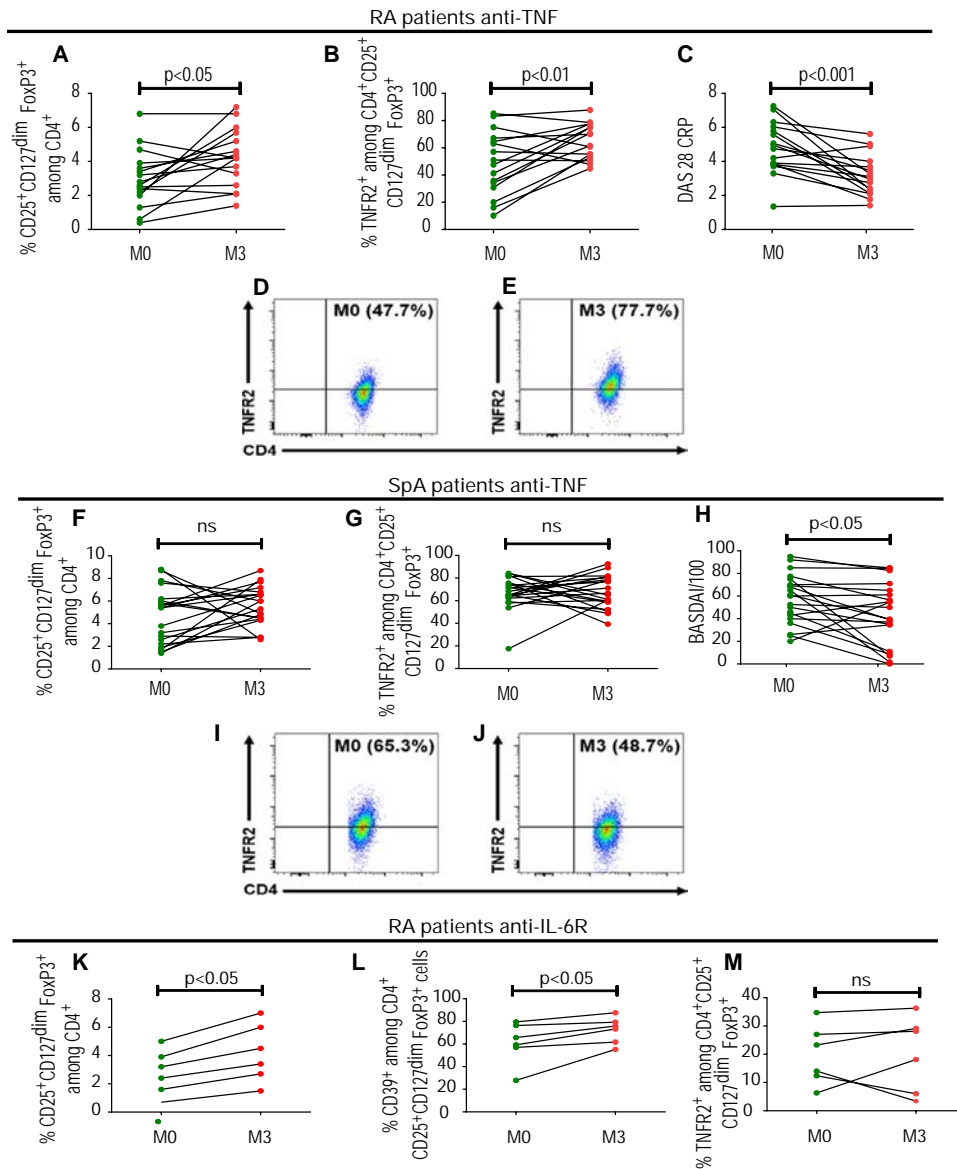


Figure 6. Evolution of peripheral blood Treg cell subpopulations from patients with rheumatoid arthritis (RA) or patients with spondyloarthritis (SpA) after treatment with anti-tumor necrosis factor (anti-TNF) or anti-interleukin-6 receptor (anti-IL-6R). Flow cytometry was used to analyze cells at baseline (M0) and at 3 months (M3) after anti-TNF treatment (etanercept $n = 8$, infliximab $n = 5$, golimumab $n = 2$, adalimumab $n = 1$, certolizumab $n = 1$) of patients with RA ($n = 16$) or patients with SpA ($n = 20$) (**A–J**) or after tocilizumab treatment of patients with RA ($n = 6$) (**K–M**). Analyses determined the percentage of Treg cells (CD4⁺CD25⁺FoxP3⁺CD127^{dim}) (**K–M**) among CD4⁺ cells (**A**, **F**, and **K**), TNF receptor type II-positive (TNFRII⁺) cells among Treg cells (**B**, **G**, and **M**), and CD39⁺ cells among Treg cells (**L**) from RA or SpA patients, and also determined the different degrees of clinical response to treatment according to the Disease Activity Score in 28 joints (DAS28) (**C**) and the Bath Ankylosing Spondylitis Disease Activity Index (BASDAI) (**H**). Representative dot plots show the frequency of TNFRII⁺ cells among Treg cells in RA patients (**D** and **E**) or SpA patients (**I** and **J**) at baseline (**D** and **I**) and 3 months (**E** and **J**) after treatment initiation. Details on the gating strategy are available from the corresponding author upon request. Each dot linked by a black line represents an individual patient. P values were determined by Wilcoxon's paired t -test. NS = not significant. Color figure can be viewed in the online issue, which is available at <http://onlinelibrary.wiley.com/doi/10.1002/art.41134/abstract>.

this phenomenon in RA is not restricted to monoclonal antibodies but is common to the entire class of anti-TNF agents. Conversely, this Treg cell subpopulation is not affected by anti-TNF treatment in patients with SpA, another disease that responds to TNF blockade. This work also integrates multilevel data that support the relevance of TNFRII⁺ Treg cells in the control of inflammation, by

showing that the adoptive transfer of TNFRII⁺ Treg cells is sufficient to ameliorate experimental arthritis. Furthermore, our data demonstrate, for the first time, an epigenetic change that may underlie the suppressive capacity of this Treg cell subset.

Consistent with previous studies in mice and humans, we showed that TNF protected against the loss of *Foxp3* expression

and induced the proliferation of Treg cells via TNFR11 *in vitro* (14,15). Moreover, TNF–TNFR11 signaling was associated with enhanced expression of CD25 (the α subunit of IL-2 receptor) by Treg cells in mice. Because Treg cells coexpressing CD25 and TNFR11 were found to be the most suppressive Treg cell subpopulation both in mice (30) and in humans (31), we aimed to determine whether this membrane phenotype is linked to the expression of the master Treg cell transcription factor *Foxp3*. Indeed, how TNFR11 signaling mediates *Foxp3* expression, and thus Treg cell stability, is unclear. Treg cell stability is regulated by numerous microenvironment inputs, including transcriptional and epigenetic programs and posttranslational modifications (32). In our study, we showed that TNFR11 expression was associated with TSDR hypomethylation and, consequently, increased Treg cell stability.

We further showed that TNF induced CD25 expression in Treg cells and also increased IL-2–induced CD25 and STAT5 phosphorylation in Treg cells. Phosphorylated STAT5 binds to demethylated CNS2, which contains the TSDR (33) and thus may stabilize *Foxp3* expression, leading to the high suppressive activity of Treg cells (34). On another note, the STAT5/STAT3 balance controls the fate of CD4+ T cells. A predominance of phospho-STAT5 leads to the proliferation of Treg cells, whereas higher STAT3 levels trigger Th17 cell differentiation (35). Thus, increased levels of CD25 and phospho-STAT5 may up-regulate Treg cell proliferation in the presence of IL-2 and may decrease Th17 cell differentiation within a control loop of TNF-mediated inflammation.

After establishing the connection between membrane TNFR11 and *Foxp3* expression, we wanted to study the functional relevance of TNFR11 signaling on Treg cells in the control of inflammation. Our results showed an exacerbation of skin inflammation and arthritis in TNFR11^{-/-} mice. It should be noted that, although the collagen-induced arthritis (CIA) model is a more appropriate mouse model for RA, we used the DTHA model in our study. Indeed, TNFR11^{-/-} mice belong to the C57BL/6 strain, but the incidence and severity of CIA are low in this strain (36). The antiinflammatory role of TNF signaling via TNFR11 has also been demonstrated in other disorders, such as experimental allergic encephalomyelitis (37,38), TNF-induced arthritis (39), allergic airway inflammation (40), and *Mycobacterium tuberculosis* infection (25). However, TNFR11 signaling can also mediate proinflammatory signals, as has been shown in a model of colitis (41), central nervous system–induced inflammation (42), experimental cerebral malaria (43), idiopathic pneumonia syndrome (44), smoke-induced pulmonary inflammation (45), and experimental glomerulonephritis (46).

This apparent discrepancy in the role of TNF raises the question as to which TNFR11-expressing cell type responds to TNF. In this study, we used adoptive transfer of WT mouse Treg cells to TNFR11^{-/-} mice, which ameliorated the experimental arthritis. This finding suggests an antiinflammatory effect of TNF via TNFR11 on Treg cells. The relevance of TNFR11 signaling on Treg cells was shown in other experimental models. In graft-versus-host disease, a blocking antibody against TNFR11 abolished the disease

control exerted by Treg cells (47), whereas TNFR11 agonists could protect against graft-versus-host disease (48) and ameliorate CIA by promoting Treg cell expansion (49). TNFR11 expression in other immunomodulatory cells, such as myeloid-derived suppressor cells (MDSCs), could also be associated with protection against inflammation, because TNFR11^{-/-} mouse MDSCs are less suppressive (50,51). Thus, the pro- and antiinflammatory effects of TNFR11 signaling features a delicate balance depending on the cell type involved. Although the actions of TNF via TNFR11 can expand Treg cells and confer higher suppressive effects to MDSCs, the same does not apply to all cells. Nonmyeloid cells expressing TNFR11, such as endothelial cells, can mediate an inflammatory signal upon stimulation with TNF (43). Eventually, TNFR11 expression by T_H17 cells is essential for full development of experimental colitis (52).

Although TNF boosts Treg cell expansion and function via TNFR11, anti-TNF monoclonal antibodies also restore Treg cell function in RA (18,53) and in experimental arthritis (13). The apparent paradox that both TNF and anti-TNF treatments can boost Treg cells suggests that, at least in some circumstances, anti-TNF treatments may block the proinflammatory activity of TNF while preserving, or even promoting, its antiinflammatory action.

Because TNFR11 is crucial for TNF-mediated Treg cell expansion, we assessed whether and how TNFR11+ Treg cells are modified by anti-TNF biologic treatments in RA and SpA. In patients with RA, we observed an increased frequency of TNFR11+ Treg cells from day 0 up to 3 months of anti-TNF treatment. Thus effect on TNFR11+ Treg cells may be treatment-specific, because tocilizumab did not affect this specific cell subpopulation. Consistent with our previous results (29), we observed an increase in the frequency of Treg cells expressing CD39 in patients receiving tocilizumab treatment. This finding suggests that, in the same disease, different targeted treatments may modulate different subsets of Treg cells. In contrast, the effect of anti-TNF treatments on Treg cells may be, at least in part, disease-specific, because we showed for the first time that these treatments had no effect on total Treg cells or TNFR11+ subpopulations in patients with SpA. Thus, anti-TNF treatments may exert their therapeutic effect by activating different mechanisms of immune regulation depending on the treated condition.

Nguyen et al showed that adalimumab, but not etanercept, expanded Treg cells *in vitro* in RA patients who were considered treatment responders (19). Adalimumab binds to membrane TNF on RA monocytes to promote Treg cell expansion via enhanced TNFR11 signaling (19). In that work, only adalimumab, and not etanercept, was associated with an expansion of Treg cells *in vivo*. In our study, all anti-TNF agents, including etanercept, induced an expansion of Treg cells and TNFR11+ Treg cells as compared to the baseline levels. This discrepancy may be explained by the fact that we longitudinally evaluated the evolution of Treg cell frequency by studying each patient before and after treatment, as their own control. This approach is justified by the fact that the baseline Treg cell frequency, and more importantly, the propor-

tion of TNFR1I1-expressing Treg cells, is highly variable between individual patients. Therefore, the frequency of these cells must be compared before and after treatment, within each patient. This approach may have allowed us to detect subtle differences in the evolution of Treg cell subpopulations that may not have been detected if we had compared the final Treg cell frequency in patients after treatment with different anti-TNF agents. This result suggests that mechanisms other than the up-regulation of membrane TNF on monocytes may be involved in etanercept-mediated Treg cell expansion. Indeed, anti-TNF monoclonal antibodies and etanercept may both induce Treg cell expansion via different mechanisms that remain to be explored.

A major limitation of this study is that the number of patients with RA who did not respond to anti-TNF treatment was too low to assess any correlations between the TNFR1I1+ Treg cell modifications and clinical response. These data are critical to establish the real importance of TNFR1I1+ Treg cell expansion in the proper response to anti-TNF treatment in RA.

TNFR1I1 signaling may be an interesting potential therapeutic target in RA. However, given the complexity of TNFR1I1 signaling on other cell types, such as conventional T cells or endothelial cells, further studies are needed to dissect the TNFR1I1-dependent pathways in those cells involved in the resolution of inflammation in autoimmune diseases such as RA.

ACKNOWLEDGMENTS

We thank Sonia Varela (animal facilities, University of Paris 13, Paris, France) for outstanding technical assistance, and Laura Smales for critically proofreading the manuscript.

AUTHOR CONTRIBUTIONS

All authors were involved in drafting the article or revising it critically for important intellectual content, and all authors approved the final version to be published. Dr. Bessis had full access to all of the data in the study and takes responsibility for the integrity of the data and the accuracy of the data analysis.


Study conception and design. Biton, Boissier, Decker, Semerano, Bessis. **Acquisition of data.** Santinon, Batignes, Mebrek, Biton, Clavel, Hervé, Lemeiter, Breckler, Busato, Tost, Zioli, Boissier, Decker, Semerano, Bessis. **Analysis and interpretation of data.** Santinon, Batignes, Mebrek, Biton, Clavel, Tost, Boissier, Decker, Semerano, Bessis.

REFERENCES

- Kalliolias GD, Ivashkiv LB. TNF biology, pathogenic mechanisms and emerging therapeutic strategies. *Nat Rev Rheumatol* 2016;12:49–62.
- Rothe J, Gehr G, Loetscher H, Lesslauer W. Tumor necrosis factor receptors: structure and function. *Immunol Res* 1992;11:81–90.
- Deng Y, Chang C, Lu Q. The inflammatory response in psoriasis: a comprehensive review. *Clin Rev Allergy Immunol* 2016;50:377–89.
- Sieper J, van der Heijde D, Dougados M, Mease PJ, Maksymowych WP, Brown MA, et al. Efficacy and safety of adalimumab in patients with non-radiographic axial spondyloarthritis: results of a randomised placebo-controlled trial (ABILITY-1). *Ann Rheum Dis* 2013;72:815–22.
- Suenaert P, Bulteel V, Lemmens L, Noman M, Geypens B, Van Assche G, et al. Anti-tumor necrosis factor treatment restores the gut barrier in Crohn's disease. *Am J Gastroenterol* 2002;97:2000–4.
- Zampeli E, Vlachoyiannopoulos PG, Tzioufas AG. Treatment of rheumatoid arthritis: unraveling the conundrum. *J Autoimmun* 2015;65:1–18.
- Liu J, Marino MW, Wong G, Grail D, Dunn A, Bettadapura J, et al. TNF is a potent anti-inflammatory cytokine in autoimmune-mediated demyelination. *Nat Med* 1998;4:78–83.
- Rabinovitch A, Suarez-Pinzon WL, Sorensen O, Rajotte RV, Power RF. TNF- α down-regulates type 1 cytokines and prolongs survival of syngeneic islet grafts in nonobese diabetic mice. *J Immunol* 1997;159:6298–303.
- Jacob CO, McDevitt HO. Tumour necrosis factor- α in murine autoimmune 'lupus' nephritis [letter]. *Nature* 1988;331:356–8.
- Kemanetzoglou E, Andreadou E. CNS demyelination with TNF- α blockers. *Curr Neurol Neurosci Rep* 2017;17:36.
- Rickard JA, Anderton H, Etemadi N, Nachbur U, Darding M, Peltzer N, et al. TNFR1-dependent cell death drives inflammation in Sharpin-deficient mice. *Elife* 2014;3:e03464.
- Fischer R, Proske M, Duffey M, Stangl H, Martinez GF, Peters N, et al. Selective activation of tumor necrosis factor receptor II induces antiinflammatory responses and alleviates experimental arthritis. *Arthritis Rheumatol* 2018;70:722–35.
- Biton J, Semerano L, Delavallée L, Lemeiter D, Laborie M, Grouard-Vogel G, et al. Interplay between TNF and regulatory T Cells in a TNF-driven murine model of arthritis. *J Immunol* 2011;186:3899–910.
- Chen X, Bäuml M, Männel DN, Howard OM, Oppenheim JJ. Interaction of TNF with TNF receptor type 2 promotes expansion and function of mouse CD4+CD25+ T regulatory cells. *J Immunol* 2007;179:154–61.
- Chen X, Wu X, Zhou Q, Howard OM, Netea MG, Oppenheim JJ. TNFR2 is critical for the stabilization of the CD4+Foxp3+ regulatory T cell phenotype in the inflammatory environment. *J Immunol* 2013;190:1076–84.
- Behrens F, Himsel A, Rehart S, Stanczyk J, Beutel B, Zimmermann SY, et al. Imbalance in distribution of functional autologous regulatory T cells in rheumatoid arthritis. *Ann Rheum Dis* 2007;66:1151–6.
- McCann FE, Perocheau DP, Ruspi G, Blazek K, Davies ML, Feldmann M, et al. Selective tumor necrosis factor receptor I blockade is antiinflammatory and reveals immunoregulatory role of tumor necrosis factor receptor II in collagen-induced arthritis. *Arthritis Rheumatol* 2014;66:2728–38.
- Ehrenstein MR, Evans JG, Singh A, Moore S, Warnes G, Isenberg DA, et al. Compromised function of regulatory T cells in rheumatoid arthritis and reversal by anti-TNF α therapy. *J Exp Med* 2004;200:277–85.
- Nguyen DX, Ehrenstein MR. Anti-TNF drives regulatory T cell expansion by paradoxically promoting membrane TNF–TNF–RII binding in rheumatoid arthritis. *J Exp Med* 2016;213:1241–53.
- Aletaha D, Neogi T, Silman AJ, Funovits J, Felson DT, Bingham CO III, et al. 2010 rheumatoid arthritis classification criteria: an American College of Rheumatology/European League Against Rheumatism collaborative initiative. *Arthritis Rheum* 2010;62:2569–81.
- Prevo ML, van't Hof MA, Kuper HH, van Leeuwen MA, van de Putte LB, van Riel PL. Modified disease activity scores that include twenty-eight-joint counts: development and validation in a prospective longitudinal study of patients with rheumatoid arthritis. *Arthritis Rheum* 1995;38:44–8.
- Van Gestel AM, Prevo ML, van't Hof MA, van Rijswijk MH, van de Putte LB, van Riel PL. Development and validation of the European League Against Rheumatism response criteria for rheumatoid arthritis: comparison with the preliminary American College of Rheumatology

- and the World Health Organization/International League Against Rheumatism criteria. *Arthritis Rheum* 1996;39:34–40.
23. Rudwaleit M, van der Heijde D, Landewé R, Akkoc N, Brandt J, Chou CT, et al. The Assessment of SpondyloArthritis international Society classification criteria for peripheral spondyloarthritis and for spondyloarthritis in general. *Ann Rheum Dis* 2010;70:25–31.
 24. Garrett S, Jenkinson T, Kennedy LG, Whitelock H, Gaisford P, Calin A. A new approach to defining disease status in ankylosing spondylitis: the Bath Ankylosing Spondylitis Disease Activity Index. *J Rheumatol* 1994;21:2286–91.
 25. Keeton R, Allie N, Dambuza I, Abel B, Hsu NJ, Sebesho B, et al. Soluble TNFRp75 regulates host protective immunity against *Mycobacterium tuberculosis*. *J Clin Invest* 2014;124:1537–51.
 26. Atkinson SM, Usher PA, Kvist PH, Markholst H, Haase C, Nansen A. Establishment and characterization of a sustained delayed-type hypersensitivity model with arthritic manifestations in C57BL/6J mice. *Arthritis Res Ther* 2012;14:R134.
 27. Tost J, Gut IG. DNA methylation analysis by pyrosequencing. *Nat Protoc* 2007;2:2265–75.
 28. Polansky JK, Kretschmer K, Freyer J, Floess S, Garbe A, Baron U, et al. DNA methylation controls *Foxp3* gene expression. *Eur J Immunol* 2008;38:1654–63.
 29. Thiolat A, Semerano L, Pers YM, Biton J, Lemeiter D, Portales P, et al. Interleukin-6 receptor blockade enhances CD39+ regulatory T cell development in rheumatoid arthritis and in experimental arthritis. *Arthritis Rheumatol* 2014;66:273–83.
 30. Chen X, Subleski JJ, Kopf H, Howard OM, Männel DN, Oppenheim JJ. Cutting edge: expression of TNFR2 defines a maximally suppressive subset of mouse CD4+CD25+FoxP3+ T regulatory cells—applicability to tumor-infiltrating T regulatory cells. *J Immunol* 2008;180:6467–71.
 31. Chen X, Subleski JJ, Hamano R, Howard OM, Wiltrot RH, Oppenheim JJ. Co-expression of TNFR2 and CD25 identifies more of the functional CD4+FOXP3+ regulatory T cells in human peripheral blood. *Eur J Immunol* 2010;40:1099–106.
 32. Lu L, Barbi J, Pan F. The regulation of immune tolerance by FOXP3 [review]. *Nat Rev Immunol* 2017;17:703–17.
 33. Rainbow DB, Yang X, Burren O, Pekalski ML, Smyth DJ, Klarqvist MD, et al. Epigenetic analysis of regulatory T cells using multiplex bisulfite sequencing. *Eur J Immunol* 2015;45:3200–3.
 34. Alvarez Salazar EK, Cortés-Hernández A, Alemán-Muench GR, Alberú J, Rodríguez-Aguilera JR, Recillas-Targa F, et al. Methylation of FOXP3 TSDR underlies the impaired suppressive function of Tregs from long-term belatacept-treated kidney transplant patients. *Front Immunol* 2017;8:219.
 35. Laurence A, Tato CM, Davidson TS, Kanno Y, Chen Z, Yao Z, et al. Interleukin-2 signaling via STAT5 constrains T helper 17 cell generation. *Immunity* 2007;26:371–81.
 36. Bessis N, Decker P, Assier E, Semerano L, Boissier MC. Arthritis models: usefulness and interpretation. *Semin Immunopathol* 2017;39:469–86.
 37. Madsen PM, Motti D, Karmally S, Szymkowski DE, Lambertsens KL, Bethea JR, et al. Oligodendroglial TNFR2 mediates membrane TNF-dependent repair in experimental autoimmune encephalomyelitis by promoting oligodendrocyte differentiation and remyelination. *J Neurosci* 2016;36:5128–43.
 38. Tsakiri N, Papadopoulos D, Denis MC, Mitsikostas DD, Kollias G. TNFR2 on non-haematopoietic cells is required for Foxp3+ Treg-cell function and disease suppression in EAE. *Eur J Immunol* 2012;42:403–12.
 39. Blüml S, Binder NB, Niederreiter B, Polzer K, Hayer S, Tauber S, et al. Antiinflammatory effects of tumor necrosis factor on hematopoietic cells in a murine model of erosive arthritis. *Arthritis Rheum* 2010;62:1608–19.
 40. Li XM, Chen X, Gu W, Guo YJ, Cheng Y, Peng J, et al. Impaired TNF/TNFR2 signaling enhances Th2 and Th17 polarization and aggravates allergic airway inflammation. *Am J Physiol Lung Cell Mol Physiol* 2017;313:L592–601.
 41. Holtmann MH, Douni E, Schütz M, Zeller G, Mudter J, Lehr HA, et al. Tumor necrosis factor-receptor 2 is up-regulated on lamina propria T cells in Crohn's disease and promotes experimental colitis in vivo. *Eur J Immunol* 2002;32:3142–51.
 42. Akassoglou K, Douni E, Bauer J, Lassmann H, Kollias G, Probert L. Exclusive tumor necrosis factor (TNF) signaling by the p75TNF receptor triggers inflammatory ischemia in the CNS of transgenic mice. *Proc Natl Acad Sci U S A* 2003;100:709–14.
 43. Stoelcker B, Hehlgans T, Weigl K, Bluethmann H, Grau GE, Männel DN. Requirement for tumor necrosis factor receptor 2 expression on vascular cells to induce experimental cerebral malaria. *Infect Immun* 2002;70:5857–9.
 44. Hildebrandt GC, Olkiewicz KM, Corrión L, Clouthier SG, Pierce EM, Liu C, et al. A role for TNF receptor type II in leukocyte infiltration into the lung during experimental idiopathic pneumonia syndrome. *Biol Blood Marrow Transplant* 2008;14:385–96.
 45. D'hulst AI, Bracke KR, Maes T, De Bleecker JL, Pauwels RA, Joos GF, et al. Role of tumour necrosis factor- α receptor p75 in cigarette smoke-induced pulmonary inflammation and emphysema. *Eur Respir J* 2006;28:102–12.
 46. Pfeifer E, Polz J, Griebl S, Mostböck S, Hehlgans T, Männel DN. Mechanisms of immune complex-mediated experimental glomerulonephritis: possible role of the balance between endogenous TNF and soluble TNF receptor type 2. *Eur Cytokine Netw* 2012;23:15–20.
 47. Leclerc M, Naserian S, Pilon C, Thiolat A, Martin GH, Pouchy C, et al. Control of GVHD by regulatory T cells depends on TNF produced by T cells and TNFR2 expressed by regulatory T cells. *Blood* 2016;128:1651–9.
 48. Chopra M, Bieh M, Steinfatt T, Brandl A, Kums J, Amich J, et al. Exogenous TNFR2 activation protects from acute GvHD via host T reg cell expansion. *J Exp Med* 2016;213:1881–900.
 49. Fischer R, Proske M, Duffey M, Stangl H, Martinez GF, Peters N, et al. Selective activation of tumor necrosis factor receptor II induces antiinflammatory responses and alleviates experimental arthritis. *Arthritis Rheumatol* 2018;70:722–35.
 50. Hu X, Li B, Li X, Zhao X, Wan L, Lin G, et al. Transmembrane TNF- α promotes suppressive activities of myeloid-derived suppressor cells via TNFR2. *J Immunol* 2014;192:1320–31.
 51. Zhao X, Rong L, Zhao X, Li X, Liu X, Deng J, et al. TNF signaling drives myeloid-derived suppressor cell accumulation. *J Clin Invest* 2012;122:4094–104.
 52. Chen X, Nie Y, Xiao H, Bian Z, Scarzello AJ, Song NY, et al. TNFR2 expression by CD4 effector T cells is required to induce full-fledged experimental colitis. *Sci Rep* 2016;6:32834.
 53. Nadkarni S, Mauri C, Ehrenstein MR. Anti-TNF- α therapy induces a distinct regulatory T cell population in patients with rheumatoid arthritis via TGF- β . *J Exp Med* 2007;204:33–9.

Learned Immunosuppressive Placebo Response Attenuates Disease Progression in a Rodent Model of Rheumatoid Arthritis

Laura Lückemann,¹  Hubert Stangl,² Rainer H. Straub,² Manfred Schedlowski,³ and Martin Hadamitzky¹

Objective. Patients with chronic inflammatory autoimmune diseases benefit from a broad spectrum of immunosuppressive and antiproliferative medication available today. However, nearly all of these therapeutic compounds have unwanted toxic side effects. Recent knowledge about the neurobiology of placebo responses indicates that associative learning procedures can be utilized for dose reduction in immunopharmacotherapy while simultaneously maintaining treatment efficacy. This study was undertaken to examine whether and to what extent a 75% reduction of pharmacologic medication in combination with learned immunosuppression affects the clinical outcome in a rodent model of type II collagen–induced arthritis.

Methods. An established protocol of taste-immune conditioning was applied in a disease model of chronic inflammatory autoimmune disease (type II collagen–induced arthritis) in rats, where a novel taste (saccharin; conditioned stimulus [CS]) was paired with an injection of the immunosuppressive drug cyclosporin A (CSA) (unconditioned stimulus [US]). Following conditioning with 3 CS/US pairings (acquisition), the animals were immunized with type II collagen and Freund's incomplete adjuvant. Fourteen days later, at the first occurrence of clinical symptoms, retrieval was started by presenting the CS together with low-dose CSA as reminder cues to prevent the conditioned response from being extinguished.

Results. This “memory-updating” procedure stabilized the learned immune response and significantly suppressed disease progression in immunized rats. Clinical arthritis score and histologic inflammatory symptoms (both $P < 0.05$) were significantly diminished by learned immunosuppression in combination with low-dose CSA (25% of the full therapeutic dose) via β -adrenoceptor–dependent mechanisms, to the same extent as with full-dose (100%) pharmacologic treatment.

Conclusion. These results indicate that learned immunosuppression appears to be mediated via β -adrenoceptors and might be beneficial as a supportive regimen in the treatment of chronic inflammatory autoimmune diseases by diminishing disease exacerbation.

INTRODUCTION

Patients with chronic inflammatory autoimmune diseases such as rheumatoid arthritis (RA) or inflammatory bowel disease require long-lasting if not continuous treatment with immunosuppressive drugs to diminish symptoms (1,2). However, there is also a drawback of therapy with most small-molecule immunosuppressive drugs, i.e. unwanted toxic side effects (nephrotoxicity, itchiness, headaches, tremors, depression, and/or anxiety), detrimentally

affecting patients' quality of life (3). In the search for strategies to overcome this disadvantage, the use of learned immunopharmacologic placebo responses to allow drug dose reduction during therapy, while simultaneously maintaining treatment efficacy (4,5), has been suggested. Such approaches are based on classic conditioning of physiologic responses and, alternatively, the bidirectional communication between the central nervous system (CNS) and the immune system (6,7). Classically conditioned or learned immunosuppressive responses have been proven effective in

Supported by the Deutsche Forschungsgemeinschaft/German Research Foundation (SFB1280 and TP A18), project 316803389 to Drs. Schedlowski and Hadamitzky and project STR 511/34-1 to Dr. Straub.

¹Laura Lückemann, PhD, Martin Hadamitzky, PhD: University Hospital Essen and University of Duisburg-Essen, Essen, Germany; ²Hubert Stangl, PhD, Rainer H. Straub, MD: University Hospital Regensburg, Regensburg, Germany; ³Manfred Schedlowski, PhD: University Hospital Essen and University of Duisburg-Essen, Essen, Germany, and Karolinska Institute, Stockholm, Sweden.

No potential conflicts of interest relevant to this article were reported.

Address correspondence to Manfred Schedlowski, PhD, University Hospital Essen, Institute of Medical Psychology and Behavioral Immunobiology, Hufelandstrasse 55, 45122 Essen, Germany. E-mail: manfred.schedlowski@uk-essen.de.

Submitted for publication July 30, 2019; accepted in revised form September 3, 2019.

experimental animal disease models, healthy subjects, and patient populations (8–11). To sustain these conditioned effects, these learned immune responses are of clinical relevance, as in rodent studies they have been shown to prolong heart allograft survival and attenuate allergic responses, as well as disease progression and mortality in autoimmune diseases (10,12–15).

In an established taste-immune learning paradigm in rats, a novel-tasting drinking solution (saccharin; conditioned stimulus [CS]) is paired with an injection of the calcineurin inhibitor and immunosuppressant cyclosporin A (CSA; unconditioned stimulus [US]). Reexposure to the CS results in reduced consumption of the saccharin (conditioned taste avoidance [CTA]) and, more importantly, a pronounced suppression of T cell functioning, as well as diminished interleukin-2 (IL-2) and interferon- γ (IFN γ) protein production and messenger expression (16–20). However, taste-associative learning extinguishes when animals are repeatedly exposed to the CS in the absence of the US (10,21). To prevent extinction of learned immunosuppression, low subtherapeutic dosages of the US were applied during the extinction process, which was ineffective in inducing CTA itself. In contrast to controls that exhibited extinguished CTA at retrieval after the presentation of saccharin only, animals additionally treated with the “reminder cues” (low or subtherapeutic dosages of the US) had CTA that remained at a level similar to that acquired at acquisition (22). We recently adapted this “memory-updating” procedure for our taste-immune model, showing that the usage of CS saccharin together with subtherapeutic CSA as reminder cues prevented conditioned immunosuppression from being extinguished in rodents (10).

The present study was undertaken to test whether and to what extent a 75% reduction of pharmacologic medication in combination with learned immunosuppression affects the clinical outcome in a rodent model of type II collagen-induced arthritis (CIA) (23–26). For this purpose, signs of inflammation (such as swollen joints, paw swelling, and grip strength) as well as histologic alterations of the paws were analyzed. In addition, we investigated the role of β -adrenoceptors (β -ARs) in modulating learned immunosuppression during the course of disease.

MATERIALS AND METHODS

Animals. Dark agouti (DA) rats (DA/HanRj; 300 gm) were housed in groups of 4 in a vivarium with controlled humidity of 55% (\pm 5%) and controlled temperature of 20°C, and were maintained on a 12-hour reversed light/dark cycle (illuminated from 7:00 PM to 7:00 AM). All experimental procedures were conducted under red light illumination. Before initiation of any experimental procedure, the animals were allowed to acclimatize to the new surroundings for 1 week after arrival. Subsequently, rats were single-housed with ad libitum access to food, with tap water available ad libitum until the water deprivation regimen started. The animal facilities and experimental procedures were in accordance with National Institutes of Health and Association for the Assess-

ment and Accreditation of Laboratory Animal Care guidelines and were approved by the Institutional Animal Care and Use Committee (LANUV; Düsseldorf, Germany).

Drugs. A stock solution of CSA (100 mg/ml; LC Laboratories) was prepared every day in 900 μ l of Miglyol (Caelo) and 100 μ l of 96% ethanol. This stock solution was diluted with sterile saline (0.9% NaCl) (Braun) to gain the required drug dose of 20 mg/kg body weight at a final injection volume of 1 ml (16,19). Nadolol pellets (Innovative Research of America) with a dosage of 5 mg/pellet and a 21-day release time (0.24 mg/day) were implanted subcutaneously on day 10 after immunization.

Study design. The standard conditioning paradigm started with a water deprivation period of 5 days, allowing animals 15 minutes of drinking at 9:00 AM and again at 5:00 PM every day (2 drinking sessions/day). Before and after each drinking session, the drinking bottles were weighed to measure fluid intake. Individual mean water consumption in the morning sessions over these days was recorded as baseline level (100%) for “normal” fluid intake. After rats had adjusted to this procedure, acquisition started on day 6. The animals were divided into 4 different treatment groups that consisted of 3 control groups (US_{low}, US_{high}, and CS₀) and 1 experimental group (CS_{slow}). During the acquisition trials, all animals received saccharin and an intraperitoneal (IP) injection of CSA in the morning session. In the evening session, all animals received water. Two days after the last acquisition day, all animals were immunized (induction of CIA described below) and received water during the morning and evening drinking sessions until day 14 before retrieval was initiated.

The animals in the conditioned group (CS_{low}) received saccharin and a low dose of CSA (5 mg/kg) in the morning sessions. The US_{low} group was included to control for low-dose pharmacologic effects on arthritis. All animals in this group received water during the morning and evening sessions and a low-dose injection of CSA (5 mg/kg) in the morning session. To compare the conditioning effect with a standard pharmacologic treatment, all animals in the US_{high} group received IP injections of CSA (20 mg/kg) during every morning session of the retrieval phase. During the 3 acquisition trials, animals in the control group for residual effects of CSA administration (CS₀) were not reexposed to the saccharin (CS) and did not receive additional CSA (Figure 1A).

Conditioned taste avoidance. After each morning and evening drinking session during acquisition and retrieval phases, the total amount of liquid consumed per session was measured by weighing the bottles before and after each drinking session. Saccharin consumption was calculated as a percentage of baseline water consumption.

Extension of the retention interval. In the established taste-immune conditioning protocol with CSA, acquisition is followed by a 3-day retention interval before retrieval is initiated. This

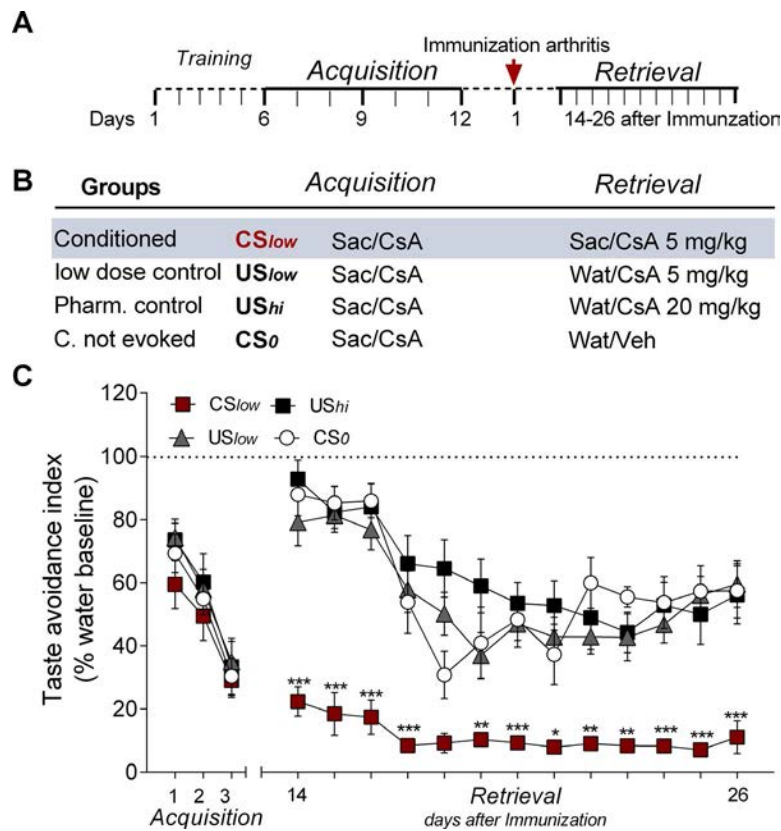


Figure 1. Paradigm of behaviorally conditioned immunosuppression in collagen-induced arthritis. **A** and **B**, Schematic representation of the protocol (**A**) and group allocation and treatment design (**B**). During the 3 acquisition trials (conditioned stimulus [CS]/unconditioned stimulus [US] pairings), animals in all groups (CS_{low}, US_{low}, US_{high}, and CS₀) received saccharin (Sac) and a 20 mg/kg injection of cyclosporin A (CSA). After the last acquisition trial, animals were immunized to induce collagen-induced arthritis. Starting on day 14 after immunization, the CS_{low} group received saccharin together with a low-dose injection of therapeutic CSA (5 mg/kg) during retrieval. Animals in the low-dose pharmacologic control group (US_{low}) received tap water (Wat) together with a 5 mg/kg injection of CSA. The pharmacologic (Pharm.) control group (US_{high}) received water together with a 20 mg/kg injection of CSA. The CS₀ group received just tap water during the drinking sessions together with an injection of NaCl vehicle (Veh). **C**, Taste avoidance index. All groups exhibited conditioned taste avoidance (CTA) in the second and third acquisition trials. During retrieval, animals in the CS_{low} group still exhibited pronounced CTA, as reflected by significantly lower fluid consumption compared to all other groups (* = $P < 0.05$; ** = $P < 0.01$; *** = $P < 0.001$, by analysis of variance). Values are the mean \pm SEM ($n = 16$ or 17 per group).

standard protocol needed to be modified for the CIA experiment by extending the retention interval to 14 days due to the late onset of symptoms after immunization. Thus, in a pilot study, we tested whether conditioned immunosuppression, reflected by CTA and inhibited IFN γ production, would still be detectable after an extended retention interval between acquisition and retrieval phases (Supplementary Figure 1, available on the *Arthritis & Rheumatology* web site at <http://onlinelibrary.wiley.com/doi/10.1002/art.41101/abstract>).

Induction of CIA. Under isoflurane anesthesia (~1.5–2% mixture with oxygen), rats received an intradermal (ID) injection of an emulsion (300 μ l) containing 150 μ l of type II collagen (#804001-sol; MD Bioproducts) and 150 μ l of Freund's incomplete adjuvant (Sigma-Aldrich) at the base of the tail. The first symptoms of the disease typically occur 14 days after injection/immunization.

Pain relief with osmotic pumps. To diminish animals' pain over the course of the experiment, all rats received analgesic medication via osmotic pumps (Alzet). These pumps were filled with 2

ml of the opioid buprenorphine (Indivior EU Limited) and implanted subcutaneously in the backs of the animals under isoflurane anesthesia on day 10 following collagen immunization (at a daily dose of 0.1 mg/kg of body weight with a pump rate of 5.0 μ l/hour).

Assessment of clinical arthritis score. The development of arthritis was monitored by daily determination of body weight and arthritis score after immunization. For scoring, each paw was evaluated separately. The maximum possible arthritis score per extremity was 4 points. One point was assigned for each of the following inflamed (slight or severe) regions: the digits, the midfeet (metatarsus/metacarpus), and the wrists/ankles. An additional point was given if the normal use of the paw was impaired and the animal was limping. The maximum possible score was 16 points. All ratings were performed by 2 experimenters (LL and MH) who were blinded with regard to animal treatment group. Animals were killed on day 28 after arthritis induction for further immunologic and histologic analyses.

Grip strength test. Grip strength measurement has initially been established to assess carrageenan-evoked muscle hyperalgesia in rats (25). In our experiments, this simple technique was used to measure motor functionality and strength in arthritic rats. Rats were placed on a 560 mm × 400 mm wire mesh grid (15 mm mesh and 3 mm wire), and grip strength was measured by attaching the tail of the rat to a spring balance (Pesola) with calibrated ranges of 0 to 500g. Since rats have the reflex to grasp the wire mesh in order to resist the pulling, the maximum force required for the traction was measured and documented (Supplementary Figure 2, available on the *Arthritis & Rheumatology* web site at <http://onlinelibrary.wiley.com/doi/10.1002/art.41101/abstract>). The first test was performed before the occurrence of symptoms (on day 7) and in the acute phase of arthritis (on day 20).

Histologic analysis. For histologic analyses and scoring, hind and front paws were collected, fixed with neutral buffered solution containing 3.7% formalin for 24–72 hours, and subsequently decalcified (RDO Rapid Decalcifier). Afterwards, the paws were washed with phosphate buffered saline (PBS; Life Technologies) and decalcified with RDO Rapid Decalcifier (Meditate) for 5 days. When the bones were dissolved, the paws were washed with PBS and dehydrated in 20% sucrose for at least 24 hours. All paws were embedded in Tissue-Tek OCT medium (Sakura Finetek), frozen in liquid nitrogen, and stored at –80°C for later histologic staining.

Paw tissue sections of 10–12 μm thickness were cut using a freezing microtome (Leica). After 1 hour of air-drying and subsequent rehydration in PBS, staining with hematoxylin and eosin (H&E) (Sigma) was performed to evaluate histologic alterations in the joints. Hind and front paws from each rat were scored separately in a blinded manner, and the mean score was calculated for each animal as follows: invasion of immune cells into the articular cavity of joints (0–4 points), invasion of immune cells into joint adjacent tissues (0–4 points), erosions of cortical bone next to the periosteum and inflammation of periosteum (0–4 points), erosions in articular and subchondral bone (0–4 points), and degradation of articular cartilage (0–4 points). Points for each extremity were totaled, and the mean was calculated for each animal, resulting in a maximum possible histologic arthritis score of 20.

Statistical analysis. Statistical analyses were performed using SigmaPlot version 12.3 and GraphPad Prism version 5. The normality of residuals was examined using Shapiro-Wilk's test, and data were log-transformed when necessary. Descriptive statistics were calculated based on the mean ± SEM. *P* values less than 0.05 were considered significant; a trend was recognized at *P* < 0.1. Behavioral data (acquisition and retrieval of CTA) were subjected to two-way analysis of variance (ANOVA) with group (treatment) as one factor and time (days) as a within-subject factor. Post hoc comparisons were performed using Bonferroni and Student-Newman-Keuls corrections. Differences in the clinical arthritis score were evaluated by two-way ANOVA with repeated

measures followed by Newman-Keuls post hoc testing. Data from the area under the curve of clinical arthritis scores were analyzed by one-way ANOVA with post hoc correction. Histologic arthritis scores were analyzed by one-way ANOVA followed by Bonferroni correction for multiple comparisons. Correlation analysis between histologic and clinical arthritis scores was performed using Pearson's correlation coefficient. The Mann-Whitney test was also performed as histologic arthritis scores in the experiments with nadolol failed normality testing.

RESULTS

Conditioned immunosuppression attenuates clinical symptoms in a rat model of CIA.

First, we tested whether the established immune-conditioning protocol pairing saccharin (CS) with CSA (US) is still retrievable following a prolonged interval between acquisition and retrieval. Three CS/US pairings resulted in pronounced CTA as well as IFN γ cytokine suppression after a 14-day retention interval (*P* < 0.001) (Supplementary Figures 1A–D, available on the *Arthritis & Rheumatology* web site at <http://onlinelibrary.wiley.com/doi/10.1002/art.41101/abstract>). The findings confirmed that this associative learning protocol can be implemented to affect disease outcome in animal models of RA. In the main experiments, acquisition was performed as described above. However, 2 days after the last CS-US pairing, all animals were immunized with type II collagen and Freund's incomplete adjuvant (Figures 1A and B). Pilot data revealed that in DA rats with experimentally induced arthritis, first clinical symptoms occurred 14 days following immunization. Importantly, daily CSA injections of 20 mg/kg (days 1–27 after immunization) were demonstrated to diminish disease progression (Supplementary Figure 3, <http://onlinelibrary.wiley.com/doi/10.1002/art.41101/abstract>). Based on these results, in the present experiments animals in the conditioned group (CS_{low}) received saccharin paired with an injection of low-dose CSA (5 mg/kg) starting from day 14 postimmunization. Animals in all other groups received water with injections of either 5 mg/kg CSA (US_{low}), 20 mg/kg CSA (US_{high}), or vehicle (CS₀). Compared to all other groups, animals in the CS_{low} group displayed CTA during the whole experiment, reflected by reduced saccharin intake (*P* < 0.05) (Figure 1C). This lack of fluid consumption, however, was compensated for in the evening, when all groups received water (Supplementary Figure 4, <http://onlinelibrary.wiley.com/doi/10.1002/art.41101/abstract>).

Along with CTA, clinical arthritis scores were analyzed daily starting on day 14 postimmunization. All animals developed clinical symptoms of arthritis, first detected on day 14 and reaching maximum scores on day 26 postimmunization (Figure 2A). Rats treated with 20 mg/kg of CSA (US_{high}) and conditioned rats (CS_{low}) that received the CS (saccharin) and only 25% (5 mg/kg) of the full therapeutic dose of CSA had significantly diminished clinical scores compared to controls US_{low} and CS₀ from day 20 to the

end of the experiment ($P < 0.05$) (Figure 2A). Moreover, additional analysis revealed a significant effect on the clinical score, indicating lower clinical arthritis scores in the US_{high} and CS_{low} groups compared to controls (US_{low} and CS₀) ($P < 0.05$), with no significant differences between the US_{high} and CS_{low} groups (Figure 2B).

To evaluate motor functionality and strength of the inflamed paws, rats were tested for grip strength on day 7 (prior to the occurrence of first symptoms) and during the acute phase of the disease on day 20 (Supplementary Figure 2A, available on the *Arthritis & Rheumatology* web site at <http://onlinelibrary.wiley.com/doi/10.1002/art.41101/abstract>). Performance in this functional test on day 20 was significantly better in the group treated with full-dose CSA as well as the conditioned group compared to the group treated with low-dose CSA and the control group that was conditioned but not evoked ($P < 0.05$) (Figure 3A). Additionally, the functional consequences of the CIA were supported by a correlation between total grip strength and clinical arthritis score ($P < 0.01$) (Supplementary Figures 2A and B).

Conditioned immunosuppression reduces histologic signs of inflammation in CIA. Consistent with changes in the clinical arthritis score, histologic analysis performed on rat front paws on day 28 revealed significant differences between treatment groups. The CS_{low} and US_{high} groups displayed milder overall inflammation compared to the US_{low} and CS₀ control groups ($P < 0.05$) (Figure 3B). In hind paws, a significant difference from controls was

observed only in the US_{high} group ($P < 0.05$); however, the sum histologic score of front and hind paws showed differences in both the US_{high} and CS_{low} groups compared to controls (data not shown). This finding was also supported by a correlation between total histologic and clinical arthritis scores ($P < 0.0001$) (Figure 3C).

The density of infiltrating immune cells and bone erosion during inflammation of the hind paws (metatarsus and ankle) was reduced in the CS_{low} group compared to the CS₀ group (Figure 3D). Moreover, detailed immunohistologic evaluation of individual anatomic regions of the paws (leukocyte infiltration, synovial hyperplasia, and bone erosion) also revealed less inflammation in CS_{low} animals compared to animals in control groups US_{high} and CS₀ ($P < 0.05$; Supplementary Figure 5, available on the *Arthritis & Rheumatology* web site at <http://onlinelibrary.wiley.com/doi/10.1002/art.41101/abstract>).

Learned immunosuppression in CIA is mediated via β -AR-dependent mechanisms. Previous studies have shown that learned suppression of calcineurin activity in T cells appears to be mainly mediated via noradrenergic innervation of lymphatic organs and β -AR-dependent mechanisms (27–29). To corroborate this hypothesis, an additional experimental approach was undertaken in our investigation, in which animals were continuously treated with the β -AR blocker nadolol (release 0.24 mg/day) via subcutaneously implanted pellets 4 days prior to the first retrieval on day 14 (Figures 4A and B and Supplementary Figure 6 [<http://onlinelibrary.wiley.com/doi/10.1002/art.41101/abstract>]). Treatment with nadolol (CS₀-NAD) alone did not decrease the

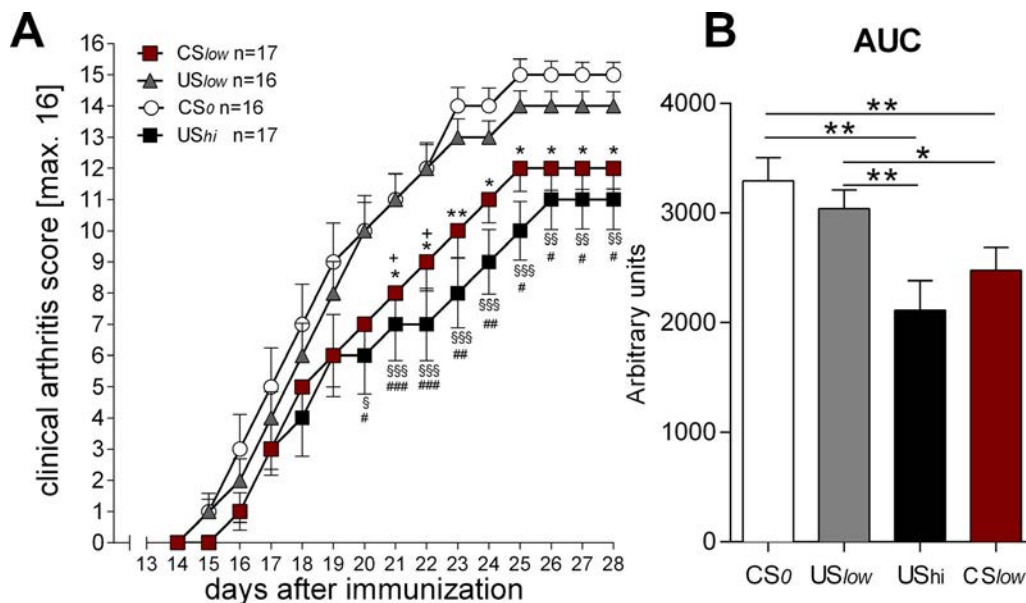


Figure 2. Behaviorally conditioned immunosuppression attenuates disease progression in collagen-induced arthritis. **A**, Clinical arthritis scores in each treatment group. During the course of the disease, behaviorally conditioned animals receiving low therapeutic doses of CSA (CS_{low}) had significantly milder clinical scores compared to the US_{low} group (+ = $P < 0.05$) and the CS₀ group (* = $P < 0.05$; ** = $P < 0.01$). The US_{high} group, which received full-dose CSA treatment, had an improved outcome compared to the CS₀ group (§ = $P < 0.05$, §§ = $P < 0.01$, and §§§ = $P < 0.001$) and US_{low} group (# = $P < 0.05$, ## = $P < 0.01$, and ### = $P < 0.001$). **B**, Area under the curve (AUC) analysis. CS_{low} group clinical scores did not significantly differ over time compared to scores in the US_{high} group. AUC in the US_{high} and US_{low} groups differed significantly, as did AUC in the CS_{low} and CS₀ groups. (* = $P < 0.05$; ** = $P < 0.01$, by analysis of variance). Values are the mean \pm SEM. max. = maximum (see Figure 1 for other definitions).

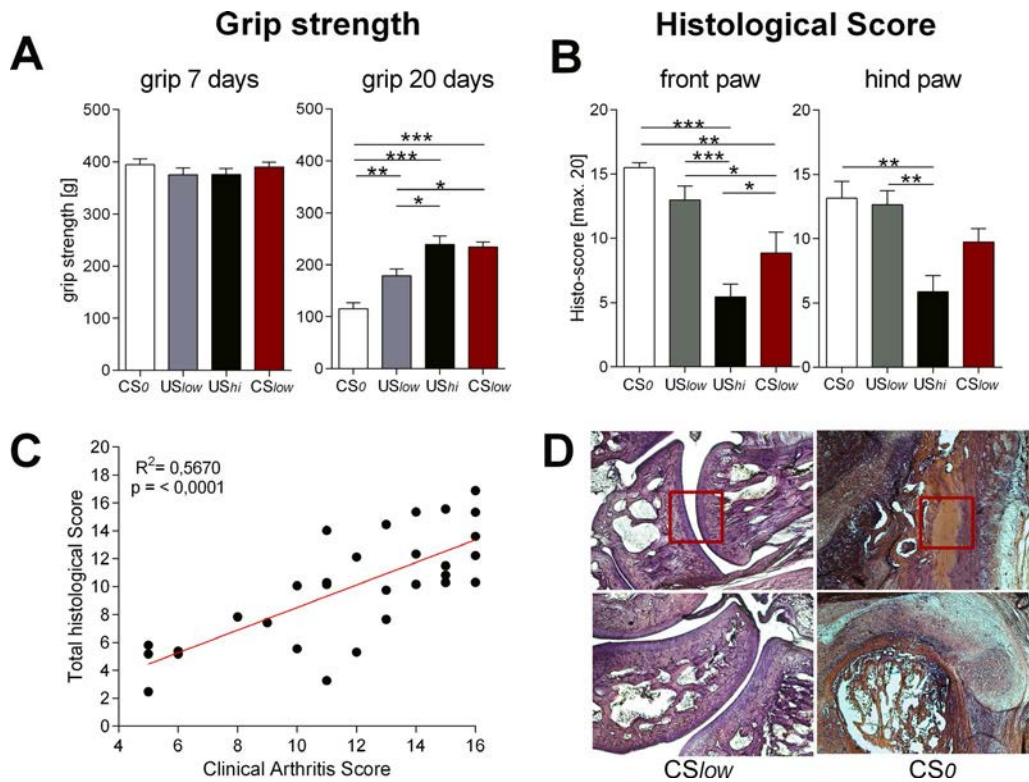


Figure 3. Conditioning ameliorates functional and histologic impairment caused by inflammation in collagen-induced arthritis. **A**, Grip strength. On day 7 after immunization, results did not differ between groups. On day 20 after immunization, all groups exhibited worsening grip strength. However, grip strength was higher in the CS_{low} animals compared to the CS₀ animals, and in the US_{high} animals compared to the US_{low} animals ($* = P < 0.05$; $** = P < 0.01$; $*** = P < 0.001$, by analysis of variance). Values are the mean \pm SEM ($n = 8$ – 10 per group). **B**, Histologic analysis. Significantly milder signs of inflammation were observed in front and hind paws obtained from CS_{low} animals compared to US_{low} and CS₀ controls ($* = P < 0.05$; $** = P < 0.01$; $*** = P < 0.001$, by analysis of variance). Values are the mean \pm SEM ($n = 6$ – 10 per group). **C**, Pearson's correlation coefficient between histologic and clinical scores ($n = 8$ or 9 per group). **D**, Hematoxylin and eosin staining of representative metatarsus tissue (top panels) and ankle tissue (bottom panels) obtained from rats in the CS_{low} and CS₀ groups. Ankle and metatarsus tissue from the CS_{low} rat exhibit mild inflammation. Ankle and metatarsus tissue from the CS₀ rat exhibit heavy bone and cartilage destruction as well as inflamed hyperplasia. Red squares indicate same region. Original magnification $\times 50$. See Figure 1 for definitions.

clinical or the histologic arthritis score when compared to the CS₀ control group. However, the significantly milder arthritis scores acquired by conditioning in the CS_{low} group (versus the CS₀ and CS₀-NAD groups) was blocked by the β -AR antagonist in the CS_{low}-NAD group ($P < 0.05$) (Figure 4C). Moreover, histologic analysis of the paws indicated that the attenuated inflammatory process in conditioned animals (CS_{low}) was blocked in the nadolol-treated animals ($P < 0.05$) (Figure 4D).

DISCUSSION

Patients with inflammatory autoimmune diseases such as RA require regular, often lifelong immunosuppressive medication, which may cause several unwanted side effects. Conditioned placebo effects in pharmacotherapy provide sophisticated approaches that may reduce drug doses and detrimental side effects without losing therapeutic efficacy (4,5). In this regard, based on the bidirectional communication between the CNS and the immune system (7,30), behavioral conditioned

immunosuppression with CSA has proven useful in animal disease models, healthy subjects, and patients (8–11,31). The present study was aimed at analyzing the potential impact of learned immunosuppression in a rat model of CIA (23). We showed that taste-immune conditioning, together with the application of only 25% of the drug dose (5 mg/kg), led to an almost identical clinical outcome as with 100% CSA administration (20 mg/kg). Conditioned animals exhibited fewer signs of inflammation, such as swollen joints and paws, as well as less bone destruction and infiltration in surrounding tissue. In addition, learned immunosuppression significantly improved performance in the functional grip strength test compared to untreated and non-conditioned controls.

Previous studies that used a taste-immune learning paradigm with CSA have shown that the learned suppression of lymphocyte proliferation and cytokine production is mediated via sympathetic nervous activity and β -AR-dependent mechanisms (15,17). Thus, we characterized the role of these receptors in learned immunosuppression during the course of inflammatory disease. We

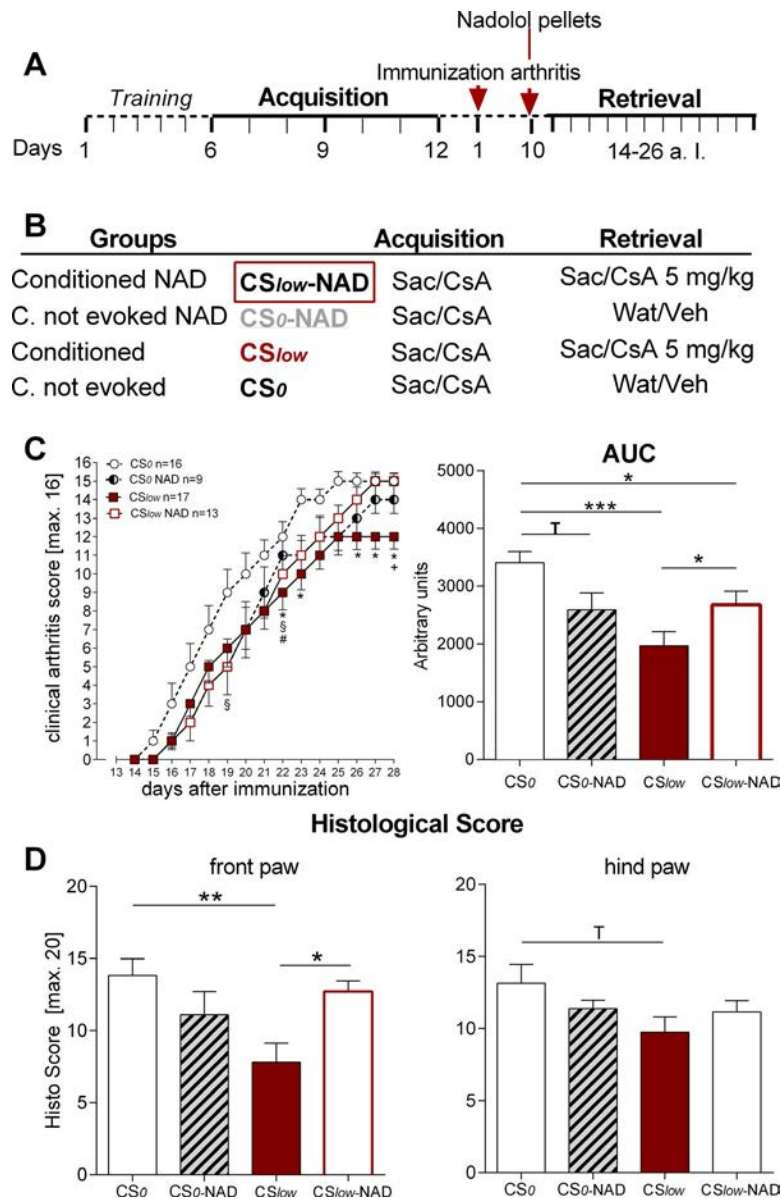


Figure 4. Behaviorally conditioned immunosuppression in collagen-induced arthritis is mediated via β -adrenoceptor-dependent mechanisms. **A** and **B**, Schematic representation of the conditioning protocol (**A**) and group allocation and treatment design (**B**). During acquisition, all animals received 3 pairings of saccharin and CSA (20 mg/kg). Two days after the third acquisition trial, the animals were immunized. Ten days after immunization (a. l.), animals in the conditioned group (CS_{low}) and control group (CS₀) were implanted with nadolol (NAD) pellets. At retrieval, CS_{low} and CS_{low}-NAD animals received saccharin together with low-dose therapeutic CSA (5 mg/kg) starting on day 14 following immunization. **C**, Clinical arthritis scores. Clinical scores were significantly milder in the CS_{low} group compared to the CS₀ group ($* = P < 0.05$), the CS_{low}-NAD group ($+ = P < 0.05$), and the CS₀-NAD group ($\# = P < 0.05$). On days 19 and 22, a significant difference between the CS_{low}-NAD group and the CS₀ group was observed ($\$ = P < 0.05$ by analysis of variance). Values are the mean \pm SEM ($n = 16$ – 18 per group). Moreover, in area under the curve (AUC) analysis, clinical scores in the CS_{low} animals were reduced compared to the CS₀ and CS_{low}-NAD groups ($* = P < 0.05$; $*** = P < 0.001$). There was a trend (T) toward milder scores in CS₀-NAD rats compared to untreated control rats ($P = 0.057$). Values are the mean \pm SEM ($n = 16$ – 18 per group). **D**, Histologic (Histo) analysis of front and hind paws. Histologic evaluation of the front paws showed significant differences between conditioned animals and controls ($* = P < 0.05$; $** = P < 0.01$, by Mann-Whitney test). Evaluation of the hind paws revealed a trend toward milder scores in CS_{low} animals compared to CS₀ animals ($P = 0.072$ by Mann-Whitney test). Values are the mean \pm SEM ($n = 7$ – 16 per group [front paws] and 7 – 11 per group [hind paws]). max. = maximum (see Figure 1 for other definitions).

observed that attenuating effects on inflammatory progression in CIA induced by conditioning were blocked by continuous application of the β -AR antagonist nadolol. Even though the precise intracellular mechanisms underlying this effect are still unknown,

previous *in vitro* and *ex vivo* data have indicated that conditioned immunosuppression seems to inhibit the calcineurin activity in T cells, thereby suppressing the production and release of cytokines and T cell activation, which is similar to the effects of CSA (27,28).

In general, the sympathetic nervous system seems to modulate the outcome of arthritis differently depending on the time point of manipulation and the target structure investigated (e.g., radiologic variables, clinical scores, plasma extravasation, leukocyte cytokine production, lymphocyte migration) (32–35). In the early phase of the disease, β -ARs typically stimulate arthritis, but this effect slows down after the onset of the disease (34,36). Similarly, the removal of the influence of the sympathetic nervous system prior to immunization and around the onset of the disease reduces arthritis severity, but this effect is not observed in later phases (36,37).

In our experiments, nadolol also partly reversed the strong effect of conditioning in the CS_{low} group, with disease severity reaching a level similar to that in the CS₀-NAD group (Figures 4B and C). This finding indicates that β -ARs have a beneficial role in conditioning, most likely via the above-mentioned calcineurin pathways. Additionally, the effect of the β -AR blockade was probably compounded by other arthritis-propagating pathways that usually play a role during the early stage of the disease (from induction to disease onset) (32–34,36,37). In other words, we observed 2 independent effects of the sympathetic nervous system, one that is beneficial and supportive for conditioning and one that is typically detrimental during the early phase of the disease.

Conditioned responses in general tend to decline progressively when subjects are reexposed to the CS in the absence of the US (38–41). However, evidence from animal and human studies has demonstrated that the extinction of learned immunosuppression could be abrogated when sub- or low-therapeutic doses of the US (CSA) were administered as reminder cues in combination with the CS during the retrieval phase (10,42–44). Such modified conditioning protocols, using reminder cues, most likely induced a memory-updating process of the learned immunosuppression during retrieval (9,10,42). The data presented here confirm these findings and extend them to experimentally induced autoimmune diseases, showing that the symptoms of RA can be abrogated by administering low therapeutic doses of the immunosuppressant drug CSA as a reminder cue combined with the CS.

The application of learned immunopharmacologic strategies in clinical situations as supportive therapy together with standard pharmacologic regimens has been suggested (4,5,45). Animal experiments indicate that this procedure can be implemented in ongoing immunosuppressive regimens, since preexposure of neither the conditioned nor the unconditioned (CSA) stimulus affected learned immunosuppression (20). Indeed, it was recently reported that in renal transplant patients, adding the conditioning process to the pharmacologic treatment further improved the immunosuppressive effect (8). Additionally, there is primary evidence that acute adverse effects of CSA are not conditioned during the learned immunosuppressive response (46).

However, there are certain limitations that need to be addressed. CSA is a potent immunosuppressive drug used in clinical

settings to prevent graft rejection after organ transplantation or to treat inflammatory autoimmune diseases (47,48). In addition, CSA is used as US in numerous established taste-immune learning protocols (9,15). However, it is not a first-line or standard option for the treatment of RA (49,50). Thus, it would be of great advantage to investigate strategies, in which effects of other, more commonly used compounds for treating RA (such as disease-modifying antirheumatic drugs) could be used in conditioning protocols as well. In addition, the precise beneficial molecular mechanisms of this β -AR-dependent learned immunosuppression superimposed on harmful β -adrenergic effects in the early phase of arthritis induction need to be further elucidated in future studies.

In conclusion, this proof-of-concept study demonstrates for the first time in a preclinical disease model the possible effectiveness of learned immunopharmacologic strategies in clinical situations as supportive therapy together with the standard pharmacologic regimen in the treatment of chronic inflammatory autoimmune diseases.

ACKNOWLEDGMENTS

We thank Elian Mireille Martinez-Gomez and Christine Wolff for technical assistance.

AUTHOR CONTRIBUTIONS

All authors were involved in drafting the article or revising it critically for important intellectual content, and all authors approved the final version to be published. Dr. Lückemann had full access to all of the data in the study and takes responsibility for the integrity of the data and the accuracy of the data analysis.

Study conception and design. Lückemann, Straub, Schedlowski, Hadamitzky.

Acquisition of data. Lückemann, Stangl, Hadamitzky.

Analysis and interpretation of data. Lückemann, Stangl, Straub, Schedlowski, Hadamitzky.

REFERENCES

- Chighizola CB, Ong VH, Meroni PL. The use of cyclosporine A in rheumatology: a 2016 comprehensive review. *Clin Rev Allergy Immunol* 2017;52:401–23.
- Fraser AG, Orchard TR, Jewell DP. The efficacy of azathioprine for the treatment of inflammatory bowel disease: a 30 year review. *Gut* 2002;50:485–9.
- Bösche K, Weissenborn K, Christians U, Witzke O, Engler H, Schedlowski M, et al. Neurobehavioral consequences of small molecule-drug immunosuppression. *Neuropharmacology* 2015;96:83–93.
- Doering BK, Rief W. Utilizing placebo mechanisms for dose reduction in pharmacotherapy. *Trends Pharmacol Sci* 2012;33:165–72.
- Schedlowski M, Enck P, Rief W, Bingel U. Neuro-bio-behavioral mechanisms of placebo and nocebo responses: implications for clinical trials and clinical practice. *Pharmacol Rev* 2015;67:697–730.
- Pavlov VA, Chavan SS, Tracey KJ. Molecular and functional neuroscience in immunity. *Annu Rev Immunol* 2018;36:783–812.
- Irwin MR, Cole SW. Reciprocal regulation of the neural and innate immune systems. *Nat Rev Immunol* 2011;11:625–32.
- Kirchhof J, Petrakova L, Brinkhoff A, Benson S, Schmidt J, Unterberdörster M, et al. Learned immunosuppressive placebo

- responses in renal transplant patients. *Proc Natl Acad Sci U S A* 2018;115:4223–7.
9. Lückemann L, Unterberdörster M, Kirchof J, Schedlowski M, Hadamitzky M. Applications and limitations of behaviorally conditioned immunopharmacological responses. *Neurobiol Learn Mem* 2017;142:91–8.
 10. Hadamitzky M, Börsche K, Wirth T, Buck B, Beetz O, Christians U, et al. Memory-updating abrogates extinction of learned immunosuppression. *Brain Behav Immun* 2016;52:40–8.
 11. Albring A, Wendt L, Benson S, Witzke O, Kribben A, Engler H, et al. Placebo effects on the immune response in humans: the role of learning and expectation. *PLoS One* 2012;7:e49477.
 12. Klosterhalfen W, Klosterhalfen S. Pavlovian conditioning of immunosuppression modifies adjuvant arthritis in rats. *Behav Neurosci* 1983;97:663–6.
 13. Exton MS, Elfers A, Jeong WY, Bull DF, Westermann J, Schedlowski M. Conditioned suppression of contact sensitivity is independent of sympathetic splenic innervation. *Am J Physiol Regul Integr Comp Physiol* 2000;279:R1310–5.
 14. Schedlowski M, Pacheco-López G. The learned immune response: Pavlov and beyond. *Brain Behav Immun* 2010;24:176–85.
 15. Ader R, Cohen N. Behaviorally conditioned immunosuppression and murine systemic lupus erythematosus. *Science* 1982;215:1534–6.
 16. Exton MS, Schult M, Donath S, Strubel T, Nagel E, Westermann J, et al. Behavioral conditioning prolongs heart allograft survival in rats. *Transplant Proc* 1998;30:2033.
 17. Exton MS, Gierse C, Meier B, Mosen M, Xie Y, Frede S, et al. Behaviorally conditioned immunosuppression in the rat is regulated via noradrenaline and β -adrenoceptors. *J Neuroimmunol* 2002;131:21–30.
 18. Pacheco-López G, Niemi MB, Kou W, Härting M, Fandrey J, Schedlowski M. Neural substrates for behaviorally conditioned immunosuppression in the rat. *J Neurosci* 2005;25:2330–7.
 19. Exton MS, von Hörsten S, Schult M, Vöge J, Strubel T, Donath S, et al. Behaviorally conditioned immunosuppression using cyclosporine A: central nervous system reduces IL-2 production via splenic innervation. *J Neuroimmunol* 1998;88:182–91.
 20. Lueckemann L, Börsche K, Engler H, Schwitalla JC, Hadamitzky M, Schedlowski M. Pre-exposure to the unconditioned or conditioned stimulus does not affect learned immunosuppression in rats. *Brain Behav Immun* 2016;51:252–7.
 21. Hadamitzky M, Orłowski K, Schwitalla JC, Börsche K, Unterberdörster M, Bendix I, et al. Transient inhibition of protein synthesis in the rat insular cortex delays extinction of conditioned taste aversion with cyclosporine A. *Neurobiol Learn Mem* 2016;133:129–35.
 22. Berman DE, Hazvi S, Stehberg J, Bahar A, Dudai Y. Conflicting processes in the extinction of conditioned taste aversion: behavioral and molecular aspects of latency, apparent stagnation, and spontaneous recovery. *Learn Mem* 2003;10:16–25.
 23. Trentham DE, Townes AS, Kang AH. Autoimmunity to type II collagen: an experimental model of arthritis. *J Exp Med* 1977;146:857–68.
 24. Choudhary N, Bhatt LK, Prabhavalkar KS. Experimental animal models for rheumatoid arthritis [review]. *Immunopharmacol Immunotoxicol* 2018;40:193–200.
 25. Kehl LJ, Trempe TM, Hargreaves KM. A new animal model for assessing mechanisms and management of muscle hyperalgesia. *Pain* 2000;85:333–43.
 26. Asquith DL, Miller AM, McInnes IB, Liew FY. Animal models of rheumatoid arthritis. *Eur J Immunol* 2009;39:2040–4.
 27. Pacheco-López G, Riether C, Doenlen R, Engler H, Niemi MB, Engler A, et al. Calcineurin inhibition in splenocytes induced by pavlovian conditioning. *FASEB J* 2009;23:1161–7.
 28. Riether C, Kavelaars A, Wirth T, Pacheco-López G, Doenlen R, Willemsen H, et al. Stimulation of β_2 -adrenergic receptors inhibits calcineurin activity in CD4(+) T cells via PKA-AKAP interaction. *Brain Behav Immun* 2011;25:59–66.
 29. Exton MS, Schult M, Donath S, Strubel T, Bode U, del Rey A, et al. Conditioned immunosuppression makes subtherapeutic cyclosporin effective via splenic innervation. *Am J Physiol* 1999;276:R1710–7.
 30. Tracey KJ. Understanding immunity requires more than immunology. *Nat Immunol* 2010;11:561–4.
 31. Klosterhalfen S, Klosterhalfen W. Conditioned cyclosporine effects but not conditioned taste aversion in immunized rats. *Behav Neurosci* 1990;104:716–24.
 32. Lubahn CL, Schaller JA, Bellinger DL, Sweeney S, Lorton D. The importance of timing of adrenergic drug delivery in relation to the induction and onset of adjuvant-induced arthritis. *Brain Behav Immun* 2004;18:563–71.
 33. Pongratz G, Straub RH. Role of peripheral nerve fibres in acute and chronic inflammation in arthritis. *Nat Rev Rheumatol* 2013;9:117–26.
 34. Levine JD, Coderre TJ, Helms C, Basbaum AI. β 2-adrenergic mechanisms in experimental arthritis. *Proc Natl Acad Sci U S A* 1988;85:4553–6.
 35. Klatt S, Stangl H, Kunath J, Lowin T, Pongratz G, Straub RH. Peripheral elimination of the sympathetic nervous system stimulates immunocyte retention in lymph nodes and ameliorates collagen type II arthritis. *Brain Behav Immun* 2016;54:201–10.
 36. Härle P, Pongratz G, Albrecht J, Turner IH, Straub RH. An early sympathetic nervous system influence exacerbates collagen-induced arthritis via CD4+ CD25+ cells. *Arthritis Rheum* 2008;58:2347–55.
 37. Schaible HG, Straub RH. Function of the sympathetic supply in acute and chronic experimental joint inflammation. *Auton Neurosci* 2014;182:55–64.
 38. Berman DE, Dudai Y. Memory extinction, learning anew, and learning the new: dissociations in the molecular machinery of learning in cortex. *Science* 2001;291:2417–9.
 39. Dudai Y. The restless engram: consolidations never end. *Annu Rev Neurosci* 2012;35:227–47.
 40. Myers KM, Carlezon WA Jr. Extinction of drug- and withdrawal-paired cues in animal models: relevance to the treatment of addiction. *Neurosci Biobehav Rev* 2010;35:285–302.
 41. Eisenberg M, Kobil T, Berman DE, Dudai Y. Stability of retrieved memory: inverse correlation with trace dominance. *Science* 2003;301:1102–4.
 42. Albring A, Wendt L, Benson S, Nissen S, Yavuz Z, Engler H, et al. Preserving learned immunosuppressive placebo response: perspectives for clinical application. *Clin Pharmacol Ther* 2014;96:247–55.
 43. Hadamitzky M, Börsche K, Engler A, Schedlowski M, Engler H. Extinction of conditioned taste aversion is related to the aversion strength and associated with c-Fos expression in the insular cortex. *Neuroscience* 2015;303:34–41.
 44. Nader K, Einarsson EÖ. Memory reconsolidation: an update. *Ann N Y Acad Sci* 2010;1191:27–41.
 45. Enck P, Bingel U, Schedlowski M, Rief W. The placebo response in medicine: minimize, maximize or personalize? *Nat Rev Drug Discov* 2013;12:191–204.
 46. Kahl AL, Kirchof J, Petrakova L, Müller J, Laubrock J, Brinkhoff A, et al. Are adverse events induced by the acute administration of calcineurin inhibitor cyclosporine A behaviorally conditioned in healthy male volunteers? *Clin Ther* 2018;40:1868–77.
 47. Lindenfeld J, Miller GG, Shakar SF, Zolty R, Lowes BD, Wolfel EE, et al. Drug therapy in the heart transplant recipient: part I—Cardiac rejection and immunosuppressive drugs. *Circulation* 2004;110:3734–40.

48. Kapturczak MH, Meier-Kriesche HU, Kaplan B. Pharmacology of calcineurin antagonists. *Transplant Proc* 2004;36:25–32.
49. Sizova L. Approaches to the treatment of early rheumatoid arthritis with disease modifying antirheumatic drugs. *Br J Clin Pharmacol* 2008;66:173–8.
50. Gerards AH, Landewé RB, Prins AP, Brujin GA, Goei Thé HS, Laan RF, et al. Cyclosporin A monotherapy versus cyclosporin A and methotrexate combination therapy in patients with early rheumatoid arthritis: a double blind randomised placebo controlled trial. *Ann Rheum Dis* 2003;62:291–6.

Errata

DOI 10.1002/art.41241

In the article by Duarte-García et al in the September 2019 issue of *Arthritis & Rheumatology* (The Epidemiology of Antiphospholipid Syndrome: A Population-Based Study [pages 1545–1552]), there were two factual errors introduced. In the first paragraph of the Case Finding and Ascertainment section of Patients and Methods on page 1546, the sentence “We queried the REP patient database for any individuals who were tested for aPL, either anti- β_2 GPI IgG or IgM antibodies or LAC IgG or IgM antibodies (by dilute Russell viper venom time [DRVVT], DRVVT mix, DRVVT confirmation, or STACLOT), for whom the test result was reported as out of range or abnormal” should have read “We queried the REP patient database for any individuals who were tested for aPL, either aCL IgG or IgM, anti- β_2 GPI IgG or IgM, or LAC (by dilute Russell viper venom time [DRVVT], DRVVT mix, DRVVT confirmation, or STACLOT) for whom the test result was reported as out of range or abnormal.” In the third paragraph of the Case Finding and Ascertainment section, the sentence “The Sydney criteria are often used in clinical research as the diagnostic classification criteria for APS and commonly used in clinical practice as a framework for diagnosis” should have read “The Sydney criteria are used in clinical research as classification criteria and commonly used in clinical practice as a framework for diagnosis.”

DOI 10.1002/art.41251

In the article by Mecoli et al in the January 2020 issue of *Arthritis & Rheumatology* (Myositis Autoantibodies: A Comparison of Results From the Oklahoma Medical Research Foundation Myositis Panel to the Euroimmun Research Line Blot [pages 192–194]), an additional acknowledgment statement should have been included. The complete Acknowledgments section should have read “We thank Dr. Ira Targoff (OMRF) for his assistance in describing OMRF laboratory methodology. We thank Dr. C. Richardson (Division of Rheumatology, Johns Hopkins University School of Medicine) for her contribution to data acquisition.”

DOI 10.1002/art.41256


In the letter by Mathian et al in the January 2020 issue of *Arthritis & Rheumatology* (Reply [page 197]), the name of the fifth author was inadvertently omitted during copyediting. The fifth author of this letter was Guy Gorochov, MD, PhD (Sorbonne Université, AP-HP, Groupement Hospitalier Pitié–Salpêtrière, French National Referral Center for Systemic Lupus Erythematosus, Antiphospholipid Antibody Syndrome and Other Autoimmune Disorders, Institut E3M, INSERM UMR-S, CIMI-Paris Paris, France).

DOI 10.1002/art.41255

In the article by Kass et al in the March 2020 issue of *Arthritis & Rheumatology* (Comparative Profiling of Serum Protein Biomarkers in Rheumatoid Arthritis–Associated Interstitial Lung Disease and Idiopathic Pulmonary Fibrosis [pages 409–419]), the first name of the eighth author was misspelled and the author's institution was shown incorrectly. The correct name (institution) of the eighth author is Juan Chen (First Hospital of Xiamen University, Xiamen, China).

We regret the errors.

Multiparameter Analysis Identifies Heterogeneity in Knee Osteoarthritis Synovial Responses

Hannah Labinsky,¹ Paul M. Panipinto,² Kaytlyn A. Ly,³ Deric K. Khuat,³ Bhanupriya Madarampalli,² Vineet Mahajan,² Jonathan Clabeaux,³ Kevin MacDonald,³ Peter J. Verdin,³ Jane H. Buckner,³ and Erika H. Noss² 

Objective. Synovial membrane inflammation is common in osteoarthritis (OA) and increases cartilage injury. However, synovial fluid and histology studies suggest that OA inflammatory responses are not homogeneous. Greater understanding of these responses may provide new insights into OA disease mechanisms. We undertook this study to develop a novel multiparameter approach to phenotype synovial responses in knee OA.

Methods. Cell composition and soluble protein production were measured by flow cytometry and multiplex enzyme-linked immunosorbent assay in synovium collected from OA patients undergoing knee replacement surgery (n = 35).

Results. Testing disaggregation conditions showed that aggressive digestion improved synovial cell yield and mesenchymal staining by flow cytometry, but it negatively impacted CD4+ T cell and CD56+ natural killer cell staining. Less aggressive digestion preserved these markers and showed highly variable T cell infiltration (range 0–43%; n = 32). Correlation analysis identified mesenchymal subpopulations associated with different nonmesenchymal populations, including macrophages and T cells (CD45+CD11b+HLA-DR+ myeloid cells with PDPN+CD73+CD90-CD34- mesenchymal cells [r = 0.65, P < 0.0001]; and CD45+CD3+ T cells with PDPN+CD73+CD90+CD34+ mesenchymal cells [r = 0.50, P = 0.003]). Interleukin-6 (IL-6) measured by flow cytometry strongly correlated with IL-6 released by ex vivo culture of synovial tissue (r = 0.59, P = 0.0012) and was highest in mesenchymal cells coexpressing CD90 and CD34. IL-6, IL-8, complement factor D, and IL-10 release correlated positively with tissue cellularity (P = 0.0042, P = 0.018, P = 0.0012, and P = 0.038, respectively). Additionally, increased CD8+ T cell numbers correlated with retinol binding protein 4 (P = 0.033). Finally, combining flow cytometry and multiplex data identified patient clusters with different types of inflammatory responses.

Conclusion. We used a novel approach to analyze OA synovium, identifying patient-specific inflammatory clusters. Our findings indicate that phenotyping synovial inflammation may provide new insights into OA patient heterogeneity and biomarker development.

INTRODUCTION

Osteoarthritis (OA) is a disabling disease of progressive mechanical joint failure, and no approved pharmacologic agents halt this progression. Although OA patients share similar radiographic findings, OA is a heterogeneous disorder with diverse

epidemiologic, structural, genetic, clinical, and pathologic risk factors/phenotypes (1–6). One consistent phenotype associated with worse clinical outcomes, including increased pain sensitization and accelerated joint damage, is joint inflammation, characterized by increased synovial tissue volume, vascularity, and proinflammatory signaling (7–12).

Presented in part by Ms Labinsky in partial fulfillment of the requirements for a Dr. Med. degree, University Medical Center of Johannes Gutenberg University, Mainz, Germany.

Ms Labinsky's work was supported by the Studienstiftung des Deutschen Volkes scholarship. Dr. Madarampalli's work was supported by NIH grant T32-AR-07198. Dr. Buckner's work was supported by NIH grant 1R01-AI-132774. Dr. Noss' work was supported by NIH grant K08-AR-063696 from the National Institute of Arthritis and Musculoskeletal and Skin Diseases and by the Rheumatology Research Foundation (Career Development Bridge Funding Award: K Supplement).

¹Hannah Labinsky, MD: University of Washington, Seattle, and University Medical Center of Johannes Gutenberg University, Mainz, Germany; ²Paul

M. Panipinto, BS, Bhanupriya Madarampalli, PhD, Vineet Mahajan, PhD, Erika H. Noss, MD, PhD: University of Washington, Seattle; ³Kaytlyn A. Ly, BS, Deric K. Khuat, BS, Jonathan Clabeaux, MD, Kevin MacDonald, MD, Peter J. Verdin, MD, Jane H. Buckner, MD: Virginia Mason Medical Center, Seattle, Washington.

No potential conflicts of interest relevant to this article were reported.

Address correspondence to Erika H. Noss, MD, PhD, 750 Republican Street, PO Box 358060, Seattle, WA 98109. E-mail: enoss@uw.edu.

Submitted for publication January 17, 2019; accepted in revised form November 5, 2019.

Although inflammation increases with OA progression, its true prevalence is difficult to estimate. Macroscopic visualization by arthroscopy, ultrasound, or magnetic resonance imaging suggests that up to 50% of patients with early OA have at least intermittent synovitis (7,8,13,14). However, microscopic examination demonstrates that synovial abnormalities are also frequent in early OA (4,15). Synovial changes are thought to arise from cellular activation by damage signals released during joint injury, resulting in areas of synovial lining hyperplasia and sublining immune infiltration. This activation increases production of proinflammatory mediators and matrix-degrading proteinases, which accelerates cartilage damage (11,12).

Synovial histology and proinflammatory mediator expression suggest considerable variability among patients in tissue injury response (4,15–20). Our objective was to use multiparameter analysis to explore synovial response diversity across a late-stage knee OA cohort, with the hope that this would provide further insight into the cellular and molecular drivers of OA pathology. To achieve this objective, matched OA synovial samples were either disaggregated for cellular analysis by flow cytometry or cultured intact to measure soluble mediator release by multiplex array. We show that correlations between these data sets provide a rich platform to investigate OA synovial responses, identifying potential tissue cell–cell interactions and clustering patients by their response networks. We also demonstrate that optimizing tissue disaggregation protocols is critical, an important reminder as synovial tissue research moves into highly detailed cellular analyses. Our results confirm that OA inflammation is far from homogeneous and indicates that further inflammatory phenotyping may provide new insights into OA pathology and patient heterogeneity.

PATIENTS AND METHODS

Patient recruitment. Thirty-five OA patients who were referred for knee replacement surgery at Virginia Mason Medical Center were recruited with approval from the Institutional Review Board at Benaroya Research Institute at Virginia Mason. Patients had a mean \pm SD age of 65.39 ± 8.33 years and a mean \pm SD body mass index (BMI) of 32.47 ± 7.72 kg/m². Twenty-three patients (66%) were female, and 32 (91%) were white (African American, $n = 1$; Asian, $n = 2$) (see Supplementary Table 1, on the *Arthritis & Rheumatology* web site at <http://onlinelibrary.wiley.com/doi/10.1002/art.41161/abstract>).

Synovial tissue processing. Knee synovium was collected during replacement surgery at surgical discretion, with patients divided equally between 3 surgeons (Supplementary Table 1). Synovial tissue was dissected into ~100-mg samples and randomly distributed between assays. Samples were weighed (mean \pm SD 106 ± 31.5 mg) and then cultured overnight in Dulbecco's modified Eagle's medium (DMEM), supplemented with 1% fetal bovine serum (FBS; Gemini),

L-glutamine, antibiotics, 2-mercaptoethanol (50 μ M), and amino acids (6-well plates, 1 sample/well). Samples for assessment of tissue soluble mediator release by enzyme-linked immunosorbent assay (ELISA) were cultured for 24 hours in media alone, and supernatants collected. Independent samples for flow cytometry were cultured in 10 μ M of monensin (Sigma-Aldrich) for 14–16 hours to block cytokine release for intracellular staining.

Synovial tissue disaggregation. Unless otherwise indicated, 12 samples per donor (~1,200 mg tissue) were minced and enzymatically digested at 37°C with gentle tube inversion every 5 minutes. Base digestion medium was DMEM with 50 μ g/ml DNase (Roche). Volume, composition, and time varied according to digestion condition (Supplementary Methods, <http://onlinelibrary.wiley.com/doi/10.1002/art.41161/abstract>). Released cells were collected in cold recovery buffer (20 ml DMEM, 10% FBS, 5 mM EDTA, 10 μ M monensin), debris was removed with 70- μ m mesh, and erythrocytes were lysed (Alfa Aesar Red Blood Cell Lysis Buffer; ThermoFisher Scientific). Live synovial cells were manually counted using trypan blue exclusion.

Flow cytometry. Human cell surface marker and intracellular interleukin-6 (IL-6) expression was analyzed by flow cytometry using the listed reagents (Supplementary Table 2, <http://onlinelibrary.wiley.com/doi/10.1002/art.41161/abstract>). Data were analyzed with Kaluza software (Beckman Coulter), with positive populations identified using isotype (IL-6) or fluorescence minus one controls. Detailed staining protocols are described in Supplementary Methods (<http://onlinelibrary.wiley.com/doi/10.1002/art.41161/abstract>).

Synovial tissue culture supernatant analysis. Supernatants from 3 independent 24-hour synovial tissue cultures per donor were stored at -20°C until testing. Concentrations of 13 soluble mediators (full list in Supplementary Methods, <http://onlinelibrary.wiley.com/doi/10.1002/art.41161/abstract>) were determined using a BioLegend LEGENDplex Human Adipokine flow cytometry-based ELISA and normalized to tissue sample weight (pg/ml/mg tissue).

Statistical analysis. Statistical analysis was performed using GraphPad Prism 7. P values less than 0.05 were considered significant. Digestion condition comparisons were summarized using the mean \pm SD, and differences were assessed by parametric testing (Student's paired t -test and one-way analysis of variance with Dunnett's multiple comparison test). Patient characteristics were summarized using the median and interquartile range (IQR), with differences assessed by Kruskal-Wallis test with Dunn's test for multiple comparisons or Spearman's rank correlation. Hierarchical clustering by correlation was performed with ClustVis (bit.cs.ut.ee/clustvis/) (21).

RESULTS

Developing a multiparameter approach to analyze OA synovium. *Assay approach.* Many studies have demonstrated heterogeneity in OA synovial responses (4,15–18,22–25), reflecting potential differences in disease pathology. To phenotype synovial response patterns in knee OA, we combined ex vivo flow cytometry and multianalyte ELISAs after limited culture of intact tissue (Figure 1A). This approach allowed simultaneous measurement of soluble mediators and cellular composition for correlation analysis. Intracellular IL-6 staining was chosen for this investigation, because IL-6 is independently associated with joint damage and has highly variable expression in joint injury (17,18,20,23,25).

Establishing culture conditions for OA tissue analysis. We first determined the amount of synovial tissue needed to accurately sample hematopoietic immune cell (CD45+), endothelial cell (CD45–CD31+), and mesenchymal cell (CD45–CD31–) populations (Supplementary Figure 1A, <http://onlinelibrary.wiley.com/doi/10.1002/art.41161/abstract>). Pooling randomly selected samples demonstrated that although cell yield increased linearly with tissue amount (Supplementary Figure 1B), low variability in the marker expression between technical replicates was seen in as little as ~400 mg of tissue (4 samples) (Supplementary Figures 1C–E). Since variability trended lower with higher tissue amounts, 12 samples (~1,200 mg) were pooled for each flow cytometry staining panel. As all flow cytometry samples were treated with the protein transport inhibitor monensin to prevent cytokine secretion (necessary for intracellular staining), we also compared the cell recovery between fresh surgical (day 0) and monensin-cultured (day 1) samples. Overnight culture with monensin decreased the cell yield by one-third, but this cell loss did not disproportionately affect the recovery of total or specific hematopoietic immune, mesenchymal, or endothelial cell populations (Supplementary Figure 2, <http://online.library.wiley.com/doi/10.1002/art.41161/abstract>), which validates this ex vivo approach to intracellular cytokine staining.

Optimizing enzymatic digestion protocols for ex vivo tissue flow cytometry. Enzymatic tissue disaggregation was chosen over mechanical disruption alone in order to facilitate release of joint cells from their connective tissue matrix. Since enzymatic digestion may limit flow staining by surface molecule cleavage, a major technical objective was to optimize digestion conditions across diverse cell markers. We tested 6 protocols derived from prior synovial or mesenchymal cell studies (26–30) (Figure 1B). All 6 enzyme cocktails included collagenase and DNase but varied based on media change, digestion time, and other added enzymes. The first 3 conditions, modified from lymph node fibroblastic reticular cell isolation (31), increased digestion efficiency by adding Dispase and replacing enzymes every 15 minutes until tissue dissolved (~2 hours). Conditions 4–6 were more characteristic of prior synovial protocols (27,30). Tissue was di-

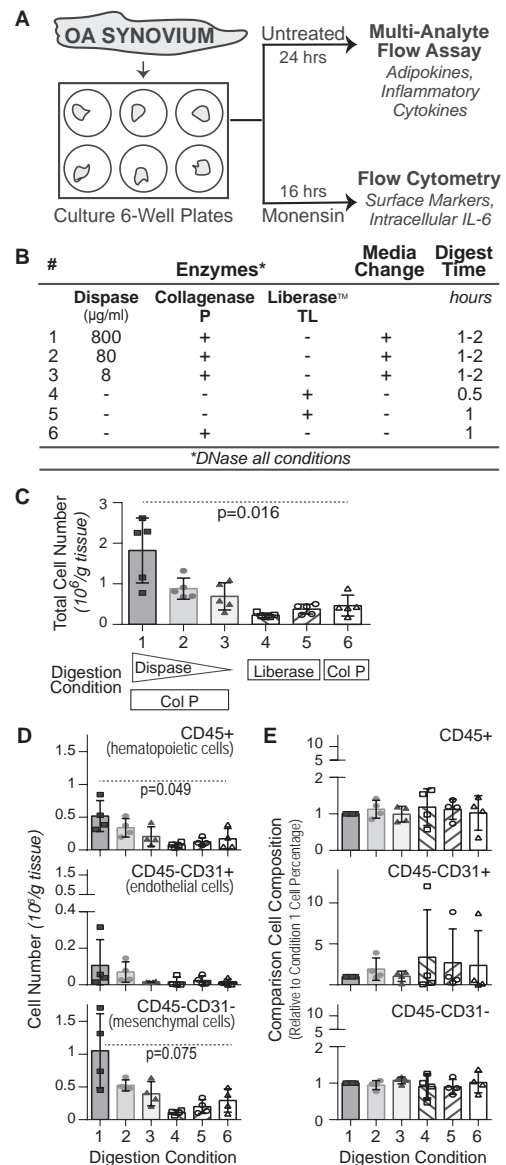


Figure 1. Influence of digestion conditions on synovial cell yield. **A**, Experimental approach. Fresh osteoarthritis (OA) synovial samples (~100 mg) were cultured overnight. Media from 3 samples were analyzed for soluble mediator release using a multianalyte, flow-based enzyme-linked immunosorbent assay. Independent samples were cultured using the protein transport inhibitor monensin prior to disaggregation for surface marker and intracellular interleukin-6 (IL-6) analysis by flow cytometry (12 samples/digestion). **B**, Digestion conditions tested for synovial disaggregation. **C**, Cell yield (per gram of tissue) for each digestion condition, determined by manual counting. **D**, Numbers of hematopoietic immune cells (CD45+), endothelial cells (CD45–CD31+), and mesenchymal cells (CD45–CD31–), calculated for each digestion condition by multiplying total cell yield by the cell percentage measured by flow cytometry. **E**, Percentage of CD45+, CD45–CD31+, and CD31–CD45– cells released by digestion condition. In **C–E**, each symbol represents an individual sample (n = 4–5); bars show the mean ± SD. P values were determined by parametric repeated measures and one-way analysis of variance. P values not shown are >0.2. Col P = collagenase P.

gested without enzyme replacement for a fixed period of time, using either commercially available Liberase TL (collagenase and thermolysin; conditions 4 and 5) or collagenase P alone (condition 6).

Dispase addition with enzyme replacement (conditions 1–3) increased average cell yields compared to fixed time digestions with Liberase TL or collagenase (Figure 1C). Cell yield in high Dispase (condition 1) averaged 1.8×10^6 cells/gm tissue, more than twice that of other conditions. Differences in cell yields were not statistically significant between other conditions, but there was a trend toward a stronger association with Dispase (conditions 2 and 3). Not surprisingly, the absolute number of hematopoietic immune cells (CD45+) and mesenchymal cells (CD45–CD31–) recovered was also highest in condition 1, with endothelial cells (CD45–CD31+) also following this trend (Figure 1D). However, no significant differences were detected in the proportion (relative percentage) of CD45+, CD45–CD31–, and CD45–CD31+ cells

isolated between conditions (Figure 1E), indicating that all major cell types were adequately sampled by all protocols. Overall, mesenchymal cells were the most abundant, followed by hematopoietic immune cells (Figure 1D), although there was wide variability among patients. Endothelial cells were significantly less abundant (median 59.9% [IQR 16.6%] for mesenchymal cells; 37.8% [IQR 16%] for hematopoietic cells; 2.11% [IQR 2.23%] for endothelial cells).

Fine-tuning digestion condition by cell type. We next tested the stability of surface marker staining under different digestion conditions. For many markers, no differences were detected, including for CD8, CD45RA, CD45RO, CD11b, HLA–DR, CD14, and CD206 (Supplementary Table 3, <http://onlinelibrary.wiley.com/doi/10.1002/art.41161/abstract>). However, digestion protocol did impact cell viability and detection of other cell populations, including CD4+ T helper cells, natural killer (NK) cells, and mesenchymal cells (Figure 2 and Supplementary Table 3).

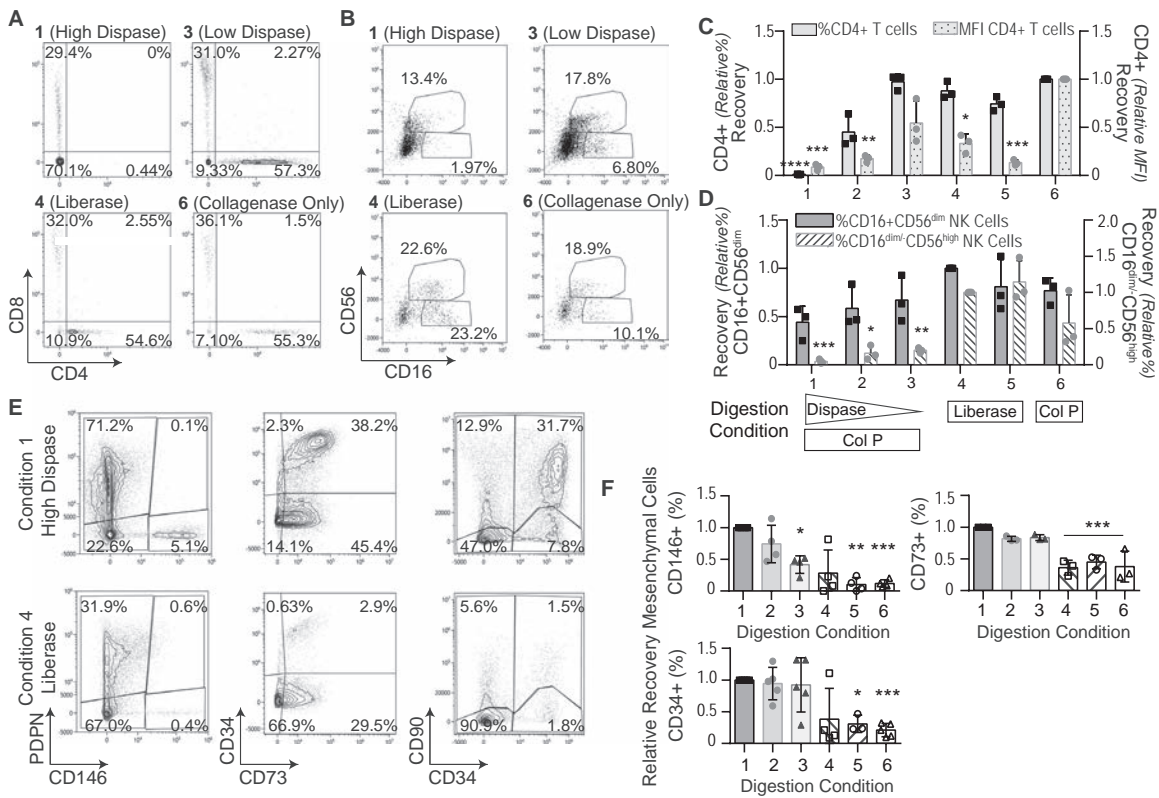


Figure 2. Optimization of disaggregation for ex vivo tissue flow cytometry. **A** and **B**, Representative CD4/CD8 cell (pregate CD45+CD3+CD11b–CD20–) staining (**A**) or natural killer (NK) cell (pregate CD45+CD3–CD11b–CD20–) staining (**B**) after digestion under different conditions (1 donor) is shown. Condition 1 included collagenase + 800 µg/ml (high) Dispase; condition 3 included collagenase + 8 µg/ml (low) Dispase; condition 4 included Liberase; and condition 6 included collagenase only. **C** and **D**, Recovery of CD4+ T cell subsets (**C**) or NK cell subsets (**D**) was compared between digestion protocols by normalizing cell percentage or mean fluorescence intensity (MFI) to that observed under the highest-expressing condition. CD4+ T cells were normalized to condition 6, and NK cells were normalized to condition 4. **E**, Representative podoplanin (PDPN), CD146, CD34, CD73, and CD90 staining on mesenchymal cells (pregate CD45–CD31–) isolated from 1 donor synovium after high Dispase (condition 1) or short Liberase (condition 4) digestion is shown. **F**, Relative recovery of CD146+, CD34+, and CD73+ mesenchymal cells was compared between digestion protocols by normalizing cell percentage for each condition to that observed under condition 1. In **C**, **D**, and **F**, each symbol represents an individual sample (n = 3–5); bars show the mean ± SD. P values were determined by repeated measures and one-way analysis of variance with Dunnett’s test for multiple comparisons. * = P ≤ 0.05; ** = P ≤ 0.01; *** = P ≤ 0.001; **** = P ≤ 0.0001. Col P = collagenase P.

Reducing Dispase significantly improved detection of CD4, the T helper cell coreceptor, as shown in representative flow plots in Figure 2A and measured by average CD4+ cell percentage and mean fluorescence intensity (MFI) (Figure 2C). CD4+ T cell percentage was similar in low Dispase (condition 3), in short Liberase (condition 4), and in collagenase alone (condition 6), while CD4 signal intensity (MFI) was strongest in collagenase alone, with addition of Dispase (conditions 1–3) or thermolysin (Liberase component; conditions 4 and 5) reducing staining brightness.

Slightly different digestion conditions facilitated detection of the following NK cell populations: CD3–CD16+CD56^{dim} and CD3–CD16^{dim}–CD56^{high} cells (Figures 2B and D). CD16+CD56^{dim} cells were detected under all conditions (Figure 2D), although detection worked best with short Liberase digestion (condition 4). CD16^{dim}–CD56^{high} NK cell detection was more difficult (Figure 2D), with staining most effective using Liberase (conditions 4–5) and detectability completely lost with Dispase addition (conditions 1–3).

In contrast to T cells and NK cells, specific mesenchymal markers are less well defined. CD146, podoplanin (PDPN), CD73, CD34, and CD90 were chosen for study based on prior histology studies (32–36) and recent synovial fibroblast flow cytometry and transcriptional analysis (29). Detection of these markers was facilitated by more aggressive, high-Dispase digestion (Figures 2E and F and Supplementary Table 3, <http://onlinelibrary.wiley.com/doi/10.1002/art.41161/abstract>). Improved staining was not solely due to increased digestion time, as marker staining (particularly for CD146) increased with dose-dependent Dispase addition (Figure 2F). Indeed, most mesenchymal markers trended toward better detection with increased Dispase concentrations (Supplementary Table 3).

These results show that reliable *ex vivo* tissue flow cytometry requires careful optimization of tissue disaggregation protocols to ensure marker stability. For this study, 2 disaggregation protocols were chosen. High-Dispase digestion (condition 1) was used for mesenchymal and hematopoietic immune cell analysis. Low-Dispase digestion (condition 3) was used for T cell analysis, as it represented the best balance between CD4 discrimination, cost, and cell yield. Further NK cell analysis was not performed in this study.

OA synovial cell analysis. *Hematopoietic immune cells.* Analysis showed that ~40% of synovial cells were hematopoietic (CD45+) in origin, with wide variability among patients (Figure 3A). CD11b+HLA-DR+ cells (majority macrophages) were most abundant (median 71.4% [IQR 29.7%]), followed by T cells (CD3+ 10.8% [IQR 14.3%]), neutrophils (CD11b+HLA-DR+CD66b+ 2.22% [IQR 2.49%]), another myeloid CD11b+HLA-DR– population (1.10% [IQR 1.13%]), and B cells (CD20+HLA-DR+ 0.310% [IQR 1.14%]) (Figure 3B). A CD45+ lineage marker–negative population (median 6.59% [IQR 9.60%]) was also detected, likely representing a mixture of other hematopoietic cells (e.g., mast cells, NK cells) and cells with marker cleavage during digestion.

OA T cells. Immune cell analysis showed high variability among donors in synovial T cell percentage (0–42.6%) (Figure 3B). Although T cell function in OA is poorly understood, animal models suggest that both CD4+ and CD8+ T cells promote pathology after injury (37,38). Therefore, OA T cells were further characterized by flow cytometry (Figure 3). As expected (39,40), CD4+ T helper cells were increased (median 58.4% [IQR 17.4%]) compared to CD8+ cytotoxic T cells (29.9% [IQR 16.1%]) (Figure 3C). However, both T cell types accumulated with increasing total T cell numbers (Supplementary Table 4, <http://onlinelibrary.wiley.com/doi/10.1002/art.41161/abstract>). Most CD4+ T cells expressed the effector/memory marker CD45RO (median 91.6% [IQR 6.25%]) (Figure 3D). Most CD8+ T cells were also effector/memory cells (CD8+CD45RO+ median 61.3% [IQR 26.6%]), but there was a higher percentage of naive CD45RA cells (21.5% [IQR 20.0%]) and cells positive for both markers (4.85% [IQR 11.4%]).

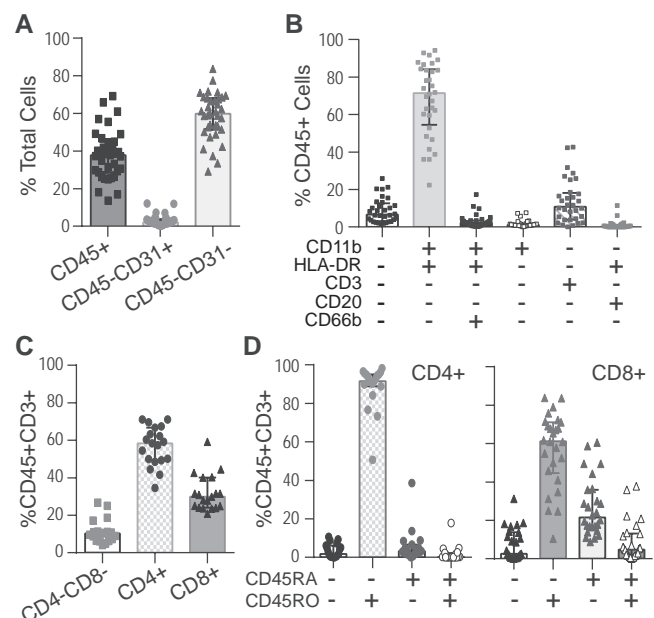


Figure 3. Wide patient variability in T cell accumulation assessed by hematopoietic immune cell analysis. **A**, Percentages of hematopoietic immune cells (CD45+), endothelial cells (CD45–CD31+), and mesenchymal cells (CD45–CD31–) in osteoarthritis synovium were measured by flow cytometry (high-Dispase digestion; n = 35). **B**, Percentages of different hematopoietic immune cell (CD45+) populations were determined using surface expression of myeloid (CD11b, HLA–DR), T cell (CD3), B cell (CD20), and neutrophil (CD66b) markers (high-Dispase digestion; n = 32). **C**, Percentages of CD4+ T helper cells and CD8+ cytotoxic T cells are shown (gate CD45+CD3+; low-Dispase digestion; n = 19). **D**, CD4+ cell (n = 19) or CD8+ cell (n = 26) expression of CD45RA+ (naive) and CD45RO+ (effector/memory) cells was analyzed (low-Dispase digestion). T cell analysis began using high-Dispase digestion. Once it was determined that CD4 staining was not reliable, digestion was switched to low Dispase, which accounts for the reduced number of donors for CD4+ cell analysis. Each symbol represents an individual sample; bars show the median and interquartile range.

Mesenchymal cells. Compared to hematopoietic immune cells, much less is known about OA mesenchymal cell (CD45–CD31–) populations. The existence of functionally distinct synovial mesenchymal/fibroblast populations is supported by recent reports showing that CD34 and/or CD90 expression skews toward different gene transcription and functional profiles (29,41). In the present analysis, vascular-associated mesenchymal cells (e.g., pericytes) were first separated by expression of CD146, also known as melanoma cell adhesion molecule (Figure 4A). CD45–CD31–CD146+ cells help regulate vascular tone and represent a small subset of total mesenchymal cells. The remaining CD146– cells, mainly synovial fibroblasts as determined by transcriptional

analysis (29), were separated into 7 populations averaging ≥1% of the total mesenchymal population based on PDPN, CD73, CD90, and CD34 surface expression (Figure 4B). The majority of cells were PDPN+CD73+, with CD90–CD34– cells the largest subset (median 32.4% [IQR 29.2%]), followed by CD90+CD34+ (20.0% [IQR 17.6%]), CD90+CD34– (16.7% [IQR 24.1%]), and CD90–CD34+ (2.68% [IQR 5.42%]). Two PDPN+CD73– subsets were also identified: CD90–CD34– cells (median 5.23% [IQR 15.4%]) and CD90+CD34– cells (1.48% [IQR 2.28%]). There was also a significant marker-negative population (median 8.28% [IQR 6.93%]), representing either a unique population and/or cells whose surface markers were cleaved during digestion.

Clues to mesenchymal cell function. To examine the possible function of different mesenchymal/fibroblast populations, associations between mesenchymal and nonmesenchymal cells were assessed. Significant correlations were found between the 2 largest mesenchymal and hematopoietic immune populations (Figures 4C–F). PDPN+CD73+CD90–CD34– cells correlated positively with CD45+CD11b+HLA–DR+ cells (largely synovial macrophages) and correlated negatively with CD45+CD3+ T cells (Figures 4C and D). This result suggests a synovial lining fibroblast population, as lining fibroblasts tightly co-compact with synovial macrophages. In contrast, PDPN+CD73+CD90+CD34+ cells correlated positively with T cells and correlated negatively with synovial macrophages (Figures 4E and F), suggesting a sublining fibroblast population. These correlations are consistent with prior histologic assessments (32,36) and tissue immunofluorescence staining (29,33–35,41), which show strong CD34 and CD90 expression in rheumatoid arthritis (RA) and OA synovial sublining. Additional correlations suggest other possible mesenchymal cell interactions with endothelial cells, T cells, B cells, and lineage-negative hematopoietic cells (Supplementary Table 5, <http://onlinelibrary.wiley.com/doi/10.1002/art.41161/abstract>).

OA IL-6 analysis in synovium. Major contribution by mesenchymal cells in OA IL-6 response. Although IL-6 is associated with increased OA pain and joint damage (9,18,19,25), OA synovial fluid IL-6 levels are highly variable, ranging from barely detectable to levels similar to those observed in RA (17). To better understand this variation, synovial cell IL-6 responses were measured ex vivo by flow cytometry (Figure 5A). Validating this approach, the number of IL-6–positive synovial cells per donor calculated by flow cytometry strongly correlated with the IL-6 released by independent synovial tissue cultures from the same donor (Figure 5B).

This analysis showed that although all cell types produce some IL-6, the cell number and intensity of expression varied significantly between different donors and cell types (Figure 5). For most donors, the percentage of IL-6–positive cells was higher in mesenchymal cells (median 13.6% [IQR 19.6%]) compared to hematopoietic cells (4.44% [IQR 17.4%]) or endothelial cells

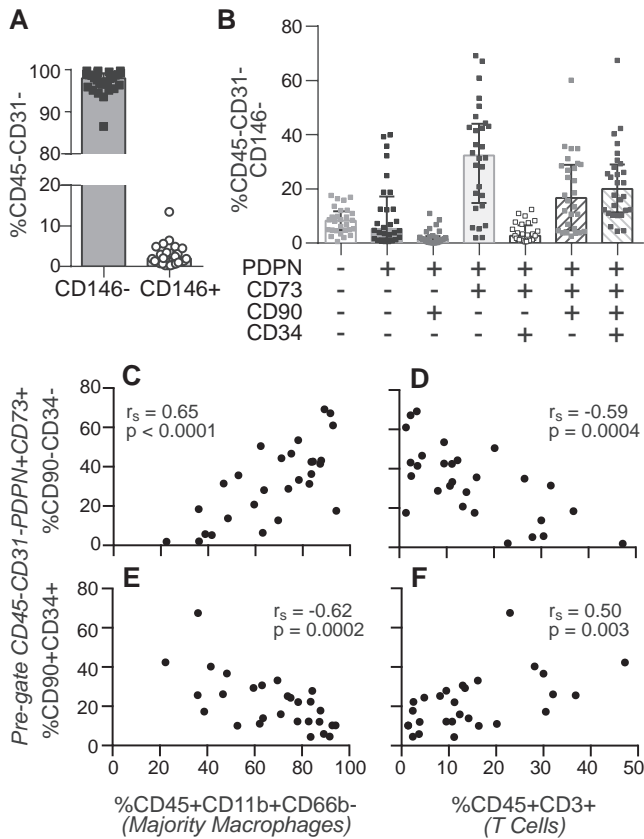


Figure 4. Correlations between synovial fibroblast and hematopoietic immune cell populations. **A**, Mean percentages of CD146+ vascular and CD146– nonvascular mesenchymal cells were analyzed in osteoarthritis synovium after high-Dispase digestion (n = 28). **B**, CD45–CD31–CD146– cells were further analyzed according to podoplanin (PDPN), CD73, CD90, and CD34 expression using tree analysis (Kaluza). Seven CD146– cell subsets with mean percent expression >1% of total number of CD146– cells were identified. In **A** and **B**, each symbol represents an individual sample; bars show the median and interquartile range. **C–F**, The mean percent expression of CD90–CD34– cells (**C** and **D**) and CD90+CD34+ cells (**E** and **F**) among mesenchymal cells was positively or negatively correlated with the mean percent expression of CD45+CD11b+CD66b– myeloid cells (**C** and **E**) and CD45+CD3+ T cells (**D** and **F**), by Spearman’s rank correlation (n = 28).

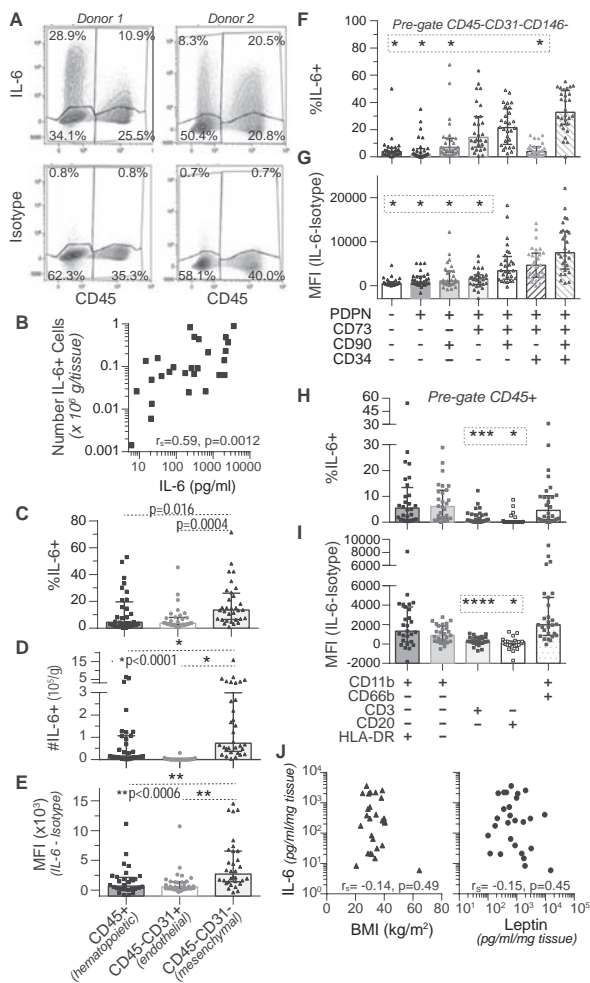


Figure 5. Diversity of interleukin-6 (IL-6) production in osteoarthritis synovium with robust mesenchymal expression. **A**, Representative synovial hematopoietic cell (CD45+) and mesenchymal cell (CD45–CD31–) intracellular IL-6 flow cytometry staining is shown, with corresponding isotype controls. **B**, IL-6 synovial tissue culture release (Adipokine Panel; LEGENDplex) correlated positively (by Spearman's rank correlation) with the total IL-6–positive cell number independently calculated by flow cytometry. Mean value of 3 independent samples per donor ($n = 27$) is shown. **C**, **F**, and **H**, The percentage of IL-6–positive cells was measured by flow cytometry in the major cell (**C**), CD146– mesenchymal cell (**F**), and CD45+ hematopoietic immune cell (**H**) populations. **D**, IL-6–positive cell number in major cell populations was calculated from the total donor cell yield. **E**, **G**, and **I**, IL-6 mean fluorescence intensity (MFI) was calculated by subtracting background signal (antibody isotype) from population IL-6 MFI for the major cell (**E**), CD146– mesenchymal cell (**G**), and CD45+ hematopoietic immune cell (**I**) populations. **J**, Synovial tissue culture IL-6 release did not correlate with the adipocyte surrogates body mass index (BMI) or leptin release. Spearman's rank correlation test was used ($n = 27$). In **C–I**, each symbol represents an individual sample; bars show the median and interquartile range. Kruskal-Wallis test with Dunn's multiple comparisons test was used to assess the significance of differences from the following reference populations: **C–E**, CD45–CD31– ($n = 32$); **F** and **G**, PDPN+CD73+CD90+CD34+ ($n = 28$); and **H** and **I**, CD11b+CD66b–CD3–CD20–HLA–DR+ ($n = 28$). * = $P \leq 0.0001$; ** = $P < 0.0006$; *** = $P = 0.007$; **** = $P = 0.004$. PDPN = podoplanin.

(3.74% [IQR 19.6%]) (Figures 5A and C). However, in a small number of donors (6 of 32), this trend was reversed, with a greater percentage of CD45+IL-6+ cells. There was also a greater number of IL-6–positive mesenchymal cells (median 0.74×10^5 [IQR 2.6×10^5] cells/gm tissue) compared to hematopoietic cells (0.16×10^5 [IQR 0.96×10^5]) or endothelial cells (0.0094×10^5 [IQR 0.023×10^5]) (Figure 5D). In addition, mesenchymal cells showed an average of 3 times more IL-6 per cell, as measured by MFI (Figure 5E). Overall, this analysis demonstrated considerable variability in IL-6 production according to synovial cell type, with mesenchymal cells proving to be a major source in most patients.

IL-6 production in synovial fibroblast subsets. Although IL-6 was expressed by all mesenchymal populations, the percentage of IL-6–positive cells was highest in the following PDPN+CD73+ populations: CD90–CD34–, CD90+CD34–, and CD90+CD34+ cells (Figure 5F). These results mirror the relative abundance of these subsets in OA synovium (Figure 4B). However, the IL-6 staining intensity (MFI) was highest in the PDPN+CD73+CD90+CD34+ (likely sublining) population and decreasing in the PDPN+CD73+CD90–CD34– (likely lining) population (Figure 5G). These results suggest the presence of an IL-6 gradient across the OA synovium, pointing to further complexity in synovial IL-6 responses.

IL-6 production in other cells. Hematopoietic cells also contribute significantly to OA IL-6 (Figures 5A, C, D, and E), with the greatest percentage of IL-6–positive cells in synovial myeloid cells/macrophages (CD11b+CD66b–) and, surprisingly, in neutrophils (CD66b+) (Figure 5H). IL-6 response was significantly lower in T cells (CD3+) and B cells (CD20+). Interestingly, IL-6 production per cell (MFI) was highest and of comparable intensity in synovial macrophages and neutrophils, roughly 5 times that of lymphocytes (Figure 5I). However, based on cell number, neutrophils likely contribute little to the total IL-6 response as they are a minor cell population (Figure 3B). Similarly, although IL-6 release was clearly detectable in endothelial cells, they also likely contribute only a small proportion to total synovial IL-6 based on cell number (Figures 5C–E). Finally, adipocytes are another potential source of synovial IL-6. As adipocytes are damaged by tissue disaggregation, their IL-6 production cannot be measured by flow cytometry. However, IL-6 release did not correlate with the adipocyte surrogates BMI or leptin release (Figure 5J), suggesting that adipocytes are not a major IL-6 source in these samples.

Understanding IL-6 responses by correlation analysis. To determine if other soluble mediators are also associated with OA IL-6 responses, correlations between IL-6 synovial culture release and a panel of 12 cytokines, chemokines, and adipokines were assessed (Figure 6A and Supplementary Table 4, <http://online.library.wiley.com/doi/10.1002.art.41161/abstract>). IL-6 most strongly correlated with IL-8, but it also directly correlated with

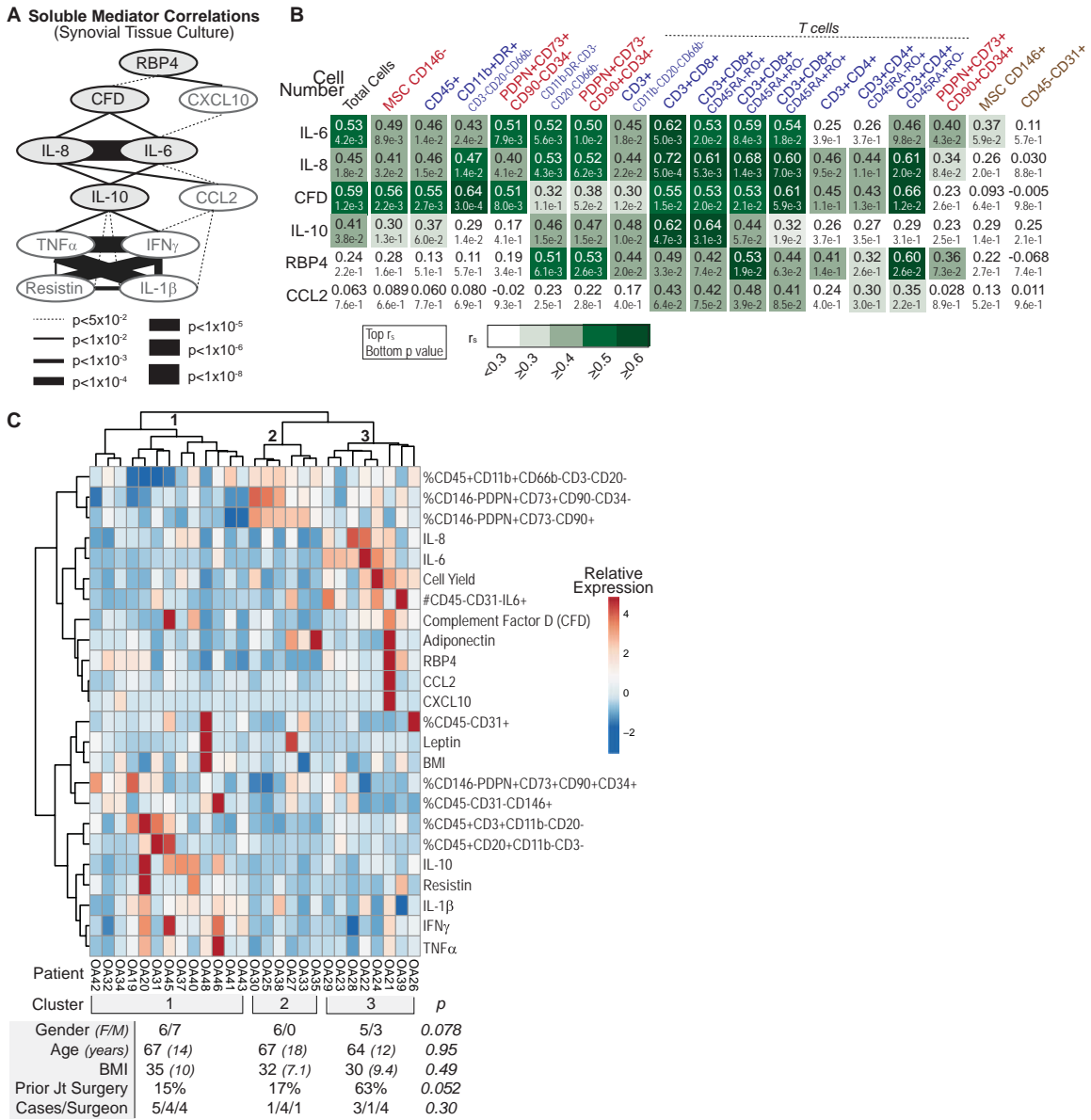


Figure 6. Correlation-based clustering using synovial soluble mediator release and cell composition revealing different osteoarthritis (OA) response patterns. **A**, Positive correlations between soluble mediators released after synovial tissue culture across multiple donors ($n = 27$). No positive correlations with adiponectin or leptin release were detected (Supplementary Table 4, <http://onlinelibrary.wiley.com/doi/10.1002/art.41161/abstract>). **B**, Strength of correlations between the indicated cell population numbers and soluble mediators ($n = 19-27$). **C**, Data obtained from analysis of OA synovium by cellular composition (flow cytometry [italics]) and soluble mediator release (multianalyte enzyme-linked immunosorbent assay [boldface]), combined with body mass index (BMI) in a correlation-based hierarchical clustering algorithm to separate different OA populations (ClustVis) (clustering method, columns and rows: correlation; clustering distance, columns and rows: Ward linkage). Limited clinical data separated by cluster are provided below the heatmap. P values were determined by Kruskal-Wallis test (continuous variables) or chi-square test (categorical variables). RBP-4 = retinol binding protein 4; CFD = complement factor D; IL-8 = interleukin-8; TNF = tumor necrosis factor; IFN = interferon; MSC = mesenchymal stem cell; PDPN = podoplanin.

complement factor D (CFD), IL-10, CCL2, and CXCL10 release (Figure 6A, Supplementary Figure 3A, and Supplementary Table 4). An additional strong expression network formed between tumor necrosis factor (TNF), interferon- γ (IFN γ), IL-1 β , and resistin, linking to IL-6 through IL-10 and CCL2 expression.

Further analysis revealed additional positive correlations between IL-6, several mediators (Figure 6A), and the numbers of total and specific synovial cell populations (Figure 6B and Supplementary Figure 3, <http://onlinelibrary.wiley.com/doi/10.1002/art.41161/abstract>). Increased total cell number correlated with IL-6, IL-8, IL-10, and CFD release, but not with other soluble

mediators such as CCL2 and TNF (Figure 6, Supplementary Figure 3, and Supplementary Table 4). In general, these 4 soluble mediators correlated with increased cell numbers across synovial cell populations, although there were exceptions (Figure 6B). IL-6 release correlated less strongly with the dominant CD45RA-RO+ CD4+ T cell population, but it did correlate with mesenchymal cells, macrophages, CD8+ T cells, and naive CD4+ T cells. IL-10 release also correlated most strongly with total T cell numbers, specifically with CD8+ T cell numbers. Finally, retinol binding protein 4 (RBP-4), and to a lesser extent CCL2 release, emerged as a distinct marker of increased T cell and/or T cell-associated mesenchymal cell numbers. These data indicate that specific groups of soluble mediators may be used to predict elements of synovial cell composition, such as increased cellularity or T cell accumulation.

Clustering of OA patients based on synovial responses.

To move beyond single correlations, we used hierarchical correlation-based clustering of flow cytometry, soluble mediator, and clinical data to determine if there were specific response patterns associated with the observed patient variability. Indeed, 3 major patterns were identified (Figure 6C). Cluster 1 was most strongly associated with increased T cells and T cell-associated cytokines (IL-10, IFN γ , and TNF), while clusters 2 and 3 were associated with increased macrophage expression (CD45+ CD11b+CD66b-CD3-CD20-). Cluster 2 showed the highest percentage of macrophages and potential lining fibroblasts (PDPN+CD73+CD90-CD34-), including a subcluster with high adiponectin expression. In contrast, cluster 3 correlated best with high total cell yield and IL-6 and IL-8 responses, especially by mesenchymal cells.

Next, we examined whether these clusters are associated with any of the limited clinical data collected (Figure 6C). There were trends toward an association of cluster 2 with female sex ($P = 0.078$) and an association of cluster 3 with prior arthroscopic or joint replacement surgery ($P = 0.052$). The clinical relevance of these findings is uncertain, as the present study did not correct for demographic and patient comorbidity confounders. However, these results highlight the possibility that phenotyping OA synovial responses may provide new insights into patient heterogeneity and disease pathology.

DISCUSSION

Synovial inflammation is associated with increased OA pain and joint damage, although there is considerable variability among patients in inflammatory responses (7,9,14,16,17,19,23,25,42). How this variability impacts disease development is hampered by a limited understanding of the cellular and molecular mechanisms active in OA synovitis. In the present study, we developed an approach using multiparameter flow cytometry and ELISA, which showed several findings relevant to OA pathology and synovial tissue research generally.

Synovial tissue flow cytometry was chosen because it increases cell identification compared to standard immunohistochemistry. However, ex vivo tissue flow cytometry requires effective tissue disaggregation without significant loss of cell viability or surface markers. We found that optimal digestion protocols depends on cell type and marker (Figure 2 and Supplementary Table 3, <http://onlinelibrary.wiley.com/doi/10.1002/art.41161/abstract>), and noted a particular difficulty staining lymphocytes and mesenchymal cells with the same protocol. Similar challenges were recently reported by the Accelerating Medicines Partnership Network, which found combining a commercial dissociator system and Liberase TL digestion optimal in their tested conditions (27).

One strength of this study is that it highlights that accurate synovial flow cytometry analysis requires clear data on how cell yield and surface marker stability are influenced by choice of disaggregation protocol. Another study strength is that it demonstrates that correlation analysis can be used to suggest potential cellular interactions. For example, with this technique we detected 2 prominent PDPN+CD73+ fibroblast populations: CD90-CD34- and CD90+CD34+ cells (Figure 4). The CD90-CD34- population correlated inversely with T cells (CD45+CD3+) and the CD90+CD34+ population correlated inversely with macrophage/myeloid cells (CD45+CD11b+CD3-CD20-CD66b-), suggesting that CD90-CD34- cells are lining fibroblasts (positively correlated with myeloid cells) and CD90+CD34+ cells are sublining fibroblasts (positively correlated with T cells). These conclusions have been independently supported by tissue staining studies showing enriched CD90 and CD34 expression in OA and RA synovial sublining (29,32,33,35,36,41). Recent ex vivo studies also support the notion that mesenchymal subpopulations may have unique functions in RA (29,41), although their role in OA remains undefined. Given that several potential cell interactions were detected using this small patient cohort (Figure 4 and Supplementary Table 5, <http://onlinelibrary.wiley.com/doi/10.1002/art.41161/abstract>), we predict that an expanded analysis will provide further guidance about how cellular niches function in synovial pathology.

Cell analysis and correlation analysis also point to potential differences in CD4+ and CD8+ T cell compartments. There was pronounced variability in T cell percentage among patients (Figure 3), which is consistent with the variable lymphocytic sublining aggregates observed in OA (39). As previously reported (39,40,43,44), CD4+ T cells were more prevalent than CD8+ cells. However, CD8+ cells showed increased variability in expression of CD45RA (naive) and CD45RO (effector/memory) markers (Figure 3D). In addition, CD8+ T cell numbers more strongly correlated with tissue release of several proinflammatory/regulatory molecules (IL-6, IL-8, CFD, IL-10, RBP-4, and CCL2) (Figure 6B). Prior studies suggest that both CD4+ and CD8+ T cells contribute to OA pathology; both subtypes have a Th1 phenotype (40,43,45,46), and the knockout of each reduces damage in

mouse OA models (37,38). The present study broadens our perspective on OA T cells, suggesting more complex roles for specific T cell subpopulations.

This study also provides the most detailed examination to date of synovial IL-6 production. Although a pathologic role for IL-6 is well recognized in RA, joint IL-6 also independently associates with OA pain and radiographic progression (9,25), and its blockade attenuates joint damage in a mouse OA model (47). Furthermore, IL-6 is one of the most variable proinflammatory cytokines in joint injury, varying 10,000-fold between patients (17,20). This study suggests that the considerable diversity in cellular IL-6 source (Figure 5) may help explain part of this patient variability. On average, IL-6 expression was highest in mesenchymal cells, although in a handful of patients, hematopoietic immune cell (mainly macrophage) expression was more dominant. This complexity suggests that defining IL-6 levels and source may be important in predicting how this cytokine affects patient outcomes.

Our study also shows the potential power of combining different data types to analyze OA patient responses (Figure 6C). Through clustering, patients were broadly categorized into a T cell/lymphocyte cluster (cluster 1) and myeloid clusters (clusters 2 and 3), with cluster 3 in particular being associated with high tissue and mesenchymal cell IL-6 and IL-8 release. There are early suggestions that these clusters reflect different patient phenotypes, with cluster 2 trending toward an association with female sex and cluster 3 with a history of prior joint surgery (arthroscopy/arthroplasty) (Figure 6C). It remains to be seen if these clusters can be better defined and how they relate to disease progression and clinical phenotypes.

There are several study limitations, including the need to dissect and culture synovial tissue for flow and ELISA analysis, which may potentially change cellular phenotypes. Additionally, tissue sampling bias may have influenced study results. Prior RA and OA studies suggest that good histologic or RNA sequencing reproducibility can be achieved with 3–4 ultrasound-guided synovial biopsy samples (15,48) or with ~150 mg tissue (27). We found low variability with 4 ~100-mg OA tissue samples, but we generally used higher tissue amounts to reduce bias. A larger confounder is that we did not control for anatomic location in sampling, an issue due to patchiness in OA inflammation and regional variations in synovial anatomy. How anatomy affects synovial responses remains an open issue in the field and requires additional comparative studies to define how synovial responses vary by distinct regional location within each patient. Finally, it is known that synovial findings change in OA as disease progresses (4,15), so a similar analysis comparing early- and late-disease tissue, along with analyzing radiographic damage and additional clinical variables, is needed in future investigations.

Despite these limitations, this study demonstrates that multiparameter investigations of OA synovial responses may

provide insight into OA patient heterogeneity and supports the possibility that synovial sampling may be a future tool in OA patient care.

AUTHOR CONTRIBUTIONS

All authors were involved in drafting the article or revising it critically for important intellectual content, and all authors approved the final version to be published. Dr. Noss had full access to all of the data in the study and takes responsibility for the integrity of the data and the accuracy of the data analysis.

Study conception and design. Labinsky, Noss.

Acquisition of data. Labinsky, Panipinto, Ly, Khuat, Madarampalli, Mahajan, Clabeaux, MacDonald, Verdin, Buckner.


Analysis and interpretation of data. Labinsky, Panipinto, Noss.

REFERENCES

- Cibrián Uhalte E, Wilkinson JM, Southam L, Zeggini E. Pathways to understanding the genomic aetiology of osteoarthritis. *Hum Mol Genet* 2017;26:R193–201.
- Beekhuizen M, Gierman LM, van Spil WE, Van Osch GJ, Huizinga TW, Saris DB, et al. An explorative study comparing levels of soluble mediators in control and osteoarthritic synovial fluid. *Osteoarthritis Cartilage* 2013;21:918–22.
- Knoop J, van der Leeden M, Thorstensson CA, Roorda LD, Lems WF, Knol DL, et al. Identification of phenotypes with different clinical outcomes in knee osteoarthritis: data from the Osteoarthritis Initiative. *Arthritis Care Res (Hoboken)* 2011;63:1535–42.
- Oehler S, Neureiter D, Meyer-Scholten C, Aigner T. Subtyping of osteoarthritic synoviopathy. *Clin Exp Rheumatol* 2002;20:633–40.
- Van Spil WE, Jansen NW, Bijlsma JW, Reijman M, DeGroot J, Welsing PM, et al. Clusters within a wide spectrum of biochemical markers for osteoarthritis: data from CHECK, a large cohort of individuals with very early symptomatic osteoarthritis. *Osteoarthritis Cartilage* 2012;20:745–54.
- Vina ER, Kwok CK. Epidemiology of osteoarthritis: literature update. *Curr Opin Rheumatol* 2018;30:160–7.
- Ayral X, Pickering EH, Woodworth TG, Mackillop N, Dougados M. Synovitis: a potential predictive factor of structural progression of medial tibiofemoral knee osteoarthritis—results of a 1 year longitudinal arthroscopic study in 422 patients. *Osteoarthritis Cartilage* 2005;13:361–7.
- Krasnokutsky S, Belitskaya-Lévy I, Bencardino J, Samuels J, Attur M, Regatte R, et al. Quantitative magnetic resonance imaging evidence of synovial proliferation is associated with radiographic severity of knee osteoarthritis. *Arthritis Rheum* 2011;63:2983–91.
- Neogi T, Guermazi A, Roemer F, Nevitt MC, Scholz J, Arendt-Nielsen L, et al. Association of joint inflammation with pain sensitization in knee osteoarthritis: the Multicenter Osteoarthritis Study. *Arthritis Rheumatol* 2016;68:654–61.
- Philp AM, Davis ET, Jones SW. Developing anti-inflammatory therapeutics for patients with osteoarthritis. *Rheumatology (Oxford)* 2017;56:869–81.
- Scanzello CR, Goldring SR. The role of synovitis in osteoarthritis pathogenesis. *Bone* 2012;51:249–57.
- Sellam J, Berenbaum F. The role of synovitis in pathophysiology and clinical symptoms of osteoarthritis. *Nat Rev Rheumatol* 2010;6:625–35.
- Beyers K, Bijlsma JW, Vriesekolk JE, van den Ende CH, den Broeder AA. The course of ultrasonographic abnormalities in knee osteoarthritis: 1 year follow up. *Osteoarthritis Cartilage* 2014;22:1651–6.

14. Guermazi A, Hayashi D, Roemer FW, Zhu Y, Niu J, Crema MD, et al. Synovitis in knee osteoarthritis assessed by contrast-enhanced magnetic resonance imaging (MRI) is associated with radiographic tibiofemoral osteoarthritis and MRI-detected widespread cartilage damage: the MOST study. *J Rheumatol* 2014;41:501–8.
15. Minten MJ, Blom A, Snijders GF, Kloppenburg M, van den Hoogen FH, den Broeder AA, et al. Exploring longitudinal associations of histologically assessed inflammation with symptoms and radiographic damage in knee osteoarthritis: combined results of three prospective cohort studies. *Osteoarthritis Cartilage* 2019;27:71–9.
16. Cuéllar VG, Cuéllar JM, Kirsch T, Strauss EJ. Correlation of synovial fluid biomarkers with cartilage pathology and associated outcomes in knee arthroscopy. *Arthroscopy* 2016;32:475–85.
17. Kaneko S, Satoh T, Chiba J, Ju C, Inoue K, Kagawa J. Interleukin-6 and interleukin-8 levels in serum and synovial fluid of patients with osteoarthritis. *Cytokines Cell Mol Ther* 2000;6:71–9.
18. Larsson S, Englund M, Struglics A, Lohmander LS. Interleukin-6 and tumor necrosis factor α in synovial fluid are associated with progression of radiographic knee osteoarthritis in subjects with previous meniscectomy. *Osteoarthritis Cartilage* 2015;23:1906–14.
19. Stannus OP, Jones G, Blizzard L, Cicuttini FM, Ding C. Associations between serum levels of inflammatory markers and change in knee pain over 5 years in older adults: a prospective cohort study. *Ann Rheum Dis* 2013;72:535–40.
20. Watt FE, Paterson E, Freidin A, Kenny M, Judge A, Saklatvala J, et al. Acute molecular changes in synovial fluid following human knee injury: association with early clinical outcomes. *Arthritis Rheumatol* 2016;68:2129–40.
21. Metsalu T, Vilo J. ClustVis: a web tool for visualizing clustering of multivariate data using Principal Component Analysis and heatmap. *Nucleic Acids Res* 2015;43:W566–70.
22. Lambert C, Dubuc JE, Montell E, Vergés J, Munaut C, Noël A, et al. Gene expression pattern of cells from inflamed and normal areas of osteoarthritis synovial membrane. *Arthritis Rheumatol* 2014;66:960–8.
23. Livshits G, Zhai G, Hart DJ, Kato BS, Wang H, Williams FM, et al. Interleukin-6 is a significant predictor of radiographic knee osteoarthritis: the Chingford Study. *Arthritis Rheum* 2009;60:2037–45.
24. Ma CH, Lv Q, Cao Y, Wang Q, Zhou XK, Ye BW, et al. Genes relevant with osteoarthritis by comparison gene expression profiles of synovial membrane of osteoarthritis patients at different stages. *Eur Rev Med Pharmacol Sci* 2014;18:431–9.
25. Stannus O, Jones G, Cicuttini F, Parameswaran V, Quinn S, Burgess J, et al. Circulating levels of IL-6 and TNF- α are associated with knee radiographic osteoarthritis and knee cartilage loss in older adults. *Osteoarthritis Cartilage* 2010;18:1441–7.
26. Autengruber A, Gereke M, Hansen G, Hennig C, Bruder D. Impact of enzymatic tissue disintegration on the level of surface molecule expression and immune cell function. *Eur J Microbiol Immunol (Bp)* 2012;2:112–20.
27. Donlin LT, Rao DA, Wei K, Slowikowski K, McGeachy MJ, Turner JD, et al. Methods for high-dimensional analysis of cells dissociated from cryopreserved synovial tissue. *Arthritis Res Ther* 2018;20:139.
28. Hagman DK, Kuzma JN, Larson I, Foster-Schubert KE, Kuan LY, Cignarella A, et al. Characterizing and quantifying leukocyte populations in human adipose tissue: impact of enzymatic tissue processing. *J Immunol Methods* 2012;386:50–9.
29. Mizoguchi F, Slowikowski K, Wei K, Marshall JL, Rao DA, Chang SK, et al. Functionally distinct disease-associated fibroblast subsets in rheumatoid arthritis. *Nat Commun* 2018;9:789.
30. Ogata Y, Mabuchi Y, Yoshida M, Suto EG, Suzuki N, Muneta T, et al. Purified human synovium mesenchymal stem cells as a good resource for cartilage regeneration. *PLoS One* 2015;10:e0129096.
31. Fletcher AL, Lukacs-Kornek V, Reynoso ED, Pinner SE, Bellemare-Pelletier A, Curry MS, et al. Lymph node fibroblastic reticular cells directly present peripheral tissue antigen under steady-state and inflammatory conditions. *J Exp Med* 2010;207:689–97.
32. Bauer S, Jendro MC, Wadler A, Kleber S, Stenner F, Dinsler R, et al. Fibroblast activation protein is expressed by rheumatoid myofibroblast-like synoviocytes. *Arthritis Res Ther* 2006;8:R171.
33. Ekwall AK, Eisler T, Anderberg C, Jin C, Karlsson N, Brissler M, et al. The tumour-associated glycoprotein podoplanin is expressed in fibroblast-like synoviocytes of the hyperplastic synovial lining layer in rheumatoid arthritis. *Arthritis Res Ther* 2011;13:R40.
34. Kurth TB, Dell'Accio F, Crouch V, Augello A, Sharpe PT, De Bari C. Functional mesenchymal stem cell niches in adult mouse knee joint synovium in vivo. *Arthritis Rheum* 2011;63:1289–300.
35. Middleton J, Americh L, Gayon R, Julien D, Mansat M, Mansat P, et al. A comparative study of endothelial cell markers expressed in chronically inflamed human tissues: MECA-79, Duffy antigen receptor for chemokines, von Willebrand factor, CD31, CD34, CD105 and CD146. *J Pathol* 2005;206:260–8.
36. Miyake K, Nishida K, Kadota Y, Yamasaki H, Nasu T, Saitou D, et al. Inflammatory cytokine-induced expression of vasohibin-1 by rheumatoid synovial fibroblasts. *Acta Med Okayama* 2009;63:349–58.
37. Hsieh JL, Shiau AL, Lee CH, Yang SJ, Lee BO, Jou IM, et al. CD8+ T cell-induced expression of tissue inhibitor of metalloproteinases-1 exacerbated osteoarthritis. *Int J Mol Sci* 2013;14:19951–70.
38. Shen PC, Wu CL, Jou IM, Lee CH, Juan HY, Lee PJ, et al. T helper cells promote disease progression of osteoarthritis by inducing macrophage inflammatory protein-1 γ . *Osteoarthritis Cartilage* 2011;19:728–36.
39. De Lange-Brokaar BJ, Ioan-Facsinay A, van Osch GJ, Zuurmond AM, Schoones J, Toes RE, et al. Synovial inflammation, immune cells and their cytokines in osteoarthritis: a review. *Osteoarthritis Cartilage* 2012;20:1484–99.
40. Li YS, Luo W, Zhu SA, Lei GH. T cells in osteoarthritis: alterations and beyond [review]. *Front Immunol* 2017;8:356.
41. Croft AP, Campos J, Jansen K, Turner JD, Marshall J, Attar M, et al. Distinct fibroblast subsets drive inflammation and damage in arthritis. *Nature* 2019;570:246–51.
42. Roemer FW, Guermazi A, Felson DT, Niu J, Nevitt MC, Crema MD, et al. Presence of MRI-detected joint effusion and synovitis increases the risk of cartilage loss in knees without osteoarthritis at 30-month follow-up: the MOST study. *Ann Rheum Dis* 2011;70:1804–9.
43. Haynes MK, Hume EL, Smith JB. Phenotypic characterization of inflammatory cells from osteoarthritic synovium and synovial fluids. *Clin Immunol* 2002;105:315–25.
44. Moradi B, Rosshirt N, Tripel E, Kirsch J, Barié A, Zeifang F, et al. Unicompartamental and bicompartamental knee osteoarthritis show different patterns of mononuclear cell infiltration and cytokine release in the affected joints. *Clin Exp Immunol* 2015;180:143–54.
45. Berner B, Akça D, Jung T, Muller GA, Reuss-Borst MA. Analysis of Th1 and Th2 cytokines expressing CD4+ and CD8+ T cells in rheumatoid arthritis by flow cytometry. *J Rheumatol* 2000;27:1128–35.
46. Ishii H, Tanaka H, Kato K, Nakamura H, Nagashima M, Yoshino S. Characterization of infiltrating T cells and Th1/Th2-type cytokines in the synovium of patients with osteoarthritis. *Osteoarthritis Cartilage* 2002;10:277–81.
47. Latourte A, Cherifi C, Maillet J, Ea HK, Bouaziz W, Funck-Brentano T, et al. Systemic inhibition of IL-6/Stat3 signalling protects against experimental osteoarthritis. *Ann Rheum Dis* 2017;76:748–55.
48. Humby F, Kelly S, Hands R, Rocher V, DiCiccio M, Ng N, et al. Use of ultrasound-guided small joint biopsy to evaluate the histopathologic response to rheumatoid arthritis therapy: recommendations for application to clinical trials. *Arthritis Rheumatol* 2015;67:2601–10.

Regulation of the Inflammatory Synovial Fibroblast Phenotype by Metastasis-Associated Lung Adenocarcinoma Transcript 1 Long Noncoding RNA in Obese Patients With Osteoarthritis

Dominika E. Nanus,¹ Susanne N. Wijesinghe,¹ Mark J. Pearson,¹ Marina R. Hadjicharalambous,² Alex Rosser,¹ Edward T. Davis,³ Mark A. Lindsay,⁴ and Simon W. Jones¹ 

Objective. To identify long noncoding RNAs (lncRNAs) associated with the inflammatory phenotype of synovial fibroblasts from obese patients with osteoarthritis (OA), and to explore the expression and function of these lncRNAs.

Methods. Synovium was collected from normal-weight patients with hip fracture (non-OA; n = 6) and from normal-weight (n = 8) and obese (n = 8) patients with hip OA. Expression of RNA was determined by RNA-sequencing and quantitative reverse transcription–polymerase chain reaction. Knockdown of lncRNA was performed using LNA-based GapmeRs. Synovial fibroblast cytokine production was measured by enzyme-linked immunosorbent assay.

Results. Synovial fibroblasts from obese patients with OA secreted greater levels of interleukin-6 (IL-6) (mean ± SEM 162 ± 21 pg/ml; $P < 0.001$) and CXCL8 (262 ± 67 pg/ml; $P < 0.05$) compared to fibroblasts from normal-weight patients with OA (IL-6, 51 ± 4 pg/ml; CXCL8, 78 ± 11 pg/ml) or non-OA patients (IL-6, 35 ± 3 pg/ml; CXCL8, 56 ± 6 pg/ml) (n = 6 patients per group). RNA-sequencing revealed that fibroblasts from obese OA patients exhibited an inflammatory transcriptome, with increased expression of proinflammatory messenger RNAs (mRNAs) as compared to that in fibroblasts from normal-weight OA or non-OA patients (>2-fold change, $P < 0.05$; n = 4 patients per group). A total of 19 lncRNAs were differentially expressed between normal-weight OA and non-OA patient fibroblasts, and a further 19 lncRNAs were differentially expressed in fibroblasts from obese OA patients compared to normal-weight OA patients (>2-fold change, $P < 0.05$ for each), which included the lncRNA for metastasis-associated lung adenocarcinoma transcript 1 (MALAT1). MALAT1 was rapidly induced upon stimulation of OA synovial fibroblasts with proinflammatory cytokines, and was up-regulated in the synovium from obese OA patients as compared to normal-weight OA patients (1.6-fold change, $P < 0.001$) or non-OA patients (6-fold change, $P < 0.001$). MALAT1 knockdown in OA synovial fibroblasts (n = 4 patients) decreased the levels of mRNA expression and protein secretion of CXCL8 (>1.5-fold change, $P < 0.01$), whereas it increased expression of mRNAs for TRIM6 (>2-fold change, $P < 0.01$), IL7R (<2-fold change, $P < 0.01$), HIST1H1C (>1.5-fold change, $P < 0.001$), and MAML3 (>1.5-fold change, $P < 0.001$). In addition, MALAT1 knockdown inhibited the proliferation of synovial fibroblasts from obese patients with OA.

Conclusion. Synovial fibroblasts from obese patients with hip OA exhibit an inflammatory phenotype. MALAT1 lncRNA may mediate joint inflammation in obese OA patients.

INTRODUCTION

Osteoarthritis (OA) has historically been considered a wear-and-tear disease of the articular cartilage. In contrast to rheumatoid

arthritis (RA), in which synovial inflammation (synovitis) is an active driver of disease (1) and targeting of synovial fluid proinflammatory cytokines is the rationale behind many of the existing RA therapeutics, OA is often referred to as a noninflammatory joint disease. As

Supported by Arthritis Research UK (grants 21530 and 21812). Dr. Lindsay's work was supported by the Biotechnology and Biological Sciences Research Council (grant BB/K00623/1).

¹Dominika E. Nanus, PhD, Susanne N. Wijesinghe, PhD, Mark J. Pearson, PhD, Alex Rosser, MSc, Simon W. Jones, PhD: University of Birmingham, Birmingham, UK; ²Marina R. Hadjicharalambous, PhD: University of Bath, Bath, UK; ³Edward T. Davis, MChB: Royal Orthopaedic Hospital, Birmingham, UK; ⁴Mark A. Lindsay, PhD: University of Birmingham, Birmingham, UK, and University of Bath, Bath, UK.

Drs. Nanus and Wijesinghe contributed equally to this work. Drs. Lindsay and Jones contributed equally to this work.

No potential conflicts of interest relevant to this article were reported.

Address correspondence to Simon W. Jones, PhD, Institute of Inflammation and Ageing, University of Birmingham, MRC-ARUK Centre for Musculoskeletal Ageing Research, Edgbaston, Birmingham B15 2TT, UK. E-mail: s.w.jones@bham.ac.uk.

Submitted for publication January 7, 2019; accepted in revised form October 31, 2019.

such, OA drug development has predominantly focused on directly targeting the catabolic and anabolic pathways of cartilage tissue, which has been of limited success (2). However, increasing evidence indicates that synovitis plays a significant role in OA joint pathology (2–4) by exacerbating cartilage damage via the induction of matrix metalloproteases and aggrecanases (5–7), and by hastening the onset of end-stage disease. Magnetic resonance imaging and histologic analyses have shown that synovitis is present at all stages of OA pathogenesis (8–10), with hyperplasia of the synovial lining (11,12), infiltration of immune cells (13,14), and expression of proinflammatory cytokines (15–17). The presence of synovitis in early OA, in patients who have minimal radiographic signs of cartilage loss (11), suggests that the emergence of synovitis may represent an opportune point for early therapeutic intervention (3).

We recently reported that the synovial fluid in OA patients who are obese contains greater levels of interleukin-6 (IL-6), tumor necrosis factor (TNF), and CXCL8, as compared to the synovial fluid in normal-weight OA patients, and that isolated synovial fibroblasts from obese OA patients secrete more IL-6 (15). Obesity may therefore drive synovial fibroblasts to adopt a more inflammatory phenotype, thereby contributing to an inflammatory environment in the joint to which the cartilage is exposed. As such, synovitis may play a particularly significant role in the onset and progression of OA in obese individuals, with implications for patient stratification in clinical testing of antiinflammatory therapeutics (3). Furthermore, determining how obesity-associated inflammation within the synovial joint tissue is regulated may lead to the development of new antiinflammatory therapies, which could be of benefit to patients diagnosed as having OA and might help prevent the onset of disease in “at-risk” obese patient populations.

In attempting to better understand the cellular regulators of synovial joint inflammation, investigators have identified long noncoding RNAs (lncRNAs) (18,19) as a central regulator of the

inflammatory response (20–24). We recently identified lncRNAs that are associated with the inflammatory response in human OA chondrocytes, which function by regulating the secretion of proinflammatory cytokines (22,25). Therefore, the aim of the present study was to characterize the transcriptome of synovial fibroblasts isolated from either obese or normal-weight patients with hip OA, as well as synovial fibroblasts from normal-weight patients with hip fracture (non-OA), in analyses using RNA-sequencing (RNA-seq) to identify lncRNAs associated with the inflammatory synovial fibroblast phenotype, and to examine the expression and functional role of metastasis-associated lung adenocarcinoma transcript 1 (MALAT1), a differentially expressed lncRNA in OA synovium.

PATIENTS AND METHODS

Patients and tissue samples. Obese and normal-weight patients with hip OA and normal-weight patients with femoral neck fracture (non-OA patients) who were scheduled to undergo elective arthroplasty were recruited for the study. Ethics approval was provided by the UK National Research Ethics Committee (approval no. 14/ES/1044), and informed consent was obtained from all patients. The characteristics of the study patients are shown in Table 1.

Synovium was collected perioperatively. A portion of synovium was snap-frozen in liquid nitrogen and pulverized for analysis of RNA expression. The remaining synovium was used for isolation of primary synovial fibroblasts.

Isolation and culture of primary fibroblasts from synovium. Synovial membrane was diced (~1 mm³) and cultured in growth medium (RPMI 1640 containing 10% fetal calf serum [FCS], 1% penicillin–streptomycin, 5% L-glutamine, 5% sodium pyruvate, and 5% nonessential amino acids [Sigma-Aldrich]).

Table 1. Characteristics of the study patients*

	Obese OA (n = 8)	Normal-weight OA (n = 8)	Non-OA (n = 6)
Demographic			
Age, years	65.1 ± 4.6	65.5 ± 2.3	69.7 ± 2.9
Female/male, %	50/50	50/50	50/50
Anthropometric			
BMI, kg/m ²	39.8 ± 3.6	23.3 ± 0.3†	22.9 ± 0.6†
Waist circumference, cm	92 ± 18.6	75 ± 8.1	–
Hip circumference, cm	100 ± 21.9	88 ± 6.4	–
WHR	0.93 ± 0.02	0.82 ± 0.05	–
OA severity measure			
Joint space width, mm	1.1 ± 1.1	0.94 ± 0.6	–
K/L radiographic grade			
Median (IQR)	4 (3.3–4)	4 (3.3–4)	–
Grade I, %	0	0	–
Grade II, %	12.5	12.5	–
Grade III, %	12.5	12.5	–
Grade IV, %	75	75	–

* Except where indicated otherwise, values are the mean ± SEM. BMI = body mass index; WHR = waist:hip circumference ratio; K/L = Kellgren/Lawrence; IQR = interquartile range.

† $P < 0.0001$ versus obese patients with osteoarthritis (OA).

Synovial fibroblasts were grown to 70–80% confluence, and phenotype was confirmed by identification of CD55-positive cells, as described previously (15).

RNA-seq analysis. Synovial fibroblasts were cultured for 24 hours in culture medium containing 0.1% FCS, without antibiotics. Total RNA was isolated using TRIzol (Life Technologies) and purified using an RNeasy column (Qiagen). RNA integrity number (RIN) values (Agilent Bioanalyzer) were >7. Paired-end and stranded 75-bp sequencing data were obtained using an Illumina HiSeq4000, carried out at the Oxford Genomics Centre (Wellcome Centre for Human Genetics, UK).

For the analysis of fibroblasts following knockdown of MALAT1 lncRNA, RNA-seq was performed using a QuantSeq 3' kit (Lexogen). Sequencing data were analyzed as previously described (25). Briefly, the paired-end reads were aligned to the human reference genome (hg38) using Hisat2 (version 2.0.4) (26) with the following command line options: `hisat2 -q --dta --rna-strandness FR -x <reference-genome.gtf> -1 <forward_strand.fa> -2 <reverse-strand file.fa> -S <output.sam>`. Using Samtools (27), output SAM files were sorted and converted to BAM files (Samtools command line `sort -@ 8 -o output.bam output.sam`) and indexed (Samtools command line `index -b output.bam`). The profile of gene expression (using the Gencode version 27 database and additional novel lncRNAs) (25) in the BAM files for each sample were determined using Stringtie (26,28), with the following command line: `stringtie <sample.BAM> -G <GenCodev26.gtf> -o <samples.gtf> -e -A <sample.txt>`. The differential expression of genes derived from Gencode version 27 and our recently generated list of novel lncRNAs implicated in the innate immune system (25) was assessed with the geometric option in Cuffdiff version 2.2.1.3 (part of the Cufflinks suite) (29), applying a significance threshold of $q < 0.05$. The command line options were as follows: `cuffdiff -FDR=0.05 --min-alignment-count=10 --library-norm-method=geometric --dispersion-method=pooled -u <reference_genome.gtf> <control_1.bam>, <control_x.bam> <activated_1.bam>, <activated_x.bam> -o <output_file_name>`.

Principal components analysis (PCA) and hierarchical clustering. The abundance of Gencode version 27–defined genes in individual samples was defined as the fragments per kilobase exon per million reads mapped (FPKM) and determined using Stringtie (RNA) as described above. PCA and hierarchical clustering on Gencode version 27 protein-coding genes that demonstrated an expression value of >1 FPKM was performed using Genesis (version 1.7.7) (30). Data were \log_2 -transformed following the addition of 1 FPKM. The threshold for reporting gene expression at FPKM >1 is based on the ability to validate sequencing data using quantitative reverse transcription–polymerase chain reaction (qRT-PCR) (31). RNA-seq data can be obtained from the Gene Expression Omnibus database (at <http://www.ncbi.nlm.nih.gov/geo/>).

Pathway analysis. Differentially expressed genes (defined as those with >1.5-fold change in expression; $P < 0.05$) were identified using DAVID and Ingenuity Pathway Analysis (IPA) software (online at <https://www.ingenuity.com>). In the DAVID analysis tool (<https://david.ncicrf.gov>), genes were analyzed using the KEGG pathway option. Using IPA software, a core functional analysis was performed to identify canonical pathways and predicted upstream regulators that were significantly associated with the differentially expressed messenger RNAs (mRNAs). The significance of the association of a given canonical pathway with the differentially expressed mRNAs was measured based on the ratio of the number of mapped differentially expressed mRNAs in the data set divided by the total number of genes that map to the canonical pathway, with P values calculated using Fisher's exact test for the association between each mRNA and the canonical pathway. For the prediction of upstream regulators, P values and Z scores were computed based on the significant overlap between genes in the data set and known targets regulated by the transcriptional regulator.

Quantitative RT-PCR. Primers for individual transcripts (see Supplementary Table 1, available on the *Arthritis & Rheumatology* web site at <http://onlinelibrary.wiley.com/doi/10.1002/art.41158/abstract>) were designed using Primer Express 3 software (Life Technologies). PCR was performed from total RNA in a 1-step reaction (iTaq Universal One-Step; BioRad). Relative expression was determined using the $\Delta\Delta C_t$ method, followed by normalization of values to those for 18S.

Inhibition of lncRNA expression using LNA GapmeRs. Primary synovial fibroblasts (obtained from 4 patients) were transfected with 2 different LNA GapmeR inhibitors (Exiqon) targeting MALAT1 lncRNA (30 nM) or with a control LNA inhibitor (30 nM), using Lipofectamine 3000 (Invitrogen). After 24 hours, the supernatants were collected for cytokine analysis by enzyme-linked immunosorbent assay (ELISA), and cells were lysed with RLT buffer (Qiagen) for RNA extraction. All RIN values (Agilent Bioanalyzer) were >8. RNA was analyzed by qRT-PCR and RNA-seq analyses (QuantSeq 3'; Lexogen). RNA-seq data were analyzed using Cuffdiff to identify differentially expressed genes.

Determination of synovial fibroblast proliferation. Proliferation of synovial fibroblasts was determined using a Cell-Titer 96 Aqueous One Solution Cell Proliferation Assay kit (Promega) in accordance with the manufacturer's instructions. Briefly, cells were cultured in 96-well plates and, following the addition of MTS reagent, the absorbance at 490 nm was measured using a microplate reader (SynergyHT; BioTek).

Statistical analysis. Data were analyzed using GraphPad Prism 6 software. Groups were compared by one-way analysis of variance with Dunnett's test for multiple comparisons. Data are

presented as the mean \pm SEM, with P values less than 0.05 defining statistically significant differences.

RESULTS

Inflammatory phenotype of synovial fibroblasts isolated from obese OA patients. Synovial fibroblasts from normal-weight non-OA patients, normal-weight OA patients, and obese OA patients ($n = 6$ patients per group) were cultured for 24 hours, and the secretion of IL-6 and CXCL8 was determined by ELISA. Compared to the normal-weight non-OA group, synovial fibroblasts from normal-weight OA patients secreted moderately more IL-6 (1.5-fold increase, $P < 0.01$), although there was no difference in the secretion of CXCL8 (Figure 1A). In contrast, the secretion of both IL-6 ($P < 0.001$) and CXCL8 ($P < 0.05$) was markedly elevated in synovial fibroblasts from obese OA patients compared to normal-weight OA and non-OA patients (Figure 1A).

Furthermore, synovial fibroblasts from obese OA patients were more highly proliferative. Thus, fibroblasts from obese OA patients exhibited a more rapid increase in cellular confluence (as determined using IncuCyte cell analysis software) over the first 24 hours following passaging, compared to either normal-weight OA

or non-OA patient fibroblasts (Figure 1B). After 7 days of culture, cell numbers of obese OA patient fibroblasts were significantly greater than those of normal-weight OA and non-OA patient fibroblasts, as determined by MTS assay (Figure 1C).

To further investigate the phenotype of these cells, we next isolated total RNA from the synovial fibroblasts obtained from all 3 patient groups ($n = 4$ patients per group) and subjected it to 75-bp, paired-end RNA-seq analysis on an Illumina 4000 (performed at the Wellcome Trust Sequencing Unit, University of Oxford, UK). Comparison of the synovial fibroblast expression profile between normal-weight patients with OA and normal-weight non-OA patients identified up-regulation of 344 mRNAs and down-regulation of 606 mRNAs (>2 -fold change, $P < 0.05$; change in FPKM >1) (Figures 2A and B, and Supplementary Tables 2 and 3, available on the *Arthritis & Rheumatology* web site at <http://onlinelibrary.wiley.com/doi/10.1002/art.41158/abstract>). We employed an FPKM cutoff value of >1 based on prior research from the Sequence Quality Control Consortium (31), which showed that this was the level that could be reliably confirmed by qRT-PCR. In addition, our previous studies have shown that lncRNAs and mRNAs have a mean expression level of 2.14 FPKM and 7.03 FPKM, respectively (23) and that cutoffs significantly higher than >1 FPKM would likely preclude large numbers of lncRNAs.

Pathway analysis (using DAVID) of these differentially expressed mRNAs in normal-weight OA patients compared to normal-weight non-OA patients revealed that the top canonical pathways that were associated with the up-regulated genes were the extracellular matrix–receptor interaction and complement/coagulation cascade pathways, whereas among the down-regulated genes, the top associated pathways were those for cell cycle, RNA replication, and cytokine–cytokine interactions (Figure 2C). This was confirmed by IPA, which identified the top pathway as cell cycle control of chromosomal replication, and also identified the top upstream regulator as CDKN2, which encodes 2 proteins (p16 INK4a and p14 arf) that regulate the cell cycle (see Supplementary Tables 4 and 5, available on the *Arthritis & Rheumatology* web site at <http://onlinelibrary.wiley.com/doi/10.1002/art.41158/abstract>).

Comparison of synovial fibroblasts between normal-weight OA patients and obese OA patients showed that a total of 377 mRNAs were up-regulated and 238 mRNAs were down-regulated (>2 -fold change, $P < 0.05$; change in FPKM >1) (Figures 2A and B, and Supplementary Tables 2 and 3 [<http://onlinelibrary.wiley.com/doi/10.1002/art.41158/abstract>]). In contrast to the comparison between the normal-weight OA and non-OA patient groups, pathway analysis revealed that the most significant up-regulated canonical pathways in obese OA patient fibroblasts were inflammation related, and included cytokine–cytokine interactions, nucleotide-binding oligomerization domain–like receptor signaling, Toll-like receptor signaling, and chemokine signaling pathways (Figure 2C). This inflammatory phenotype was confirmed using IPA (Supplementary Table 4 [<http://onlinelibrary.wiley.com/doi/10.1002/art.41158/abstract>]).

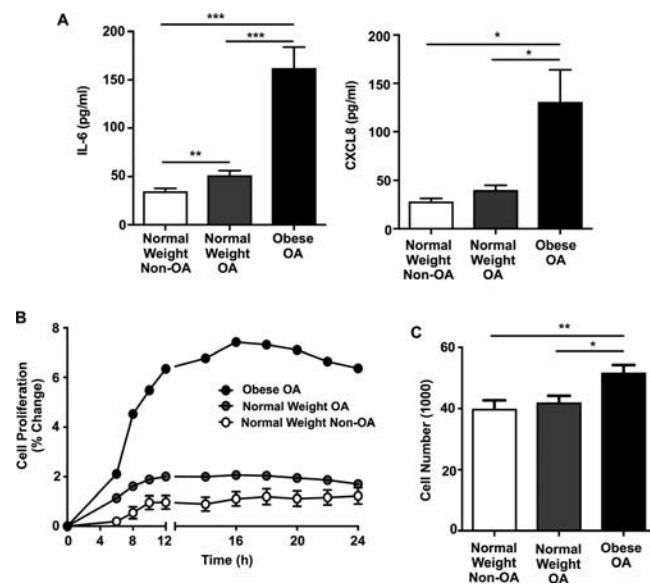


Figure 1. Inflammatory phenotype of synovial fibroblasts from obese patients with hip osteoarthritis (OA). **A**, Protein secretion of interleukin-6 (IL-6) and CXCL8 in primary synovial fibroblasts from normal-weight non-OA, normal-weight OA, and obese OA patients ($n = 6$ per group), as quantified in culture supernatants by enzyme-linked immunosorbent assay. **B**, Percentage increase in confluency of synovial fibroblasts over 24 hours ($n = 3$ patients per group), as measured by IncuCyte cell analysis. **C**, Proliferation of synovial fibroblasts after 7 days of culture ($n = 3$ patients per group), as measured by MTS assay. Results are the mean \pm SEM. * = $P < 0.05$, ** = $P < 0.01$; *** = $P < 0.001$, by analysis of variance with Bonferroni's post hoc test.

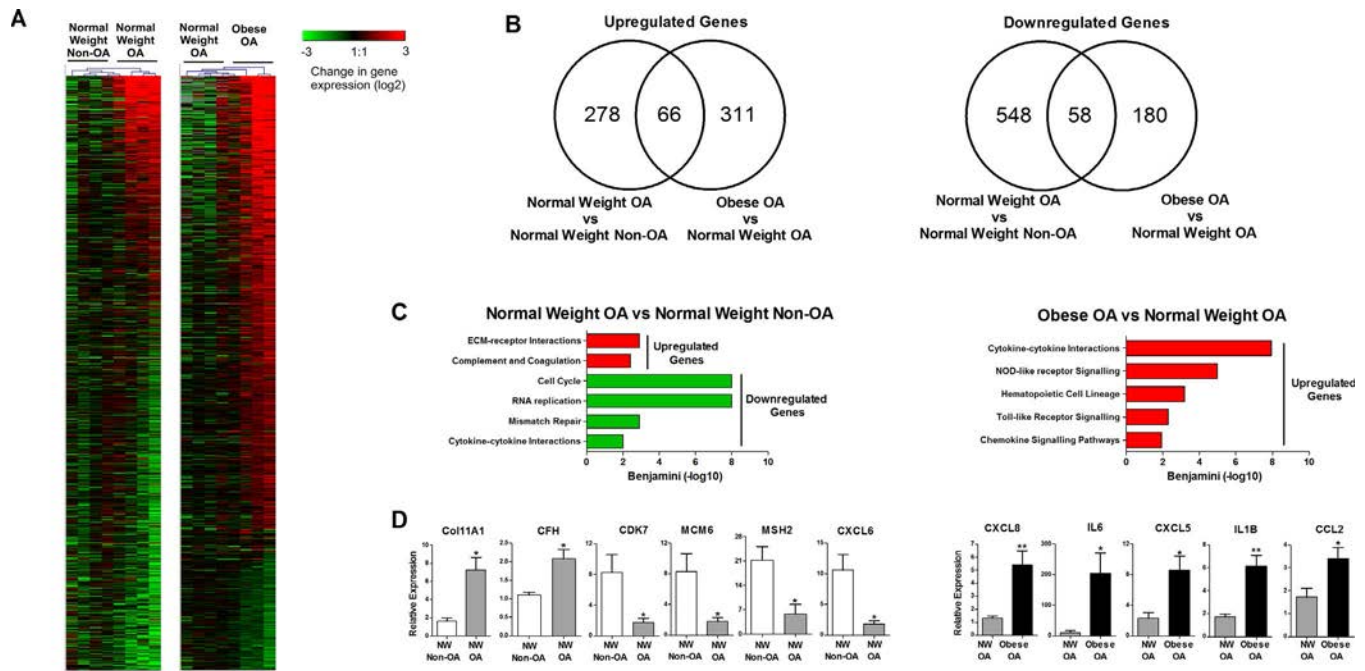


Figure 2. Differentially expressed mRNAs in osteoarthritis (OA) synovial fibroblasts identified using RNA-sequencing (RNA-seq) analysis. **A**, Heatmap showing fold increase in mRNA expression in synovial fibroblasts from normal-weight (NW) non-OA, normal-weight OA, and obese OA patients ($n = 4$ per group), as determined by RNA-seq. Dendrograms were created using the average linkage weighted-pair group method with arithmetic mean. **B**, Venn diagrams of the number of differentially expressed mRNAs (defined as >2 -fold change in expression [$P < 0.05$]) and absolute change in expression of >1 fragments per kilobase exon per million reads mapped between normal-weight non-OA and normal-weight OA patient fibroblasts, and between normal-weight OA and obese OA patient fibroblasts. **C**, Top canonical pathways of the differentially expressed mRNAs between normal-weight OA and normal-weight non-OA patient fibroblasts, and between obese OA and normal-weight OA patient fibroblasts, as determined by DAVID pathway analysis. **D**, Differential mRNA expression of genes representing each of the canonical pathways between normal-weight non-OA and normal-weight OA patient fibroblasts ($n = 3$ per group), and between normal-weight OA and obese OA patient fibroblasts ($n = 4$ per group), as determined by quantitative reverse transcription–polymerase chain reaction. * = $P < 0.05$; ** = $P < 0.01$. ECM = extracellular matrix; NOD = nucleotide-binding oligomerization domain.

We then selected key representative genes for each of the identified significant canonical pathways and performed qRT-PCR analysis of independent samples to validate the differential expression of each gene between normal-weight non-OA and normal-weight OA patient fibroblasts ($n = 3$ patients) or between normal-weight OA and obese OA patient fibroblasts ($n = 4$ patients). The expression of Col11A1 and CFH was confirmed to be significantly up-regulated while the expression of CDK7, MCM6, MSH2, and CXCL6 was confirmed to be significantly down-regulated in fibroblasts from normal-weight OA patients as compared to fibroblasts from normal-weight non-OA patients. The expression of CXCL8, IL6, CXCL5, IL1 β , and CCL2 was found to be significantly increased in synovial fibroblasts from obese OA patients as compared to fibroblasts from normal-weight OA patients (Figure 2D).

Identification of lncRNAs associated with the inflammatory phenotype of synovial fibroblasts from obese OA patients. We next analyzed the RNA-seq data to identify lncRNAs that were differentially expressed in synovial fibroblasts between the groups. Initial comparison of normal-weight

OA patient fibroblasts and non-OA patient fibroblasts uncovered 19 lncRNAs that were differentially expressed (>2 -fold change, $P < 0.05$; change in FPKM >1) (Supplementary Table 6, available on the *Arthritis & Rheumatology* web site at <http://onlinelibrary.wiley.com/doi/10.1002/art.41158/abstract>). This included 16 long intergenic noncoding RNAs (lincRNAs) and 3 antisense lncRNAs, of which 10 lincRNAs were up-regulated and 6 were down-regulated in normal-weight OA patient fibroblasts compared to normal-weight non-OA patient fibroblasts (Figures 3A and B).

Comparison between synovial fibroblasts from obese OA patients and synovial fibroblasts from normal-weight OA patients identified a total of 19 differentially expressed lncRNAs (Supplementary Table 6 [<http://onlinelibrary.wiley.com/doi/10.1002/art.41158/abstract>]). Again, this included both antisense and lincRNAs, of which the majority were lincRNAs (15). We observed that 9 lincRNAs were up-regulated and 6 were down-regulated in obese OA patient fibroblasts compared to normal-weight OA patient fibroblasts (Figures 3A and B). Among these lincRNAs, MALAT1 demonstrated the largest absolute increase in expression, rising from 37 FPKM in normal-weight OA to 79 FPKM in obese OA (Supplementary Table 6).

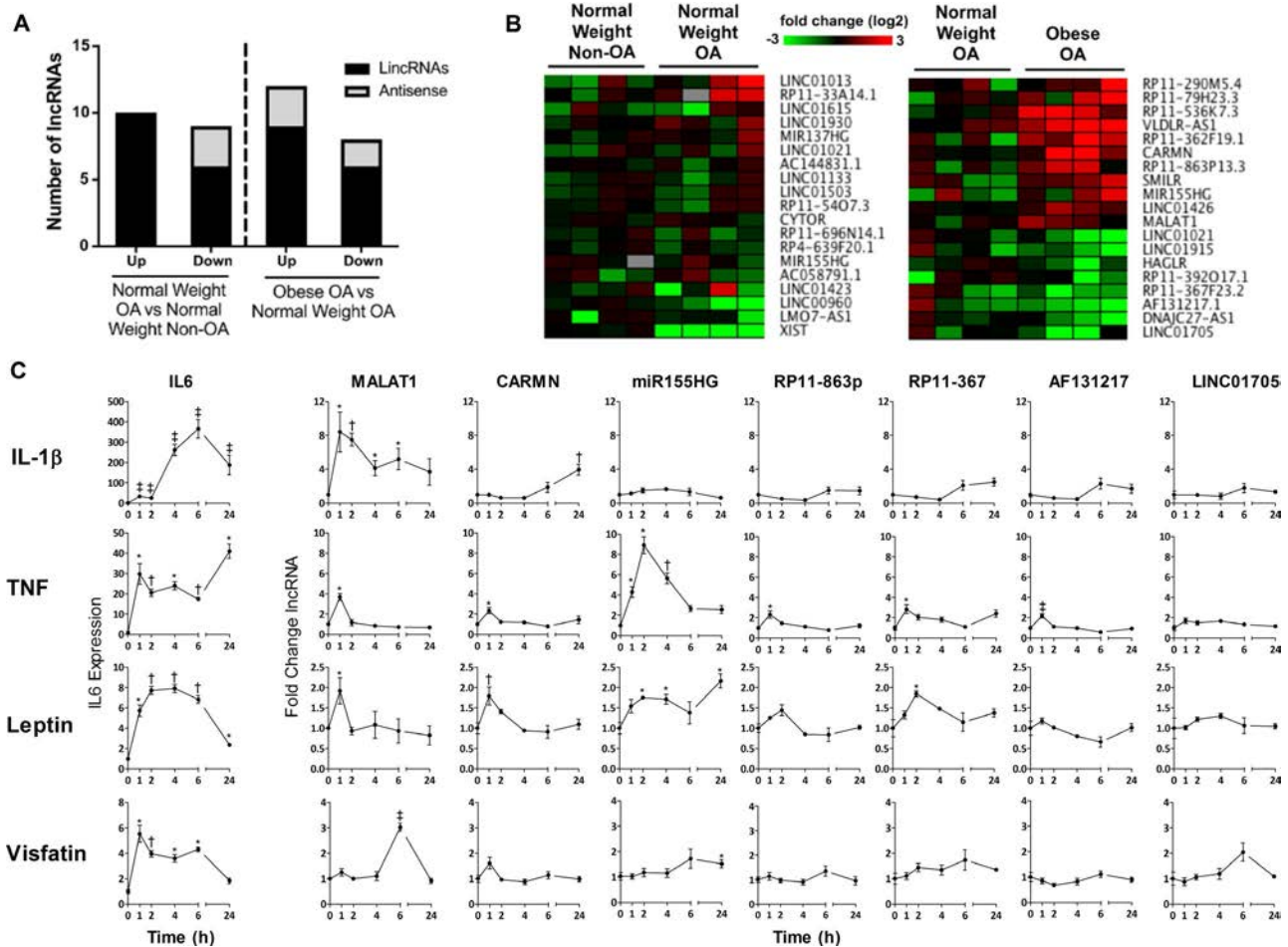


Figure 3. Inflammation-associated long noncoding RNAs (lincRNAs) in osteoarthritis (OA) synovial fibroblasts. **A**, Categorization of the differentially expressed lincRNAs, including antisense and long intergenic noncoding RNAs (lincRNAs), between normal-weight OA and non-OA patient fibroblasts and between obese OA and normal-weight OA patient fibroblasts, as identified by RNA-sequencing. **B**, Heatmaps of differentially expressed lincRNAs in normal-weight non-OA, normal-weight OA, and obese OA patient synovial fibroblasts. **C**, Time course of expression of IL6 mRNA and lincRNAs, as determined by quantitative reverse transcription-polymerase chain reaction in primary human OA synovial fibroblasts over 24 hours following exposure to either interleukin-1 β (IL-1 β) (1 ng/ml), tumor necrosis factor (TNF) (10 ng/ml), leptin (100 ng/ml), or visfatin (100 ng/ml). Results are the mean \pm SEM ($n = 3$). * = $P < 0.05$; † = $P < 0.01$; ‡ = $P < 0.001$ versus time 0, by analysis of variance with repeated measures. Color figure can be viewed in the online issue, which is available at <http://onlinelibrary.wiley.com/doi/10.1002/art.41158/abstract>.

Rapid induction of obesity-associated lincRNAs in response to cytokine stimulation of OA synovial fibroblasts.

Of the lincRNAs differentially expressed between normal-weight OA and obese OA synovial fibroblasts, we selected 7 (namely, MALAT1 as well as the lincRNAs CARMN, AF131217.1, miR155HG, LINC01705, RP11-863p13.3, and RP11-367F23.2) and examined their expression in response to an inflammatory challenge. To this end, OA fibroblasts were stimulated with either IL-1 β (1 ng/ml), TNF (10 ng/ml), leptin (100 ng/ml), or visfatin (100 ng/ml), and the time course of expression of the 7 lincRNAs and of IL6 mRNA was measured over 24 hours.

As expected, stimulation of OA fibroblasts with either IL-1 β , TNF, leptin, or visfatin induced an increase in IL6 mRNA expression (Figure 3C). Examination of lincRNA expression in the OA synovial fibroblasts showed that only the expression of MALAT1 and

CARMN were significantly increased in response to stimulation with each of the 4 cytokines, with MALAT1 demonstrating the largest fold changes (Figure 3C). Furthermore, expression of miR155HG increased in response to TNF and leptin, RP11-863p and RP11-367 increased in response to IL-1 β , TNF, and leptin, AF131217 increased in response to TNF, and LINC01705 increased in response to visfatin (Figure 3C). Notably, we found that the synovial fluid cytokine concentrations of TNF ($P < 0.01$) and leptin ($P < 0.05$) were significantly elevated in obese OA patients compared to normal-weight OA patients, and both were significantly correlated with the expression of MALAT1, IL6, and CXCL8 in obese OA patients (see Supplementary Figure 1, available on the *Arthritis & Rheumatology* web site at <http://onlinelibrary.wiley.com/doi/10.1002/art.41158/abstract>). The level of IL-1 β was also elevated in synovial fluid from obese OA patients com-

pared to normal-weight OA patients, although this difference did not reach statistical significance ($P = 0.07$). Nevertheless, IL-1 β synovial fluid concentrations were significantly correlated with the expression of MALAT1 ($P < 0.01$) (Supplementary Figure 1). Given that MALAT1 showed both the largest absolute change in expression between normal-weight OA and obese OA patient fibroblasts and was ubiquitously induced (with the largest fold changes) in response to inflammatory mediators, subsequent studies were focused on elucidating the in vivo relevance and function of MALAT1.

Differential expression of MALAT1 in inflammatory OA synovial tissue. To examine the potential in vivo relevance of MALAT1, we extracted total RNA from the synovium of normal-weight non-OA patients ($n = 6$), normal-weight OA patients ($n = 8$), and obese OA patients ($n = 8$). Expression of MALAT1 was significantly up-regulated in normal-weight OA patient synovium compared to normal-weight non-OA patient synovium, and was further increased in obese OA patient synovium (Figure 4A). Interestingly, down-regulation of MALAT1 mRNA expression was associated with increased expression of the inflammatory genes IL6 and CXCL8 (Figure 4A).

Regulation of the inflammatory response and cell proliferation by MALAT1 in fibroblasts from obese OA patients. Subsequently, we undertook knockdown studies to ascertain whether changes in MALAT1 expression could be causally linked to the increased inflammatory and proliferative response of synovial fibroblasts from obese OA patients. To this end, fibroblasts from obese OA patients were transfected with 2 different LNA GapmeRs targeting MALAT1 or with a nontargeting control LNA (each at 30 nM; Exiqon). Both MALAT1 LNAs produced a >90% knockdown in expression of MALAT1 mRNA after 24 hours, compared to cells transfected with the nontargeting control LNA (Figure 4B). Fibroblasts depleted of MALAT1 expressed significantly reduced levels of CXCL8 mRNA and CXCL8 protein secretion (Figure 4C). Furthermore, fibroblasts depleted of MALAT1 also displayed significantly reduced cellular proliferation as compared to fibroblasts transfected with control LNA, both at 48 hours and after 5 days of culture (Figure 4D).

To further investigate the role of MALAT1 on the OA synovial fibroblast transcriptome, we then performed an additional MALAT1 loss-of-function study. To this end, OA synovial fibroblasts ($n = 4$ patients) were transfected for 24 hours with 1 of 2 different LNA GapmeRs targeting MALAT1 or with a nontargeting control LNA (each at 30 nM; Exiqon), and total RNA was subjected to RNA-seq analysis (Lexogen).

In total, RNA-seq identified 28 mRNAs, including CXCL8 mRNA, that were differentially expressed (>1.5 fold, $P < 0.05$) following MALAT1 knockdown, with comparable findings yielded by both MALAT1 LNA GapmeRs (Figures 5A and B, and Supplementary Tables 7 and 8, available on the *Arthritis & Rheumatology*

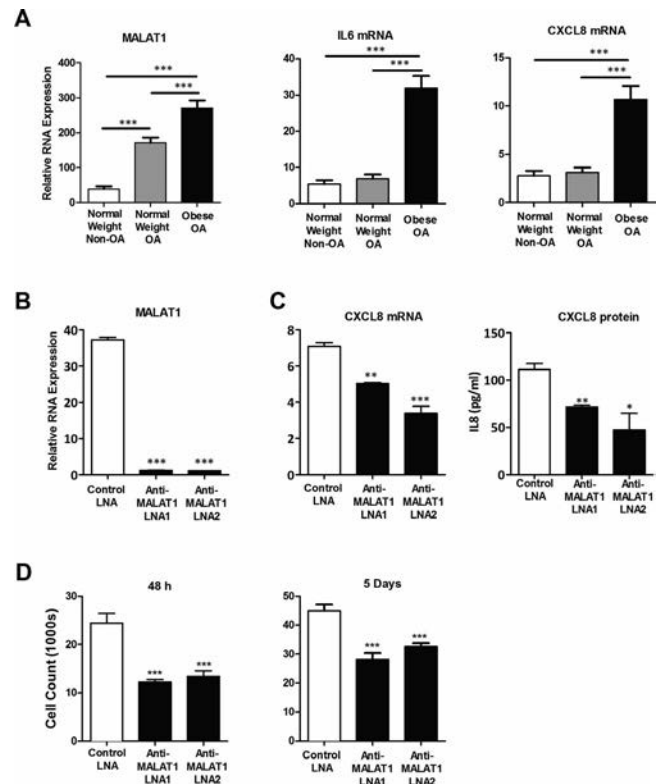


Figure 4. Expression and functional role of the long noncoding RNA (lncRNA) for metastasis-associated lung adenocarcinoma transcript 1 (MALAT1) in osteoarthritis (OA) synovial tissue. **A**, Differential expression of MALAT1 lncRNA and inflammatory IL6 and CXCL8 mRNAs in normal-weight non-OA ($n = 6$), normal-weight OA ($n = 8$), and obese OA ($n = 8$) patient synovial tissue. Expression was determined by quantitative reverse transcription–polymerase chain reaction (qRT-PCR), with values normalized to the values for 18S. * = $P < 0.05$; ** = $P < 0.01$; *** = $P < 0.001$, by analysis of variance (ANOVA) with Bonferroni's post hoc test. **B**, LNA-mediated knockdown of MALAT1 in OA synovial fibroblasts. Synovial fibroblasts were transfected for 24 hours with either a control LNA or 2 different MALAT1 LNA GapmeRs. MALAT1 knockdown was determined by qRT-PCR, with values normalized to the values for 18S. **C**, Effect of LNA-mediated MALAT1 knockdown using 2 different MALAT1 LNA GapmeRs on the expression of CXCL8 mRNA and secretion of CXCL8 protein in OA fibroblasts ($n = 4$ patients). Expression of mRNA was determined by qRT-PCR, with values normalized to the values for 18S. CXCL8 protein was measured by enzyme-linked immunosorbent assay. In **B** and **C**, * = $P < 0.05$; ** = $P < 0.01$; *** = $P < 0.001$ versus control LNA-transfected fibroblasts, by ANOVA with Dunnett's post hoc test. **D**, Effect of LNA-mediated knockdown of MALAT1 on the proliferation of OA synovial fibroblasts 48 hours and 5 days posttransfection, as determined by MTS assay. *** = $P < 0.001$ versus control LNA-transfected fibroblasts, by ANOVA. Results are the mean \pm SEM.

web site at <http://onlinelibrary.wiley.com/doi/10.1002/art.41158/abstract>).

The effect of MALAT1 knockdown on the differential expression of the mRNAs for CXCL8, TRIM6, IL7R, HIST1H1C, and MAML3 was then validated by qRT-PCR, and a significant correlation in the fold change data was observed between the RNA-seq

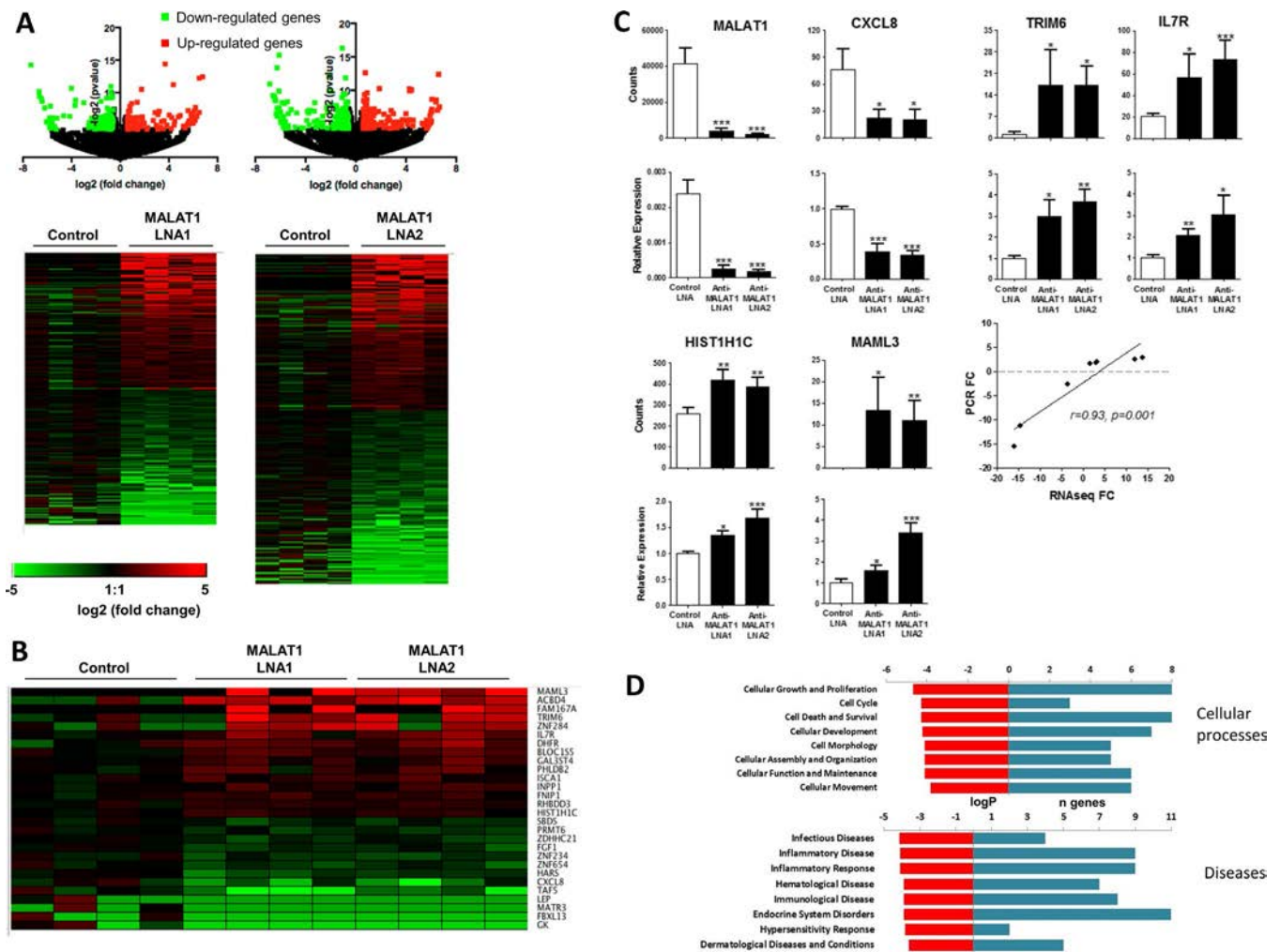


Figure 5. RNA-sequencing (RNA-seq) analysis of the effects of knockdown of the metastasis-associated lung adenocarcinoma transcript 1 (MALAT1) long noncoding RNA in OA synovial fibroblasts. **A**, Volcano plots and heatmaps of RNA-seq data showing fold change (FC) in the differentially expressed mRNAs (fold change >1.5, $P < 0.05$) after knockdown with either MALAT1 LNA1 or MALAT1 LNA2 GapmeRs compared to control LNA ($n = 4$ patients per group). **B**, Heatmap of expression of mRNAs for the 28 differentially expressed genes (fold change >1.5, $P < 0.05$), following knockdown with the MALAT1 GapmeRs compared to control LNA. **C**, Comparison of RNA-seq counts with quantitative reverse transcription–polymerase chain reaction (qRT-PCR) relative expression data for the MALAT1, CXCL8, TRIM6, IL7R, HIST1H1c, and MAML3 genes, and Pearson's analysis of correlation between the PCR fold change data and RNA-seq fold change data. Results are the mean \pm SEM. * = $P < 0.05$; ** = $P < 0.01$; *** = $P < 0.001$ versus control LNA-transfected fibroblasts, by analysis of variance with Dunnett's post hoc test. **D**, Top cellular processes and disease functions as determined by Ingenuity Pathway Analysis of the differentially expressed mRNAs (fold change >1.5, $P < 0.05$) following MALAT1 knockdown. Color figure can be viewed in the online issue, which is available at <http://onlinelibrary.wiley.com/doi/10.1002/art.41158/abstract>.

and qRT-PCR analyses ($r = 0.93$, $P = 0.001$) (Figure 5C). Further investigation using pathway analysis of the 28 differential mRNAs revealed that the most significantly affected cellular processes included those for cellular growth and proliferation, while the most significantly affected disease functions included inflammatory response and inflammatory disorders (Figure 5D).

DISCUSSION

The role of synovitis as a disease driver in OA has been largely understudied, with OA tissue often being used as a noninflamma-

tory control in comparative studies of patients with rheumatoid arthritis. Importantly, in the present study we demonstrate, for the first time, that synovial fibroblasts isolated from the synovium of patients with hip OA exhibit a more inflammatory and proliferative phenotype in those patients who are obese, compared to normal-weight OA patients.

Synovial fibroblasts from obese OA patients secreted greater protein amounts of IL-6 and CXCL8 than did synovial fibroblasts from normal-weight OA patients. Notably, OA disease processes in the absence of obesity had little effect on the inflammatory phenotype of the synovial tissue. For example, synovial tissue mRNA

expression and protein secretion of CXCL8 from isolated synovial fibroblasts did not differ between normal-weight OA patients and normal-weight patients without OA. Likewise, there was no difference in the synovial tissue expression of IL-6 between non-OA and OA patients of normal weight, and only a small increase in IL-6 secretion in synovial fibroblasts from normal-weight OA patients compared to synovial fibroblasts from non-OA patients. Furthermore, the proliferative activity of fibroblasts was similar between non-OA and normal-weight OA.

Transcriptomics analysis of synovial fibroblasts revealed that obese OA patient synovial fibroblasts exhibited differential expression of a plethora of inflammatory mRNAs (including cytokines, chemokines, and their receptors), compared to normal-weight OA patient fibroblasts. Pathway analysis of these differentially expressed mRNAs predicted a significant role of activation chemokine signaling pathways.

These findings may have important implications for patient stratification. Clinical trials of antiinflammatory therapies in OA have produced disappointing results (3). Adalimumab, a TNF-neutralizing antibody, was deemed ineffective at reducing disease activity in patients with erosive hand OA (32). Similarly, treatment of knee OA patients with AMG108, an IL-1 β receptor-neutralizing antibody, failed to significantly reduce pain (33). However, these trials did not select patients based on their degree of synovial inflammation. Notably, in a clinical trial of the effectiveness of adalimumab to alleviate knee pain in OA, 40% of patients had a 50% improvement in their pain score (34). Our data would suggest that the degree of synovial inflammation in the patients recruited for these studies would have been dependent on their body mass index. Given our findings, it would be pertinent to consider whether those patients who responded were obese and exhibited greater synovial inflammation.

In addition to coding genes, our study has identified several lncRNAs that are differentially expressed in OA patient fibroblasts compared to non-OA patient fibroblasts, as well as lncRNAs that are differentially expressed in obese OA patient fibroblasts compared to normal-weight OA patient fibroblasts. Given the potential clinical implications of the inflammatory phenotype of synovial fibroblasts in obese patients with OA, it was notable that the majority of the differentially expressed lncRNAs were classified as lincRNAs. Evidence has emerged to indicate that lincRNAs are central regulators of the inflammatory response in multiple cell types. Indeed, we recently identified lincRNAs associated with the human OA chondrocyte inflammatory response, which were induced in response to an inflammatory challenge and functioned to mediate the production of IL-6 (22).

In the present study we found that the expression of obesity-associated lincRNAs in synovial fibroblasts was modulated by stimulation with proinflammatory cytokines and adipokines. Of the lincRNAs investigated, MALAT1 was the most responsive to proinflammatory challenge, being rapidly induced following stimulation of synovial fibroblasts. This induction was transient, with MALAT1 expression returning to baseline levels within 24 hours,

and occurred prior to an increase in the expression of IL6 and CXCL8 mRNA. Such rapid and transient expression in response to an inflammatory challenge is indicative of MALAT1 being an important regulator of synovial fibroblast inflammation, which is supported by our finding that depletion of MALAT1 from obese OA patient synovial fibroblasts reduced the expression and secretion of CXCL8, and globally had an impact on mRNAs that regulate cellular growth and proliferation and the inflammatory response, including IL7R, TRIM6, HIST1H1C, and MAML3. There is precedent for a role of MALAT1 as a regulator of inflammation, including the regulation of CXCL8. In hepatocellular carcinoma cells, MALAT1 knockdown decreased the expression of CXCL8 and IL-6 (35). In human endothelial cells, depletion of MALAT1 with small interfering RNA (siRNA) reduced the expression of TNF and IL-6 (36,37), while MALAT1 knockdown in monocytes from patients with systemic lupus erythematosus reduced the expression of IL-21 (38). In vivo, inflammation markers, including IL-6, IL-1 β , TNF, and interferon- γ , were all suppressed in MALAT1-knockout diabetic mice compared to wild-type mice (36). Mechanistically, MALAT1 has recently been reported to bind to and modulate NF- κ B activity, thereby regulating the lipopolysaccharide-induced inflammatory response (39,40).

We also found that depletion of MALAT1 reduced the proliferation of synovial fibroblasts from obese OA patients, suggesting that targeted inhibition of MALAT1 in the synovial joint could have the dual action of reducing both synovial inflammation and hyperplasia. Several studies using cancer cell models have demonstrated that MALAT1 is a regulator of cellular proliferation. Knockdown of MALAT1 by siRNA in non-small cell lung cancer A549 cells inhibited their proliferation both in vitro and in a xenograft tumor growth model (41). Similarly, knockdown of MALAT1 inhibited the proliferation of the human triple-negative breast cancer cell line MDA-MB-453 (42).

It is important to note that our study only examined the synovium from patients with hip OA. Similar to the knee, the hip is a weight-bearing joint. Therefore, the obesity-associated inflammatory synovial fibroblast phenotype described herein may be initiated and promoted by excess loading on the joint. However, obesity is associated with OA in both weight-bearing and non-weight-bearing joints, supporting the notion that the effect of obesity is not simply attributable to increased joint loading. Indeed, it is known that obesity is associated with increased circulatory levels of proinflammatory cytokines and adipokines (43,44). We previously reported that the adipokine resistin is elevated systemically and more highly expressed in the synovial joint tissue in obese patients with hip OA as compared to normal-weight patients with hip OA (45), and it was recently found that patients with hand OA exhibit increased circulatory levels of resistin (46). Thus, the obesity-associated inflammatory synovial fibroblast phenotype may be replicated in non-weight-bearing OA joints.

In summary, these data demonstrate that obesity in OA patients is associated with an inflammatory synovial fibroblast

phenotype, and further supports the notion that lncRNAs, and in particular MALAT1, are central regulators of the inflammatory response in the OA synovial joint. Determining the effect of obesity on the inflammatory phenotype of synovial tissue in both weight-bearing and non-weight-bearing joints and the relationship to the expression and functional role of lncRNAs will provide new insights into our understanding of how OA joint inflammation is regulated, and may lead to the development of novel anti-inflammatory disease-modifying therapies or to the repurposing of existing therapies for OA.

ACKNOWLEDGMENTS

The authors would like to acknowledge all study participants and also the research staff at The Royal Orthopaedic Hospital NHS Foundation Trust (Birmingham, UK), Russell's Hall Hospital (Dudley, UK), and Kings Mill Hospital (Sutton in Ashfield, UK) for obtaining informed consent and performing patient screenings. In addition, the authors acknowledge the contributions of the orthopaedic surgeons David Dunlop, Matthew Revell, and Sohail Quraishi.

AUTHOR CONTRIBUTIONS

All authors were involved in drafting the article or revising it critically for important intellectual content, and all authors approved the final version to be published. Dr. Jones had full access to all of the data in the study and takes responsibility for the integrity of the data and the accuracy of the data analysis.

Study conception and design. Lindsay, Jones.

Acquisition of data. Nanus, Wijesinghe, Pearson, Hadjicharalambous, Rosser, Davis, Lindsay, Jones.

Analysis and interpretation of data. Lindsay, Jones.

REFERENCES

- Ganesan R, Rasool M. Fibroblast-like synoviocytes-dependent effector molecules as a critical mediator for rheumatoid arthritis: current status and future directions [review]. *Int Rev Immunol* 2017;36:20–30.
- Tonge DP, Pearson MJ, Jones SW. The hallmarks of osteoarthritis and the potential to develop personalised disease-modifying pharmacological therapeutics. *Osteoarthritis Cartilage* 2014;22:609–21.
- Philp AM, Davis ET, Jones SW. Developing anti-inflammatory therapeutics for patients with osteoarthritis. *Rheumatology (Oxford)* 2017;56:869–81.
- Mathiessen A, Conaghan PG. Synovitis in osteoarthritis: current understanding with therapeutic implications [review]. *Arthritis Res Ther* 2017;19:18.
- Jones SW, Brockbank SM, Clements KM, Le Good N, Campbell D, Read SJ, et al. Mitogen-activated protein kinase-activated protein kinase 2 (MK2) modulates key biological pathways associated with OA disease pathology. *Osteoarthritis Cartilage* 2009;17:124–31.
- Brown KK, Heitmeyer SA, Hookfin EB, Hsieh L, Buchalova M, Taiwo YO, et al. P38 MAP kinase inhibitors as potential therapeutics for the treatment of joint degeneration and pain associated with osteoarthritis. *J Inflamm (Lond)* 2008;5:22.
- Kapoor M, Martel-Pelletier J, Lajeunesse D, Pelletier JP, Fahmi H. Role of proinflammatory cytokines in the pathophysiology of osteoarthritis. *Nat Rev Rheumatol* 2011;7:33–42.
- Fernandez-Madrid F, Karvonen RL, Teitge RA, Miller PR, An T, Negendank WG. Synovial thickening detected by MR imaging in osteoarthritis of the knee confirmed by biopsy as synovitis. *Magn Reson Imaging* 1995;13:177–83.
- Oehler S, Neureiter D, Meyer-Scholten C, Aigner T. Subtyping of osteoarthritic synoviopathy. *Clin Exp Rheumatol* 2002;20:633–40.
- Rhodes LA, Conaghan PG, Radjenovic A, Grainger AJ, Emery P, McGonagle D. Further evidence that a cartilage-pannus junction synovitis predilection is not a specific feature of rheumatoid arthritis. *Ann Rheum Dis* 2005;64:1347–9.
- Myers SL, Brandt KD, Ehlich JW, Braunstein EM, Shelbourne KD, Heck DA, et al. Synovial inflammation in patients with early osteoarthritis of the knee. *J Rheumatol* 1990;17:1662–9.
- Korkusuz P, Dagdeviren A, Eksioglu F, Ors U. Immunohistological analysis of normal and osteoarthritic human synovial tissue. *Bull Hosp Jt Dis* 2005;63:63–9.
- De Lange-Brokaar BJ, Ioan-Facsinay A, van Osch GJ, Zuurmond AM, Schoones J, Toes RE, et al. Synovial inflammation, immune cells and their cytokines in osteoarthritis: a review. *Osteoarthritis Cartilage* 2012;20:1484–99.
- Revell PA, Mayston V, Lalor P, Mapp P. The synovial membrane in osteoarthritis: a histological study including the characterisation of the cellular infiltrate present in inflammatory osteoarthritis using monoclonal antibodies. *Ann Rheum Dis* 1988;47:300–7.
- Pearson MJ, Herndler-Brandstetter D, Tariq MA, Nicholson TA, Philp AM, Smith HL, et al. IL-6 secretion in osteoarthritis patients is mediated by chondrocyte-synovial fibroblast cross-talk and is enhanced by obesity. *Sci Rep* 2017;7:3451.
- Deleuran B, Lemche P, Kristensen M, Chu CQ, Field M, Jensen J, et al. Localisation of interleukin 8 in the synovial membrane, cartilage-pannus junction and chondrocytes in rheumatoid arthritis. *Scand J Rheumatol* 1994;23:2–7.
- Hulejová H, Baresová V, Klézil Z, Polanská M, Adam M, Senolt L. Increased level of cytokines and matrix metalloproteinases in osteoarthritic subchondral bone. *Cytokine* 2007;38:151–6.
- Cabili MN, Trapnell C, Goff L, Koziol M, Tazon-Vega B, Regev A, et al. Integrative annotation of human large intergenic noncoding RNAs reveals global properties and specific subclasses. *Genes Dev* 2011;25:1915–27.
- Mercer TR, Gerhardt DJ, Dinger ME, Crawford J, Trapnell C, Jeddloh JA, et al. Targeted RNA sequencing reveals the deep complexity of the human transcriptome. *Nat Biotechnol* 2011;30:99–104.
- Austin PJ, Tsitsiou E, Boardman C, Jones SW, Lindsay MA, Adcock IM, et al. Transcriptional profiling identifies the long noncoding RNA plasmacytoma variant translocation (PVT1) as a novel regulator of the asthmatic phenotype in human airway smooth muscle. *J Allergy Clin Immunol* 2017;139:780–9.
- Pearson MJ, Jones SW. Long noncoding RNAs in the regulation of inflammatory pathways in rheumatoid arthritis and osteoarthritis [review]. *Arthritis Rheumatol* 2016;68:2575–83.
- Pearson MJ, Philp AM, Heward JA, Roux BT, Walsh DA, Davis ET, et al. Long intergenic noncoding RNAs mediate the human chondrocyte inflammatory response and are differentially expressed in osteoarthritis cartilage. *Arthritis Rheumatol* 2016;68:845–56.
- Ilott NE, Heward JA, Roux B, Tsitsiou E, Fenwick PS, Lenzi L, et al. Corrigendum: long non-coding RNAs and enhancer RNAs regulate the lipopolysaccharide-induced inflammatory response in human monocytes. *Nat Commun* 2015;6:6814.
- Hamann PD, Roux BT, Heward JA, Love S, McHugh NJ, Jones SW, et al. Transcriptional profiling identifies differential expression of long non-coding RNAs in Jo-1 associated and inclusion body myositis. *Sci Rep* 2017;7:8024.

25. Roux BT, Heward JA, Donnelly LE, Jones SW, Lindsay MA. Catalog of differentially expressed long non-coding RNA following activation of human and mouse innate immune response. *Front Immunol* 2017;8:1038.
26. Pertea M, Kim D, Pertea GM, Leek JT, Salzberg SL. Transcript-level expression analysis of RNA-seq experiments with HISAT, StringTie and Ballgown. *Nat Protoc* 2016;11:1650–67.
27. Li H, Handsaker B, Wysoker A, Fennell T, Ruan J, Homer N, et al. The Sequence Alignment/Map format and SAMtools. *Bioinformatics* 2009;25:2078–9.
28. Pertea M, Pertea GM, Antonescu CM, Chang TC, Mendell JT, Salzberg SL. StringTie enables improved reconstruction of a transcriptome from RNA-seq reads. *Nat Biotechnol* 2015;33:290–5.
29. Trapnell C, Williams BA, Pertea G, Mortazavi A, Kwan G, van Baren MJ, et al. Transcript assembly and quantification by RNA-Seq reveals unannotated transcripts and isoform switching during cell differentiation. *Nat Biotechnol* 2010;28:511–5.
30. Sturn A, Quackenbush J, Trajanoski Z. Genesis: cluster analysis of microarray data. *Bioinformatics* 2002;18:207–8.
31. SEQC/MAQC-III Consortium. A comprehensive assessment of RNA-seq accuracy, reproducibility and information content by the Sequencing Quality Control Consortium. *Nat Biotechnol* 2014;32:903–14.
32. Verbruggen G, Wittoek R, Vander Cruyssen B, Elewaut D. Tumour necrosis factor blockade for the treatment of erosive osteoarthritis of the interphalangeal finger joints: a double blind, randomised trial on structure modification. *Ann Rheum Dis* 2012;71:891–8.
33. Cohen SB, Proudman S, Kivitz AJ, Burch FX, Donohue JP, Burstein D, et al. A randomized, double-blind study of AMG 108 (a fully human monoclonal antibody to IL-1R1) in patients with osteoarthritis of the knee. *Arthritis Res Ther* 2011;13:R125.
34. Maksymowych WP, Russell AS, Chiu P, Yan A, Jones N, Clare T, et al. Targeting tumour necrosis factor alleviates signs and symptoms of inflammatory osteoarthritis of the knee. *Arthritis Res Ther* 2012;14:R206.
35. Huang M, Wang H, Hu X, Cao X. lncRNA MALAT1 binds chromatin remodeling subunit BRG1 to epigenetically promote inflammation-related hepatocellular carcinoma progression. *Oncoimmunology* 2018;8:e1518628.
36. Biswas S, Thomas AA, Chen S, Aref-Eshghi E, Feng B, Gonder J, et al. MALAT1: an epigenetic regulator of inflammation in diabetic retinopathy. *Sci Rep* 2018;8:6526.
37. Puthanveetil P, Chen S, Feng B, Gautam A, Chakrabarti S. Long non-coding RNA MALAT1 regulates hyperglycaemia induced inflammatory process in the endothelial cells. *J Cell Mol Med* 2015;19:1418–25.
38. Yang H, Liang N, Wang M, Fei Y, Sun J, Li Z, et al. Long noncoding RNA MALAT-1 is a novel inflammatory regulator in human systemic lupus erythematosus. *Oncotarget* 2017;8:77400–6.
39. Zhao G, Su Z, Song D, Mao Y, Mao X. The long noncoding RNA MALAT1 regulates the lipopolysaccharide-induced inflammatory response through its interaction with NF- κ B. *FEBS Lett* 2016;590:2884–95.
40. Zhou HJ, Wang LQ, Wang DB, Yu JB, Zhu Y, Xu QS, et al. Long noncoding RNA MALAT1 contributes to inflammatory response of microglia following spinal cord injury via the modulation of a miR-199b/IKK β /NF- κ B signaling pathway. *Am J Physiol Cell Physiol* 2018;315:C52–61.
41. Ma J, Wu K, Liu K, Miao R. Effects of MALAT1 on proliferation and apoptosis of human non-small cell lung cancer A549 cells in vitro and tumor xenograft growth in vivo by modulating autophagy. *Cancer Biomark* 2018;22:63–72.
42. Zuo Y, Li Y, Zhou Z, Ma M, Fu K. Long non-coding RNA MALAT1 promotes proliferation and invasion via targeting miR-129-5p in triple-negative breast cancer. *Biomed Pharmacother* 2017;95:922–8.
43. Ellulu MS, Patimah I, Khaza'ai H, Rahmat A, Abed Y. Obesity and inflammation: the linking mechanism and the complications. *Arch Med Sci* 2017;13:851–63.
44. Scherer PE. Adipose tissue: from lipid storage compartment to endocrine organ. *Diabetes* 2006;55:1537–45.
45. Philp AM, Collier RL, Grover LM, Davis ET, Jones SW. Resistin promotes the abnormal type I collagen phenotype of subchondral bone in obese patients with end stage hip osteoarthritis. *Sci Rep* 2017;7:4042.
46. Fioravanti A, Cheleschi S, De Palma A, Addimanda O, Mancarella L, Pignotti E, et al. Can adipokines serum levels be used as biomarkers of hand osteoarthritis? *Biomarkers* 2018;23:265–70.

GRK5 Inhibition Attenuates Cartilage Degradation via Decreased NF- κ B Signaling

Takuya Sueishi,¹ Yukio Akasaki,¹ Norio Goto,¹ Ichiro Kurakazu,¹ Masakazu Toya,¹ Masanari Kuwahara,¹ Taisuke Uchida,¹ Mitsumasa Hayashida,¹ Hidetoshi Tsushima,¹ Hirofumi Bekki,² Martin K. Lotz,³ and Yasuharu Nakashima¹

Objective. NF- κ B–dependent signaling is an important modulator in osteoarthritis (OA), and G protein–coupled receptor kinase 5 (GRK5) regulates the NF- κ B pathway. This study was undertaken to investigate the functional involvement of GRK5 in OA pathogenesis.

Methods. GRK5 expression in normal and OA human knee joints was analyzed immunohistochemically. Gain- or loss-of-function experiments were performed using human and mouse chondrocytes. OA was induced in GRK5-knockout mice by destabilization of the medial meniscus, and histologic examination was performed. OA was also induced in wild-type mice, which were then treated with an intraarticular injection of amlexanox, a selective GRK5 inhibitor, every 5 days for 8 weeks.

Results. GRK5 protein expression was increased in human OA cartilage. In vitro, expression levels of OA-related factors and NF- κ B transcriptional activation were down-regulated by suppression of the *GRK5* gene in human OA chondrocytes (3.49-fold decrease in *IL6* [$P < 0.01$], 2.43-fold decrease in *MMP13* [$P < 0.01$], and 2.66-fold decrease in *ADAMTS4* [$P < 0.01$]). Conversely, GRK5 overexpression significantly increased the expression of OA-related catabolic mediators and NF- κ B transcriptional activation. On Western blot analysis, GRK5 deletion reduced I κ B α phosphorylation (up to 4.4-fold decrease [$P < 0.05$]) and decreased p65 nuclear translocation (up to 6.4-fold decrease [$P < 0.01$]) in mouse chondrocytes. In vivo, both GRK5 deletion and intraarticular amlexanox protected mouse cartilage against OA.

Conclusion. Our results suggest that GRK5 regulates cartilage degradation through a catabolic response mediated by NF- κ B signaling, and is a potential target for OA treatment. Furthermore, amlexanox may be a major compound in relevant drugs.

INTRODUCTION

Osteoarthritis (OA) is a degenerative disease driven in part by signaling mechanisms induced by stress- and inflammation-induced factors (1). NF- κ B signaling is known to be widely involved in OA pathophysiology and cartilage homeostasis through various mechanisms, including cell survival, differentiation, and inflammation, and is induced in OA chondrocytes during aging and inflammation (2–4). Therefore, targeted strategies that interfere with NF- κ B signaling may be novel therapeutic options for OA treatment (5).

In the resting state, NF- κ B dimers are inactive in the cytoplasm because of their association with I κ B. When IKK is activated by extracellular stimuli, I κ B proteins are phosphorylated at Ser^{32/36} and degraded. Following this activity, NF- κ B dimers are released, then migrate to the nucleus, leading to specific gene transactivation (6).

A previous study demonstrated that G protein–coupled receptor kinase 5 (GRK5) independently phosphorylated I κ B α at the same Ser^{32/36} phosphorylated by IKK in a mouse macrophage cell line (7). Consistent with this biochemical finding, another study using GRK5-knockout mice found that GRK5 positively regulated

Supported by the Japan Society for the Promotion of Science (Grant-in-Aid for Young Scientists [A] 17H05097).

¹Takuya Sueishi, MD, Yukio Akasaki, MD, PhD, Norio Goto, MD, PhD, Ichiro Kurakazu, MD, Masakazu Toya, MD, Masanari Kuwahara, MD, Taisuke Uchida, MD, Mitsumasa Hayashida, MD, PhD, Hidetoshi Tsushima, MD, PhD, Yasuharu Nakashima, MD, PhD: Kyushu University Graduate School of Medical Sciences, Fukuoka, Japan; ²Hirofumi Bekki, MD, PhD: Kyushu University Graduate School of Medical Sciences, Fukuoka, Japan, and Scripps Research Institute, San Diego,

California; ³Martin K. Lotz, MD: Scripps Research Institute, San Diego, California.

No potential conflicts of interest relevant to this article were reported.

Address correspondence to Yukio Akasaki, MD, PhD, Kyushu University Graduate School of Medical Sciences, Department of Orthopedic Surgery, 3-1-1 Maidashi, Higashi-ku, Fukuoka City, Fukuoka 812-8582, Japan. E-mail: akasaki@ortho.med.kyushu-u.ac.jp.

Submitted for publication February 24, 2019; accepted in revised form October 29, 2019.

the NF- κ B pathway in cardiomyocytes (8). In addition, I κ B α phosphorylation and p65 nuclear translocation were significantly reduced in lipopolysaccharide (LPS)-treated, GRK5-deficient peritoneal macrophages (9). However, another group reported the opposite results; namely, that interaction between GRK5 and I κ B α promoted the nuclear accumulation of I κ B α , resulting in inhibition of NF- κ B activity in endothelial cells (10). Thus, the role of GRK5 in the NF- κ B pathway remains a subject of controversy. GRKs, which comprise 7 subfamilies, have been functionally linked to a number of cell signaling processes, related not only to their role in G protein-coupled receptor (GPCR) phosphorylation and desensitization (11), but also to their ability to phosphorylate a number of intracellular signaling proteins (12,13). In particular, GRK5 has been reported to phosphorylate histone deacetylase 5 (HDAC-5) (14), arrestin 2 (15), and p53 (16), as well as I κ B α . Therefore, GRK5 has been proposed to be a critical kinase in the pathogenesis of several conditions, including endotoxemia (9), cardiac hypertrophy (14), sepsis (17), Alzheimer's disease (18), and cancer (19).

It was hypothesized that GRK5 plays an important role in the pathogenesis of OA because of its ubiquitous expression and ability to regulate NF- κ B signaling. This study aimed to investigate the functional involvement of GRK5 in OA pathogenesis using cartilage tissue and cells from both humans and GRK5-knockout mice. Identifying the mechanisms whereby GRK5 regulates OA progression may provide new insights into the development of potential therapies.

MATERIALS AND METHODS

Clinical samples. Human knee joints from individuals ages 17–88 years were obtained at autopsy with the approval of the Scripps Human Subjects Committee, or obtained from patients undergoing total knee arthroplasty, with the approval of the Ethics Committee of Kyushu University Hospital. The entire femoral condyles of normal knee joints were harvested from 5 donors (mean \pm SD age 29.8 \pm 10.0 years [range 17–43 years]; OA grade I) with no history of joint disease. Human OA joints were obtained from 5 donors (mean \pm SD age 68.6 \pm 18.5 years [range 49–88 years]; OA grade III–IV). Written informed consent was obtained from all subjects.

Immunohistochemical analysis of human knee joints. Osteochondral slabs were fixed in 4% paraformaldehyde for 2 days. After decalcification, the femoral condyles were cut (into 4- μ m-thick sections) along the sagittal plane and embedded in paraffin. The severity of OA was classified based on the degree of cartilage surface fibrillation. Slightly and severely fibrillated areas were collected from the weight-bearing regions of each of the 5 OA donors. Antigen retrieval was performed overnight with 1 mM EDTA at pH 8.0. Endogenous peroxidase activity was blocked by 3% hydrogen peroxidase in methanol for 30 minutes. For the

blocking procedure, each specimen was placed in normal horse serum for 20 minutes, then incubated for 1 hour at room temperature with primary anti-GRK5 antibody (Proteintech). Finally, the samples were counterstained with hematoxylin.

Quantification of positive cells in human cartilage.

GRK5 localization in each cartilage zone was systematically assessed by counting the number of positive cells in 3 images in each zone under 40 \times magnification, starting from the cartilage surface and continuing to the deep zone. The identification of each zone was based on previously reported characteristics (20). The frequency of positive cells was expressed as a percentage relative to the total number of cells counted in each zone with the BZ-II Analyzer software program (Keyence).

Cell isolation from human OA knee joints.

Human articular cartilage fragments were collected aseptically from OA patients who had undergone knee joint arthroplasty at Kyushu University Hospital. The cartilage fragments were then digested with 2 mg/ml of collagenase for 12 hours. Chondrocytes were then cultured in a 10-cm dish in Dulbecco's modified Eagle's medium (DMEM)/F-12 with 10% fetal bovine serum (FBS), then used in the experiments at the time of subconfluence (1–2 weeks or less in primary culture). Normal human chondrocytes were purchased from Lonza.

Small interfering RNA (siRNA) transfection and quantitative real-time polymerase chain reaction (PCR).

Human OA chondrocytes were seeded in 12-well plates at a density of 0.75×10^5 cells/well with DMEM and 10% FBS. After 1 day, siRNA targeting GRK5 (siGRK5) (8 nM) was transfected into cells using Lipofectamine RNAiMAX (ThermoFisher Scientific). Small interfering GRK5 and control siRNA (siCtrl) were purchased from Santa Cruz Biotechnology. Thirty-six hours after transfection, cells were serum-starved for 12 hours, then stimulated with LPS (10 μ g/ml) or interleukin-1 β (IL-1 β ; 1 ng/ml) for 6 hours. Total RNA was extracted using TRIzol reagent (ThermoFisher Scientific). Complementary DNA (cDNA) was synthesized using a PrimeScript RT Reagent kit (Takara Bio), and the resulting cDNA was amplified with PCR using a commercially available kit (SYBR Premix Ex Taq; Takara Bio). All PCR reactions were performed using a LightCycler 2.0 Instrument (Roche). Expression levels of *IL6*, *MMP13*, *ADAMTS4*, *ADAMTS5*, *NOS2*, and *GAPDH* were examined. The relative ratio of each target gene to *GAPDH* was calculated. The primers are listed in Supplementary Table 1, available on the *Arthritis & Rheumatology* web site at <http://onlinelibrary.wiley.com/doi/10.1002/art.41152/abstract>.

Luciferase assay. Small interfering RNA-transfected human OA chondrocytes were simultaneously transfected with pNL3.2 (NlucP/NF- κ B-RE/Hygro; Promega), and pGL-CMV (luc2/CMV/Neo; Promega) vectors using Lipofectamine 3000

(ThermoFisher Scientific). Thirty-six hours after transfection, cells were serum-starved for 12 hours, then stimulated with LPS (10 $\mu\text{g/ml}$) for 6 hours. Lysates were prepared and analyzed using a Dual Luciferase System (Promega).

Amlexanox treatment of human OA chondrocytes.

After human OA chondrocytes were serum-starved for 12 hours, they were treated for 48 hours with 10 μM or 100 μM amlexanox (MedChem Express), previously identified to be a GRK5 inhibitor (21). After amlexanox treatment for 48 hours, cells were stimulated with LPS (10 $\mu\text{g/ml}$) for 6 hours.

Enzyme-linked immunosorbent assay (ELISA). After amlexanox treatment for 48 hours, human OA chondrocytes were stimulated with LPS (10 $\mu\text{g/ml}$) for 24 hours. The concentrations of IL-6 and matrix metalloproteinase 13 (MMP-13) in the supernatant were measured using Human IL6 and MMP13 ELISA kits (R&D Systems).

GRK5 overexpression. Recombinant adenoviral vector encoding constitutively active GRK5 and control Ad-GFP were purchased from Vector BioLabs. Normal chondrocytes were infected with adenovirus using Lipofectamine 3000 at 100 multiplicities of infection with or without amlexanox (100 μM). Thirty-six hours after infection, cells were serum-starved for 12 hours, then stimulated with LPS (10 $\mu\text{g/ml}$) for 6 hours. Fifty-four hours after infection, cells were collected.

Cytotoxicity assay. Human OA chondrocytes were seeded into the wells of a 96-well plate at a density of 5,000 cells/well and cultured overnight. Then 10 μl of amlexanox solution was added at various concentrations (10 μM and 100 μM). A Cell Counting Kit-8 (CCK-8) assay (Dojindo) was then performed at 24, 48, and 72 hours after amlexanox treatment according to the instructions of the manufacturer.

Mice. GRK5-deficient mice (GRK5^{-/-}) and wild-type (WT) mice with a C57BL/6 background were used in all animal experiments. GRK5^{-/-} mice were obtained from Dr. Kurose (Kyushu University). These GRK5-deficient mice were general knockout mice originally generated by Dr. R. T. Premont (Duke University, Durham, NC) (22). The sequences of the primers used for genotyping are shown in Supplementary Table 2, available on the *Arthritis & Rheumatology* web site at <http://onlinelibrary.wiley.com/doi/10.1002/art.41152/abstract>. All experiments were performed according to the guidelines of Kyushu University.

Histologic sections of growth plate from mice at embryonic day 16.5 and postnatal day 0 were stained with hematoxylin and eosin. Histologic sections of knee joints from 4-week-old mice ($n = 5$) were stained with toluidine blue to measure the thickness of growth plate cartilage and total articular cartilage in 2 images per section. Double staining of mouse embryo skeletons was

performed with a solution containing alizarin red S and Alcian blue 8 GX (Sigma-Aldrich).

Isolation of cells from mouse knee joints. Immature chondrocytes were obtained from 5-day-old GRK5^{-/-} and WT mice and cultured as described previously (23). Under clean operating conditions, the femurs were dislocated, and the soft tissues around the joints were discarded. Isolated femoral condyles and tibial plateau from 2 litters were agitated until all soft tissues detached from the cartilage pieces; the cartilage was then digested with 2 mg/ml of collagenase for 12 hours with moderate stirring. Chondrocytes were plated and maintained in DMEM/F-12 with 10% FBS, then used in experiments at the time of confluence (1–2 weeks in primary culture).

Protein extraction and quantitative Western blot analysis. Whole-cell protein extracts were obtained using Cell Lysis Buffer or radioimmunoprecipitation assay buffer (Sigma-Aldrich). Nuclear extracts were isolated using Nuclear and Cytoplasmic Extraction Reagents (ThermoFisher Scientific). The Western blot analysis was performed with an automated system (Wes; ProteinSimple). Briefly, extract samples (800 ng/lane) were mixed with a master mixture to a final concentration of 1 \times sample buffer, 1 \times fluorescent molecular weight markers, and 40 mM dithiothreitol, and then heated at 95°C for 5 minutes. The samples, blocking reagent, primary antibodies, horseradish peroxidase-conjugated secondary antibodies, chemiluminescent substrate, and separation and stacking matrices were dispensed into designated plate wells. The electrophoresis and immunodetection steps were performed using a 12–230-kd capillary system. Digital images were analyzed and quantified with Compass software (ProteinSimple) after normalization to lamin B1 and GAPDH. Phospho-IkBa was normalized to total IkBa. The primary antibodies were phospho-IkBa, total-IkBa, p65 (all from Cell Signaling Technology), lamin B1 (Abcam), and GAPDH (Cell Signaling Technology).

Mouse OA model. OA was induced by destabilization of the medial meniscus (DMM) in 12-week-old male GRK5^{-/-} and WT mice as previously described (24). Sham surgery was performed in a separate group of mice using the same approach without DMM. All experimental groups consisted of 10 mice. The mice were killed 8 weeks after the operation and subjected to histologic analysis. Knee sections in the sagittal plane were stained with Safranin O–fast green. Histologic evaluations were performed using 2 sections of weight-bearing area per mouse. OA severity was quantified by Osteoarthritis Research Society International (OARS) histopathology grading (on a scale of 0–12) (25) by 2 independent observers in a blinded manner, and the scores were averaged to minimize observer bias. Osteophyte maturity was evaluated by examining anteromedial tibial regions in each mouse and was scored by 2 observers using a previously described scoring system (26). Synovial inflammation was also scored by 2 observers using a previously described scoring system (with a scale of 0–3) (27).

Application of amlexanox to mice in the OA model.

DMM or sham operations were performed on the left knee joints of mice. The injection solution comprised 10 mM amlexanox stock solution (MedChemExpress) diluted with saline.

Ten microliters of either 100 μ M amlexanox or saline as vehicle was injected into the intraarticular spaces of the mouse knee joints every 5 days for 8 weeks. All experimental groups consisted of 7 mice. Mice were killed at 20 weeks of age.

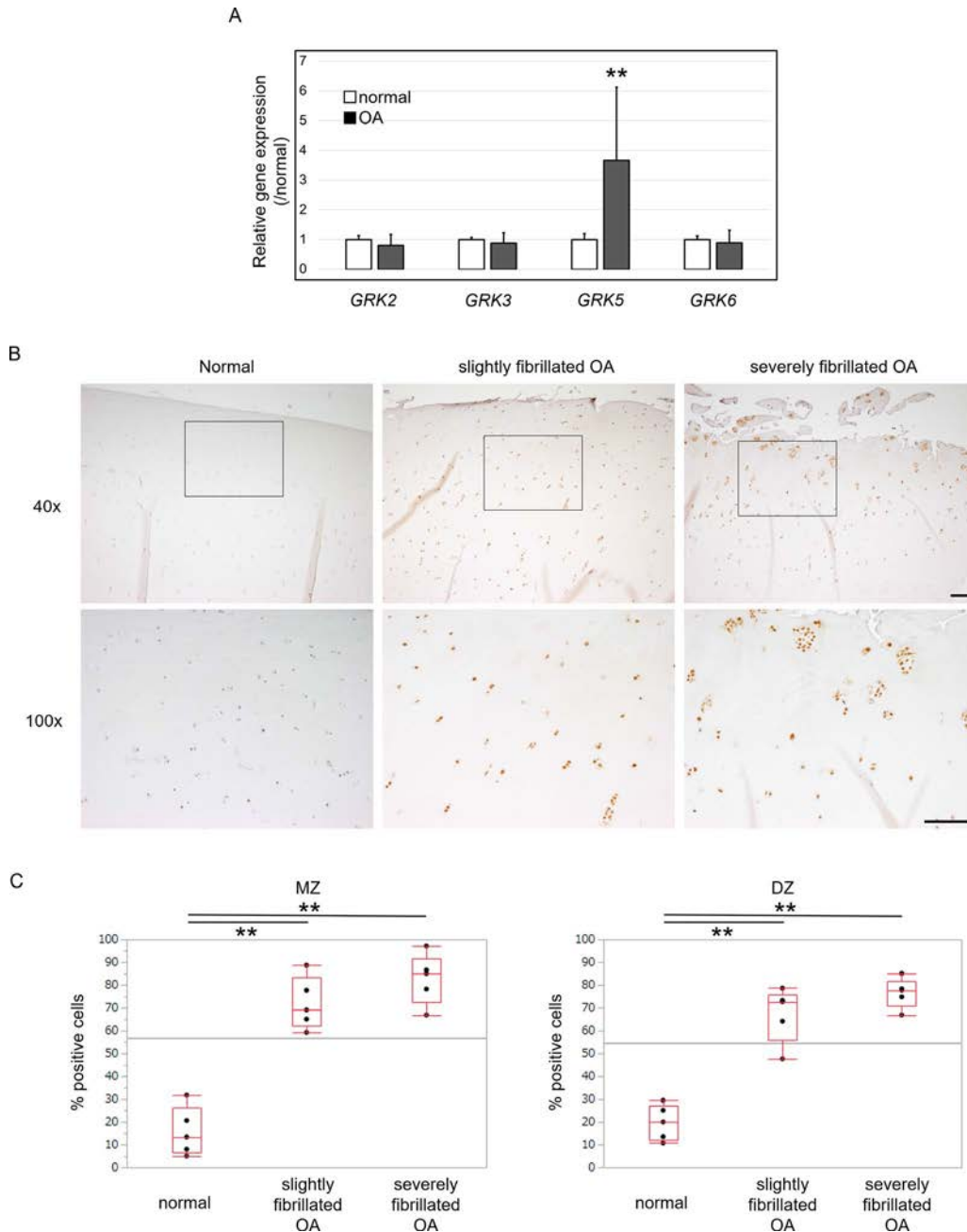


Figure 1. G protein-coupled receptor kinase 5 (GRK5) expression in human cartilage. **A**, Relative expression of messenger RNA for the *GRK2*, *GRK3*, *GRK5*, and *GRK6* genes in normal human chondrocytes (Lonza) and chondrocytes from patients with osteoarthritis (OA). Values are the mean \pm SD ($n = 8$ per group). ** = $P < 0.01$ versus normal chondrocytes. **B**, Representative immunohistochemical staining for GRK5 in normal cartilage, slightly fibrillated OA cartilage, and severely fibrillated OA cartilage. The severity of OA was classified based on the degree of cartilage surface fibrillation in the weight-bearing area. Bottom panels show higher-magnification views of the boxed areas in the top panels. Bars = 100 μ m. **C**, Quantification of GRK5-positive cells in the middle zone (MZ) and deep zone (DZ) in normal cartilage, slightly fibrillated OA cartilage, and severely fibrillated OA cartilage. Data are shown as box plots, where the boxes represent the 25th to 75th percentiles, the lines within the boxes represent the median, and the lines outside the boxes represent the 10th and 90th percentiles. Circles indicate individual samples ($n = 5$ per group). ** = $P < 0.01$. Color figure can be viewed in the online issue, which is available at <http://onlinelibrary.wiley.com/doi/10.1002/art.41152/abstract>.

Immunofluorescence staining of mouse embryo and knee joints.

Sections were stained with primary antibodies at room temperature for 1 hour, then incubated with Alexa Fluor-conjugated secondary antibodies (ThermoFisher Scientific). The following primary antibodies were used: GRK5 (Protein-tech), MMP-13 (Abcam), and IL-6 (Cell Signaling Technology). The numbers of GRK5-positive, MMP-13-positive, and IL-6-positive cells in the mouse model were quantified by counting immunopositive cells in sagittal sections of the knee joint at 400× magnification ($n = 10$ per group). The percentages of positively stained cells in 2 fields per section were counted using the BZ-II Analyzer software program. TUNEL staining was performed with an In Situ Cell Death Detection Kit (Takara Bio). The number of TUNEL-positive cells was quantified as described above.

Statistical analysis. Data normality was assessed by the Shapiro-Wilk test. When the distribution was normal, statistically significant differences between groups were determined by Student's *t*-test or the Tukey-Kramer test. When the distribu-

tion was not normal, the Wilcoxon test or Steel-Dwass test was used. Statistically significant differences between 4 groups were determined by the Steel-Dwass test. Results are reported as the mean \pm SD. *P* values less than 0.05 were considered significant.

RESULTS

Significant increase in GRK5 protein expression in human OA cartilage and colocalization of GRK5 protein expression with MMP-13/ADAMTS4 expression.

We initially compared the expression of the *GRK2*, *GRK3*, *GRK5*, and *GRK6* genes, which are ubiquitously expressed in humans, in normal chondrocytes versus OA chondrocytes isolated from human cartilage. *GRK5* expression was significantly higher in OA compared to normal chondrocytes, whereas expression of the other *GRKs* did not differ between normal and OA chondrocytes (Figure 1A). In immunohistochemical analysis, normal cartilage showed minimal GRK5 expression and a low percentage of GRK5-positive cells in all zones (Figure 1B). In contrast, in areas of severely fibrillated OA

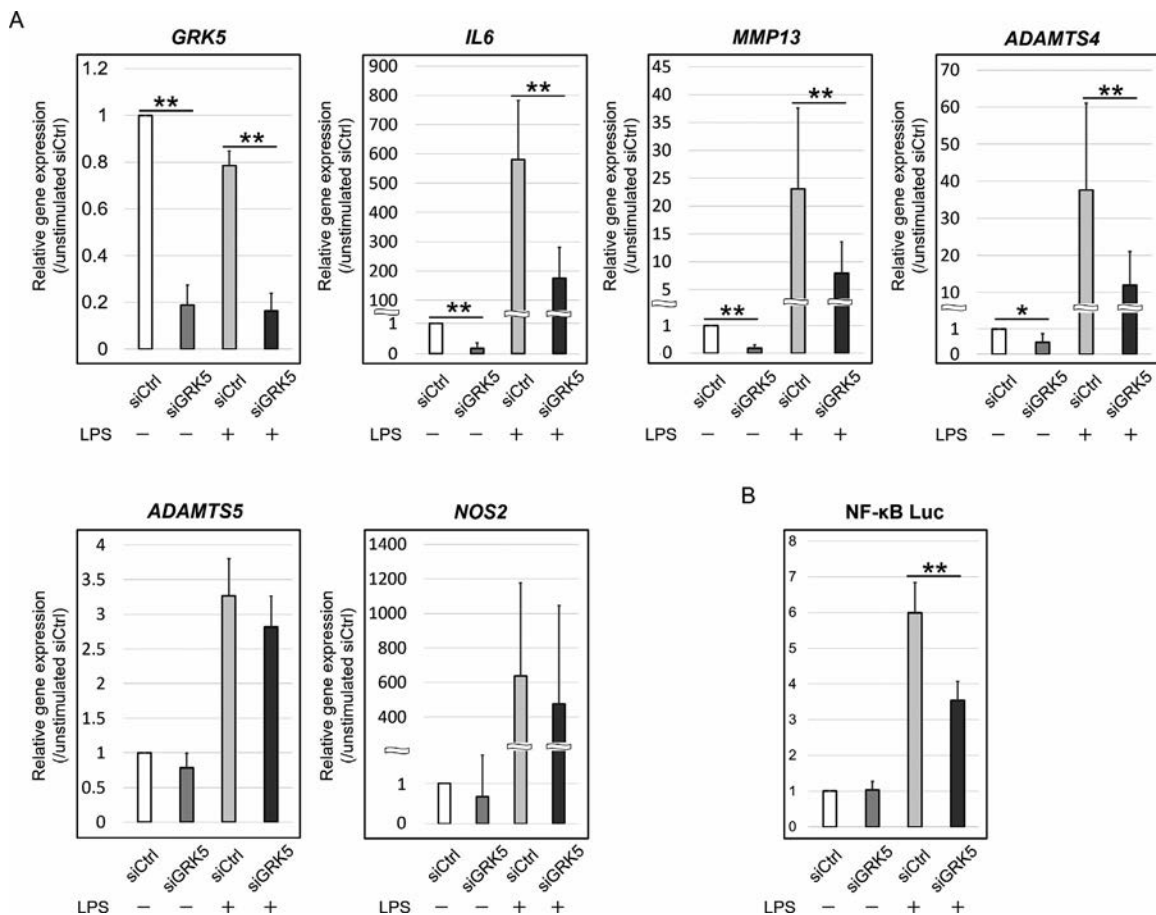


Figure 2. Effects of knockdown of *GRK5* by small interfering RNA (siRNA) on the gene expression levels of catabolic factors and NF- κ B transcriptional activation in osteoarthritic (OA) human chondrocytes. **A**, Changes in gene expression in response to lipopolysaccharide (LPS) in human OA chondrocytes transfected with siRNA targeting GRK5 (siGRK5). Values are the mean \pm SD ($n = 5$ donors per group). **B**, NF- κ B transcriptional activation in siGRK5-transfected human OA chondrocytes. Values are the mean \pm SD ($n = 3$ donors per group). * = $P < 0.05$; ** = $P < 0.01$. siCtrl = control siRNA.

cartilage, chondrocytes that formed clusters in the middle zones strongly expressed GRK5. In both middle and deep zones, the GRK5-positive cell rates in OA cartilage were significantly higher than those in normal cartilage (Figure 1C). The distribution pattern of GRK5 expression was similar to those of MMP-13 and ADAMTS4 in severely fibrillated OA cartilage (Supplementary Figure 1, available on the *Arthritis & Rheumatology* web site at <http://onlinelibrary.wiley.com/doi/10.1002/art.41152/abstract>).

Attenuation of expression of *IL6*, *MMP13*, and *ADAMTS4* genes, as well as NF- κ B transcriptional activation, upon GRK5 knockdown by siRNA in human OA chondrocytes. To explore the involvement of GRK5 in OA pathogenesis, the effects of GRK5 knockdown on inflammatory and catabolic gene expression and NF- κ B transcriptional activation were analyzed using siGRK5-transfected human OA chondrocytes stimulated with LPS. GRK5 knockdown by siRNA significantly attenuated the gene expression of *IL6* (3.49-fold decrease), *MMP13* (2.43-fold decrease), and *ADAMTS4* (2.66-fold decrease) compared to siCtrl in the presence of LPS (Figure 2A). In contrast, *ADAMTS5* and *NOS2* expression were not significantly altered by down-regulation of GRK5. Similarly, the expression levels of the genes *IL6*, *MMP13*, and *ADAMTS4* were significantly attenuated by GRK5 knockdown in the presence of IL-1 β (Supplementary Figure 2, available on the *Arthritis & Rheumatology* web site at <http://onlinelibrary.wiley.com/doi/10.1002/art.41152/abstract>). LPS-induced NF- κ B transcription activity was significantly attenuated by GRK5 knockdown (Figure 2B).

Suppression of inflammatory and catabolic gene expression, and of NF- κ B transcriptional activation, upon GRK5 inhibition by amlexanox in human OA chondrocytes. Amlexanox, a selective GRK5 inhibitor (21), was used to analyze the effect of GRK5 inhibition in human OA chondrocytes. In a CCK-8 assay, 72 hours of amlexanox treatment at concentrations of 10 μ M and 100 μ M did not significantly affect cell proliferation (Supplementary Figure 3, available on the *Arthritis & Rheumatology* web site at <http://onlinelibrary.wiley.com/doi/10.1002/art.41152/abstract>). LPS-induced expression of *IL6*, *MMP13*, and *ADAMTS5* genes was significantly suppressed in a dose-dependent manner by 48 hours of pretreatment with amlexanox (Figure 3A). Amlexanox at a concentration of 100 μ M significantly attenuated the LPS-induced gene expression of *IL6*, *MMP13*, *ADAMTS4*, *ADAMTS5*, and *NOS2*. Amlexanox significantly suppressed LPS-induced NF- κ B transcription activity at concentrations of 10 and 100 μ M (Figure 3C).

Induction of inflammatory and catabolic gene expression and NF- κ B transcriptional activation by GRK5 overexpression in normal human chondrocytes. GRK5 overexpression in normal human chondrocytes significantly increased the expression of *IL6*, *MMP13*, *ADAMTS4*, *ADAMTS5*,

and *NOS2* genes stimulated with LPS, and these increases were significantly suppressed by amlexanox treatment (Figure 3D). In the same manner, NF- κ B transcription activity enhanced by GRK5 overexpression was attenuated by amlexanox treatment (Figure 3E).

Inhibition of IL-1 β -induced I κ B α phosphorylation and p65 nuclear translocation by GRK5 knockout in mouse chondrocytes. Chondrocytes from GRK5-knockout mice were isolated for the following analyses. The expression levels of *Il6*, *Mmp13*, *Adamts4*, and *Adamts5* genes were significantly attenuated in GRK5-knockout mice compared to WT mice in the presence of IL-1 β (Figure 4A). This finding was consistent with the results in human chondrocytes transfected with siGRK5. In a quantitative Western blot assay (Supplementary Figure 4, available on the *Arthritis & Rheumatology* web site at <http://onlinelibrary.wiley.com/doi/10.1002/art.41152/abstract>), GRK5 knockout significantly inhibited the phosphorylation of I κ B α at Ser^{32/36} at 10 and 20 minutes after IL-1 β stimulation (up to 4.4-fold decrease [$P < 0.05$]) (Figure 4B). In addition, subsequent p65 nuclear translocation at 20 and 40 minutes after stimulation was not increased in GRK5-deficient mouse chondrocytes, as shown by proteins in nuclear extracts (up to 6.4-fold decrease [$P < 0.01$]) (Figure 4C).

GRK5 knockout does not exacerbate cartilage degeneration in a mouse model of OA. To examine the in vivo effect of GRK5 deletion on OA development, a DMM model was generated using GRK5-knockout and WT mice. GRK5-knockout mice developed and grew without any abnormality from the embryonic stage (embryonic day 16.5) to delivery (postnatal day 0) (Supplementary Figures 5 and 6, available on the *Arthritis & Rheumatology* web site at <http://onlinelibrary.wiley.com/doi/10.1002/art.41152/abstract>). Growth plate and articular cartilage thickness were not significantly different between GRK5-knockout mice and WT mice at 4 weeks of age (Figure 5A). Body weight did not differ significantly between the 2 strains at 4, 8, 12, or 20 weeks of age (Figure 5B).

Sham-operated mice showed no structural cartilage change, with no significant difference in OARSI scores between the 2 strains. The knee joints of WT mice showed moderate-to-severe cartilage degeneration 8 weeks after DMM surgery (Figure 5C). In contrast, cartilage degradation in GRK5-knockout mice was only mild. The average OARSI score in GRK5-knockout mice was significantly lower than that in WT mice 8 weeks after DMM (Figure 5C).

Osteophyte maturity slightly increased after DMM surgery, with no significant difference between genotypes (Figure 5C). Synovial inflammation was not observed in either group (Supplementary Figure 7A, available on the *Arthritis & Rheumatology* web site at <http://onlinelibrary.wiley.com/doi/10.1002/art.41152/abstract>). Chondrocyte apoptosis determined by TUNEL staining was significantly suppressed by GRK5 knockout (Figure 5D). Compared to

sham surgery, DMM surgery significantly increased the number of cells expressing GRK5 in WT mice (Figure 5E). After OA induction, the rates of cells positive for IL-6 and MMP-13 in GRK5-knockout mice were significantly lower than those in WT mice (Figures 5F and G).

Delayed cartilage degradation in mice with OA treated with intraarticular injection of amlexanox. Finally, we examined the effects of amlexanox on cartilage degradation in the OA mouse model. Amlexanox solution or saline was injected into the

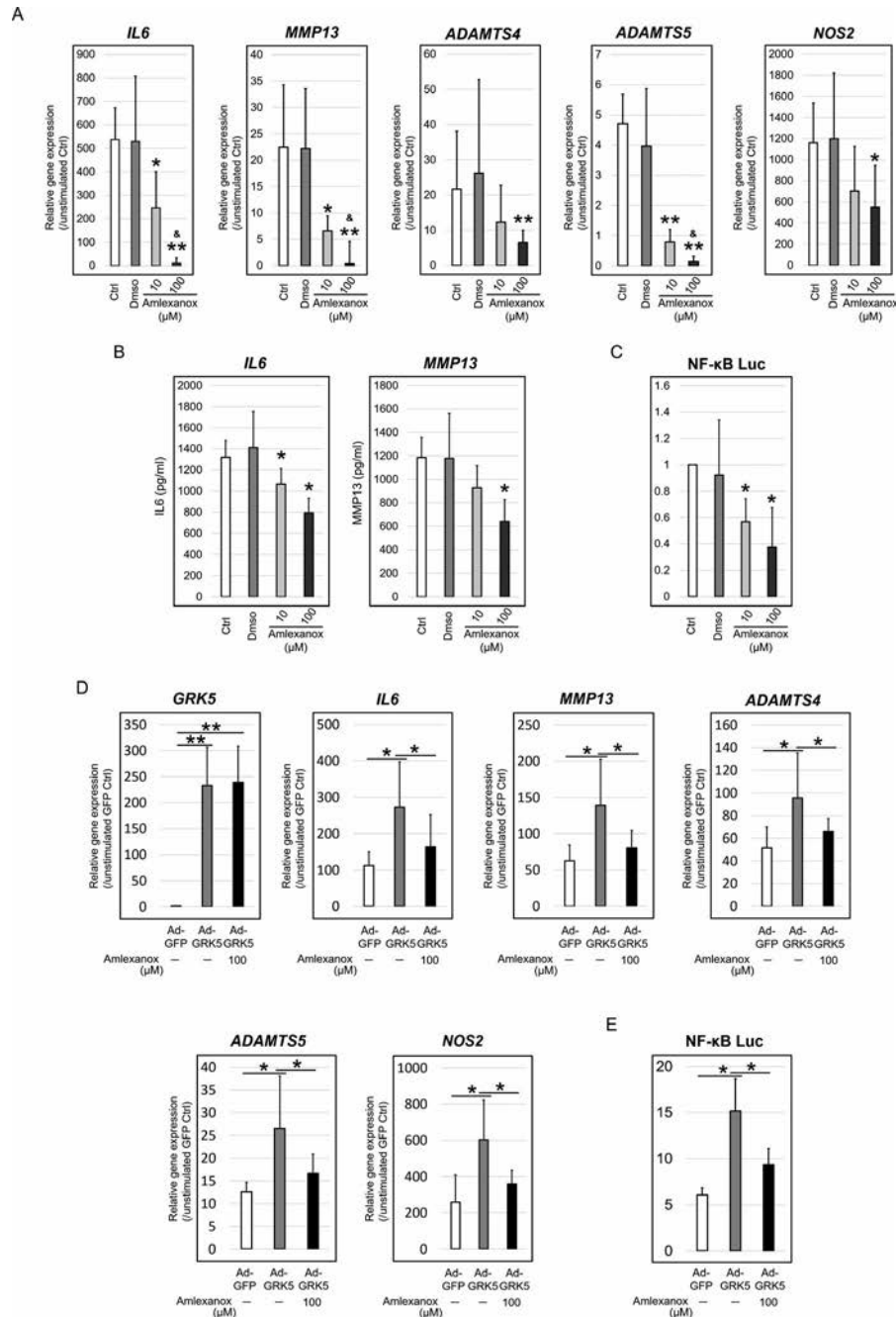


Figure 3. Effects of amlexanox and overexpression of G protein-coupled receptor kinase 5 (GRK5) on the expression of catabolic factors and NF- κ B transcriptional activation in human osteoarthritic (OA) chondrocytes. **A**, Changes in lipopolysaccharide (LPS)-induced *IL6*, *MMP13*, *ADAMTS4*, *ADAMTS5*, and *NOS2* gene expression in human OA chondrocytes treated with amlexanox. **B**, Changes in LPS-induced interleukin-6 (IL-6) and matrix metalloproteinase 13 (MMP-13) protein levels in the supernatant in human OA chondrocytes treated with amlexanox. **C**, Changes in LPS-induced NF- κ B transcriptional activation in human OA chondrocytes treated with amlexanox. **D**, Expression of inflammatory and cartilage catabolic genes in LPS-stimulated normal human chondrocytes with overexpression of GRK5, left untreated or treated with amlexanox. **E**, NF- κ B transcriptional activation in LPS-stimulated normal human chondrocytes with overexpression of GRK5, left untreated or treated with amlexanox. Values are the mean \pm SD ($n = 6$ donors per group in **A**, 3 donors per group in **B** and **E**, and 4 donors per group in **C** and **D**). * = $P < 0.05$; ** = $P < 0.01$, versus control in **A**, **B**, and **C** and versus the indicated group in **D** and **E**; & = $P < 0.05$ versus amlexanox 10 μ M.

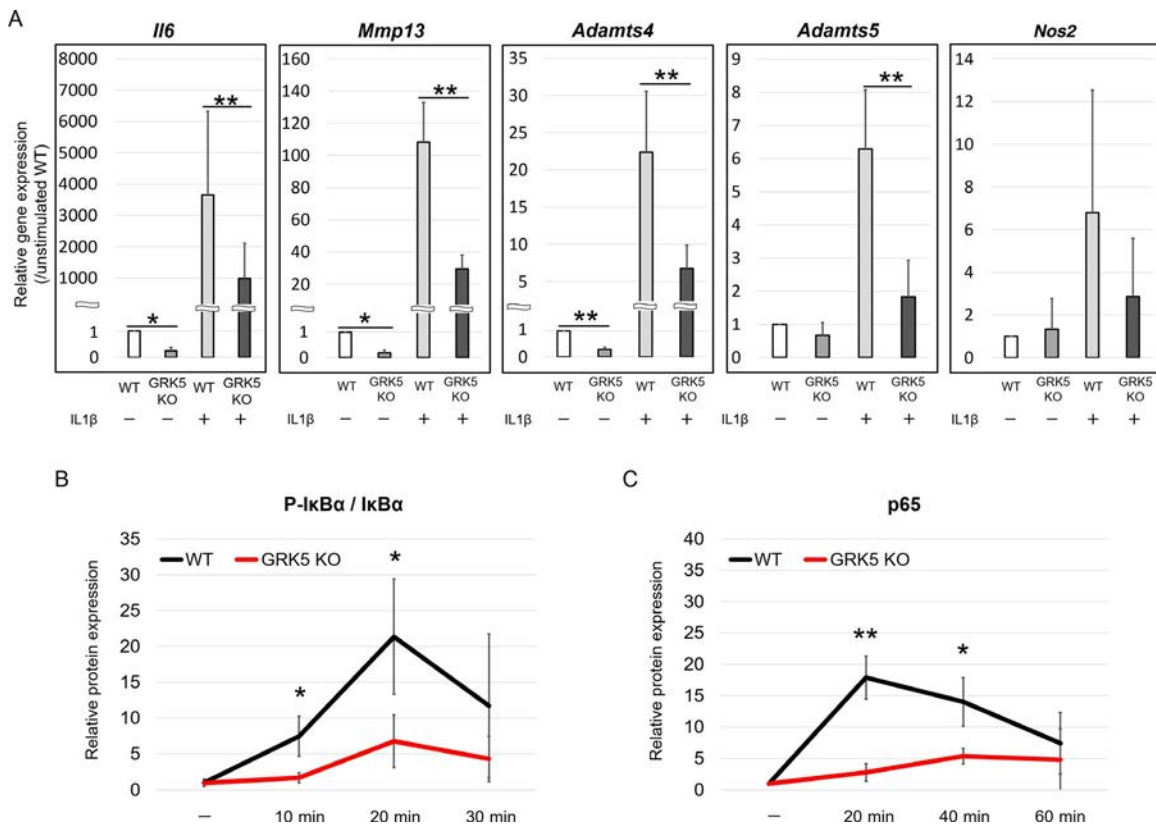


Figure 4. Effects of G protein-coupled receptor kinase 5 (GRK5) knockout (KO) on gene expression of catabolic factors, I κ B α phosphorylation, and p65 nuclear translocation in mouse chondrocytes. **A**, Changes in osteoarthritis (OA)-related gene expression in chondrocytes from wild-type (WT) mice and GRK5-knockout mice in response to stimulation with interleukin-1 β (IL-1 β). Values are the mean \pm SD ($n = 6$ mice per group). * = $P < 0.05$; ** = $P < 0.01$. **B**, Changes over time in IL-1 β -induced I κ B α phosphorylation in chondrocytes from WT mice and GRK5-knockout mice. Phospho-I κ B α was normalized to total I κ B α . **C**, Changes over time in IL-1 β -induced p65 nuclear translocation in chondrocytes from WT mice and GRK5-knockout mice. In **B** and **C**, values are the mean \pm SD ($n = 4$ mice per group). * = $P < 0.05$; ** = $P < 0.01$, versus GRK5-knockout mice at the same time point. Color figure can be viewed in the online issue, which is available at <http://onlinelibrary.wiley.com/doi/10.1002/art.41152/abstract>.

joint space of DMM and sham-operated mouse knees every 5 days for 8 weeks (Figure 6A). Histologic analysis 8 weeks after DMM surgery revealed that the mouse knee joints treated with 100 μ M of amlexanox had a significantly lower OARSI score than those treated with vehicle control, without any significant effect on osteophyte formation or synovitis (Figure 6B) (Supplementary Figure 7B, available on the *Arthritis & Rheumatology* web site at <http://onlinelibrary.wiley.com/doi/10.1002/art.41152/abstract>). Sham-operated mice injected with saline or amlexanox showed no structural cartilage damage related to the use of a needle for injection (Figure 6B). There was a significantly lower rate of TUNEL-positive cells in the group treated with amlexanox than in the group treated with saline (Figure 6C). Importantly, compared to vehicle, intraarticular injection of amlexanox significantly decreased the number of cells expressing IL-6 and MMP-13 in articular cartilage (Figures 6D and E).

DISCUSSION

This is the first study to characterize GRK5 protein expression in cartilage tissue and its functional involvement in OA pathogen-

esis. GRK5 was more highly expressed in human cartilage from OA patients than from healthy controls, suggesting that GRK5 is deeply involved in OA pathogenesis. In in vitro experiments, the OA-related catabolic mediators *IL6*, *MMP13*, and *ADAMTS4* were down-regulated by loss of GRK5 function in human and mouse chondrocytes. Conversely, adenoviral overexpression of GRK5 resulted in increased expression of OA-related catabolic factors. Further mechanistic analyses demonstrated that GRK5 was a key factor for phosphorylation of I κ B α at Ser^{32/36} and subsequent p65 nuclear translocation in chondrocytes. In in vivo experiments, GRK5-knockout mice were resistant to DMM-induced cartilage degradation. In addition, intraarticular administration of the GRK5 inhibitor amlexanox showed protective effects against cartilage degradation and DMM-induced expression of catabolic factors. Taken together, our results suggested that GRK5 inhibition acted via NF- κ B signaling to decrease cartilage degradation by suppressing the catabolic response.

In this study, all experimental manipulations to lower GRK5 function resulted in suppressive effects on catabolic factors; this finding confirmed that GRK5 is an exacerbating factor of OA

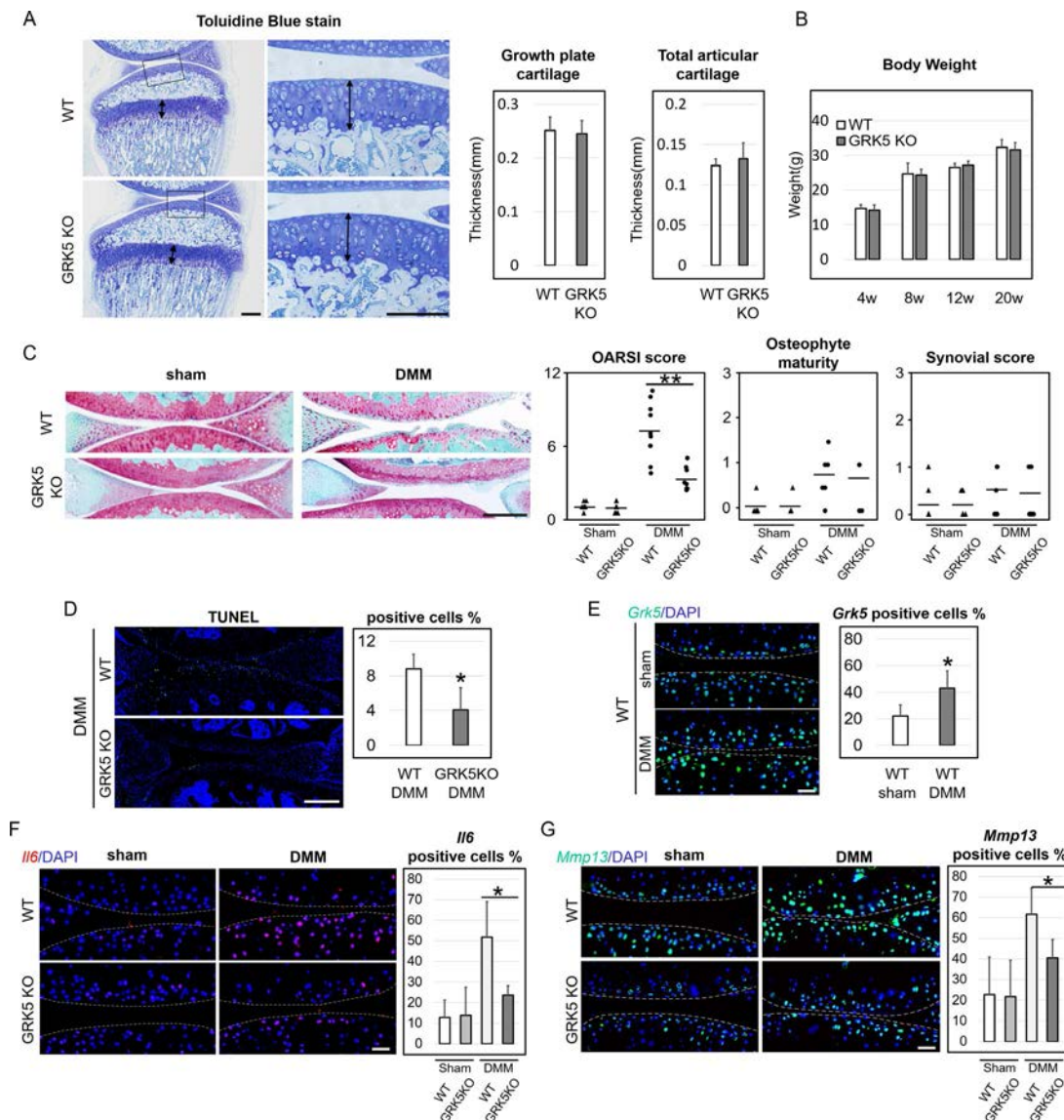


Figure 5. In vivo effect of G protein-coupled receptor kinase 5 (GRK5) deletion on osteoarthritis (OA) in a destabilized medial meniscus (DMM) model in GRK5-knockout (GRK5-KO) mice. **A**, Left, Toluidine blue staining of semi-serial histologic sagittal sections of the proximal tibia from a 4-week-old wild-type (WT) mouse and a 4-week-old GRK5-knockout mouse. Right panels show higher-magnification views of the boxed areas in the left panels. **Arrows** indicate weight-bearing areas. Bars = 100 μ m. Right, Thickness of growth plate cartilage and total articular cartilage at the vertex of the articular surface of the weight-bearing areas in WT and GRK5-knockout mice. Values are the mean \pm SD ($n = 4$ mice per group). **B**, Body weight of WT and GRK5-knockout mice at the indicated ages. Values are the mean \pm SD ($n = 5$ mice per group). **C**, Left, Safranin O-fast green staining of the knee joints of WT and GRK5-knockout mice subjected to sham operation or DMM. Bar = 100 μ m. Right, Cartilage degradation, as measured by OA Research Society International (OARSi) score, osteophyte maturity, and synovitis in WT and GRK5-knockout mice subjected to sham operation or DMM. Horizontal lines show the mean; symbols represent individual mice ($n = 10$ per group). ** = $P < 0.01$. **D**, Left, DAPI (blue) staining of nuclei for TUNEL-positive cells in WT and GRK5-knockout mice 8 weeks after DMM surgery. Bar = 40 μ m. Right, Rates of TUNEL-positive cells in the indicated mouse strains. Values are the mean \pm SD ($n = 10$ mice per group). * = $P < 0.05$. **E**, Left, Representative immunofluorescence images of GRK5-positive cells (green) in WT and GRK5-knockout mice 8 weeks after DMM surgery. Bar = 40 μ m. Right, Rates of GRK5-positive cells in the indicated mouse strains. Values are the mean \pm SD ($n = 10$ mice per group). * = $P < 0.05$. **F** and **G**, Representative immunofluorescence images (left panels) and rates of cells positive for interleukin-6 (IL-6; red) (**F**) and matrix metalloproteinase 13 (MMP-13; green) (**G**) (right panels) in WT and GRK5-knockout mice 8 weeks after DMM surgery. Bars = 40 μ m. Values are the mean \pm SD ($n = 10$ mice per group). * = $P < 0.05$.

pathogenesis. Until now, no study has evaluated the functional role of GRK5 in the joint tissue such as cartilage and bone. Regarding other tissues and disorders, in the heart, GRK5 overexpression was reported to worsen heart failure and cardiac hypertrophy as a

nuclear HDAC kinase independent of any action directly on GPCRs (14,28). In the prostate, GRK5 was highly expressed in aggressive prostate cancer cells, and the loss of GRK5 activity resulted in decreased prostate tumor growth (19). In polymicrobial sepsis,

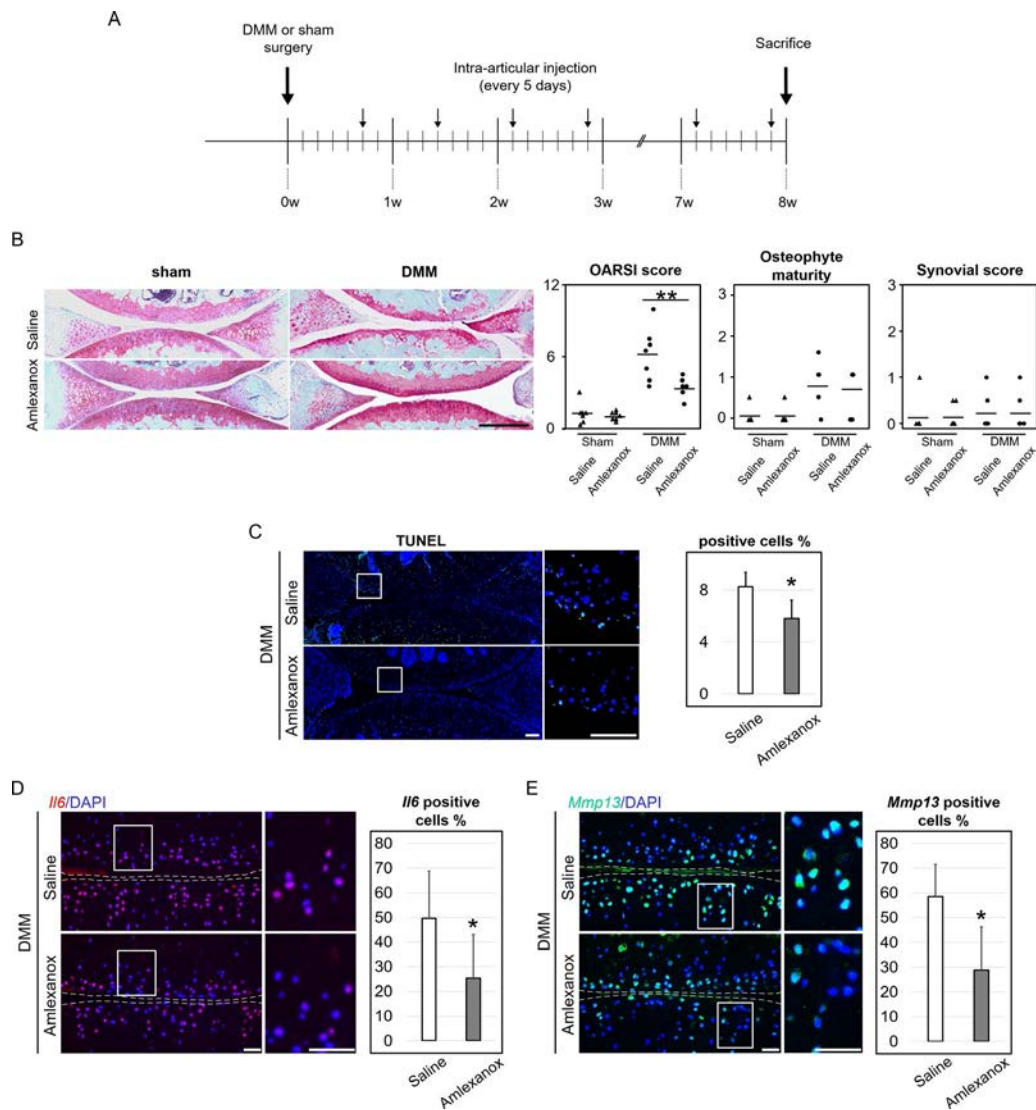


Figure 6. In vivo effect of intraarticular administration of amlexanox on osteoarthritis (OA) development in wild-type (WT) mice subjected to destabilization of the medial meniscus (DMM). **A**, Schematic representation of the timeline for the surgical procedure for OA induction and intraarticular injection of treatment (saline or amlexanox) in WT mice. **B**, Left, Histologic assessment by Safranin O–fast green staining of the knee joints of WT mice subjected to sham surgery or DMM and treated with saline or amlexanox. Bar = 100 μ m. Right, Cartilage degradation, as measured by OA Research Society International (OARSI) score, osteophyte maturity, and synovitis in the indicated groups. Horizontal lines show the mean; symbols represent individual mice ($n = 7$ per group). $** = P < 0.01$. **C**, DAPI (blue) staining of nuclei for TUNEL-positive cells 8 weeks after DMM surgery in WT mice treated with saline or amlexanox. Right panels show higher-magnification views of the boxed areas in the left panels. Bars = 40 μ m. Right, Rates of TUNEL-positive cells in WT mice subjected to DMM and treated with saline or amlexanox. Values are the mean \pm SD ($n = 7$ mice per group). $* = P < 0.05$. **D**, Left, Representative immunofluorescence images of staining for interleukin-6 (IL-6) (red) 8 weeks after surgery in mice subjected to DMM and treated with saline or amlexanox. Right panels show higher-magnification views of the boxed areas in the left panels. Bars = 40 μ m. Right, Rates of IL-6–positive cells in mice subjected to DMM and treated with saline or amlexanox. Values are the mean \pm SD ($n = 7$ mice per group). $* = P < 0.05$. **E**, Left, Representative immunofluorescence images of staining for matrix metalloproteinase (MMP-13) (green) 8 weeks after surgery in mice subjected to DMM and treated with saline or amlexanox. Right panels show higher-magnification views of the boxed areas in the left panels. Bars = 40 μ m. Right, Rates of MMP-13–positive cells in mice subjected to DMM and treated with saline or amlexanox. Values are the mean \pm SD ($n = 7$ mice per group). $* = P < 0.05$. Color figure can be viewed in the online issue, which is available at <http://onlinelibrary.wiley.com/doi/10.1002/art.41152/abstract>.

NF- κ B activation in sepsis-induced inflammation was significantly inhibited by GRK5 knockout, and mortality was significantly prevented in GRK5-knockout mice in the presence of antibiotics (17). On the other hand, in a mouse model of Alzheimer's disease, GRK5 deficiency accelerated β -amyloid accumulation via impaired cholin-

ergic activity (18). Taken together, these findings and the results of the present study indicate that GRK5 is deeply involved in a diversity of pathogenesis and mostly functions as a progression factor.

Mice with knockout of different GRKs show different phenotypes; GRK2-knockout mice experience embryonic death due

to cardiac abnormalities, but mice with knockout of other GRKs develop normally (29). In most studies that used GRK5-knockout mice, phenotypes caused by inhibition of GPCR desensitization were not obvious, likely due to compensation by other GRKs, whereas 2 studies found disease-related phenotypic changes associated with GPCR desensitization (22,30). GRK1, GRK4, and GRK7 have a limited tissue distribution; in contrast, GRK2, GRK3, GRK5, and GRK6 are ubiquitously expressed (31,32). Thus, most GPCRs in the body are potentially regulated by 4 of these kinases. In contrast, several GRKs have been reported to show disease-specific functions by interacting with intracellular substrates in a GPCR-independent manner (33–36). In particular, GRK5 is one of the most important kinases that phosphorylate I κ B α in NF- κ B activation (8,9,17).

It was previously demonstrated that in mouse macrophages, GRK5 independently phosphorylated I κ B α at the same Ser^{32/36} sites phosphorylated by IKK (7). Consistent with those findings, the present study showed that GRK5 deficiency significantly decreased I κ B α phosphorylation at Ser^{32/36} in chondrocytes; however, it remains unclear whether GRK5 phosphorylated I κ B α independently of IKK. Recently, Ohba et al reported that GRK6 also directly phosphorylated I κ B α at Ser^{32/36} independently of IKK, and that kinase activation, a conformational change in GRK6, was required for the promotion of NF- κ B signaling after tumor necrosis factor stimulation in macrophages (36). In the present study, one possible reason GRK6 did not compensate for I κ B α phosphorylation decreased by GRK5 deletion is that GRK6 expression was not induced at a pathologically significant level in OA chondrocytes compared to GRK5.

The activity of the NF- κ B signaling pathway has been found to be closely associated with OA development (3,4,37), although targeted therapeutic strategies to inhibit NF- κ B activity and thus limit OA progression have not yet been established. Intraarticular administration of decoy oligodeoxynucleotides that inhibit NF- κ B activation was previously shown to reduce OA progression (38). However, the half-life of free oligodeoxynucleotides was found to be too short to achieve a sufficient therapeutic effect (39). Other studies showed that using an adenoviral vector or peptide nanoparticle to deliver siRNA targeting NF- κ B p65 into knee joints suppressed cartilage degradation in rat and mouse OA models (40,41). The transfection efficacy of viral-based vectors was excellent, but safety concerns remain (42–44). In the present study, amlexanox, a selective inhibitor of GRK5, successfully inhibited phosphorylation of I κ B α at Ser^{32/36} and subsequently NF- κ B activation. Amlexanox was originally developed for the treatment of asthma, allergic rhinitis, and aphthous ulcers (43,44), and given its established safety record and low cost, it may be an interesting candidate for OA treatment.

This study had some limitations. First, we observed inconsistent effects of GRK5 inhibition on *ADAMTS5* and *NOS2* gene expression depending on the experimental approach. In particular, GRK5 down-regulation by siRNA in human chondrocytes did

not decrease *ADAMTS5* or *NOS2* expression even though NF- κ B activity was reduced. Similarly, GRK5 knockout in mouse chondrocytes did not decrease *Nos2* expression. Although there was no clear explanation for these findings, we believe that various experimental conditions, such as the differences in degree of GRK5 down-regulation and cell species, could be potentially influential factors. Second, the effect of intraarticular amlexanox injection was validated at a single time point, 8 weeks after surgery. Ideally, additional analysis at different time points would be conducted for elucidating further therapeutic efficacy of amlexanox.

In conclusion, our results suggest that GRK5 regulates cartilage degradation through a catabolic response mediated by NF- κ B signaling, and is a potential target for OA treatment. Furthermore, amlexanox may be a major compound in relevant drugs.

ACKNOWLEDGMENTS

The authors thank Hitoshi Kurose, Michio Nakaya, Akiomi Nagasaka, and Yuki Ohba for providing GRK5-knockout mice and technical support. The authors also thank the anonymous peer reviewers of this manuscript for their constructive comments. The authors thank the staff of the Research Support Center, Research Center for Human Disease Modeling, Kyushu University Graduate School of Medical Sciences.

AUTHOR CONTRIBUTIONS

All authors were involved in drafting the article or revising it critically for important intellectual content, and all authors approved the final version to be published. Dr. Akasaki had full access to all of the data in the study and takes responsibility for the integrity of the data and the accuracy of the data analysis.

Study conception and design. Sueishi, Akasaki, Hayashida, Tsushima, Lotz, Nakashima.

Acquisition of data. Sueishi.


Analysis and interpretation of data. Sueishi, Akasaki, Goto, Kurakazu, Toya, Kuwahara, Uchida, Bekki.

REFERENCES

1. Lotz M, Loeser RF. Effects of aging on articular cartilage homeostasis. *Bone* 2012;51:241–8.
2. Bonizzi G, Karin M. The two NF- κ B activation pathways and their role in innate and adaptive immunity. *Trends Immunol* 2004;25:280–8.
3. Kobayashi H, Chang SH, Mori D, Itoh S, Hirata M, Hosaka Y, et al. Biphasic regulation of chondrocytes by Rel α through induction of anti-apoptotic and catabolic target genes. *Nat Commun* 2016;7:13336.
4. Saito T, Fukai A, Mabuchi A, Ikeda T, Yano F, Ohba S, et al. Transcriptional regulation of endochondral ossification by HIF-2 α during skeletal growth and osteoarthritis development. *Nat Med* 2010;16:678–86.
5. Choi MC, Jo J, Park J, Kang HK, Park Y. NF- κ B signaling pathways in osteoarthritic cartilage destruction. *Cells* 2019;8:E734.
6. Bhatt D, Ghosh S. Regulation of the NF- κ B-mediated transcription of inflammatory genes [review]. *Front Immunol* 2014;5:71.
7. Patial S, Luo J, Porter KJ, Benovic JL, Parameswaran N. G-protein-coupled-receptor kinases mediate TNF α -induced NF κ B

- signalling via direct interaction with and phosphorylation of I κ B α . *Biochem J* 2009;425:169–78.
8. Islam KN, Bae JW, Gao E, Koch WJ. Regulation of nuclear factor κ B (NF- κ B) in the nucleus of cardiomyocytes by G protein-coupled receptor kinase 5 (GRK5). *J Biol Chem* 2013;288:35683–9.
 9. Patial S, Shahi S, Saini Y, Lee T, Packiriswamy N, Appledorn DM, et al. G-protein coupled receptor kinase 5 mediates lipopolysaccharide-induced NF κ B activation in primary macrophages and modulates inflammation in vivo in mice. *J Cell Physiol* 2011;226:1323–33.
 10. Sorriento D, Ciccarelli M, Santulli G, Campanile A, Altobelli GG, Cimmini V, et al. The G-protein-coupled receptor kinase 5 inhibits NF κ B transcriptional activity by inducing nuclear accumulation of I κ B α . *Proc Natl Acad Sci U S A* 2008;105:17818–23.
 11. Ribas C, Penela P, Murga C, Salcedo A, García-Hoz C, Jurado-Pueyo M, et al. The G protein-coupled receptor kinase (GRK) interactome: role of GRKs in GPCR regulation and signaling. *Biochim Biophys Acta* 2007;1768:913–22.
 12. Watari K, Nakaya M, Kurose H. Multiple functions of G protein-coupled receptor kinases [review]. *J Mol Signal* 2014;9:1.
 13. Gurevich EV, Tesmer JJ, Mushegian A, Gurevich VV. G protein-coupled receptor kinases: more than just kinases and not only for GPCRs. *Pharmacol Ther* 2012;133:40–69.
 14. Martini JS, Raake P, Vinge LE, DeGeorge BR Jr, Chuprun JK, Harris DM, et al. Uncovering G protein-coupled receptor kinase-5 as a histone deacetylase kinase in the nucleus of cardiomyocytes. *Proc Natl Acad Sci U S A* 2008;105:12457–62.
 15. Barthelet G, Carrat G, Cassier E, Barker B, Gaven F, Pillot M, et al. B-arrestin1 phosphorylation by GRK5 regulates G protein-independent 5-HT $_4$ receptor signalling. *EMBO J* 2009;28:2706–18.
 16. Chen X, Zhu H, Yuan M, Fu J, Zhou Y, Ma L. G-protein-coupled receptor kinase 5 phosphorylates p53 and inhibits DNA damage-induced apoptosis. *J Biol Chem* 2010;285:12823–30.
 17. Packiriswamy N, Lee T, Raghavendra PB, Durairaj H, Wang H, Parameswaran N. G-protein-coupled receptor kinase-5 mediates inflammation but does not regulate cellular infiltration or bacterial load in a polymicrobial sepsis model in mice. *J Innate Immun* 2013;5:401–13.
 18. Cheng S, Li L, He S, Liu J, Sun Y, He M, et al. GRK5 deficiency accelerates β -amyloid accumulation in Tg2576 mice via impaired cholinergic activity. *J Biol Chem* 2010;285:41541–8.
 19. Kim JI, Chakraborty P, Wang Z, Daaka Y. G-protein coupled receptor kinase 5 regulates prostate tumor growth. *J Urol* 2012;187:322–9.
 20. Gulak F, Alexopoulos LG, Upton ML, Youn I, Choi JB, Cao L, et al. The pericellular matrix as a transducer of biomechanical and biochemical signals in articular cartilage. *Ann N Y Acad Sci* 2006;1068:498–512.
 21. Homan KT, Wu E, Cannavo A, Koch WJ, Tesmer JJ. Identification and characterization of amlexanox as a G protein-coupled receptor kinase 5 inhibitor. *Molecules* 2014;19:16937–49.
 22. Premont RT, Gainetdinov RR. Physiological roles of G protein-coupled receptor kinases and arrestins. *Annu Rev Physiol* 2007;69:511–34.
 23. Salvat C, Pigenet A, Humbert L, Berenbaum F, Thirion S. Immature murine articular chondrocytes in primary culture: a new tool for investigating cartilage. *Osteoarthritis Cartilage* 2005;13:243–9.
 24. Glasson SS, Blanchet TJ, Morris EA. The surgical destabilization of the medial meniscus (DMM) model of osteoarthritis in the 129/SvEv mouse. *Osteoarthritis Cartilage* 2007;15:1061–9.
 25. Glasson SS, Chambers MG, Van Den Berg WB, Little CB. The OARSI histopathology initiative—recommendations for histological assessments of osteoarthritis in the mouse. *Osteoarthritis Cartilage* 2010;18 Suppl 3:S17–23.
 26. Little CB, Barai A, Burkhardt D, Smith SM, Fosang AJ, Werb Z, et al. Matrix metalloproteinase 13-deficient mice are resistant to osteoarthritic cartilage erosion but not chondrocyte hypertrophy or osteophyte development. *Arthritis Rheum* 2009;60:3723–33.
 27. Midwood K, Sacre S, Piccinini AM, Inglis J, Trebaul A, Chan E, et al. Tenascin-C is an endogenous activator of Toll-like receptor 4 that is essential for maintaining inflammation in arthritic joint disease. *Nat Med* 2009;15:774–80.
 28. Chen EP, Bittner HB, Akhter SA, Koch WJ, Davis RD. Myocardial function in hearts with transgenic overexpression of the G protein-coupled receptor kinase 5. *Ann Thorac Surg* 2001;71:1320–4.
 29. Matkovich SJ, Divan A, Klanke JL, Hammer DJ, Marreez Y, Odley AM, et al. Cardiac-specific ablation of G-protein receptor kinase 2 redefines its roles in heart development and β -adrenergic signaling. *Circ Res* 2006;99:996–1003.
 30. Liu J, Rasul I, Sun Y, Wu G, Li L, Premont RT, et al. GRK5 deficiency leads to reduced hippocampal acetylcholine level via impaired presynaptic M2/M4 autoreceptor desensitization. *J Biol Chem* 2009;284:19564–71.
 31. Hisatomi O, Matsuda S, Satoh T, Kotaka S, Imanishi Y, Tokunaga F. A novel subtype of G-protein-coupled receptor kinase, GRK7, in teleost cone photoreceptors. *FEBS Lett* 1998;424:159–64.
 32. Premont RT, Macrae AD, Stoffel RH, Chung N, Pitcher JA, Ambrose C, et al. Characterization of the G protein-coupled receptor kinase GRK4: identification of four splice variants. *J Biol Chem* 1996;271:6403–10.
 33. Usui I, Imamura T, Babendure JL, Satoh H, Lu JC, Hupfeld CJ, et al. G protein-coupled receptor kinase 2 mediates endothelin-1-induced insulin resistance via the inhibition of both G α q/11 and insulin receptor substrate-1 pathways in 3T3-L1 adipocytes. *Mol Endocrinol* 2005;19:2760–8.
 34. Peregrin S, Jurado-Pueyo M, Campos PM, Sanz-Moreno V, Ruiz-Gomez A, Crespo P, et al. Phosphorylation of p38 by GRK2 at the docking groove unveils a novel mechanism for inactivating p38MAPK. *Curr Biol* 2006;16:2042–7.
 35. Lafarga V, Aymerich I, Tapia O, Mayor F Jr, Penela P. A novel GRK2/HDAC6 interaction modulates cell spreading and motility. *EMBO J* 2012;31:856–69.
 36. Ohba Y, Nakaya M, Watari K, Nagasaka A, Kurose H. GRK6 phosphorylates I κ B α at Ser(32)/Ser(36) and enhances TNF- α -induced inflammation. *Biochem Biophys Res Commun* 2015;461:307–13.
 37. Marcu KB, Otero M, Olivetto E, Borzi RM, Goldring MB. NF- κ B signaling: multiple angles to target OA. *Curr Drug Targets* 2010;11:599–613.
 38. Roman-Blas JA, Jimenez SA. NF- κ B as a potential therapeutic target in osteoarthritis and rheumatoid arthritis. *Osteoarthritis Cartilage* 2006;14:839–48.
 39. De Stefano D. Oligonucleotides decoy to NF- κ B: becoming a reality? *Discov Med* 2011;12:97–105.
 40. Chen LX, Lin L, Wang HJ, Wei XL, Fu X, Zhang JY, et al. Suppression of early experimental osteoarthritis by in vivo delivery of the adenoviral vector-mediated NF- κ Bp65-specific siRNA. *Osteoarthritis Cartilage* 2008;16:174–84.
 41. Yan H, Duan X, Pan H, Holguin N, Rai MF, Akk A, et al. Suppression of NF- κ B activity via nanoparticle-based siRNA delivery alters early cartilage responses to injury. *Proc Natl Acad Sci U S A* 2016;113:E6199–208.
 42. Wang D, Gao G. State-of-the-art human gene therapy: part 1—gene delivery technologies. *Discov Med* 2014;18:67–77.
 43. Makino H, Saijo T, Ashida Y, Kuriki H, Maki Y. Mechanism of action of an antiallergic agent, amlexanox (AA-673), in inhibiting histamine release from mast cells: acceleration of cAMP generation and inhibition of phosphodiesterase. *Int Arch Allergy Appl Immunol* 1987;82:66–71.
 44. Bell J. Amlexanox for the treatment of recurrent aphthous ulcers. *Clin Drug Investig* 2005;25:555–66.

Intergenerational Transmission of Diet-Induced Obesity, Metabolic Imbalance, and Osteoarthritis in Mice

Natalia S. Harasymowicz,¹  Yun-Rak Choi,² Chia-Lung Wu,¹ Leanne Iannucci,¹ Ruhang Tang,¹ and Farshid Guilak¹

Objective. Obesity and osteoarthritis (OA) are 2 major public health issues affecting millions of people worldwide. Whereas parental obesity affects the predisposition to diseases such as cancer or diabetes in children, transgenerational influences on musculoskeletal conditions such as OA are poorly understood. This study was undertaken to assess the intergenerational effects of a parental/grandparental high-fat diet on the metabolic and skeletal phenotype, systemic inflammation, and predisposition to OA in 2 generations of offspring in mice.

Methods. Metabolic phenotype and predisposition to OA were investigated in the first and second (F1 and F2) generations of offspring (n = 10–16 mice per sex per diet) bred from mice fed a high-fat diet (HFD) or a low-fat control diet. OA was induced by destabilizing the medial meniscus. OA, synovitis, and adipose tissue inflammation were determined histologically, while bone changes were measured using micro-computed tomography. Serum and synovial cytokines were measured by multiplex assay.

Results. Parental high-fat feeding showed an intergenerational effect, with inheritance of increased weight gain (up to 19% in the F1 generation and 9% in F2), metabolic imbalance, and injury-induced OA in at least 2 generations of mice, despite the fact that the offspring were fed the low-fat diet. Strikingly, both F1 and F2 female mice showed an increased predisposition to injury-induced OA (48% higher predisposition in F1 and 19% in F2 female mice fed the HFD) and developed bone microarchitectural changes that were attributable to parental and grandparental high-fat feeding.

Conclusion. The results of this study reveal a detrimental effect of parental HFD and obesity on the musculoskeletal integrity of 2 generations of offspring, indicating the importance of further investigation of these effects. An improved understanding of the mechanisms involved in the transmissibility of diet-induced changes through multiple generations may help in the development of future therapies that would target the effects of obesity on OA and related conditions.

INTRODUCTION

Osteoarthritis (OA) is the most common arthritic joint disease and the top indication for total joint replacement surgery, affecting more than 250 million people worldwide (1). One of the primary risk factors for OA is obesity and its associated metabolic syndrome (2). However, the mechanisms linking obesity and OA are multifactorial and are not fully understood. Whereas it was originally believed that the link between OA and obesity was simply attributable to increased “wear-and-tear” of excessive joint loading, it is now apparent that numerous additional factors

associated with obesity, such as systemic inflammation or a high-fat diet (HFD), may also be critical mediators of OA (3). Furthermore, a familial predisposition to OA in human subjects has been confirmed to possess strong polygenetic and environmental risk (4). Previous animal studies have demonstrated that diet-induced obesity greatly affects the progression of OA. For instance, a diet rich in saturated fat with an excess of proinflammatory fatty acids (FAs) (i.e., omega-6 FAs) increases the predisposition to OA (5,6).

In addition to the direct effects of obesity on OA, growing evidence is now showing that prenatal and postnatal development are affected by both nutrition and environmental stimuli, particularly in

Supported in part by the NIH (grants AR-50245, AR-48852, AG-15768, AR-48182, AG-46927, AR-073752, OD-10707, AR-060719, and AR-057235), the Arthritis Foundation, and the Nancy Taylor Foundation for Chronic Diseases.

¹Natalia S. Harasymowicz, PhD, Chia-Lung Wu, PhD, Leanne Iannucci, BSc, Ruhang Tang, PhD, Farshid Guilak, PhD: Washington University in St. Louis and Shriners Hospitals for Children, St. Louis, Missouri; ²Yun-Rak Choi, MD, PhD: Washington University in St. Louis and Shriners Hospitals for Children,

St. Louis, Missouri, and Yonsei University College of Medicine, Seoul, South Korea.

No potential conflicts of interest relevant to this article were reported.

Address correspondence to Farshid Guilak, PhD, Washington University, Center of Regenerative Medicine, Couch Biomedical Research Building, Room 3121, PO Box 8233, St. Louis, MO 63110. E-mail: guilak@wustl.edu.

Submitted for publication June 23, 2019; accepted in revised form October 17, 2019.

the context of obesity (7). The health of future offspring is thought to be influenced by diet and exercise aspects of parental lifestyle (8). Some diseases in children, such as cancer (9) and type 2 diabetes mellitus, have been shown to correlate with both maternal (10) and paternal obesity (11). Several mechanisms are postulated to play an important role in mediating these changes, including epigenetic modifications of reproductive cells (12), disturbance in hypothalamic hunger/satiety signaling (10), and finally, the role of intrauterine (13) and maternal microbiome milieu (14) during development.

These previous findings suggest that parental obesity may be an important factor in the heritability of obesity and metabolic dysfunction, and therefore may also influence the pathogenesis and susceptibility to musculoskeletal diseases such as OA. We studied the intergenerational effects of obesity on the metabolic and skeletal phenotype, systemic inflammation, and predisposition to OA in 2 generations (F1 and F2) of offspring bred from mice fed either an HFD or a low-fat control diet (Figure 1A). We hypothesized that, despite the fact that the offspring were fed the low-fat control diet postweaning, the offspring would exhibit disturbed metabolism and an “obese-like” phenotype, and thus would have an increased predisposition to develop injury-induced OA.

MATERIALS AND METHODS

Animal studies and experimental design. All experimental procedures were approved by and conducted in accordance with the Institutional Animal Care and Use Committee guidelines of Washington University in St. Louis. C57BL/6J mice were purchased from The Jackson Laboratory. Mice were housed in a 12-hour light/12-hour dark cycle with access to water and food ad libitum. At age 4 weeks, mice were allocated to receive either the low-fat control diet (Research Diets product no. D11120103) or the HFD (Research Diets product no. D11120105) for 11–15 weeks. The contents of these diets (details provided in Supplementary Table 1, available on the *Arthritis & Rheumatology* web site at <http://onlinelibrary.wiley.com/doi/10.1002/art.41147/abstract>) have been reported previously (5). Two groups of breeding pairs (F0 breeders) were formed: F0 Control (F0 mice receiving the low-fat control diet) and F0 HFD (F0 mice receiving HFD) ($n = 6$ mice per breeding group). The F1 generation of offspring (both sexes) was then collected, forming F1 Control and F1 HFD groups. A subset of F1 mice ($n = 4$ mice per breeding group) was also used to create the F2 generation (both sexes), forming F2 Control and F2

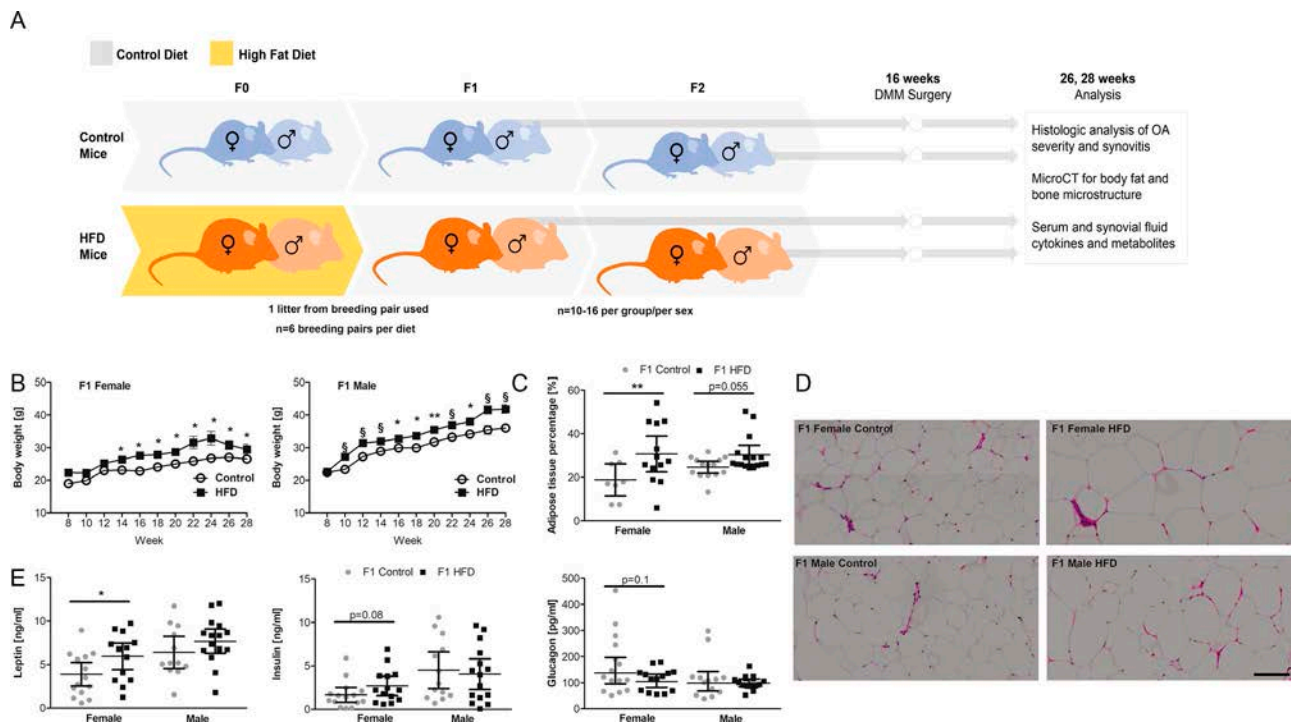


Figure 1. Parental high-fat diet (HFD) affects weight gain, adiposity, and the metabolic profile in the first (F1) generation of offspring. **A**, Study design. F0-generation mice were fed either a low-fat control diet (10% fat by kcal) or an HFD (60% fat by kcal). The F1 generation was fed the control diet after weaning. Destabilization of the medial meniscus (DMM) surgery was performed on the left knee at age 16 weeks, and mice were scanned with a micro-computed tomography (micro-CT) scanner for body fat analysis at age 26 weeks. Animals were killed at age 28 weeks for further analysis, according to sex and parental diet group. OA = osteoarthritis. **B**, Longitudinal body weight. **C**, Adipose tissue content assessed by micro-CT. **D**, Representative images of tissue samples showing histologic staining with hematoxylin and eosin to detect subcutaneous adipose tissue. Bar = 100 μm . **E**, Serum levels of adipokines (leptin, insulin, and glucagon). In **B**, **C**, and **E**, results are shown as the mean \pm 95% confidence interval ($n = 10$ –16 mice per sex and per parental diet group). Symbols in **C** and **E** represent individual mice. * = $P < 0.05$; ** = $P < 0.01$; § = $P < 0.001$, by repeated measures one-way analysis of variance in **B** or Mann-Whitney U test in **C** and **E**. Color figure can be viewed in the online issue, which is available at <http://onlinelibrary.wiley.com/doi/10.1002/art.41147/abstract>.

HFD groups. The F1 breeder mice were siblings of the F1 offspring, obtained from the same litter as used for the main experiments.

One litter per breeding pair was used, and 1–5 offspring per litter per sex was collected. F1 and F2 mice were allocated to receive the low-fat control diet throughout the study (Figure 1A). Offspring were housed separately from the breeders after weaning, and siblings from the same litter were housed together.

The F1 and F2 offspring mice underwent destabilization of the medial meniscus (DMM) surgery at age 16 weeks; thereafter, the animals were killed at age 28 weeks. At that time, the knee joints, visceral adipose tissue (AT), subcutaneous AT, serum, and synovial fluid were collected.

Body weight and composition. Mice were weighed biweekly. Body fat content was measured in the mice at age 26 weeks, using a micro-computed tomography (micro-CT) scanner (SkyScan 1176; Bruker) with a 35- μ m isotropic voxel resolution (357 μ A, 500 msec integration time, 1 frame averaging). A 1-mm aluminum filter was used to reduce the effects of beam hardening. Images were reconstructed using NRecon software (with 30% beam hardening and 20 ring artifact correction).

For in vivo scans, mice were anesthetized using 2–3% isoflurane inhalation. Scans were reconstructed for the abdominal region (between the proximal end of L1 and the distal end of L6 (as shown in Supplementary Figure 1A, available on the *Arthritis & Rheumatology* web site at <http://onlinelibrary.wiley.com/doi/10.1002/art.41147/abstract>) to quantify representative AT content in each animal. The AT percentage was measured using a modified script provided by CTan software (SkyScan 1176; Bruker), which delineated the percentage threshold for AT as compared to that for other tissues, as previously described (15). Briefly, the algorithm separated the mouse body from the background to provide the total tissue volume, while the AT threshold delineated total fat mass from lean mass and bone (see Supplementary Figures 1B and C at <http://onlinelibrary.wiley.com/doi/10.1002/art.41147/abstract>), forming the AT percentage values for each scanned mouse.

OA and synovitis assessments. At age 16 weeks, all mice underwent DMM surgery to induce knee OA in the left hind limb, as previously described (16). To evaluate the effects of parental diet on OA development, the mice were killed at age 28 weeks. Briefly, both the left and right hind limbs were harvested and fixed in 10% neutral buffered formalin. Limbs were then decalcified in Cal-Ex solution (Fisher Scientific), dehydrated, and embedded in paraffin. The joint was sectioned in the coronal plane at a thickness of 8 μ m.

Joint sections were stained with hematoxylin, fast green, and Safranin O to determine the development of OA and formation of osteophytes. For evaluation of synovitis, sections were stained with hematoxylin and eosin (H&E) to reveal infiltrated cells and synovial structure. Three independent, blinded graders (YRC, CLW, and RT) scored the joint sections for OA using a modified

Mankin scoring system (17), and scored osteophytes and synovitis using a previously established protocol (18). Scores were averaged among the graders for the whole joint (total Mankin score of OA, synovitis score) or medial part of the joint (total medial osteophyte score).

Measurement of serum and synovial fluid cytokine levels. Serum and synovial fluid from the DMM-operated mouse limbs and contralateral control limbs were collected as described previously (5). For determination of cytokine and adipokine levels in the serum and synovial fluid, a multiplexed bead assay (Discovery Luminex 31-plex; Eve Technologies) was used to determine the concentration of eotaxin, granulocyte colony-stimulating factor, granulocyte-macrophage colony-stimulating factor, interferon- γ (IFN γ), interleukin-1 α (IL-1 α), IL-1 β , IL-2, IL-3, IL-4, IL-5, IL-6, IL-7, IL-9, IL-10, IL-12 (p40), IL-12 (p70), IL-13, IL-15, IL-17A, IFN γ -inducible 10-kd protein, keratinocyte chemoattractant, leukemia inhibitory factor, lipopolysaccharide-induced CXC chemokine, monocyte chemoattractant protein 1, monokine induced by IFN γ , macrophage inflammatory protein 1 α (MIP-1 α), MIP-1 β , MIP-2, RANTES, tumor necrosis factor (TNF), and vascular endothelial growth factor. A mouse metabolic array (MRDMET; Eve Technologies) was used to measure the levels of amylin, C-peptide, ghrelin, glucagon, insulin, leptin, phosphoprotein, peptide YY, and resistin in the serum.

Bone microstructural analysis. Bone structural and morphologic changes were measured in the intact hind limbs of mice by micro-CT (SkyScan 1176; Bruker) with an 8.75- μ m isotropic voxel resolution (500 μ A, 500 msec integration time, 4 frame averaging). A 1-mm aluminum filter was used to reduce the effects of beam hardening. Images were reconstructed using NRecon software (with 30% beam hardening and 20 ring artifact correction). Subchondral/trabecular regions were segmented using CTan automatic thresholding software. The tibial and femoral epiphyses were selected using the subchondral plate and growth plate as references. The tibial metaphysis was defined as the 1-mm region directly below the growth plate.

Hydroxyapatite calibration phantoms were used to calibrate the bone density values (all in mg/cm³). Micro-CT limb images were analyzed for bone volume/total volume (BV/TV), trabecular bone number (Tb.N), trabecular bone thickness (Tb.Th), trabecular bone separation (Tb.Sp), and bone mineral density (BMD).

Detection of AT macrophages by immunofluorescence. Samples of visceral AT were collected, flash-frozen in OCT compound, and cryosectioned at a thickness of 5 μ m. Tissue slides were then fixed in acetone, followed by incubation with Fc-receptor blocking in 2.5% goat serum (Vector Laboratories) and incubation with a cocktail of primary antibodies containing Alexa

Fluor 488–conjugated anti-CD11b and phycoerythrin-conjugated CD11c (BioLegend). Nuclei were stained with DAPI. Samples were imaged using fluorescence microscopy (VS120; Olympus).

Histologic assessment of AT. Samples of visceral AT were fixed in 10% neutral buffered formalin, paraffin-embedded, and cut into 5- μ m sections. Sections were deparaffinized, rehydrated, and stained with a standard H&E method. Samples were imaged using fluorescence microscopy (VS120; Olympus). Further details are provided in the Supplementary Methods, available on the *Arthritis & Rheumatology* web site at <http://online.library.wiley.com/doi/10.1002/art.41147/abstract>.

Real-time polymerase chain reaction (PCR). RNA from visceral AT (n= 5–9 samples per group) was obtained using a Total RNA Purification kit (Norgen Biotek). RNA purity was assessed by NanoDrop absorbance measurement with 260 nm/280 nm and 260 nm/230 nm absorbance ratios of >1.9. One microgram of RNA was reverse transcribed using iSCRIPT (Bio-Rad) in accordance with the instructions of the suppliers. Real-time PCR was conducted on a QuantStudio (ThermoFisher). Ten nanograms of complementary DNA was analyzed. The primer concentration was used at 10 μ M. The reactions were performed in duplicate for each analyzed gene.

Reactions using SYBR Green chemistry were also subjected to melting curve analysis. The amplification curves and efficiency of amplification of each gene were validated, and the efficiency values ranged from 95% to 105%. Values for target gene expression were normalized to the average value for 3 housekeeping genes (Rip32 [for ribosomal protein 32], Ppia [for peptidylprolyl isomerase A], and Gapdh [for glyceraldehyde-3-phosphate dehydrogenase]). Relative messenger RNA (mRNA) expression was assessed using the $2^{-\Delta\Delta C_t}$ method, with the lowest threshold cycle (C_t) value of the group serving as a calibrator (according to the method described by Livak and Schmittgen [19]). The primer sequences used for assessment of gene expression were as follows: for *Lep*, forward GGGCTTCACCCCATCTGAG and reverse AAGGCCAGCAGATGGAGGAG; for *Lepr*, forward CTGCAGTCTTCGGGGATGTG and reverse TGGGCTGCAGTGACATCAGA; for *Cd36*, forward GACG TGGCAAAGAACAGCAG and reverse GGCTCCATTGGGCTGTACAA; for *AdipoQ*, forward CCCTCCACCCAAGGGAACCTT and reverse TCCAGGAGTGCCATCTCTGC; for *AdipoR1*, forward TGCC TCAGGAAGAGGAGGAG and reverse TTTCAGCCAGTCAGGAAGCA; for *AdipoR2*, forward GCTCAGAAAAGGGCACCAAC and reverse ATCATGACACTCGGGCTCCT; for *Pparg*, forward GCCC TGGAACTGCAGCTAAA and reverse GTGCTCTGTGACGATCTGCCT; for *Fabp4*, forward TGTGATGCCTTTGTGGGAAC and reverse ATGCCTGCCACTTTCCTTGT; for *Rpl32*, forward GGTGAAGCCCAAGATCGTCA and reverse CTCCGCACCCTGTTGTCAAT; for *Ppia*, forward AGGATTCATGTGCCAGCGTG and reverse TTGCCATGACAAGATGCCA; and for *Gapdh*, forward GGCAAATTCACGGCACAGT and reverse GTCTCGTCTCCTGGAAGATGG.

Statistical analysis. Statistical analyses were performed using IBM SPSS software, with significance reported at the 95% confidence level. All data are presented as the mean \pm 95% confidence interval. Regular two-way analysis of variance (ANOVA), Mann-Whitney U test, or repeated measures two-way ANOVA was used for group comparisons, followed by Bonferroni's test for multiple comparisons where appropriate. The right (non-DMM-operated) contralateral leg was used as a control. All analyses were performed within separate sex groups. Spearman's bivariate regression was used to evaluate the association between the left (DMM-operated) joint OA score and other outcomes. The Spearman's rank-order correlation test was conducted to assess correlations between the left joint OA score and 52 separate measurements, including weight, serum cytokine levels, and adipokine levels, as well as synovial fluid cytokine levels.

RESULTS

F1 offspring. *Weight gain, adiposity, and metabolic profile.* Female and male F1 HFD mice were significantly heavier than their corresponding F1 Control mice (Figure 1B). F1 HFD females had a significantly higher percentage of AT than did F1 Control females, and there was a trend ($P = 0.055$) toward increased abdominal fat in F1 HFD males compared to F1 Control males (Figure 1C).

We observed increased adipocyte hypertrophy in the subcutaneous AT from both female and male F1 HFD mice compared to their F1 Control counterparts (Figure 1D). Furthermore, in female F1 HFD mice compared to female F1 Control mice, the serum leptin levels were significantly higher, insulin trended toward higher levels, and glucagon trended toward lower levels (Figure 1E). In F1 male mice, no significant differences were found in the serum adipokine levels of leptin, insulin, or glucagon between the diet groups. Levels of other serum adipokines did not differ between the diet groups (see Supplementary Figures 2A–E, available on the *Arthritis & Rheumatology* web site at <http://onlinelibrary.wiley.com/doi/10.1002/art.41147/abstract>).

Systemic and local inflammation. Serum IL-1 β levels trended higher in female F1 HFD mice compared to female F1 Control mice, whereas there was no change in serum TNF and IL-6 levels. Serum levels of IL-1 α , IL-10, and IP-10 were significantly lower in female F1 HFD mice compared to female F1 Control mice. There was a trend toward higher levels of IL-17 in female F1 HFD mice compared to female F1 Control mice (Figure 2A). Levels of other cytokines did not differ between the analyzed groups (see Supplementary Table 2, available on the *Arthritis & Rheumatology* web site at <http://onlinelibrary.wiley.com/doi/10.1002/art.41147/abstract>).

Visceral AT from F1 HFD offspring had a higher content of fibrotic areas when compared to their sex-matched controls

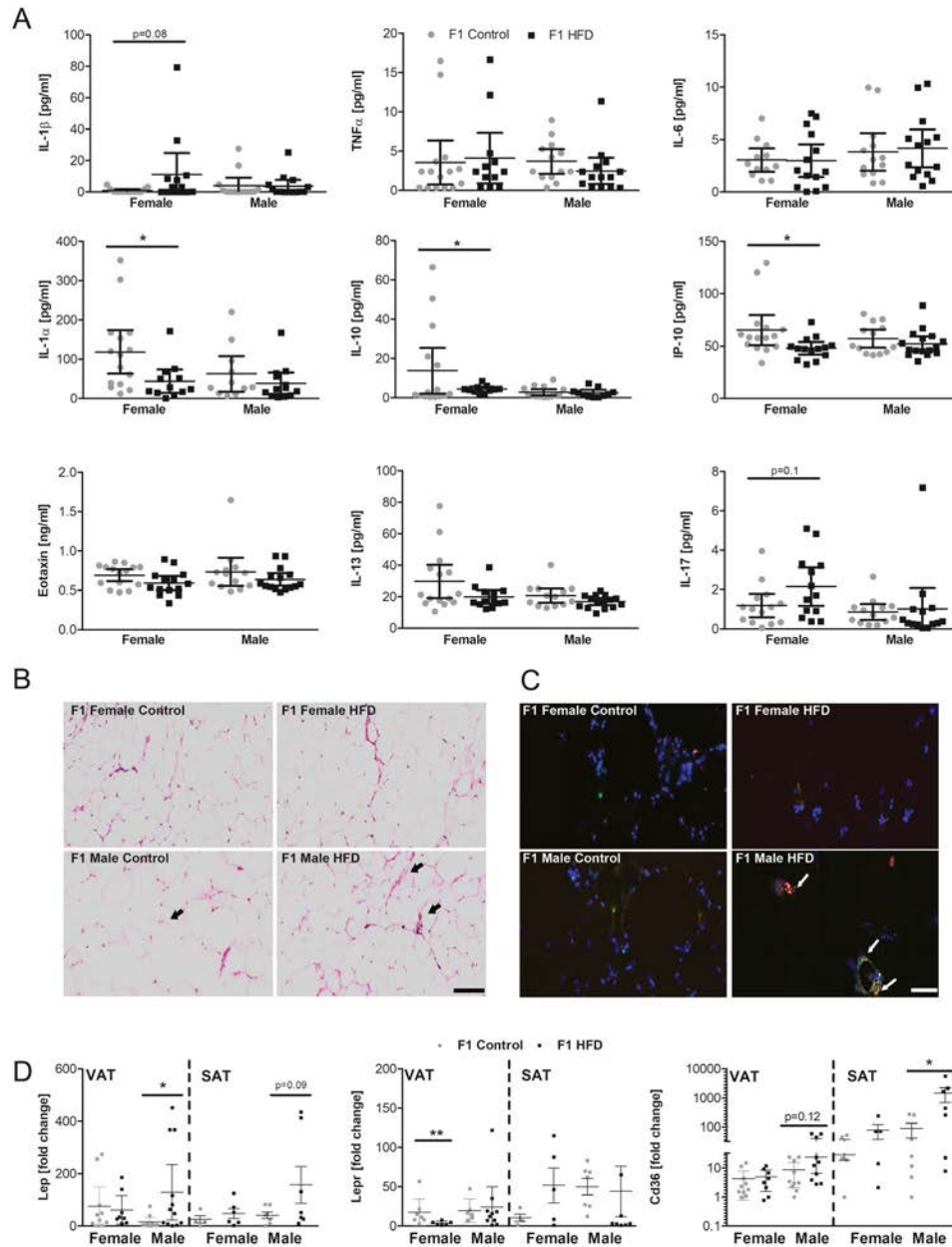


Figure 2. Parental HFD affects the immune profile of the F1 generation of offspring. **A**, Serum levels of the cytokines interleukin-1 β (IL-1 β), tumor necrosis factor (TNF), IL-6, IL-1 α , IL-10, interferon- γ -inducible 10-kd protein (IP-10), eotaxin, IL-13, and IL-17 in each group. **B**, Representative images of histologic staining with hematoxylin and eosin to detect visceral adipose tissue (VAT) in each group. **Arrows** indicate fibrosis. Bar = 100 μ m. **C**, Immunohistochemical staining of visceral AT for CD11b (green), CD11c (red), and nuclei (blue) among M1 (proinflammatory) macrophages. **Arrows** indicate double-positive cells. Bar = 100 μ m. **D**, Fold change in expression of the leptin (Lep), leptin receptor (Lepr), and Cd36 genes in visceral AT and subcutaneous AT (SAT). Symbols in **A** and **D** represent individual mice; horizontal lines with bars show the mean \pm 95% confidence interval ($n = 6$ –16 mice per sex and per diet group). * $P < 0.05$; ** = $P < 0.01$, by Mann-Whitney U test. See Figure 1 for other definitions. Color figure can be viewed in the online issue, which is available at <http://onlinelibrary.wiley.com/doi/10.1002/art.41147/abstract>.

(Figure 2B and Supplementary Figures 3A–D, available on the *Arthritis & Rheumatology* web site at <http://onlinelibrary.wiley.com/doi/10.1002/art.41147/abstract>). Furthermore, CD11b+CD11c+ labeling indicated an increased number of M1-like macrophages in visceral AT from male F1 HFD mice compared to male F1 Control mice. The number of M1-like macrophages in the visceral AT was comparable in female mice of both diet groups (Figure 2C

and Supplementary Figure 3E [<http://onlinelibrary.wiley.com/doi/10.1002/art.41147/abstract>]).

Gene expression analysis of the visceral AT showed significantly higher Lep levels and a trend toward higher Cd36 levels in male F1 HFD mice, but significantly lower Lepr levels in female F1 HFD mice, compared to their sex-matched controls. Similar trends in the subcutaneous AT were seen in terms of higher Lep

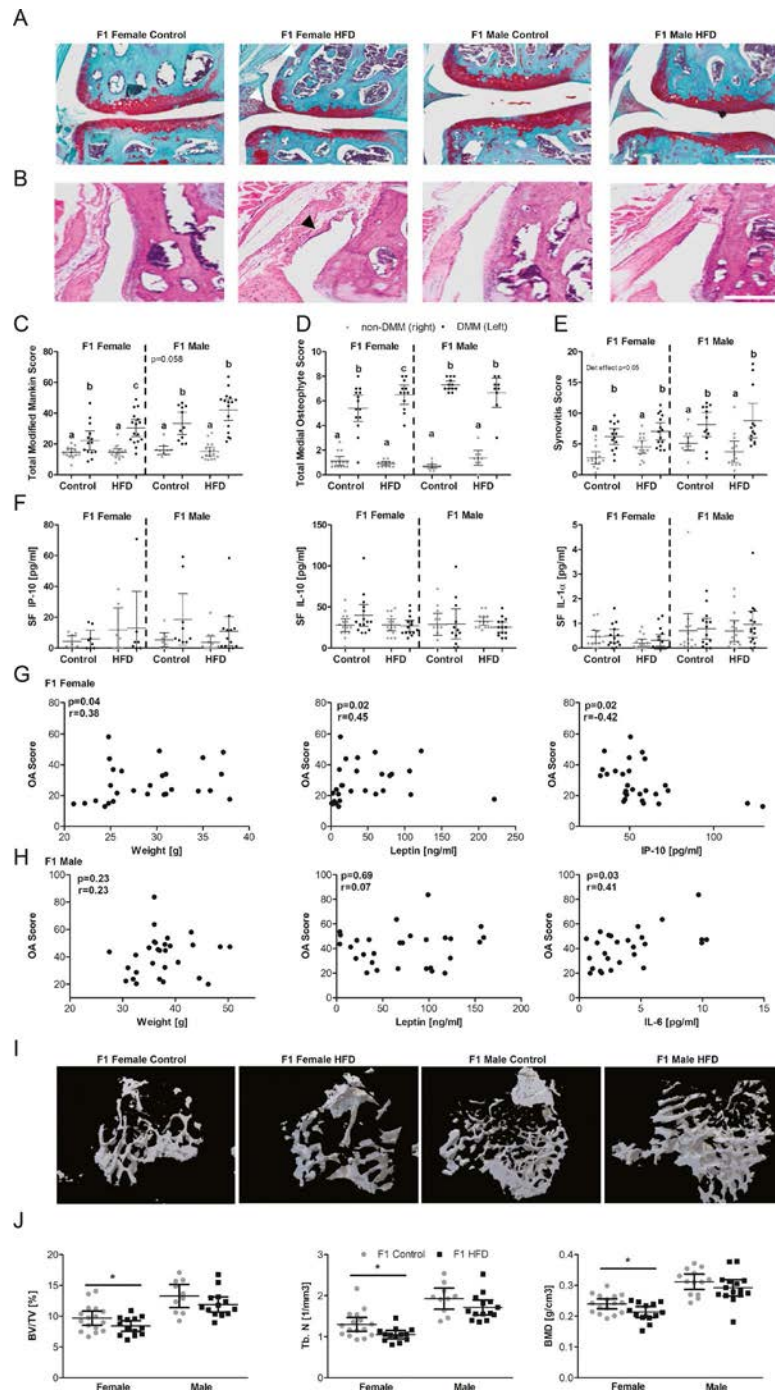


Figure 3. Parental HFD affects the musculoskeletal integrity of F1 offspring. **A**, Representative images show Safranin O–fast green staining of the DMM-operated knee joints. Bar = 100 μ m. **B**, Representative images show hematoxylin and eosin staining of the medial femoral condyles of DMM-operated joints. **Arrowhead** indicates evident synovitis. Bar = 100 μ m. **C–F**, DMM-operated joints (left knee) were compared to non–DMM-operated control joints (contralateral right knee) to assess the total modified Mankin score of OA (**C**), total medial osteophyte score (**D**), total synovitis score (**E**), and synovial fluid (SF) levels of interferon- γ -inducible 10-kd protein (IP-10), interleukin-10 (IL-10), and IL-1 α (**F**). **G** and **H**, Spearman's correlation tests assessed bivariate correlations between the total OA score in the DMM-operated (left) knee joint and weight, serum leptin levels, and serum IP-10 or IL-6 levels in F1 females (**G**) or F1 males (**H**). **I**, Representative images show reconstructed micro-CT images of the tibial metaphysis from each group. **J**, Micro-CT analysis of the tibial metaphysis from DMM-operated joints examined the trabecular bone fraction bone volume/total volume (BV/TV), trabecular bone number (Tb.N), and bone mineral density (BMD). Symbols in **C–F** and **J** represent individual mice; horizontal lines with bars show the mean \pm 95% confidence interval ($n = 10$ –16 mice per sex and per diet group). Groups not sharing the same letter (a, b, or c) are significantly different ($P < 0.05$ by two-way analysis of variance with Bonferroni post hoc analysis) within each sex. * = $P < 0.05$ by Mann-Whitney U test. See Figure 1 for other definitions.

expression and significantly higher Cd36 expression in male F1 HFD mice compared to male F1 Control mice (Figure 2D).

OA severity, osteophyte formation, and synovitis. A modified Mankin scoring system was used to analyze the severity of DMM-induced OA in F1 mice (5). Comparison by two-way ANOVA within each sex revealed that there was a significantly higher predisposition to injury-induced OA in female F1 HFD mice, with a similar trend ($P = 0.058$) in male F1 HFD mice, compared to their corresponding F1 Control mice (Figures 3A and C).

Osteophyte formation was detected in the DMM-operated joints (Figure 3A), with the total medial osteophyte score being significantly higher in female F1 HFD mice compared to female F1 Control mice (Figure 3D). Furthermore, although there was no significant interaction, we found that there was a significant parental diet effect on the total synovitis score in female F1 HFD mice compared to female F1 Control mice (Figures 3B and E and Supplementary Figures 4A–C, available on the *Arthritis & Rheumatology* web site at <http://onlinelibrary.wiley.com/doi/10.1002/art.41147/abstract>). There were no significant differences in synovial fluid cytokine levels in the analyzed F1 offspring group (Figure 3F). In addition, we did not observe any significant differences in the synovial F4/80+ macrophage influx between the analyzed groups (see Supplementary Figures 5A, C, and D, available on the *Arthritis & Rheumatology* web site at <http://onlinelibrary.wiley.com/doi/10.1002/art.41147/abstract>).

Total Mankin scores of OA in the DMM-operated joints correlated positively with weight and with the serum leptin levels in F1 females, but not in F1 males. Moreover, serum IP-10 levels correlated negatively with the total OA score in F1 females, while the serum IL-6 level showed a positive correlation with the total OA score in F1 males (Figures 3G and H).

Bone microstructure changes. Micro-CT imaging revealed differences in the bone microstructure in F1 mice (Figure 3I). The BV/TV, BMD, and Tb.N of the tibial metaphysis were each significantly lower in female F1 HFD mice compared to female F1 Control mice (Figure 3J). In addition, female F1 HFD mice displayed a significantly lower BV/TV and Tb.Th of the trabecular bone in the medial femoral condyle, but no major differences were detected in the tibial plateau epiphysis (see Supplementary Figures 6A–D, available on the *Arthritis & Rheumatology* web site at <http://onlinelibrary.wiley.com/doi/10.1002/art.41147/abstract>). In male F1 mice, we did not observe any major significant changes in bone microstructure, regardless of the diet fed to the parents.

F2 offspring. Weight gain, adiposity, and metabolic profile. The female F2 HFD and Control groups of mice did not differ in weight, whereas the male F2 HFD mice were significantly heavier than the male F2 Control mice (Figure 4A). Male F2 HFD mice also had a significantly higher percentage of AT compared to male F2 Control mice (Figure 4B). There was no noticeable difference in adipocyte size in the subcutaneous AT of female F2 mice in either diet group, while a trend toward enhanced adipocyte hypertrophy was present in male F2 HFD mice compared to male F2 Control mice (Figure 4C and Supplementary Figure 3A [<http://onlinelibrary.wiley.com/doi/10.1002/art.41147/abstract>]). In addition, we observed a trend toward a lower glucagon level in female F2 HFD mice, and toward higher serum levels of insulin and leptin, as well as lower serum levels of resistin, in male F2 HFD mice compared to male F2 Control mice (Figure 4D and Supplementary Figure 7A, available on the *Arthritis & Rheumatology* web site at <http://onlinelibrary.wiley.com/doi/10.1002/art.41147/abstract>). Levels of other serum adipokines did not

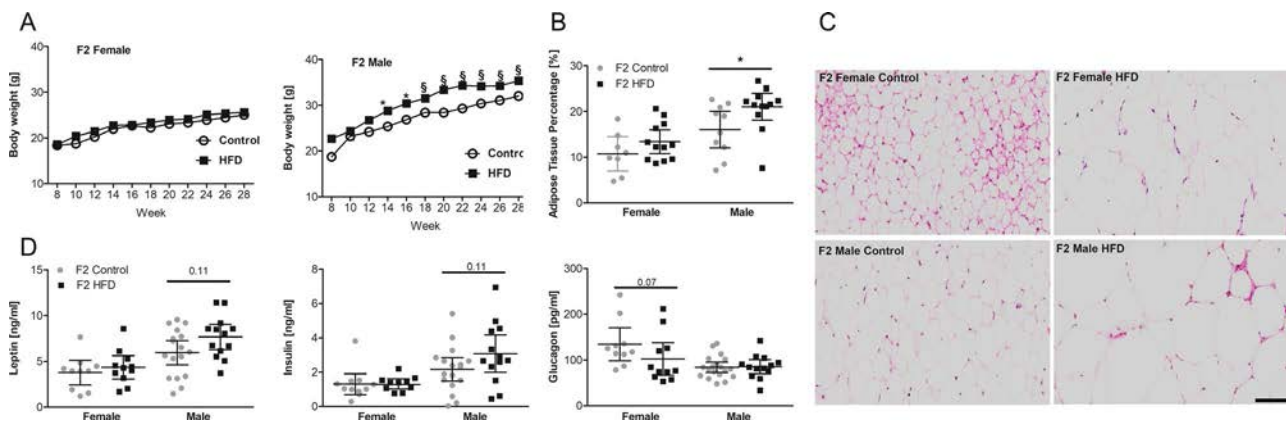


Figure 4. Grandparental HFD affects weight gain, adiposity, and the metabolic profile in F2 offspring. The F2 generation was fed the control diet after weaning, and DMM surgery was performed on the left knee at age 16 weeks. Mice were scanned with a micro-CT scanner for body fat analysis at age 26 weeks. Animals were killed at age 28 weeks for further analysis, according to sex and grandparental diet group. **A**, Mean longitudinal body weight. **B**, Adipose tissue content assessed by micro-CT. **C**, Representative images of tissue samples showing histologic staining with hematoxylin and eosin to detect subcutaneous adipose tissue. Bar = 100 μ m. **D**, Serum levels of adipokines (leptin, insulin, and glucagon). Symbols in **B** and **D** represent individual mice; horizontal lines with bars show the mean \pm 95% confidence interval ($n = 10$ –16 mice per sex and per diet group). * = $P < 0.05$; § = $P < 0.001$, by one-way analysis of variance in **A** or Mann-Whitney U test in **B** and **D**. See Figure 1 for definitions. Color figure can be viewed in the online issue, which is available at <http://onlinelibrary.wiley.com/doi/10.1002/art.41147/abstract>.

differ between the analyzed groups (Supplementary Figures 7B–E [<http://onlinelibrary.wiley.com/doi/10.1002/art.41147/abstract>]).

Systemic and local inflammation. Similar to the findings in the F1 generation of offspring mice, we found that serum IL-1 β trended toward higher levels, whereas serum IP-10 levels were significantly lower, in female F2 HFD mice compared to

female F2 Control mice (Figure 5A). No significant differences were observed in the levels of other cytokines, including IL-10, between the female F2 mice of either diet group (see Supplementary Table 3, available on the *Arthritis & Rheumatology* web site at <http://onlinelibrary.wiley.com/doi/10.1002/art.41147/abstract>). We also did not find any significant difference in serum cytokine levels between F2 male mice of either diet group.

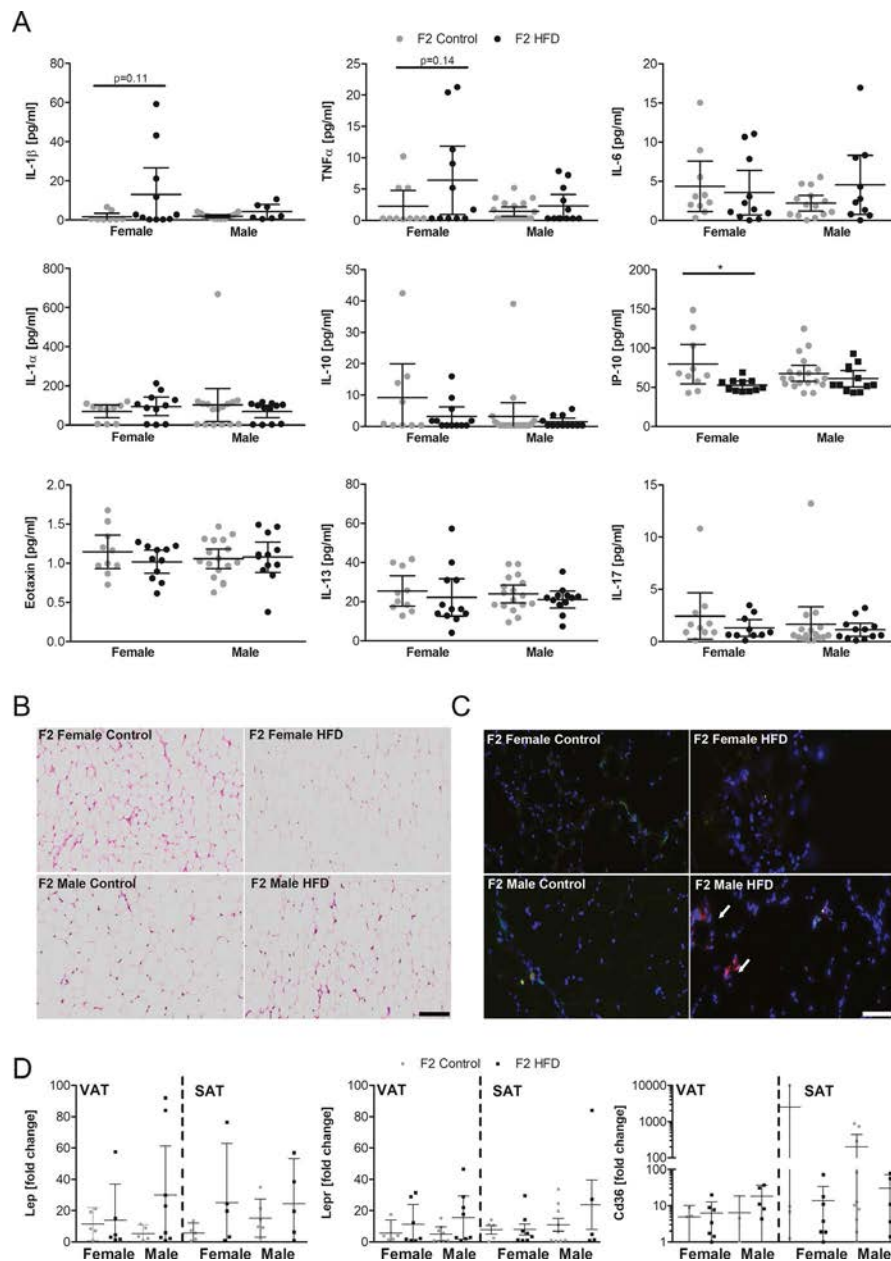


Figure 5. Grandparental HFD affects the immune profile of F2 offspring. **A**, Serum levels of interleukin-1 β (IL-1 β), tumor necrosis factor (TNF), IL-6, IL-1 α , IL-10, interferon- γ -inducible 10-kd protein (IP-10), eotaxin, IL-13, and IL-17 in each group. **B**, Representative images of histologic staining with hematoxylin and eosin to detect visceral adipose tissue (VAT) in each group. Bar = 100 μ m. **C**, Immunohistochemical staining of visceral AT for CD11b (green), CD11c (red), and nuclei (blue) among M1 (proinflammatory) macrophages. **Arrows** indicate double-positive cells. Bar = 100 μ m. **D**, Fold change in expression of the leptin (Lep), leptin receptor (Lepr), and Cd36 genes in visceral AT and subcutaneous AT (SAT). Symbols in **A** and **D** represent individual mice; horizontal lines with bars show the mean \pm 95% confidence interval ($n = 5$ –16 mice per sex and per diet group). * = $P < 0.05$ by Mann-Whitney U test. See Figure 1 for other definitions. Color figure can be viewed in the online issue, which is available at <http://onlinelibrary.wiley.com/doi/10.1002/art.41147/abstract>.

Furthermore, we did not observe any remarkable differences in fibrosis among the analyzed groups, although there was a trend toward a higher number of M1-like macrophages in male F2 HFD mice compared to male F2 Control mice (Figures 5B and C and Supplementary Figure 3E [<http://onlinelibrary.wiley.com/doi/10.1002/art.41147/abstract>]).

Gene expression analysis of the visceral AT and subcutaneous AT from the F2 offspring groups showed no significant differences in the levels of *Lep*, *Lepr*, or *Cd36* genes (Figure 5D).

OA severity, osteophyte formation, and synovitis. We found that female F2 mice from HFD-fed grandparents had a significantly higher predisposition to develop OA, while there was no difference in OA development in male F2 mice of either grandparental diet group (Figures 6A and C). We also found that the osteophyte scores were not affected by grandparental diet in the analyzed groups of F2 mice (Figure 6D and Supplementary Figures 4D–F, <http://onlinelibrary.wiley.com/doi/10.1002/art.41147/abstract>). Interestingly, there was a significantly higher total synovitis score in the male F2 HFD mice compared to the male F2 Control mice (Figures 6B and E).

We did not find differences in the synovial fluid cytokine levels in any of the analyzed F2 offspring (Figure 6F and Supplementary Table 3, available on the *Arthritis & Rheumatology* web site at <http://onlinelibrary.wiley.com/doi/10.1002/art.41147/abstract>). In addition, we did not observe significant differences in the presence of synovial F4/80+ macrophages in the analyzed groups of F2 mice (see Supplementary Figure 5B, <http://onlinelibrary.wiley.com/doi/10.1002/art.41147/abstract>).

The total Mankin scores of OA assessed in the DMM-operated joints did not correlate with the weight and serum leptin levels in female and male F2 mice. However, the serum C-peptide level correlated positively with the total OA score in female F2 mice, and the serum insulin level showed a positive correlation with the total OA score in male F2 mice (Figures 6G and H).

Bone microstructure changes. Bones of F2 mice were imaged with micro-CT (Figure 6I). The BV/TV and Tb.N, but not the BMD, of the tibial metaphysis were significantly lower in female F2 HFD mice compared to female F2 Control mice (Figure 6J). In addition, female F2 HFD mice displayed significantly lower trabecular bone BV/TV in the epiphysis of the lateral femoral condyle, while male F2 HFD mice had significantly lower BV/TV in the lateral tibial plateau, as compared to their corresponding Control mice (Supplementary Figures 8A–D and 9A–D, available on the *Arthritis & Rheumatology* web site at <http://onlinelibrary.wiley.com/doi/10.1002/art.41147/abstract>).

DISCUSSION

Our findings show that high-fat feeding has an intergenerational effect on the inheritance of increased risk of weight gain, metabolic imbalance, and OA in mice for at least 2 generations of offspring. Both F1 and F2 offspring groups, despite being

allocated to receive the standard low-fat control diet, demonstrated a dysregulated systemic metabolism, weight gain, and disturbed musculoskeletal integrity. Strikingly, both F1 and F2 female mice showed an increased predisposition to injury-induced OA and severe bone microarchitectural changes that were attributed to parental and grandparental high-fat feeding. These findings indicate that in addition to well-characterized genetic factors (20), the heritability of OA risk may involve epigenetic factors secondary to diet-induced obesity (21) that may be passed through multiple generations of offspring.

Significantly higher weight and AT content in F1 (male and female) offspring and F2 male offspring of HFD-fed parents, in comparison to offspring of low-fat control diet-fed parents, is consistent with the results of previous studies in which it was shown that combined parental diet had a cumulative effect on weight gain and adiposity in multiple generations of offspring. For instance, it has been reported that maternal fructose consumption during pregnancy increases metabolic syndrome and AT content in F1 female mice (22), while maternal high-fat feeding increases adiposity in adult male rats (23). Paternal hyperglycemia was also shown to affect obesity predisposition in offspring (24), and maternal obesity leads to an increased weight gain across multiple generations (25). While the mechanisms involved in this process remain to be determined, it has been postulated that reduced quality of oocyte and sperm cells due to an HFD, epigenetic modifications, dysregulated hypothalamic signaling, the effect of the maternal microbiome (14), and intrauterine nutrient transfer (7) may each play an essential role.

Leptin and insulin signaling have been postulated as being key contributors in fetal programming. Dysregulated leptin hypothalamic signaling in leptin-sensitive neurons of overfeeding mothers has been shown to be passed on to male offspring, and in fact, to mediate an “obese” phenotype in future generations (26). Several previous studies have also shown that both maternal hyperglycemia (27) and paternal obesity lead to a modification in insulin sensitivity and glucose tolerance (28). In the present study we show that there are significant sex-dependent differences in circulating leptin, insulin, and glucagon levels, as well as differences in *Lepr* gene expression, within both F1 and F2 HFD offspring as compared to their controls. The serum leptin level significantly correlated with the OA score in F1 females, but not in any of the other analyzed groups, while serum insulin levels correlated significantly with the OA score only in the male F2 offspring group. Interestingly, leptin is postulated to be a key mediator in the pathogenesis of OA (29), while the loss of leptin signaling is protective against obesity-induced OA in mice (30). Moreover, circulating leptin levels differ between male and female mice, and leptin has been shown to affect males and females differently (31). Although we did not investigate fasting metabolite levels in our animal cohort, the data presented imply that both leptin and glucose metabolism may be significantly affected in offspring in a sex-dependent manner.

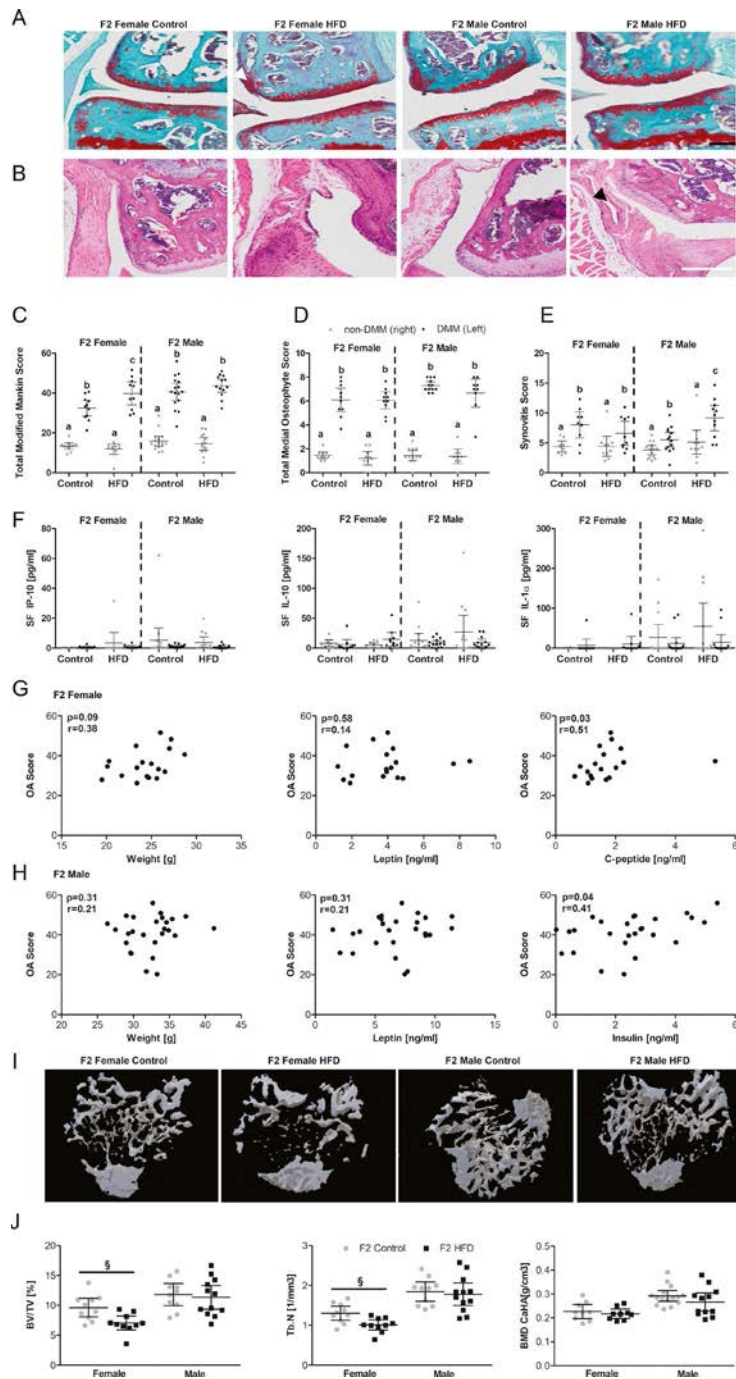


Figure 6. Grandparental HFD affects the musculoskeletal integrity of F2 offspring. **A**, Representative images show Safranin O–fast green staining of the DMM-operated knee joints. Bar = 100 μ m. **B**, Representative images show hematoxylin and eosin staining of the medial femoral condyles of DMM-operated joints. **Arrowhead** indicates evident synovitis. Bar = 100 μ m. **C–F**, DMM-operated joints (left knee) were compared to non–DMM-operated control joints (contralateral right knee) to assess the total modified Mankin score of OA (**C**), total medial osteophyte score (**D**), total synovitis score (**E**), and synovial fluid (SF) levels of interferon- γ -inducible 10-kd protein (IP-10), interleukin-10 (IL-10), and IL-1 α (**F**). **G** and **H**, Spearman's correlation tests were used to assess bivariate correlations between the total OA score in the DMM-operated (left) knee joint and weight, serum leptin levels, and serum C-peptide or insulin levels in F2 females (**G**) or F2 males (**H**). **I**, Representative images show reconstructed micro-CT images of the tibial metaphysis from each group. **J**, Micro-CT analysis of the tibial metaphysis from DMM-operated joints examined trabecular bone fraction bone volume/total volume (BV/TV), trabecular bone number (Tb.N), and bone mineral density (BMD). Symbols in **C–F** and **J** represent individual mice; horizontal lines with bars show the mean \pm 95% confidence interval ($n = 10$ –16 mice per sex and per diet group). Groups not sharing the same letter (a, b, or c) are significantly different ($P < 0.05$ by two-way analysis of variance with Bonferroni post hoc analysis) within each sex. $\S = P < 0.001$ by Mann-Whitney U test. See Figure 1 for other definitions. Color figure can be viewed in the online issue, which is available at <http://onlinelibrary.wiley.com/doi/10.1002/art.41147/abstract>.

Obesity-induced systemic and local inflammation plays an important role in the progression of OA damage. The results of the present study and other previous studies have shown that immune cells colocalize within the knee joint during obesity-induced OA (32–34). In addition, the systemic proinflammatory milieu has been shown to be important in the pathogenesis of OA, potentially through interactions with local injury-induced inflammation (18). Before we addressed the ramifications of obesity as it relates to the development and progression of OA in our mouse study, we showed that obesity-related local and systemic immune changes are affected by parental and grandparental HFD. Local AT inflammation, as indicated by AT fibrosis and CD11b+CD11c+ macrophage infiltration, was mainly observed in male F1 and F2 HFD mice, although no serum proinflammatory cytokines were significantly affected in these groups. However, we found that serum levels of proinflammatory IL-1 β trended higher in female F1 HFD mice, whereas serum levels of antiinflammatory IL-10 were significantly lower in female F1 and F2 HFD mice, compared to their Control groups.

Studies have suggested that immune cells play an important role in mediating the transgenerational effect of obesity in offspring. For instance, recent studies have shown that monocytes and macrophages obtained from cord blood of obese mothers had significantly changed levels of IL-1 β and IL-10, as well as significant differences in DNA methylation of IL-10 promoter in those cells (35). Furthermore, children born to obese mothers were observed as having a significantly lower number of eosinophils and CD4+ T helper cells and a reduced monocyte response to inflammation (36).

Finally, the findings in our study show, unexpectedly, that serum IP-10 levels were significantly lower in both female F1 and female F2 HFD mice compared to their Control groups, and this was negatively correlated with the OA score in the female F1 group. The maternal diet has been proposed as a regulator of the fate of hematopoietic cells (37). Indeed, our findings and those of others are consistent with this notion, as they indicate that the immunometabolism in offspring of mice having received an HFD is compromised, potentially leading to observed changes in body composition and musculoskeletal integrity (for a summary of these intergenerational effects, see Supplementary Table 4, available on the *Arthritis & Rheumatology* web site at <http://onlinelibrary.wiley.com/doi/10.1002/art.41147/abstract>).

Although OA has been historically considered to be a “wear and tear” disease, it is now commonly accepted that OA-related changes are attributable to multifactorial processes affecting multiple joint tissues and are correlated with the progression of systemic and local inflammation. We and other groups have previously shown that injury-induced OA is significantly affected by obesity (5,18,38). In addition, previous studies in humans have also indicated a strong correlation of obesity with the familial predisposition to OA (39–41). In the present study we also show that there are significant changes in the predisposition to injury-induced

OA, particularly in female F1 and F2 HFD mice, despite the fact that there were changes in body weight or composition in both male and female offspring. Furthermore, we did not find any significant differences in local synovial fluid cytokine levels or synovial F4/80+ macrophage content in the joints of the offspring, which may suggest that factors beyond injury-induced inflammation play an important role in the intergenerational inheritance of OA. The mechanisms modulating the inheritability of cartilage damage remain to be determined, but epigenetic regulation has become a central mechanism in the hypothesis of fetal developmental programming affected by parental obesity (42). For example, grandparental HFD-induced obesity has been shown to affect the skeletal muscle transcriptome transgenerationally (43). In addition, maternal HFD has been shown to impair muscle mitochondria in female offspring (44).

Regardless of whether OA is surgically induced, the structure and integrity of the subchondral bone are postulated to play an important role in the progression of OA (45). Previous studies showed that maternal diabetes affects bone health and growth in offspring (46). Similarly, the results of our study show that HFD affects the bone structure of only female offspring in the F1 and F2 generations; trabecular bone BV/TV, Tb. N, and BMD across the tibial metaphysis and femoral condyle of the knee joint were found to be significantly impacted in the female F1 and F2 HFD offspring. Previous studies have shown that maternal HFD impairs offspring skeletal development by affecting osteoblast differentiation and promoting cell senescence (47,48). Furthermore, intra-uterine exposure to HFD was shown to negatively regulate the bone microstructure (49). There are several factors that could possibly explain these observations. For instance, Liang et al pointed out that the observed HFD-mediated reduction in bone quality may, in fact, mirror the findings from human epidemiologic studies in which it was demonstrated that HFD-induced delayed skeletal development is associated with bone fragility during aging (49). Furthermore, the detrimental effect of the microbiome on bone quality due to HFD has been postulated as an important mechanism in reducing bone microarchitectural changes (50).

It is important to note several points that may influence the interpretation of our findings. Although we did not examine the role of the microbiome in this study, it has been reported that the obesity-induced microbiome may play an important role in musculoskeletal integrity (50). For example, obesity can significantly disrupt the gut microbiome, which has a detrimental role in OA progression (33). In addition, parental HFD has been shown to affect the microbiome of offspring, predisposing them to autoimmune diseases (51).

Another potential limitation of the current study is the lack of direct measurement of the dysfunction in glucose metabolism and insulin resistance in offspring, which would allow further understanding of the potential role of metabolic syndrome in the observed outcomes. Furthermore, the described disturbance in leptin and its satiety/hunger role could possibly be explained by analysis of food intake in studied mice.

In conclusion, our results indicate that high-fat feeding of mice plays a sex-dependent detrimental role in musculoskeletal integrity in at least 2 generations of offspring. We showed that offspring metabolism, adiposity, immune profile, and cartilage and bone integrity are significantly affected by parental high-fat feeding. These findings have significant implications for the inheritability mechanism of obesity-triggered OA, and such findings should prompt an in-depth investigation of the role of epigenetic and environmental stimuli as factors in the progression of OA. Future studies confirming the beneficial role of maternal and paternal diet, exercise, and microbiome interventions may benefit the musculoskeletal integrity of offspring and perhaps mitigate the observed transgenerational inheritance of a predisposition to OA.

ACKNOWLEDGMENTS

The authors thank Sara Oswald for providing technical writing support for the manuscript, and Nicholas Benshoff for technical support.

AUTHOR CONTRIBUTIONS

All authors were involved in drafting the article or revising it critically for important intellectual content, and all authors approved the final version to be published. Dr. Guilak had full access to all of the data in the study and takes responsibility for the integrity of the data and the accuracy of the data analysis.

Study conception and design. Harasymowicz, Guilak.

Acquisition of data. Harasymowicz, Choi, Wu, Iannucci, Tang.




Analysis and interpretation of data. Harasymowicz, Choi, Wu, Iannucci, Tang.

REFERENCES

- Vos T, Flaxman AD, Naghavi M, Lozano R, Michaud C, Ezzati M, et al. Years lived with disability (YLDs) for 1160 sequelae of 289 diseases and injuries 1990–2010: a systematic analysis for the Global Burden of Disease Study 2010. *Lancet* 2012;380:2163–96.
- Felson DT, Lawrence RC, Dieppe PA, Hirsch R, Helmick CG, Jordan JM, et al. Osteoarthritis: new insights. Part 1: the disease and its risk factors. *Ann Intern Med* 2000;133:635–46.
- Thijssen E, van Caam A, van der Kraan PM. Obesity and osteoarthritis, more than just wear and tear: pivotal roles for inflamed adipose tissue and dyslipidaemia in obesity-induced osteoarthritis. *Rheumatology (Oxford)* 2015;54:588–600.
- Felson DT, Couropmitree NN, Chaisson CE, Hannan MT, Zhang Y, McAlindon TE, et al. Evidence for a Mendelian gene in a segregation analysis of generalized radiographic osteoarthritis: the Framingham Study. *Arthritis Rheum* 1998;41:1064–71.
- Wu CL, Jain D, McNeill JN, Little D, Anderson JA, Huebner JL, et al. Dietary fatty acid content regulates wound repair and the pathogenesis of osteoarthritis following joint injury. *Ann Rheum Dis* 2015;74:2076–83.
- Griffin TM, Huebner JL, Kraus VB, Yan Z, Guilak F. Induction of osteoarthritis and metabolic inflammation by a very high-fat diet in mice: effects of short-term exercise. *Arthritis Rheum* 2012;64:443–53.
- Ross MG, Desai M. Developmental programming of offspring obesity, adipogenesis, and appetite. *Clin Obstet Gynecol* 2013;56:529–36.
- McGreevy KR, Tezanos P, Ferreira-Villar I, Pallé A, Moreno-Serrano M, Esteve-Codina A, et al. Intergenerational transmission of the positive effects of physical exercise on brain and cognition. *Proc Natl Acad Sci U S A* 2019;116:10103–12.
- Contreras ZA, Ritz B, Virk J, Cockburn M, Heck JE. Maternal pre-pregnancy and gestational diabetes, obesity, gestational weight gain, and risk of cancer in young children: a population-based study in California. *Cancer Causes Control* 2016;27:1273–85.
- Wilson PW, Meigs JB, Sullivan L, Fox CS, Nathan DM, D'Agostino RB Sr. Prediction of incident diabetes mellitus in middle-aged adults: the Framingham Offspring Study. *Arch Intern Med* 2007;167:1068–74.
- Öst A, Lempradl A, Casas E, Weigert M, Tiko T, Deniz M, et al. Paternal diet defines offspring chromatin state and intergenerational obesity. *Cell* 2014;159:1352–64.
- Jaeger K, Saben JL, Moley KH. Transmission of metabolic dysfunction across generations. *Physiology (Bethesda)* 2017;32:51–9.
- Oestreich AK, Moley KH. Developmental and transmittable origins of obesity-associated health disorders. *Trends Genet* 2017;33:399–407.
- Li Y. Epigenetic mechanisms link maternal diets and gut microbiome to obesity in the offspring [review]. *Front Genet* 2018;9:342.
- De Langhe E, Vande Velde G, Hostens J, Himmelreich U, Nemery B, Luyten FP, et al. Quantification of lung fibrosis and emphysema in mice using automated micro-computed tomography. *PLoS One* 2012;7:e43123.
- Glasson SS, Blanchet TJ, Morris EA. The surgical destabilization of the medial meniscus (DMM) model of osteoarthritis in the 129/SvEv mouse. *Osteoarthritis Cartilage* 2007;15:1061–9.
- Olson SA, Furman BD, Kraus VB, Huebner JL, Guilak F. Therapeutic opportunities to prevent post-traumatic arthritis: lessons from the natural history of arthritis after articular fracture. *J Orthop Res* 2015;33:1266–77.
- Louder CR, Furman BD, Huebner JL, Kraus VB, Olson SA, Guilak F. Diet-induced obesity significantly increases the severity of posttraumatic arthritis in mice. *Arthritis Rheum* 2012;64:3220–30.
- Livak KJ, Schmittgen TD. Analysis of relative gene expression data using real-time quantitative PCR and the $2^{-\Delta\Delta CT}$ method. *Methods* 2001;25:402–8.
- Bomer N, den Hollander W, Ramos YF, Meulenbelt I. Translating genomics into mechanisms of disease: osteoarthritis. *Best Pract Res Clin Rheumatol* 2015;29:683–91.
- Little D, Wu CL, D'Amico R, Corcoran D, Gregory S, Guilak F. Epigenetic analysis of adipose stem cells in obesity identifies dysregulation of critical pathways in musculoskeletal regeneration and disease [poster]. Presented at the ORS Annual Meeting; 2015 March 28–31; Las Vegas.
- Saad AF, Dickerson J, Kechichian TB, Yin H, Gamble P, Salazar A, et al. High-fructose diet in pregnancy leads to fetal programming of hypertension, insulin resistance, and obesity in adult offspring. *Am J Obstet Gynecol* 2016;215:378.
- Lecoutre S, Deracinois B, Laborie C, Eberlé D, Guinez C, Panchenko PE, et al. Depot- and sex-specific effects of maternal obesity in offspring's adipose tissue. *J Endocrinol* 2016;230:39–53.
- Shi X, Li X, Hou Y, Cao X, Zhang Y, Wang H, et al. Paternal hyperglycemia in rats exacerbates the development of obesity in offspring. *J Endocrinol* 2017;234:175–86.
- Masuyama H, Mitsui T, Eguchi T, Tamada S, Hiramatsu Y. The effects of paternal high-fat diet exposure on offspring metabolism with epigenetic changes in the mouse adiponectin and leptin gene promoters. *Am J Physiol Endocrinol Metab* 2016;311:E236–45.
- Wang H, Ji J, Yu Y, Wei X, Chai S, Liu D, et al. Neonatal overfeeding in female mice predisposes the development of obesity in their

- male offspring via altered central leptin signalling. *J Neuroendocrinol* 2015;27:600–8.
27. Song Y, Li J, Zhao Y, Zhang Q, Liu Z, Li J, et al. Severe maternal hyperglycemia exacerbates the development of insulin resistance and fatty liver in the offspring on high fat diet. *Exp Diabetes Res* 2012;2012:254976.
 28. Park JH, Yoo Y, Cho M, Lim J, Lindroth AM, Park YJ. Diet-induced obesity leads to metabolic dysregulation in offspring via endoplasmic reticulum stress in a sex-specific manner. *Int J Obes (Lond)* 2018;42:244–51.
 29. Datta P, Zhang Y, Parousis A, Sharma A, Rossomacha E, Endisha H, et al. High-fat diet-induced acceleration of osteoarthritis is associated with a distinct and sustained plasma metabolite signature. *Sci Rep* 2017;7:8205.
 30. Griffin TM, Huebner JL, Kraus VB, Guilak F. Extreme obesity due to impaired leptin signaling in mice does not cause knee osteoarthritis. *Arthritis Rheum* 2009;60:2935–44.
 31. Guo K, Mogen J, Struzzi S, Zhang Y. Preadipocyte transplantation: an in vivo study of direct leptin signaling on adipocyte morphogenesis and cell size. *Am J Physiol Regul Integr Comp Physiol* 2009;296:R1339–47.
 32. Sun AR, Panchal SK, Friis T, Sekar S, Crawford R, Brown L, et al. Obesity-associated metabolic syndrome spontaneously induces infiltration of pro-inflammatory macrophage in synovium and promotes osteoarthritis. *PLoS One* 2017;12:e0183693.
 33. Schott EM, Farnsworth CW, Grier A, Lillis JA, Soniwala S, Dadourian GH, et al. Targeting the gut microbiome to treat the osteoarthritis of obesity. *JCI Insight* 2018;3:95997.
 34. Wu CL, McNeill J, Goon K, Little D, Kimmerling K, Huebner J, et al. Conditional macrophage depletion increases inflammation and does not inhibit the development of osteoarthritis in obese macrophage Fas-induced apoptosis–transgenic mice. *Arthritis Rheumatol* 2017;69:1772–83.
 35. Cifuentes-Zúñiga F, Arroyo-Jousse V, Soto-Carrasco G, Casanello P, Uauy R, Krause BJ, et al. IL-10 expression in macrophages from neonates born from obese mothers is suppressed by IL-4 and LPS/INF γ . *J Cell Physiol* 2017;232:3693–701.
 36. Wilson RM, Marshall NE, Jeske DR, Purnell JQ, Thornburg K, Messaoudi I. Maternal obesity alters immune cell frequencies and responses in umbilical cord blood samples. *Pediatr Allergy Immunol* 2015;26:344–51.
 37. Kamimae-Lanning AN, Krasnow SM, Goloviznina NA, Zhu X, Roth-Carter QR, Levasseur PR, et al. Maternal high-fat diet and obesity compromise fetal hematopoiesis. *Mol Metab* 2015;4:25–38.
 38. Mooney RA, Sampson ER, Lerea J, Rosier RN, Zuscik MJ. High-fat diet accelerates progression of osteoarthritis after meniscal/ligamentous injury. *Arthritis Res Ther* 2011;13:R198.
 39. Khan HI, Aitken D, Chou L, McBride A, Ding C, Blizzard L, et al. A family history of knee joint replacement increases the progression of knee radiographic osteoarthritis and medial tibial cartilage volume loss over 10 years. *Osteoarthritis Cartilage* 2015;23:203–9.
 40. Pan F, Blizzard L, Tian J, Cicuttini F, Winzenberg T, Ding C, et al. The interaction between weight and family history of total knee replacement with knee cartilage: a 10-year prospective study. *Osteoarthritis Cartilage* 2017;25:227–33.
 41. Loughlin J. Familial inheritance of osteoarthritis: documented family subsets. *Clin Orthop Relat Res* 2004 Suppl:S22–5.
 42. Ruchat SM, Hivert MF, Bouchard L. Epigenetic programming of obesity and diabetes by in utero exposure to gestational diabetes mellitus. *Nutr Rev* 2013;71 Suppl 1:S88–94.
 43. Alm PS, de Castro Barbosa T, Barrès R, Krook A, Zierath JR. Grandpaternal-induced transgenerational dietary reprogramming of the unfolded protein response in skeletal muscle. *Mol Metab* 2017;6:621–30.
 44. Khamoui AV, Desai M, Ross MG, Rossiter HB. Sex-specific effects of maternal and postweaning high-fat diet on skeletal muscle mitochondrial respiration. *J Dev Orig Health Dis* 2018;9:670–7.
 45. Li G, Yin J, Gao J, Cheng TS, Pavlos NJ, Zhang C, et al. Subchondral bone in osteoarthritis: insight into risk factors and microstructural changes [review]. *Arthritis Res Ther* 2013;15:223.
 46. Zhao J, Weiler HA. Long-term effects of gestational diabetes on offspring health are more pronounced in skeletal growth than body composition and glucose tolerance. *Br J Nutr* 2010;104:1641–9.
 47. Chen JR, Lazarenko OP, Blackburn ML, Rose S, Frye RE, Badger TM, et al. Maternal obesity programs senescence signaling and glucose metabolism in osteo-progenitors from rat and human. *Endocrinology* 2016;157:4172–83.
 48. Chen JR, Lazarenko OP, Zhao H, Alund AW, Shankar K. Maternal obesity impairs skeletal development in adult offspring. *J Endocrinol* 2018;239:33–47.
 49. Liang C, Oest ME, Prater MR. Intrauterine exposure to high saturated fat diet elevates risk of adult-onset chronic diseases in C57BL/6 mice. *Birth Defects Res B Dev Reprod Toxicol* 2009;86:377–84.
 50. Hernandez CJ. The microbiome and bone and joint disease [review]. *Curr Rheumatol Rep* 2017;19:77.
 51. Myles IA, Fontecilla NM, Janelsins BM, Vithayathil PJ, Segre JA, Datta SK. Parental dietary fat intake alters offspring microbiome and immunity. *J Immunol* 2013;191:3200–9.

Interleukin-17 Inhibition in Spondyloarthritis Is Associated With Subclinical Gut Microbiome Perturbations and a Distinctive Interleukin-25–Driven Intestinal Inflammation

Julia Manasson,¹  David S. Wallach,² Giuliana Guggino,³ Matthew Stapylton,² Michelle H. Badri,⁴ Gary Solomon,¹ Soumya M. Reddy,¹ Roxana Coras,⁵  Alexander A. Aksenov,⁶ Drew R. Jones,¹ Parvathy V. Girija,¹ Andrea L. Neimann,¹ Adriana Heguy,¹ Leopoldo N. Segal,¹ Pieter C. Dorrestein,⁶ Richard Bonneau,⁷ Monica Guma,⁵  Francesco Ciccia,⁸ Carles Ubeda,⁹ Jose C. Clemente,² and Jose U. Scher¹

Objective. To characterize the ecological effects of biologic therapies on the gut bacterial and fungal microbiome in psoriatic arthritis (PsA)/spondyloarthritis (SpA) patients.

Methods. Fecal samples from PsA/SpA patients pre- and posttreatment with tumor necrosis factor inhibitors (TNFi; n = 15) or an anti-interleukin-17A monoclonal antibody inhibitor (IL-17i; n = 14) underwent sequencing (16S ribosomal RNA, internal transcribed spacer and shotgun metagenomics) and computational microbiome analysis. Fecal levels of fatty acid metabolites and cytokines/proteins implicated in PsA/SpA pathogenesis or intestinal inflammation were correlated with sequence data. Additionally, ileal biopsies obtained from SpA patients who developed clinically overt Crohn's disease (CD) after treatment with IL-17i (n = 5) were analyzed for expression of IL-23/Th17–related cytokines, IL-25/IL-17E–producing cells, and type 2 innate lymphoid cells (ILC2s).

Results. There were significant shifts in abundance of specific taxa after treatment with IL-17i compared to TNFi, particularly Clostridiales ($P = 0.016$) and *Candida albicans* ($P = 0.041$). These subclinical alterations correlated with changes in bacterial community co-occurrence, metabolic pathways, IL-23/Th17–related cytokines, and various fatty acids. Ileal biopsies showed that clinically overt CD was associated with expansion of IL-25/IL-17E–producing tuft cells and ILC2s ($P < 0.05$), compared to pre-IL-17i treatment levels.

Conclusion. In a subgroup of SpA patients, the initiation of IL-17A blockade correlated with features of subclinical gut inflammation and intestinal dysbiosis of certain bacterial and fungal taxa, most notably *C albicans*. Further, IL-17i–related CD was associated with overexpression of IL-25/IL-17E–producing tuft cells and ILC2s. These results may help to explain the potential link between inhibition of a specific IL-17 pathway and the (sub)clinical gut inflammation observed in SpA.

Supported by the Colton Center for Autoimmunity. Dr. Manasson's work was supported by the Group for Research and Assessment of Psoriasis and Psoriatic Arthritis 2017 Pilot Research Grant and the National Institute of Arthritis and Musculoskeletal and Skin Diseases, NIH (grant T32-AR-069515). Mr. Wallach, Mr. Stapylton, and Dr. Clemente's work was supported by the National Institute of Diabetes and Digestive and Kidney Diseases, NIH (grant R01-DK-114038). Dr. Heguy's work was supported by the National Cancer Institute, NIH (Cancer Center Support grant P30-CA-016087) at the Laura and Isaac Perlmutter Cancer Center. Dr. Cora and Dr. Guma's work was supported by the National Institute of Arthritis and Musculoskeletal and Skin Diseases, NIH (grant R01-AR-073324). Dr. Scher's work was supported by the National Institute of Arthritis and Musculoskeletal and Skin Diseases, NIH (grant R03-AR-072182), the Colton Center for Autoimmunity, the Rheumatology Research Foundation, the Riley Family Foundation, and the Snyder Family Foundation.

¹Julia Manasson, MD, Gary Solomon, MD, Soumya M. Reddy, MD, Drew R. Jones, PhD, Parvathy V. Girija, MS, Andrea L. Neimann, MD, MSCE, Adriana Heguy, PhD, Leopoldo N. Segal, MD, Jose U. Scher, MD: New York University School of Medicine, New York, New York; ²David S. Wallach, BA, Matthew Stapylton, BA, Jose C. Clemente, PhD: Icahn School of Medicine at Mount Sinai, New York, New York; ³Giuliana Guggino, MD, PhD: University of Palermo, Palermo, Italy; ⁴Michelle H. Badri, BS: New York University, New York, New York; ⁵Roxana Coras, MD, Monica Guma, MD, PhD: University of California, San Diego; ⁶Alexander A. Aksenov, PhD, Pieter C. Dorrestein, PhD:

Skaggs School of Pharmacy and Pharmaceutical Sciences at the University of California, San Diego; ⁷Richard Bonneau, PhD: Simons Foundation, New York University, Center for Data Science, and Courant Institute of Mathematical Sciences, New York, New York; ⁸Francesco Ciccia, MD, PhD: University of Naples, Naples, Italy; ⁹Carles Ubeda, PhD: La Fundación para el Fomento de la Investigación Sanitaria y Biomédica de la Comunitat Valenciana, Valencia, Spain, and CIBERESP, Madrid, Spain.

Dr. Solomon has received consulting fees, speaking fees, and/or honoraria from AbbVie (less than \$10,000). Dr. Reddy has received consulting fees, speaking fees, and/or honoraria from Novartis, Pfizer, UCB, AbbVie, Amgen, and Janssen (less than \$10,000 each). Dr. Scher has received consulting fees, speaking fees, and/or honoraria from Bristol-Myers Squibb, UCB, and Janssen (less than \$10,000 each) and from Novartis (more than \$10,000). No other disclosures relevant to this article were reported.

Address correspondence to Jose C. Clemente, PhD, Icahn School of Medicine at Mount Sinai, Department of Genetics and Genomic Sciences, Icahn Institute for Genomics and Multiscale Biology, 1470 Madison Avenue, CSM 8-107, New York, NY 10029 (e-mail: jose.clemente@mssm.edu); or to Jose U. Scher, MD, New York University School of Medicine, Division of Rheumatology and Psoriatic Arthritis Center, 301 East 17th Street, Room 1608, New York, NY 10003 (e-mail: jose.scher@nyulangone.org).

Submitted for publication February 6, 2019; accepted in revised form November 12, 2019.

INTRODUCTION

The microbiome, the collection of microorganisms that co-inhabit human surfaces, serves many important functions, ranging from carbohydrate metabolism and synthesis of essential vitamins to immune system modulation and protection from pathogens (1). Intestinal dysbiosis (i.e., the imbalance in the composition of gut microbiota), has been implicated in the development of autoimmune disorders and chronic inflammatory arthritis, including axial and peripheral spondyloarthritis (SpA) (2), ankylosing spondylitis (AS) (3), psoriatic arthritis (PsA) (4), reactive arthritis (5), and inflammatory bowel disease (IBD) (6).

Notably, the microbiome can affect the metabolism, bioavailability, efficacy, and toxicity of drugs (7). Recent examples include novel checkpoint inhibitors (8,9), whose anticancer efficacy and safety are also microbiome-dependent. Conversely, several drugs, including those that lack known antibiotic properties, can alter the gut microbial composition (10). Of direct relevance to autoimmune and chronic inflammatory arthritis, interleukin-17A (IL-17A) blockade has been associated with candidiasis (11) and exacerbation of Crohn's disease (CD) (12), a condition linked to higher frequencies of *Candida albicans* colonization (13). This is not unexpected since IL-17A is known to provide protection against extracellular pathogens and maintain intestinal epithelial health (14).

In this study, we characterized the ecological effects of the most commonly prescribed biologic therapies in PsA and SpA on the gut bacterial and fungal microbiome. We hypothesized that biologic therapy, particularly IL-17A inhibition, would perturb the gut bacterial and fungal communities, altering their interrelationships and causing downstream changes in gut metabolite and local cytokine production. We further examined ileal biopsy specimens from patients who developed gut inflammation after treatment with IL-17i, and characterized changes in adhesive/invasive bacterial scores and local immune responses.

PATIENTS AND METHODS

Patient recruitment. Adult PsA/SpA patients were recruited from the New York University (NYU) clinics prior to initiating biologic therapy. Fifteen patients analyzed in the TNFi cohort were either naive to prior biologic treatment (93.3%) or had brief exposure >1 year prior to enrollment (6.7%). They were compared to 15 age-, sex-, and ethnicity-matched controls to determine differences between healthy and PsA/SpA subjects. A different set of 14 patients in the IL-17i cohort were also compared to the TNFi cohort, of which 9 (64.3%) were inadequate responders to TNFi, warranting the switch to IL-17i therapy (secukinumab). This allowed us to observe the natural history of microbiome fluctuation in a typical clinical progression of biologic therapy for SpA and psoriatic disease. Ileal biopsy specimens were analyzed from an additional cohort (University of Palermo)

of 5 HLA-B27-positive SpA patients (all diagnosed as having AS) who developed CD after treatment with secukinumab, compared to 5 who did not.

Patient evaluation and sample collection. For the TNFi and IL-17i NYU cohorts, demographic and clinical data were recorded. Fecal samples were collected for microbiome, metagenomic, metabolomic, and cytokine/inflammatory protein analyses. Blood was collected for basic laboratory testing and HLA typing. In the TNFi cohort, samples were collected at baseline and 6 months after starting therapy (maintenance visit; mean \pm SD 27 \pm 10 weeks). In the IL-17i cohort, samples were collected at baseline, 5 weeks after starting therapy (loading visit; mean \pm SD 7 \pm 2 weeks), and 3 months after starting therapy (maintenance visit; mean \pm SD 17 \pm 5 weeks). All 14 patients provided samples at the baseline and loading visits, and 9 provided samples at the maintenance visit. For the SpA (AS) cohorts, ileal biopsy samples were collected before (at baseline) and after initiation of IL-17i therapy (post-IL-17i), and used for histologic, immunohistochemical, and messenger RNA quantification analyses.

DNA extraction, 16S ribosomal RNA (rRNA) and internal transcribed spacer (ITS) gene sequencing, and data analysis. Gut bacterial and fungal DNA was extracted and sequenced as previously described (15). Bacterial microbiota composition was determined by sequencing the V4 hypervariable region of bacterial 16S rRNA (Illumina MiSeq platform) (5). Fungal microbiota composition was determined by sequencing the fungal ITS1 region using published primers (16). Obtained sequences were demultiplexed and clustered into operational taxonomic units (OTUs) with closed-reference OTU picking using Quantitative Insights into Microbial Ecology (QIIME), version 1.9.1 (17). QIIME and R software, version 3.4.3 (18), were used to calculate alpha and beta diversity, taxa summary, and the change in taxa relative abundance in the NYU cohorts. The Linear discriminant analysis effect size (LEfSe) tool, version 1.0.7 (19), was used to identify differentially abundant bacterial taxa between groups.

Co-occurrence networks. Taxa were summarized at the genus level and pruned to $\geq 0.1\%$ relative abundance in ≥ 2 samples. Co-occurrence of taxa was calculated using SparCC (20), and results were validated with 10 rarefactions of the input table. Significantly co-occurring taxa ($P < 0.05$) were kept for further analysis. Cytoscape, version 3.2.1 (21), was used to visualize the co-occurrence networks.

Shotgun sequencing and metagenomic analysis. DNA libraries were generated following the Nextera XT Illumina protocol and sequenced on the Illumina NextSeq platform. Raw sequencing reads were processed using HUMAnN2 (22). The Kruskal-Wallis test was used to identify differentially abundant enzymatic pathways in the TNFi and IL-17i cohorts.

Measurement of fecal cytokines/proteins and fatty acid metabolites. Fecal protein was extracted (4) and used to measure PsA/SpA-related cytokines and inflammatory proteins with multiplex and enzyme-linked immunosorbent assays. Short-, medium-, and long-chain fatty acid (FA) levels were measured using gas chromatography mass spectrometry (GC-MS) and liquid chromatography mass spectrometry (LC-MS) methods.

Metadata correlation analysis. Spearman's correlations were performed on pooled pre- and posttreatment samples to identify bacterial and fungal taxa that significantly correlate with cytokines/proteins and FAs. Using QIIME, OTUs were grouped at the genus level and tables pruned to contain only OTUs with >0.5% relative abundance in ≥ 2 samples, followed by Spearman's correlations with false discovery rate (FDR) correction. Associations with genera that achieved FDRs of <0.1 and <0.2

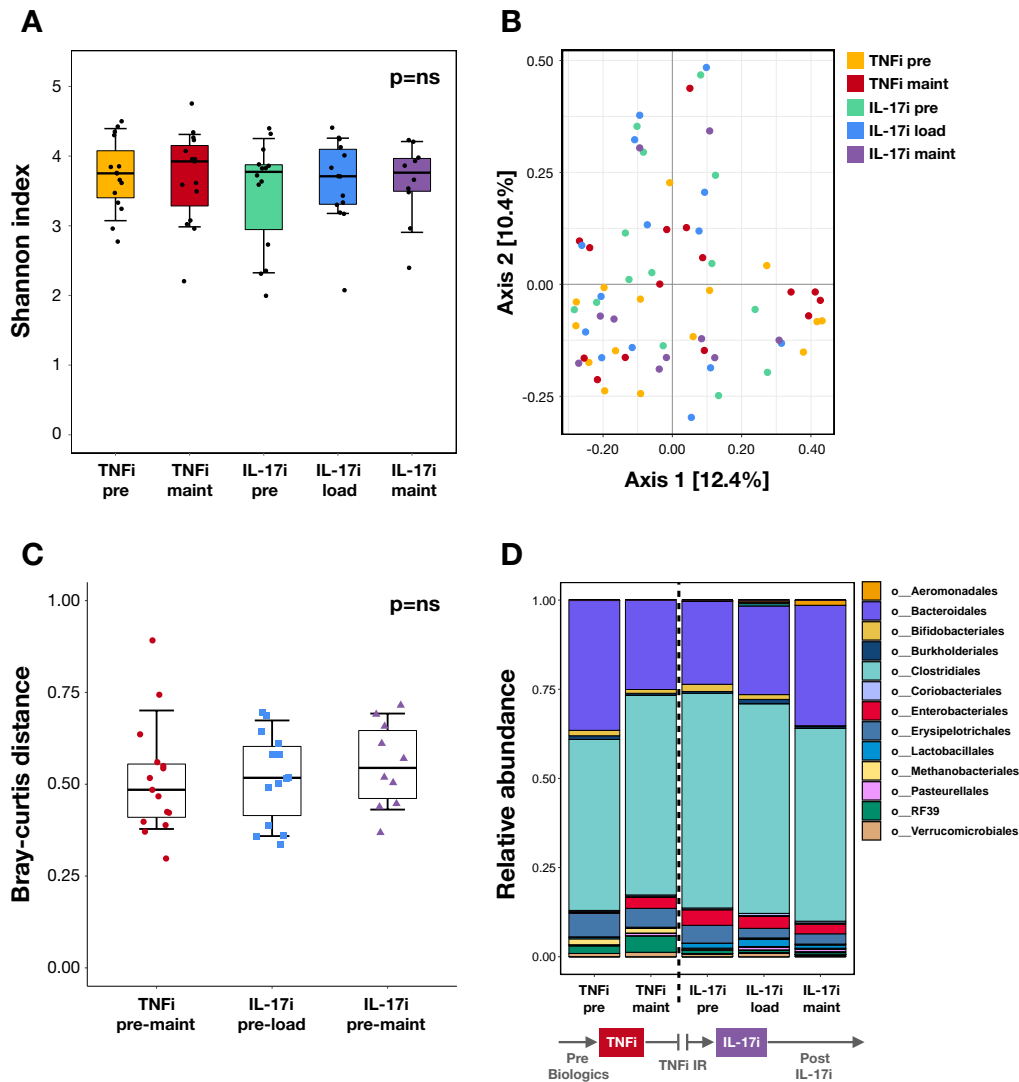


Figure 1. Bacterial composition at different stages of tumor necrosis factor inhibitor (TNFi) therapy and interleukin-17 inhibitor (IL-17i) therapy. **A**, Alpha diversity as measured by the Shannon diversity index. There were no significant differences (ns) between pre- and posttreatment visits in the TNFi (baseline [pre] versus 6-month [maintenance] visits) and IL-17i (baseline [pre] versus 5-week [loading] and baseline [pre] versus 3-month [maintenance] visits) cohorts by Wilcoxon's signed rank test. **B**, Principal coordinates analysis plot of beta diversity as measured by the Bray-Curtis distance. No distinct clustering patterns were identified. **C**, Community dissimilarity pre- to posttreatment with TNFi (distance measured between baseline and maintenance visits) and IL-17i (distance measured between baseline and loading visits and between baseline and maintenance visits). No significant differences were seen when comparing TNFi to IL-17i by Mann-Whitney U test. **D**, Mean relative abundance of taxa at the order level pre-TNFi treatment to post-IL-17i treatment. Relative abundance is shown in parts per unit. Legend lists only the top taxa. In **A** and **C**, data are shown as box plots, where each box represents the interquartile range (IQR). Lines inside the boxes represent the median. Whiskers represent the 10th and 90th percentiles. O = order; IR = inadequate responders. Color figure can be viewed in the online issue, which is available at <http://onlinelibrary.wiley.com/doi/10.1002/art.41169/abstract>.

were plotted as correlograms based on previously published thresholds (4).

Biopsy specimen collection, processing, and analysis. Ileal mucosal biopsy specimens were collected from 10 additional SpA patients before and after IL-17i therapy (5 patients who developed CD and 5 controls who did not). Presence of adherent and invasive bacteria was assessed using Warthin-Starry staining and antibodies directed against bacterial lipopolysaccharide, as previously described (23). Messenger RNA levels of tight junction proteins Occludin and Claudin 1 were assessed with reverse transcriptase–polymerase chain reaction (RT-PCR). In the 5 subjects who developed CD, ileal biopsy specimens were histologically evaluated for inflammation using hematoxylin and eosin and immunoperoxidase staining, as previously described (24). Expression of IL-25/IL-17E, IL-25R/IL-17RB, IL-17A, IL-23p19, and IL-13 was assessed with RT-PCR and immunohistochemical staining. Type 2 innate lymphoid cells (ILC2s) were identified and quantified by techniques based on confocal microscopy and flow cytometry of lamina propria mononuclear cells. Detailed methods for analyses, sequencing, cytokine/protein measurement, GC-MS, LC-MS, and biopsy specimen collection/processing, as well as links to publicly available data can be found in the Supplementary Methods (available on the *Arthritis & Rheumatology* web site at <http://onlinelibrary.wiley.com/doi/10.1002/art.41169/abstract>).

RESULTS

Baseline characteristics. Characteristics of the TNFi and IL-17i cohorts are shown in Supplementary Table 1 (<http://onlinelibrary.wiley.com/doi/10.1002/art.41169/abstract>). The IL-17i cohort tended to be older (P not significant) and female-predominant (P not significant), compared to the TNFi cohort. Body mass index was comparable in both cohorts. Phenotypically, the majority of patients had PsA, with a small minority diagnosed as having axial SpA. All patients from the TNFi cohort had psoriasis (mostly mild) and either peripheral PsA (53.3%) or a combination of peripheral and axial PsA (46.7%). The average tender and swollen joint counts were 5.5 and 3.6, respectively. In the IL-17i cohort, 9 patients had psoriasis (64.3%) and were diagnosed as having either peripheral PsA (35.7%), axial PsA (7.1%), a combination of peripheral and axial PsA (28.6%), or axial SpA (21.4%). One patient had predominantly skin disease. Very few patients in both cohorts were HLA-B27–positive and about one-third of patients in each cohort had elevated CRP (28.6% in IL-17i versus 33.3% in TNFi; P not significant).

PsA/SpA characterized by intestinal bacterial dysbiosis. Using 16S rRNA gene sequencing, we compared the intestinal microbiota of biologic-naïve PsA/SpA patients (TNFi baseline) to age-, sex-, race-, and ethnicity-matched healthy controls. We noted an expansion of Clostridiales (order) and

Erysipelotrichales (order), as well as a reduction of Bacteroidales (order) relative abundance in PsA/SpA, compared to healthy subjects (Supplementary Figure 1A, <http://onlinelibrary.wiley.com/doi/10.1002/art.41169/abstract>). Furthermore, and as previously shown by our group, several low abundance taxa were overrepresented in healthy controls, the majority of which belong to the Bacteroidales order (Supplementary Figure 1B).

Distinctive features in intestinal bacterial perturbations after TNFi and IL-17i therapies. We next analyzed the microbiota of fecal samples from subjects pre- and posttreatment with TNFi and IL-17i. Neither alpha nor beta diversity were significantly different within each cohort (Figures 1A and B and Supplementary Figure 2, <http://onlinelibrary.wiley.com/doi/10.1002/art.41169/abstract>). We then analyzed whether there were community dissimilarities over time between the TNFi and IL-17i cohorts. While changes in beta diversity did not show significant differences (Figure 1C), there were noticeable perturbations in specific taxa. In particular, there was an expansion of Clostridiales and a reduction of Bacteroidales at the TNFi maintenance visit compared to baseline, and an opposite reduction of Clostridiales with concomitant expansion of Bacteroidales at the IL-17i maintenance visit (Figure 1D). Furthermore, we observed high variability in therapy response in specific patients. There were prominent shifts in Clostridiales relative abundance (both expansion and reduction) with IL-17i therapy, which were not pronounced with TNFi therapy ($P < 0.005$ and $P < 0.05$, respectively) (Figures 2A–C).

We found a similar pattern at higher taxonomic levels, particularly with Firmicutes (phylum) (Supplementary Figures 3A–C, <http://onlinelibrary.wiley.com/doi/10.1002/art.41169/abstract>) and Clostridia (class) (Supplementary Figures 3D–F). In contrast, most patients had a reduction of Bacteroidales relative abundance with TNFi, and about one-third of patients showed expansion with IL-17i (Figures 2D–F). Additional taxa of interest are summarized in Supplementary Table 2 (<http://onlinelibrary.wiley.com/doi/10.1002/art.41169/abstract>).

IL-17i disrupts bacterial interactions in the gut. To further explore perturbations in the bacterial community, we performed a network analysis to identify groups of intestinal bacteria that co-occur with one another before and after biologic therapy with TNFi (Supplementary Figures 4A, 4B, and 14 and Supplementary Table 3A) or IL-17i (Figure 3, Supplementary Figures 15A and B, and Supplementary Table 3B, <http://onlinelibrary.wiley.com/doi/10.1002/art.41169/abstract>). At the pre-TNFi phase, there were 2 clusters dominated by *Bacteroides* and Ruminococcaceae (family) that became less prominent (nodes arranged in a linear structure rather than in clusters) with treatment (Supplementary Figures 4A, 4B, and 14 and Supplementary Table 3A). In contrast, in the pre-IL-17i phase, there was a strong positive correlation between *Bacteroides* and Ruminococcaceae, with nodes arranged in a linear structure. However, post-IL-17i *Bacteroides* and Ruminococcaceae

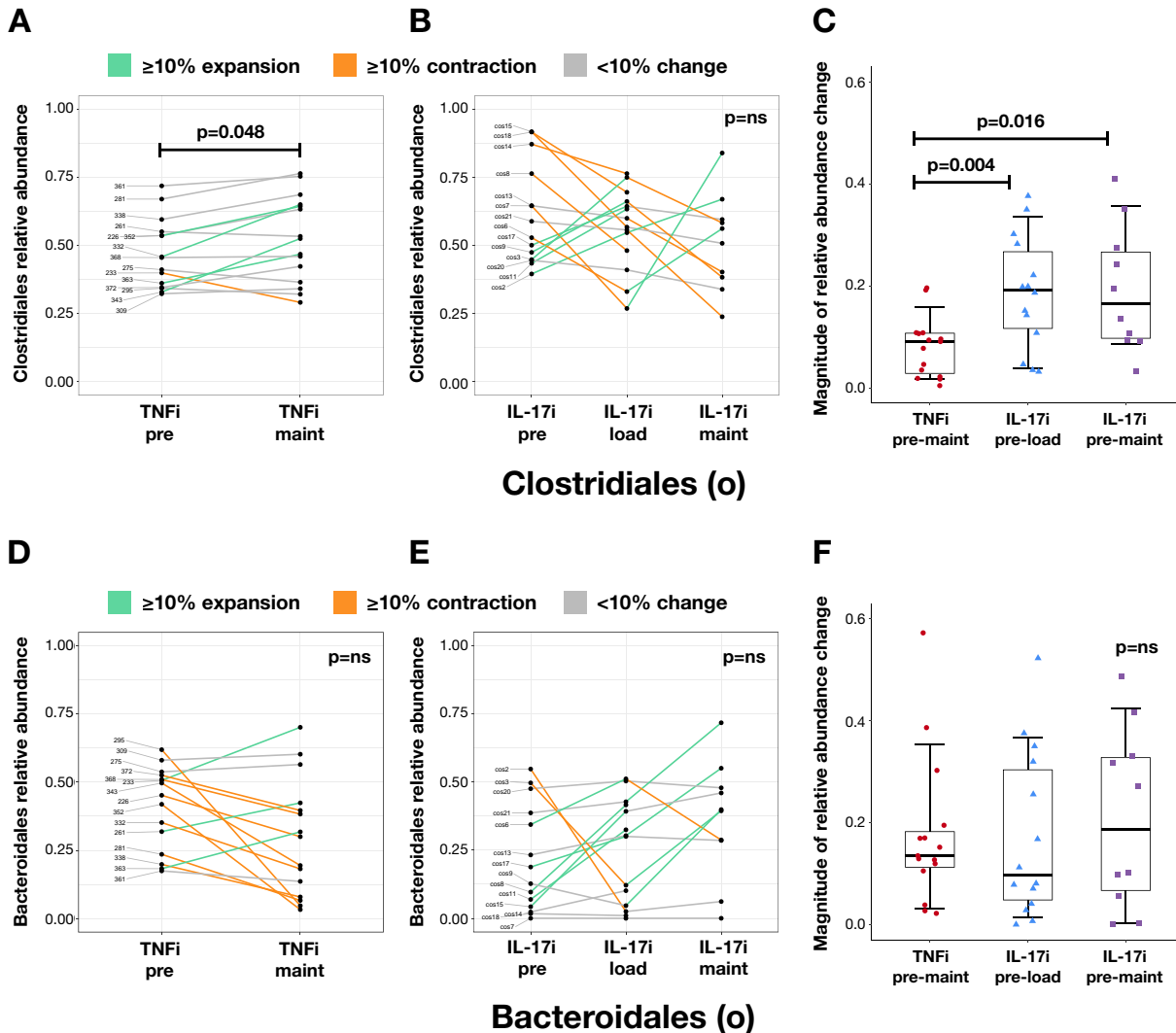


Figure 2. Changes in Clostridiales and Bacteroidales relative abundance with TNFi therapy and IL-17i therapy. Changes in relative abundance of Clostridiales (order) and Bacteroidales (order) with TNFi therapy (**A** and **D**, respectively) and with IL-17i therapy (**B** and **E**, respectively) are shown. Each line represents an individual patient. Relative abundance is shown in parts per unit. Magnitude of change in relative abundance pre- to posttreatment with TNFi (measured between baseline and maintenance visits) and IL-17i (measured between baseline and loading visits and between baseline and maintenance visits) (**C** and **F**, respectively) is also shown. In **C** and **F**, data are shown as box plots, where each box represents the IQR. Lines inside the boxes represent the median. Whiskers represent the 10th and 90th percentiles. Statistical comparisons within each cohort were calculated by Wilcoxon's signed rank test. Statistical comparisons between TNFi and IL-17i cohorts were calculated by Mann-Whitney U test. See Figure 1 for other definitions.

separated into 2 negatively correlated clusters (Figure 3, Supplementary Figures 15A and B, and Supplementary Table 3B).

Of note, the pre-IL-17i network differed markedly from the pre-TNFi network, likely reflecting prior exposure to TNFi in this group (i.e., altered baseline). In addition, the pre-IL-17i network showed differences with the post-TNFi network, which could be partially due to different durations of exposure to biologic agents. Overall, however, these findings suggest that biologic therapy is not only associated with perturbations at the level of the individual taxon but also with changes in the interconnectivity and co-occurrence among specific bacteria, especially with IL-17i, where positive symbiotic correlations became negative associations after treatment.

Intestinal *Candida* expansion with IL-17i treatment. Using ITS sequencing, we analyzed changes in fungal microbiota following biologic therapy. Akin to results from the bacterial data, alpha and beta diversity were not significantly different in the TNFi- or IL-17i-treated cohorts (alpha diversity displayed in Figure 4A and Supplementary Figure 5, <http://onlinelibrary.wiley.com/doi/10.1002/art.41169/abstract>; beta diversity displayed in Figures 4B and C). However, there were noticeable perturbations in specific fungal taxa. These included an expansion of Saccharomycetales (order) at the TNFi and IL-17i maintenance visits relative to baseline, both on average (Figure 4D) and in the majority of patients in each

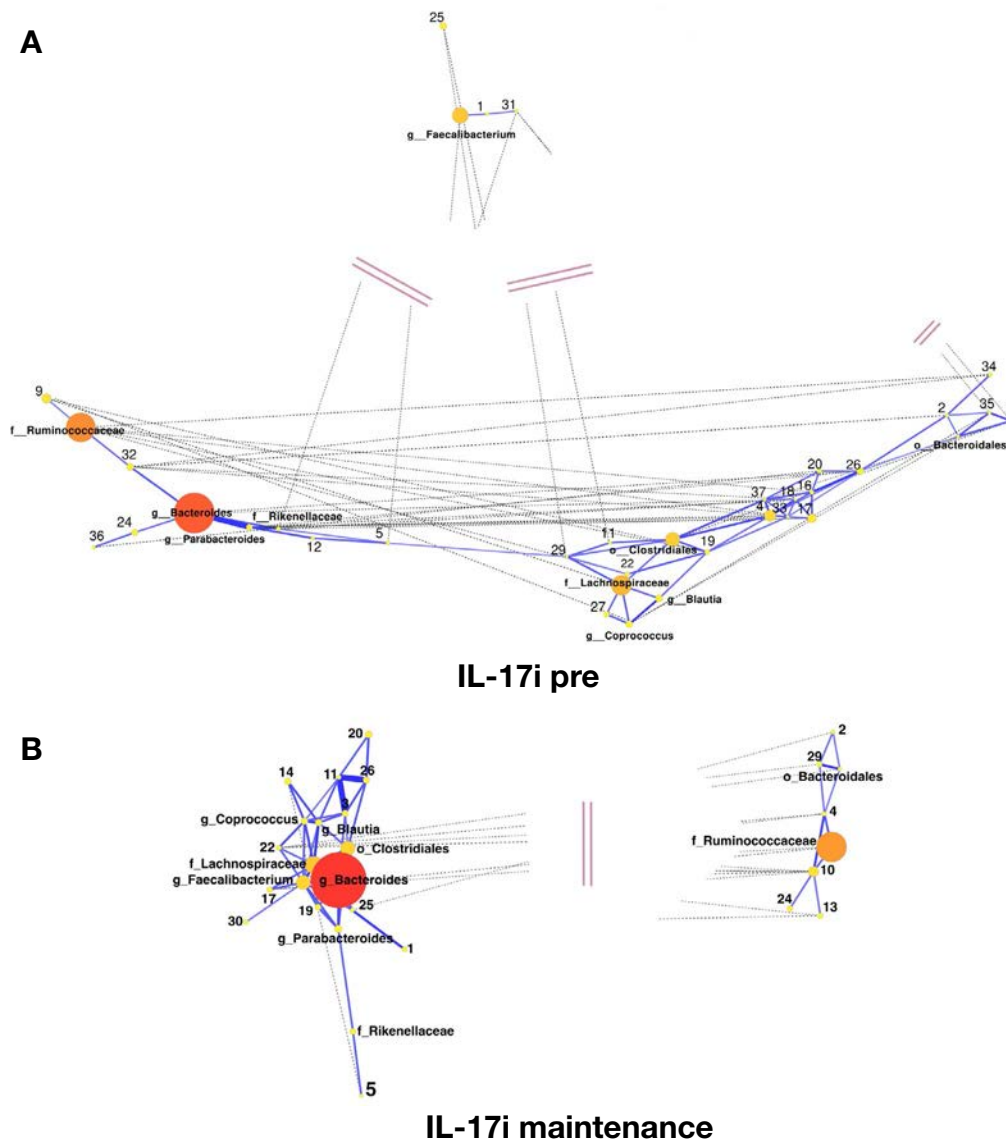


Figure 3. Co-occurrence networks of bacterial taxa pre- and posttreatment with IL-17i. **A**, IL-17i baseline visit. **B**, IL-17i maintenance visit. Nodes represent individual taxa, with the size and color denoting relative abundance (large red nodes = high abundance; medium orange nodes = medium abundance; small yellow nodes = low abundance). Edges represent significant correlations between taxa, with solid lines corresponding to positive correlations and dashed lines corresponding to negative correlations. Edge lengths are inversely proportional to correlation strength. Double lines represent truncated edge distances. G = genus; F = family (see Figure 1 for other definitions). Color figure can be viewed in the online issue, which is available at <http://onlinelibrary.wiley.com/doi/10.1002/art.41169/abstract>.

cohort (Supplementary Figures 6A–C, <http://onlinelibrary.wiley.com/doi/10.1002/art.41169/abstract>).

There were notable IL-17i treatment-specific differences in a subset of patients, including a robust expansion of *Candida* (29% of cohort) (Figure 5B) and *C albicans* (21% of cohort) (Figure 5E). A smaller subset of patients demonstrated a similar magnitude in reduction of *Candida* (14% of cohort) (Figure 5B) and *C albicans* (7% of cohort) (Figure 5E). Moreover, the magnitude of change in *C albicans* relative abundance (expansion or reduction) was significantly higher with IL-17i compared to TNFi between baseline and maintenance visits ($P < 0.05$) (Figure 5F). In contrast, several patients showed a robust expansion of *Saccharomyces cerevi-*

siae, mostly in the TNFi cohort (40% of cohort) (Supplementary Figure 6D, <http://onlinelibrary.wiley.com/doi/10.1002/art.41169/abstract>). Correspondingly, the magnitude of *S cerevisiae* relative abundance change was significantly higher in TNFi compared to IL-17i between baseline and maintenance visits ($P < 0.05$) (Supplementary Figure 6F). Additional taxa of interest are summarized in Supplementary Table 4 (<http://onlinelibrary.wiley.com/doi/10.1002/art.41169/abstract>).

We then performed differential enrichment analysis to identify bacterial taxa that could distinguish subjects with high *Candida* and *C albicans* expansion (“expanders”) from all other patients pre- and posttreatment with IL-17i (none achieved

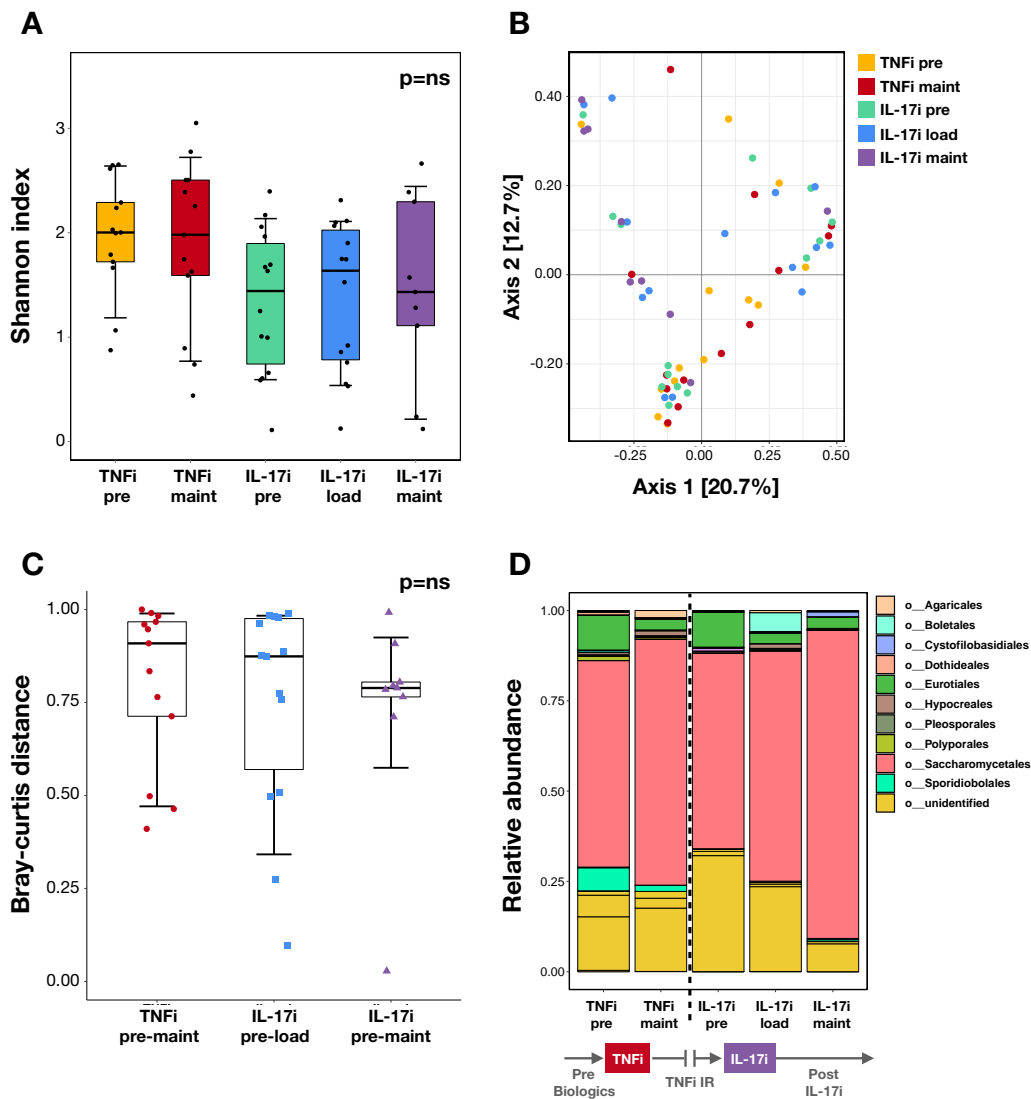


Figure 4. Fungal composition at different stages of TNFi therapy and IL-17i therapy. **A**, Alpha diversity as measured by the Shannon diversity index. There were no significant differences between pre- and posttreatment in the TNFi (baseline versus maintenance visits) and IL-17i (baseline versus loading and baseline versus maintenance visits) cohorts by Wilcoxon's signed rank test. **B**, Principal coordinates analysis plot of beta diversity as measured by the Bray-Curtis distance. No distinct clustering patterns were identified. **C**, Community dissimilarity pre- to posttreatment with TNFi (distance measured between baseline and maintenance visits) and IL-17i (distance measured between baseline and loading visits and between baseline and maintenance visits). No significant differences were seen when comparing TNFi to IL-17i by Mann-Whitney U test. **D**, Mean relative abundance of taxa at the order level pre-TNFi treatment to post-IL-17i treatment. Relative abundance is shown in parts per unit. Legend lists only the top taxa. In **A** and **C**, data are shown as box plots, where each box represents the IQR. Lines inside the boxes represent the median. Whiskers represent the 10th and 90th percentiles. See Figure 1 for definitions. Color figure can be viewed in the online issue, which is available at <http://onlinelibrary.wiley.com/doi/10.1002/art.41169/abstract>.

FDR) (Supplementary Figures 7 and 8, respectively). Pretreatment, *Candida* expanders associated with a higher abundance of taxa from the Clostridiales order, most notably *Faecalibacterium* (Supplementary Figure 7A, <http://onlinelibrary.wiley.com/doi/10.1002/art.41169/abstract>). At the maintenance visit, *Candida* expanders were distinguished by higher abundance of Bacteroidetes and taxa within the Bacteroidetes phylum (i.e., *Bacteroides*) (Supplementary Figure 7B). In the case of *C. albicans*, the most prominent taxon distinguishing high expanders at the pretreatment visit was the Veillonellaceae family, also belonging

to the Clostridiales order (Supplementary Figure 8A, <http://onlinelibrary.wiley.com/doi/10.1002/art.41169/abstract>). Posttreatment, expanders were again characterized by higher abundance of Bacteroidaceae and *Bacteroides* (Supplementary Figure 8B).

Microbial gene pathway perturbations after biologic therapy. Shotgun sequencing and metagenomic analysis were performed to identify functional changes that occur in response to biologic therapy. We identified several differentially abundant microbial pathways in both cohorts. In the TNFi-treated patients,

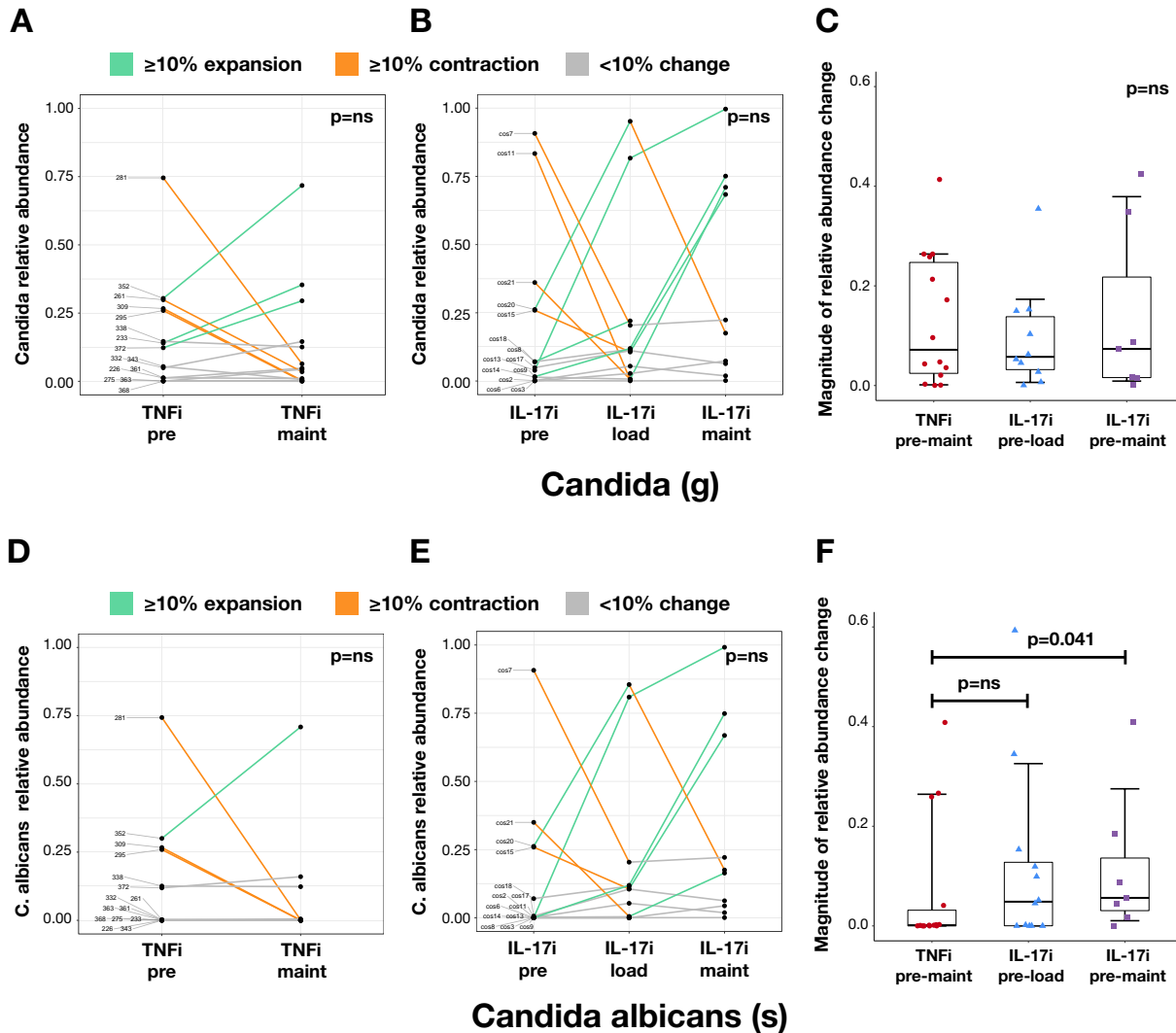


Figure 5. Changes in *Candida* and *Candida albicans* relative abundance with TNFi and IL-17i therapy. Changes in relative abundance of *Candida* and *C. albicans* with TNFi therapy (**A** and **D**, respectively) and IL-17i therapy (**B** and **E**, respectively) are shown. Each line represents an individual subject. Relative abundance is shown in parts per unit. Magnitude of change in relative abundance pre- to posttreatment with TNFi (measured between baseline and maintenance visits) and IL-17i (measured between baseline and loading visits and between baseline and maintenance visits) (**C** and **F**, respectively) is shown. In **C** and **F**, data are shown as box plots, where each box represents the IQR. Lines inside the boxes represent the median. Whiskers represent the 10th and 90th percentiles. Statistical comparisons within each cohort were calculated by Wilcoxon's signed rank test. Statistical comparisons between TNFi and IL-17i cohorts were calculated by Mann-Whitney U test. G = genus; S = species (see Figure 1 for other definitions).

the majority of pathways that changed with therapy were related to nucleotide metabolism (Supplementary Figure 9 and Supplementary Table 5, <http://onlinelibrary.wiley.com/doi/10.1002/art.41169/abstract>). In contrast, pathways that changed with IL-17i therapy were related to cell wall, vitamin, carbohydrate, and amino acid metabolism, particularly tryptophan (Supplementary Figure 10 and Supplementary Table 6, <http://onlinelibrary.wiley.com/doi/10.1002/art.41169/abstract>).

Changes in key bacterial and fungal taxa correlate with fecal levels of IL-23/Th17 cytokines and immunomodulatory metabolites. We measured levels of cytokines and proteins that have been implicated in either PsA/SpA pathogenesis

and/or intestinal inflammation, including IL-12, IL-23, the IL-17 family, calprotectin, CCL20, and secretory IgA (sIgA). We also measured short-, medium-, and long-chain FAs. We found several correlations between these metadata and intestinal microbiota at the genus level in TNFi- and IL-17i-treated patients (Supplementary Figures 11 and 12 and Supplementary Tables 7 and 8, <http://onlinelibrary.wiley.com/doi/10.1002/art.41169/abstract>).

Interestingly, the TNFi cohort had mostly negative correlations with cytokines and other metadata, whereas the IL-17i cohort had mostly positive correlations. In the TNFi cohort, *Bacteroides* positively correlated with CCL20, sIgA, and several cytokines involved in the IL-23/Th17 axis. In contrast, *Prevotella*

and *Catenibacterium* negatively correlated with the same cytokines and inflammatory proteins. In addition, several taxa from the Clostridiales and Bacteroidales orders negatively correlated with calprotectin (Supplementary Figures 11A and 12A, <http://onlinelibrary.wiley.com/doi/10.1002/art.41169/abstract>). In the IL-17i cohort, members of the Bacteroidales order had strong positive correlations with IL-25/IL-17E, while members of the Clostridiales order showed weak positive correlations with IL-21 and/or IL-23. Of interest, *Faecalibacterium* correlated positively with propionic acid and negatively with octanoic acid, while taxa of the Clostridiales order positively correlated with several long-chain FAs. Of the fungal taxa, *Candida* positively correlated with slgA and negatively correlated with valeric acid and stearic acid (Supplementary Figures 11B and 12B, <http://onlinelibrary.wiley.com/doi/10.1002/art.41169/abstract>).

IL-17i-induced CD is characterized by decreased bacterial counts and simultaneous expansion of both IL-25/IL-17E-producing tuft cells and ILC2s in the lamina propria.

The described observations in gut microbiota dynamics following TNFi and IL-17i treatment were seen in patients exposed to their respective therapies for relatively short periods of time. Despite correlations with fecal levels of intestinal inflammatory mediators, none of the participants developed clinically evident gut inflammation. Therefore, and to further characterize the effects of IL-17A inhibition on gut immunity and inflammation, we examined ileal biopsy samples from an additional cohort of SpA (AS) patients who developed clinically overt CD after IL-17i exposure. All 5 patients demonstrated reduction in adherent and invasive bacteria in nonlesional ileal biopsy samples via Warthin-Stary staining and lipopolysaccharide immunostaining,

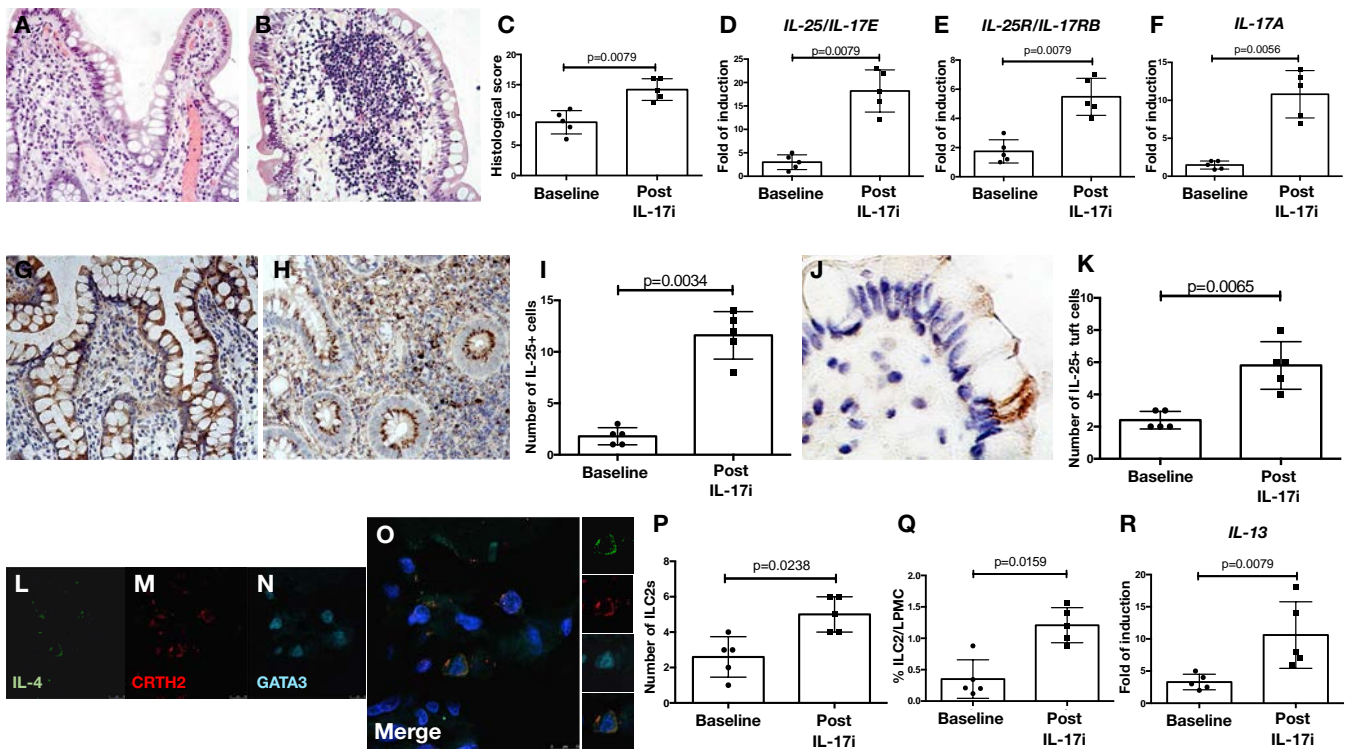


Figure 6. Interleukin-25 (IL-25)-driven inflammation characterizes colitis seen in spondyloarthritis (SpA) (ankylosing spondylitis) patients after IL-17 inhibitor (IL-17i) therapy. **A** and **B**, Representative hematoxylin and eosin-stained images demonstrating histologic changes in the ileum of SpA patients at baseline (**A**) and after the onset of clinically evident Crohn's disease (CD) during treatment with IL-17i (secukinumab) (**B**). **C**, Histologic score in SpA ileal samples at baseline and after the onset of CD. **D–F**, Relative mRNA levels of IL-25/IL-17E (**D**), IL-25R/IL-17RB (**E**), and IL-17A (**F**) in SpA patients at baseline and after the onset of CD, as assessed by reverse transcriptase–polymerase chain reaction (RT-PCR). **G** and **H**, Representative images showing IL-25 immunostaining in SpA ileal samples at baseline and after the onset of CD. **I**, Number of IL-25–positive cells in SpA patients. **J**, Representative image showing the expression of IL-25/IL-17E in the context of specialized gut epithelial cells that were morphologically identified as tuft cells in the gut of SpA patients after the onset of CD during treatment with secukinumab. **K**, Number of IL-25–positive tuft cells at baseline and after the onset of CD. **L–N**, Representative confocal microscopy images of IL-4 (**L**), chemoattractant receptor–like molecule expressed on Th2 cells (CRTH2) (**M**), and GATA-3 (**N**) in SpA ileal tissue after the onset of CD during treatment with secukinumab. **O**, Merged triple-stained image showing IL-4/CRTH2/GATA-3–positive type 2 innate lymphoid cell (ILC2) colocalization in the gut of SpA patients. **P**, Number of ILC2s in the gut of SpA patients. **Q**, Percentage of ILC2s evaluated by flow cytometry in the gut of SpA patients at baseline and after the onset of CD during treatment with secukinumab. **R**, Relative mRNA levels of IL-13 in the ileum of SpA patients at baseline and after the onset of CD, as assessed by RT-PCR. Symbols represent individual samples; bars with whiskers show the median with interquartile range. Statistical comparisons were calculated by Student's *t*-test and Mann-Whitney U test.

as well as increased expression of 2 tight junction proteins, Occludin and Claudin 1 (Supplementary Figure 13, <http://onlinelibrary.wiley.com/doi/10.1002/art.41169/abstract>). Curiously, the same pattern was observed in 5 control SpA (AS) subjects who were also treated with IL-17i but did not develop CD.

In those with colitis, histologic evaluation of ileal samples pre- and post-IL-7i treatment clearly demonstrated the presence of a Crohn's-like inflammation after therapy (Figures 6A–C). This inflammation was characterized by increased expression of IL-25/IL-17E, IL-25R/IL-17RB, and IL-17A post-IL-17i, as evaluated by RT-PCR (Figures 6D–F) and immunohistochemistry (Figures 6G–K), and increased numbers of IL-25/IL-17E-positive tuft cells (Figures 6J and K), which are chemosensory cells lining the intestinal epithelium, known to secrete IL-25/IL-17E in response to parasitic infections (25). There were no changes in IL-23 levels. The higher expression of IL-25/IL-17E was accompanied by expansion of ILC2s ($P < 0.05$), defined as CD3–IL-4+CRHT2+GATA3+ cells by confocal microscopy (Figures 6L–P) or Lin–(ST2–)CD45+IL-25R+KLRG1+Thy1+ cells by flow cytometry (Figure 6Q), as well as increased production of IL-13 (Figure 6R).

DISCUSSION

We describe, for the first time, the effects of 2 biologic therapies (i.e., TNFi and IL-17i) on the intestinal microbiome of PsA and SpA patients. Through our longitudinal study approach, we were able to directly discern changes in the microbiome before and after therapy. Consistent with our previous findings, we observed intestinal dysbiosis in PsA/SpA patients prior to the initiation of biologic therapy. Although variations in specific taxa differed from our previous study (4), this was unsurprising given that microbiome sequencing was performed using different platforms. After biologic therapy, patients demonstrated further bacterial and fungal perturbations, which were more prominent with IL-17i and characterized by significant changes in Clostridiales and related taxa. This is relevant because *Clostridia* contribute to the maintenance of intestinal homeostasis (26), with many species producing butyrate, a short-chain FA that can induce the differentiation of colonic regulatory T cells (Treg cells) (27), which are critical for self-tolerance and prevention of autoimmune disease. Moreover, *Clostridia* species play a physiologic role in gut protection since early inoculation with *Clostridium* renders mice resistant to the development of colitis (28). In humans, low abundance of *Faecalibacterium prausnitzii* not only associates with IBD but also correlates with both ulcerative colitis (UC) disease activity (29) and postoperative recurrence of CD (30).

In the present study, IL-17i led to a robust expansion of *Candida* and *C albicans* in a subgroup of patients of varying clinical phenotypes, with a few patients demonstrating a reduction. We also found that at the pretreatment stage, these *Candida* and *C albicans* expanders were associated with a higher abundance of taxa from the Clostridiales order. Similarly, *Candida* expand-

ers were associated with a higher abundance of *Bacteroides* (and related taxa) posttreatment. A variant of this relationship was seen in a recent study showing that commensal Clostridia and Bacteroidetes were critical for the prevention of *C albicans* intestinal colonization in mice (31).

Other groups have demonstrated microbial changes after biologic therapies. For example, CD patients had a significant decrease in *Escherichia coli* after adalimumab (a TNFi), which was shown to shift their microbiome closer to the composition of healthy individuals (32). Furthermore, CD patients who responded to ustekinumab, an IL-12/23 inhibitor, had higher bacterial diversity pretreatment, while several taxa (e.g., *Faecalibacterium*) distinguished responders from nonresponders (33). In axial SpA, patients who improved with TNFi had a stable microbiome, which was less prone to perturbations with treatment. Additionally, patients who responded to TNFi tended to have higher taxa diversity prior to treatment (34).

Our study showed that bacterial and fungal dysbiosis do not happen in isolation. As indicated in our network analysis, treatment with IL-17i turned positive mutualistic associations between taxa into negative ones, particularly *Bacteroides* and Ruminococcaceae, a member of the Clostridiales order. In turn, changes in the relative abundance of key taxa correlated with shifts in intestinal levels of IL-23/Th17-related cytokines and beneficial short-chain FAs such as propionic acid, linked to Treg cell expansion and abrogation of gut inflammation (27,35). In the fungal community, changes in *Candida* correlated positively with slgA and negatively with valeric acid, which has been associated with IL-10 production and reduction of IL-17A (36). Moreover, metagenomic analysis demonstrated that treatment with IL-17i was associated with up-regulation of L-tryptophan biosynthesis. This is relevant because in vitro binding of a tryptophan-derived photoproduct enhances Th17 cell development and IL-17A expression (37). The reasons for these findings are likely multifactorial but it is possible that, in response to IL-17 blockers, microbial-derived tryptophan is overproduced as a positive feed-forward loop in order to maintain Th17 cell homeostasis in the lamina propria.

Some of the unfavorable associations with *Candida* are not surprising, as prior work suggests that this taxon may be linked to gut inflammation and CD (38). In fact, *C albicans* was shown to be an immunogen for anti-*Saccharomyces cerevisiae* antibodies (ASCA), a sensitive serologic marker for IBD (39). Moreover, families with CD (both affected and unaffected relatives) are more frequently colonized by *C albicans* (13), and the abundance of a different *Candida* species, *Candida tropicalis*, is significantly higher in CD compared to nondiseased first-degree relatives, positively correlating with ASCA levels (40). The role of fungal flora in the development of IBD is further supported by the fact that mice lacking dectin 1 have increased susceptibility to dextran sulfate sodium (DSS)-induced colitis (41). Dectin 1, a receptor for β -glucan found in fungal cell walls, recognizes fungal organisms and induces a strong Th17 response upon binding (42). In the SKG

mouse model, systemic exposure to curdian (1,3- β -glucan aggregates) results in the development of a SpA phenotype and CD-like colitis, while inhibition of dectin 1 can prevent the onset of arthritis (43). Because IL-17 confers protection from extracellular pathogens, IL-17 inhibition is likely to allow fungal outgrowth, as in observed cases of candidiasis during IL-17i clinical trials (44,45). IL-17i has also been shown to exacerbate CD in some patients (12), which has led to the hypothesis that IL-17 inhibition could prompt intestinal *C. albicans* expansion and downstream intestinal inflammation (42).

In our study, IL-17i resulted in CD-like inflammation in a small cohort of SpA (AS) patients and a reduction in adhesive/invasive bacterial scores in patients who developed CD (nonlesional ileum) as well as those who did not (healthy ileum). This may be related to the normalization of tight junction expression after treatment, which was observed as independent of clinically overt CD. Remarkably, ileal biopsy samples from patients who developed colitis demonstrated significantly higher levels of IL-25/IL-17E-producing tuft cells and concomitant expansion of IL-13-producing ILC2s compared to pretreatment levels. These data differ from findings in naturally occurring CD, where gut mucosal levels of IL-25/IL-17E not only are reduced, but also are inversely correlated with endoscopic disease severity (46). Furthermore, a number of studies have demonstrated significant alterations in specific subsets of ILC1 and ILC3 rather than ILC2 cells in naturally occurring CD (47). These differences may be attributable to the underlying diagnosis of AS in the cohort, which is known to be associated with clinical and subclinical gut inflammation. Therefore, it is possible that patients had a priori subclinical gut inflammation and were predisposed to CD. Alternatively, ILC2 expansion may actually correlate with treatment efficacy as a recent study showed that higher circulating ILC2 counts are associated with PsA remission (48).

Taken together, our results suggest that IL-17i-induced CD is driven by divergent pathways compared to typical, "idiopathic" CD. It is, however, essential to note that while IBD exacerbation was frequently observed following IL-17i in CD studies (up to 10%) (12), exacerbations of (or de novo) IBD occurred in <1% of SpA patients enrolled in randomized clinical trials (11,49). Nevertheless, several confirmed cases in routine clinical practice have since been reported (50–52).

Perturbations seen with IL-17i may be specifically related to the inhibition of IL-17A, one of several IL-17 isoforms. This was elegantly demonstrated in IL-17F^{-/-} mice which, unlike IL-17A^{-/-} animals, were resistant to DSS-induced colitis compared to wild-type controls (53). Importantly, the attenuation of colitis in IL-17F^{-/-} mice was linked to overexpansion of Treg cells in the lamina propria and a higher abundance of commensal *Clostridia* (53). Pretreatment with a monoclonal antibody against IL-17F also attenuated colitis (53). Thus, unlike IL-17A inhibition, which may promote deleterious effects on the intestine, blockade of IL-17F or other isoforms (e.g., IL-17E) may have a rather positive outcome and abrogate inflammation in rodents. Whether this is true in human disease will require demonstration in clinical trials.

Limitations of our study include small cohort sizes, subject recruitment from geographically different regions and dietary practices, a phenotypically heterogeneous population, and different drugs used in the TNFi cohort. Although specific microbiota perturbations were pronounced in both bacterial and fungal communities, these results will require validation in larger prospective cohorts, especially since the TNFi cohort was naive to treatment with biologic agents, but the majority of patients in the IL-17i cohort were previously treated with a TNFi. Extending our results would also help us understand whether baseline gut microbiota can be used as predictors of biologic therapy response, as in the case of cancer immunotherapies. In addition, current databases for taxa identification are significantly more comprehensive for bacteria relative to fungi. However, we utilized the same publicly available databases cited by a number of other publications, allowing for data comparison across studies. Improvement in fungal genome sequencing and expansion of taxonomic tools in the near future should enhance our ability to classify these communities in further detail. Given the correlative nature of microbiome studies, it is possible that shifts in *Candida* (and other bacterial taxa) rather follow changes in immune pressure after local inflammation. Although further work is needed to elucidate directionality, recent human and animal studies imply that candidiasis is likely involved in the pathogenesis of IBD. Finally, the present study is not mechanistic in nature and cannot address how microbial fluctuations correlate with disease outcomes. Future research is therefore needed.

In summary, our findings demonstrate that biologic therapies in PsA and SpA not only modulate immune cell response but also are associated with perturbations in specific bacterial and fungal taxa. IL-17i leads to significant changes in Clostridiales and notable expansion of *Candida* and *C. albicans* in more than a quarter of patients, which are accompanied by changes in metabolic pathways and levels of PsA/SpA-related cytokines, proinflammatory molecules, and FA production. Furthermore, IL-17i-induced CD in human SpA differs from idiopathic CD and appears to be driven by diverging IL-17 family pathways (i.e., IL-25/IL-17E). Moving forward, these IL-17i-induced microbial and immune perturbations should be explored, perhaps through a machine learning model, and incorporated into the clinic by predicting which individuals are susceptible to adverse outcomes from IL-17A and related therapies such as candidiasis and (sub)clinical gut inflammation. Ultimately, understanding the downstream effects of these perturbations could allow for the development of precision medicine approaches in PsA, SpA, and related rheumatic diseases.

ACKNOWLEDGMENTS

We would like to acknowledge Michael Colin, Kristen Lee, Gary Zagon, and Pamela Rosenthal for recruiting patients to our study. We would also like to thank Rhina Medina and Luz Alvarado for coordinating and collecting patient samples, Yonghua Li for helping set up the 16S rRNA sequencing runs, and Benjamin

Wu for his advice with preliminary data analysis. We would like to acknowledge the NYU Langone Genome Technology Center for 16S rRNA sequencing, María Jose Garzón and the Sequencing and Bioinformatics Service of FISABIO for ITS sequencing, as well as the University of California, San Diego, Skaggs School of Pharmacy and Pharmaceutical Sciences and the NYU Metabolomics Core Resource Laboratory for performing metabolomics. Although not included in this manuscript, we would like to thank Sergei Korolov and Lu Yang for the animal work related to this project.

AUTHOR CONTRIBUTIONS

All authors were involved in drafting the article or revising it critically for important intellectual content, and all authors approved the final version to be published. Dr. Manasson had full access to all of the data in the study and takes responsibility for the integrity of the data and the accuracy of the data analysis.

Study conception and design. Manasson, Guggino, Ciccía, Clemente, Scher.

Acquisition of data. Manasson, Guggino, Solomon, Reddy, Coras, Akse nov, Jones, Girija, Neimann, Heguy, Dorrestein, Guma, Ciccía, Scher.







Analysis and interpretation of data. Manasson, Wallach, Guggino, Stapy lton, Badri, Segal, Bonneau, Ciccía, Ubeda, Clemente, Scher.

REFERENCES

- Clemente JC, Manasson J, Scher JU. The role of the gut microbiome in systemic inflammatory disease [review]. *BMJ* 2018;360:j5145.
- Tito RY, Cypers H, Joossens M, Varkas G, Van Praet L, Glorieus E, et al. *Dialister* as a microbial marker of disease activity in spondyloarthritis. *Arthritis Rheumatol* 2017;69:114–21.
- Costello ME, Ciccía F, Willner D, Warrington N, Robinson PC, Gardiner B, et al. Intestinal dysbiosis in ankylosing spondylitis. *Arthritis Rheumatol* 2015;67:686–91.
- Scher JU, Ubeda C, Artacho A, Attur M, Isaac S, Reddy SM, et al. Decreased bacterial diversity characterizes the altered gut microbiota in patients with psoriatic arthritis, resembling dysbiosis in inflammatory bowel disease. *Arthritis Rheumatol* 2015;67:128–39.
- Manasson J, Shen N, Garcia Ferrer HR, Ubeda C, Iraheta I, Heguy A, et al. Gut microbiota perturbations in reactive arthritis and postinfectious spondyloarthritis. *Arthritis Rheumatol* 2018;70:242–54.
- Sokol H, Leducq V, Aschard H, Pham HP, Jegou S, Landman C, et al. Fungal microbiota dysbiosis in IBD. *Gut* 2017;66:1039–48.
- Koppel N, Maini Rekdal V, Balskus EP. Chemical transformation of xenobiotics by the human gut microbiota [review]. *Science* 2017;356:eaag2770.
- Gopalakrishnan V, Spencer CN, Nezi L, Reuben A, Andrews MC, Karpinets TV, et al. Gut microbiome modulates response to anti-PD-1 immunotherapy in melanoma patients. *Science* 2018;359:97–103.
- Dubin K, Callahan MK, Ren B, Khanin R, Viale A, Ling L, et al. Intestinal microbiome analyses identify melanoma patients at risk for checkpoint-blockade-induced colitis. *Nat Commun* 2016;7:10391.
- Maier L, Pruteanu M, Kuhn M, Zeller G, Telzerow A, Anderson EE, et al. Extensive impact of non-antibiotic drugs on human gut bacteria. *Nature* 2018;555:623–8.
- McInnes IB, Mease PJ, Kirkham B, Kavanaugh A, Ritchlin CT, Rahman P, et al. Secukinumab, a human anti-interleukin-17A monoclonal antibody, in patients with psoriatic arthritis (FUTURE 2): a randomised, double-blind, placebo-controlled, phase 3 trial. *Lancet* 2015;386:1137–46.
- Hueber W, Sands BE, Lewitzky S, Vandemeulebroecke M, Reinisch W, Higgins PD, et al. Secukinumab, a human anti-IL-17A monoclonal antibody, for moderate to severe Crohn's disease: unexpected results of a randomised, double-blind placebo-controlled trial. *Gut* 2012;61:1693–700.
- Standaert-Vitse A, Sendid B, Joossens M, François N, Vandewalle-El Khoury P, Branche J, et al. *Candida albicans* colonization and ASCA in familial Crohn's disease. *Am J Gastroenterol* 2009;104:1745–53.
- Curtis MM, Way SS. Interleukin-17 in host defence against bacterial, mycobacterial and fungal pathogens. *Immunology* 2009;126:177–85.
- Scher JU, Joshua V, Artacho A, Abdollahi-Roodsaz S, Öckinger J, Kullberg S, et al. The lung microbiota in early rheumatoid arthritis and autoimmunity. *Microbiome* 2016;4:60.
- Toju H, Tanabe AS, Yamamoto S, Sato H. High-coverage ITS primers for the DNA-based identification of ascomycetes and basidiomycetes in environmental samples. *PLoS One* 2012;7:e40863.
- Caporaso JG, Kuczynski J, Stombaugh J, Bittinger K, Bushman FD, Costello EK, et al. QIIME allows analysis of high-throughput community sequencing data [letter]. *Nat Methods* 2010;7:335–6.
- R Core Team (2018). R: a language and environment for statistical computing. URL: <https://www.R-project.org/>.
- Segata N, Izard J, Waldron L, Gevers D, Miropolsky L, Garrett WS, et al. Metagenomic biomarker discovery and explanation. *Genome Biol* 2011;12:R60.
- Friedman J, Alm EJ. Inferring correlation networks from genomic survey data. *PLoS Comput Biol* 2012;8:e1002687.
- Shannon P, Markiel A, Ozier O, Baliga NS, Wang JT, Ramage D, et al. Cytoscape: a software environment for integrated models of biomolecular interaction networks. *Genome Res* 2003;13:2498–504.
- Franzosa EA, McIver LJ, Rahnava rd G, Thompson LR, Schirmer M, Weingart G, et al. Species-level functional profiling of metagenomes and metatranscriptomes. *Nat Methods* 2018;15:962–8.
- Ciccía F, Guggino G, Zeng M, Thomas R, Ranganathan V, Rahman A, et al. Proinflammatory CX₃CR1+CD59+tumor necrosis factor-like molecule 1A+interleukin-23+ monocytes are expanded in patients with ankylosing spondylitis and modulate innate lymphoid cell 3 immune functions. *Arthritis Rheumatol* 2018;70:2003–13.
- Baert FJ, D'Haens GR, Peeters M, Hiele MI, Schaible TF, Shealy D, et al. Tumor necrosis factor α antibody (infliximab) therapy profoundly down-regulates the inflammation in Crohn's ileocolitis. *Gastroenterology* 1999;116:22–8.
- Von Moltke J, Ji M, Liang HE, Locksley RM. Tuft-cell-derived IL-25 regulates an intestinal ILC2-epithelial response circuit. *Nature* 2016;529:221–5.
- Lopetuso LR, Scaldaferrì F, Petito V, Gasbarrini A. Commensal Clostridia: leading players in the maintenance of gut homeostasis [review]. *Gut Pathog* 2013;5:23.
- Furusawa Y, Obata Y, Fukuda S, Endo TA, Nakato G, Takahashi D, et al. Commensal microbe-derived butyrate induces the differentiation of colonic regulatory T cells. *Nature* 2013;504:446–50.
- Atarashi K, Tanoue T, Shima T, Imaoka A, Kuwahara T, Momose Y, et al. Induction of colonic regulatory T cells by indigenous Clostridium species. *Science* 2011;331:337–41.
- Machiels K, Joossens M, Sabino J, De Preter V, Arijis I, Eeckhaut V, et al. A decrease of the butyrate-producing species *Roseburia hominis* and *Faecalibacterium prausnitzii* defines dysbiosis in patients with ulcerative colitis. *Gut* 2014;63:1275–83.
- Sokol H, Pigneur B, Watterlot L, Lakhdari O, Bermúdez-Humarán LG, Gratadoux JJ, et al. *Faecalibacterium prausnitzii* is an anti-inflammatory commensal bacterium identified by gut microbiota analysis of Crohn disease patients. *Proc Natl Acad Sci U S A* 2008;105:16731–6.

31. Fan D, Coughlin LA, Neubauer MM, Kim J, Kim MS, Zhan X, et al. Activation of HIF-1 α and LL-37 by commensal bacteria inhibits *Candida albicans* colonization. *Nat Med* 2015;21:808–14.
32. Busquets D, Mas-de-Xaxars T, López-Siles M, Martínez-Medina M, Bahí A, Sàbat M, et al. Anti-tumour necrosis factor treatment with adalimumab induces changes in the microbiota of Crohn's disease. *J Crohns Colitis* 2015;9:899–906.
33. Doherty MK, Ding T, Koumpouras C, Telesco SE, Monast C, Das A, et al. Fecal microbiota signatures are associated with response to ustekinumab therapy among Crohn's disease patients. *MBio* 2018;9:e02120–17.
34. Bazin T, Hooks KB, Barnetche T, Truchetet ME, Enaud R, Richez C, et al. Microbiota composition may predict anti-TNF α response in spondyloarthritis patients: an exploratory study. *Sci Rep* 2018;8:5446.
35. Smith PM, Howitt MR, Panikov N, Michaud M, Gallini CA, Bohlooly YM, et al. The microbial metabolites, short-chain fatty acids, regulate colonic Treg cell homeostasis. *Science* 2013;341:569–73.
36. Luu M, Pautz S, Kohl V, Singh R, Romero R, Lucas S, et al. The short-chain fatty acid pentanoate suppresses autoimmunity by modulating the metabolic-epigenetic crosstalk in lymphocytes. *Nat Commun* 2019;10:760.
37. Veldhoen M, Hirota K, Westendorf AM, Buer J, Dumoutier L, Renauld JC, et al. The aryl hydrocarbon receptor links TH17-cell-mediated autoimmunity to environmental toxins [letter]. *Nature* 2008;453:106–9.
38. Gerard R, Sendid B, Colombel JF, Poulain D, Jouault T. An immunological link between *Candida albicans* colonization and Crohn's disease. *Crit Rev Microbiol* 2015;41:135–9.
39. Standaert-Vitse A, Jouault T, Vandewalle P, Mille C, Seddik M, Sendid B, et al. *Candida albicans* is an immunogen for anti-*Saccharomyces cerevisiae* antibody markers of Crohn's disease. *Gastroenterology* 2006;130:1764–75.
40. Hoarau G, Mukherjee PK, Gower-Rousseau C, Hager C, Chandra J, Retuerto MA, et al. Bacteriome and mycobiome interactions underscore microbial dysbiosis in familial Crohn's disease. *MBio* 2016;7:e01250–16.
41. Iliev ID, Funari VA, Taylor KD, Nguyen Q, Reyes CN, Strom SP, et al. Interactions between commensal fungi and the C-type lectin receptor Dectin-1 influence colitis. *Science* 2012;336:1314–7.
42. Colombel JF, Sendid B, Jouault T, Poulain D. Secukinumab failure in Crohn's disease: the yeast connection? [letter]. *Gut* 2013;62:800–1.
43. Yoshitomi H, Sakaguchi N, Kobayashi K, Brown GD, Tagami T, Sakihama T, et al. A role for fungal β -glucans and their receptor Dectin-1 in the induction of autoimmune arthritis in genetically susceptible mice. *J Exp Med* 2005;201:949–60.
44. Mease PJ, McInnes IB, Kirkham B, Kavanaugh A, Rahman P, van der Heijde D, et al. Secukinumab inhibition of interleukin-17A in patients with psoriatic arthritis. *N Engl J Med* 2015;373:1329–39.
45. Van der Heijde D, Gladman DD, Kishimoto M, Okada M, Rathmann SS, Moriarty SR, et al. Efficacy and safety of ixekizumab in patients with active psoriatic arthritis: 52-week results from a phase III study (SPIRIT-P1). *J Rheumatol* 2018;45:367–77.
46. Su J, Chen T, Ji XY, Liu C, Yadav PK, Wu R, et al. IL-25 downregulates Th1/Th17 immune response in an IL-10-dependent manner in inflammatory bowel disease. *Inflamm Bowel Dis* 2013;19:720–8.
47. Sonnenberg GF. Regulation of intestinal health and disease by innate lymphoid cells. *Int Immunol* 2014;26:501–7.
48. Soare A, Weber S, Maul L, Rauber S, Gheorghiu AM, Luber M, et al. Cutting edge: homeostasis of innate lymphoid cells is imbalanced in psoriatic arthritis. *J Immunol* 2018;200:1249–54.
49. Mease P, Roussou E, Burmester GR, Goupille P, Gottlieb A, Moriarty SR, et al. Safety of ixekizumab in patients with psoriatic arthritis: results from a pooled analysis of three clinical trials. *Arthritis Care Res (Hoboken)* 2019;71:367–78.
50. Fobelo Lozano MJ, Serrano Giménez R, Castro Fernández M. Emergence of inflammatory bowel disease during treatment with secukinumab. *J Crohns Colitis* 2018;12:1131–3.
51. Philipose J, Ahmed M, Idiculla PS, Mulrooney SM, Gumaste VV. Severe de novo ulcerative colitis following ixekizumab therapy. *Case Rep Gastroenterol* 2018;12:617–21.
52. Ehrlich D, Jamaluddin N, Pisegna J, Padua D. A challenging case of severe ulcerative colitis following the initiation of secukinumab for ankylosing spondylitis. *Case Rep Gastrointest Med* 2018;2018:9679287.
53. Tang C, Kakuta S, Shimizu K, Kadoki M, Kamiya T, Shimazu T, et al. Suppression of IL-17F, but not of IL-17A, provides protection against colitis by inducing Treg cells through modification of the intestinal microbiota. *Nat Immunol* 2018;19:755–65.

Prediction of Damage Accrual in Systemic Lupus Erythematosus Using the Systemic Lupus International Collaborating Clinics Frailty Index

Alexandra Legge,¹ Susan Kirkland,¹ Kenneth Rockwood,¹ Pantelis Andreou,¹ Sang-Cheol Bae,² Caroline Gordon,³  Juanita Romero-Diaz,⁴ Jorge Sanchez-Guerrero,⁴ Daniel J. Wallace,⁵ Sasha Bernatsky,⁶ Ann E. Clarke,⁷  Joan T. Merrill,⁸ Ellen M. Ginzler,⁹ Paul R. Fortin,¹⁰ Dafna D. Gladman,¹¹ Murray B. Urowitz,¹¹  Ian N. Bruce,¹² David A. Isenberg,¹³  Anisur Rahman,¹³ Graciela S. Alarcón,¹⁴ Michelle Petri,¹⁵  Munther A. Khamashta,¹⁶ M. A. Dooley,¹⁷ Rosalind Ramsey-Goldman,¹⁸ Susan Manzi,¹⁹ Asad A. Zoma,²⁰ Cynthia Aranow,²¹ Meggan Mackay,²¹ Guillermo Ruiz-Irastorza,²² S. Sam Lim,²³ Murat Inanc,²⁴ Ronald F. van Vollenhoven,²⁵ Andreas Jonsen,²⁶ Ola Nived,²⁶ Manuel Ramos-Casals,²⁷ Diane L. Kamen,²⁸ Kenneth C. Kalunian,²⁹ Soren Jacobsen,³⁰ Christine A. Peschken,³¹ Anca Askanase,³² and John G. Hanly³³ 

Objective. The Systemic Lupus International Collaborating Clinics (SLICC) frailty index (FI) has been shown to predict mortality, but its association with other important outcomes is unknown. We examined the association of baseline SLICC FI values with damage accrual in the SLICC inception cohort.

Methods. The baseline visit was defined as the first visit at which both organ damage (SLICC/American College of Rheumatology Damage Index [SDI]) and health-related quality of life (Short Form 36) were assessed. Baseline SLICC FI scores were calculated. Damage accrual was measured by the increase in SDI between the baseline assessment and the last study visit. Multivariable negative binomial regression was used to estimate the association between baseline SLICC FI values and the rate of increase in the SDI during follow-up, adjusting for relevant demographic and clinical characteristics.

Results. The 1,549 systemic lupus erythematosus (SLE) patients eligible for this analysis were mostly female (88.7%) with a mean \pm SD age of 35.7 ± 13.3 years and a median disease duration of 1.2 years (interquartile range 0.9–1.5 years) at baseline. The mean \pm SD baseline SLICC FI was 0.17 ± 0.08 . Over a mean \pm SD follow-up of 7.2 ± 3.7 years, 653 patients (42.2%) had an increase in SDI. Higher baseline SLICC FI values (per 0.05 increase) were associated with higher rates of increase in the SDI during follow-up (incidence rate ratio [IRR] 1.19 [95% confidence interval 1.13–1.25]), after adjusting for age, sex, ethnicity/region, education, baseline SLE Disease Activity Index 2000, baseline SDI, and baseline use of glucocorticoids, antimalarials, and immunosuppressive agents.

Conclusion. Our findings indicate that the SLICC FI predicts damage accrual in incident SLE, which further supports the SLICC FI as a valid health measure in SLE.

The views expressed are those of the authors and not necessarily those of the NHS, the NIHR, or the Department of Health.

Supported by the Canadian Institutes of Health Research (grant MOP-88526). The Hopkins Lupus Cohort is supported by the NIH (grants AR-43727 and AR-69572). The Montreal General Hospital Lupus Clinic is supported in part by the Singer Family Fund for Lupus Research. Dr. Rockwood's work was supported by the Dalhousie Medical Research Foundation, the Canadian Institutes of Health Research, the QEII Health Sciences Centre Foundation (Foundation Family Innovation Fund), and the Capital Health Research Fund. Dr. Bae's work was supported in part by the Ministry of Science & ICT of the Republic of Korea (grant NRF-2017M3A9B4050335). Dr. Gordon's work was supported by Lupus UK, the Sandwell and West Birmingham Hospitals NHS Trust, and the NIHR/Wellcome Trust Birmingham Clinical Research Facility. Dr. Clarke's work was supported by the University of Calgary and the Arthritis Society. Dr. Fortin's work was supported by Université Laval and the Arthritis Society. Dr. Bruce's work was supported by Arthritis Research UK, the NIHR Manchester Biomedical Centre, and the NIHR/Wellcome Trust Manchester Clinical Research Facility. Drs. Isenberg and Rahman's work was supported by

the NIHR University College London Hospitals Biomedical Research Center. Dr. Dooley's work was supported by the NIH (grant RR-00046). Dr. Ramsey-Goldman's work was supported by the NIH (grants 5UL-1TR-001422-02 [formerly 8UL-1TR-000150], UL-1RR-025741, K24-AR-02318, and P60-AR-064464 [formerly P60-AR-48098]). Dr. Ruiz-Irastorza's work was supported by the Department of Education, Universities, and Research of the Basque Government. Dr. Jacobsen's was supported by the Danish Rheumatism Association (grant A3865) and the Novo Nordisk Foundation (grant A05990).

¹Alexandra Legge, MD, Susan Kirkland, PhD, Kenneth Rockwood, MD, Pantelis Andreou, PhD: Dalhousie University, Halifax, Nova Scotia, Canada; ²Sang-Cheol Bae, MD, PhD: Hanyang University Hospital for Rheumatic Diseases, Seoul, Korea; ³Caroline Gordon, MD: University of Birmingham College of Medical and Dental Sciences, Birmingham, UK; ⁴Juanita Romero-Diaz, MD, MSc, Jorge Sanchez-Guerrero, MD, MSc: Instituto Nacional de Ciencias Médicas y Nutrición Salvador Zubiran, Mexico City, Mexico; ⁵Daniel J. Wallace, MD: Cedars-Sinai Medical Center and David Geffen School of Medicine at University of California, Los Angeles; ⁶Sasha Bernatsky, MD, PhD: McGill University, Montreal, Quebec, Canada; ⁷Ann E. Clarke, MD, MSc:

INTRODUCTION

The clinical course of systemic lupus erythematosus (SLE) is variable and challenging to predict. In geriatric medicine (1) and other disciplines (2–5), susceptibility to adverse outcomes is quantified using the construct of frailty, defined as increased vulnerability due to diminished ability to respond to physiologic stressors (6). One approach to operationalizing frailty is through a frailty index (FI) (7), which measures the accumulation of health deficits across multiple systems (8). Individuals with few deficits are considered relatively fit, while those with more health problems are considered increasingly frail (9). The validity of the FI approach is well-established in nonlupus populations (7,10–13). Recently, in the Systemic Lupus International Collaborating Clinics (SLICC) inception cohort, we constructed the first FI for SLE patients (14) and demonstrated an association between higher SLICC FI values and increased mortality risk (15).

Organ damage is a core disease domain in SLE (16). It is evaluated using the SLICC/American College of Rheumatology (ACR) Damage Index (SDI) (17), which measures damage occurring after the diagnosis of SLE, regardless of attribution (17,18). Among SLE patients, higher SDI scores are associated with increased mortality (19–24), higher health care costs (25), greater activity limitations (26), and lower health-related quality of life (19,27). Since organ damage accumulates at different rates in individual patients (20), predicting which SLE patients are likely to experience greater damage accrual would be valuable.

We hypothesized that the SLICC FI would identify which SLE patients are most likely to accumulate organ damage over time. The primary objective of this study was to estimate the association between baseline SLICC FI values and the rate of damage accrual

in the SLICC inception cohort. Preexisting organ damage also predicts future damage in SLE (19,20). Therefore, a secondary aim was to compare the abilities of the SLICC FI and the SDI for the prediction of damage accrual.

PATIENTS AND METHODS

Data source. This was a secondary analysis of longitudinal data from the SLICC inception cohort. SLICC comprises 52 investigators at 43 academic centers in 16 countries. From 1999 to 2011, an inception cohort of SLE patients was recruited from 31 SLICC sites in Europe, Asia, and North America. In total, 1,826 SLE patients were enrolled within 15 months of SLE diagnosis (28). Data were collected per a standardized protocol, submitted to the coordinating centers at the University of Toronto and Dalhousie University, and entered into centralized databases. The study was approved by the institutional research ethics boards of all participating centers, and all participants provided written informed consent.

Clinical and laboratory assessments. Patients were evaluated at enrollment and annually for the following variables: demographic features (age, sex, race/ethnicity, and years of post-secondary education), physical measurements (blood pressure, height, and weight), medication use (glucocorticoids, antimalarials, and immunosuppressive agents), individual ACR classification criteria for SLE (28), medical comorbidities, neuropsychiatric events (29,30), SLE disease activity (SLE Disease Activity Index 2000 [SLEDAI-2K]) (31), cumulative organ damage (SDI) (17), and health-related quality of life (Medical Outcomes Study Short Form 36 [SF-36]) (32). Pertinent laboratory investigations were performed locally at each visit (19). Antibodies to cardiolipin,

University of Calgary Cumming School of Medicine, Calgary, Alberta, Canada; ⁹Joan T. Merrill, MD: Oklahoma Medical Research Foundation, Oklahoma City; ⁹Ellen M. Ginzler, MD, MPH: SUNY Downstate Medical Center, New York, New York; ¹⁰Paul R. Fortin, MD, MPH: CHU de Quebec-Université Laval, Quebec City, Quebec, Canada; ¹¹Dafna D. Gladman, MD, Murray B. Urowitz, MD: Toronto Western Hospital and University of Toronto, Toronto, Ontario, Canada; ¹²Ian N. Bruce, MD: Arthritis Research UK Epidemiology Unit, University of Manchester, NIHR Manchester Musculoskeletal Biomedical Research Centre, and Manchester University NHS Foundation Trust, Manchester, UK; ¹³David A. Isenberg, MD, Anisur Rahman, MD, PhD: University College London, London, UK; ¹⁴Graciela S. Alarcón, MD, MPH: University of Alabama at Birmingham; ¹⁵Michelle Petri, MD, MPH: Johns Hopkins University School of Medicine, Baltimore, Maryland; ¹⁶Munther A. Khamashta, MD: St. Thomas Hospital and King's College London GKT School of Medical Education, London, UK; ¹⁷M. A. Dooley, MD, MPH: University of North Carolina at Chapel Hill; ¹⁸Rosalind Ramsey-Goldman, MD, DrPH: Northwestern University and Feinberg School of Medicine, Chicago, Illinois; ¹⁹Susan Manzi, MD, MPH: Lupus Center of Excellence, Allegheny Health Network, Pittsburgh, Pennsylvania; ²⁰Asad A. Zoma, MD: Hairmyres Hospital, East Kilbride, UK; ²¹Cynthia Aranow, MD, Meggan Mackay, MD: Feinstein Institute for Medical Research, Manhasset, New York; ²²Guillermo Ruiz-Irastorza, MD: Hospital Universitario Cruces, University of the Basque Country, Barakaldo, Spain; ²³S. Sam Lim, MD, MPH: Emory University School of Medicine, Atlanta, Georgia; ²⁴Murat Inanc, MD: Istanbul University, Istanbul, Turkey; ²⁵Ronald F. van Vollenhoven, MD: Karolinska Institute, Stockholm, Sweden; ²⁶Andreas Jonsen, MD, PhD, Ola Nived, MD, PhD: Lund University, Lund, Sweden; ²⁷Manuel Ramos-Casals, MD: Institut d'Investigacions Biomèdiques August Pi i Sunyer and Hospital Clínic, Barcelona, Barcelona, Spain; ²⁸Diane L. Kamen,

MD: Medical University of South Carolina, Charleston; ²⁹Kenneth C. Kalunian, MD: University of California, San Diego School of Medicine; ³⁰Soren Jacobsen, MD, DMSc: Rigshospitalet, Copenhagen University Hospital, Copenhagen, Denmark; ³¹Christine A. Peschken, MD: University of Manitoba, Winnipeg, Manitoba, Canada; ³²Anca Askanase, MD, MPH: Hospital for Joint Diseases, New York University, New York, New York; ³³John G. Hanly, MD: Queen Elizabeth II Health Sciences Center and Dalhousie University, Halifax, Nova Scotia, Canada.

Dr. Rockwood has received consulting fees, speaking fees, and/or honoraria from Baxter, Baxalta, Shire, Hollister, Nutricia, Roche, Otsuka, and Lundbeck (less than \$10,000 each), and research support from Pfizer Canada and Sanofi Canada. Dr. Wallace has received consulting fees, speaking fees, and/or honoraria from Merck, EMD Serono, Pfizer, Eli Lilly, and Glenmark (less than \$10,000 each). Dr. Clarke has received consulting fees from MedImmune/AstraZeneca, Exagen Diagnostics, and Bristol-Myers Squibb (less than \$10,000 each). Dr. Inanc has received consulting fees from MSD, AbbVie, Roche, Novartis, Bristol-Myers Squibb, and Pfizer (less than \$10,000 each). Dr. van Vollenhoven has received consulting fees, speaking fees, and/or honoraria from AbbVie, AstraZeneca, Biotest, Biogen, Bristol-Myers Squibb, Celgene, Gilead, GlaxoSmithKline, Janssen, Eli Lilly, Novartis, Pfizer, and UCB (less than \$10,000 each) and research support from AbbVie, Bristol-Myers Squibb, GlaxoSmithKline, Pfizer, and UCB. No other disclosures relevant to this article were reported.

Address correspondence to John G. Hanly, MD, Nova Scotia Rehabilitation Center, 2nd Floor, Division of Rheumatology, 1341 Summer Street, Halifax, Nova Scotia B3H 4K4, Canada. E-mail: john.hanly@nshealth.ca.

Submitted for publication August 14, 2019; accepted in revised form October 15, 2019.

β_2 -glycoprotein I, and the lupus anticoagulant were measured at a central laboratory at the Oklahoma Medical Research Foundation as previously described (33).

Construction of the SLICC FI. The procedure for SLICC FI construction has been described in detail previously (14). Briefly, we established a baseline data set of 1,683 patients, consisting of the first visit at which both the SDI and SF-36 had been completed. Variables were included in the SLICC FI if they met the standard criteria for a health deficit, defined as any symptom, disease process, functional impairment, or laboratory abnormality that 1) is acquired, 2) is associated with chronological age, 3) is associated with adverse health outcomes, 4) is present in $\geq 1\%$ and $\leq 80\%$ of the sample, and 5) has nonmissing values for $\geq 95\%$ of the sample (7). Of 222 candidate variables, 48 health deficits met the inclusion criteria, spanning multiple organ systems and incorporating organ damage, disease activity, comorbidities, and functional status (14). For each of the 48 health deficits, patients were assigned a score between 0 (complete absence of the deficit) and 1 (deficit fully present) using definitions from the SLE literature (17,28,29,31,32). More detailed information has been published previously (15).

Calculation of baseline SLICC FI scores. A baseline SLICC FI score was calculated for each patient as the sum of their individual health deficit scores divided by the total number of deficits. For example, an individual in whom 12 of the 48 health deficits in the SLICC FI are fully present at baseline would have a baseline SLICC FI score of $12/48 = 0.25$. Each additional health deficit increases the SLICC FI score by 0.021.

Measurement of organ damage accrual. To measure damage accrual, we calculated the change in SDI during follow-up for each patient by subtracting their baseline SDI score from their SDI score at last follow-up. Patients with no follow-up assessments after their baseline visit ($n = 134$) were excluded.

Statistical analysis. Descriptive statistics were calculated for baseline demographic and clinical characteristics, baseline SLICC FI values, and change in SDI values during follow-up. Using a frailty cutoff value established in non-SLE populations (12,34,35), we compared the rate of change in SDI score between patients classified as frail (SLICC FI > 0.21) at baseline and those who were not (SLICC FI ≤ 0.21). We also compared rates of damage accrual between those with organ damage (SDI > 0) at baseline and those without (SDI 0).

We initially fit Poisson regression models for the change in SDI score during follow-up, using likelihood ratio tests to evaluate for overdispersion. However, all Poisson models demonstrated overdispersion, and therefore negative binomial models were fit instead. To account for differential duration of patient follow-up, we considered the rate of change in SDI as

the outcome of interest by including follow-up time (patient-years) as an offset. All models were evaluated for goodness of fit and assessed for multicollinearity between independent variables.

First, a univariable model was constructed with baseline SLICC FI (per 0.05 increase) as the independent variable. To identify potential confounders of the relationship between the baseline SLICC FI and damage accrual, we considered baseline demographic and clinical variables associated with damage accrual in SLE (19,20). Univariable models for rate of change in SDI were constructed for each potential confounder.

A multivariable model for the rate of damage accrual included the baseline SLICC FI, as well as any potentially confounding variables with P values less than 0.1 in univariable analyses. Similarly, univariable and multivariable models were constructed for the rate of damage accrual with 1) baseline SDI score (per 1-unit increase) as the independent variable of interest; and 2) both baseline SLICC FI and SDI scores as independent variables in the same model. We then used likelihood ratio tests to compare the multivariable model containing both baseline SLICC FI and SDI scores to the multivariable models containing 1) the baseline SLICC FI alone and 2) the baseline SDI alone. We compared the relative performance of these alternative models using Akaike's information criterion (AIC), with smaller AIC values indicating better predictive quality. Data analysis was conducted using Stata/IC, version 14 (StataCorp).

Sensitivity analysis. The SLICC FI contains health deficits that overlap with items captured by the SDI. To determine the relationship between baseline SLICC FI scores and damage accrual independent of the baseline SDI, we repeated the above analyses after removing overlapping SDI items from the SLICC FI and recalculating SLICC FI scores using the remaining 33 health deficits. We investigated whether the SLICC FI could predict damage accrual in patients without baseline damage by reassessing the association of baseline SLICC FI scores with the rate of change in the SDI in a subgroup of patients without baseline damage (baseline SDI 0).

To address differential durations of follow-up, we selected different follow-up time cut points, based approximately on the 10th percentile (2.5 years), 25th percentile (5 years), 50th percentile (7.5 years), 75th percentile (10 years), and 90th percentile (12.5 years) in the data set. We then repeated the above analyses separately for patients with follow-up time above versus below each cut point.

RESULTS

Baseline patient characteristics. There were 1,549 patients (92.0% of the baseline data set) with ≥ 1 follow-up visit such that 2 data points were available to model change in SDI score. Baseline demographic and clinical characteristics are

shown in Table 1. The median SLE disease duration at baseline was 1.2 years (interquartile range [IQR] 0.9–1.5 years), and most patients ($n = 1,300$ [83.9%]) had their baseline visit within 2 years of SLE diagnosis.

At the baseline assessment, SLICC FI values ranged from 0.004 to 0.510, with a median of 0.16 (IQR 0.11–0.22) and a mean \pm SD of 0.17 ± 0.08 . In total, 422 patients (27.2%) were classified as frail at baseline (SLICC FI >0.21). There were 370 patients (23.9%) with preexisting organ damage (SDI >0) at baseline and 1,179 patients (76.1%) without baseline organ damage (SDI 0). Baseline SLICC FI scores were higher among patients with baseline organ damage (mean baseline SLICC FI 0.203) than among those without damage at baseline (mean

Table 1. Baseline demographic and clinical characteristics of the SLE patients in the SLICC inception cohort eligible for the analysis of organ damage accrual ($n = 1,549$)*

Age at baseline, mean \pm SD years	35.7 \pm 13.3
Sex	
Female	1,374 (88.7)
Male	175 (11.3)
Race/ethnicity	
White	767 (49.5)
Black	249 (16.1)
Asian	245 (15.8)
Hispanic	236 (15.2)
Other	52 (3.4)
Region	
US	393 (25.4)
Canada	377 (24.3)
Mexico	192 (12.4)
Europe	433 (28.0)
Asia	154 (9.9)
Postsecondary education	782 (51.2)
SLE disease duration, median (IQR) years	1.2 (0.9–1.5)
SLEDAI-2K, median (IQR)	2 (0–6)
Baseline SDI of 0	1,179 (76.1)
Medications	
Glucocorticoids	1,089 (70.3)
Antimalarials	1,048 (67.7)
Immunosuppressive agents	631 (40.8)
Comorbidities	
Antihypertensive agent use	460 (29.8)
Diabetes mellitus	33 (2.2)
Current smoker	224 (14.5)
Body mass index, mean \pm SD kg/m ²	25.7 \pm 6.0
Antiphospholipid antibody positivity	
Lupus anticoagulant	209 (22.8)
Anticardiolipin	119 (13.1)
Anti- β_2 -glycoprotein I	135 (14.8)

* Data were missing for 21 patients (1.4%) for postsecondary education, 5 patients (0.3%) for Systemic Lupus Erythematosus Disease Activity Index 2000 (SLEDAI-2K) score and antihypertensive agent use, 2 patients (0.1%) for antimalarial use and immunosuppressive agent use, 34 patients (2.2%) for diabetes mellitus, 63 patients (4.1%) for body mass index, 631 patients (40.7%) for lupus anticoagulant, and 638 patients (41.2%) for anticardiolipin and anti- β_2 -glycoprotein I. Except where indicated otherwise, values are the number (%). SLE = systemic lupus erythematosus; SLICC = Systemic Lupus International Collaborating Clinics; IQR = interquartile range; SDI = SLICC/American College of Rheumatology Damage Index.

baseline SLICC FI 0.155), and this difference was statistically significant ($P < 0.0001$ by t -test).

Excluded patients. A total of 134 patients (8.0% of the baseline data set) were excluded from this analysis. One patient was excluded due to insufficient baseline data for calculation of a baseline SLICC FI score. The remaining 133 patients were excluded due to lack of available follow-up data to model changes in SDI score. Eight patients died prior to their next follow-up visit, while 125 patients were lost to clinic follow-up. There were no significant baseline differences between excluded and nonexcluded patients with respect to age, sex, education level, marital status, cigarette smoking, SLEDAI-2K score, therapeutic exposures, or specific SLE manifestations (data not shown). There were differences between the excluded and nonexcluded patients with regard to race/ethnicity, which were largely explained by a higher proportion of excluded patients at study sites within the US (data not shown). SLE disease duration at baseline was longer among excluded patients (median 15.6 months versus 14.0 months among nonexcluded patients; $P = 0.003$). Baseline SDI scores were slightly higher among excluded patients (mean 0.54 versus 0.40 among nonexcluded patients; $P = 0.05$). However, this difference in baseline SDI values was no longer statistically significant after accounting for differences in baseline disease duration.

Organ damage accrual. Over a mean \pm SD follow-up of 7.2 ± 3.7 years and 11,189 patient-years, there were 896 patients (57.8%) with no change in SDI score. There were 332 patients (21.4%) with an increase of 1, 178 patients (11.5%) with an increase of 2, and 143 patients (9.2%) with an increase of ≥ 3 in SDI score during follow-up.

Baseline SLICC FI and organ damage accrual. Patients classified as frail at baseline demonstrated a rate of increase in SDI per patient-year of follow-up that was twice the rate observed among patients who were classified as nonfrail, with an incidence rate ratio (IRR) of 1.98 (95% confidence interval [95% CI] 1.68–2.34). Patients with damage at baseline (SDI >0) demonstrated a higher rate of change in SDI score during follow-up compared to patients without baseline organ damage (IRR 1.70 [95% CI 1.43–2.01]).

Unadjusted models for organ damage accrual. In unadjusted analysis, each 0.05 increase in baseline SLICC FI was associated with a 26% increase in the rate of change in the SDI (IRR 1.26 [95% CI 1.20–1.33]). Similarly, each 1-point increase in baseline SDI was associated with a 31% increase in the rate of subsequent damage accrual (IRR 1.31 [95% CI 1.20–1.43]). When baseline SLICC FI (IRR 1.23 [95% CI 1.17–1.30]) and baseline SDI (IRR 1.19 [95% CI 1.09–1.31]) were included in the same model, both measures maintained independent associations with the rate of damage accrual.

Identification of other factors associated with damage accrual in univariable analysis. Older age, male sex, glucocorticoid use, immunosuppressive agent use, and higher disease activity (SLEDAI-2K) at baseline were associated with a higher rate of increase in the SDI score during follow-up (Table 2).

Table 2. Univariable negative binomial regression models for the association of baseline demographic and clinical variables with the change in SDI score during follow-up among SLE patients in the SLICC inception cohort (n = 1,549)*

Independent variable	IRR (95% CI)	P
Baseline age (years)	1.015 (1.010–1.020)	<0.0001
Male sex	1.66 (1.33–2.07)	<0.0001
Race/ethnicity		
White	Referent	–
Hispanic	1.37 (1.09–1.73)	0.007
Black	1.82 (1.46–2.26)	<0.001
Asian	0.72 (0.56–0.92)	0.008
Other	1.55 (1.04–2.31)	0.030
Geographic location		
US	Referent	–
Canada	0.53 (0.42–0.66)	<0.001
Mexico	0.77 (0.59–1.02)	0.064
Europe	0.52 (0.42–0.64)	<0.001
Asia	0.38 (0.28–0.52)	<0.001
Postsecondary education†		
No	Referent	–
Yes	0.80 (0.68–0.95)	0.009
Cigarette smoking		
No	Referent	–
Yes	1.09 (0.87–1.36)	0.449
Glucocorticoid use at baseline		
No	Referent	–
Yes	1.49 (1.24–1.78)	<0.0001
Immunosuppressive agent use at baseline		
No	Referent	–
Yes	1.44 (1.22–1.70)	<0.0001
Antimalarial use at baseline		
No	Referent	–
Yes	0.79 (0.67–0.94)	0.007
SLEDAI-2K at baseline (per 1.0)	1.05 (1.03–1.07)	<0.0001
SLE disease duration at baseline (years)	1.00 (0.99–1.01)	0.528
Lupus anticoagulant positivity at baseline‡		
No	Referent	–
Yes	1.19 (0.94–1.50)	0.152
Anticardiolipin positivity at baseline‡		
No	Referent	–
Yes	1.23 (0.92–1.65)	0.164
Anti-β ₂ -glycoprotein I positivity at baseline‡		
No	Referent	–
Yes	1.06 (0.76–1.50)	0.727

* IRR = incidence rate ratio; 95% CI = 95% confidence interval (see Table 1 for other definitions).

† A “missing” indicator was included for the 1.4% of patients for whom this data was lacking.

‡ Analysis included 911 patients with complete antiphospholipid antibody data.

Table 3. Multivariable negative binomial regression models for the association of baseline SLICC FI and SDI scores with the change in SDI score during follow-up among SLE patients in the SLICC inception cohort*

	Univariable model (n = 1,549)	Multivariable model (n = 1,539)†
IRR (95% CI)		
Model 1: SLICC FI (per 0.05 increase)	1.26 (1.20–1.33)	1.20 (1.14–1.27)
Model 2: SDI (per 1.0 increase)	1.31 (1.20–1.43)	1.17 (1.07–1.28)
Model 3: SLICC FI and SDI		
SLICC FI (per 0.05 increase)	1.23 (1.17–1.30)	1.19 (1.13–1.25)
SDI (per 1.0 increase)	1.19 (1.09–1.31)	1.10 (1.01–1.21)
Overall model comparisons, LR test statistic (P)		
Model 1 versus model 3	15.35 (<0.001)	5.18 (0.023)
Model 2 versus model 3	67.64 (<0.001)	40.49 (<0.001)
AIC		
Model 1: SLICC FI	3,735.12	3,566.78
Model 2: SDI	3,787.41	3,602.09
Model 3: SLICC FI and SDI	3,721.78	3,563.60

* FI = frailty index; IRR = incidence rate ratio; 95% CI = 95% confidence interval; LR = likelihood ratio; AIC = Akaike's information criterion (see Table 1 for other definitions).

† Adjusted for the baseline characteristics age, sex, glucocorticoid use, antimalarial use, immunosuppressive agent use, ethnicity/location, postsecondary education, and SLEDAI-2K.

Antimalarial use and postsecondary education at baseline were associated with lower rates of damage accrual (Table 2). There were also differences in the rate of increase in the SDI based on race/ethnicity and geographic region (Table 2). Since the effects of race/ethnicity and geographic region could not be evaluated independent of one another, a combined ethnicity/region variable was created for multivariable analysis.

Multivariable models for organ damage accrual. The relationship between the baseline SLICC FI and the rate of increase in the SDI during follow-up remained largely unchanged following multivariable adjustment (Table 3). Each 0.05 increase in the baseline SLICC FI was associated with a 20% increase in the rate of subsequent damage accrual (IRR 1.20 [95% CI 1.14–1.27]) after adjusting for baseline age, sex, glucocorticoid use, antimalarial use, immunosuppressive agent use, ethnicity/location, postsecondary education, and SLEDAI-2K.

Baseline SDI scores also remained significantly associated with the rate of further damage accrual after multivariable adjustment (Table 3). In the multivariable model including both the baseline SLICC FI and baseline SDI as independent variables, both measures maintained statistically significant associations with the rate of increase in the SDI per patient-year of follow-up (Table 3). Compared to the models containing either the baseline SLICC FI or the baseline SDI alone, the model containing both baseline SLICC FI and SDI scores was superior for predicting the rate of subsequent damage accrual (Table 3). In particular, the addition of the baseline SLICC FI to the model containing

the baseline SDI alone was associated with significant improvement in model fit (for model 2 versus model 3, likelihood ratio test statistic 40.49 [$P < 0.001$]) and relative predictive quality (AIC 3602.1 for model 2 versus 3563.6 for model 3).

Results of the sensitivity analysis. The association between higher baseline SLICC FI values and higher rates of damage accrual remained statistically significant when the above analyses were repeated after removing all SDI-related items from the SLICC FI (Table 4). We also repeated the above analyses in the subgroup of patients without preexisting organ damage (SDI 0) at baseline. Among these 1,179 patients, those classified as frail at baseline (SLICC FI > 0.21) accrued organ damage at a rate that was 89% higher than in nonfrail individuals (IRR 1.89 [95% CI 1.51–2.36]). In multivariable analysis, each 0.05 increase in baseline SLICC FI was associated with a 21% increase in the rate of change in the SDI during follow-up (IRR 1.21 [95% CI 1.14–1.30]) after adjusting for baseline age, sex, glucocorticoid use, antimalarial use, immunosuppressive agent use, ethnicity/location, postsecondary education, and SLEDAI-2K.

The main analyses were then repeated in subgroups stratified by follow-up time (Table 5). The relationship between baseline SLICC FI scores and subsequent damage accrual was maintained in all subgroups, with the exception of the small subset of patients ($n = 188$) who were followed up for ≤ 2.5 years after their baseline assessment. This may have been related to the small sample size,

Table 4. Negative binomial regression models for the association of baseline SLICC FI and SDI scores with the change in SDI score during follow-up among SLE patients, excluding damage-related health deficits from the SLICC FI*

	Univariable model ($n = 1,549$)	Multivariable model ($n = 1,539$)†
IRR (95% CI)		
Model 1: SLICC FI (per 0.05 increase)‡	1.17 (1.12–1.21)	1.13 (1.09–1.17)
Model 2: SDI (per 1.0 increase)	1.31 (1.20–1.43)	1.17 (1.07–1.28)
Model 3: SLICC FI and SDI		
SLICC FI (per 0.05 increase)‡	1.15 (1.11–1.20)	1.12 (1.08–1.16)
SDI (per 1.0 increase)	1.26 (1.15–1.37)	1.15 (1.05–1.25)
Overall model comparisons, LR test statistic (P)		
Model 1 versus model 3	26.46 (< 0.0001)	10.74 (0.001)
Model 2 versus model 3	61.25 (< 0.0001)	35.72 (0.0001)
AIC		
Model 1: SLICC FI	3,752.61	3,577.12
Model 2: SDI	3,787.41	3,602.09
Model 3: SLICC FI and SDI	3,728.16	3,568.37

* IRR = incidence rate ratio; 95% CI = 95% confidence interval; LR = likelihood ratio; AIC = Akaike’s information criterion (see Table 1 for other definitions).

† Adjusted for the baseline characteristics age, sex, glucocorticoid use, antimalarial use, immunosuppressive agent use, ethnicity/location, postsecondary education, and SLEDAI-2K.

‡ Baseline SLICC frailty index (FI) calculated using the 33 health deficits not related to organ damage.

Table 5. Negative binomial regression models for the association between baseline SLICC FI values and the change in SDI score during follow-up among SLE patients, stratified by follow-up time*

	Univariable model	Full multivariable model†
Cut point 2.5 years follow-up		
≤ 2.5 years follow-up ($n = 188$)	1.09 (0.91–1.30)	0.93 (0.77–1.11)
> 2.5 years follow-up ($n = 1,361$)	1.27 (1.21–1.34)	1.22 (1.16–1.29)
Cut point 5.0 years follow-up		
≤ 5.0 years follow-up ($n = 486$)	1.23 (1.11–1.36)	1.15 (1.04–1.27)
> 5.0 years follow-up ($n = 1,063$)	1.26 (1.19–1.33)	1.22 (1.15–1.29)
Cut point 7.5 years follow-up		
≤ 7.5 years follow-up ($n = 825$)	1.22 (1.14–1.32)	1.14 (1.06–1.22)
> 7.5 years follow-up ($n = 724$)	1.30 (1.22–1.37)	1.25 (1.17–1.34)
Cut point 10.0 years follow-up		
≤ 10.0 years follow-up ($n = 1,184$)	1.26 (1.19–1.33)	1.18 (1.12–1.26)
> 10.0 years follow-up ($n = 365$)	1.27 (1.17–1.38)	1.22 (1.12–1.34)
Cut point 12.5 years follow-up		
≤ 12.5 years follow-up ($n = 1,395$)	1.25 (1.18–1.32)	1.19 (1.13–1.25)
> 12.5 years follow-up ($n = 154$)	1.42 (1.25–1.62)	1.35 (1.16–1.56)

* Values are the incidence rate ratio per 0.05 increase in baseline SLICC frailty index (FI) score (95% confidence interval). See Table 1 for other definitions.

† Adjusted for the baseline characteristics age, sex, glucocorticoid use, antimalarial use, immunosuppressive agent use, ethnicity/location, postsecondary education, and SLEDAI-2K.

as well as a low event rate, as most of these patients (75.5%; $n = 142$) did not experience any damage accrual during follow-up.

DISCUSSION

In a well-characterized, international cohort of recently diagnosed SLE patients, we have demonstrated an association between higher baseline SLICC FI values and higher rates of increase in the SDI during follow-up, independent of other demographic and clinical characteristics known to predict damage accrual in SLE. This finding adds to our previous work that demonstrated that the SLICC FI predicts mortality in SLE (15) and further supports the notion that the SLICC FI is a valid and robust measure for predicting clinically meaningful outcomes among SLE patients.

The association between the SLICC FI and organ damage accrual in SLE is consistent with prior work investigating frailty in nonlupus populations. For example, in addition to mortality, frailty indices can predict other important health outcomes, including falls, fractures, health service utilization, hospitalizations, institutionalization, and multimorbidity (11–13,36,37). The ability of baseline SLICC FI values to predict future damage accrual is also consistent with the theoretical basis of the deficit accumulation approach to frailty. Since frailty represents a loss of physiologic reserve with resultant inability to withstand future insults (8), it is expected that SLE patients with higher baseline SLICC FI values will be more likely to sustain organ damage when faced with new health threats.

Given the importance of preexisting damage, measured using the SDI, for predicting subsequent damage accumulation

in SLE (19,21,22), some may question whether the ability of the SLICC FI to predict damage accrual is heavily reliant upon the baseline SDI score. However, our sensitivity analysis demonstrated persistence of the relationship between baseline SLICC FI values and the rate of damage accrual during follow-up even when all SDI-related items were removed from the index. This suggests that it is not only organ damage, but the global effect of deficit accumulation, that drives the association between baseline SLICC FI values and the rate of subsequent damage accrual. This highlights a key strength of the deficit accumulation approach to frailty—it is the cumulative impact of all health deficits, and not the specific nature of the individual deficits, that is important (9,38).

We found that the baseline SLICC FI and the baseline SDI were both significant predictors of the rate of damage accrual during follow-up. Thus, these two instruments are likely measuring separate constructs that each provide valuable prognostic information. Since many SLE patients will remain free of organ damage captured by the SDI for several years after diagnosis (20), the added prognostic value of the SLICC FI when compared with the SDI may be most evident early in the disease course. For example, even in our subgroup analysis of patients without organ damage at baseline, the baseline SLICC FI remained a significant predictor of damage accrual over time.

Importantly, this study focused on predictors of damage accrual based on information available to clinicians early in the course of incident SLE. As a result, our analysis does not account for the complex variations in disease activity, therapeutic exposures, and frailty that subsequently occur over the course of follow-up. While the current analysis provides relevant information for clinical decision-making early in disease, the impact of changes in frailty over time on the risk of adverse outcomes remains to be determined. Future work will investigate how the trajectories of SLICC FI scores over multiple time points are related to the risk of future adverse health outcomes in incident SLE. It would also be valuable to determine whether SLICC FI scores are more strongly associated with the development of certain types of organ damage. While damage accrual in this sample was not sufficient to facilitate an analysis of the association between baseline SLICC FI values and individual damage items, this is an objective for future studies.

Our study has some limitations. First, observation time differed between patients, which could introduce bias if the association between the SLICC FI and damage accrual were to vary depending on follow-up time. However, our sensitivity analysis stratified by length of follow-up demonstrated a consistent association between baseline SLICC FI values and the rate of damage accrual across strata, suggesting that this was not a major concern. Second, our analysis assumed a constant rate of damage accrual throughout the follow-up period and thus could not account for potential accelerations or decelerations in the average

rate of change in SDI score over time. However, consistent with the results of previous studies conducted in a variety of different health care systems (19,21,39,40), we found a steady, linear rate of increase in mean SDI score during follow-up, suggesting that our assumption about the constant rate of damage accrual among SLE patients is valid. Third, 277 patients (15.2% of the SLICC cohort) were excluded due to missing baseline or follow-up data. This raises the possibility of selection bias due to exclusion of more severe SLE cases with early mortality. However, the demographic and clinical characteristics of the patients included in our analysis were comparable to those of the excluded patients, and were similar to those reported in previous studies of the SLICC cohort (19,30), suggesting that our data set remained representative of the overall cohort. Last, it should be acknowledged that the SLICC FI has been constructed and evaluated in a cohort of relatively young, incident SLE patients. It remains unclear whether these findings can be generalized to older patients with longstanding SLE. Therefore, external validation of the SLICC FI in prevalent SLE cohorts is required.

In conclusion, the SLICC FI predicts damage accrual among patients with SLE, which is clinically relevant given the association of organ damage with increased mortality risk (19–24), lower quality of life (19,27), and increased health care costs (25). The SLICC FI holds potential value as a prognostic tool for identifying SLE patients who are at increased risk for the development of significant organ damage. Since frailty is potentially reversible (1), the SLICC FI may also be useful as an outcome measure in future intervention studies.

AUTHOR CONTRIBUTIONS

All authors were involved in drafting the article or revising it critically for important intellectual content, and all authors approved the final version to be published. Dr. Hanly had full access to all of the data in the study and takes responsibility for the integrity of the data and the accuracy of the data analysis.

Study conception and design. Legge, Kirkland, Rockwood, Andreou, Romero-Diaz, Merrill, Fortin, Gladman, Urowitz, Bruce, Alarcón, Petri, Khamashta, Zoma, Nived, Askanase, Hanly.

Acquisition of data. Legge, Kirkland, Rockwood, Andreou, Bae, Gordon, Romero-Diaz, Sanchez-Guerrero, Wallace, Bernatsky, Clarke, Merrill, Ginzler, Fortin, Gladman, Urowitz, Bruce, Isenberg, Rahman, Alarcón, Petri, Khamashta, Dooley, Ramsey-Goldman, Manzi, Zoma, Aranow, Mackay, Ruiz-Irastorza, Lim, Inanc, van Vollenhoven, Nived, Ramos-Casals, Kamen, Kalunian, Jacobsen, Peschken, Askanase, Hanly.

Analysis and interpretation of data. Legge, Kirkland, Rockwood, Andreou, Gordon, Romero-Diaz, Wallace, Bernatsky, Clarke, Fortin, Urowitz, Bruce, Khamashta, Ramsey-Goldman, Zoma, Inanc, van Vollenhoven, Jonsen, Askanase, Hanly.

REFERENCES

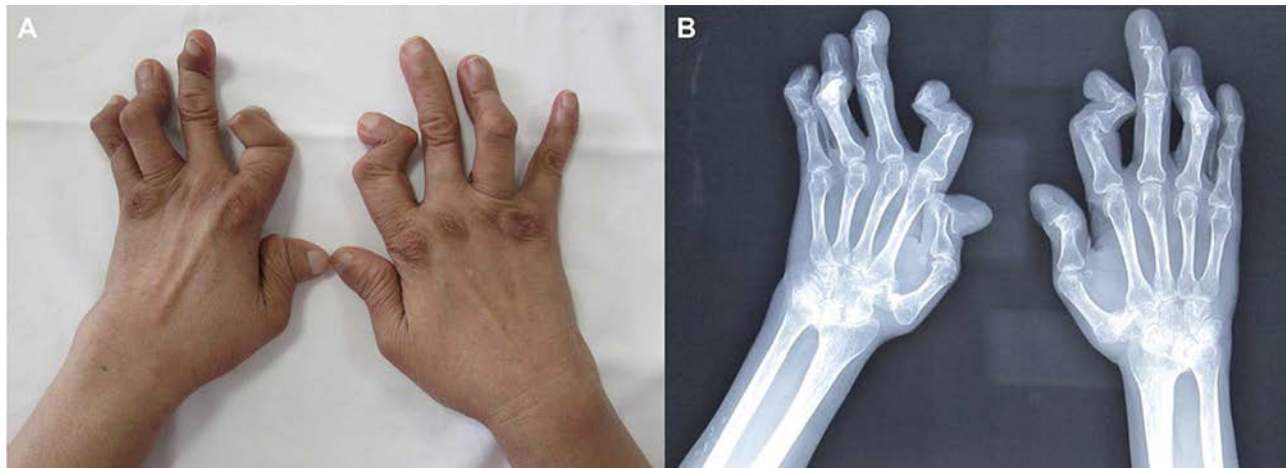
1. Clegg A, Young J, Iliffe S, Rikkert MO, Rockwood K. Frailty in elderly people. *Lancet* 2013;381:752–62.
2. Partridge JS, Harari D, Dhosi JK. Frailty in the older surgical patient: a review. *Age Ageing* 2012;41:142–7.
3. Abel GA, Klepin HD. Frailty and the management of hematologic malignancies. *Blood* 2018;131:515–24.

4. Ness KK, Armstrong GT, Kundu M, Wilson CL, Tchkonja T, Kirkland JL. Frailty in childhood cancer survivors. *Cancer* 2015; 121:1540–7.
5. Brothers TD, Kirkland S, Guaraldi G, Falutz J, Theou O, Johnston BL, et al. Frailty in people aging with human immunodeficiency virus (HIV) infection. *J Infect Dis* 2014;210:1170–9.
6. Fulop T, Larbi A, Witkowski JM, McElhaney J, Loeb M, Mitnitski A, et al. Aging, frailty and age-related diseases. *Biogerontology* 2010; 11:547–63.
7. Searle SD, Mitnitski A, Gahbauer EA, Gill TM, Rockwood K. A standard procedure for creating a frailty index. *BMC Geriatr* 2008; 8:24.
8. Mitnitski A, Rockwood K. Aging as a process of deficit accumulation: its utility and origin. *Interdiscip Top Gerontol* 2015;40: 85–98.
9. Theou O, Walston J, Rockwood K. Operationalizing frailty using the frailty phenotype and deficit accumulation approaches. *Interdiscip Top Gerontol Geriatr* 2015;41:66–73.
10. Mitnitski A, Song X, Skoog I, Broe GA, Cox JL, Grunfeld E, et al. Relative fitness and frailty of elderly men and women in developed countries and their relationship with mortality. *J Am Geriatr Soc* 2005; 53:2184–9.
11. Rockwood MR, MacDonald E, Sutton E, Rockwood K, Canadian Scleroderma Research Group, Baron M. Frailty index to measure health status in people with systemic sclerosis. *J Rheumatol* 2014;41:698–705.
12. Rockwood K, Song X, Mitnitski A. Changes in relative fitness and frailty across the adult lifespan: evidence from the Canadian National Population Health Survey. *CMAJ* 2011;183:E487–94.
13. Guaraldi G, Brothers TD, Zona S, Stentarelli C, Carli F, Malagoli A, et al. A frailty index predicts survival and incident multimorbidity independent of markers of HIV disease severity. *AIDS* 2015;29:1633–41.
14. Legge A, Kirkland S, Rockwood K, Andreou P, Bae SC, Gordon C, et al. Construction of a frailty index as a novel health measure in systemic lupus erythematosus. *J Rheumatol* 2019. E-pub ahead of print.
15. Legge A, Kirkland S, Rockwood K, Andreou P, Bae SC, Gordon C, et al. Evaluating the properties of a frailty index and its association with mortality risk among patients with systemic lupus erythematosus. *Arthritis Rheumatol* 2019;71:1297–307.
16. Strand V, Chu AD. Measuring outcomes in systemic lupus erythematosus clinical trials. *Expert Rev Pharmacoecon Outcomes Res* 2011;11:455–68.
17. Gladman D, Ginzler E, Goldsmith C, Fortin P, Liang M, Urowitz M, et al. The development and initial validation of the Systemic Lupus International Collaborating Clinics/American College of Rheumatology damage index for systemic lupus erythematosus. *Arthritis Rheum* 1996;39:363–9.
18. Gladman DD, Urowitz MB, Goldsmith CH, Fortin P, Ginzler E, Gordon C, et al. The reliability of the Systemic Lupus International Collaborating Clinics/American College of Rheumatology damage index in patients with Systemic Lupus Erythematosus. *Arthritis Rheum* 1997;40:809–13.
19. Bruce IN, O’Keeffe AG, Farewell V, Hanly JG, Manzi S, Su L, et al. Factors associated with damage accrual in patients with systemic lupus erythematosus: results from the Systemic Lupus International Collaborating Clinics (SLICC) Inception Cohort. *Ann Rheum Dis* 2015;74:1706–13.
20. Sutton EJ, Davidson JE, Bruce IN. The Systemic Lupus International Collaborating Clinics (SLICC) damage index: a systematic literature review. *Semin Arthritis Rheum* 2013;43:352–61.
21. Alarcón GS, Roseman JM, McGwin G Jr, Uribe A, Bastian HM, Fessler BJ, et al. Systemic lupus erythematosus in three ethnic groups. XX. Damage as a predictor of further damage. *Rheumatology (Oxford)* 2004;43:202–5.
22. Cardoso CR, Signorelli FV, Papi JA, Salles GF. Initial and accrued damage as predictors of mortality in Brazilian patients with systemic lupus erythematosus: a cohort study. *Lupus* 2008;17: 1042–8.
23. Rahman P, Gladman DD, Urowitz MB, Hallett D, Tam LS. Early damage as measured by the SLICC/ACR damage index is a predictor of mortality in systemic lupus erythematosus. *Lupus* 2001;10:93–6.
24. Nived O, Jönsen A, Bengtsson AA, Bengtsson C, Sturfelt G. High predictive value of the Systemic Lupus International Collaborating Clinics/American College of Rheumatology damage index for survival in systemic lupus erythematosus [abstract]. *J Rheumatol* 2002;29:1398–400.
25. Jönsen A, Bengtsson AA, Hjalte F, Petersson IF, Willim M, Nived O. Total cost and cost predictors in systemic lupus erythematosus—8-years follow-up of a Swedish inception cohort. *Lupus* 2015;24:1248–56.
26. Björk M, Dahlström Ö, Wetterö J, Sjöwall C. Quality of life and acquired organ damage are intimately related to activity limitations in patients with systemic lupus erythematosus. *BMC Musculoskelet Disord* 2015;16:188.
27. Mok CC, Ho LY, Cheung MY, Yu KL, To CH. Effect of disease activity and damage on quality of life in patients with systemic lupus erythematosus: a 2-year prospective study. *Scand J Rheumatol* 2009;38:121–7.
28. Hochberg MC. for the Diagnostic and Therapeutic Criteria Committee of the American College of Rheumatology. Updating the American College of Rheumatology revised criteria for the classification of systemic lupus erythematosus [letter]. *Arthritis Rheum* 1997;40:1725.
29. ACR Ad Hoc Committee on Neuropsychiatric Lupus Nomenclature. The American College of Rheumatology nomenclature and case definitions for neuropsychiatric lupus syndromes. *Arthritis Rheum* 1999;42:599–608.
30. Hanly JG, Urowitz MB, Sanchez-Guerrero J, Bae SC, Gordon C, Wallace DJ, et al, for the Systemic Lupus International Collaborating Clinics. Neuropsychiatric events at the time of diagnosis of systemic lupus erythematosus: an international inception cohort study. *Arthritis Rheum* 2007;56:265–73.
31. Gladman DD, Ibañez D, Urowitz MB. Systemic lupus erythematosus disease activity index 2000. *J Rheumatol* 2002;29:288–91.
32. Ware JE Jr, Sherbourne CD. The MOS 36-item short-form health survey (SF-36). I. Conceptual framework and item selection. *Med Care* 1992;30:473–83.
33. Hanly JG, Urowitz MB, Siannis F, Farewell V, Gordon C, Bae SC, et al, for the Systemic Lupus International Collaborating Clinics. Autoantibodies and neuropsychiatric events at the time of systemic lupus erythematosus diagnosis: results from an international inception cohort study. *Arthritis Rheum* 2008;58:843–53.
34. Rockwood K, Song X, MacKnight C, Bergman H, Hogan DB, McDowell I, et al. A global clinical measure of fitness and frailty in elderly people. *CMAJ* 2005;173:489–95.
35. Rockwood K, Andrew M, Mitnitski A. A comparison of two approaches to measuring frailty in elderly people. *J Gerontol A Biol Sci Med Sci* 2007;62A:738–43.
36. Rockwood K, Mitnitski A, Song X, Steen B, Skoog I. Long-term risks of death and institutionalization of elderly people in relation to deficit accumulation at age 70. *J Am Geriatr Soc* 2006;54:975–9.

37. Fang X, Shi J, Song X, Mitnitski A, Tang Z, Wang C, et al. Frailty in relation to the risk of falls, fractures, and mortality in older Chinese adults: results from the Beijing Longitudinal Study of Aging. *J Nutr Health Aging* 2012;16:903–7.
38. Rutenberg AD, Mitnitski AB, Farrell SG, Rockwood K. Unifying aging and frailty through complex dynamical networks [review]. *Exp Gerontol* 2018;107:126–9.
39. Gladman DD, Urowitz MB, Rahman P, Ibañez D, Tam LS. Accrual of organ damage over time in patients with systemic lupus erythematosus. *J Rheumatol* 2003;30:1955–9.
40. Frodlund M, Reid S, Wetterö J, Dahlström Ö, Sjöwall C, Leonard D. The majority of Swedish systemic lupus erythematosus patients are still affected by irreversible organ impairment: factors related to damage accrual in two regional cohorts. *Lupus* 2019;28:1261–72.

DOI 10.1002/art.41183


Clinical Images: Jaccoud's arthropathy




The patient, a 55-year-old woman, presented with a 10-year history of progressive deformity of the hands and feet. The patient had been diagnosed as having systemic lupus erythematosus (SLE) 10 years previously, with high-titer antinuclear antibody (ANA) positivity, low complement levels, oral ulcers, arthritis, and deep vein thrombosis in the left leg. The patient did not adhere to treatment and only took low-dose prednisone and warfarin intermittently. There was severe deformation of the interphalangeal joints of the hands (A) and feet, but most of the joints were reducible. ANA, anti-Ro/SSA, and anti-RNP antibodies were all positive; anti-cyclic citrullinated peptide antibodies and rheumatoid factor were absent. Radiography of the hands and wrists showed severe luxation and subluxation of the interphalangeal joints and multiple mild erosive lesions below the articular surfaces of the metacarpal and wrist joints (B). Jaccoud's arthropathy has been described in patients with chronic rheumatic diseases, especially SLE (1). Joint deformity is caused by tendon and ligament laxity. Its features may be easily confused with deformities seen in rheumatoid arthritis. While previously regarded as a nonerosive arthritis, it is now accepted that imaging can reveal erosions (2,3).

Supported by the Peking Union Medical College Medical Education Quality Project 2019 (2019zlgc0104).

1. Ceccarelli F, Massaro L, Perricone C, Pendolino M, Cipriano E, Truglia S, et al. Jaccoud's arthropathy in systemic lupus erythematosus: clinical, laboratory and ultrasonographic features. *Clin Exp Rheumatol* 2017;35:674–7.
2. Park JK, Carrino JA, Baer AN. Occult erosions in Jaccoud arthropathy [letter]. *J Clin Rheumatol* 2012;18:277–8.
3. Santiago MB, Galvão V, Ribeiro DS, Santos WD, da Hora PR, Mota AP, et al. Severe Jaccoud's arthropathy in systemic lupus erythematosus. *Rheumatol Int* 2015;35:1773–7.

Wen Shi, MD
 Yang Jiao, MD, MPH 
 Department of General Internal Medicine,
 Peking Union Medical College Hospital
 and Peking Union Medical College
 Beijing, China

Diagnostic Assessment Strategies and Disease Subsets in Giant Cell Arteritis: Data From an International Observational Cohort

K. Bates Gribbons,¹ Cristina Ponte,² Anthea Craven,³ Joanna C. Robson,⁴ Ravi Suppiah,⁵ Raashid Luqmani,³ Richard Watts,⁶ Peter A. Merkel,⁷ and Peter C. Grayson¹ 

Objective. Diagnostic assessment in giant cell arteritis (GCA) is rapidly changing as vascular imaging becomes more available. This study was undertaken to determine if clinical GCA subsets have distinct profiles or reflect differential diagnostic assessments.

Methods. Patients were recruited from an international cohort and divided into 4 subsets based on a temporal artery (TA) abnormality (positive TA biopsy [TAB] or halo sign on TA ultrasound [TA-US]) and/or evidence of large vessel (LV) involvement on imaging: 1) both TA abnormality and LV involvement (TA+/LV+ GCA); 2) TA abnormality without LV involvement (TA+/LV– GCA); 3) LV involvement without TA abnormality (TA–/LV+ GCA); and 4) clinically diagnosed GCA without LV involvement or TA abnormality (TA–/LV– GCA).

Results. Nine hundred forty-one patients with GCA were recruited from 72 international study sites. Most patients received multiple forms of diagnostic assessment, including TAB (n = 705 [75%]), TA-US (n = 328 [35%]), and LV imaging (n = 534 [57%]). Assessment using TAB, TA-US, and LV imaging confirmed the diagnosis of GCA in 66%, 79%, and 40% of cases, respectively. GCA subsets had distinct profiles independent of diagnostic assessment strategies. TA+/LV– were the most common subset (51%), with a high burden of cranial ischemia. Those in the TA–/LV– subset (26%) had a high prevalence of cranial ischemia and musculoskeletal symptoms. Patients in the TA–/LV+ subset (12%) had prevalent upper extremity vascular abnormalities and a low prevalence of vision loss, and those in the TA+/LV+ subset (11%) were older and had a high prevalence of cranial ischemia, constitutional symptoms, and elevated acute-phase reactant levels.

Conclusion. Vascular imaging is increasingly incorporated into the diagnostic assessment of GCA and identifies clinical subsets of patients based on involvement of temporal and extracranial arteries.

INTRODUCTION

Giant cell arteritis (GCA) is a rare form of vasculitis that causes inflammation of the medium-sized and large arteries. GCA is a heterogeneous disease (1) in which symptoms and the extent of arterial involvement often vary between patients. Traditionally, GCA was thought to be confined to the cranial arteries; however,

many patients also have evidence of large vessel (LV) involvement (2–5). GCA patients with LV involvement often present with different clinical features than are found in patients with cranial GCA, but the extent to which patients have overlapping versus distinct cranial and extracranial disease is not well characterized (5–9).

A temporal artery biopsy (TAB) demonstrating mononuclear cell infiltration or granulomatous inflammation remains the

Supported by the Intramural Research Program at the National Institute of Arthritis and Musculoskeletal and Skin Diseases, NIH (grant ZIA-AR-041199). The Diagnostic and Classification Criteria for Vasculitis study was coordinated at the University of Oxford with support from the NIHR Musculoskeletal Biomedical Research Unit, University of Oxford, Vasculitis Foundation, American College of Rheumatology, and European League Against Rheumatism.

¹K. Bates Gribbons, BS, Peter C. Grayson, MD, MSc: National Institute of Arthritis and Musculoskeletal and Skin Diseases, NIH, Bethesda, Maryland; ²Cristina Ponte, MD: Hospital de Santa Maria and Centro Hospitalar Universitário Lisboa Norte, Lisbon, Portugal; ³Anthea Craven, BS, Raashid Luqmani, MD: University of Oxford, Oxford, UK; ⁴Joanna C. Robson, MD, PhD: University of the West of England, Bristol, UK; ⁵Ravi Suppiah, MD: Auckland District Health Board, Auckland, New Zealand; ⁶Richard Watts, MD: University of East Anglia Norwich Medical School, Norwich, UK, and University of

Oxford, Oxford, UK; ⁷Peter A. Merkel, MD, MPH: University of Pennsylvania, Philadelphia.

Dr. Merkel has received consulting fees from AbbVie, AstraZeneca, Biogen, Boehringer Ingelheim, Bristol-Myers Squibb, Celgene, ChemoCentryx, CSL Behring, Genentech/Roche, Genzyme/Sanofi, GlaxoSmithKline, InflaRx, Insmad, Janssen, Kiniksa, and Sparrow (less than \$10,000 each), research support from AstraZeneca, Boehringer Ingelheim, Bristol-Myers Squibb, Celgene, ChemoCentryx, Genentech/Roche, Genzyme/Sanofi, GlaxoSmithKline, InflaRx, Kypha, and Terumo BCT, and royalties for UpToDate. No other disclosures relevant to this article were reported.

Address correspondence to Peter C. Grayson, MD, MSc, National Institute of Arthritis and Musculoskeletal and Skin Diseases, NIH, 10 Center Drive, Building 10, 10 North Room 311D, Bethesda, MD 20892. E-mail: peter.grayson@nih.gov.

Submitted for publication July 17, 2019; accepted in revised form November 7, 2019.

gold standard for the diagnosis of GCA. Although highly specific by definition, the sensitivity of TABs has decreased over time, highlighting that many patients with GCA are diagnosed without histologic evidence of arteritis (10–13). Patients with suspected GCA are increasingly diagnosed using TA ultrasound (TA-US) (14). A homogeneous, hypoechoic wall thickening of the TA, termed the “halo sign,” has been proposed as a diagnostic equivalent of a positive TAB (15). Additionally, LV imaging has become an increasingly common form of diagnostic assessment and clinical evaluation in GCA. A substantial percentage of patients with GCA, with or without a positive TAB, have LV involvement, with estimates ranging from 20% to 67% by angiography, 83% by ^{18}F -fluorodeoxyglucose–positron emission tomography (^{18}F -FDG-PET) imaging, and 100% by autopsy (2–5,16–18).

Patients can receive a diagnosis of GCA based on a combination of cranial and LV assessments. With the expansion of diagnostic modalities in GCA, the extent to which cranial GCA and LV GCA are distinct entities, or whether co-occurrence is undetected, is poorly understood. The objectives of this study were to 1) detail the assessment strategies currently utilized to diagnose GCA using data collected within a large, international observational cohort and 2) determine if subsets of GCA, defined by TAB and vascular imaging, are associated with distinct clinical profiles or merely reflect differential diagnostic testing.

PATIENTS AND METHODS

Patient selection. The Diagnostic and Classification Criteria for Vasculitis (DCVAS) is an international observational cohort of patients with vasculitis (19,20). Patients were enrolled within 2 years from the time of diagnosis. Only physician-submitted cases, with a diagnosis of GCA confirmed by an expert panel review, were included in this study.

Clinical variables. Comprehensive demographic, clinical, and vascular imaging data were collected using standardized forms. Data were available for the following clinical aspects of disease: visual changes and other symptoms of cranial ischemia; pulmonary, musculoskeletal, and constitutional symptoms; vascular abnormalities; and laboratory findings. All variables were recorded only if present by the time of diagnosis.

Vascular abnormalities. TA physical examination abnormalities were defined as tenderness, diminished or absent pulse, and/or a nodular, cord-like TA. Blood pressure (BP) was recorded in both arms, and BP difference between the arms was categorized as either <10 mm Hg or ≥ 10 mm Hg. Pulse abnormality was defined as diminished or absent pulse in either the upper limbs (subclavian, axillary, brachial, or radial arteries) or lower limbs (femoral, popliteal, posterior tibial, or dorsalis pedis arteries). Bruits in the abdominal aorta, carotid, subclavian, axillary, or renal arteries were recorded.

Laboratory findings. The maximum values of the erythrocyte sedimentation rate (ESR) and C-reactive protein level by the time of diagnosis were recorded. Anemia was defined as hemoglobin <10 gm/dl, hypoalbuminemia was defined as albumin <30 gm/liter, and thrombocytosis was defined as platelet count $>500 \times 10^9$ /liter.

Temporal artery biopsies. TABs were performed at the discretion of the physician. A positive TAB result was recorded if active vasculitis was histologically evident as assessed by the pathologist at the local level.

LV and TA imaging. TA ultrasonography was performed in a subset of patients at the discretion of the submitting physician. A positive TA-US result was recorded if the presence of a halo sign was reported by the submitting physician.

LV involvement was assessed in a subset of patients, using a combination of angiography (magnetic resonance, computed tomography, or catheter-based), ultrasonography, or ^{18}F -FDG-PET imaging. Clinical radiologists or nuclear medicine physicians at each participating institution assessed vascular imaging data. Angiographic and ultrasound damage was defined as stenosis, occlusion, or aneurysm. Wall thickness was not included in the definition of arterial damage. ^{18}F -FDG-PET scans were assessed according to local practices (21). LV involvement was recorded if arterial damage or abnormal FDG uptake was present and attributed to vasculitis, according to the reader, within 14 arterial territories of interest: right and left carotid, subclavian, axillary, iliofemoral, and renal arteries; mesenteric arteries; and ascending, descending, and abdominal aorta.

Subset definitions. Patients were divided into 4 subsets based on TAB, TA-US, and/or LV imaging findings. Patients with evidence of both LV involvement on imaging and either a positive TAB or halo sign on TA-US were classified as having TA+/LV+ GCA. Patients with a TAB showing definite vasculitis or a halo sign seen on TA-US but without evidence of LV involvement on imaging were classified as having TA+/LV– GCA. Patients with evidence of LV involvement on imaging without a positive TAB or halo sign on TA-US were classified as having TA–/LV+ GCA. Patients with a clinical diagnosis of GCA but without evidence of LV involvement on imaging, positive TAB, or a halo sign on TA-US were classified as having TA–/LV– GCA. Clinical differences were analyzed between the 4 subsets.

Restricted cohort. Since TAB, TA-US, and LV imaging assessments were performed at the discretion of the treating physician, patients could have received different diagnostic assessments. To determine the extent to which differences between the subsets were related to clinical differences versus diagnostic bias from differential assessments, analyses were performed in a restricted cohort of patients who received both TA assessment (TAB or TA-US) and LV imaging, and the results were compared to data from the overall cohort.

Statistical analysis. Chi-square, Mann-Whitney, and Kruskal-Wallis tests were used, as appropriate. *P* values less than 0.05 were considered significant. Nominal logistic regression was used to analyze the association between the clinical decision to undergo a specific diagnostic test and clinical features of disease. All analyses were performed using GraphPad Prism V.7.0a.

RESULTS

Patient characteristics. A total of 941 patients with GCA were included, representing 72 study sites, 26 countries, and 5 continents. Demographic information is listed in Table 1.

Diagnostic assessment strategies in the DCVAS cohort. Patients received vascular assessments at the submitting physician's discretion. In general, 705 patients (75%) had a TAB, 328 patients (35%) had TA-US, 534 patients (57%) had LV imaging, and 431 patients (45.8%) had both LV and TA assessments (Table 1). Only 33 patients (3.5%) did not have any diagnostic testing performed beyond clinical assessment (see Supplementary Table 1, available on the *Arthritis & Rheumatology* web site at <http://onlinelibrary.wiley.com/doi/10.1002/art.41165/abstract>).

Diagnostic assessment by demographics. The use of the various diagnostic assessments differed between patients based on demographics, including age and sex. Male patients were more likely to undergo a TAB compared to female patients (male 81.4% versus female 71.6%; *P* = 0.001). In logistic regression models, male patients were 34% more likely to undergo a TAB compared to female patients independent of symptoms of cranial ischemia, age at diagnosis, TA

abnormality on physical examination, and LV involvement on imaging (see Supplementary Table 2, available on the *Arthritis & Rheumatology* web site at <http://onlinelibrary.wiley.com/doi/10.1002/art.41165/abstract>). There was no difference in the rate of TA-US by sex (male 36.8% versus female 33.9%; *P* = 0.38) or LV imaging (male 57.7% versus female 56.3%; *P* = 0.70). Male and female patients were equally likely to have a positive TAB (male 61.6% versus female 64.3%; *P* = 0.51) and evidence of LV involvement on imaging (male 36.2% versus female 42.6%; *P* = 0.16). Male patients were more likely than female patients to have a halo sign on TA-US (85.0% versus 75.4%; *P* = 0.05).

Patients who underwent TAB were older (mean 73.4 years versus 70.5 years; *P* < 0.0001), and patients who had LV imaging were younger (mean 71.9 years versus 73.8 years; *P* = 0.0009). There was no significant difference in age between patients who did and those who did not undergo a TA-US (mean 72.8 years versus 72.6 years; *P* = 0.71).

Diagnostic assessment by continent. Diagnostic assessment differed among patients based on the continent in which they were seen. The percentage of patients who underwent a TAB did not differ significantly between continents (North America 82.8%, Europe 73.1%, Asia 82.8%, Oceania [defined as the islands of the Central and South Pacific, including Australia] 88.9%) (Figure 1). Patients from European centers were more likely to have undergone TA-US (North America 2.7%, Europe 41.0%, Asia 13.8%, Oceania 0.0%). LV imaging was performed in approximately half of patients from North American, European, and Asian centers, but less commonly in Oceanian centers (North America 58.6%, Europe 57.7%, Asia 51.7%, Oceania 11.1%).

Table 1. Demographic characteristics and diagnostic assessment of giant cell arteritis patients in the overall cohort and by subset*

	Overall (n = 941)	TA-/LV- (n = 245)	TA+/LV- (n = 480)	TA+/LV+ (n = 100)	TA-/LV+ (n = 116)
Age, mean ± SD years†	72.6 ± 9.0	71.0 ± 8.5	74.1 ± 9.2	74.2 ± 7.9	68.6 ± 8.6
Female‡	634 (67.4)	173 (70.6)	309 (64.4)	64 (64.0)	88 (75.9)
Continent					
Europe	783 (83.2)	187 (23.9)	411 (52.4)	92 (11.8)	93 (11.9)
North America	111 (11.8)	38 (34.2)	50 (45.1)	5 (4.5)	18 (16.2)
Asia	29 (3.1)	15 (51.7)	7 (24.1)	3 (10.3)	4 (13.8)
Oceania	18 (1.9)	5 (27.8)	12 (66.7)	0 (0.0)	1 (5.6)
Diagnostic assessment					
TAB	705 (75.0)	174 (71.0)	430 (89.6)	74 (74.0)	27 (23.3)
TA-US	328 (35.0)	22 (9.0)	225 (46.9)	61 (61.0)	20 (17.2)
LV imaging	534 (57)	90 (36.7)	228 (47.3)	100 (100)	116 (100)
Angiography	227 (24.1)	54 (22.1)	65 (13.5)	52 (52.0)	56 (48.3)
Ultrasonography	307 (32.6)	36 (14.8)	160 (33.3)	58 (58.0)	53 (45.7)
¹⁸ F-FDG-PET	175 (18.6)	21 (8.6)	29 (6.0)	45 (45.0)	80 (69.0)
Comprehensive§	431 (45.8)	59 (24.1)	227 (47.3)	100 (100)	45 (38.8)

* Except where indicated otherwise, values are the number (%). TA-/LV- = patients without evidence of temporal artery (TA) or large vessel (LV) involvement; TA+/LV- = patients with TA involvement; TA+/LV+ = patients with both TA and LV involvement; TA-/LV+ = patients with LV involvement; TAB = TA biopsy; TA-US = TA ultrasound; ¹⁸F-FDG-PET = ¹⁸F-fluorodeoxyglucose-positron emission tomography.

† *P* < 0.001, by Kruskal-Wallis test comparing across all subgroups.

‡ *P* = 0.049, by Kruskal-Wallis test comparing across all subgroups.

§ A comprehensive diagnostic assessment was performed on patients who underwent both TA and LV assessments.

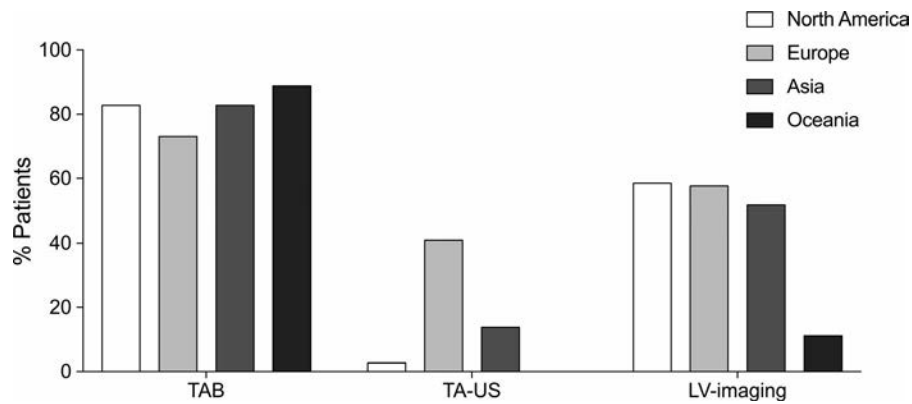


Figure 1. Diagnostic assessment of giant cell arteritis by continent. The percentage of patients with giant cell arteritis who underwent a temporal artery biopsy (TAB), temporal artery ultrasound (TA-US), or large vessel (LV) imaging from North American, European, Asian, and Oceanian study centers was calculated.

Patients receiving multiple forms of diagnostic assessment. Most patients underwent multiple forms of diagnostic assessment. The majority of patients who underwent a TAB received additional vascular imaging regardless of the TAB result (TAB positive 57.2%, TAB negative 56.2%) (see Supplementary Table 1, available on the *Arthritis & Rheumatology* web site at <http://onlinelibrary.wiley.com/doi/10.1002/art.41165/abstract>). Vascular imaging was performed in 86.1% of patients who did not receive TAB (Supplementary Table 1 and Figure 2). Disease was confirmed in 70.0% of these patients. TA-US was rarely used alone as a form of vascular assessment. Only 1.1% of patients received TA-US without another form of vascular assessment, compared to 10.9% of patients who received only LV imaging and 32.3% of patients who received only TAB.

TAB results were not associated with LV imaging or TA-US results (Figure 2). Patients with a positive TAB and those with a negative TAB were equally likely to have evidence of LV involvement on imaging (positive TAB 31% versus negative TAB 27%; $P = 0.54$). Similarly, patients with a positive TAB and those with a negative TAB were equally likely to have a halo sign on TA-US (positive TAB 82% versus negative TAB 76%; $P = 0.38$).

Clinical GCA subsets in the overall cohort. Subsets of GCA were defined according to cranial and LV involvement. Among the overall cohort, patients were characterized into 1 of 4 subsets: 480 patients (51.0%) as having TA+/LV- GCA, 245 patients (26.0%) as having TA-/LV- GCA, 116 patients (12.3%) as having TA-/LV+ GCA, and 100 patients (10.6%) as having

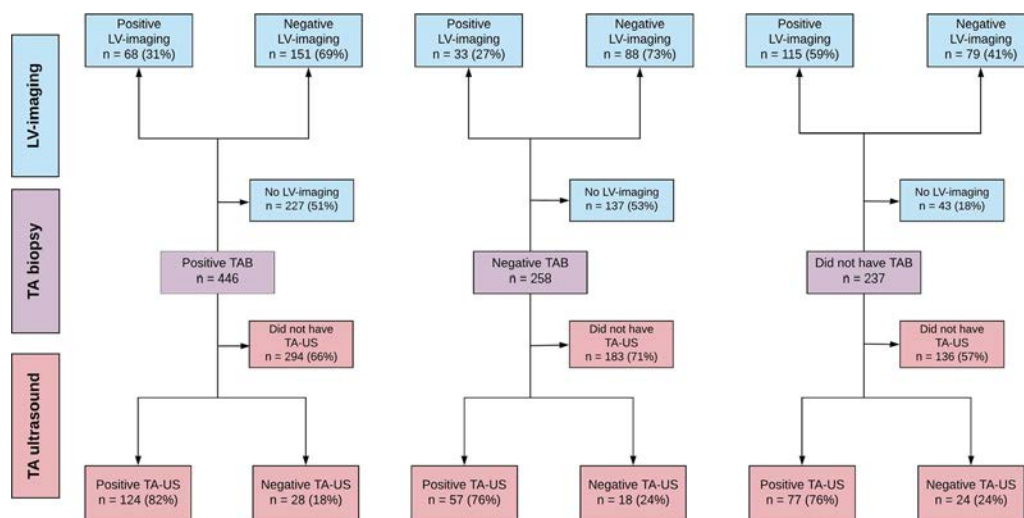


Figure 2. Diagnostic assessment of giant cell arteritis (GCA) by temporal artery biopsy (TAB) results. Large vessel (LV) imaging and temporal artery ultrasound (TA-US) results were stratified by whether TAB was diagnostic for GCA (positive TAB), was nondiagnostic for GCA (negative TAB), or was not performed (did not have TAB). A positive TA-US result was recorded based on the presence of a halo sign. A positive LV imaging result was recorded based on evidence of vasculitic involvement of the aorta or branch arteries on angiography, ultrasonography, or ^{18}F -fluorodeoxyglucose-positron emission tomography imaging.

TA+/LV+ GCA. Demographic characteristics and assessment strategies in the overall cohort and by subset are shown in Table 1.

Clinical GCA subsets in the restricted cohort. Clinical subsets of GCA were characterized in a restricted cohort of patients who had both temporal and large artery assessments. Of the 431 patients in the restricted cohort (46% of the overall cohort), 340 (79%) underwent TAB, 258 (60%) underwent TA-US, and all patients received LV imaging. Compared to patients who did not have assessment of both the temporal and large arteries, patients who had comprehensive assessment were older, more likely male, and presented more frequently with fever, weight loss,

syncope, scalp tenderness, arm claudication, upper extremity pulse abnormality, or elevated ESR ($P < 0.01$). All 4 clinical subgroups were again represented in the restricted cohort, including 59 patients (14%) in the TA-/LV- GCA subset, 227 patients (53%) in the TA+/LV- GCA subset, 100 patients (23%) in the TA+/LV+ GCA subset, and 45 patients (10%) in the TA-/LV+ GCA subset (Table 2).

Subset diagnosed by TAB or TA-US in the restricted cohort. Patients in the TA+/LV- GCA subset had a high prevalence of TA abnormalities on physical examination, visual changes, and other symptoms of cranial ischemia, including amaurosis fugax, sudden ongoing vision loss, jaw claudication, scalp tenderness,

Table 2. Clinical associations in patients with giant cell arteritis who had both TA and LV assessments (restricted cohort)*

	TA-/LV- (n = 59)	TA+/LV- (n = 227)	TA+/LV+ (n = 100)	TA-/LV+ (n = 45)	P
Age, mean \pm SD years	69.34 \pm 7.54	73.67 \pm 7.98	74.17 \pm 7.93	70.31 \pm 9.32	<0.001
Female	41 (69.5)	142 (62.6)	64 (64.0)	28 (62.2)	0.794
Diagnostic assessment, no./no. assessed					
Positive TAB	0/54	151/185	68/74	0/27	<0.001
Halo sign on TA-US	0/14	148/163	55/61	0/20	<0.001
Temporal artery abnormality	20 (33.9)	145 (63.9)	51 (51.0)	7 (15.6)	<0.001
Visual changes	19 (32.2)	82 (36.1)	25 (25.0)	7 (15.6)	0.03
Amaurosis fugax	7 (11.9)	37 (16.3)	6 (6.0)	4 (8.9)	0.06
Sudden visual loss	9 (15.3)	34 (14.9)	9 (9.0)	1 (2.2)	0.06
Blurred vision	8 (13.6)	38 (16.7)	16 (16.0)	5 (11.1)	0.77
Ischemic cranial symptoms	53 (89.8)	201 (88.5)	78 (78.0)	24 (53.3)	<0.001
Jaw claudication	25 (42.4)	125 (55.1)	42 (42.0)	10 (22.2)	<0.001
Scalp tenderness	22 (37.3)	68 (29.9)	21 (21.0)	10 (22.2)	0.11
Headache	49 (83.1)	178 (78.4)	69 (69.0)	20 (44.4)	<0.001
Pulmonary symptoms	6 (10.2)	24 (10.6)	16 (16.0)	9 (20.0)	0.22
Dyspnea	4 (6.8)	10 (4.4)	9 (9.0)	2 (4.4)	0.40
Nonproductive cough	3 (5.1)	16 (7.1)	8 (8.0)	8 (17.8)	0.08
Musculoskeletal symptoms	28 (47.5)	88 (38.8)	45 (45.0)	22 (48.9)	0.41
Morning stiffness >1 hour	16 (27.1)	34 (14.9)	14 (14.0)	7 (15.6)	0.12
Neck or torso	8 (13.6)	19 (8.4)	8 (8.0)	8 (17.8)	0.17
Hip and thighs	12 (20.3)	33 (14.5)	15 (15.0)	6 (13.3)	0.71
Muscle tenderness	11 (18.6)	17 (7.5)	13 (13.0)	1 (2.2)	0.01
Myalgia	17 (28.8)	67 (29.5)	33 (33.0)	12 (26.7)	0.87
Vascular abnormalities	24 (40.7)	58 (25.6)	37 (37.0)	18 (40.0)	0.03
Arm claudication	5 (8.5)	1 (0.44)	1 (1.0)	6 (13.3)	<0.001
Leg claudication	8 (13.6)	6 (2.6)	4 (4.0)	2 (4.4)	0.005
Any bruit	9 (15.3)	18 (7.9)	16 (16.0)	8 (17.8)	0.06
Pulse abnormality					
Upper limb	2 (3.4)	3 (1.3)	4 (4.0)	8 (17.8)	<0.001
Lower limb	4 (6.8)	20 (8.8)	15 (15.0)	4 (8.9)	0.27
Absent blood pressure	0 (0.0)	0 (0.0)	1 (1.0)	1 (2.2)	0.17
Blood pressure difference	14 (23.7)	31 (13.7)	15 (15.0)	11 (24.4)	0.12
Constitutional symptoms	33 (55.9)	117 (51.5)	68 (68.0)	28 (62.2)	0.04
Night sweats	12 (20.3)	52 (22.9)	29 (29.0)	13 (18.9)	0.49
Fever, >38°C	15 (25.4)	45 (19.8)	30 (30.0)	13 (28.9)	0.19
Weight loss	21 (35.6)	80 (35.2)	52 (52.0)	20 (44.4)	0.03
Laboratory findings	24 (40.7)	66 (29.1)	38 (38.0)	15 (33.3)	0.23
ESR, mean \pm SD mm/hour	75.8 \pm 34	69.2 \pm 31	80.9 \pm 32	80.6 \pm 31	0.009
CRP, median (range) mg/liter	51.7 (22–150)	68 (34–128)	75.9 (46–139)	50 (26–90)	0.06
Anemia	11 (18.6)	25 (11.0)	22 (22.0)	15 (33.3)	0.001
Hypoalbuminemia	12 (20.3)	30 (13.2)	24 (24.0)	7 (15.6)	0.10
Thrombocytosis	26 (27.1)	35 (15.4)	25 (25.0)	11 (24.4)	0.07

* Except where indicated otherwise, values are the number (%). ESR = erythrocyte sedimentation rate; CRP = C-reactive protein (see Table 1 for other definitions).

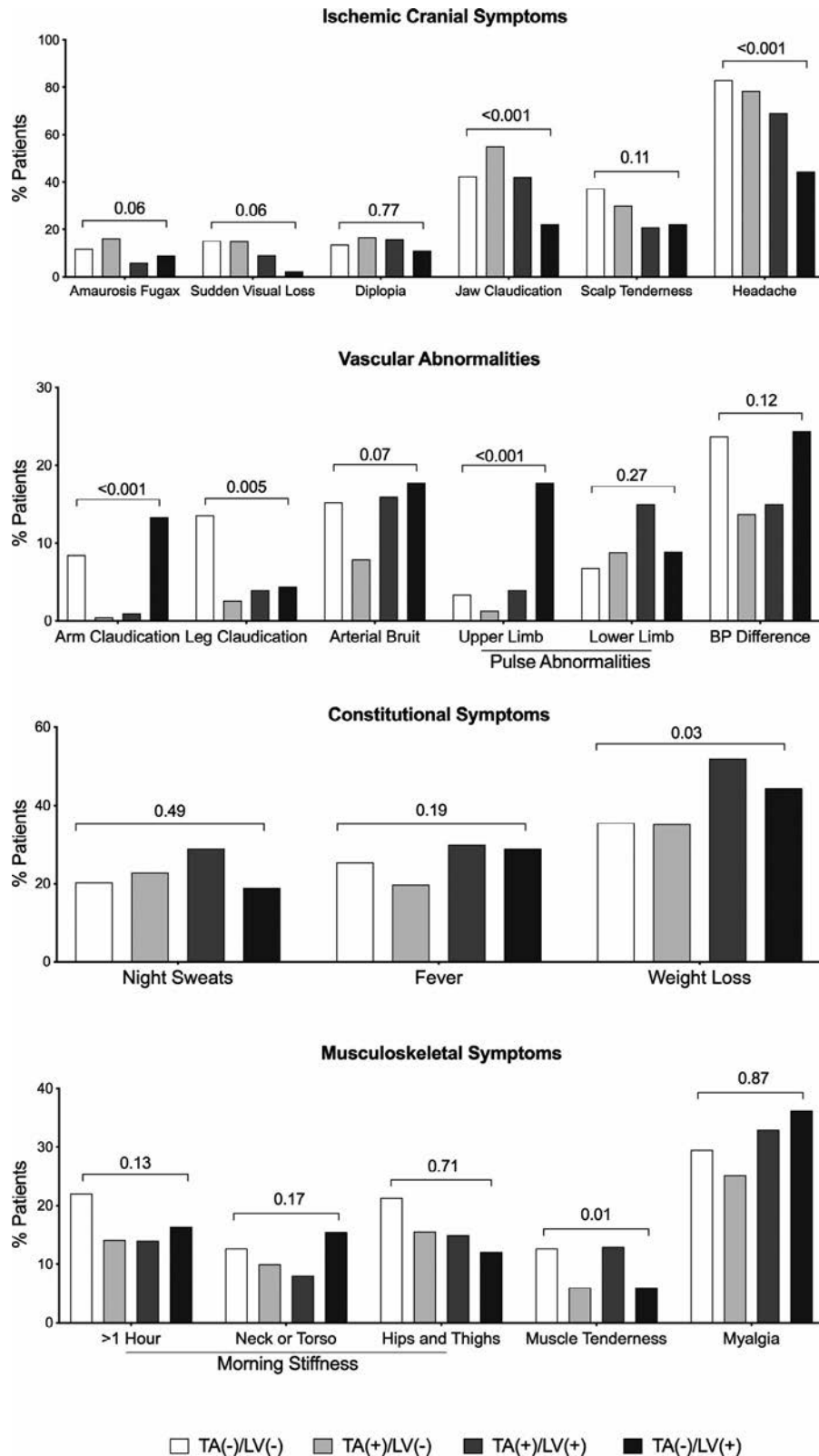


Figure 3. Clinical characteristics of patients in the restricted cohort by giant cell arteritis subset. Differences in the prevalence of ischemic cranial symptoms, vascular abnormalities, constitutional symptoms, and musculoskeletal symptoms are shown. Numbers above the horizontal bars are *P* values. TA-/LV- = patients without evidence of temporal artery (TA) or large vessel (LV) involvement; TA+/LV- = patients with TA involvement; TA+/LV+ = patients with both TA and LV involvement; TA-/LV+ = patients with LV involvement; BP = blood pressure.

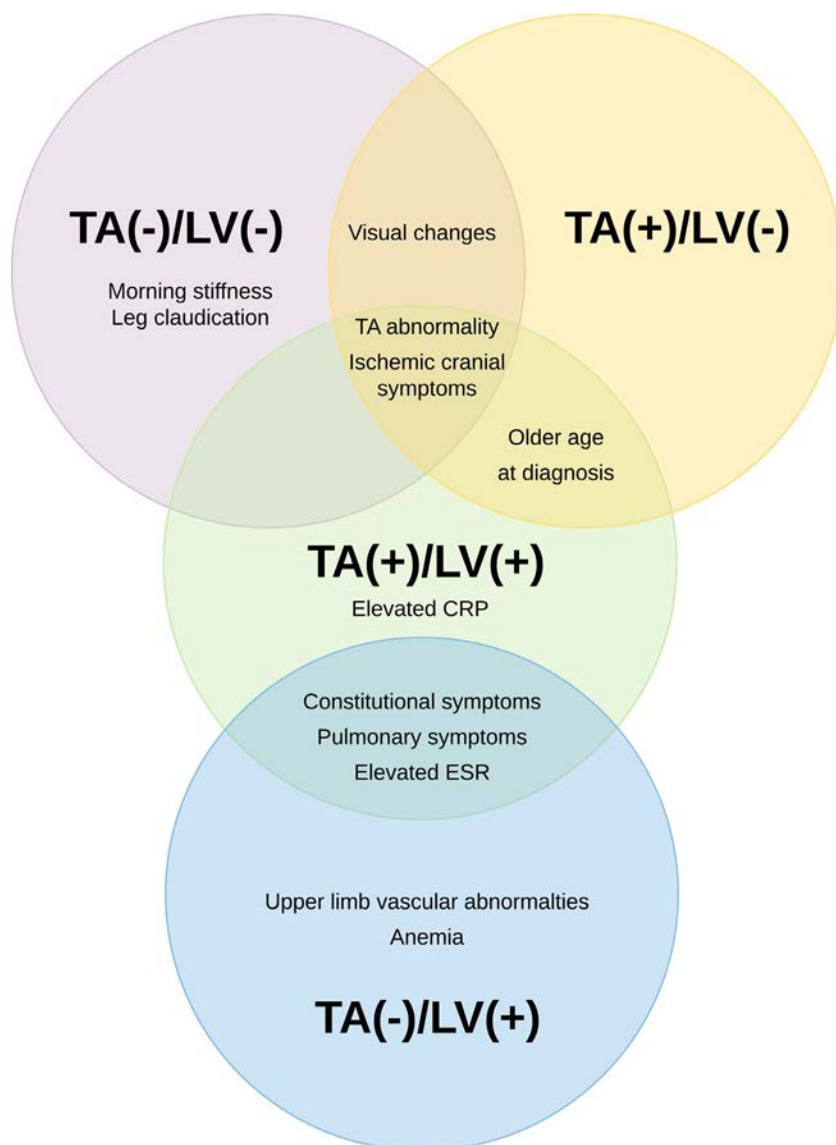


Figure 4. Clinical profile of patients with giant cell arteritis (GCA) in the restricted cohort by clinical subset. Some of the defining clinical features of each GCA subset are displayed. ESR = erythrocyte sedimentation rate (see Figure 3 for other definitions).

and new-onset headache. Patients in the TA+/LV- GCA subset were older than patients without TA involvement and had a low prevalence of vascular abnormalities, laboratory abnormalities, and constitutional and musculoskeletal symptoms compared to other subsets (Table 2).

Subset diagnosed by clinical symptoms but without confirmatory histologic or imaging findings in the restricted cohort. Patients in the TA-/LV- GCA subset were most similar to patients in the TA+/LV- GCA subset (Table 2 and Figure 3). When compared to the TA+/LV- GCA subset, patients in the TA-/LV- subset had a similarly high prevalence of visual changes and other symptoms of cranial ischemia, including sudden ongoing vision loss, jaw claudication, scalp tenderness, and headache. Patients in the TA-/LV- subset had a high prevalence of musculoskeletal symptoms, including the highest prevalence of morning stiffness

≥1 hour, morning stiffness in the hips and thighs, and muscle tenderness. Despite normal LV assessment by imaging, a proportion of patients in the TA-/LV- subset had leg claudication (14%), arterial bruits (15%), and BP difference between the arms of ≥10 mm Hg (24%).

Subset diagnosed by LV imaging abnormalities in the restricted cohort. Patients in the TA-/LV+ GCA subset had significantly fewer symptoms of cranial ischemia and TA abnormalities compared to the other subsets (Table 2 and Figure 3). Those in the TA-/LV+ GCA subset had a high prevalence of vascular symptoms (i.e., arm claudication) and vascular abnormalities on examination (i.e., vascular bruit, upper limb pulse abnormality, BP difference between arms of ≥10 mm Hg), pulmonary symptoms (i.e., nonproductive cough), and constitutional symptoms (i.e., fever, weight loss).

Subset diagnosed by TA and LV imaging abnormalities in the restricted cohort. The clinical profile of the TA+/LV+ GCA subset included features similar to those found in the TA+/LV- GCA and TA-/LV+ GCA subsets, as well as features that were not seen in either subset (Table 2 and Figure 3). Patients in the TA+/LV+ GCA subset had a high prevalence of TA abnormalities and ischemic cranial symptoms, significantly higher than the TA-/LV+ GCA subset but lower than the TA+/LV- GCA subset, including jaw claudication and new-onset headache. Although the overall prevalence of ischemic cranial symptoms was similar between the TA+/LV+ GCA and TA+/LV- GCA subsets, patients in the TA+/LV+ GCA subset were less likely to experience visual changes, including amaurosis fugax and sudden ongoing vision loss. Patients in the TA+/LV+ GCA and TA-/LV+ GCA subsets had a similarly high prevalence of vascular abnormalities, including bruit and lower limb pulse abnormality, and constitutional symptoms (i.e., night sweats, fever, weight loss) (Table 2 and Figure 3). However, patients in the TA+/LV+ GCA subset had significantly fewer vascular symptoms and examination abnormalities of the upper limbs compared to those in the TA-/LV+ GCA subset, including arm claudication and upper limb pulse abnormality. Patients in the TA+/LV+ GCA subset had a high prevalence of laboratory abnormalities, including elevated acute-phase reactant levels (Table 2).

Clinical GCA subsets in the overall versus the restricted cohort. A summary of the clinical subsets observed in the restricted cohort is provided in Figure 4. In general, the clinical associations were consistent between the GCA subsets in the overall cohort and the subsets in the restricted cohort, with only minor differences (see Supplementary Table 3, available on the *Arthritis & Rheumatology* web site at <http://onlinelibrary.wiley.com/doi/10.1002/art.41165/abstract>). In the overall cohort compared to the restricted cohort, there was no difference in prevalence of the TA+/LV- GCA subset (51% versus 53%; $P = 0.57$) or the TA-/LV+ GCA subset (12% versus 10%; $P = 0.31$). Patients in the restricted cohort were less likely to have TA-/LV- GCA (14% versus overall cohort 26%; $P < 0.0001$) and more likely to have TA+/LV+ GCA (23% versus overall cohort 11%; $P < 0.0001$). Unlike the restricted cohort, differences in sex were observed between the clinical subsets using data from the overall cohort (Table 1). Within the overall cohort, the percentage of patients who were female was higher in the TA-/LV+ subset compared to the other subsets, and the percentage who were male was higher in the TA+/LV- and TA+/LV+ subsets. Compared to patients in the TA-/LV- subset in the restricted cohort, patients in the TA-/LV- GCA subset in the overall cohort had a significantly lower prevalence of leg claudication (restricted cohort 13.6% versus overall cohort 4.9%; $P < 0.0001$) and arterial bruit (restricted cohort 15.3% versus overall cohort 7.0%; $P = 0.04$).

DISCUSSION

Diagnostic assessment in GCA is rapidly changing, as noninvasive vascular imaging techniques become increasingly available to categorize the extent of arterial involvement. Data from this study demonstrate how clinicians across the world use different diagnostic assessment strategies to assess arterial involvement in GCA. Although TAB is still the most common form of diagnostic assessment, noninvasive techniques such as ultrasonography, angiography, and PET imaging are increasingly used to assess disease in GCA. Patients who have isolated or overlapping cranial and LV involvement are now more frequently recognized. This study also details the characteristics of clinical subsets based on documented involvement of the cranial or large arteries. Besides differences in the extent of vascular involvement, patients in these subsets have different clinical profiles that likely reflect underlying biologic differences. These findings should inform clinicians on the clinical variability among patients with GCA and aid in researching more homogeneous patient populations.

TAB remains the diagnostic gold standard for GCA; however, the sensitivity of TAB has declined in recent years (22). Decreasing sensitivity is due in part to the growing practice of using vascular imaging as a diagnostic surrogate for biopsy to detect arterial involvement in and beyond the temporal arteries. Three-quarters of patients with a physician-confirmed diagnosis of GCA in the DCVAS cohort underwent TAB to diagnose GCA, but one-third of those biopsies were not diagnostic. Of those with a nondiagnostic TAB, 32.6% had evidence of vascular involvement by vascular imaging and 67.4% were diagnosed based on clinical symptoms alone. Vascular imaging was used as an alternative method to diagnose GCA in one-quarter of patients who did not have a TAB.

Vascular imaging techniques are being used to complement TAB and to capture the full extent of arterial disease. More than half of the patients who had a TAB had additional vascular imaging, independent of TAB results. Of the patients receiving a TAB, ~50% had LV imaging and ~30% had TA-US. Regional practices strongly influenced diagnostic assessment strategies, as TA-US was performed mostly at European centers. Patients who had TA-US also typically had concomitant TAB, although recent recommendations suggest that TA-US may be a diagnostic surrogate for TAB in patients in whom a clinical diagnosis of GCA is highly suspected (23). Patients with a negative TAB and those with a positive TAB were equally likely to have a halo sign on TA-US, suggesting that TA-US and TAB may identify different aspects of disease.

The increased use of vascular imaging in both the assessment and the evaluation of patients with suspected GCA has seemingly expanded the definition of GCA, with more patients now receiving this diagnosis. This evolution of clinical practice may result in not only a larger population of individuals receiving a GCA diagnosis, but also a change in the relative prevalence of different clinical characteristics of the condition labeled as GCA.

Clinical subsets of GCA have been proposed to account for the significant clinical heterogeneity seen among patients with GCA. Patients with LV involvement often present with different clinical features when compared to patients with cranial GCA, but the extent to which patients have overlapping versus distinct cranial and extracranial disease is not well characterized. In this study, clinical subsets were created a priori based on documented cranial and LV involvement. Different clinical profiles were observed in patients with GCA based on whether or not disease was detected in the cranial or large arteries. Restriction of analyses to a subset of patients who had comprehensive TA and LV assessments confirmed that these clinical differences were not simply the product of differential diagnostic testing. However, some bias in diagnostic assessment was also observed. Women were less likely than men to undergo TAB to confirm a GCA diagnosis, independent of differences in the presenting clinical features of disease.

The TA+/LV- GCA subset represents patients with a traditional GCA clinical profile. These patients had a high burden of symptoms of cranial ischemia and visual changes, and had limited evidence of LV involvement. Patients with isolated LV involvement differed substantially from patients with isolated TA involvement in their demographic and presenting clinical features. Patients in the TA-/LV+ GCA subset had a high burden of upper extremity vascular abnormalities, and constitutional and pulmonary symptoms.

A subset of patients with GCA have overlapping cranial and LV abnormalities, leading to speculation that the extent of arterial involvement may be underdetected in patients with isolated cranial or LV involvement. More of these patients were identified in the restricted cohort, where assessment of both the temporal and large arteries was performed. However, in the DCVAS cohort, patients with overlapping cranial and LV involvement had unique clinical associations, confirming that patients with overlapping disease represent an independent subgroup that is not merely due to underdetection of arterial involvement in the other subgroups. Patients with overlapping disease were older and had a high prevalence of cranial ischemia similar to patients with isolated cranial disease, and had a high prevalence of vascular abnormalities, bruits, and constitutional symptoms similar to patients with isolated LV disease. Patients with overlapping disease also had a high prevalence of laboratory abnormalities and constitutional symptoms. Similar to prior studies (6), patients with LV involvement, including those with overlapping disease, were less likely than patients without LV involvement to have visual changes.

In the DCVAS cohort, almost all patients had some form of arterial assessment, but one-quarter of patients did not have diagnostic confirmation of either cranial or extracranial artery involvement. The clinical profile of these patients was nearly indistinguishable from that of patients in the TA+/LV- GCA subgroup. Patients in the DCVAS cohort also had an increased burden of polymyalgia rheumatica (PMR)-like symptoms and had vascular examination abnormalities and symptoms associated with the

large arteries in the absence of corresponding imaging findings. Even in the setting of negative diagnostic assessment, these patients were diagnosed as having GCA, most likely due to the suggestive pattern of symptoms of cranial ischemia and PMR-like symptoms.

This study has potential limitations to consider. Diagnostic and imaging assessments were not standardized across the cohort. TA or LV involvement may have been underdetected. Additionally, standardized definitions for a diagnostic TAB or halo sign on TA-US were not used, and instead were at the discretion of the submitting physician. LV imaging was not standardized in the DCVAS cohort. Different rates of LV involvement in GCA have been described based on modality, and there is no gold standard for assessing LV involvement in GCA. LV involvement may be overestimated due to difficulty distinguishing between atherosclerosis and vasculitis on imaging, particularly in the lower extremities. Treatment data were not available in the DCVAS cohort, and use of glucocorticoids in particular may have impacted the performance characteristics of diagnostic testing. There is circularity in subgrouping based on documented arterial involvement, since vascular assessment may be driven by the presenting clinical symptoms. However, in the restricted cohort, where patients had cranial and LV assessments, all 4 subgroups exhibited a similar pattern of clinical symptoms as in the overall cohort. The majority of participating centers in the DCVAS cohort are tertiary research hospitals; therefore, diagnostic assessment may not be fully representative of general practice. Long-term outcome data were not available in the DCVAS cohort, and might reveal other signs and symptoms of GCA and/or increased prevalence of involvement of the large arteries at later stages of disease.

With the widespread adoption of vascular imaging into clinical practice, clinical variability among patients with GCA is increasingly being recognized. Previous studies have shown that patients with GCA can differ in their systemic inflammatory response, extent of arterial involvement, and treatment response (6), and suggest that there are distinct subgroups of GCA with potentially divergent disease etiology. Identifying subgroups may lead to stratified clinical decision-making and enable research into differences in disease pathology. In this study, subsets of patients with GCA had distinct clinical profiles based on cranial or large artery involvement. The extent to which differences in biologic mechanisms of disease underlie these subsets is unknown. Prospective studies to assess potential differences in disease risk factors, response to treatment, and long-term outcomes among subsets of patients with GCA are warranted. Comprehensive vascular assessment of the cranial and large arteries should be considered in the diagnostic assessment of all patients with suspected GCA.

AUTHOR CONTRIBUTIONS

All authors were involved in drafting the article or revising it critically for important intellectual content, and all authors approved the final version

to be published. Dr. Gribbons had full access to all the data in the study and takes responsibility for the integrity of the data and the accuracy of the data analysis.

Study conception and design. Gribbons, Ponte, Craven, Robson, Suppiah, Luqmani, Watts, Merkel, Grayson.




Acquisition of data. Gribbons, Ponte, Craven, Robson, Suppiah, Luqmani, Watts, Merkel, Grayson.

Analysis and interpretation of data. Gribbons, Ponte, Craven, Robson, Suppiah, Luqmani, Watts, Merkel, Grayson.

REFERENCES

- Buttgereit F, Dejaco C, Matteson EL, Dasgupta B. Polymyalgia rheumatica and giant cell arteritis: a systematic review. *JAMA* 2016; 315:2442–58.
- García-Martínez A, Hernández-Rodríguez J, Arguis P, Paredes P, Segarra M, Lozano E, et al. Development of aortic aneurysm/dilatation during the followup of patients with giant cell arteritis: a cross-sectional screening of fifty-four prospectively followed patients. *Arthritis Rheum* 2008;59:422–30.
- Nueninghoff DM, Hunder GG, Christianson TJ, McClelland RL, Matteson EL. Incidence and predictors of large-artery complication (aortic aneurysm, aortic dissection, and/or large-artery stenosis) in patients with giant cell arteritis: a population-based study over 50 years. *Arthritis Rheum* 2003;48:3522–31.
- Cid MC, Prieto-González S, Arguis P, Espígol-Frigolé G, Butjosa M, Hernández-Rodríguez J, et al. The spectrum of vascular involvement in giant-cell arteritis: clinical consequences of detrimental vascular remodelling at different sites. *APMIS Suppl* 2009;10–20.
- Prieto-González S, Arguis P, García-Martínez A, Espígol-Frigolé G, Tavera-Bahillo I, Butjosa M, et al. Large vessel involvement in biopsy-proven giant cell arteritis: prospective study in 40 newly diagnosed patients using CT angiography. *Ann Rheum Dis* 2012;71:1170–6.
- Van der Geest KS, Sandovici M, van Sleen Y, Sanders JS, Bos NA, Abdulahad WH, et al. What is the current evidence for disease subsets in giant cell arteritis? [review]. *Arthritis Rheumatol* 2018; 70:1366–76.
- Muratore F, Kermani TA, Crowson CS, Green AB, Salvarani C, Matteson EL, et al. Large-vessel giant cell arteritis: a cohort study. *Rheumatology (Oxford)* 2015;54:463–70.
- De Boysson H, Liozon E, Lambert M, Dumont A, Boutemy J, Maigné G, et al. Giant-cell arteritis: do we treat patients with large-vessel involvement differently? *Am J Med* 2017;130:992–5.
- De Boysson H, Liozon E, Ly KH, Dumont A, Delmas C, Aouba A. The different clinical patterns of giant cell arteritis. *Clin Exp Rheumatol* 2019;37 Suppl 117:57–60.
- Luqmani R, Lee E, Singh S, Gillett M, Schmidt WA, Bradburn M, et al. The role of ultrasound compared to biopsy of temporal arteries in the diagnosis and treatment of giant cell arteritis (TABUL): a diagnostic accuracy and cost-effectiveness study. *Health Technol Assess* 2016;20:1–238.
- Hunder GG. Giant cell arteritis and polymyalgia rheumatica. *Med Clin North Am* 1997;81:195–219.
- Hedges TR III, Gieger GL, Albert DM. The clinical value of negative temporal artery biopsy specimens. *Arch Ophthalmol* 1983;101: 1251–4.
- Roth AM, Milsow L, Keltner JL. The ultimate diagnoses of patients undergoing temporal artery biopsies. *Arch Ophthalmol* 1984; 102:901–3.
- Nesher G, Shemesh D, Mates M, Sonnenblick M, Abramowitz HB. The predictive value of the halo sign in color Doppler ultrasonography of the temporal arteries for diagnosing giant cell arteritis [abstract]. *J Rheumatol* 2002;29:1224–6.
- Chrysidis S, Duftner C, Dejaco C, Schäfer VS, Ramiro S, Carrara G, et al. Definitions and reliability assessment of elementary ultrasound lesions in giant cell arteritis: a study from the OMERACT Large Vessel Vasculitis Ultrasound Working Group. *RMD Open* 2018;4:e000598.
- Blockmans D, de Ceuninck L, Vanderschueren S, Knockaert D, Mortelmans L, Bobbaers H. Repetitive ¹⁸F-fluorodeoxyglucose positron emission tomography in giant cell arteritis: a prospective study of 35 patients. *Arthritis Rheum* 2006;55:131–7.
- Ostberg G. Morphological changes in the large arteries in polymyalgia arteritica. *Acta Med Scand Suppl* 1972;533:135–59.
- Ostberg G. An arteritis with special reference to polymyalgia arteritica. *Acta Pathol Microbiol Scand Suppl* 1973;237:1–59.
- Luqmani RA, Suppiah R, Grayson PC, Merkel PA, Watts R. Nomenclature and classification of vasculitis—update on the ACR/EULAR Diagnosis and Classification of Vasculitis Study (DCVAS) [review]. *Clin Exp Immunol* 2011;164 Suppl 1:11–3.
- Craven A, Robson J, Ponte C, Grayson PC, Suppiah R, Judge A, et al. ACR/EULAR-endorsed study to develop Diagnostic and Classification Criteria for Vasculitis (DCVAS). *Clin Exp Nephrol* 2013; 17:619–21.
- Slart RH, Glaudemans AW, Chareonthaitawee P, Tregliab G, Besson FL, Bley TA, et al. FDG-PET/CT(A) imaging in large vessel vasculitis and polymyalgia rheumatica: joint procedural recommendation of the EANM, SNMMI, and the PET Interest Group (PIG), and endorsed by the ASNC [review]. *Eur J Nucl Med Mol Imaging* 2018;45:1250–69.
- Rubenstein E, Maldini C, Gonzalez-Chiappe S, Chevret S, Mahr A. Sensitivity of temporal artery biopsy in the diagnosis of giant cell arteritis: a systematic review and meta-analysis. *Rheumatology (Oxford)* 2019. E-pub ahead of print.
- Dejaco C, Ramiro S, Duftner C, Besson FL, Bley TA, Blockmans D, et al. EULAR recommendations for the use of imaging in large vessel vasculitis in clinical practice. *Ann Rheum Dis* 2018;77:636–43.

Increased T Cell Plasticity With Dysregulation of Follicular Helper T, Peripheral Helper T, and Treg Cell Responses in Children With Juvenile Idiopathic Arthritis and Down Syndrome–Associated Arthritis

C. Foley,¹  A. Floudas,² M. Canavan,² M. Binięcka,³ E. J. MacDermott,⁴ D. J. Veale,³ R. H. Mullan,⁵ 
O. G. Killeen,⁴ and U. Fearon² 

Objective. Juvenile idiopathic arthritis (JIA) is the most common inflammatory arthritis in children; however, an aggressive, erosive arthritis of little-known immunologic mechanism occurs 20 times more frequently in children with Down syndrome. This study was undertaken to characterize T cell and B cell polyreactivity, follicular helper T (Tfh) cell, peripheral helper T (Tph) cell, and Treg cell responses, and synovial inflammation in Down syndrome–associated arthritis (DA).

Methods. Multiparametric flow cytometric analysis and Simplified Presentation of Incredibly Complex Evaluations (SPICE) software were used to examine peripheral blood B cell populations and T cell cytokine responses in patients with DA, JIA, Down syndrome (trisomy 21 [T21]), and in healthy controls. Tfh and Tph cell frequency and origin, in addition to Treg cell frequency, were also evaluated. Synovial inflammation was assessed by immunohistology.

Results. Expansion of IgM-only memory B cells was demonstrated in DA compared to JIA (mean \pm SEM 22.48 \pm 3.278 versus 9.011 \pm 1.317; $P = 0.005$), paralleled by decreased frequency of transitional B cells. T cell responses in DA were characterized by marked functional plasticity, as was evident from the increased frequency of polyfunctional CD8+ Th cells ($P < 0.05$), CD161+ Th cells ($P < 0.05$), and CD8– Th cells ($P < 0.001$), and positivity for tumor necrosis factor, interferon- γ , interleukin-17A, or granulocyte–macrophage colony-stimulating factor, compared to all other groups. Significant expansion of CXCR3+CCR6+ (Th1/Th17) Tfh cells ($P = 0.003$) and CXCR3+CCR6+ Tph cells ($P = 0.01$), paralleled by a decrease in CXCR3–CCR6– (Th2) Tfh cells was observed in DA compared to T21. Treg cells were significantly reduced in DA compared to T21 (mean \pm SEM 7.111 \pm 0.9518 versus 11.96 \pm 1.055 versus; $P = 0.0028$), with a specific reduction in the naive:memory Treg cell ratio. Marked synovial tissue inflammation and increased T cell and B cell infiltrations were demonstrated in DA compared to JIA.

Conclusion. DA is more common and more aggressive than JIA. It is characterized by increased polyreactive Th, Tfh, and Tph cell responses, reduced Treg cell frequency, and evidence of increased synovial inflammation, all of which are potentially distinct from JIA and T21.

INTRODUCTION

Down syndrome (trisomy 21 [T21]) is the most common chromosomal abnormality globally, with 1 in 700 children in the US born with it each year, and its prevalence is increasing. We

have recently identified the largest reported cohort of children with Down syndrome and a newly described form of aggressive, erosive, inflammatory arthritis, classified as Down syndrome–associated arthritis (DA). DA prevalence (1 in 50) is estimated to be 20 times greater than that of JIA and much higher than its

The views expressed herein are those of the authors and do not represent those of any health care organization or commercial interest.

Supported by National Children's Research Centre at Our Lady's Children's Hospital at Crumlin, Arthritis Ireland, Down Syndrome Ireland, and the Health Research Board of Ireland.

¹C. Foley, PhD: Our Lady's Children's Hospital at Crumlin and Trinity College Dublin, Dublin, Ireland; ²A. Floudas, PhD, M. Canavan, PhD, U. Fearon, PhD: Trinity College Dublin, Dublin, Ireland; ³M. Binięcka, PhD, D. J. Veale, MD: Centre for Arthritis and Rheumatic Diseases EULAR Centre of Excellence, St. Vincent's University Hospital, and University College Dublin, Dublin, Ireland;

⁴E. J. MacDermott, MD, O. G. Killeen, MD: Our Lady's Children's Hospital at Crumlin, Dublin, Ireland; ⁵R. H. Mullan, PhD: Tallaght University Hospital and Trinity College Dublin, Dublin, Ireland.

Drs. Foley and Floudas contributed equally to this work.

No potential conflicts of interest relevant to this article were reported.

Address correspondence to U. Fearon, PhD, Trinity College Dublin, College Green, Dublin 2, County Dublin, Ireland. E-mail: fearonu@tcd.ie.

Submitted for publication April 16, 2019; accepted in revised form October 24, 2019.

previously reported prevalence of 8.7 in 1,000 (1,2). With little information available regarding clinical and epidemiologic characteristics of this inflammatory arthritis and a lack of awareness about the increased risk of arthritis in children with T21, this group is at a potentially greater risk of long-term complications.

To better understand the immunologic factors contributing to the pathogenesis of DA, we first need to consider the immune system in T21 and JIA. In T21, there is a reported decrease in Treg cell capacity to suppress effector T cell responses (3). Further evidence suggests a failure of central tolerance mediated by reduced availability of thymic antigens, thereby facilitating the escape of potentially autoreactive T cells from the thymus (4). While the extent of B cell contribution to T21 remains unclear, one study suggests that IgM-expressing nonswitched memory B cells (CD27+IgD+IgM+) show reduced proliferation capacity and somatic hypermutation potential. Generalized B cell lymphopenia has also been reported, with a reduction in transitional (CD38^{high}CD24^{high}) and switched memory B cells (5).

Characterizing immunologic features of DA is further complicated by the complexity of JIA, a clinically heterogeneous autoimmune disease (6,7). Similar to T21, impaired Treg suppressive function with restricted clonotypic expansion has been reported in JIA, which potentially limits the array of immune responses that Treg cells are able to control. Importantly, Th17 plasticity leading to CD161+ Th17 cells expressing interferon- γ (IFN γ) has previously been identified in the joints of JIA patients, with the cytokine environment of the inflamed joint promoting this effect (8). Epigenetic polymorphisms of the T cell compartment can be indicative of remission maintenance and are associated with clinical pathology of JIA, while the transcription factor cAMP response element contributes to the CD161+ T cell proinflammatory profile in JIA synovial fluid (9,10). Accumulation of switched memory B cells in the synovial fluid of JIA patients has also been reported, along with a potential decrease in regulatory B cell-enriched peripheral blood B cells (CD24^{high}CD38^{high}) (11,12).

Due to the lack of information on the unique immunologic features of DA and the implications this may have for treatment, we performed an in-depth characterization of B cell and T cell responses in children with DA. We found alterations in both B cell and T cell compartments, with increased IgM-only memory B cells in DA compared to T21, as well as increased T cell polyfunctionality in DA compared to T21 and JIA. Traditionally, CD4+ T cells have been categorized in populations based on expression of a key cytokine, including Th1 (IFN γ -positive), Th17 (interleukin-17A [IL-17A]-positive), Th22 (IL-22-positive), etc. However, recent studies demonstrate the importance of T cell plasticity and polyfunctionality in infection and autoimmunity (8,13,14). Elevated T cell proinflammatory cytokine responses in DA, compared to JIA, were evident due to the marked increase in tumor necrosis factor (TNF)-positive and IFN γ -positive CD8- T cells and a significantly higher proportion of CD8-, CD8+, and Th17-lineage T cells (CD161+) expressing multiple proinflammatory

cytokines simultaneously and thus exhibiting polyfunctionality. We also showed differential distribution of follicular helper T (Tfh) cell (CD3+CD8-CXCR5+ICOS+/-PD-1+/-) subsets and peripheral helper T (Tph) cell (CD3+CD8-CXCR5-ICOS+/-PD-1+) subsets in DA, with significant expansion of CXCR3+CCR6+ (Th1/Th17) Tfh cells and CXCR3+CCR6+ Tph cells, paralleled by decreased CXCR3-CCR6- (Th2) Tfh cells observed in DA compared to healthy controls and children with T21. Decreased Treg cell (CD3+CD8-CD127-CD39+/-Foxp3+CD25+) frequency and evidence of increased synovial inflammation and cellular infiltration in DA highlight the potentially distinct (from JIA) immunologic profile of DA.

PATIENTS AND METHODS

Patients and sample collection. Children with DA and children with JIA were recruited from the National Centre for Paediatric Rheumatology (NCPR) at Our Lady's Children's Hospital, Crumlin (OLCHC). Based on clinical manifestation, laboratory findings, and pattern of joint involvement, arthritis in children with Down syndrome is a polyarticular form of rheumatoid factor (RF)-negative inflammatory arthritis found in children and young people with T21 (2). Therefore, children with polyarticular RF-negative JIA were included in all comparative studies (see Supplementary Table 1, on the *Arthritis & Rheumatology* web site at <http://online.library.wiley.com/doi/10.1002/art.41150/abstract>). Children with T21 were recruited from musculoskeletal screening clinics set up and run by clinicians at the NCPR. These children had a diagnosis of Down syndrome but no evidence of past or present arthritis. Healthy controls included children without Down syndrome and with no medical history of inflammatory or autoimmune disease who were recruited from the orthopedic department at OLCHC. Fully informed parental consent and participant assent was obtained for all subjects who provided blood and synovial tissue. The OLCHC Ethics Committee granted approval for this study.

Flow cytometric analysis. For the flow cytometric analysis of peripheral blood B cells and Tfh cells, 1×10^6 peripheral blood mononuclear cells (PBMCs) were used per sample. Cells were washed in ice-cold phosphate buffered saline (PBS) prior to incubation with Live/Dead Fixable Near-IR dye (ThermoFisher). An Fc receptor blocking step was performed by incubating the cells with TruStain FcX Fc blocking solution (BioLegend). Cells were then stained for 30 minutes at 4°C with the following antibodies: anti-CD38 (HIT2; BioLegend), anti-CD24 (ML5; BD Biosciences), anti-CD20 (2H7; BD Biosciences), anti-CD27 (O323; BioLegend), anti-IgM (G20-127; BD Biosciences), anti-CD138 (MI15; BioLegend), anti-CD45 (H130; BioLegend), anti-CD19 (HIB19; BioLegend), anti-CD40 (5C3; BioLegend), anti-IgD (1A6-2) or anti-CD45RO (UCHL1) (both from BioLegend), anti-CD57 (HNK-1), anti-programmed death 1 (anti-PD-1) (EH12.2H7), anti-CD4 (A161A1), anti-CD3 (OKT3), anti-CCR6 (G034E3), anti-CXCR5

(J252D4), anti-CXCR3 (G025H7), anti-CCR7 (G043H7), anti-CD45 (HI30), and anti-CD161 (HP-3G10) (all from BioLegend). For further details on antibodies used and fluorochrome conjugates please refer to Supplementary Tables 2 and 3 (<http://onlinelibrary.wiley.com/doi/10.1002/art.41150/abstract>).

For Th cell and Treg cell characterization and cytokine detection, cells were subjected to a cell surface staining step with the following antibodies: anti-CD3 (B27; BD Bioscience), anti-CD8 (SK1; eBioscience), anti-CD161 (HP-3G10) or anti-CD3 (SK7) (both from eBioscience), anti-CD4 (A161A1), anti-CD45RO (UCHL1), anti-CD39 (A1), anti-CD152 (BNI3), anti-CD25 (BC96), anti-CCR7 (G043H7), and anti-CD45 (HI30) (all from BioLegend). For intracellular staining, cells were fixed and permeabilized using a FoxP3 staining buffer set (eBiosciences) followed by staining with the following antibodies: anti-IL-17A (BL168; BioLegend), anti-granulocyte-macrophage colony-stimulating factor (anti-GM-CSF) (BVD2-21C11; BioLegend), anti-tumor necrosis factor (anti-TNF) (Mab11; eBioscience), anti-IFN γ (B27; BD Biosciences) or anti-FoxP3 (150D; BioLegend), and anti-Ki-67 (Ki-67; BioLegend). For further details on antibodies used and fluorochrome conjugates, please refer to Supplementary Tables 2 and 3 (<http://onlinelibrary.wiley.com/doi/10.1002/art.41150/abstract>). Acquisition was performed on a 3-laser Beckman Coulter CyAn ADP analyzer or a 4-laser BD LSR Fortessa II cell analyzer. Software-assisted compensation was performed with the use of single antibody-stained compensation beads (BD Biosciences). Data were analyzed using FlowJo, version 10 (Treestar), with a t-distributed Stochastic Neighbor embedding (tSNE) add-on, and Simplified Presentation of Incredibly Complex Evaluations (SPICE), version 6 (15). Doublet cell exclusion was performed, and Florescence Minus One controls were used to determine gating parameters.

Cell stimulation. For PBMC stimulation and cytokine detection, 2×10^5 cells were placed in each well of a flat bottom 96-well plate in 100 μ l of cRPMI (RPMI GlutaMAX, 10% fetal bovine serum, and penicillin/streptomycin) (ThermoFisher). Cells were then stimulated with Cell Stimulation Cocktail (phorbol myristate acetate/ionomycin) (eBioscience) for 1 hour prior to the addition of 0.05 μ g/ml brefeldin A (ThermoFisher) for 5 hours of incubation. Cells were analyzed by flow cytometry.

Immunohistologic analysis of DA and JIA synovial membrane. Synovial biopsy samples (JIA, $n = 4$; DA, $n = 3$) were obtained by ultrasound-guided biopsy at the time of therapeutic arthrocentesis, before intraarticular steroid delivery, and were cryopreserved by snap-freezing in OCT (Sigma-Aldrich), followed by storage at -80°C (clinical characteristics available in Supplementary Table 4, <http://onlinelibrary.wiley.com/doi/10.1002/art.41150/abstract>). Seven-micrometer sections were cut, and a routine 3-stage immunoperoxidase labeling technique incorporating avidin-biotin-immunoperoxidase complex (Dako) was used. Sections were incubated with primary mouse anti-CD3 and anti-CD20 monoclonal

antibodies (Dako) at room temperature for 1 hour. Color was developed in solution containing diaminobenzidine tetrahydrochloride (0.5% H_2O_2 in PBS, pH 7.6) (Sigma-Aldrich). Slides were counterstained with hematoxylin (Sigma-Aldrich) and mounted using DPX according to instructions from the manufacturer (Dako). For overall inflammation and vascularity, a scoring range of 0–3 was used. For cell-specific markers, a well-established semi-quantitative scoring method (range 0–4) was used as previously described (16). Briefly, a score of 1 is representative of 5–24% of cells being positive for the cell-specific marker, a score of 2 represents 25–49%, 3 represents 50–74%, and 4 represents 75–100% of cells being positive for the cell-specific marker.

Statistical analysis. Statistical analysis was performed using GraphPad Prism software, version 7. One-way or two-way analysis of variance with Tukey's multiple comparisons test and Student's unpaired 2-tailed t -test were used as indicated. P values less than 0.05 were considered significant.

RESULTS

Increased IgM-only memory B cells in patients with DA. Patient demographics are described in Supplementary Table 1 (<http://onlinelibrary.wiley.com/doi/10.1002/art.41150/abstract>). Following the identification of CD19+CD20+/- cells, B cells were further analyzed based on the expression of membrane-bound IgD and the memory B cell marker CD27, allowing for the identification of 4 major B cell subpopulations with distinct functionalities: naive B cells (IgD+CD27-), nonswitched memory B cells (IgD+CD27+), double-negative memory B cells (IgD-CD27-), and switched memory B cells (IgD-CD27+) (Figure 1A and Supplementary Figure 1A, <http://onlinelibrary.wiley.com/doi/10.1002/art.41150/abstract>). In accordance with previous findings (5), the frequency of B cells in patients with T21 was significantly reduced when compared to healthy controls ($P = 0.03$). Children with DA showed a greater reduction in B cell frequency compared to healthy controls ($P < 0.001$) and children with T21 ($P < 0.05$) (Figure 1B). There was also a significant decrease in memory B cells (CD27+) in children with T21 compared to healthy controls ($P < 0.01$), with memory B cell frequency restored in DA (Figure 1B). Interestingly, the peripheral blood IgM-only germinal center-like B cells (IgM+IgD-CD27+) recently described in humans (17) were significantly increased within the IgD-CD27+ memory compartment in DA compared to healthy controls and JIA ($P = 0.01$ and $P = 0.005$, respectively) (Figure 1C). No differences were observed in the frequency of circulating plasma cells (CD138^{high}CD27^{high}) between DA and all other groups (Figure 1D).

Transitional B cells (CD24^{high}CD38^{high}) are enriched in potentially immunoregulatory IL-10-producing cells (18). We found a decrease, although not statistically significant, in the frequency of transitional B cells in JIA and DA compared to healthy controls and T21, respectively (Figure 1E).

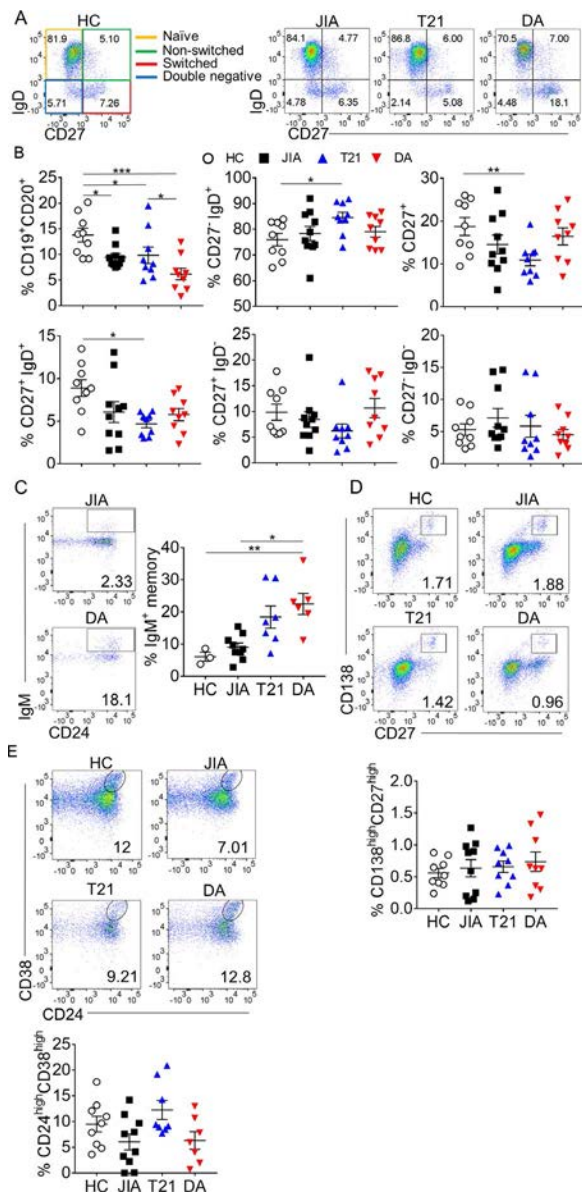


Figure 1. Peripheral blood B cell subpopulation distribution and increased IgM-only memory B cells in Down syndrome-associated arthritis (DA). **A**, Representative flow cytometric analysis plots for the identification of B cell subpopulations based on expression of CD27 and IgD in healthy controls (HCs) and in children with juvenile idiopathic arthritis (JIA), Down syndrome (trisomy 21 [T21]), or DA. **B**, Frequency of the indicated B cell populations in the peripheral blood of healthy controls and children with JIA, T21, or DA. **C**, Gating example and overall frequency of IgM-only memory B cells in peripheral blood from the indicated groups. **D**, Representative flow cytometric analysis plots for the identification of plasma cells (CD138+CD27^{high}) and frequency of plasma cells in peripheral blood from the indicated groups. **E**, Representative gating for the identification of transitional B cells (CD24^{high}CD38^{high}) and frequency of transitional B cells in peripheral blood from all groups. In **B**, **C**, and **E**, each symbol represents an individual sample ($n = 10\text{--}11$ per group); bars show the mean \pm SEM. Statistical analysis was performed by one-way analysis of variance with Tukey's multiple comparisons test. * = $P < 0.05$; ** = $P < 0.01$; *** = $P < 0.001$.

Increase in proinflammatory cytokine responses of

CD8⁻ and CD8⁺ T cells in DA. Previous studies of JIA have identified increased frequency of IFN γ - and IL-17A-expressing T cells, highlighting potential pathogenic roles for Th1 (IFN γ) and Th17 (IL-17A) cells (19). Following stimulation *in vitro*, we identified proinflammatory cytokine-producing CD8⁺ and CD8⁻ T cells in healthy controls and in patients with JIA, T21, and DA (Supplementary Figure 2, <http://onlinelibrary.wiley.com/doi/10.1002/art.41150/abstract>). Children with DA had the highest levels of cytokine production compared to patients with T21 or JIA and healthy controls, with significant increases in TNF, IFN γ , and IL-17A CD8⁺ T cell responses ($P < 0.05$ for all) (Figures 2A and B).

CD161 is a novel marker for all T cell subsets that are or have been producing IL-17A. Some Th17 cells, due to increased functional plasticity, can convert to ex-Th17. These cells no longer produce IL-17A but have instead switched to IFN γ production. During this transition from Th17 to ex-Th17 cells, they maintain CD161 expression (20). In the present study, the majority of IL-17A-producing cells resided within the CD8⁻CD161⁺ T cell compartment (Figure 2C), with a substantial population producing TNF and IFN γ (Figure 2D). A higher frequency of CD8⁻CD161⁺ T cells was observed in DA compared to all other groups (Figures 2E–G). Marked differences in the proinflammatory cytokine production of CD8⁺ T cells were also evident, with significant increases in the frequency of TNF- and IFN γ -producing CD8⁺ T cells in DA compared to JIA ($P = 0.017$ and $P = 0.003$ respectively) (Figures 2H–J).

Increased T cell polyfunctionality in DA.

T cell functional plasticity provides flexibility to the immune system and is needed for adequate response to pathogens. Previous studies have shown correlations between T cell polyfunctionality and disease progression of rheumatoid arthritis (RA) and psoriatic arthritis (PsA) (14,21). Polyfunctional CD8⁻ T cells have a unique transcriptional profile in comparison to monofunctional T cells, and this is indicative of stark differences in their activation, trafficking, and metabolism (22). In order to identify polyfunctional T cells, we used the SPICE algorithm. SPICE is a supervised algorithm that uses labeled flow cytometric data for the visualization of complex data sets and the identification of cell populations that express combinations of different markers. In the present study, using multidimensional SPICE analysis, we demonstrated a dramatic increase in CD8⁻ T cell polyfunctionality in DA compared to all other groups (Figure 2K). This was characterized by an increased frequency of cells simultaneously producing multiples of the proinflammatory cytokines TNF, IFN γ , GM-CSF, and IL-17A ($P < 0.001$) (Figure 2K). Increased polyfunctionality was also a characteristic of CD161⁺CD8⁻ and CD8⁺ T cells, with significantly higher frequency in DA compared to T21, JIA, or healthy controls (Figure 2K). These results indicate a global dysregulation of T cell plasticity in DA that could be an important contributor to disease progression.

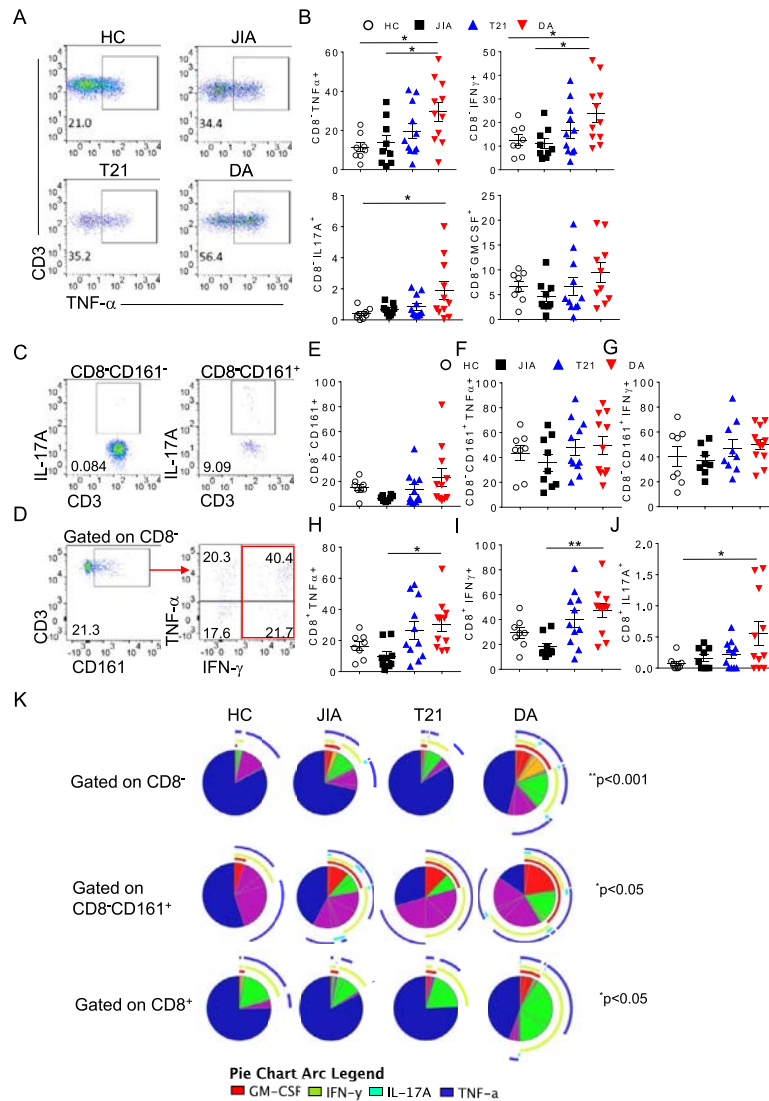


Figure 2. Increased T cell proinflammatory cytokine responses and T cell polyfunctionality in DA. **A**, Representative flow cytometry analysis plots and overall frequency of CD8⁺ peripheral blood T cells expressing tumor necrosis factor (TNF) in the indicated groups. **B**, Frequency of CD8⁺ peripheral blood T cells expressing TNF, interferon- γ (IFN γ), interleukin-17A (IL-17A), or granulocyte-macrophage colony-stimulating factor (GM-CSF) in the indicated groups. **C**, Representative flow cytometry analysis plots showing the expression of IL-17A by CD8⁺CD161⁻ or CD8⁺CD161⁺ (Th17-lineage) cells. **D**, Gating for the identification of IFN γ -producing ex-Th17 cells. **E–G**, Frequency of total CD8⁺CD161⁺ cells (**E**), TNF-expressing CD8⁺CD161⁺ cells (**F**), and IFN γ -expressing CD8⁺CD161⁺ cells (**G**) in all groups. **H–J**, Proinflammatory cytokine expression by CD8⁺ cells in the indicated groups. **K**, Simplified Presentation of Incredibly Complex Evaluations analysis for the identification of T cells (of the indicated populations) expressing multiple proinflammatory cytokines. Pie segments indicate frequency of cells producing different combinations of cytokines. Surrounding arcs denote the specific cytokines produced by the cells in each pie segment. In **B**, **E–G**, and **H–J**, each symbol represents an individual sample ($n = 8–11$ per group); bars show the mean \pm SEM. Statistical analysis was performed by one-way analysis of variance with Tukey's multiple comparisons test. * = $P < 0.05$; ** = $P < 0.001$. See Figure 1 for other definitions.

Dysregulated Tfh and Tph responses in DA due to increased CXCR3⁺/CCR6⁺ cells. Tfh cells are instrumental in their capacity to provide B cell help for optimal T cell-dependent antibody responses to occur. CXCR5⁺CD4⁺ Tfh cells have differential cytokine profiles and capacity to provide B cell help, which are reflected by the expression of CXCR3 and CCR6 (23). CXCR3⁺CCR6⁻ Tfh cells are of Th1 descent, CXCR3⁻CCR6⁺ Tfh cells are of Th17 descent, CXCR3⁻CCR6⁻ Tfh cells are of Th2 descent, and CXCR3⁺CCR6⁺ Tfh cells are of dual Th1/Th17

descent (23,24). While we observed no differences in the frequency of peripheral blood Tfh cells between groups (Figure 3A), significant differences were demonstrated in the Tfh subpopulation distribution. In children with DA, there was a significant expansion of CXCR3⁺CCR6⁺ double-positive (Th1/Th17) Tfh cells compared to healthy controls, JIA, and T21 ($P = 0.009$, $P = 0.0232$, and $P = 0.0034$, respectively), with a specific decrease in CXCR3⁻CCR6⁻ (Th2) Tfh T cells compared to healthy controls and T21 ($P = 0.03$ and $P = 0.018$, respectively) (Figure 3B).

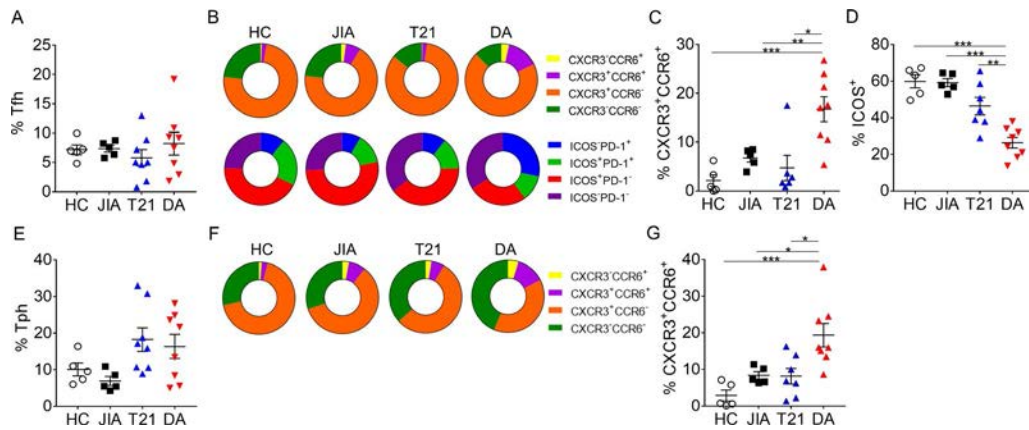


Figure 3. Enhanced follicular helper T (Tfh) and peripheral helper T (Tph) cell plasticity with increased Th1/Th17-like cells. **A**, Total Tfh cell frequency in all groups. **B**, Subpopulation distribution, showing the frequency of CXCR3+CCR6+ and Inducible costimulator (ICOS)–positive Tfh cells in all groups. **C**, CXCR3+CCR6+ Tfh cell frequency. **D**, ICOS-positive Tfh cell frequency. **E**, Total Tph cell frequency. **F**, Subpopulation distribution, showing the frequency of CXCR3+CCR6+ Tph cells in all groups. **G**, CXCR3+CCR6+ Tph cell frequency. In **A**, **C**, **D**, **E**, and **G**, each symbol represents an individual sample ($n = 5\text{--}8$ per group); bars show the mean \pm SEM. Statistical analysis was performed by one-way analysis of variance with Tukey's multiple comparisons test. * = $P < 0.05$; ** = $P < 0.01$; *** = $P < 0.001$. PD-1 = programmed death 1 (see Figure 1 for other definitions).

Inducible costimulator (ICOS) expression by Tfh cells has previously been shown to maintain the Tfh phenotype and prevent Tfh cells from returning to their previous non-Tfh state (25). Interestingly, we found that ICOS-positive Tfh cells were significantly decreased in DA compared to all other groups ($P < 0.0001$ versus JIA and healthy controls; $P = 0.0022$ versus T21) (Figures 3B and D). A recent study has revealed that CXCR5– T cells that express PD-1 (Tph) can have a potential B cell helper function that resembles that of conventional Tfh cells (26). We examined the frequency of Tph cells in the peripheral blood of healthy controls and children with JIA, T21, and DA (Supplementary Figure 3, <http://onlinelibrary.wiley.com/doi/10.1002/art.41150/abstract>). A nonsignificant increase in the frequency of Tph cells in T21 and DA was observed (Figure 3E), and similar to the observed increase in CXCR3+CCR6+ (Th1/Th17) Tfh cells, we noted a significant increase in CXCR3+CCR6+ Tph cells in DA compared to healthy controls, JIA, and T21 ($P = 0.0008$, $P = 0.0276$, and $P = 0.04$, respectively) (Figures 3F and G). These results highlight a potentially pathogenic dysregulation of Tfh responses in DA that favors the expansion of plastic CXCR3+CCR6+ (Th1/Th17) Tfh and Tph cells.

Impaired Treg cell responses in DA with reduced cell frequency and altered naive:memory Treg cell ratio.

In order to assess Treg cell frequency, activation, and memory status, we performed unbiased, unsupervised, multidimensional analysis of flow cytometric data (27) (Figure 4A). Following pre-gating on CD8– T cells, clustering was performed using the tSNE algorithm. T-distributed SNE is an unsupervised algorithm (i.e., does not require data labeled by the user) that performs dimensionality reduction of complex data by clustering cells that have similar expression profiles. Therefore, tSNE performs unbiased analysis and can be used for data exploration in order to identify

novel cell populations, and it also assists with data visualization as cell clusters can be more clearly distinguished without the need for multiple conventional flow cytometry scatter plots.

Our analysis revealed 2 distinct Treg cell populations present in all samples tested, and tSNE analysis validation was performed by conventional 2-dimensional gating (Supplementary Figure 4, <http://onlinelibrary.wiley.com/doi/10.1002/art.41150/abstract>). These 2 populations correspond to naive and memory Treg cells (Figure 4A). In DA, there was a statistically significant reduction in the frequency of Treg cells compared to T21 ($P = 0.016$), with a reduction in the naive:memory Treg cell ratio (Figures 4B and C). Although not statistically significant, alterations in proliferating T cells were observed, with an increase in Ki67+ T cells in T21 and DA (Figure 4D). Interestingly, there was a strong negative correlation between the frequency of peripheral blood Tph cells and Treg cells, specifically for DA patients, with high Tph cell frequency observed in patients with low Treg cell frequency (Figure 4E). These results highlight an impairment in Treg cell responses in DA compared to T21.

Evidence of increased synovial pathology and inflammation in DA.

In DA synovial tissue, there was evidence to suggest an overall increase in inflammation, with increased vascularity and lining layer thickness, compared to that of JIA tissue (Figures 5A and B), which may contribute to the more erosive disease observed in DA compared to JIA. Furthermore, an increase in the number of CD20+ B cells (Figures 5C and D) and CD3+ T cells (Figures 5E and F) was observed in DA compared to JIA.

DISCUSSION

We recently showed that the estimated prevalence of DA is 20 times greater than that of JIA (2). DA is a newly characterized,

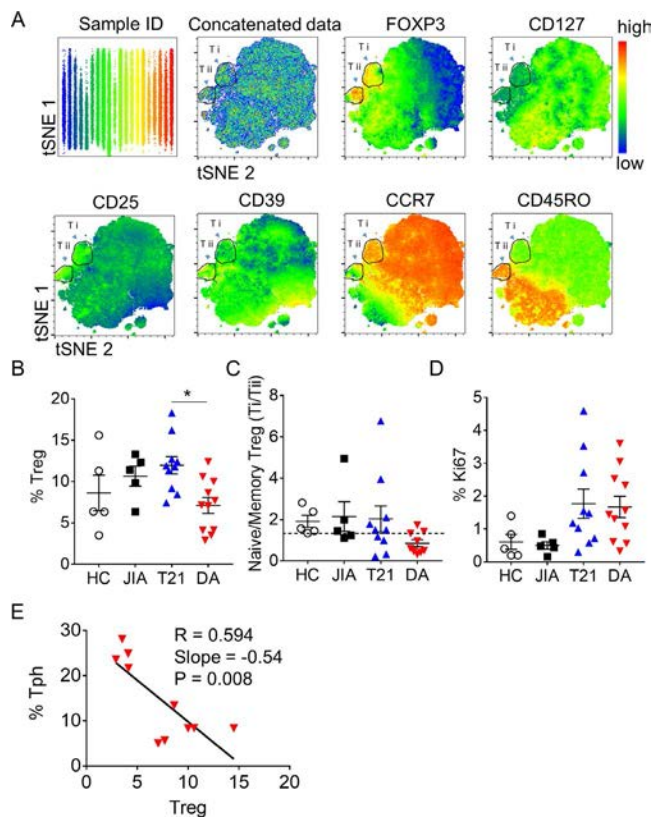


Figure 4. Treg cell identification by unsupervised clustering and reduced Treg cell frequency in DA. Multiparametric flow cytometric data on total CD8⁻ cells were subjected to unsupervised clustering by t-distributed Stochastic Neighbor embedding (tSNE) algorithm following data concatenation. Data concatenation and relative expression by the indicated parameters are shown. **A**, Identification of Treg cell populations. On the basis of FoxP3, CD25, CD127, and CD45RO expression of CD8⁻ T cells, 2 populations of Treg cells were identified: naive Treg cells (Ti) (CD25+CD127-FoxP3+CD45RO⁻) and memory Treg cells (Tii) (CD25+CD127-FoxP3+CD45RO⁺). **B**, Frequency of peripheral blood Treg cells in the indicated groups. **C**, Naive:memory Treg cell ratios. **D**, Frequency of Ki67⁺ CD3⁺ T cells. **E**, Correlation between peripheral helper T (Tph) cell frequency and Treg cell frequency in DA patient peripheral blood samples. In **B–E**, each symbol represents an individual sample ($n = 5–10$ per group); bars show the mean \pm SEM. Statistical analysis was performed by one-way analysis of variance with Tukey's multiple comparisons test. * = $P < 0.05$. See Figure 1 for other definitions.

aggressive, erosive arthritis, with little information on the underlying immune dysregulation. Therefore, effective treatment of DA is currently hindered. In the present study, we examined for the first time the adaptive immune system in children with DA, with a specific focus on identifying whether defects in immune regulation drive the clinically aggressive, erosive phenotype observed. We identified an expansion of IgM-only memory B cells in DA compared to JIA, and a decreased frequency of transitional B cells that could contribute to a failure of immune regulation. Importantly, proinflammatory cytokine TNF and IFN γ responses by CD8⁻ T cells and TNF and IL-17A responses by CD8⁺ T cells were higher in

DA compared to JIA. The increased proinflammatory cytokine responses were associated with increased T cell plasticity as evident by marked polyreactivity of CD8⁺, CD8⁻, and ex-Th17 cells in DA compared to JIA. The observed enhanced T cell plasticity in DA was not restricted to cytokine production, as an analysis

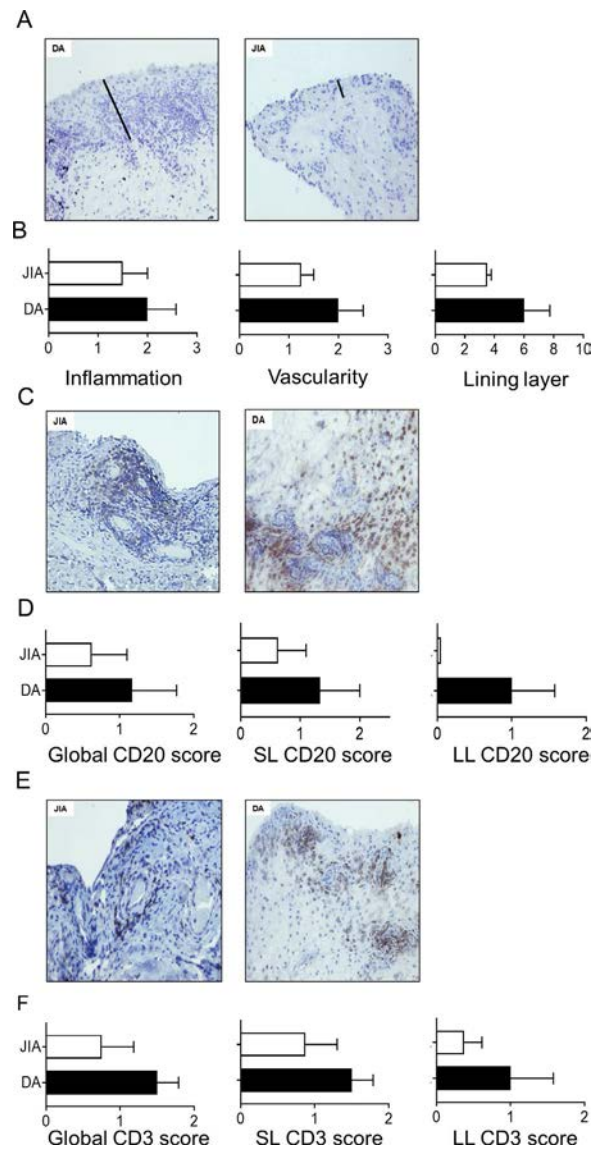


Figure 5. Increased synovial inflammation and cellular infiltration in DA compared to JIA. **A**, Representative images of DA and JIA synovial tissue biopsy sections stained with hematoxylin. Lines indicate synovial lining layer thickness. **B**, JIA and DA synovial inflammation and vascularity scores and lining layer thickness (number of cells). **C**, Representative immunohistochemistry staining for the identification of CD20⁺ cells in the synovial tissue of JIA and DA patients. **D**, Global, sublining (SL), and lining layer (LL) scores for the presence of CD20-expressing cells. **E**, Representative immunohistochemistry staining for the identification of CD3⁺ cells in the synovial tissue of JIA and DA patients. **F**, Global, sublining, and lining layer scores for the presence of CD3-expressing cells. Original magnification $\times 20$. Bars show the mean \pm SEM. See Figure 1 for other definitions.

of Tfh and the recently described Tph cells showed an elevated frequency of plastic Th1/Th17-like cells within these populations. An additional contributing factor in DA immune dysregulation is the significant reduction in the frequency of Treg cells in DA compared to T21, as well as an inverse correlation between the frequency of Tph and Treg cells in DA. Finally, evidence suggests the presence of increased synovial tissue inflammation and tissue infiltration of T and B cells in DA compared to JIA. Taken together, these results indicate that DA is potentially distinct from JIA and manifests with more aggressive proinflammatory, polyfunctional Th, Tfh, and Tph cell responses, accompanied by reduced Treg cell frequency and increased synovial pathology.

In this study, we show that despite B cell lymphopenia in DA, there is an increased relative frequency of IgM-only-producing CD27+IgD- memory B cells. These cells differ from nonswitched memory B cells (IgM+IgD+CD27+) and may represent a population that has exited the germinal center early or that was formed outside of a germinal center (17). There are no studies to date on B cell distribution in DA, and the extent to which B cells contribute to the features of T21 is currently a matter of debate due to the limited (and at times conflicting) findings on peripheral blood B cell population distribution and serum immunoglobulin levels. One study suggests that B cells are altered in T21. Despite normal serum Ig levels, IgM-expressing nonswitched memory B cells (IgM+IgD+CD27+) show reduced proliferation capacity and somatic hypermutation potential (28). Deficiency in natural effector B cells could result in an increased risk of infection, which is characteristic of T21 (28). Generalized B cell lymphopenia has also been reported, with reduction in transitional (CD38^{high}CD24^{high}) and switched memory B cells. Interestingly, however, under Toll-like receptor 9 stimulation, T21-derived B cells have been shown to differentiate into antibody-producing plasma cells and proliferate at a higher degree than control-derived B cells (5).

T cell responses in DA are characterized by marked functional plasticity, as evidenced by the increased frequency of polyfunctional CD8+, CD8-, and CD161+ Th cells. Previous studies have highlighted the role of CD4+ T cells producing multiple cytokines simultaneously in the pathogenesis and progression of spondyloarthritis, RA, and PsA (14,21,29). These cells are molecularly distinct from monofunctional T cells and are subject to differential chemotaxis, activation, and metabolism (22). Among the Th subsets, CD161+ Th cells and ex-Th17 cells have increased polyfunctionality (20,21). Ex-Th17 cells can be identified based on expression of CD161, a marker of the Th17 lineage, and a switch from IL-17A production to IFN γ production. CD161+ Th cells and ex-Th17 cells have previously been reported to accumulate at the site of inflammation in RA, PsA, and, importantly, JIA (14,20,30). The pathogenic nature of these cells is further exacerbated by their increased survival, cytokine production, and resistance to Treg cell-mediated suppression (20). Herein, we report that in DA there is an increased frequency of proinflammatory cytokine-producing T cells and increased polyfunctionality that is not

restricted to CD8- T cell responses but is evident in CD8+ and CD161+ Th cells. This shows a generalized dysregulation of T cell plasticity in DA over that in JIA, which is a potentially important contributor to disease pathophysiology.

We also demonstrated that dysregulated plasticity is present in the Tfh compartment, with enhanced Tfh responses of a CXCR3+CCR6+ hybrid Th1/Th17-origin cell population. Tfh cell plasticity in DA may be associated with the reduced ICOS expression, since high expression of ICOS has previously been shown to act as an enforcing factor of Tfh cell lineage commitment (25). We performed an analysis of the newly described Tph cells under the CXCR3/CCR6 paradigm, and, similar to findings in the Tfh compartment, CXCR3+CCR6+ Tph cells were increased in DA. In addition to mirroring the observed increased plasticity of Th cells in DA, dysregulated Tfh and Tph cell responses could promote a pathogenic T cell-dependent antibody repertoire.

We performed unbiased multidimensional clustering analysis for the identification of Treg cell populations and, similar to previous findings (27), identified 2 distinct populations: naive and memory Treg cells (31). Notably, we observed a decrease in Treg cells in DA compared to T21 as well as an inverse correlation between the frequencies of Tph and Treg cells in DA. Naive and memory Treg cells reportedly have similar suppressive potential, but a reduced frequency of naive T cells has previously been associated with autoimmune disorders, and memory Treg cells are potentially less able to maintain FoxP3 expression and their own suppressive capacity (31-33). Previous studies in RA have shown no defect in the suppressive capacity of naive or memory peripheral blood Treg cells, but in T21 this suppressive capacity was diminished (31-34). Defective Treg cell responses have also been reported in JIA, with restricted T cell receptor repertoire and a clonotypic expansion profile similar to findings in other arthritides, which can limit the array of T cell responses these cells are able to suppress (35). The enhanced proinflammatory and diminished regulatory processes in the peripheral blood of children with DA is reflected by the increased inflammation and immune cell infiltration in a joint affected by DA compared to JIA. Interestingly, synovial inflammation in DA does not correlate with erythrocyte sedimentation rate (ESR). As we have previously demonstrated in the largest DA patient cohort to date, ESR levels in children with DA are significantly lower than in children with JIA and are of low diagnostic or prognostic value (2). This further highlights the need for careful and thorough examination of suspected DA.

The relatively increased duration of disease in children with DA compared to children with JIA (Supplementary Table 1, <http://online.library.wiley.com/doi/10.1002/art.41150/abstract>) is a potential confounding factor that might influence the differences observed between the 2 groups. Although this is a limitation of the study, it emphasizes the increased need for awareness regarding the diagnosis of DA, as DA diagnoses are significantly delayed

compared to JIA diagnoses (2). Additionally, due to the size of the patient cohort, a potential effect of biologic treatment on the immunologic features of DA cannot be excluded, despite preliminary data suggesting that the immune phenotype observed is independent of treatment or disease duration.

In conclusion, we have for the first time identified an underlying immune system dysregulation in DA, which is potentially more aggressive than JIA and is characterized by enhanced polyreactive T, Tfh, and Tph cell responses, reduced Treg cell frequency, and increased synovial inflammation. The accumulation of this altered immune profile can influence disease progression in DA. A more comprehensive understanding of these mechanisms will lead to improved diagnostic and prognostic outcomes for this disease.

AUTHOR CONTRIBUTIONS

All authors were involved in drafting the article or revising it critically for important intellectual content, and all authors approved the final version to be published. Dr. Fearon had full access to all of the data in the study and takes responsibility for the integrity of the data and the accuracy of the data analysis.

Study conception and design. Foley, Floudas, MacDermott, Veale, Killeen, Fearon.

Acquisition of data. Foley, Floudas, Canavan, Biniacka, Veale, Mullan, Killeen.




Analysis and interpretation of data. Foley, Floudas, Canavan, Biniacka, Mullan, Fearon.

REFERENCES

1. Yancey CL, Zmijewski C, Athreya BH, Doughty RA. Arthropathy of Down's syndrome. *Arthritis Rheum* 1984;27:929–34.
2. Foley C, Killeen OG. Musculoskeletal anomalies in children with Down syndrome: an observational study. *Arch Dis Child* 2019;104:482–7.
3. Pellegrini FP, Marinoni M, Frangione V, Tedeschi A, Gandini V, Ciglia F, et al. Down syndrome, autoimmunity and T regulatory cells. *Clin Exp Immunol* 2012;169:238–43.
4. Giménez-Barcons M, Casteràs A, Armengol Mdel P, Porta E, Correa PA, Marín A, et al. Autoimmune predisposition in Down syndrome may result from a partial central tolerance failure due to insufficient intrathymic expression of AIRE and peripheral antigens. *J Immunol* 2014;193:3872–9.
5. Carsetti R, Valentini D, Marcellini V, Scarsella M, Marasco E, Giustini F, et al. Reduced numbers of switched memory B cells with high terminal differentiation potential in Down syndrome. *Eur J Immunol* 2015;45:903–14.
6. Moore TL. Immune complexes in juvenile idiopathic arthritis [review]. *Front Immunol* 2016;7:177.
7. Ravelli A, Martini A. Juvenile idiopathic arthritis. *Lancet* 2007;369:767–78.
8. Nistala K, Adams S, Cambrook H, Ursu S, Olivito B, de Jager W, et al. Th17 plasticity in human autoimmune arthritis is driven by the inflammatory environment. *Proc Natl Acad Sci U S A* 2010;107:14751–6.
9. Spreafico R, Rossetti M, Whitaker JW, Wang W, Lovell DJ, Albani S. Epipolymorphisms associated with the clinical outcome of autoimmune arthritis affect CD4⁺ T cell activation pathways. *Proc Natl Acad Sci U S A* 2016;113:13845–50.
10. Ohl K, Nickel H, Moncrieffe H, Klemm P, Scheufen A, Föll D, et al. The transcription factor CREM drives an inflammatory phenotype of T cells in oligoarticular juvenile idiopathic arthritis. *Pediatr Rheumatol Online J* 2018;16:39.
11. Zhao Y, Shen M, Feng Y, He R, Xu X, Xie Y, et al. Regulatory B cells induced by pancreatic cancer cell-derived interleukin-18 promote immune tolerance via the PD-1/PD-L1 pathway. *Oncotarget* 2017;9:14803–14.
12. Corcione A, Ferlito F, Gattorno M, Gregorio A, Pistorio A, Gastaldi R, et al. Phenotypic and functional characterization of switch memory B cells from patients with oligoarticular juvenile idiopathic arthritis. *Arthritis Res Ther* 2009;11:R150.
13. Duvall MG, Precopio ML, Ambrozak DA, Jaye A, McMichael AJ, Whittle HC, et al. Polyfunctional T cell responses are a hallmark of HIV-2 infection. *Eur J Immunol* 2008;38:350–63.
14. Wade SM, Canavan M, McGarry T, Low C, Wade SC, Mullan RH, et al. Association of synovial tissue polyfunctional T-cells with DAPSA in psoriatic arthritis. *Ann Rheum Dis* 2019;78:350–4.
15. Roederer M, Nozzi JL, Nason MC. SPICE: exploration and analysis of post-cytometric complex multivariate datasets. *Cytometry A* 2011;79:167–74.
16. Biniacka M, Kennedy A, Fearon U, Ng CT, Veale DJ, O'Sullivan JN. Oxidative damage in synovial tissue is associated with in vivo hypoxic status in the arthritic joint. *Ann Rheum Dis* 2010;69:1172–8.
17. Seifert M, Przekopowicz M, Taudien S, Lollies A, Ronge V, Drees B, et al. Functional capacities of human IgM memory B cells in early inflammatory responses and secondary germinal center reactions. *Proc Natl Acad Sci U S A* 2015;112:E546–55.
18. Iwata Y, Matsushita T, Horikawa M, DiIorio DJ, Yanaba K, Venturi GM, et al. Characterization of a rare IL-10-competent B-cell subset in humans that parallels mouse regulatory B10 cells. *Blood* 2011;117:530–41.
19. Nistala K, Moncrieffe H, Newton KR, Varsani H, Hunter P, Wedderburn LR. Interleukin-17-producing T cells are enriched in the joints of children with arthritis, but have a reciprocal relationship to regulatory T cell numbers. *Arthritis Rheum* 2008;58:875–87.
20. Basdeo SA, Cluxton D, Sulaimani J, Moran B, Canavan M, Orr C, et al. Ex-Th17 (nonclassical Th1) cells are functionally distinct from classical Th1 and Th17 cells and are not constrained by regulatory T cells. *J Immunol* 2017;198:2249–59.
21. Basdeo SA, Moran B, Cluxton D, Canavan M, McCormick J, Connolly M, et al. Polyfunctional, pathogenic CD161⁺ Th17 lineage cells are resistant to regulatory T cell-mediated suppression in the context of autoimmunity. *J Immunol* 2015;195:528–40.
22. Burel JG, Apte SH, Groves PL, McCarthy JS, Doolan DL. Polyfunctional and IFN- γ monofunctional human CD4⁺ T cell populations are molecularly distinct. *JCI Insight* 2017;2:e87499.
23. Morita R, Schmitt N, Benteibibel SE, Ranganathan R, Bourdery L, Zurawski G, et al. Human blood CXCR5⁺CD4⁺ T cells are counterparts of T follicular cells and contain specific subsets that differentially support antibody secretion. *Immunity* 2011;34:P108–21.
24. Ma CS, Wong N, Rao G, Avery DT, Torpy J, Hambridge T, et al. Monogenic mutations differentially affect the quantity and quality of T follicular helper cells in patients with human primary immunodeficiencies. *J Allergy Clin Immunol* 2015;136:993–1006.
25. Weber JP, Fuhrmann F, Feist RK, Lahmann A, Al Baz MS, Gentz LJ, et al. ICOS maintains the T follicular helper cell phenotype by down-regulating Kruppel-like factor 2. *J Exp Med* 2015;212:217–33.
26. Rao DA, Gurish MF, Marshall JL, Slowikowski K, Fonseka CY, Liu Y, et al. Pathologically expanded peripheral T helper cell subset drives B cells in rheumatoid arthritis. *Nature* 2017;542:110–4.
27. Kordasti S, Costantini B, Seidl T, Perez Abellan P, Martinez Llordella M, McLornan D, et al. Deep phenotyping of Tregs identifies an immune signature for idiopathic aplastic anemia and predicts response to treatment. *Blood* 2016;128:1193–205.
28. Verstegen RH, Driessen GJ, Bartol SJ, van Noesel CJ, Boon L, van der Burg M, et al. Defective B-cell memory in patients with Down syndrome. *J Allergy Clin Immunol* 2014;134:1346–53.

29. Jandus C, Bioley G, Rivals JP, Dudler J, Speiser D, Romero P. Increased numbers of circulating polyfunctional Th17 memory cells in patients with seronegative spondylarthritides. *Arthritis Rheum* 2008;58:2307–17.
30. Cosmi L, Cimaz R, Maggi L, Santarlaschi V, Capone M, Borriello F, et al. Evidence of the transient nature of the Th17 phenotype of CD4⁺CD161⁺ T cells in the synovial fluid of patients with juvenile idiopathic arthritis. *Arthritis Rheum* 2011;63:2504–15.
31. Venken K, Hellings N, Broekmans T, Hensen K, Rummens JL, Stinissen P. Natural naive CD4⁺CD25⁺CD127^{low} regulatory T cell (Treg) development and function are disturbed in multiple sclerosis patients: recovery of memory Treg homeostasis during disease progression. *J Immunol* 2008;180:6411–20.
32. Hoffmann P, Eder R, Boeld TJ, Doser K, Piseshka B, Andreesen R, et al. Only the CD45RA⁺ subpopulation of CD4⁺CD25^{high} T cells gives rise to homogeneous regulatory T-cell lines upon in vitro expansion. *Blood* 2006;108:4260–7.
33. Booth NJ, McQuaid AJ, Sobande T, Kissane S, Agius E, Jackson SE, et al. Different proliferative potential and migratory characteristics of human CD4⁺ regulatory T cells that express either CD45RA or CD45RO. *J Immunol* 2010;184:4317–26.
34. Walter GJ, Fleskens V, Frederiksen KS, Rajasekhar M, Menon B, Gerwien JG, et al. Phenotypic, functional, and gene expression profiling of peripheral CD45RA⁺ and CD45RO⁺ CD4⁺CD25⁺CD127^{low} Treg cells in patients with chronic rheumatoid arthritis. *Arthritis Rheumatol* 2016;68:103–16.
35. Henderson LA, Volpi S, Frugoni F, Janssen E, Kim S, Sundel RP, et al. Next-generation sequencing reveals restriction and clonotypic expansion of Treg cells in juvenile idiopathic arthritis. *Arthritis Rheumatol* 2016;68:1758–68.

Disease Severity Linked to Increase in Autoantibody Diversity in IgG4-Related Disease

Hang Liu,¹ Cory A. Perugino,² Musie Ghebremichael,³ Zachary S. Wallace,⁴  Sydney B. Montesi,⁴ John H. Stone,⁴  and Shiv Pillai³ 

Objective. Four autoantigens have been described recently in IgG4-related disease (IgG4-RD): prohibitin, annexin A11, laminin 511-E8, and galectin-3. However, no external validation has been performed, and the possibility that some individuals break tolerance to more than 1 autoantigen has not been explored. We undertook this study to evaluate the relative frequencies of antibody responses against these autoantigens in order to explore the role of adaptive immune response in IgG4-RD.

Methods. Autoantibody responses against prohibitin, annexin A11, and laminin 511-E8 were measured among a clinically diverse cohort of IgG4-RD patients (n = 100) using enzyme-linked immunosorbent assays. Autoantibody responses were correlated with disease severity and organ distribution.

Results. The frequencies of IgG4 autoantibody responses against prohibitin (10%), annexin A11 (12%), and laminin 511-E8 (7%) were not significantly different from those of controls. A portion of the cohort (n = 86) had been analyzed previously at our center for anti-galectin-3 antibody responses, with 25 patients (29%) having IgG4 anti-galectin-3 antibodies. Of these 86 patients, 32 (37%) had IgG4 antibodies to ≥ 1 of the 4 autoantigens and 12 (14%) showed reactivity with ≥ 2 of the tested antigens. The subset of patients with ≥ 2 autoantibodies had higher total levels of IgG1, IgG2, IgG4, and C-reactive protein, were more commonly hypocomplementemic, and were more likely to have visceral organ involvement.

Conclusion. Antibodies against prohibitin, annexin A11, and laminin 511-E8 were found in only a small portion of patients with IgG4-RD. A subset of IgG4-RD patients, however, had IgG4 antibodies against ≥ 2 autoantigens. These patients presented with robust IgG subclass elevations, complement consumption, and visceral organ involvement. This broader break in immunologic tolerance in IgG4-RD was associated with more severe disease.

INTRODUCTION

IgG4-related disease (IgG4-RD) is an insidiously progressive autoimmune fibrotic disease of unknown etiology that often presents with tumor-like masses involving multiple organs (1). Seemingly disparate organ manifestations are unified by the pathologic findings of a dense lymphoplasmacytic infiltrate, fibrosis in a “storiform” pattern (derived from the word “storea,” Latin for woven mat), and obliterative phlebitis, with prominent

IgG4-positive plasma cells noted on immunostaining (2). Characteristics of this disease include the oligoclonal expansion of both plasmablasts and tissue-infiltrating CD4-positive cytotoxic T lymphocytes, the identification of specific autoantigens as B cell targets, and consistent clinical responsiveness to B cell depletion (3–11). These observations support the possibility that IgG4-RD is an autoimmune disease, with an important role for adaptive immune responses in the associated tissue fibrosis.

Supported by grants from the NIH Autoimmune Centers of Excellence to Drs. Stone and Pillai (UM1-AI-144295 and U19-AI-110495). Drs. Perugino and Wallace’s work was supported by a Rheumatology Research Foundation Scientist Development award. Dr. Ghebremichael’s work was supported by a grant from the National Institute of Allergy and Infectious Diseases, NIH (P30-AI-060354). Dr. Montesi’s work was supported by the Parker B. Francis Foundation and the Scleroderma Foundation.

¹Hang Liu, MD: Ragon Institute of MGH, MIT and Harvard, Cambridge, Massachusetts, and First Affiliated Hospital of China Medical University, Shenyang, China; ²Cory A. Perugino, DO: Ragon Institute of MGH, MIT and Harvard, Cambridge, Massachusetts, and Massachusetts General Hospital, Boston; ³Musie Ghebremichael, PhD, Shiv Pillai, MBBS, PhD: Ragon Institute of MGH, MIT and Harvard, Cambridge, Massachusetts; ⁴Zachary S. Wallace,

MD, MSc, Sydney B. Montesi, MD, John H. Stone, MD, MPH: Massachusetts General Hospital, Boston.

Drs. Liu and Perugino contributed equally to this work.

Dr. Perugino has received consulting fees and/or honoraria from UCB and Bristol-Myers Squibb (less than \$10,000 each). Dr. Stone has received consulting fees and/or honoraria from Xencor and Genentech (less than \$10,000 each). Dr. Pillai has received consulting fees and/or honoraria from SAB Biotherapeutics and Apbro Corp (less than \$10,000 each). No other disclosures relevant to this article were reported.

Address correspondence to Shiv Pillai, MBBS, PhD, Ragon Institute of MGH, MIT and Harvard, 400 Technology Square, Cambridge, MA 02139. E-mail: pillai@helix.mgh.harvard.edu.

Submitted for publication May 24, 2019; accepted in revised form October 11, 2019.

Since 2015, 4 autoantigens have been described as potential triggers for IgG4-RD: prohibitin, annexin A11, laminin 511-E8, and galectin-3 (5–8). However, validation of these findings using external patient cohorts and characterization of the relationship between these specific autoantigens has yet to be achieved. Furthermore, annexin A11 and laminin 511-E8 have been reported only in the organ-specific contexts of IgG4-related autoimmune pancreatitis (AIP) and IgG4-related autoimmune cholangitis (AIC) for the former, and AIP for the latter (6,8). In order to explore the role of the adaptive immune response in IgG4-RD, we examined the relative frequencies of antibody responses against prohibitin, annexin A11, laminin 511-E8, and galectin-3 using a large, clinically diverse cohort of patients with IgG4-RD. We analyzed these 4 autoantibodies for correlation with organ distribution, disease severity, and co-occurrence with each other.

PATIENTS AND METHODS

Patient cohorts. One hundred patients with IgG4-RD were recruited between January 10, 2012 and June 25, 2018 through the Division of Rheumatology, Allergy and Immunology at Massachusetts General Hospital. IgG4-RD was defined by the fulfillment of either established histopathologic or comprehensive diagnostic criteria (2,12). The cohort of 100 IgG4-RD patients included those with involvement of the major salivary glands ($n = 55$), pancreas ($n = 32$), lacrimal glands ($n = 31$), kidneys ($n = 21$), retroperitoneum ($n = 20$), lungs ($n = 18$), and/or biliary tract ($n = 14$) (Table 1). Information regarding demographics, treatment, disease activity, laboratory parameters, and disease manifestations was extracted from the medical records. Disease activity was quantified using the IgG4-RD Responder Index, with active disease defined as a score of ≥ 1 (13). All patients had active disease at the time of sample collection despite the fact that 14% were receiving some form of immunosuppression. Seventy-six patients had an elevated serum IgG4 level, and 30 were hypocomplementemic at the time of sampling. The cohort consisted primarily of white patients ($n = 69$), with only 12 patients being of Asian descent (Table 1). Visceral organ involvement was defined by the presence of lung, pancreas, bile duct, or kidney involvement. We clustered our cohort into subsets of patients according to their number of autoantibody responses (no response, 1 response, and ≥ 2 responses) and compared clinical parameters among these groups.

To control for nonspecific observations that may arise in the setting of any chronic fibroinflammatory disease, we used idiopathic pulmonary fibrosis (IPF) plasma samples as a disease control. Samples from IPF patients ($n = 50$) were obtained through Massachusetts General Hospital's Division of Pulmonary & Critical Care Medicine's Biorepository of Interstitial Lung Diseases, as previously described (14). Samples from 50 age- and sex-matched healthy donors were obtained through the Division of Rheumatology, Allergy and Immunology at Massachusetts General Hospital and through Partners HealthCare Biobank, an enterprise-wide

Table 1. Demographic, clinical, and laboratory data on the IgG4-RD cohort ($n = 100$)*

Demographic data	
Age at onset, median (IQR) years	55 (44–66)
Age at diagnosis, median (IQR) years	61 (49–69)
Male sex	68
Ethnicity	
White	69
Asian	12
Hispanic	5
African American	4
Other	10
Clinical data	
Clinically active disease	100
IgG4-RD Responder Index, median (IQR) score	4 (2–6)
Receiving treatment	14
Organ involvement	
Multiorgan involvement	68
No. of organs involved, median (IQR)	3 (2–4)
Salivary glands	55
Lymph nodes	41
Submandibular glands	48
Pancreas	32
Parotid glands	26
Lacrimal glands	31
Lungs	18
Retroperitoneum	20
Kidney	21
Bile ducts	14
Laboratory parameters	
Elevated total IgG ($>1,295$ mg/dl)	63
Elevated serum IgG1 (>928.6 mg/dl)	43
Elevated serum IgG2 (>700.3 mg/dl)	39
Elevated serum IgG3 (>176.1 mg/dl)	36
Elevated serum IgG4 (>86.4 mg/dl)	76
Elevated serum IgE (>114 kU/liter)	54
Low serum IgM (<53 mg/dl)	39
Hypocomplementemia (C3 <81 mg/dl or C4 <12 mg/dl)	30
Elevated CRP (>8.0 mg/liter)	35
Elevated ESR (>13 mm/hour)	63

* Except where indicated otherwise, values are the percent. IgG4-RD = IgG4-related disease; IQR = interquartile range; CRP = C-reactive protein; ESR = erythrocyte sedimentation rate.

repository of samples obtained from consenting subjects. For healthy controls, we excluded those with any history of malignancy, autoimmune disease, or recurrent/chronic infections by review of the medical records. All studies were approved by the Partners Institutional Review Board, and written informed consent was obtained prior to sample collection. Plasma was collected from subjects, separated by centrifugation, and stored at -80°C until the time of use. Autoantibody diversity was defined as antibody responses to ≥ 2 self antigens from an individual subject.

Enzyme-linked immunosorbent assays (ELISAs).

ELISAs for antibodies against prohibitin, annexin A11, and laminin 511-E8 were performed as previously described in the identification of galectin-3 autoantibody responses in the context of IgG4-RD (7). Briefly, alternating rows of 96-well

plates were coated with antigen to allow for negative control wells (bovine serum albumin [BSA] only) specific for each sample tested. Plate coating concentrations and plasma dilutions used for each antigen were consistent with those in previous studies: prohibitin (no. 178465; Abcam) (coating concentration 0.5 µg/ml, plasma dilution 1:100), annexin A11 (no. 101050; Abcam) (coating concentration 1 µg/ml, plasma dilution 1:100), and laminin 511-E8 (no. 892011; Nacalai) (coating concentration 2 µg/ml, plasma dilution 1:20). Each plasma sample was tested in triplicate with corresponding triplicate BSA-only wells without antigen coating to control for nonspecific protein–protein and protein–plate interactions. Secondary antibodies included rabbit anti-human IgG (no. 6759; Abcam), mouse anti-human IgG1 (no. 99774; Abcam), and mouse anti-human IgG4 (no. 99817; Abcam). The same mouse anti-human IgG4 secondary antibody that was previously used to identify anti-galectin-3 responses in IgG4-RD was employed in the current study. If any individual well deviated by >50% from its respective replicates, that well was not included in the calculation of the average absorbance. A cut-off value of 2 standard deviations above the mean in healthy donors was used to categorically define a positive antibody response.

Statistical analysis. Descriptive measures such as median, interquartile range, frequency, and percentage were used to summarize the data. The Mann-Whitney test was used to compare continuous variables between 2 groups. For comparisons between >2 groups, the Kruskal-Wallis test with Dunn’s post hoc analysis was used. Regression analyses using logistic regression models were utilized to assess the predictors of diverse autoantibody responses. The maximum likelihood method was used to estimate model parameters, and significance was tested using Wald’s test statistic. *P* values (2-sided) less than 0.05 were considered significant. Statistical analysis was performed using SAS 9.4 and GraphPad Prism 8.0.

RESULTS

Low frequencies of IgG4 antibodies against prohibitin, annexin A11, and laminin 511-E8 in systemic IgG4-RD.

The frequencies of antibodies were similar across all 3 autoantigens: 10% for prohibitin, 12% for annexin A11, and 7% for laminin 511-E8 (Figures 1A–C). None of these frequencies among the IgG4-RD patients differed significantly from those in controls.

To investigate consistency with previously published data related to laminin 511-E8, we examined total IgG and IgG1-specific

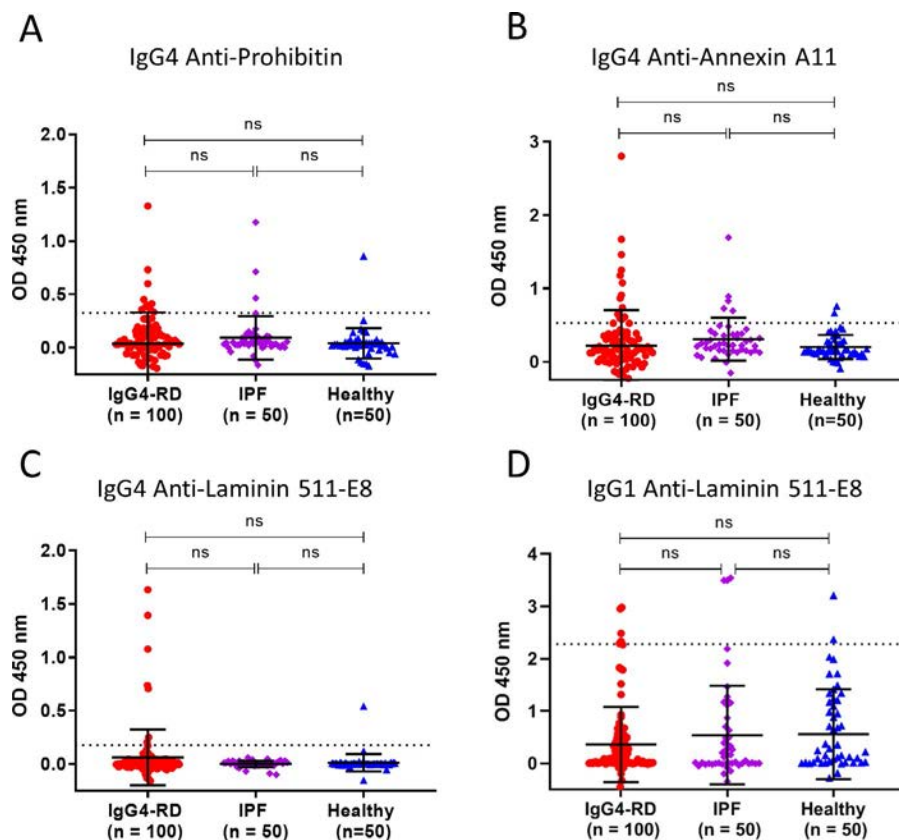


Figure 1. Frequencies of autoantibody responses against prohibitin (A), annexin A11 (B), and laminin 511-E8 (C) and against IgG1 laminin 511-E8 (D) among patients with systemic IgG4-related disease (IgG4-RD). Symbols represent individual subjects; bars show the mean ± SD. Dotted lines show the cutoff for positivity (2 SD above the mean in healthy donors). IPF = idiopathic pulmonary fibrosis; NS = not significant. Color figure can be viewed in the online issue, which is available at <http://onlinelibrary.wiley.com/doi/10.1002/art.41140/abstract>.

responses against this antigen among our cohort, but observed only a low frequency of reactivity using either of these secondary antibodies (1% for IgG and 6% for IgG1) (Figure 1D and Supplementary Figure 1A, on the *Arthritis & Rheumatology* web site at <http://onlinelibrary.wiley.com/doi/10.1002/art.41140/abstract>). For IgG anti-laminin 511-E8 responses, we observed higher frequencies among both control groups compared to IgG4-RD patients (Supplementary Figure 1A). To understand the discrepancy in IgG4 and total IgG antibody response frequencies against laminin 511-E8, we studied the relative sensitivity of each of these secondary antibodies in detecting purified human IgG4. We observed the ability of the anti-human IgG4 secondary antibody to detect plate-bound IgG4 at a concentration of 1 ng/well. In contrast, the anti-human IgG secondary antibody required a 10-fold greater coating concentration in order to generate a comparable colorimetric signal on ELISA (Supplementary Figure 1B).

Frequencies of annexin A11 and laminin 511-E8 autoantibodies are not increased in patients with pancreatobiliary disease. Because annexin A11 and laminin 511-E8 have been described in smaller IgG4-RD cohorts with high frequencies of pancreatobiliary involvement (annexin A11) or pancreatic involvement (laminin 511-E8) (6,8), we evaluated the frequency of those antibody responses within the corresponding subset of organ involvement in our cohort. We found that 22% of the AIP or AIC patients had IgG4 antibody responses against annexin A11. For laminin 511-E8, we observed IgG4 antibodies among 12.5% of the AIP patients.

In contrast to annexin A11 and laminin 511-E8, only anti-prohibitin antibodies had been reported in the context of multiorgan systemic IgG4-RD (5), thereby permitting a direct comparison to the present cohort. The frequency of anti-prohibitin responses observed among the systemic and clinically diverse cohort was 10%.

We also assessed whether antibody responses against annexin A11 or laminin 511-E8 could be predicted by stratifying

our cohort based on specific organ involvement, with the stratifications designed to reflect the patient populations from the studies in which antibodies to annexin A11 and laminin 511-E8 were originally identified. We therefore compared annexin A11 autoantibody responses between IgG4-RD patients with AIP or AIC and those without such involvement and compared laminin 511-E8 responses between IgG4-RD patients with and without pancreatic involvement. No significant differences were seen between the groups (Figures 2A and B), suggesting that these autoantigen responses are not predicted by such organ-specific involvement.

Reactivity against multiple autoantigens in a subset of IgG4-RD patients. We previously reported that 28% of subjects from a cohort of 121 IgG4-RD patients had autoantibodies directed against galectin-3 (7). We examined the reactivity in patients in the present cohort who had data available regarding galectin-3 antibody responses ($n = 86$). Among these patients, 32 (37%) had IgG4 reactivity with ≥ 1 of the 4 autoantigens. We also explored the number of specific autoantibody responses for each patient with ≥ 1 autoantibody response. The majority of these patients (62.5%; $n = 20$) showed reactivity with only 1 of the 4 autoantigens, but 12 patients (37.5%) reacted with ≥ 2 autoantigens. Five patients (15.6%), 4 patients (12.5%), and 3 patients (9.4%) responded to 2, 3, or all 4 autoantigens, respectively (Figure 3A).

When analyzing the overlapping reactivity between these 4 autoantigens, we did not observe any IgG4 anti-laminin 511-E8 responses in isolation (Figure 3B). All 7 patients with IgG4 anti-laminin 511-E8 responses also showed reactivity with ≥ 1 other autoantigen studied. Galectin-3, the autoantigen with the highest baseline frequency of reactivity in this cohort, had the highest proportion of isolated autoantibody responses. Fourteen (56%) of the 25 patients with anti-galectin-3 antibodies had no response to any of the other 3 autoantigens studied. Overall, we did not observe any specific clustering in co-occurrence of antibody responses among the 4 autoantigens tested (Figure 3B).

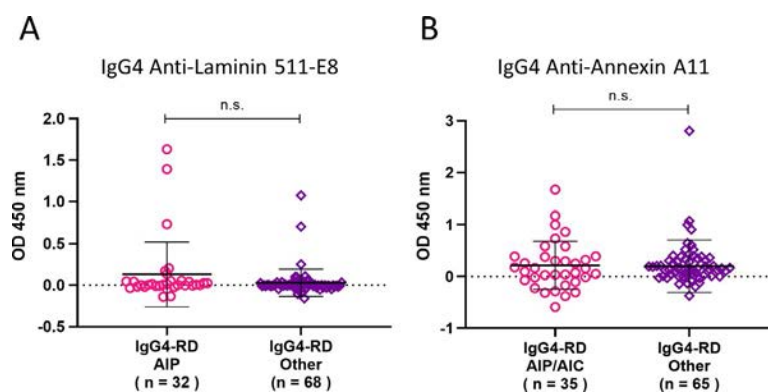


Figure 2. Responses to annexin A11 and laminin 511-E8 autoantibodies according to pancreatobiliary involvement (autoimmune pancreatitis [AIP] or autoimmune cholangitis [AIC]). IgG4 anti-laminin 511-E8 (A) and IgG4 anti-annexin A11 (B) antibody responses in IgG4-related disease (IgG4-RD) patients with pancreatic or biliary involvement and those without such involvement are shown. Symbols represent individual subjects; bars show the mean \pm SD. NS = not significant. Color figure can be viewed in the online issue, which is available at <http://onlinelibrary.wiley.com/doi/10.1002/art.41140/abstract>.

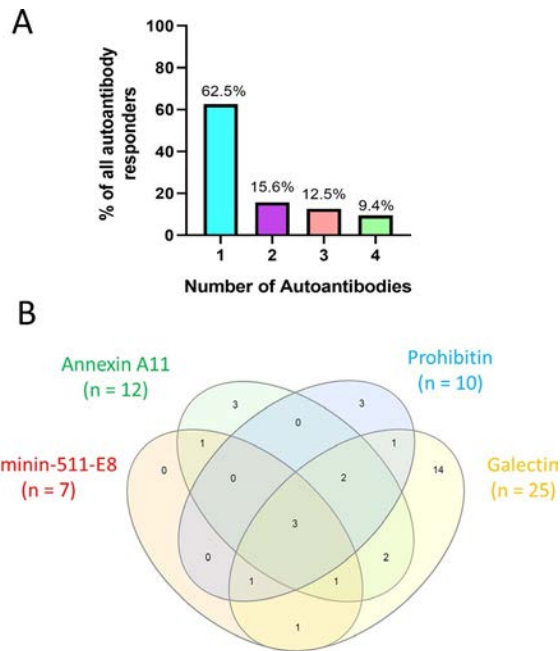


Figure 3. B cell responses of IgG4-related disease (IgG4-RD) patients to autoantigens. **A**, Percentages of subject reactivity with number of specific autoantibodies (among 32 patients with response to ≥ 1 autoantibody). **B**, Overlap in antigen reactivity between annexin A11, laminin 511-E8, prohibitin, and galectin-3 among all subjects with response to ≥ 1 IgG4 autoantibody (n = 32).

Correlation of disease severity with T-dependent B cell responses to multiple autoantigens in patients with IgG4-RD. We examined the correlation between the number of specific autoantibody responses per patient and the severity of the clinical phenotype. No clinical phenotypic differences were observed between the group with no autoantibody responses

and those with a single autoantibody response (data not shown). Given the similarities between these groups, we then compared the subset of patients with ≥ 2 autoantibody responses, representing 14% of our cohort (n = 12), to all other patients and observed a distinctly more severe clinical phenotype among patients in this subset. Higher levels of IgG1, IgG2, IgG4, and C-reactive protein (CRP), greater complement consumption, and more frequent visceral organ involvement were associated with diverse autoantibody responses (Figure 4).

DISCUSSION

Considerable insight into the immunologic mechanisms of IgG4-RD has been achieved in the last decade, but few systematic efforts to identify the antigens driving this immune response have been undertaken (15). Given the protean clinical nature of IgG4-RD and the possibility that a diverse array of proteins may be involved in driving the disease in different patients, external validation of any proposed autoantigen in this disease is essential. In the present study, we leveraged a large, clinically diverse cohort of IgG4-RD patients to assess the frequency of antibody responses against 3 antigens recently described as being associated with IgG4-RD: annexin A11, laminin 511-E8, and prohibitin. We observed IgG4-specific autoantibody responses against each of these proteins, but the frequency of such responses was relatively low among our cohort compared to the results from the 3 cohorts in which these autoantibody responses were initially described (5,6,8).

For these 3 autoantibodies, the low frequency observed in IgG4-RD patients is similar to the frequency observed in controls. With antibody response frequencies of only 7%, 10%, 12%, and 28% for laminin 511-E8, prohibitin, annexin A11, and galectin-3,

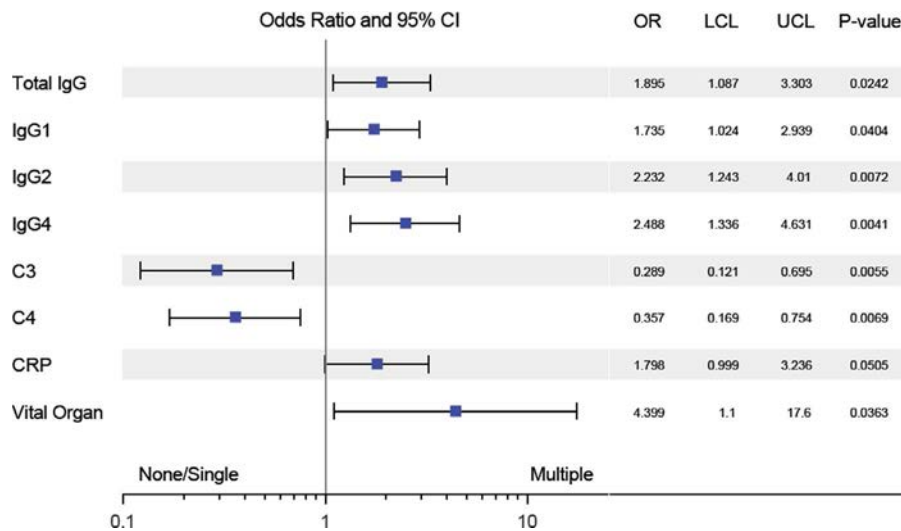


Figure 4. Association of disease severity in IgG4-related disease (IgG4-RD) and response to multiple autoantibodies. Forest plot shows the odds ratio (OR) and 95% confidence interval (95% CI) for multiple autoantigen responses in relation to the presence of increased levels of different categorical and continuous variables. Variables favoring response to 1 or no autoantigens and those favoring response to multiple autoantigens are shown. LCL = lower control limit; UCL = upper control limit; CRP = C-reactive protein. Color figure can be viewed in the online issue, which is available at <http://onlinelibrary.wiley.com/doi/10.1002/art.41140/abstract>.

respectively, it seems clear that none of these autoantigens constitutes a dominant antigen in the context of IgG4-RD. Additionally, we did not observe any organ-specific enrichment for pancreatic or biliary involvement among the patients with autoantibodies directed against annexin A11 and laminin 511-E8 (6,8). The frequencies of antibody responses against these 2 autoantigens among subsets of our patients with AIP or AIC were comparable to those previously reported: 22% versus 18% for annexin A11 in AIP/AIC patients (6), and 12.5% versus 10% for laminin 511-E8 in AIP patients (8).

Some of the antibody response frequencies observed among patients in this cohort were widely discrepant from those previously reported. Anti-laminin 511-E8 IgG was detected in only 1% of our IgG4-RD cohort, which is comparable to the 1.6% response frequency observed among controls by Shiokawa et al, but markedly below the 51% frequency reported in their cohort of IgG4-related AIP patients (8). Similarly, although anti-prohibitin IgG4 was reported to occur in 73% of IgG4-RD patients with diverse organ manifestations (5), we found only 10% IgG4 reactivity among the patients in our similarly diverse cohort. One possible explanation for these discrepancies may be related to genetic differences between the studied cohorts. For example, HLA class II molecules that are more prevalent among East Asian populations compared to white populations may be much more efficient at presenting immune-dominant peptides from laminin 511-E8 or prohibitin to follicular helper T cells, thereby permitting such IgG or IgG4 antibody responses. This possibility highlights the importance of cross-validation studies in patients of both East Asian and Western descent. More exuberant serum IgG4 increases were recently demonstrated to occur among East Asian patients with IgG4-RD compared to other patients (16). Such ethnic comparisons will be important in understanding the generalizability of regional findings related to IgG4-RD.

Autoantibody responses are surrogate markers of autoreactive B cell clones that have evaded normal tolerance mechanisms. In IgG4-RD, the oligoclonal proliferation of antibody-producing cells has been tied to disease activity, and the marked clinical responsiveness to B cell depletion reinforces the importance of B cells in the pathophysiology of IgG4-RD (3,9,17–19). Whether this is related to cytokine secretion, the elaboration of pathogenic autoantibodies, the presentation of antigen to disease-driving CD4+ cytotoxic T cells, a direct cytotoxic effect of B cell subsets, or a combination of these effector functions remains unknown. The adoptive transfer of purified immunoglobulin from IgG4-RD patients to mice results in disease within organs typically affected by IgG4-RD, suggesting the possibility that antibodies may have a direct pathogenic role in IgG4-RD (20). The finding that a distinct subset of IgG4-RD patients with multiple autoantibodies of differing specificity suggests that some patients have a more flagrant breach of B cell tolerance compared to others. This subset of patients was clinically marked by a robust humoral immune response (higher IgG, IgG1, IgG2, IgG4 levels), greater comple-

ment consumption (low C3 or C4 levels), more systemic inflammation (higher CRP levels), and more severe disease (higher likelihood of visceral organ involvement). These correlations suggest that patients with diverse B cell autoantigen responses have a more severe clinical phenotype.

The correlation of hypocomplementemia with diverse autoantibody responses supports the possibility that immune complexes are relevant to the disease process in a subset of patients with IgG4-RD (21,22). However, it is also possible that in patients with more severe disease, breaking of immune tolerance is more efficient, higher nonpathogenic antibody titers against self antigens are generated, and the transient formation of circulating immune complexes, and thus hypocomplementemia, is induced. These findings could also merely represent epiphenomena of limited relevance to the pathogenesis of IgG4-RD.

The IgG4-RD Responder Index is designed to measure disease activity longitudinally on an individual basis but is not suited to comparisons of disease severity across subjects (13). For instance, a patient with asymptomatic disease confined to the lacrimal, parotid, and submandibular glands would be assigned a score of 6, while a patient admitted to the hospital with obstructive jaundice secondary to a pancreatic mass would be given a score of 4. Similarly, the number of organs involved, or multiple organ involvement versus single organ involvement, is susceptible to limitations in broadly assessing disease severity.

Without a validated tool to gauge disease severity, we used the likelihood of having visceral organ involvement (lung, pancreas, bile ducts, kidney) as a surrogate indicator of disease severity. In contrast to patients with disease limited to the lacrimal or salivary glands, those with visceral organ involvement generally require more urgent therapeutic intervention. This clinical phenotype of visceral organ involvement did correlate with the number of different autoantibody responses per individual patient. Our group recently described the clustering of IgG4-RD patients based on the clinical phenotypes of organ distribution, with certain clusters being distinguished by visceral organ involvement (23). The positive correlation of more severe disease involvement with IgG4 autoantibody diversity supports the possibility that such antibodies may be pathogenic in IgG4-RD. Additional studies of IgG4 autoantibodies in the pathophysiology of IgG4-RD and their relationship to disease severity are warranted.

A potential limitation of the present study is the inclusion of samples from patients exhibiting galectin-3 autoantibody responses, from our previously described IgG4-RD cohort (7). The plasma samples utilized here to validate anti-annexin A11, anti-laminin 511-E8, and anti-prohibitin autoantibody responses were chosen based on sample availability. Among the 86 patients used for the current validation studies who also had available data regarding galectin-3 responses, 25 (29%) had known IgG4 anti-galectin-3 autoantibody responses. This response rate was comparable to the anti-galectin-3 response frequency we previously reported among the larger cohort of 121 IgG4-RD patients

(28%), which suggests that the patients used in the current analysis were reflective of the greater cohort. Moreover, as a means of eliminating detection bias, the same healthy subject and IPF plasma samples that had previously been used in our work on galectin-3 (7) were used in the present study.

In summary, we evaluated prohibitin, annexin A11, and laminin 511-E8 as autoantigens in IgG4-RD using a large and clinically diverse cohort of IgG4-RD patients. Antibodies to these autoantigens were observed only at a low frequency in the present cohort, were equally frequent in control subjects, and were not associated with specific organ involvement. We identified the presence of a subset of IgG4-RD patients with multiple autoantigen B cell responses who were clinically characterized by more severe disease with higher IgG4 levels, more complement consumption, higher CRP levels, and more visceral organ involvement. While these findings suggest the underlying importance of B cell tolerance and the potential pathogenicity of autoantibodies in IgG4-RD, they also highlight the unmet need for identifying a dominant and specific antigen that may drive the pathogenesis of IgG4-RD. Such a discovery would create a novel diagnostic option and broaden our understanding of this immune-mediated fibrotic disease.

AUTHOR CONTRIBUTIONS

All authors were involved in drafting the article or revising it critically for important intellectual content, and all authors approved the final version to be published. Dr. Pillai had full access to all of the data in the study and takes responsibility for the integrity of the data and the accuracy of the data analysis.

Study conception and design. Perugino.

Acquisition of data. Liu, Perugino, Wallace, Montesi, Stone, Pillai.

Analysis and interpretation of data. Liu, Perugino, Ghebremichael, Pillai.

REFERENCES

- Kamisawa T, Zen Y, Pillai S, Stone JH. IgG4-related disease. *Lancet* 2015;385:1460–71.
- Deshpande V, Zen Y, Chan JK, Yi EE, Sato Y, Yoshino T, et al. Consensus statement on the pathology of IgG4-related disease. *Mod Pathol* 2012;25:1181–92.
- Mattoo H, Mahajan VS, Della-Torre E, Sekigami Y, Carruthers M, Wallace ZS, et al. De novo oligoclonal expansions of circulating plasmablasts in active and relapsing IgG4-related disease. *J Allergy Clin Immunol* 2014;134:679–87.
- Mattoo H, Mahajan VS, Maehara T, Deshpande V, Della-Torre E, Wallace ZS, et al. Clonal expansion of CD4⁺ cytotoxic T lymphocytes in patients with IgG₄-related disease. *J Allergy Clin Immunol* 2016;138:825–38.
- Du H, Shi L, Chen P, Yang W, Xun Y, Yang C, et al. Prohibitin is involved in patients with IgG4 related disease. *PLoS One* 2015;10:e0125331.
- Hubers LM, Vos H, Schuurman AR, Erken R, Oude Elferink RP, Burgering B, et al. Annexin A11 is targeted by IgG4 and IgG1 autoantibodies in IgG4-related disease. *Gut* 2018;67:728–35.
- Perugino CA, AlSalem SB, Mattoo H, Della-Torre E, Mahajan V, Ganesh G, et al. Identification of galectin-3 as an autoantigen in patients with IgG₄-related disease. *J Allergy Clin Immunol* 2019;143:736–45.
- Shiokawa M, Kodama Y, Sekiguchi K, Kuwada T, Tomono T, Kuriyama K, et al. Laminin 511 is a target antigen in autoimmune pancreatitis. *Sci Transl Med* 2018;10:eaq0997.
- Carruthers MN, Topazian MD, Khosroshahi A, Witzig TE, Wallace ZS, Hart PA, et al. Rituximab for IgG4-related disease: a prospective, open-label trial. *Ann Rheum Dis* 2015;74:1171–7.
- Majumder S, Mohapatra S, Lennon RJ, Piovezani Ramos G, Postier N, Gleeson FC, et al. Rituximab maintenance therapy reduces rate of relapse of pancreaticobiliary immunoglobulin G4-related disease. *Clin Gastroenterol Hepatol* 2018;16:1947–53.
- Ebbo M, Grados A, Samson M, Groh M, Loundou A, Rigolet A, et al. Long-term efficacy and safety of rituximab in IgG4-related disease: data from a French nationwide study of thirty-three patients. *PLoS One* 2017;12:e0183844.
- Umehara H, Okazaki K, Masaki Y, Kawano M, Yamamoto M, Saeki T, et al. Comprehensive diagnostic criteria for IgG4-related disease (IgG4-RD), 2011. *Mod Rheumatol* 2012;22:21–30.
- Wallace ZS, Khosroshahi A, Carruthers MD, Perugino CA, Choi H, Campochiaro C, et al. An international, multi-specialty validation study of the IgG4-Related Disease Responder Index. *Arthritis Care Res (Hoboken)* 2018;70:1671–8.
- Lagares D, Ghassemi-Kakroodi P, Tremblay C, Santos A, Probst CK, Franklin A, et al. ADAM10-mediated ephrin-B2 shedding promotes myofibroblast activation and organ fibrosis. *Nat Med* 2017;23:1405–15.
- Perugino CA, Mattoo H, Mahajan VS, Maehara T, Wallace ZS, Pillai S, et al. IgG4-related disease: insights into human immunology and targeted therapies. *Arthritis Rheumatol* 2017;69:1722–32.
- Qi R, Chen LY, Park S, Irvine R, Seidman MA, Kelsall JT, et al. Utility of serum IgG4 levels in a multiethnic population. *Am J Med Sci* 2018;355:61–6.
- Wallace ZS, Mattoo H, Carruthers M, Mahajan VS, Della Torre E, Lee H, et al. Plasmablasts as a biomarker for IgG4-related disease, independent of serum IgG4 concentrations. *Ann Rheum Dis* 2015;74:190–5.
- Doorenspleet ME, Hubers LM, Culver EL, Maillette de Buy Wenniger LJ, Klarenbeek PL, Chapman RW, et al. Immunoglobulin G4⁺ B-cell receptor clones distinguish immunoglobulin G 4-related disease from primary sclerosing cholangitis and biliary/pancreatic malignancies. *Hepatology* 2016;64:501–7.
- Della-Torre E, Feeney E, Deshpande V, Mattoo H, Mahajan V, Kulikova M, et al. B-cell depletion attenuates serological biomarkers of fibrosis and myofibroblast activation in IgG4-related disease. *Ann Rheum Dis* 2015;74:2236–43.
- Shiokawa M, Kodama Y, Kuriyama K, Yoshimura K, Tomono T, Morita T, et al. Pathogenicity of IgG in patients with IgG4-related disease. *Gut* 2016;65:1322–32.
- Cornell LD. IgG4-related kidney disease. *Semin Diagn Pathol* 2012;29:245–250.
- Zhang P, Cornell LD. IgG4-related tubulointerstitial nephritis. *Adv Chronic Kidney Dis* 2017;24:94–100.
- Wallace ZS, Zhang Y, Perugino CA, Naden R, Choi HK, Stone JH, et al. Clinical phenotypes of IgG4-related disease: an analysis of two international cross-sectional cohorts. *Ann Rheum Dis* 2019;78:406–12.

LETTERS

DOI 10.1002/art.41148

Additional analyses to confirm relationship of hydroxychloroquine blood levels to retinopathy: comment on the article by Petri et al

To the Editor:

We read with great interest the report by Petri et al describing their study of the association between hydroxychloroquine (HCQ) blood levels and frequency of HCQ retinopathy (Petri M, Elkhalfa M, Li J, Magder LS, Goldman DW. Hydroxychloroquine blood levels predict hydroxychloroquine retinopathy. *Arthritis Rheumatol* 2020;72:448–53). The authors concluded that monitoring HCQ blood levels has clinical value in predicting retinopathy. However, some issues remain to be resolved.

First, mean or maximum HCQ blood levels were used to investigate the relationship with risk of HCQ retinopathy in this study. We noted no rigidly bound treatment intervals (quarterly or more frequently if necessary) in the prospective study, and a considerable variation in HCQ blood levels over time, in the 492 patients with median of 7 measurements. Therefore, we believe time-adjusted mean HCQ blood levels would be more appropriate and should be applied to strengthen the reliability of the key finding (Ibañez D, Urowitz MB, Gladman DD. Summarizing disease features over time. I. Adjusted mean SLEDAI derivation and application to an index of disease activity in lupus. *J Rheumatol* 2003;30:1977–82). Furthermore, as the risk of HCQ toxicity is closely associated with duration of HCQ intake, we think an additional subgroup analysis according to duration of HCQ intake or using Cox regression models could be performed to demonstrate the (independent) value of HCQ blood levels in predicting retinopathy. Finally, patients with a diagnosis of “no” or “possible” HCQ toxicity were classified as not having toxicity, with only those for whom “yes” was recorded categorized as having it. Although this approach is acceptable, we strongly suggest that a sensitivity analysis excluding individuals with “possible” HCQ toxicity or classifying them into the “yes” group should be conducted.

Wen-hui Xie, PhD 
Zhuo-li Zhang, MD, PhD
*Peking University First Hospital
Beijing, China*

DOI 10.1002/art.41146

Reply

To the Editor:


We thank Drs. Xie and Zhang for their suggestions regarding additional analyses of our data we could perform. In response, we have conducted the suggested analyses.

First, as suggested, we reclassified patients based on their time-adjusted mean HCQ blood levels. Tertiles of time-adjusted mean levels ($n = 164$ per tertile) were as follows: 0–739 ng/ml, 740–1,180 ng/ml, and 1,181–3,466 ng/ml. In the lowest, intermediate, and highest tertiles, respectively, the number of patients exhibiting HCQ toxicity was 2 (1.2%), 5 (3.1%), and 14 (8.5%) ($P = 0.0036$, P for trend = 0.0010). Thus, the observed relationship between HCQ blood levels and risk of toxicity in this analysis was very similar to the findings presented in our published article.

Second, we used logistic regression to determine whether there was still a statistically significant association between mean HCQ blood levels and retinopathy after adjustment for duration of HCQ treatment. The results were again similar to those described in our article, as well as those reported above ($P = 0.016$, P for trend = 0.003).

Third, we performed a sensitivity analysis in which patients in the “possible” retinopathy group were included with the “yes” group. In this analysis, the estimated risk of retinopathy doubled to 8.6%. However, almost all of the relationships with predictors were similar to those described in the article. One exception was that, after inclusion of the patients with “possible” retinopathy in the “yes” group, we found a statistically significant association with body mass index (BMI) ($P = 0.0032$), with higher rates of retinopathy among those with a BMI of >25 kg/m².

There are always multiple decisions to be made when analyzing data. It is reassuring that in this case, the main conclusions were not affected by the decisions we made.

Michelle Petri, MD, MPH 
Jessica Li, MPH
Johns Hopkins University School of Medicine
Laurence S. Magder, PhD, MPH
University of Maryland School of Medicine
Daniel W. Goldman, PhD, MCS
*Johns Hopkins University School of Medicine
Baltimore, MD*

DOI 10.1002/art.41178

Does leukopenia influence performance of the new European League Against Rheumatism/American College of Rheumatology classification criteria in an African-descendent population with childhood-onset systemic lupus erythematosus? Comment on the article by Aringer et al

To the Editor:

We read with great interest the article by Dr. Aringer et al, describing the development of the 2019 European League

Table 1. Performance measures for the new EULAR/ACR criteria in classifying childhood-onset SLE at first visit/baseline and at 1-year follow-up, excluding patients who fulfilled the hematologic domain through isolated leukopenia*

Time of assessment, cutoff point	Sensitivity, % (95% CI)	Specificity, % (95% CI)	PPV, %	NPV, %	Cutoff point accuracy, % (95% CI)
First visit/baseline					
Total score ≥ 10	83.7 (75.1–90.2)	70.4 (59.2–80.0)	78.4	77.0	77.8 (71.2–83.6)
Total score ≥ 13	74.0 (64.5–82.1)	92.6 (84.6–97.2)	92.8	73.5	82.2 (75.9–87.4)
1-year follow-up					
Total score ≥ 10	94.3 (88.1–97.9)	61.5 (49.8–72.3)	76.9	88.9	80.4 (74.0–85.9)
Total score ≥ 13	89.6 (82.2–94.7)	88.5 (79.2–94.6)	91.4	86.3	89.1 (83.7–93.2)


* EULAR = European League Against Rheumatism; ACR = American College of Rheumatology; 95% CI = 95% confidence interval; PPV = positive predictive value; NPV = negative predictive value.

Against Rheumatism (EULAR)/American College of Rheumatology (ACR) classification criteria for systemic lupus erythematosus (SLE) (1). These new criteria include positive antinuclear antibody (ANA) as an obligatory entry criterion and additive weighted criteria grouped in 7 clinical and 3 immunologic domains. Patients accumulating ≥ 10 points are classified as having SLE. The new EULAR/ACR criteria set has strong operating characteristics, with excellent sensitivity and specificity compared to the 1997 update to the 1982 ACR criteria for the classification of SLE and the Systemic Lupus International Collaborating Clinics 2012 criteria (2,3).

Our group recently published a study that assessed the performance of the new EULAR/ACR classification criteria in a population with childhood-onset SLE and controls with other defined rheumatic diseases that often are difficult to distinguish from childhood-onset SLE in daily clinical practice (4). Both our childhood-onset SLE group and the control patients were all positive for ANA, which may constitute an external validation since the original derivation and validation cohorts did not include patients with childhood-onset SLE, as stated by Aringer et al (1). We found that in the juvenile population, the EULAR/ACR SLE criteria set could still be used to classify patients as having childhood-onset SLE, but with a cutoff of ≥ 13 rather than ≥ 10 .

We subsequently tested the hypothesis raised by Aringer et al that leukocyte counts of $< 4,000/\text{mm}^3$ may have an influence on criteria performance in African American cohorts. Although each individual criterion was counted only when not better explained by another condition, we were interested in testing the idea that by excluding from the performance analysis those patients in our childhood-onset SLE cohort who fulfilled the hematologic domain through isolated leukopenia, a score of ≥ 13 , would still be most appropriate to classify childhood-onset SLE.

We found that a score of ≥ 13 did in fact result in higher specificity ($P < 0.001$), positive predictive value, and cutoff point accuracy, at first visit and 1-year follow-up (Table 1). We conclude that a total EULAR/ACR score of ≥ 13 would still be most appropriate to classify childhood-onset SLE based on our study, which included a predominantly African-descendent population, even if patients who fulfilled the hematologic domain due to leukopenia alone were excluded from the performance analysis.

Adriana R. Fonseca, MD, MSc 
 Marta C. F. Rodrigues, MD, MSc
 Flavio Sztajn bok, MD, PhD
 Marcelo G. P. Land, MD, PhD
 Sheila K. F. de Oliveira, MD, PhD
 Universidade Federal do Rio de Janeiro
 Rio de Janeiro, Brazil

1. Aringer M, Costenbader K, Daikh D, Brinks R, Mosca M, Ramsey-Goldman R, et al. 2019 European League Against Rheumatism/American College of Rheumatology classification criteria for systemic lupus erythematosus. *Arthritis Rheumatol* 2019;71:1400–12.
2. Hochberg MC, for the Diagnostic and Therapeutic Criteria Committee of the American College of Rheumatology. Updating the American College of Rheumatology revised criteria for the classification of systemic lupus erythematosus [letter]. *Arthritis Rheum* 1997;40:1725.
3. Petri M, Orbai AM, Alarcon GS, Gordon C, Merrill JT, Fortin PR, et al. Derivation and validation of the Systemic Lupus International Collaborating Clinics classification criteria for systemic lupus erythematosus. *Arthritis Rheum* 2012;64:2677–86.
4. Rodrigues Fonseca A, Felix Rodrigues MC, Sztajn bok FR, Gerardin Poirot Land M, Knupp Feitosa de Oliveira S. Comparison among ACR1997, SLICC and the new EULAR/ACR classification criteria in childhood-onset systemic lupus erythematosus. *Adv Rheumatol* 2019;59:20.

DOI 10.1002/art.41177

Reply


To the Editor:


Dr. Fonseca and colleagues refer to their analysis of the new EULAR/ACR 2019 criteria in a group of 122 patients with childhood-onset SLE and 89 patients with other diagnoses mimicking SLE (1). This analysis was published before the full contents of the EULAR/ACR 2019 criteria were available, which may explain why some important aspects were not taken into account. Using the EULAR/ACR criteria under these conditions, Fonseca et al found a sensitivity of 87.7% at the first visit (close to the 89.3% sensitivity of the Systemic Lupus International Collaborating Clinics [SLICC] criteria [2]). However, specificity was lower in their pediatric control cohort of 89 subjects (67%) than in our adult non-SLE validation cohort of 574 subjects (93%).

While unfortunately details on the exact distribution of the EULAR/ACR criteria items were not provided by Fonseca et al (1), the data on the SLICC criteria items listed suggest that item attribution for the EULAR/ACR criteria may not have been correctly performed. For example, 25% of the non-SLE patients in their sample had an acute cutaneous lupus erythematosus (ACLE) rash (1). If this were true ACLE by the EULAR/ACR definition ("Malar rash or generalized maculopapular rash observed by a clinician. If skin biopsy is performed, typical changes must be present [interface vacuolar dermatitis consisting of a perivascular lymphohistiocytic infiltrate, often with dermal mucin noted. Perivascular neutrophilic infiltrate may be present early in the course]), many of these patients would be expected to have SLE, as it is a highly specific manifestation and carries a weight of 6 points in the EULAR/ACR criteria. However, if these were other rashes and not true ACLE, they should not be attributed to SLE according to the guidelines for scoring the EULAR/ACR criteria.

The EULAR/ACR SLE criteria attribution rule specifies that items should only be counted if there is no more likely alternative (3). In essence, if the scorer believes that a manifestation is more likely due to another cause than to SLE, it should not be scored for classification according to the new criteria. In addition, in the study by Fonseca and colleagues, 5.6% of the pediatric patients without SLE had SLE-specific antibodies to double-stranded DNA by *Criethidia luciliae* test and/or anti-Sm antibodies, which would also have to be explained, since these are also specific and heavily weighted criteria, carrying 6 points in the EULAR/ACR 2019 criteria.

We are grateful to Fonseca and colleagues for their efforts to test the new criteria in a South American pediatric population and for their reiteration that leukopenia in patients of African descent is common and may lead to misclassification if not correctly attributed to ethnicity. The significant prevalence of SLE-specific items in their non-SLE patient population (1), however, sheds doubt on the correct use of the EULAR/ACR 2019 SLE classification criteria attribution rule or, less likely, the non-SLE diagnoses in this cohort. This may explain some of the discrepancies between their cohort and the EULAR/ACR SLE criteria validation cohort.

Martin Aringer, MD 
 University Medical Center
 and TU Dresden Faculty of Medicine Carl Gustav Carus
 Dresden, Germany
 Karen H. Costenbader, MD, MPH
 Brigham and Women's Hospital
 and Harvard Medical School
 Boston, MA
 Thomas Dörner, MD
 Charité-Universitätsmedizin Berlin
 Freie Universität Berlin
 Humboldt-Universität zu Berlin
 and Berlin Institute of Health
 Berlin, Germany

Sindhu R. Johnson, MD, PhD, FRCPC 
 Toronto Western Hospital
 Mount Sinai Hospital
 and University of Toronto
 Toronto, Ontario, Canada

1. Rodrigues Fonseca A, Felix Rodrigues MC, Sztajn bok FR, Gerardin Poirot Land M, Knupp Feitosa de Oliveira S. Comparison among ACR1997, SLICC and the new EULAR/ACR classification criteria in childhood-onset systemic lupus erythematosus. *Adv Rheumatol* 2019;59:20.
2. Petri M, Orbai AM, Alarcon GS, Gordon C, Merrill JT, Fortin PR, et al. Derivation and validation of the Systemic Lupus International Collaborating Clinics classification criteria for systemic lupus erythematosus. *Arthritis Rheum* 2012;64:2677–86.
3. Tedeschi SK, Johnson SR, Boumpas D, Daikh D, Dörner T, Jayne D, et al. Developing and refining new candidate criteria for systemic lupus erythematosus classification: an international collaboration. *Arthritis Care Res (Hoboken)* 2018;70:571–81.

DOI 10.1002/art.41198

CD4+ T cells as key players in the immunopathology of Takayasu arteritis: comment on the article by Zhang et al

To the Editor:


I read with interest the report by Zhang et al, describing their study demonstrating that CD4+ T cells isolated from patients with Takayasu arteritis (TAK) are biased to detect the spontaneous differentiation of Th1 and Th17 cells because of hyperactivity of mechanistic target of rapamycin complex 1 (mTORC1) (1). Subsequently, using human artery-NSG mouse chimeras, they showed that mTORC1 inhibition, by either rapamycin or RNAi technology, effectively abrogated the maldifferentiation of TAK CD4+ T cells and vascular inflammation (1). The data presented are convincing; however, I would like to add some comments.

First, TAK and giant cell arteritis (GCA) are categorized as large vessel vasculitides in which vascular inflammation is considered to be mediated by Th1 and Th17 cells (2,3). CD8+ T cells are rarely seen in GCA (2,3), whereas cytotoxic CD8+ T cells are implicated in the pathogenesis of TAK, with perforin expression believed to play a key role (4). Zhang et al did not test mTORC1 activity in TAK CD8+ T cells. Thus, an unanswered question, whether mTORC1 hyperactivity is specific to TAK CD4+ T cells, remains.

Second, the authors mainly focused on effector CD4+ T cell differentiation into Th1 and Th17 cells. However, a previous study from their group showed that CD8+ Treg cells, but not CD4+ Treg cells, are deficient and dysfunctional in GCA (5). It remains unclear whether TAK shares this phenotype with GCA.

Third, the authors established a vasculitis model by engrafting human aortic arteries into the backs of the NSG mice into which TAK peripheral blood mononuclear cells were then injected. CD3+ T cells extracted from the artery grafts were predominantly CD4+ T cells (Figure 5C of the article). A very important question is

why CD4+ T cells, not CD8+ T cells, are selectively recruited to the vascular lesion. Is mTORC1 activity in TAK CD4+ T cells related to this phenomenon? The elucidation of the molecular mechanism underlying this selective recruitment may lead to identification of a novel therapeutic target in both TAK and GCA.

Ryu Watanabe, MD, PhD 
Osaki Citizen Hospital
Osaki, Japan
and Tohoku University Graduate School of Medicine
Sendai, Japan

1. Zhang J, Zhao L, Wang J, Chen Z, Sun M, Zhao J, et al. Targeting mechanistic target of rapamycin complex 1 restricts proinflammatory T cell differentiation and ameliorates Takayasu arteritis. *Arthritis Rheumatol* 2019;72:303–15.
2. Weyand CM, Goronzy JJ. Immune mechanisms in medium and large-vessel vasculitis. *Nat Rev Rheumatol* 2013;9:731–40.
3. Watanabe R, Hosgur E, Zhang H, Wen Z, Berry G, Goronzy JJ, et al. Pro-inflammatory and anti-inflammatory T cells in giant cell arteritis. *Joint Bone Spine* 2017;84:421–6.
4. Seko Y, Minota S, Kawasaki A, Shinkai Y, Maeda K, Yagita H, et al. Perforin-secreting killer cell infiltration and expression of a 65-kD heat-shock protein in aortic tissue of patients with Takayasu's arteritis. *J Clin Invest* 1994;93:750–8.
5. Wen Z, Shimojima Y, Shirai T, Li Y, Ju J, Yang Z, et al. NADPH oxidase deficiency underlies dysfunction of aged CD8+ Tregs. *J Clin Invest* 2016;126:1953–67.

DOI 10.1002/art.41197

Reply

To the Editor:

Dr. Watanabe raises 3 questions that are relevant to our study: first, whether mTORC1 hyperactivity is restricted to CD4+ T cells; second, whether functional CD8+ Treg cells are defi-

cient; and third, whether mTORC1 hyperactivity in CD4+ T cells accounts for their infiltration of arterial lesions. To address these questions, we recruited 6 patients with TAK and 5 age-matched healthy donors and analyzed mTORC1 activity in CD8+ T cells (1), NADPH oxidase 2 (NOX-2) expression in CD8+ Treg cells (2), and the function of mTORC1 in CD4+ T cell mobility (3). Written informed consent was provided by all subjects, and this study was approved by the Ethics Committee of Soochow University.

After stimulation of CD8+ T cells from patients with TAK and healthy donors with anti-CD3/CD28 beads, higher mTORC1 activity was identified in TAK patient T cells (Figure 1A). This observation is supported by earlier reports that, while perforin^{high} CD8+ T cells have been implicated in arterial lesions in TAK patients (4), mTORC1 activity is associated with the production of effector molecules such as perforin in CD8+ T cells (5). Such findings suggest that mTORC1 hyperactivity might be a common feature in T cells, reinforcing the critical involvement of mTORC1 in TAK pathogenesis.

Treg cells are critical for maintaining immune hemostasis and thus preventing autoimmune inflammation. CD8+ Treg cells suppress the activation of CD4+ T cells by transferring NOX-2-containing exosomes, and such functional NOX-2+CD8+ Treg cells are diminished in older adults (2). Of importance, NOX-2+CD8+ Treg cells are essentially absent in patients with GCA, an age-related, autoimmune, large vessel vasculitis (2,6). In contrast, NOX-2 expression in CD8+ Treg cells of TAK patients was generally comparable with that in age-matched healthy donors (Figure 1B), indicating that a deficiency of NOX-2+CD8+ Treg cells is specific to GCA.

In the humanized TAK model, we observed significant infiltration of CD4+ T cells in the arterial lesion. This phenomenon is similar in the human GCA model and is also in accordance with clinical and pathologic observations (7,8). Since inhibition of mTORC1 by rapamycin abrogated the migration of CD4+ T cells

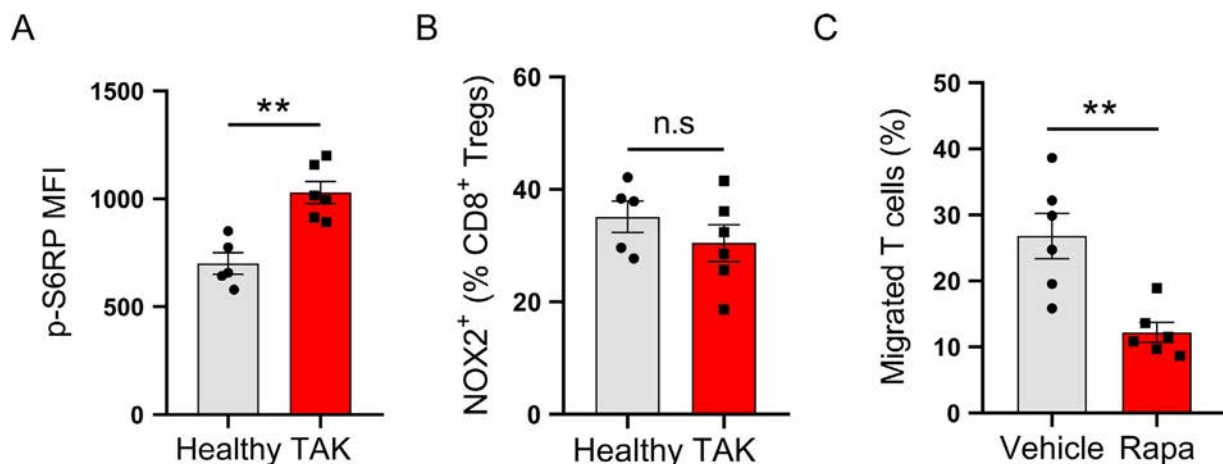


Figure 1. **A**, CD8+ T cells from TAK patients (n = 6) or healthy donors (n = 5) were isolated and stimulated with anti-CD3/CD28 beads (cell:bead ratio 2:1) for 3 days, then analyzed for mTORC1 activity by quantifying intracellular levels of phosphorylated ribosomal protein S6 (S6RP). **B**, CD8+FoxP3+ Treg cells were gated from fresh peripheral blood mononuclear cells and analyzed by flow cytometry for membrane NADPH oxidase 2 (NOX-2) expression. **C**, CD4+CD45RA+ T cells were stimulated with anti-CD3/CD28 beads (cell:bead ratio 2:1) for 2 days in the presence or absence of rapamycin (RAPA) (10 μ M), and analyzed for cell migration by Transwell assay. Symbols represent individual subjects; bars show the mean \pm SEM. ** = $P < 0.01$ by Student's *t*-test. MFI = mean fluorescence intensity; NS = not significant.

(Figure 1C), high mTORC1 levels are clearly related to CD4+ T cell infiltration of the arterial lesion. However, we do not believe hyperactivity of mTORC1 could solely account for the dominant infiltration of CD4+ T cells, given our finding of mTORC1 hyperactivity in TAK CD8+ T cells as well. Rather, we speculate that arterial tissue-resident cells might constitute a unique microenvironment that biases the recruitment of CD4+ T cells. Future studies to address this question would potentially be relevant for the development of novel therapeutic targets for both GCA and TAK.

Supported by the Soochow University's Start-Up Research Fund for Distinguished Professors.

Xiyu Liu, MD, PhD
*Japan Union Hospital of Jilin University
 Changchun, China*
 Wanwan Jiang, BS
 Ying Wang, BS
*Soochow University
 Suzhou, China*
 Mengyao Sun, MD
The First Hospital of Jilin University
 Zhibo Li, MD, PhD 
 Zhenke Wen, MD, PhD 
*The Second Hospital of Jilin University
 Changchun, China*

1. Wen Z, Jin K, Shen Y, Yang Z, Li Y, Wu B, et al. N-myristoyltransferase deficiency impairs activation of kinase AMPK and promotes synovial tissue inflammation. *Nat Immunol* 2019;20:313–25.
2. Wen Z, Shimojima Y, Shirai T, Li Y, Ju J, Yang Z, et al. NADPH oxidase deficiency underlies dysfunction of aged CD8+ Tregs. *J Clin Invest* 2016;126:1953–67.
3. Shen Y, Wen Z, Li Y, Matteson EL, Hong J, Goronzy JJ, et al. Metabolic control of the scaffold protein TKS5 in tissue-invasive, proinflammatory T cells. *Nat Immunol* 2017;18:1025–34.
4. Seko Y, Minota S, Kawasaki A, Shinkai Y, Maeda K, Yagita H, et al. Perforin-secreting killer cell infiltration and expression of a 65-kD heat-shock protein in aortic tissue of patients with Takayasu's arteritis. *J Clin Invest* 1994;93:750–8.
5. Ito D, Nojima S, Nishide M, Okuno T, Takamatsu H, Kang S, et al. mTOR complex signaling through the SEMA4A-plexin B2 axis is required for optimal activation and differentiation of CD8+ T Cells. *J Immunol* 2015;195:934–43.
6. Collison J. Vasculitis syndromes: dysfunctional CD8 T_{REG} cells implicated in GCA. *Nat Rev Rheumatol* 2016;12:314.
7. Wen Z, Shen Y, Berry G, Shahram F, Li Y, Watanabe R, et al. The microvascular niche instructs T cells in large vessel vasculitis via the VEGF-Jagged1-Notch pathway. *Sci Transl Med* 2017;9:eaal3322.
8. Saadoun D, Garrido M, Comarmond C, Desbois AC, Domont F, Savey L, et al. Th1 and Th17 cytokines drive inflammation in Takayasu arteritis. *Arthritis Rheumatol* 2015;67:1353–60.

ACR Announcements

AMERICAN COLLEGE OF RHEUMATOLOGY
2200 Lake Boulevard NE, Atlanta, Georgia 30319-5312
www.rheumatology.org

ACR Meetings

Annual Meeting

November 6–11, 2020, Washington, DC

November 5–10, 2021, San Francisco

Pediatric Rheumatology Symposium

April 29–May 2, 2020, New Orleans

For additional information, visit rheumatology.org/Learning-Center/Educational-Activities.

Applications Invited for *Arthritis Care & Research* Editor-in-Chief (2021–2026 Term)

The American College of Rheumatology Committee on Journal Publications announces the search for the position of Editor, *Arthritis Care & Research*. The official term of the next *Arthritis Care & Research* editorship is July 1, 2021–June 30, 2026; however, some of the duties of the new Editor will begin during a transition period starting April 1, 2021. ACR/ARP members who are considering applying for this prestigious and rewarding position should submit a nonbinding letter of intent by May 4, 2020 to the Managing Editor, Maggie Parry, at mparry@rheumatology.org, and are also encouraged to contact the current Editor-in-Chief, Dr. Marian Hannan, to discuss details. Initial contact should be made via e-mail to Hannan@hsl.harvard.edu. Applications will be due by June 15, 2020 and will be reviewed during the summer of 2020. Application materials are available on the ACR web site at <https://www.rheumatology.org/Learning-Center/Publications-Communications/Journals/AC-R>.

Nominations for ACR Awards of Distinction and Masters Due May 15

The ACR has many Awards of Distinction, including the Presidential Gold Medal. Members who wish to nominate a colleague or mentor for an Award of Distinction must complete the online form at www.rheumatology.org by May 15, 2020. The nomination process includes a letter of nomination, 2 additional letters of recommendation, and a copy of the nominee's curriculum vitae. Recognition as a Master of the American College of Rheumatology is one of the highest honors the ACR bestows. The designation of Master is conferred on ACR members age 65 or older who have made outstanding contributions to the field of rheumatology through scholarly achievements and/or service to their patients, students, and the profession. To nominate someone for a Master designation, members must complete the online nomination form at www.rheumatology.org and include a letter of nomination, 2 supporting letters from voting members of the ACR, and the nominee's curriculum vitae. Nominees for ACR Master must have reached the age of 65 before October 1, 2020.

ACR Invites Nominations for Volunteer Positions

The ACR encourages all members to participate in forming policy and conducting activities by assuming positions of leadership in the organization. Positions are available in all areas of the work of the American College of Rheumatology and the Rheumatology Research Foundation. Please visit www.rheumatology.org for information about nominating yourself or a colleague for a volunteer position with the College. The deadline for volunteer nominations is June 1, 2020. Letters of recommendation are not required but are preferred.